THE MINOR INTRUSIONS AND STRUCTURE OF THE CARLINGFORD COMPLEX, EIRE.

by

T.J. Halsall B.Sc., Leicester.

A thesis submitted for the degree of Doctor of Philosophy in the University of Leicester, June 1974.

T.J.HALSALL, Ph.D. THESIS 1974.

THE MINOR INTRUSIONS AND STRUCTURE OF THE CARLINGFORD COMPLEX, EIRE.

by T. J. Halsall, B.Sc.

Abstract

The Carlingford volcanic complex has an intense swarm of minor intrusions associated with it. Field work demonstrates that the swarm is composite, having involved the repeated injection of magma as dykes, cone sheets and complementary cone sheets in at least three rythmic cycles. Three major rock series are represented in these bodies: the tholeiitic basalt - craignurite series, the alkali basalt series and the high alumina basalt series, other rock types such as felsites, quartz feldspar porphyries and lamprophyres are present in minor proportions.

Analysis of the structure of individual swarms suggests that basaltic magma was injected into the crust as an elongate ridge like body culminating in a cupola beneath the complex, from which cone sheet and radial dyke swarms emerged; linear dyke swarms arose from the ridge crest.

Detailed geochemical investigations show, that the main magma series were derived by fractionation from basaltic parents; that two fractionation paths are represented in the alkali basalt series (the trachy basalt - tristanite series and hawaiite - mugearite - benmorite series); that craignurites represent a true fractionation product of tholeiitic magma and are petrochemically distinct from icelandites.

Basalt fractionation at Carlingford was dominated by the separation of olivine and plagioclase at low pressure while the petrochemistry of the rocks suggests that the three parental stems - tholeiitic basalt, alkali basalt and high alumina basalt, were derived from a common parent by fractionation at higher pressure. Time relations indicate that common parent to be olivine tholeiite magma which it is suggested was formed at depths in excess of 60 km. Miscellaneous rock types, including felsites, lamprophyres and quartz feldspar porphyries are shown to have been derived by melting of crustal rocks during the injection of basic magma within the complex.

T. J. HALSALL

JUNE 1974.

CONTENTS

	Page Numbers
INTRODUCTION	1 - 5
Acknowledgements	4
CHAPTER I	6 - 26
The Petrology and Petrochronology of the Carlingford Complex	
Abstract	6
Introduction	6
Structure	7
Petrology	9
a) Alkali dolerites and derivatives	10
b) Transition dolerites	11
c) Tholeiitic dolerites	11
d) High alumina gabbros and feldsparphyric dolerites	12
e) Quartz dolerites	13
f) Craignurites and craignuritic felsites	14
g) Miscellaneous	15
Relative ages of intrusions	16
Techniques of relative dating	17
Petrochronology of the minor intrusions	22
Absolute age of the Carlingford igneous rocks	24
Conclusions	25
CHAPTER II	27 - 75
The Structural Development of the Carlingford Igneous Complex	
Abstract	27
Introduction	27
A. Major Structures	28 - 42
The Palaeozoic rocks	28

Page Numbers

The Tertiary lavas 30

The early gabbros 33

The layered gabbros 34

Volcanic vents 35

The Carlingford granophyre 36

Faulting 39

B. Minor Intrusions 43 - 69

The dyke swarms 43

Cone sheets and related intrusions 49

The complementary cone-sheets 56

The minor intrusions of Cycle One 57

The minor intrusions of Cycle Two 60

The high alumina gabbro, feldsparphyric dolerite cone sheet swarm 65

The minor intrusions of Cycle Three 67

The occurrence of xenoliths within the minor intrusions 68

C. The Substructure of the Complex 69 - 74

Summary 74 - 75

CHAPTER 3 76 - 97

The Classification of the Tertiary Igneous Rocks of Carlingford

Abstract 76

Introduction 76

Petrological Classification 78 - 81

Alkali dolerite series 78

Tholeiitic dolerites and quartz dolerites 78

Transition dolerites and picrites 79

High alumina gabbros and feldsparphyric dolerites 80

Page Numbers

Craignurite - craignuritic felsite series 80

Rhyolites, felsites and quartz porphyries 81

Lamprophyres 81

Chemical Classification 81 - 93

Processing the analytical data 81

Distinction between the alkaline and tholeiitic series 84

The transition dolerites 86

The high iron transition dolerites 87

The high alumina basalt series 87

The tholeiitic basalt series 88

The basalt "andesite" boundary 89

Subdivision of the alkali basalt series 89

Craignurites and craignuritic felsites 90

High alumina craignurites 92

Rhyolitesand quartz feldspar porphyries 93

The biotite felsites and lamprophyres 93

Summary 93 - 97

CHAPTER 4 98 - 133

The Petrology and Petrochemistry of the Alkali Dolerites and Related Rocks

Abstract 98

Introduction 98

Petrology 99 - 110

a) The alkali dolerites of Cycle I 101

b) The alkaline rocks of Cycle II 102

c) The alkaline rocks of Cycle III 103

	Page Numbers
Mineralogy of the Cycle III alkali dolerites	105 - 110
Petrochemistry	110 - 131
Composition in terms of major elements	110
Trace elements	116
Fractionation trends	126
CHAPTER 5	134 - 165
The Petrology and Petrochemistry of the High Alumina Basalt Series.	
Abstract	134
Introduction	134
Petrography	135 - 138
Mineralogy of the Feldsparphyric Dolerites	138 - 142
Petrochemistry	142 - 157
Composition in terms of major elements	143
Trace elements	149
Petrogenesis	157 - 164
The true nature of the high alumina gabbros and feldsparphyric dolerites	157
Fractionation trends	160
Summary	165
CHAPTER 6	166 - 206
The Petrology, Mineralogy and Petrochemistry of the Tholeiitic Basalt - Craignurite Series	
Abstract	166
Introduction	166
Petrography	167 - 174
Mineralogy	174 - 181

Page Numbers

Petrochemistry 181 - 203

Composition in terms of major elements 181

Trace elements 188

Fractionation trends 198

Summary 204 - 205

CHAPTER 7 206 - 217

The Petrochemistry and Petrogenesis of a Quartz Dolerite - Craignuritic Felsite Composite Cone-Sheet at Carlingford

Abstract 206

Introduction 206

Description 207

Petrochemistry 208

Petrogenesis 211

Conclusions 214

Summary 215

CHAPTER 8 218 - 248

The Petrochemistry of the Country Rocks, Gabbro Xenoliths, Lamprophyres and Acid Rocks in the Carlingford Complex.

Abstract 218

Introduction 218

Composition of the sedimentary country rocks 219

Composition of a Caledonian minette dyke 222

The composition of the basaltic lavas 223

The origin of the gabbro xenoliths 224

The composition of the quartz feldspar porphyries 226

The composition of the biotite felsites 227

Page Numbers

The composition of a rhyolite 228

The composition of the felsite sample 839 228

The composition of the lamprophyres 232

The origin of the acid magmas 234

The origin of the lamprophyres 241

Summary 245

CHAPTER 9 249 - 274

The Origin of Basaltic Magmas Occurring Within the Carlingford Complex

Abstract 249

Introduction 249

Summary of Carlingford fractionation trends 250

Reconsideration of the Carlingford time sequence 252

Primitive and primary magmas 254

The origin of parental alkali basalt magmas 262

The generation of high alumina basalt magmas 266

The role of PO_2 in Carlingford fractionation trends 267

The occurrence of spinel xenocrysts 271

Conclusions 272

Summary 273

CHAPTER 10 275 - 280

A Summary and Synthesis of the Magmatic Processes which took place in the Carlingford Complex.

Abstract 275

Introduction 275

Processes within the mantle 275

Page Numbers

Processes within the crust 277

Conclusion 279

APPENDIX I 281 - 292

Analytical Techniques

Introduction 282

Sample preparation 282

XRF Nottingham 283

a) Major elements 283

b) Trace elements 283

c) Standards 283

d) Operating conditions 286

XRF Reading 286

Wet analysis Leicester 286

Wet analysis Reading 289

a) Sample splitting 289

b) Sample decomposition 289

c) Analytical methods 289

Microprobe analysis 291

APPENDIX II 293 - 298

Composition of Carlingford Alkaline Rocks

APPENDIX III 299 - 302

Composition of Carlingford High Alumina Basalts

Page Numbers

APPENDIX IV 303 - 319

Composition of Carlingford Tholeiitic Basalts and Craignurites

APPENDIX V 320 - 323

Composition of Miscellaneous Carlingford Rocks

APPENDIX VI 324 - 328

C.I.P.W. Norms of Carlingford Alkaline Rocks

APPENDIX VII 329 - 333

C.I.P.W. Norms of Carlingford High Alumina Basalts

APPENDIX VIII 334 - 356

C.I.P.W. Norms of Rocks in the Tholeiitic Basalt-Craignurite Series

APPENDIX IX 357 - 363

C.I.P.W. Norms of Miscellaneous Carlingford Rocks

APPENDIX X 364 - 368

Trace Element Concentrations in Rocks of the Alkali Basalt Series

APPENDIX XI 369 - 372

Trace Element Concentrations in Rocks of the High Alumina Basalt Series

Page Numbers

APPENDIX XII 373 - 387

Trace Element Concentrations in Rocks of the Tholeiitic Basalt - Craignurite Series

APPENDIX XIII 388 - 393

Trace Element Concentrations in Miscellaneous Carlingford Rocks

APPENDIX XIV 394 - 407

Duplicate XRF and Wet Analyses of Carlingford Rocks

APPENDIX XV 408 - 417

Analyses of Carlingford Rocks Prepared at Reading by XRF

APPENDIX XVI 418 - 438

Identity, Age and Locality of Analysed Carlingford Rocks, and Structures of Source Bodies

BIBLIOGRAPHY 439 - 465

INTRODUCTION

This account of the structure, petrology and petrochemistry of the Carlingford Complex is the product of five years research initiated in September 1968. Much of the work was carried out during the tenurship of a three year N.E.R.C. studentship and a further year as a temporary lecturer in the Department of Geology, Leicester University. The majority of analytical work was carried out at Nottingham University during that period, using X-ray fluorescence spectrometry. Since October 1972 the author has held the post of Lecturer in Geology at Reading University, which has enabled the investigation to be continued and completed thus far.

The aim of the project as originally conceived was to investigate the petrochemistry and petrochemical behaviour of basaltic magmas in the Carlingford Complex in the light of their petrography, time relations (petrochronology) and structural setting; to define precisely the nature and significance of Hebridean intermediate magma types occurring there; to investigate processes of magma genesis associated with the complex both in the crust and in the mantle in the light of the petrochemical, petrographic and petrochronological data; and to apply the conclusions arrived at to a consideration of the genesis of basaltic magmas in general, particularly the current petrogenetic models based largely on experimental petrology. It was considered at the outset that minor intrusions provide the most representative sample of the magma types available in a Tertiary central complex, and that the intensity of the Carlingford dyke and cone-sheet swarms provided abundant field data enabling the

erection of a detailed petrochronological sequence based largely on cross cutting relationships and chilling phenomena.

The entire investigation is based on some fifteen weeks field work carried out in September and October 1968, and July and August 1969, and a collection of some 1431 samples collected during those periods. Further material was kindly provided by Dr. M.J. Le Bas from his extensive collections.

This report is subdivided into ten chapters. Chapter 1 considers briefly the petrology of the complex and the erection of the petrochronological sequence, which is critical to investigation as a whole. Chapter 2 is a structural interpretation based on the three dimensional geometry and time relations of the dyke and cone-sheet swarms.

The classification outlined in petrological terms in Chapter 1, is adopted in Chapter 2 as it stands but defined more rigorously on the basis of petrochemistry in Chapter 3. The two schemes are not entirely consistant with one another, but the use of a petrographic classification enables incorporation of a large quantity of material which could not otherwise be included, as petrochemical data is not available in the case of the rocks in question. Such discrepancies which arise as a result of these minor inconsistancies are too few in number and too minor in substance to discount the structural interpretation put forward.

Chapters 4,5 and 6 describe the petrographic and petrochemical trends exhibited by the three principal series of igneous rocks exhibited in the complex (the alkali basalt series, the high alumina

basalt series and the tholeiitic basalt - craignurite series, respectively). A rigorous statistical approach to this data has not been adopted, due largely to the pressure of time, the trends described have been defined diagramatically. Such a statistical investigation of the data may yield further information of significance in the future.

Chapter 7 describes the structure and petrochemistry of a composite cone-sheet and outlines the process of hybridization which took place during its emplacement. The petrochemistry and petrogenesis of miscellaneous rock types, including country rocks, Tertiary lavas and intrusive rocks not covered in previous chapters, are described in Chapter 8.

Chapter 9 discussed the origin of the three magma series described in Chapters 4.5 and 6 in the light of experimental petrology. Chapter 10 is a brief synthesis of petrogenetic process in the complex during the Tertiary based on the conclusions drawn in previous chapters, including Chapters 1 and 2.

The abundant petrochemical data, on which many of the results depend, are listed in Apendices II, III, IV and V (major element determinations, Nottingham XRF), X, XI, XII and XIII (trace element determinations, Nottingham XRF), V, and XV (Reading XRF). CIPW norms of the analyses listed in Appendices II to V are set out in Appendices VI, VII, VIII and IX. Duplicate analyses, carried out by wet methods, Reading XRF or Durham XRF, are listed for comparison with the Nottingham XRF results in Appendix XIV. Appendix XIV shows that there is reasonable agreement between major element compositions determined by different methods and laboratories, there are inconsistances between

trace element concentrations determined at Nottingham and those determined at Reading, in some cases however. In order to retain internal consistancy, the petrochemical interpretations set out in Chapters 4, 5 and 6, are based entirely on the 262 analyses carried out at Nottingham except where, only Reading data is available in the case of some elements. The trends described are thus meaningful in themselves, but trace element concentrations quoted should not be treated as absolute values. The analytical techniques adopted, including those for microprobe analysis, are described in Appendix I.

Appendix XVI consists of a list of specimen localities and their identities.

In conclusion it must be stated that this thesis is not regarded as a complete account of those aspects of the Carlingford Complex encompassed by its title. The reader will appreciate that large fields require further examination and that some problems have been merely touched in passing. Detailed studies of the mineralogy and mineralogical distribution of trace elements in Carlingford rocks; the use of opaque mineral studies in geothermometry and oxygen barometry; the erection of a palaeomagnetic chronology which could be compared with the time sequence set out herein, could all bear fruitful results for example.

Acknowledgements.

I gratefully acknowledge the advise, guidence and unceasing encouragement of Dr. M.J. Le Bas which was forthcoming throughout the period of this investigation; the assistance and advise of Dr. P.K.

Harvey, Dr. D. Field and Dr. R.B. Elliot of Nottingham University and for their generous provision of XRF facilities; also for the invaluable friendship of Dr. C. Barber without whose help in overcoming the vagaries of computers it would have been impossible to complete the analytical programme undertaken.

I wish to thank Professor P.C. Sylvester Bradley and the staff of the Leicester Department for advice, assistance and constant inspiration.

I thankfully acknowledge the encouragement and advice of Professor P. Allen and many helpful discussions with my colleagues at Reading, also the assistance of Dr. A. Parker and of Dr. G.A.R. Till in the fields of X-ray analysis and computing respectively.

I also wish to thank the technical staff of the Geology Departments at Leicester, Nottingham and Reading and in particular Mr.A.G. Cross and Mr. J.L. Watkins for their assistance with illustrations, and Mrs. A. Fuller and Mrs. L. Garland for typing the thesis.

I gratefully acknowledge the N.E.R.C. studentship which made possible the first three years of this investigation.

Finally, I must asknowledge the forebearance and affection of my wife and family, which has encouraged me throughout the period in question, and the special contribution made by my wife and by Mrs. S.E. Nightingale in correcting the manuscript and assisting to draft the figures.

T.J.H. January 1974.

CHAPTER 1

THE PETROLOGY AND PETROCHRONOLOGY OF THE CARLINGFORD COMPLEX

Abstract.

The structure of the numerous minor intrusions of the Carlingford Tertiary Complex is outlined and their petrology described. A schematic petrochronological sequence is set out and justified on the basis of field relations and comparative petrology. The petrochronological sequence indicates a rhythmic repetition of the principle magma types present in the area.

Introduction

The Carlingford Complex, an igneous centre in the British Tertiary Province, forms a mountainous peninsula on the east coast of Ireland immediately south of the Ulster border and some 50 miles north of Dublin (see Fig. 1.1) It is one of three Tertiary igneous complexes in the area; the granites of the Mourne Mountains crop out some 5 miles to the north east, across Carlingford Lough, while the Slieve Gullion Complex lies immediately to the north west.

The complex was first mapped in the 19th Century by the Irish Survey (Traill 1878). The complex and its petrology has previously been discussed by Hamilton (1839), Griffith (1840), Haughton (1856, 1858, 1876), Rose (1863) and Von Lasaulx (1878). Traills map shows a series of large masses of basic rock capping the higher ground, a granite and an intense swarm of basic minor intrusions, all cutting argillaceous Silurian sediments and Carboniferous Limestone. Sollas (1894) and more recently Nockolds (1935, 1937, 1938) have described the complex acid-basic hybridization of the larger intrusive masses

Figure 1.1

Distribution of Tertiary dyke swarms and intrusive centres, including Carlingford, in the British Isles (After Richey and Thomas 1930 Fig. 4 p. 53).

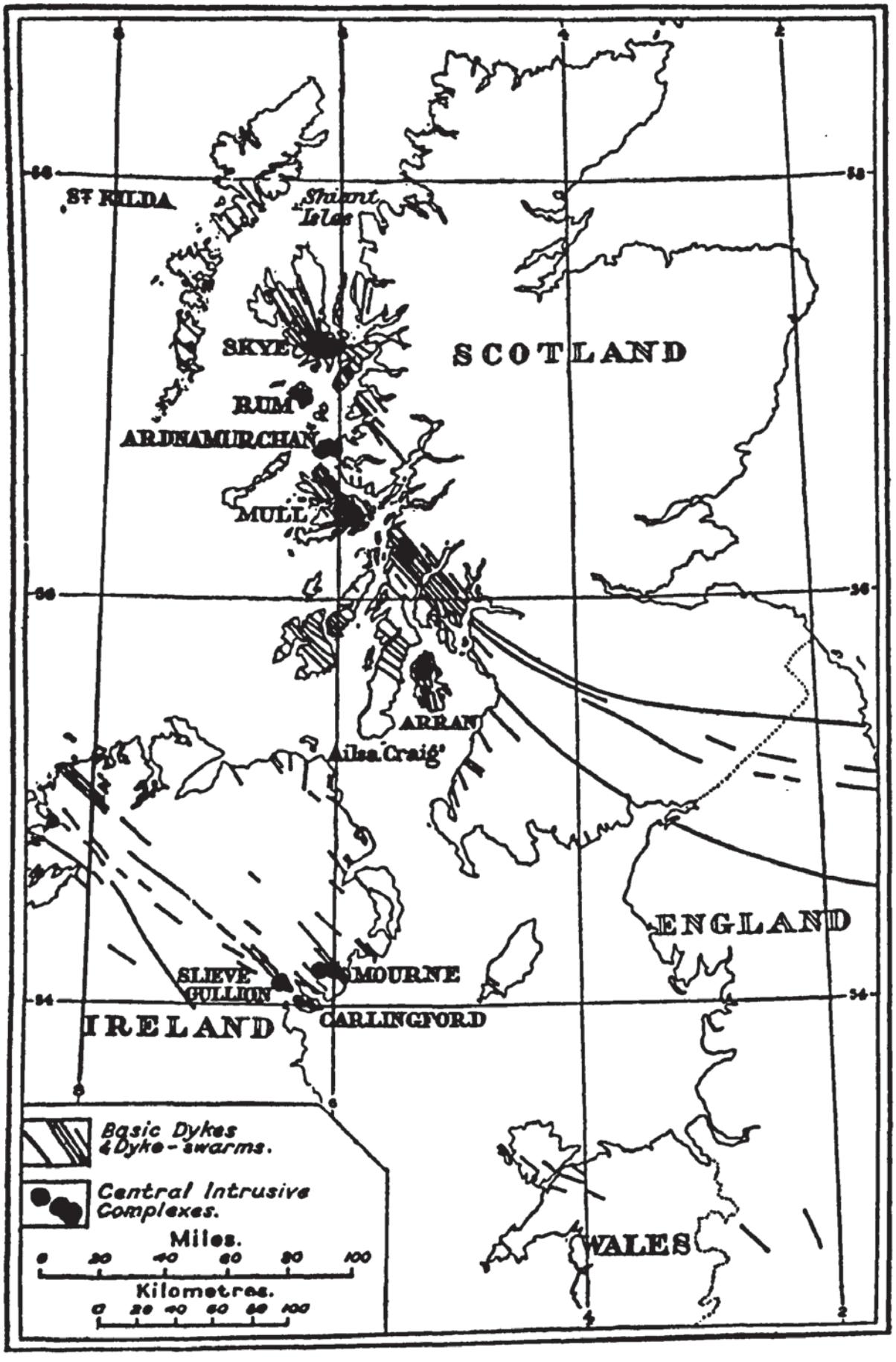

in the complex, the structure of which bodies have been discussed by Richey (1932) and Le Bas (1960, 1967). The work of Richey and Le Bas has shown that outliers of basaltic lava(Richey 1932, Le Bas 1965a) and a series of volcanic vents of Tertiary age (Le Bas 1955) are present in the area. The metamorphic effects of intrusive basic magma on Silurian Country rock at Carlingford have been discussed by Harry (1952, 1954) and Le Bas (1960, 1970b), Le Bas has also described the effects of contamination of the Carlingford gabbro by limestone (1965b) and by Silurian argillites and Tertiary basalts (1970a and b). A gravity survey of the area has been carried out by Cook and Murphy (1952) and the Carlingford Peninsula is covered by the Geological Survey Aeromagnetic Map Sheet 7 (Bullerwell 1964). The Tertiary age of the complex, originally established by Richey on the basis of field relations (1932), has recently been confirmed by Evans, Fitch and Miller (1973) on the basis of radiometric dating of samples of igneous material from the centre.

The object of the current investigation is to elucidate the structure, petrology and petrochronology of the abundant minor intrusions of the area. The latter are shown on Map 1 and subsequent inset maps. The boundaries of the major rock units are largely taken from Le Bas' maps, the minor intrusions were mapped by the present author who was, in large part, able to confirm the accuracy of Traills survey work.

Structure.

The country rocks into which the Tertiary intrusions were emplaced, consist of tightly folded Silurian argillites with isolated minette

dykes of Caledonian age, overlain unconformably by gently folded Carboniferous Limestone and capped by extrusive Tertiary basalts.

The ring like outcrop pattern of the major gabbro masses led Richey to suggest that they formed a discontinuous basic ring dyke (Richey 1932). Le Bas was later able to show that the majority of these gabbro masses form part of a layered gabbro lopolith, intruded by the granite and subsequently dissected by erosion to give their present form; and that the gabbros of Trumpet Hill, Drumenagh Hill and Rock Marshall are plug like intrusions forming an earlier Tertiary event (Le Bas 1960).

The granite (a granophyre) has the form of a flat topped dome interpreted as the top of a ring dyke by Le Bas (1967).

The minor intrusions of the complex include: cone sheets, as defined by Anderson (Bailey et al.1924 Ps 11-12), some of which have the form of transgressive sills where they cut Carboniferous Limestone, and which in total constitute about 66% of all minor intrusions of Tertiary age in the area, (some 792 have been recorded during the current investigation); sheets which dip radially outwards from the cone sheet focii and referred to below as complementary cone sheets, they constitute about 4% of the minor intrusions; and near vertical dykes which in total constitute the remaining 30% of the swarm, some 360 dykes have been mapped.

The cone sheets and complementary cone sheets focus on an elliptical area at the centre of the complex near Spellickanee, with its long axis directed north west - south east (see Fig. 1.2) and at an average depth of about 3 km. below the present surface.

The azimuths of the dyke trends for the whole complex have been

Figure 1.2

Map of the Carlingford Peninsula showing the distribution of cone-sheets (heavy lines with down-dip symbol) and cone-sheet focii. For details of distribution of major rock units see Map 1.

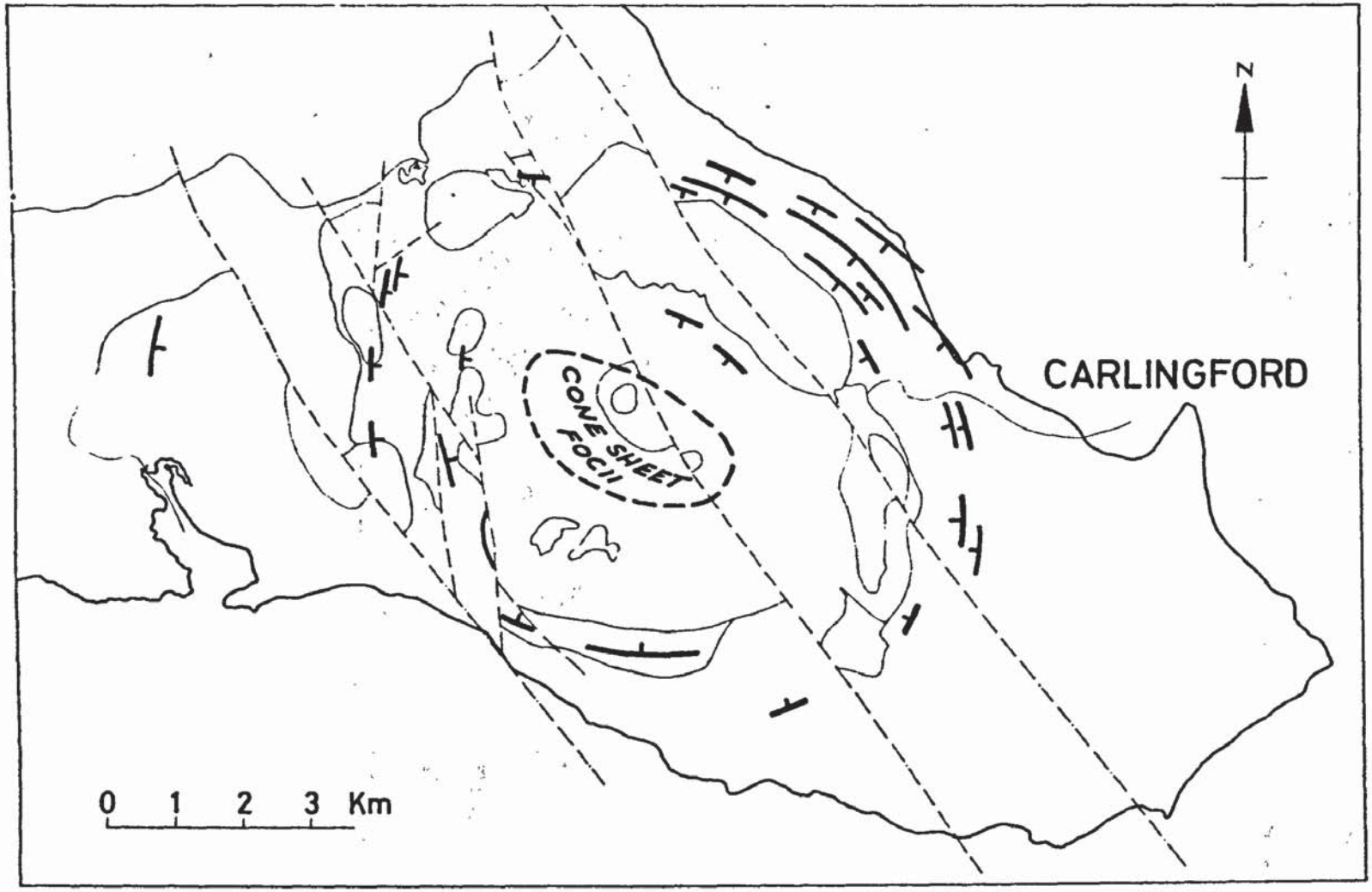

Figure 1.3

Rose diagram of dyke trend azimuths in the Carlingford Complex as a whole, for a total of 327 dykes, where peak height from the base circle is proportional to the number of dykes per 10° arc ($001^{\circ} - 010^{\circ}$ inc., $011^{\circ} - 020^{\circ}$ inc., etc., etc.). All azimuths are measured from True North.

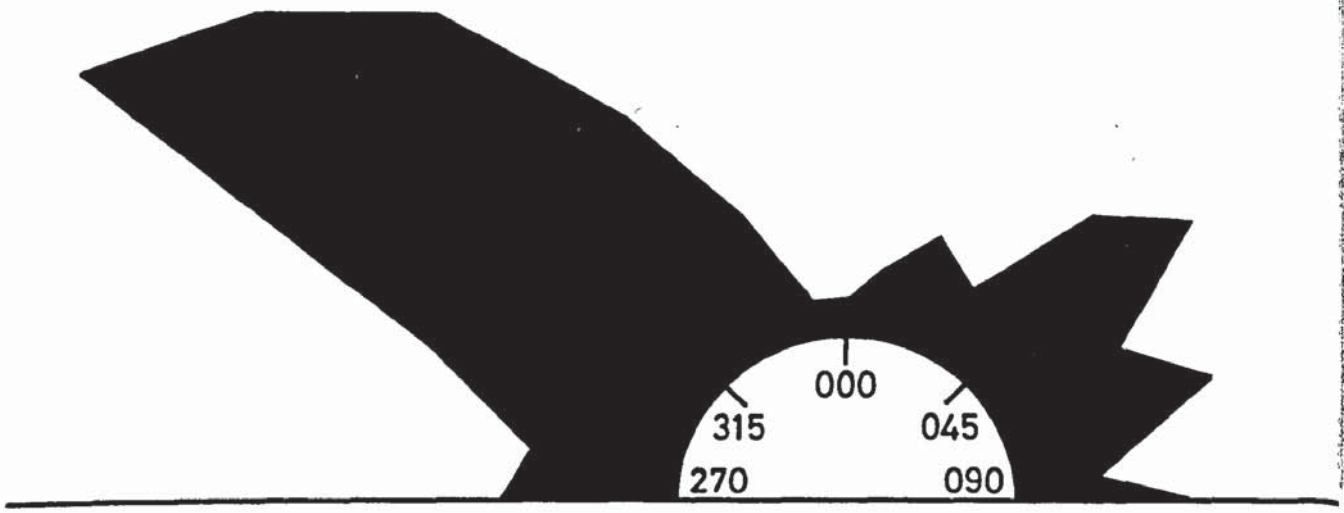

plotted as a rose diagram of numbers of dykes every 10° interval from true north (Fig. 1.3) which shows that there are several axes of dyke injection. The majority of dykes - about 60 percent of the total - have the north west - south east trend typical of Tertiary centres in Britain (Richey 1939), however dykes with other trends do occur, most notably a series with a north east - south west axis trending 050° true, on average. In order to show the variation of dyke trends with geographical location within the complex the Carlingford Peninsula was divided into eight sub areas, each of about 80 square kilometres, and the dykes trends for each area plotted separately as rose diagrams (Fig. 1.4). The lack of data in the subareas forming the southern part of the peninsula (subareas 5,6 & 7) largely results from paucity of exposure there. Figure 1.4 shows that some of the dykes have a radial distribution about the centre of the complex and the cone sheet focal axis, however it is not considered by the author that they constitute a single radial swarm, and it will be demonstrated below that a number of superimposed dyke swarms are present, some of the individual swarms may be radial to the complex.

Traversing the peninsula are a series of fractures which postdate igneous activity within the complex. The most significant of these are a series of north west - south east trending tear faults with a consider -able horizontal displacement in a dextral sense, other faults trend north - south and north east - south west.

Petrology.

The petrology of the gabbros and granophyres of the Carlingford

Figure 1.4

Rose diagrams of dyke trend azimuths for dykes within eight sub areas of the Carlingford Complex, each of approximately 80 square kilometres. The number of dykes in each sub area is indicated in the lower right hand corner, no data is available for area 5. Peak height from the origin is proportional to the number of dykes per 10° arc (001° - 010° inc., 011° - 020° inc., etc., etc.). All azimuths are measured from True North.

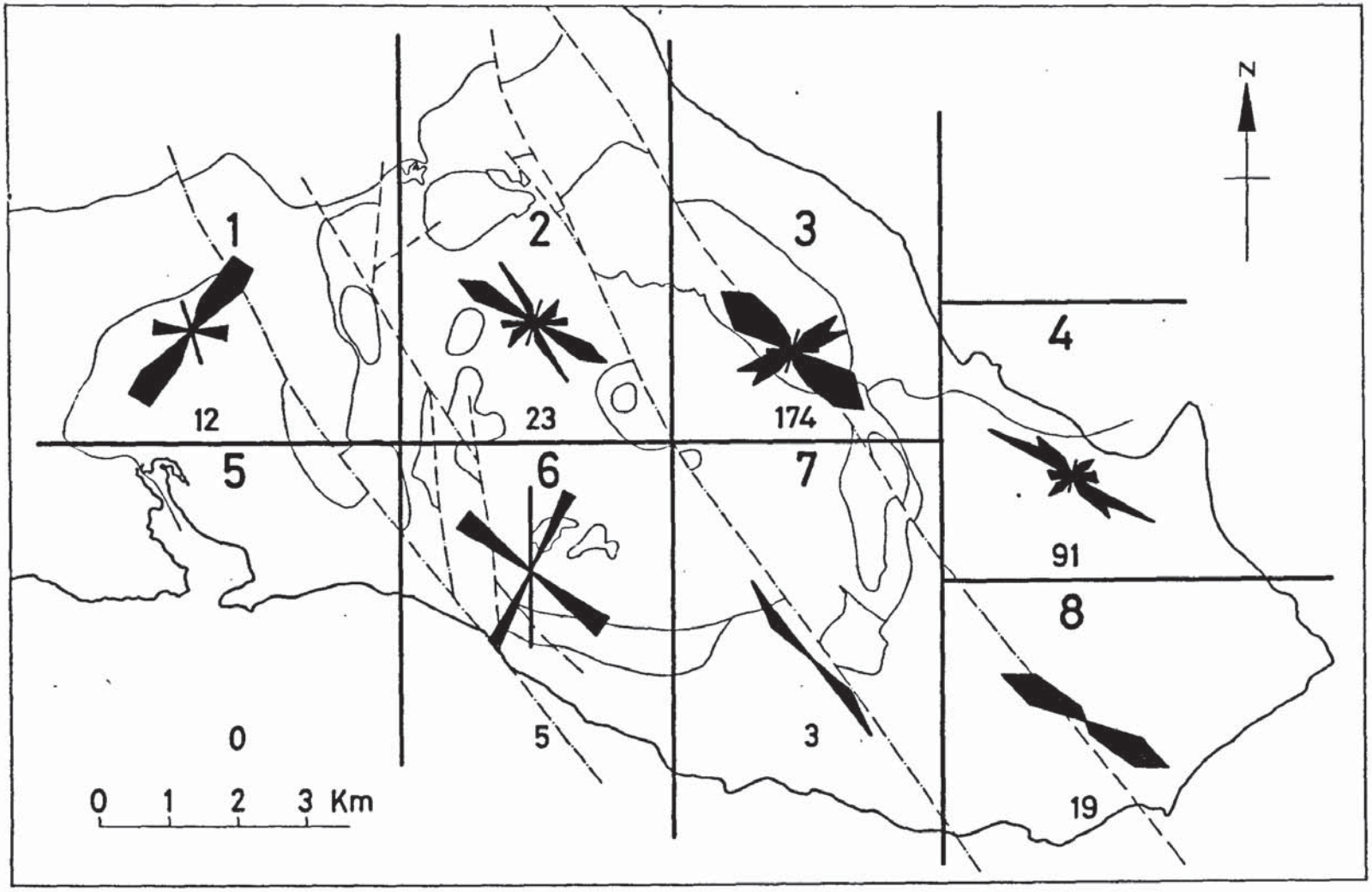

Complex has been discussed in detail by Le Bas (1960, 1965b, 1967, 1970a, 1970b) and will not be further considered here. A variety of rock types are present in the minor intrusions of the area, the majority falling within six petrological suites discussed below. The remaining types are considered together under the miscellaneous heading.

a) Alkali dolerites and derivatives.

Alkali dolerites and related rocks are almost totally restricted to dykes, of which they constitute some 28% of those mapped. They are readily identifiable in the field by their marked spheroidal weathering. Olivine is usually present and some of the more picritic varieties may contain as much as 30 percent in the mode.

The alkali dolerites are typically medium grained and holocrystalline with subophitic textures, often with some alignment of the prismatic minerals. The more siliceous members of the suite however tend to be fine grained, and show a marked development of the trachytic texture . The basic varieties which comprise the majority of rocks in this group are characterised by the presence of titan augite (up to 40 percent in the mode) which is usually a distinct pink or lilac colour in thin section. Plagioclase is basic, either bytownite or calcic labradorite in the more basic varieties, giving way to andesine and oligoclase in feldspathic derivatives.

The rocks in this suite are generally aphyric but phenocrysts of basic plagioclase do occur. Olivine phenocrysts are abundant in the picritic varieties and some basaltic types. Amygdales of chlorite, calcite or siderite are often present in abundance, particularly near

the margins of some dykes reflecting the distribution of CO_2 and H_2O noted in a basic dyke in Ardnamurchan by Wells and Smith (1973).*

The majority of alkaline rocks in the area show intense alteration with replacement of ferromagnesium minerals by chlorite, and the introduction of calcite; olivine, if present, is invariably pseudomorphed by iddingsite, bowlingite,chlorite or calcite.

b) Transition dolerites.

Rocks defined petrographically as "transition dolerites" occur as cone sheets, complementary cone sheets and dykes, and comprise about 15% of all minor intrusions in the complex.

Typically they consist of ophitic or subophitic augite, calcic labradorite or bytownite plagioclase and subhedral skeletal titanomagnetite. Olivine is often present and may constitute more than 20% of the rock though it is usually replaced by bowlingite, chlorite or calcite. Chlorite frequently occurs as an alteration product and secondary pyrite is present in some transition dolerites. Phenocrysts, when present, are usually basic plagioclase or olivine, though pyroxene xenocrysts and xenoliths of gabbro and/or hornfelsed sediment are sometimes present. Primary quartz, hypersthene, zeolite or feldspathoid are always absent. These rocks give way to tholeiitic dolerites with the appearance of a glassy or granophyric mesostasis.

c) Tholeiitic dolerites

Tholeiitic dolerites comprise approximately 28% of all minor intrusions in the complex, occurringas cone sheets, complementary cone sheets and dykes. They consist of subophitic or granular clinopyroxene, labradorite plagioclase and granular titanomagnetite with varying

* NOTE : ABSTRACT ONLY. SINCE THE TIME OF WRITING, THIS PAPER HAS BEEN PUBLISHED IN FULL (WELLS, SMITH AND BOWLES, 1974).

quantities of interstitial material. The latter is usually brown glass, chlorite, or a granophyric intergrowth of quartz and feldspar. Olivine may comprise up to 12 percent in the mode. Textures are typically basaltic.

Phenocrysts, when present, are usually labradorite or olivine, though augite phenocrysts/xenocrysts or gabbro xenoliths may also be present. Corroded brown spinel xenocrysts occur in some tholeiitic dolerites. When altered, the tholeiitic dolerites usually contain chlorite, replacing the ferromagnesium minerals, and frequently secondary quartz, calcite and pyrite.

With increasing proportions of mesostasis or free quartz the tholeiitic dolerites grade into the quartz dolerites.

d) High alumina gabbros and feldsparphyric dolerites.

This group of rocks is readily identified in the field by its coarse gabbroic or porphyritic texture.

The feldsparphyric dolerites occur almost exclusively as cone sheets comprising about 20% of all such intrusions. The less abundant high alumina gabbros occur both as cone sheets and as dykes - possibly a radial swarm.

The feldsparphyric dolerites are characterised by abundant labradorite - bytownite phenocrysts (between 30 and 60 percent in the mode) and are equivalent to Bailey's "Porphyritic Central Magma Type" (Bailey et al.1924). The matrix in these rocks is petrologically identical with that of some of the tholeiitic dolerites, it consists of ophitic to subophitic augite, labradorite lathes and titano-magnetite, olivine is frequently, but not invariably, present, as are

interstitial phases. Le Bas has shown that removal of the plagioclase phenocrysts from the analysed composition of a feldsparphyric dolerite (Le Bas specimen 72, Specimen 172 in the current study) leaves a composition which is essentially tholeiitic (Le Bas 1955 pg 238).

With increase in the grain size of the matrix the feldsparphyric dolerites grade into the high alumina gabbros, this, in some cases, takes place within a single intrusion, the feldsparphyric dolerite, specimen 172, grading into the high alumina gabbro, specimen 177, within about 200 metres along the outcrop of a cone sheet. Olivine is invariably present in the gabbros while interstitial mesostasis is absent, otherwise the gabbroic texture is all that distinguishes them from the feldsparphyric dolerites. The gabbros are petrologically identical with those of the layered gabbro lopolith described by Le Bas (1960) emphasising the significance of this rock type within the complex.

Rocks of this suite sometimes contain xenoliths of olivine gabbro. They are also particularly susceptable to uralitization and chloritization of their ferromagnesium minerals.

e) Quartz dolerites.

Quartz dolerites comprise approximately 20% of all minor intrusions at Carlingford, occurring as dykes, cone sheets and complementary cone sheets. The principal minerals present in these rocks are prismatic clinopyroxenes, andesine or labradorite plagioclase, and titanomagnetite sometimes accompanied by iron sulphide. Interstitial glass is present in some varieties and free quartz is often abundant, both

in the interstices and as a late development in cavities where it is often accompanied by calcite.

The texture of medium grained rocks is essentially doleritic, chilled rocks show well developed variolitic textures or in some cases occur as tachylites. Phenocrysts, when present, are plagioclase or clinopyroxene ; gabbro xenoliths also occur in some rocks. Many quartz dolerites have suffered secondary pyritization.

The quartz dolerites grade into craignuritic varieties with decreasing groundmass pyroxene and corresponding increasing proportions of quartz and sodic plagioclase.

f). Craignurites and craignuritic felsites.

Craignurites (Bailey et al.1924) and related rocks occur as both dykes and cone sheets, constituting at least 10% of all minor intrusions mapped.

The craignurites themselves are characterised by the craignuritic texture, which is one of elongate clinopyroxene prisms, set in a feldspathic matrix. The matrix may be glassy or crystalline, frequently with quartz occurring throughout the groundmass as irregular crystals. Groundmass feldspar is typically oligoclase or andesine in composition and often shows hopper crystal development, particularly when embedded in glass. Ore is not usually present in abundance in these rocks though titanomagnetite with a rod-like habit and iron sulphide often occur in small quantities. Phenocrysts, when present, include plagioclase and clinopyroxene.

In more feldspathic varieties groundmass pyroxene is greatly reduced in quantity and occurs as small prisms, usually chloritized, set

in a matrix of finely intergrown quartz and feldspar, or glass. These craignuritic felsites correspond with Bailey's leidleites, if aphyric, and inninmorites if porphyritic (Bailey et al, 1924).

g). Miscellaneous

Other rock types occur in the area in limited quantities. Lamprophyres consisting of euhedral hornblende, phenocrysts set in a feldspathic matrix, occur in the northern part of the area. They are vogesites and spessartites which grade into rocks of camptonitic character as defined by Hatch, Wells and Wells (1961, pg. 383) and there is some difficulty in attributing an age to them. Many are similar to the vogesites of the Ards Peninsula which are considered to be Caledonian in age by Reynolds (1931), however they occur as sheets which may be interpreted from their attitude as Tertiary cone sheets and complementary cone sheets related to the Carlingford centre. Camptonitic lamprophyre dykes, some bearing hornblende, are associated with many of the Tertiary volcanic centres of the Hebridean Province, and are attributed to the Tertiary by Bailey (Bailey et al.1924 Chapter XXXV). None of the Carlingford lamprophyre sheets are seen to cut dykes of known Tertiary age, however biotite felsite dykes and cone sheets, which are perhaps related to the lamprophyres, do postdate known Tertiary dykes. On that basis the lamprophyres are tentatively attributed to the Tertiary.

The biotite felsites consist of phenocrysts of green biotite and plagioclase set in a medium grained granitic matrix of quartz, alkali feldspar and mica.

Quartz-porphyries consisting of embayed subhedral phenocrysts of

quartz, subhedral phenocrysts of plagioclase, and occasional micro-xenoliths of granophyre, and a fine grained quartzofeldspathic matrix, occur as dykes in the northern part of the area (specimens 1203, 1212) and also in the vicinity of Whitestown in the south east (specimen 810). A felsite consisting of subhedral clinopyroxene crystals set in a fine grained quartzofeldspathic matrix occurs as the upper layer of a composite cone sheet near Mullatee (specimen 839).

Two northwest - southeast dykes which crop out in a stream about two kilometres north east of Spellickanee, have a gabbroic texture and consist of labradorite, subophitic augite and granular ore with large interstitial patches of granophyre and abundant epidote (see specimen 1292). The presence of the granophyre patches and epidote result from the effects of the granophyre which these dykes cut, and which must still have been hot and probably undergoing pneumatolitic crystallization, at the time of their intrusion.

Relative ages of intrusions.

The sequence of major episodes in the development of the Carlingford Complex during the Tertiary has been established by Le Bas (1960, 65a and 67) and may be summarized as follows:

1. Extrusion of basalt lavas.
2. Intrusion of the layered gabbros.
3. Development of the volcanic vents.
4. Intrusion of the Carlingford granophyre.
5. Development of north west - south east trending tear faults.

The intrusion of the "Early" gabbro plugs of Trumpet Hill, Drumenagh Hill and Rock Marshall may be related to the extrusion of the lavas and certainly preceded the emplacement of the layered gabbros (Le Bas 1960).

The relative ages of the minor intrusions of the Carlingford Complex have been established during the current research and can be set against the framework provided by Le Bas' scheme.

Techniques of relative dating

The following techniques were employed to determine the relative ages of the minor intrusions and the rock types: incorporated within them:

1. Detailed field studies of cross cutting relationships at dyke (etc) intersections.

2. Investigation of the petrology of minor intrusions cutting major intrusive masses.

3. Correlation of petrologically similar types and the recognition of rock types occurring only once in the sequence.

4. Investigations of chilling phenomena of one rock against another, particularly in composite and multiple intrusions.

5. Petrological investigation of the metamorphic affects of: a) the layered gabbros; and b) the granophyre, on minor intrusions within their respective aureoles.

6. Study of the distribution of pyritization of minor intrusions.

7. Investigation of the nature of xenoliths incorporated in minor intrusions.

Figure 1.5

Localities of inset maps and figures: a = Map 2; b = Map 3; c = Map 4; d = Map 5; e = Map 6; f = Fig. 1.6 g = Fig. 1.7; h = Fig. 1.8. For details of distribution of major rocks units see Map 1.

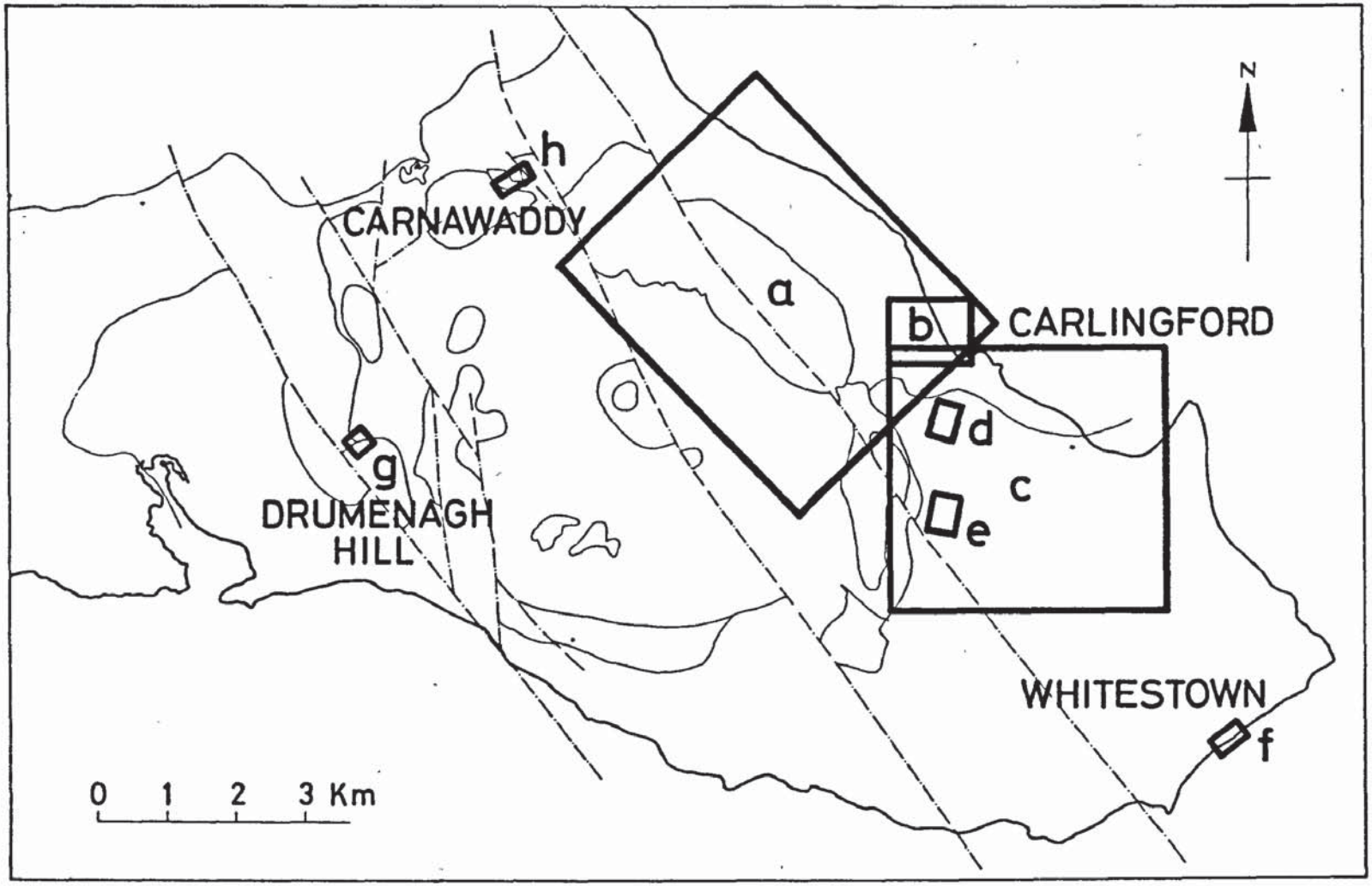

The investigation of cross cutting dyke intersections in South Arran by the current author proved successful in determining the age relationships of minor intrusions there (Halsall and Le Bas 1971). Study of some 300 intersections of dykes and cone sheets, and other cross cutting relationships at Carlingford has established the relative ages of large numbers of individual intrusions. The technique requires petrological correlation of the individual intrusions at such intersections with others elsewhere, in order to complete a sequence in many cases. Figure 1.5 indicates the geographical location of the inset Maps 2,3,4,5 and 6, and Figures 1.6, 1.7, and 1.8 which give details of dyke and cone sheet outcrop patterns and cross cutting relations in the areas of the Carlingford Complex depicted.

Rocks of all the main petrological suites cut the gabbros and granophyre. The apparent lack of minor intrusions shown cutting the granophyre on the accompanying maps is the result of poor exposure due to drift cover, rather than an absence of dykes etc., the latter are seen to be present wherever exposure is good. Minor intrusions are not as numerous cutting the gabbros as in the surrounding country rock. This is partly due to the fact that the gabbros postdate many minor intrusions (as does the granophyre) but is also a function of the resistance of these massive rocks to the formation of fractures suitable for intrusion. Many dykes and cone sheets which can be shown to post-date the gabbros on other evidence, fail to pass from the Silurian sediments on Carlingford Mountain into the lopolith, and in some cases are deflected as they approach the contact.

Correlation of similar rock types proved difficult as many were

Figure 1.6

Geology of the shore at Whitestown (Fig. 1.5f). See Map 1 for legend, numbers refer to sample numbers.

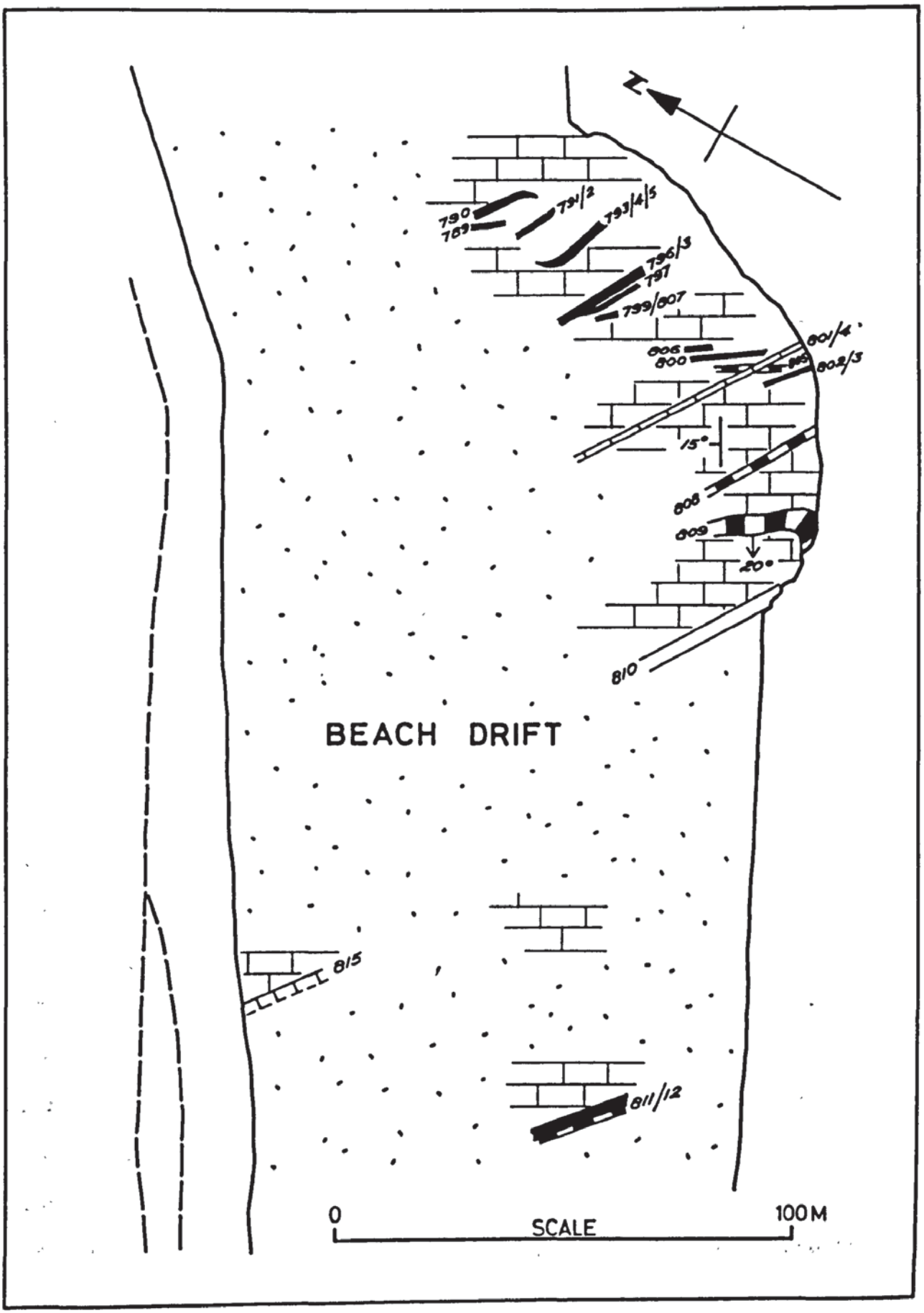

repeatedly injected and variation within each petrological suite is wide. The high alumina gabbros and feldsparphyric dolerites are a readily distinguishable group in the field, and form a clearly defined petrological suite. They occur once only in any single sequence of relative ages established in any part of the centre, and on that basis are assumed to have been formed by a single intrusive episode throughout the complex. It can be shown that emplacement of individual intrusions of this type either immediately preceded or immediately postdated the emplacement of the Carlingford granophyre, and it is therefore assumed that these two intrusive episodes are intimately associated.

Relatively few composite and multiple intrusions were encountered within the complex, but internal contacts within those present proved useful in confirming the sequences established by investigation of cross cutting relations.

The presence or absence of the effects of thermal metamorphism in minor intrusions cropping out within the aureoles of the gabbros and granophyre proved extremely useful in establishing the relative ages of the various bodies. As recognised by Le Bas (1960), the intrusion of the layered gabbro induced intense metamorphism in the surrounding country rocks. Two zones were recognized during the current survey, an outer zone, the limits of which some 200-300 feet below the base of the gabbro are marked by the lines X-X' and X''-X'' on maps 2 and 4 respectively, is recognised in the field by a distinct induration of the country rocks. In thin section it can be seen that basaltic intrusions affected by metamorphism in this zone show the development of a distinctly dusty appearance due to the growth of small magnetite

Figure 1.7

Geology of the quarry at Drumenagh Hill (Fig. 1.5g). Numbers refer to sample numbers.

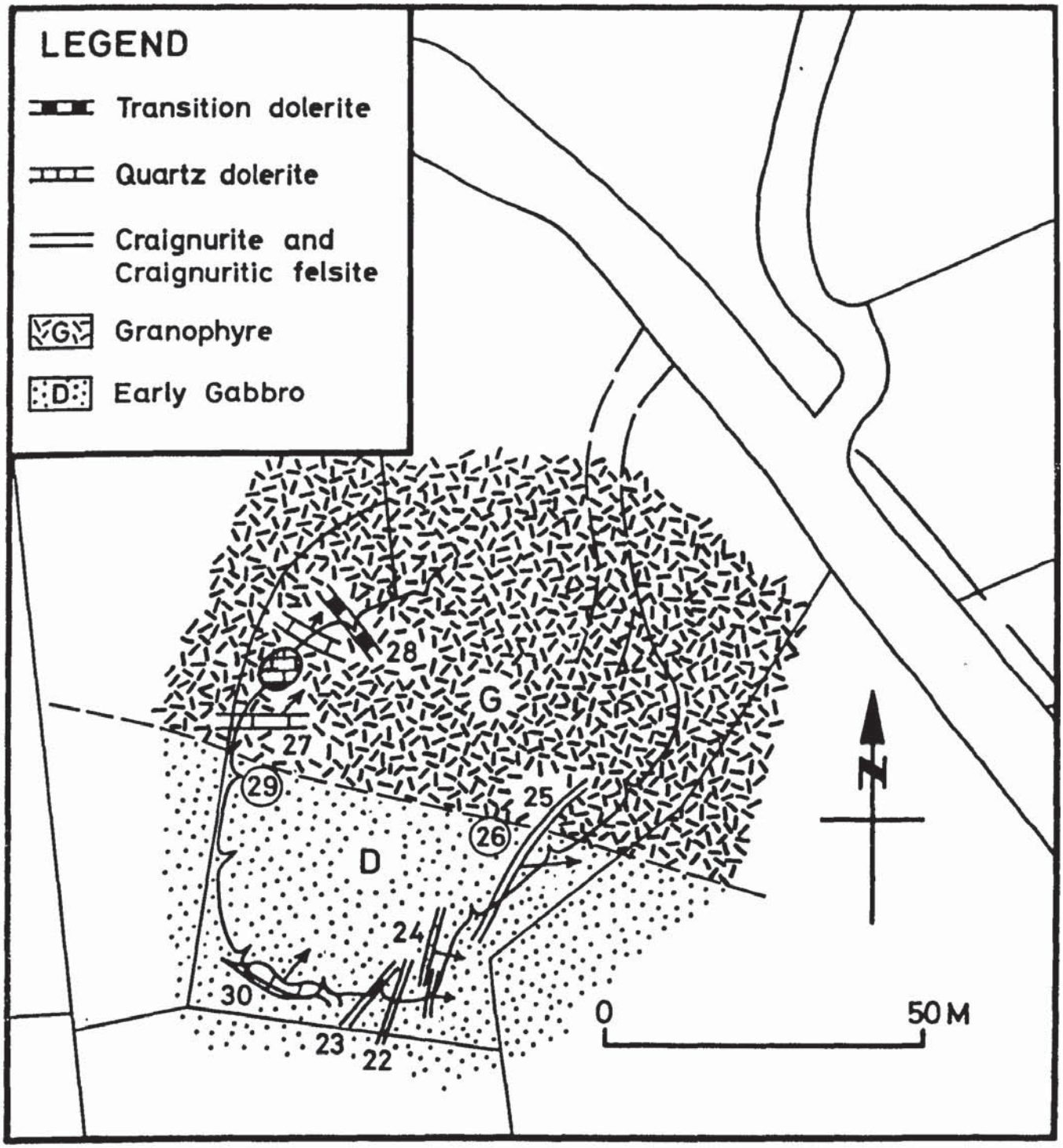

crystals in the pyroxene and pre-existing chlorite (specimen 530). Within the inner zone of the aureole, extending about 100 feet below the base of the gabbro and indicated by the lines Z-Z' and Z'-Z" on maps 2 and 4 respectively, complete recrystallization of the country rock and minor intrusions has given rise to pyroxene hornfelses. In thin section it can be seen that the original ophitic textures in dolerites in the inner zone have been completely replaced by granular hornfelsic textures as a result of recrystallization of pyroxenes and plagioclase, and that plagioclase phenocrysts have been completely recrystallized as a mosaic of small crystals. Well developed flakes of brown biotite and granular ore have grown in many rocks in the inner zone.

In contrast, the alteration resulting from the intrusion of the granophyre is, on the one hand, more widespread extending more than a kilometre from the outcrop of the granite contacts in some places, but at the same time far less intense. Its principal effects were to replace both plagioclase (saussuritization), and chlorite associated with quartz and calcite in amygdales, by epidote (Deer, Howie and Zussman 1966 p.67), and to uralitize and chloritize pyroxenes in basic rocks (specimen 172 for example). In many rocks finely divided brown biotite was formed, and frequently silicification with the introduction of secondary quartz also took place.

It has been noted above that some dykes cutting the granophyre have suffered its pneumatolytic effects. Some dykes cutting layer 1 of the layered gabbro (Le Bas 1960) have suffered metamorphism, presumably as the result of the subsequent injection of later layers

Figure 1.8

Geology of the area to the north east of Carnawaddy (Fig. 1.5h)
See Map 1. for legend, numbers refer to sample numbers.

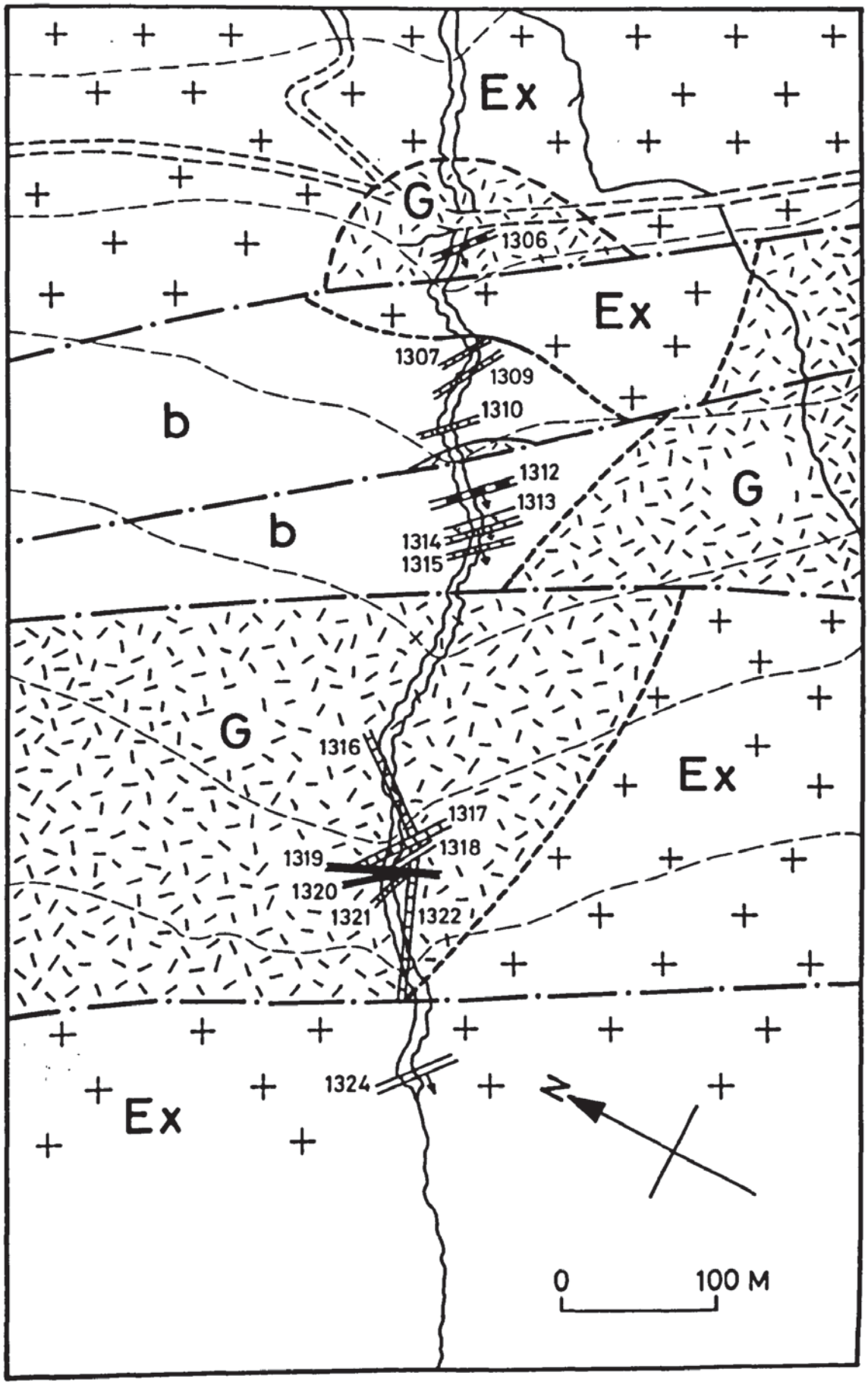

(specimen 1264 for example). It is clear that intrusive activity within the complex was almost continuous, one event following rapidly on another.

An investigation of the distribution of pyritization in minor intrusions indicates that this is, with few exceptions, limited to an area within 2 kilometres of the granophyre contact, and that it is largely absent from dykes postdating the intrusion of the latter (see Fig. 1.9). This indicates that the majority of pyritization at least is related to the emplacement of the granophyre, probably as a result of deuteric volatile activity following the intrusion of that mass, which either introduced iron sulphide into the surrounding rocks or served to concentrate and redistribute finely disseminated sulphides already present. It follows that the majority of minor intrusions showing pyritization are pregranophyre in age.

Many of the minor intrusions contain xenocrysts and xenoliths, the latter ranging in size from microxenoliths a few millimetres in diameter to larger masses up to 2 metres across. The majority of these xenoliths comprise fragments of olivine gabbro identical in their petrology with the layered gabbros (specimens 12, 373), fragments of hornfelsed sediment (specimen 134), granophyre (specimen 1212) and a variety of dolerites also occur. By their nature xenoliths represent fragments of the solid rock through which the later intrusion which encloses them passed, serving to establish the relative ages of the two rock types. It is suggested that the gabbro and hornfels xenoliths are largely derived from the gabbro mass which fed the layered gabbro and its surrounding sedimentary envelope.

Figure 1.9

Sketch map showing the distribution of pyritisation in the minor intrusions of the Carlingford Complex. Dot indicates locality of pyritised sample, heavy lines delineate granophyre outcrop.

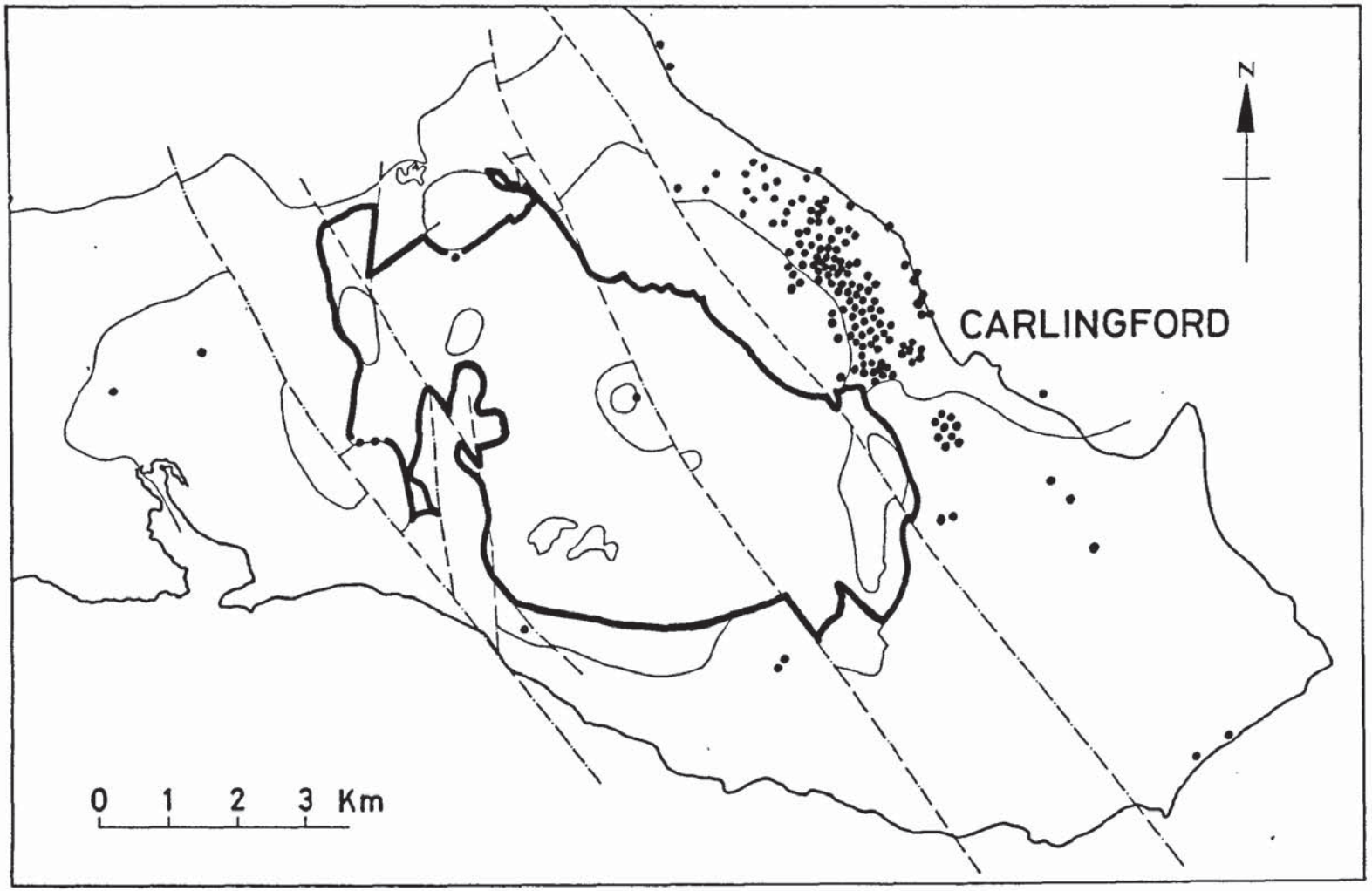

Petrochronology of the Minor Intrusions

A series of time sequences derived by the methods described above, including at least one sequence from each of the areas shown on Maps 2,3,4,5, and 6, and Figures 1.6, 1.7 and 1.8, are tabulated in Figure 1.10. Each sequence is subdivided into episodes, the smallest clearly defined series of events within the sequence, whose relative age can be established with some confidence. Where episodes have been unambiguously related in time to other episodes within any one sequence, they are separated by solid lines within the columns. Dotted lines represent correlation between episodes within sequences from different areas. On the basis of these correlations the following sequence of magmatic activity within the complex is proposed:

1. Extrusion of basalt lavas and emplacement of early gabbro plugs, this may be, in part, coeval with 2 and 3.
2. Intrusion of quartz dolerite and craignurite dykes and cone sheets.
3. Intrusion of transition dolerite and tholeiitic dolerite dykes, cone sheets and complementary cone sheets.
4. Emplacement of the layered gabbros. *
5. Intrusion of felsite dykes and cone sheets.
6. Intrusion of a swarm of alkali dolerite and picrite dykes.
7. Intrusion of a second series of quartz dolerite and craignurite dykes, cone sheets and complementary cone sheets.
8. Intrusion of a second series of transition dolerite and tholeiitic dolerite dykes and cone sheets (there may be

* NOTE A FEW ALKALI DOLERITE DYKES WERE INTRUDED PRIOR TO THE EMPLACEMENT OF THE LAYERED GABBROS. THEY ARE NOT INCLUDED IN THIS SCHEME.

Figure 1.10

Petrochronological sequences for area of the Carlingford Complex depicted in inset maps and figures. The time sequences are set out in column form in order of decreasing age upwards. Correlations between columns are indicated by horizontal broken lines, solid lines within columns separate clearly defined episodes.

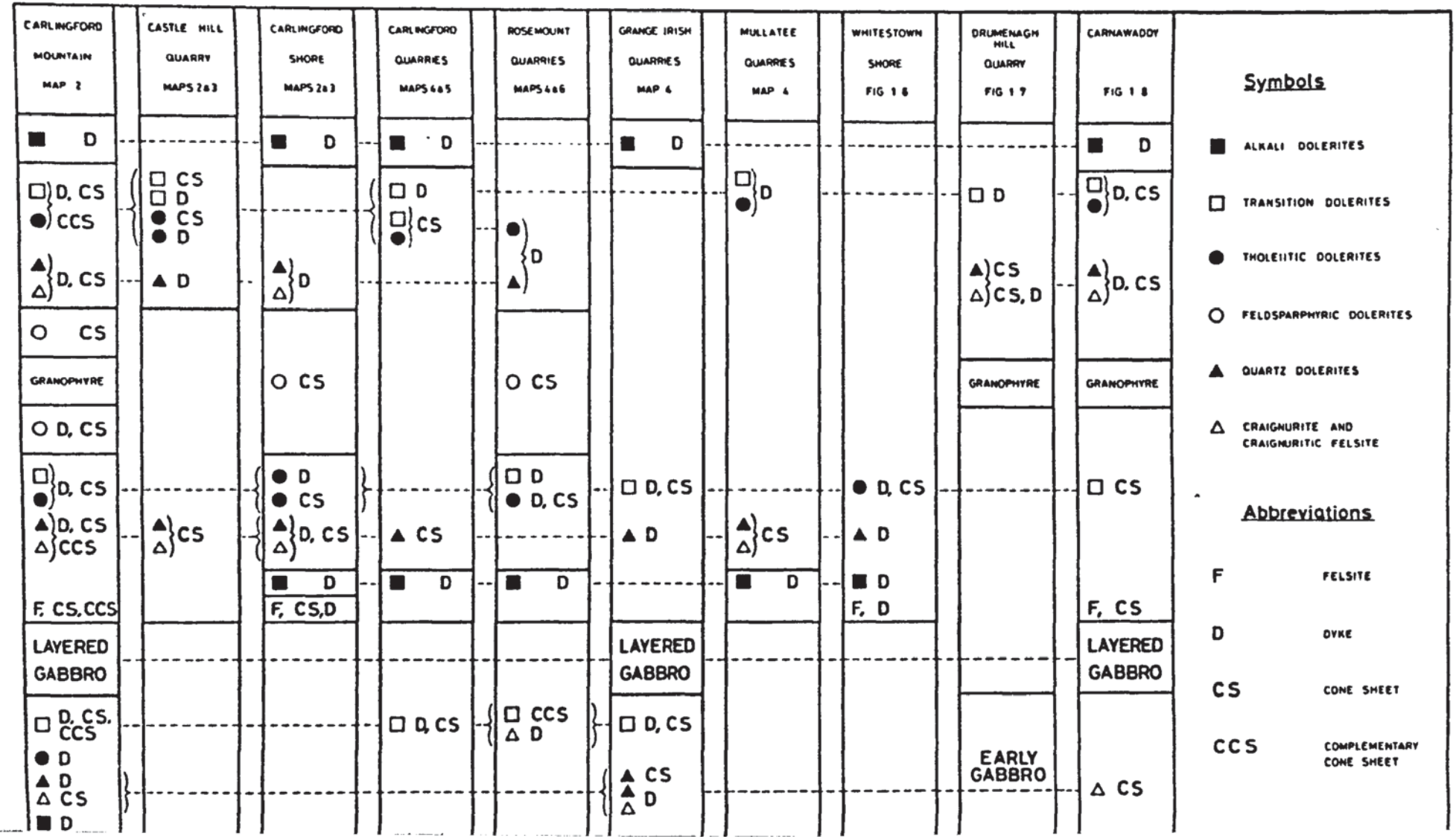

considerable overlap with 7 above).

9. Explosive volcanism at the surface (may be coeval with 5 or 7 or 8).

10. Intrusion of high alumina gabbros and feldsparphyric dolerites as dykes and cone sheets, and emplacement of Carlingford granophyre.

11. Intrusion of a third series of quartz dolerite and craignurite dykes and and cone sheets.

12. Intrusion of a third series of transition dolerite and tholeiitic dolerite dykes, cone sheets and complementary cone sheets.

13. Intrusion of a series of alkali dolerite dykes.

This sequence is summarized in Figure 1.11. It is schematic and a number of tentative correlations have had to be made, the relative age of the basalt lavas and the minor intrusions which predate the layered gabbros,and the volcanic vents and minor intrusions injected between the emplacement of the layered gabbros and the Carlingford granophyre are equally uncertain. However, a rhythmic repetition of a pattern is clearly defined, with quartz dolerite and craignurite dykes and cone sheets repeatedly followed by tholeiitic and transition dolerite intrusions, suggesting that magmatic activity took place in cycles. Three such cycles have been recognised and are numbered I, II, III, from oldest to youngest in Figure 1.11. Episodes within the cycles are lettered. Many episodes represented in this sequence as single events, probably actually consisted of a whole series of distinct episodes, Cycle II may in fact represent two or more such cycles, others

Figure 1.11

Diagrammatic petrochronology of intrusive events in the Carlingford complex as a whole. The sequence is divided into three cycles each subdivided into episodes lettered in order of decreasing age left to right. Solid lines indicate relative age range of intrusive events in the sequence, dotted lines limits of possible age range where uncertain.

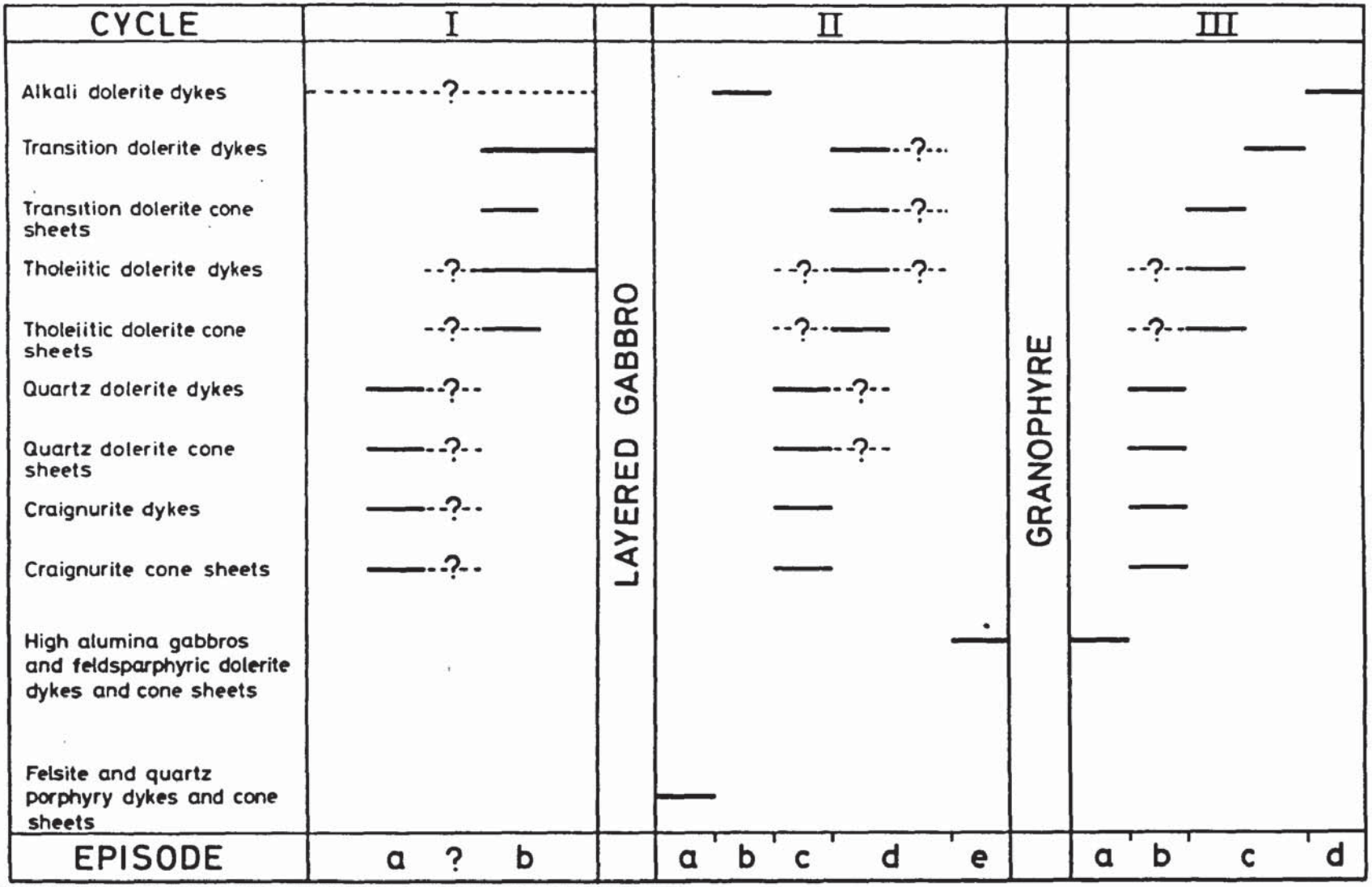

not recognised may also be present. Minor variations within cycles are represented by the appearance of alkali dolerites and felsitic rocks.

There is some evidence, from isolated dyke intersections, that within each episode dykes with a north west - south east trend were emplaced before cone sheets, complementary cone sheets or other dyke swarms, including radial swarms. There is also evidence that the tholeiitic dolerites appear before the transition dolerites in each cycle, bridging the gap between the latter and the quartz dolerites which tend to appear after the craignurites (see Figure 1.10).

Absolute age of the Carlingford igneous rocks.

Evans, Fitch and Miller (1973) recently reported ages for Tertiary igneous rocks from a number of localities, including one from Carlingford. Using the Potassium Argon method of Miller and Brown (1965) they concluded that the minimum age of the Antrim basalts is 60.2 m.y. and that igneous activity within the British Tertiary Provence as a whole, including Antrim, began 65 - 66 m.y. ago. In view of the fact that the majority of the intrusions of the Carlingford Complex postdate lavas correlated with those of Antrim (Le Bas 1965) it is certain that most were formed less than 65 m.y. ago,and possibly less than 60.2 m.y. The minimum age of a basalt dyke cutting the gabbros of Barnavave is reported as 58.5 m.y. by Evans et al.(1973 P432), they do not say whether the intrusion cuts the Carlingford granophyre which is later than the gabbro, so it is possible that the former is younger than 58.5 m.y. However, they claim that the dyke is fresh which suggests that it postdates the granophyre, further if it were older than the

granophyre it may be assumed that the deuteric activity associated with that body would have overprinted the age of the dyke itself, Evans et al. suggest that overprinting by later mineralization has taken place in a number of Tertiary rocks and did so readily. Thus it may be assumed that the minimum age of the Carlingford granophyre is 58.5 m.y.

The figures suggest that the intrusive activity attributed to Cycle I in part took place between 60.2 and 66 m.y. assuming that it is coeval with the extrusion of the Antrim Lavas, that the intrusive activity of Cycle II took place between 58.5 m.y. and 60.2 m.y. and that the intrusions of Cycle III may have been emplaced after 58.5 m.y.

Evans, Fitch and Miller suggest that the nearby Mourne Granites are not younger than 58.0 m.y. and that igneous activity within the British Tertiary Provence as a whole probably ceased about 50 m.y. ago (1973 ps. 433 and 434).

Conclusions

The Carlingford Complex displays a variety of minor intrusions in an intense composite swarm. A wide range of rock types are represented in these bodies but, with the exception of alkali dolerites and relatively unimportant felsites and lamprophyres, all are related by intermediate petrological types with the transition dolerites and/or tholeiitic dolerites. A schematic chronological sequence of minor intrusive episodes, related to the time sequence already established by Le Bas, shows a rhythmic repetition of the main rock types in the sequence, craignurite, quartz dolerite, tholeiitic

dolerite, transition dolerite, punctuated by the emplacement of the layered gabbros, the granophyre, high alumina gabbro and feldspar-phyric dolerite intrusions, and alkali dolerite dykes. The repeated appearance of these magmas in sequence indicates that they are related by processes which were fundamental to petrogenesis within the complex, processes which were not accidental occurrences but which were repeated throughout the development of the complex in the early Tertiary.

CHAPTER 2

THE STRUCTURE AND STRUCTURAL DEVELOPMENT OF THE CARLINGFORD IGNEOUS COMPLEX.

Abstract.

An igneous centre, such as that of Carlingford, is the product of a complex intrusive history, involving repeated injection of magma under a variety of stress regimes each giving rise to different forms of intrusion. The form of the minor intrusions and other structures in the Carlingford complex are considered herein and the history of the structural development of the centre outlined. A hypothesis involving repeated injection of basaltic magma as ridge and dome like masses is put forward to explain that development.

Introduction.

It has been shown that the Carlingford complex consists of remnant outliers of extrusive basalt of Tertiary age lying unconformably on folded Palaeozoic sediments, intruded by a gabbro lopolith, volcanic vents and a granophyre ring-dyke or plug (Le Bas 1960, 1965a, 1967); and that both country rock and the igneous masses themselves are cut and intruded by a series of dyke and cone-sheet swarms (see Chapter 1 above). The minor intrusions can be related to a series of three intrusive cycles. Cycle I predating the layered gabbro; Cycle II postdating the gabbro, cut by the Carlingford granophyre and in part coeval with the volcanic vents; and Cycle III postdating the granophyre. To some extent this scheme is over-

simplified, probably many more cycles of activity took place within the complex but cannot now be recognised individually. Each major event within the three Cycles is referred to as an episode, episodes are numbered and lettered according to the scheme set out in Chapter 1. (Figure 1.11.).

The form and structure of the major rock masses and the minor intrusions of each episode are studied in turn below in the context of their relationships to each other in time and space. Mechanisms of igneous intrusion have been discussed by many workers, most noteably Daly (1903a, b, 1908), Grout (1918), Anderson (Bailey et al. 1924 and Anderson 1936), Richey (1928, 1932 and 1939), Billings (1945), Ode (1957), Garson (Garson and Smith 1958 and Garson 1959), Robson and Barr (1964) and Roberts (1970). The development of igneous structures at Carlingford are considered below in the light of this work.

A. MAJOR STRUCTURES.

The Palaeozoic Rocks

a). The oldest rocks exposed in the area are well bedded argillites, gritty sandstones and greywackes of Lower Llandovery age (Charlesworth et al 1960 p. 432). They have been folded into a series of isoclines striking north east - south west throughout their outcrop in the Carlingford Peninsula (the northern and western flanks of the complex, see Map 1). The beds are inclined at high angles and are, in places, near vertical (see Fig. 2.1.). This folding is consistant with that resulting from Caledonian movements elsewhere in Ireland and the Southern Uplands (Walton 1963).

Figure 2.1

Sketch map showing the relationship of fold structures in the Palaeozoic sediments and Tertiary lavas to the contacts of the Carlingford granophyre. Heavy lines delineate granophyre outcrop, synclinal axis indicated X——X. A = area veined by granophyre offshoots; B = masses of basic rock located by boreholes.

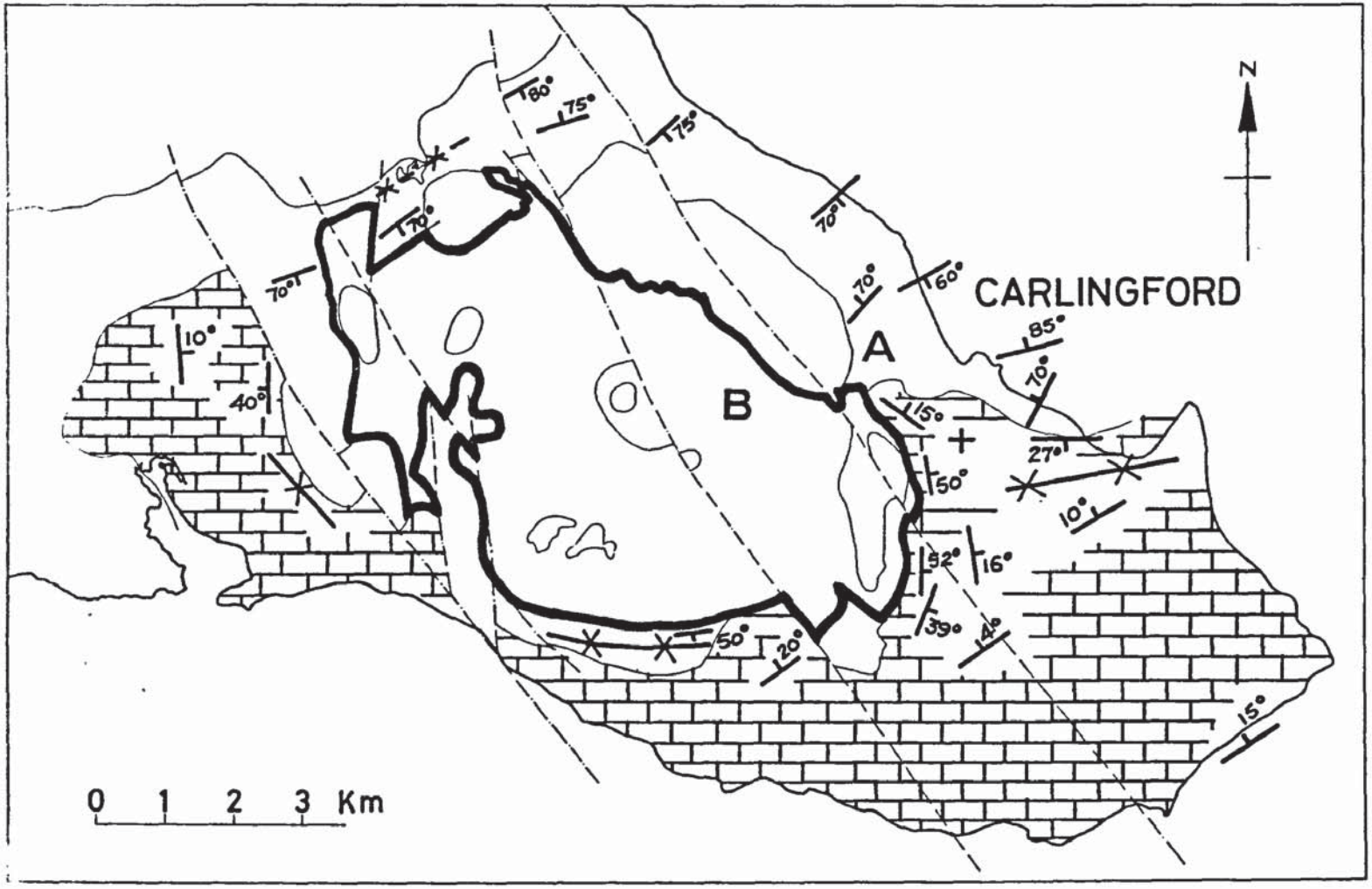

b). Cutting the Silurian sediments, but in part deformed by the Caledonian movements, are a series of minette dykes in the form of pods and lenses. These dykes are petrologically similar to those described by Reynolds from the Ards Peninsula (1931).

c). Carboniferous Limestone of d^1 and d^2 age crop out on the eastern, southern and south western flanks of the complex (Traill 1878) where they overlie the Silurian rocks with marked angular discontinuity. The limestones, which are fossiliferous and dark blue grey or black in colour, have suffered gentle folding, the trend of the fold axes varying from east north east - west south west, to the east of the complex, to north west - south east, on its south western flanks (see Fig. 2.1). The angle of dip of the fold limbs rarely exceeds 20°, the folding probably resulting from the Hercynian orogeny which affected southern Ireland (Anderson and Owen 1968).

Near the contacts of the limestone with the intrusive gabbros and granophyres the angle of dip is considerably increased, angles in excess of 50° being recorded east of Barnavave (see Fig. 2.1). At such localities the direction of dip is always away from the intrusive masses and the strike of the beds parallel to their contacts. Such a deformation of Hercynian Structures must have resulted from the intrusion of the igneous rocks, the sheet like form of the layered gabbro (see below) precludes the latter having contributed to it, and hence it may largely be attributed to the forceful emplacement of the granophyre.

Le Bas attributes the up doming of the limestone unconformity over the complex to cone-sheet injection (Le Bas 1971). The importance

of cone-sheet injection in this phenomenon is confirmed (see below), however it is probable that the emplacement of the granophyre also had considerable influence in this updoming.

The Tertiary Lavas.

Tertiary lavas occur as outliers at Rockmarshall on the southern flank of the complex, to the west of Carnawaddy, possibly at Spellickanee, and at at least three localities on Carlingford Mountain (see Maps 1 and 2). They also occur as xenoliths within the layered gabbros and as an extensive screen separating layers 3 and 4 (Le Bas 1960, 1970b). Lavas occurringwithin or adjacent to the layered gabbros are intensely metamorphosed.

These outliers represent remnants of basaltic flows which probably covered the area around Carlingford and Slieve Gullion, where they also occur (Richey and Thomas 1932), and possibly were continuous with the lavas of the Antrim Plateau. The flows were extruded onto an eroded land surface of Palaeozoic sediments. Those to the west of Carnawaddy lie in a shallow valley running north east - south west, Silurian sediments crop out higher up the slopes on both sides of this valley, capped on the east by the gabbros of Carnawaddy and cut on the north west by the granophyre of Clermont Carn. It is possible that this outlier is a remnant lying in a reexcavated valley of the Tertiary land surface, an alternative interpretation however is that both the lavas and underlying Palaeozoics have been folded into a periferal syncline by the subsequent emplacement of the Carlingford granophyre.

The largest of the basalt outliers occurs on the southern flank

of the complex. It has a synclinal structure (see Fig. 2.1), tholeiitic basalts of the limbs flanking alkali basalts and hawaiitic basalts in the core (Le Bas 1965a). The axis of the syncline runs almost east-west parallel to the steep contact of the lavas with the intrusive granophyre. The angle of dip of the flows in the syncline is of the order of 20 - 30° except where the granophyre contact is approached where it increases to about 50°. Folding of Tertiary age possibly associated with alpine movements has taken place in north east Ireland but gave rise only to warping and gentle folds (Anderson and Owen 1968 p.2), thus the Rockmarshallsyncline must also be the result of deformation induced by the emplacement of the Carlingford granophyre.

The hornfelsed lavas at Cloughmore 2 km. north west of Slieve Foye occur as a faulted elongate outcrop adjacent to the layered gabbro and were first mapped as hornfelsed Silurian sediments by Traill (1878). This view was also taken by Richey (1932) who interpreted these rocks as a sedimentary screen separating the gabbros of Carlingford Mountain, which he considered to be part of a ring dyke, from the granophyre. Le Bas (1955) subsequently interpreted them as vents cutting the gabbro on the basis of the following evidence:

i) close petrological examination shows that the rocks are volcanic rather than sedimentary in origin.

ii) Breccias are present.

iii) Many of the contacts of the outcrops are steep.

iv) The outcrops occur within a gabbro lopolith and can be interpreted as cutting it.

v) Volcanic vents are present elsewhere in the area.

Re-examination of the Cloughmore outcrop and its petrology has brought the following points to light:

a) The rocks are intensely hornfelsed in many cases with complete recrystallization of the pyroxenes. This degree of metamorphism could only result from the emplacement of the layered gabbro, the metamorphic effects of the later granophyre are nowhere so intense, (see Chapter 1 above). These rocks therefore clearly predate the layered gabbro in age, the vents of Slievenaglogh and Annaloughan are post gabbro in age (see below).

b) The predominant rock type present is metabasalt. Breccias have been formed by faulting.

c) The steep contacts of the masses are faults which show up clearly as such on aerial photographs. The irregularity of some boundaries suggest that the contact between the gabbros and metabasalts is in fact at a low angle.

d) Some contacts show the gabbro intruding the hornfelses.

This evidence indicates that the metabasalts are lavas underlying the layered gabbro and intruded by it rather than vents cutting it.

The nature of the volcanics outcropping near Spellickanee is uncertain. (see Map 1). The larger mass entirely surrounded by gabbro largely consists of metabasalt, both were mapped as hornfelsed Silurian sediments by Traill (1878). Fragmental rocks are also present and may be hornfelsed vent agglomerates, inter basaltic tuffs, or fault breccias. The volcanic rocks occupy the higher ground and

the contacts with the surrounding gabbros are steep but their nature is uncertain. The metamorphic effects of the Carlingford granophyre are pervasive and obliterate any evidence of hornfelsing of the volcanics by the gabbro, if present initially. On the basis of the data currently available it is uncertain whether the Spellickanee Volcanics form part of a vent cutting the layered gabbro, or are a large xenolith or pendant of basalt lavas and tuffs engulfed by the gabbro or projecting into it from its roof. In view of the Cloughmore occurrence the latter interpretation is preferred. The smaller outcrop of volcanics some 1250 metres south east of Spellickanee is discussed under "Volcanic Vents" below.

The source of the lavas has not been clearly identified and may lie outside the area. None of the numerous basalt dykes in the complex show evidence of being lava feeders (see below).

The Early Gabbros

The early gabbros occur only on the south west of the complex. The Rockmarshallmass is fault bounded on two sides and its contact with the Carboniferous Limestones to the south is drift covered, hence the exact form of this intrusion is uncertain but is probably similar to that of the Trumpet Hill-Drumenagh Hill mass.

The gabbros of Trumpet Hill and Drumenagh Hill form steep sided eliptical eminances separated by a narrow valley. Their form is that of an elongate vertical sided plug, long axis north west - south east, cut and displaced by a north west - south east dextral tear fault.

Le Bas interprets these gabbros as being earlier than both the layered gabbro and the Carlingford granophyre (Le Bas 1970a p 76).

They intrude Carboniferous Limestone and Silurian sediments but are cut by the granophyre. Petrologically similar gabbros were emplaced early in the development of the Slieve Gullion Complex at Cashel, Forkhill and Mullaghbawn (Richey and Thomas 1932).

The form of the Trumpet Hill - Drumenagh Hill intrusion is similar to that of Slemish, Co. Antrim (Preston 1963) which has been interpreted as a lava feeder, as are others in Antrim at Corkey and Trosk (Walker 1959), Tieveragh and Tievebulliagh (Tomkeieff 1940) and Carnmoney and Glasmollen (Patterson and Swaine 1957). It is probable therefore that the early gabbro plugs of Carlingford and Slieve Gullion were also lava feeders.

The Layered Gabbros

The structure of the layered gabbros has been discussed in detail by Le Bas (1960), who demonstrated the lopolithic form of the intrusion. He suggested that the floor of the intrusion was funnel shaped, however, although the floor can be shown to dip inwards in places, elsewhere it is horizontal.

The lopolith was intruded at the base of the Tertiary lavas along the plane of weakness formed by the unconformity separating them from the underlying Palaeozoic sediments. The unconformity did not separate cleanly however and patches of lava remained attached to the sediments beneath, these are now exposed at the base of the gabbro north east of Slieve Foye and at Cloughmore.

The feeder, or feeders, for the gabbros have not been identified but these presumably occur within the area now occupied by the

granophyre which later intruded the lopolith , there is evidence that it/they lay about 1 km. north-west of Spellikanee (see below under "The Minor Intrusions of Cycle II ", a).

Volcanic Vents.

Le Bas (1955) reported the presence of a series of volcanic vents cutting the layered gabbros and in turn being cut by the Carlingford granophyre. He identified four areas where volcanic vents occur; Slievenaghlogh, Annaloughan, Spellikanee and Cloughmore. The "vents" at Cloughmore and the larger "vent" at Spellikanee have been reinterpreted as outliers of Tertiary basalt and are disucssed as such above.

The vents of Slievenaghlogh and Annaloughan contain well developed agglomerates with large fragments of gabbro, dolerite, basalt, hornfelsed Silurian sediment and a granophyre of a type similar to, but clearly older than, the Carlingford granophyre itself (Le Bas 1967). The Slievenaglogh vents cut the layered gabbros, and together with that of Annaloughan are broken up by faulting and show metamorphism veining and alteration resulting from the intrusion of the Carlingford granophyre.

The small patch of volcanics which crops out 1250 metres south east of Spellikanee include metabasalts, fragmental rocks possibly tuffs, and other rock types similar to those occurring in many minor intrusions in the area. No unquestionably solid exposure has been located in the area and it is possible that the abundant loose blocks of basic igneous rock occurring there have been derived from minor intrusions higher up the hillside. If on the other hand they do

reflect the solid geology at this locality it is possible that a vent is present as indicated on Map 1.

The presence of vents containing breccias such as those of Slievenaglogh and Annaloughan reflect changes in the style of igneous activity towards explosive external volcanism similar to that which occurred in Mull (Bailey et al. 1924), Skye (Harker 1904, Ray 1960) and Arran (Tyrrell 1928, King 1954), and which took place at Carlingford between the emplacement of the layered gabbros and the granophyre.

The Carlingford Granophyre

The form of the Carlingford granophyre, the "later granophyre" of (Le Bas (1967), was first ascribed to that of a ring dyke by Richey (1932). Le Bas subsequently accepted this interpretation (1960, 1967). As now exposed the granophyre has a dome like structure occupying some 30 square kilometres at the surface. It has a somewhat flattened roof indicated by the low angle of the contacts with the layered gabbros on Carlingford Mountain. The flanks dip outwards steeply, in the south near Rockmarshal the contact is nearly vertical, while to the north east of Slieve Foye it runs close beneath the surface of the hillside, sending a series of offshoot veins to cut the Silurian sediments at the locality marked A on Figure 2.1. and extensively altering and uralitizing earlier basic dykes and cone sheets in the area. Such a form is consistant with that of a ring dyke (Richey 1928), a bell jar intrusion (Du Toit 1920),or plug (Frankel 1968).

The classic ring-dyke as described by Anderson (1936) is a permitted passive intrusion emplaced largely by the collapse of a

cylinder of country rock into a magma chamber by movement along steeply inclined annular shear fractures. However, as has been noted above, the country rocks, into which the granophyre was emplaced, show the development of periferal folding similar to the periferal synclines of Mull (Rast, Diggens and Rast 1968, Anderson and Owen 1968 P 146) and updoming, indicating that the intrusion of this body was at least in part forceful, similar updoming is produced by the diapiric emplacement of salt domes (Gussow 1968) - see Figure 2.2. The periferal deformation and doming at Carlingford is by no means as extensive as that induced by the Arran Granite (Bailey 1926) and could not account alone for the space requirements of the granophyre mass. Daly (1903a, b, 1908) and Billings (1945) have suggested that piecemeal stoping plays an important role in the emplacement of some ring dykes.

The altitude of the lower contacts of the gabbro masses of Barnavave, Cooley, Doolargy and Spellikanee, 250 metres, 50 metres, 150 metres and 150 metres above sea level respectively, is much lower than that of the gabbro-granophyre contact of Carlingford Mountain and Carnawaddy at 300 - 400 metres above sea level. This suggests that these gabbro masses are now below the level of the roof of the granophyre though it may in part be the result of faulting (see below). The gabbros of Barnavave and Cooley are extensively contaminated by the granophyre which is in turn basified (Nockolds 1935, 1937, 1938, Sollas 1894), similar assimilation of gabbro by the granophyre is present at Doolargy. It is proposed that the gabbro masses in question are in fact large xenoliths which have foundered into the granophyre, the resulting total immersion leading to

Figure 2.2

Cross section of Reitbrook oil field, Germany showing deformation associated with the diapiric emplacement of a salt dome. (After Gussow 1968).

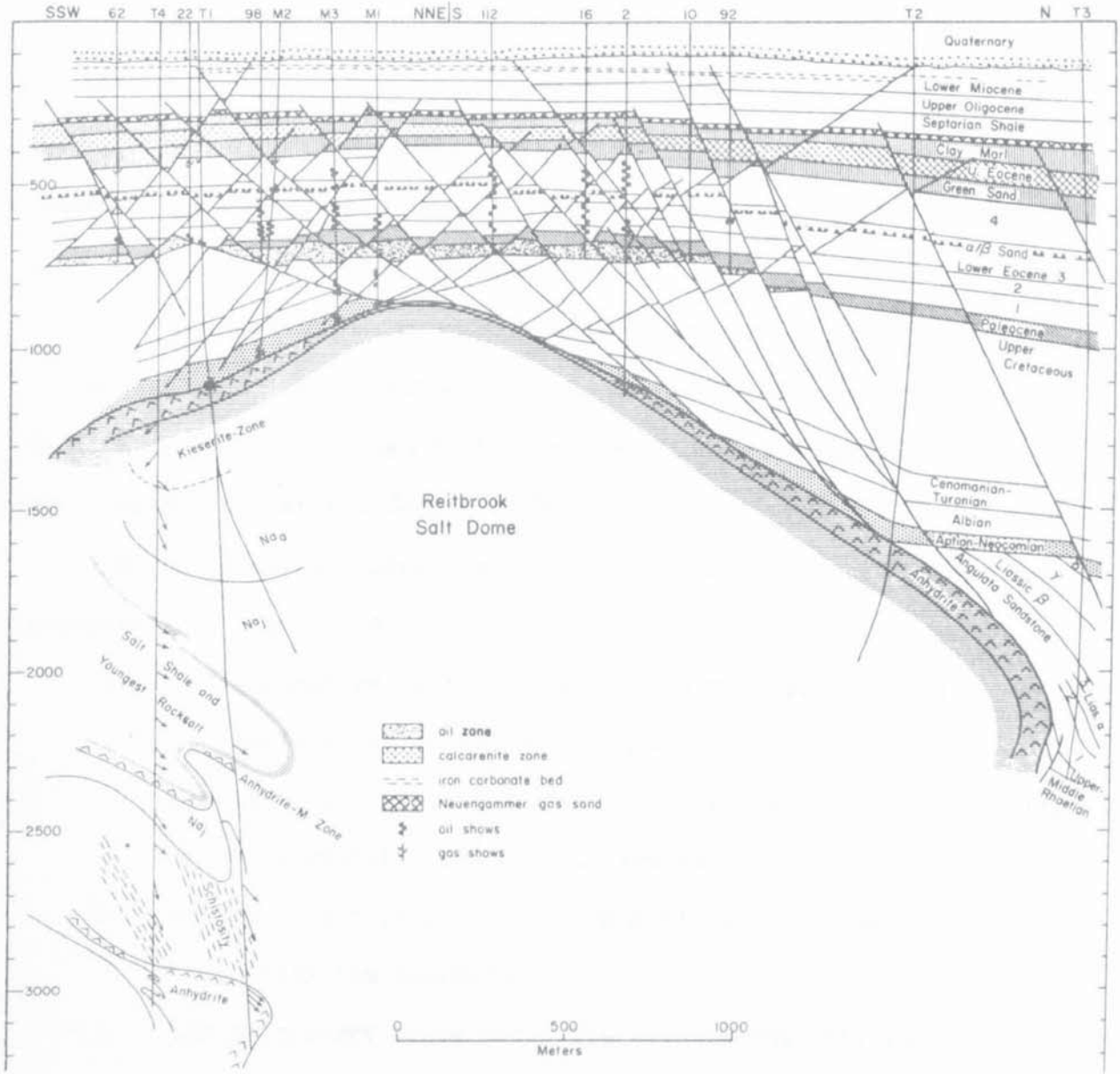

assimilation and hybridization. The gabbros of Carlingford Mountain immediately adjacent to the granophyre and forming its roof, although altered and uralitised, are not so hybridised.

Coring operations northeast of Spellikanee within the vicinity of locality B Figure 2.1. have revealed the presence of large masses of basic material in an area, and at a level, where granophyre is expected (Le Bas private communication). These masses are probably also megaxenoliths within the granophyre.

Le Bas attributes the petrogenesis of the Carlingford granophyre to melting of Silurian sediments by large masses of basic magma at depth (Le Bas 1967) though that interpretation has recently been challenged (Meighan and Gamble 1973).

The mechanism proposed for the development of the granophyre is summarized in Figure 2.3.

1. The granophyre melt is formed by melting of Silurian sediments adjacent to basic magma or possibly by fractionation of that magma, and starts to rise diapirically under hydrostatic pressure in the manner of a salt dome.
2. A plug like column of acid magma rises, updoming and fracturing its carapace.
3. The granophyre magma works its way upwards into the fractured carapace spalling off blocks of all sizes which sink into the magma as xenoliths.

The granophyre was thus emplaced by a combination of forceful diapiric emplacement and stoping and is therefore not a ring dyke as such, but rather a dome or plug.

Figure 2.3

Diagrammatic representation of the mechanism of emplacement of the Carlingford granophyre:

1. generation of the magma
2. initiation of upward diapiric movement
3. emplacement by combination of forceful diapirism and stoping.

The diagram indicates the plug like form of the intrusion. For further discussion see text.

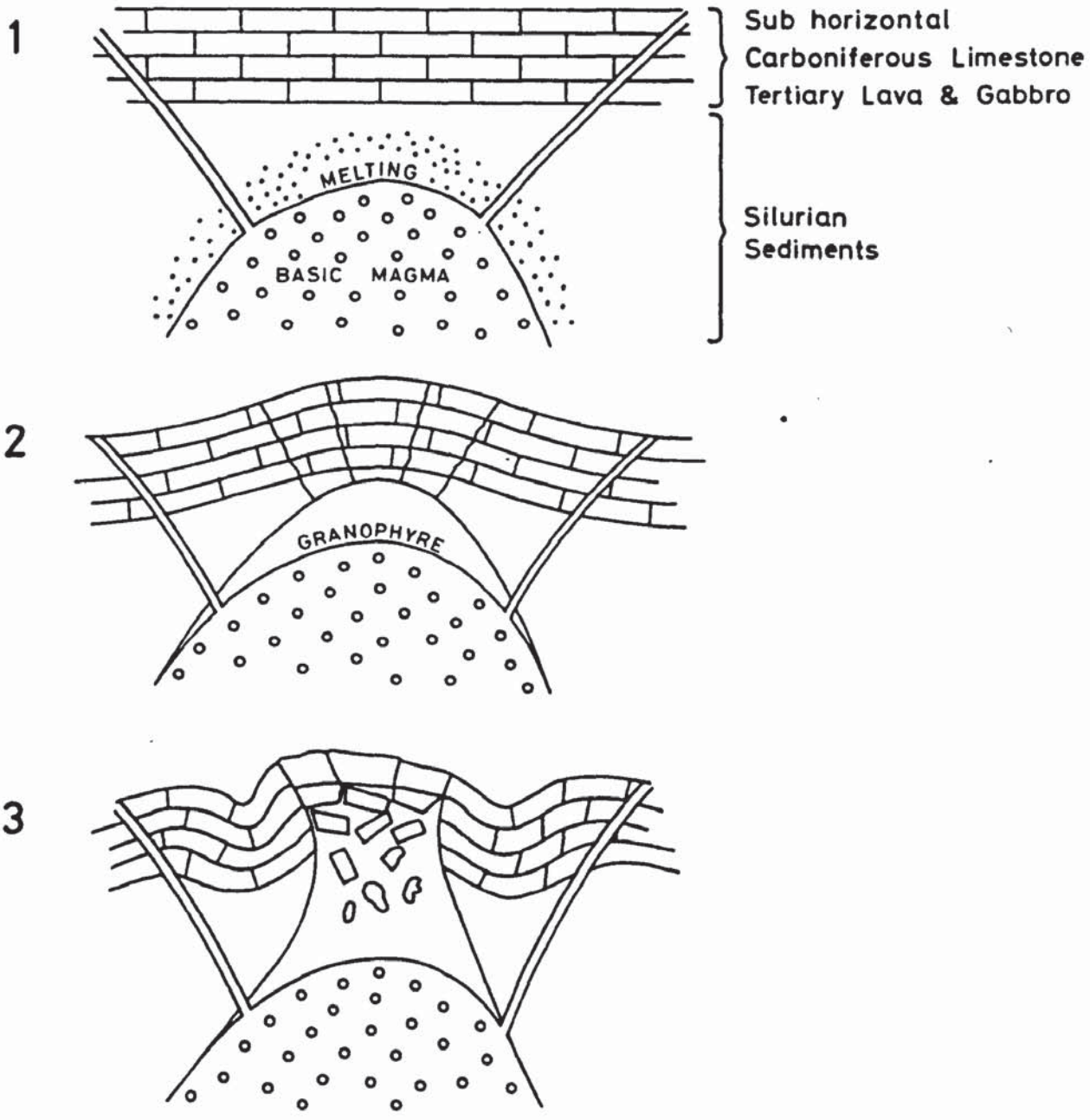

Faulting

A complex fault system traverses the complex. The fracture pattern is dominated by major faults trending north west - south east which continue northwest through the Slieve Gullion complex (see maps by Richey and Thomas 1932). The most important faults are lettered for convenience on Figure 2.4, Figure 2.5 is a rose diagram showing the azimuths of the trends of the principal fractures.

Fault A - A' (Fig. 2.4), which cuts the Trumpet Hill - Drumenagh Hill plug, displaces it about 1 km. to the south east on the north east side of the fault plane. As the plug is essentially vertical this displacement must be the result of strike slip movement in a dextral sense. That a vertical component of movement is also present is indicated by the fact that the two halves of the plug are not equal in outcrop length along the fault plane at the surface, and that the fault forms the boundary between Carboniferous and Silurian strata in this area. As the Carboniferous Limestone occurs only to the south west of the fault north of Trumpet Hill, it is inferred that it downthrows to the southwest.

The prominant fault C - C' which traverses the centre of the complex consistantly gives rise to a dextral displacement of boundaries it crosses along its whole outcrop (it extends over 20 kilometres through Carlingford and Slieve Gullion), suggesting again a dextral strike slip component of the order of 1250 metres in this case. It also has a vertical component of at least 60 metres down-throw to the south west as shown by its displacement of the layered gabbros north east of Carnawaddy. Probably this fault is not a single fracture but consists of a series of parallel fractures, such

Figure 2.4

Sketch map of the Carlingford Complex showing the distribution of fractures which are indicated as heavy lines. Significant faults are lettered for convenience.

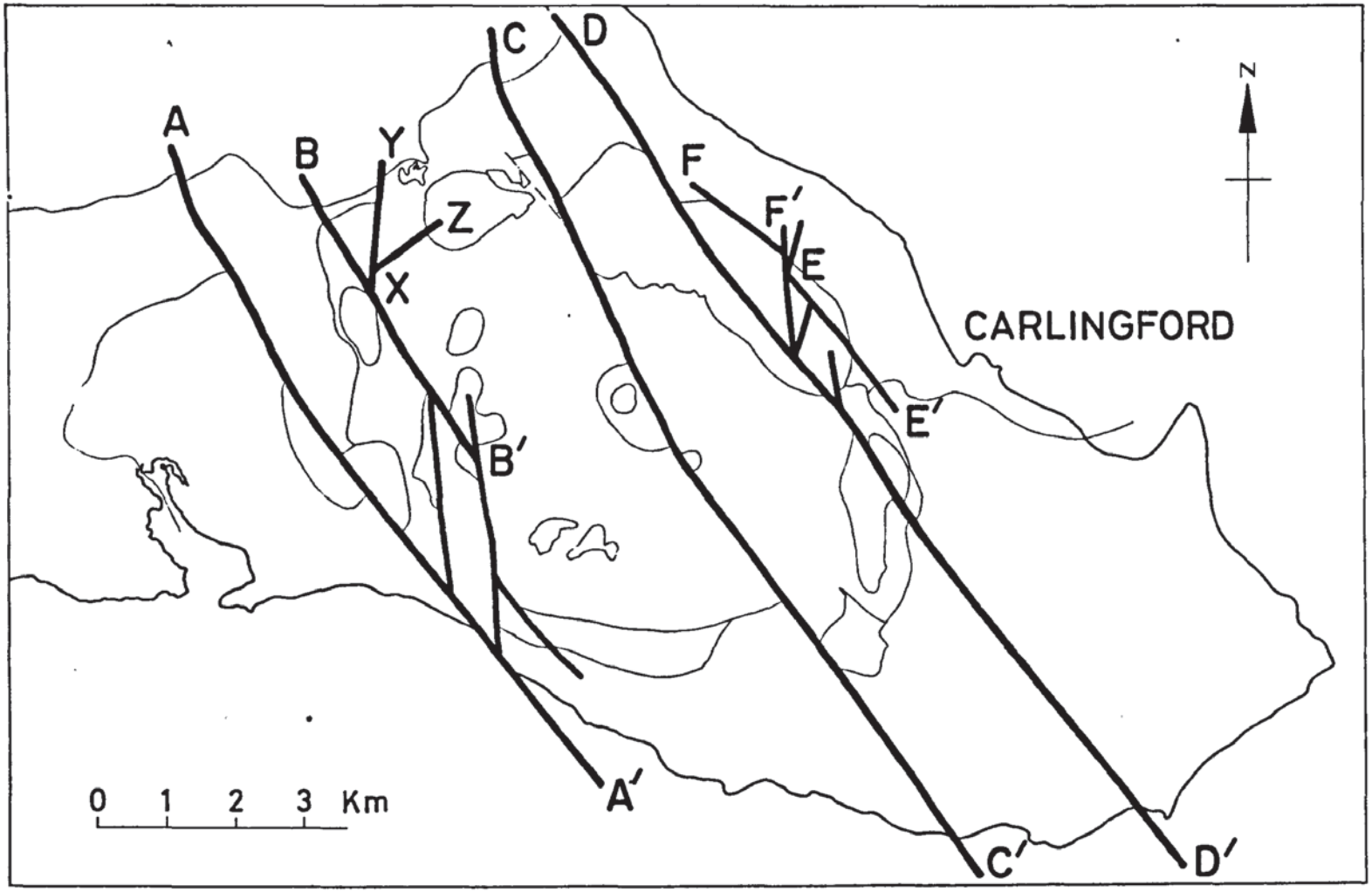

Figure 2.5

Rose diagram of fault trend azimuths in the Carlingford complex as a whole. Peak height from the base circle is proportional to the total known outcrop length of fracture planes within each 10° arc (001° - 010° inc., 011° - 020° inc., etc., etc.). All azimuths are measured from True North.

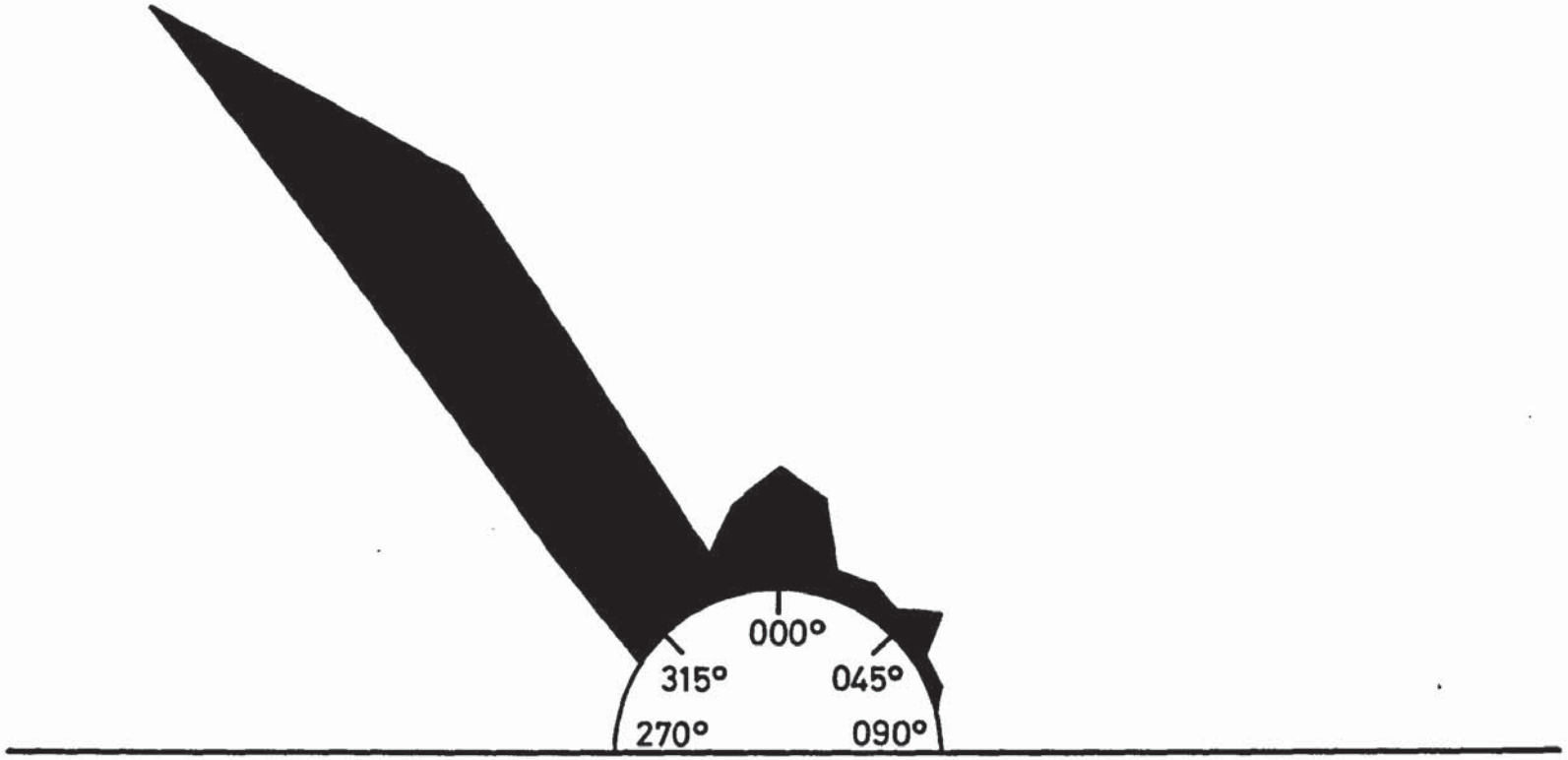

a series of faults cut the gabbros and granophyre in a stream to the north east of Carnawaddy (see Fig. 1.8).

Faults B - B', D - D' (forms a deep cleft where it traverses Barnavave) and F - F' (interpreted as a normal igneous contact by Richey 1932) also downthrow to the south west. The displacement of geological boundaries is not inconsistant with an element of dextral strike slip movement on these faults too, which is also the case with fault E - E'.

A second set of fractures trending north-south (see Fig. 2.5) branch from the northwest tear faults at angles of 35 - 40°. Fault B - B' dies out at its south eastern end in a series of north - south fractures which are normal faults downthrowing to the west. The north - south fault X-Y downthrows to the east. Similar fractures interconnect D - D', E - E' and F - F' on Carlingford Mountain to form a complex fracture pattern.

Fractures trending north east - south west (see Fig. 2.5) are also present but are not so extensively developed. One of these, X-Z (Fig. 2.4) has a normal component downthrowing to the north west. Others offset the metabasalts of Cloughmore. No strike slip movement can be demonstrated on these fractures but is not precluded.

The north west, north south and north east faults can all be attributed to a single fracture system in which the principal direction of failure lay along the north west - south east tear faults. The north - south normal faults are secondary fractures equivalent to the tension gashes developed between shear planes in the experiments of Reidel (1929) and Cloos (1932). The acute angles

between the secondary faults and the shear planes (tear faults) point in the direction of relative movement of the fault blocks (Sherbon Hills 1963 p 171-174),confirming the dextral movement attributed to these fractures.

The north east - south west faults represent complementary 1st order tear fractures (Sherbon Hills 1963 p 201), only feebly developed and largely incipient. Normal movement on both the north west and north east faults has probably been superimposed on the shear fractures subsequent to their initiation.

The stress pattern giving rise to such a fracture system can be resolved in terms of three principal stress directions mutually at right angles, the maximum and minimum stress directions (P max and P min Fig. 2.6) horizontal and oblique to the shear planes, the intermediate stress direction (P int) vertical (Sherbon Hills 1963 p 178-179). The north south secondary faults at Carlingford would be parallel to the maximum stress direction (P max) in such a system (De Sitter 1964 p 158), indicating that the Carlingford fault system could have been induced by a north - south compressive stress. However, in view of the consistant dominance of the north west - south east shear fractures it is probable that they were induced by a horizontal shear couple rather than by compression (Sherbon Hills 1963 p. 202). Such a shear couple might be produced by differential movement of crustal plates during the opening of the Atlantic in the Tertiary. It is of considerable significance that the major north west - south east fractures run parallel to the principal direction of dyke injection at Carlingford, and throughout the British Tertiary

Figure 2.6

Resolution of the stress pattern giving rise to the Carlingford tear fault system into three mutually perpendicular stress directions, maximum stress (P max.), intermediate stress (P int.), and minimum stress (P min.). Planes represent north west - south east and north east - south west shear planes equivalent to the tear faults and complementary first order tear fractures respectively.

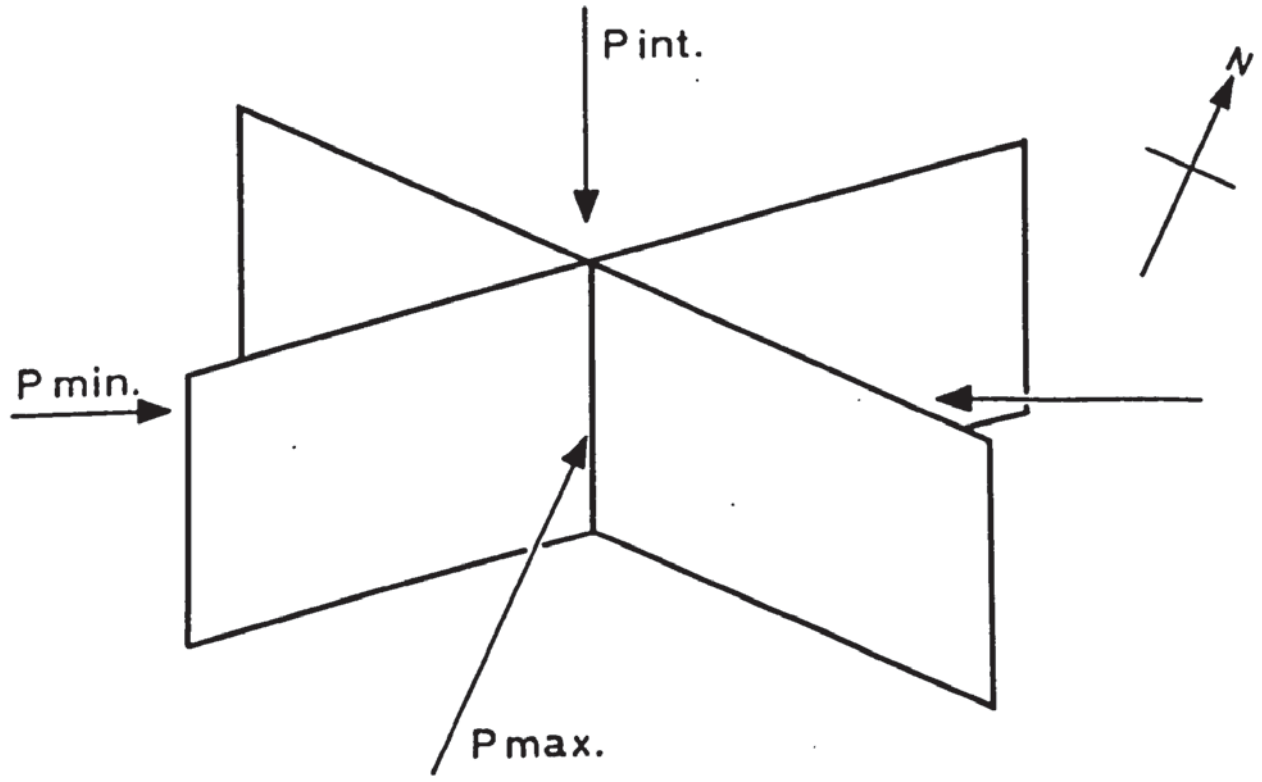

Province in general (Richey 1939 p 420) indicating a genetic relationship between these structures.

Small faults and fractures unrelated to this fracture system also occur within the complex, some of these cut the vents of Slievenagologh and Annaloughan. One such fracture, trending north east on the northern flank of Carlingford Mountain, is occupied by a dyke and displaced by faults of the post intrusive episode discussed above. These fractures are attributed to the break up of the country rock envelope surrounding the granophyre during its diapiric emplacement (see above).

The north west - south east tear faults cut and displace the Carlingford granophyre and some minor intrusions of Cycle III, no minor intrusion can be shown to cut or occupy any of these fractures, and it is therefore assumed that they postdate all intrusive events in the complex. In view of their considerable lateral displacement it is necessary to 'put back' their movement in order to interpret the structural development of the minor intrusions of the complex - particularly the cone sheets. Consequently, a base map has been prepared (Fig. 2.7) on which the movement on faults A - A', B - B', C - C' and D - D' have been 'put back'. The displacement assumed for each fault in this reconstruction is indicated on Fig. 2.7. it has been chosen such that boundaries crossed by the fault in question match up where possible. It will be noted that the complex takes on a more circular plan as a result of these adjustments. This reconstruction is used as a base map for plotting cone sheet focii etc. below.

Figure 2.7

Pre-fault reconstruction of geological boundaries in the Carlingford Complex. The displacement on the major fractures A - A', B - B', C - C', D - D' has been put back by a sinistral adjustment, the correction applied is indicated in each case.

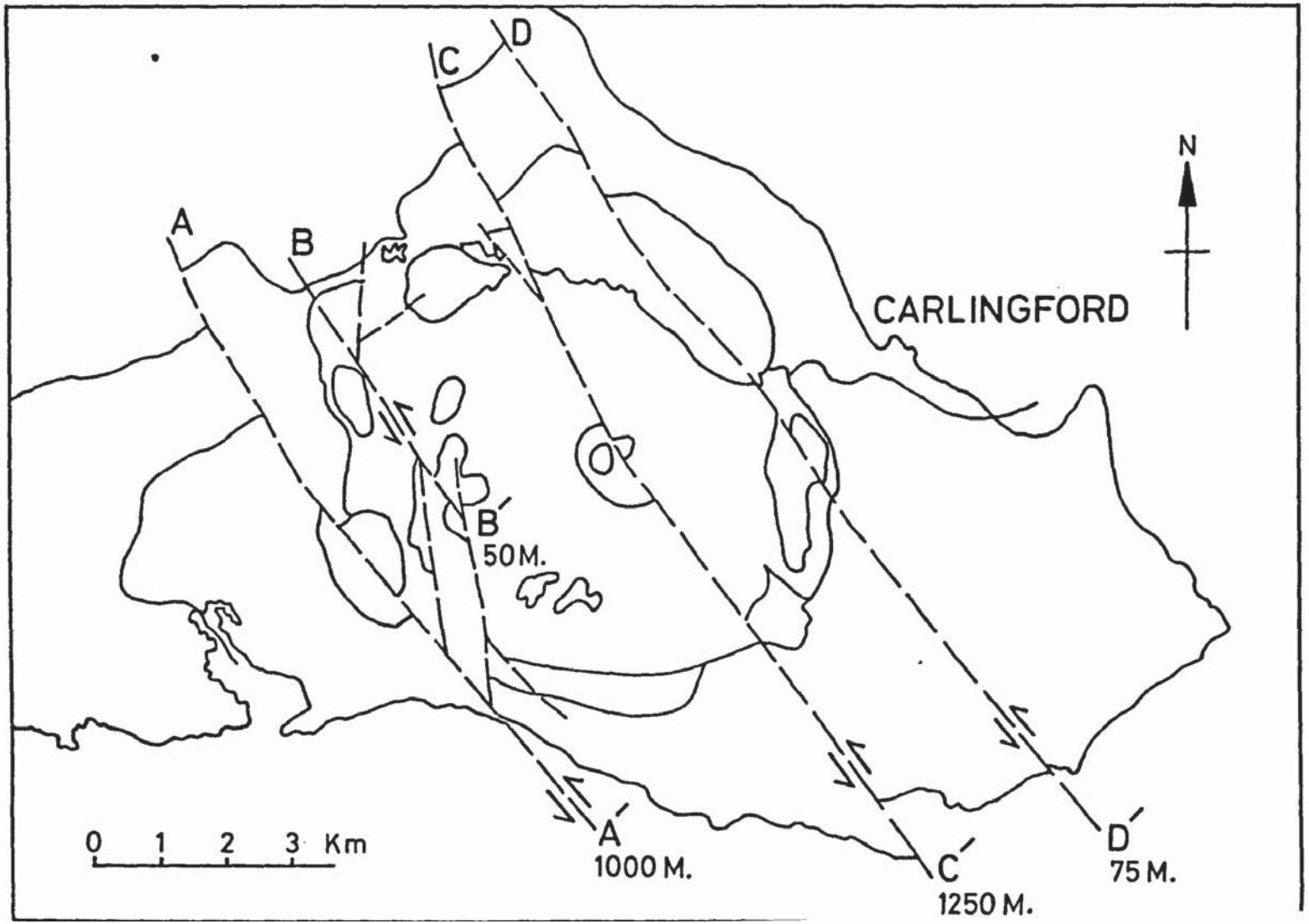

B. MINOR INTRUSIONS

The Dyke Swarms

Frankel (1968) defines dykes as, "discordant tabular injected bodies, thin in comparison with length. They are vertical or near vertical when emplaced, and fairly uniform in width with little deviation in linear outcrop". The majority of the Carlingford dykes fall within this definition, some however are inclined at angles little in excess of 60° from horizontal, these can be distinguished from cone-sheets and complementary cone-sheets only where they do not dip towards or directly away from cone-sheet focii (see below).

As noted in Chapter 1 above, intense dyke injection has taken place in the Carlingford Peninsula along a number of trend axes, most dominant of which are north west - south east (300 - 320° True) and north east - south west (050° True), a minor east west axis is also present but north - south dykes are largely absent (Fig. 1.3). The radial element apparent in Fig. 1.4 above, does not reflect the structure of a single dyke system, but developed by repeated injection in a least three cycles, of a series of superimposed dyke swarms (see Chapter 1). These episodes are discussed individually below as far as possible.

Fig. 2.8 is a thickness frequency histogram showing the thickness of some 300 measured dykes, taking individual sheets within multiple and composite intrusions separately. The diagram distinguishes between north west, north east and east - west trending dykes and shows that the thickness distribution is similar in each

Figure 2.8

Thickness frequency histogram for 300 dykes, the ornament distinguishes those with north west, north east and east west trends. Peak height reflects the number of dykes within the thickness limits indicated.

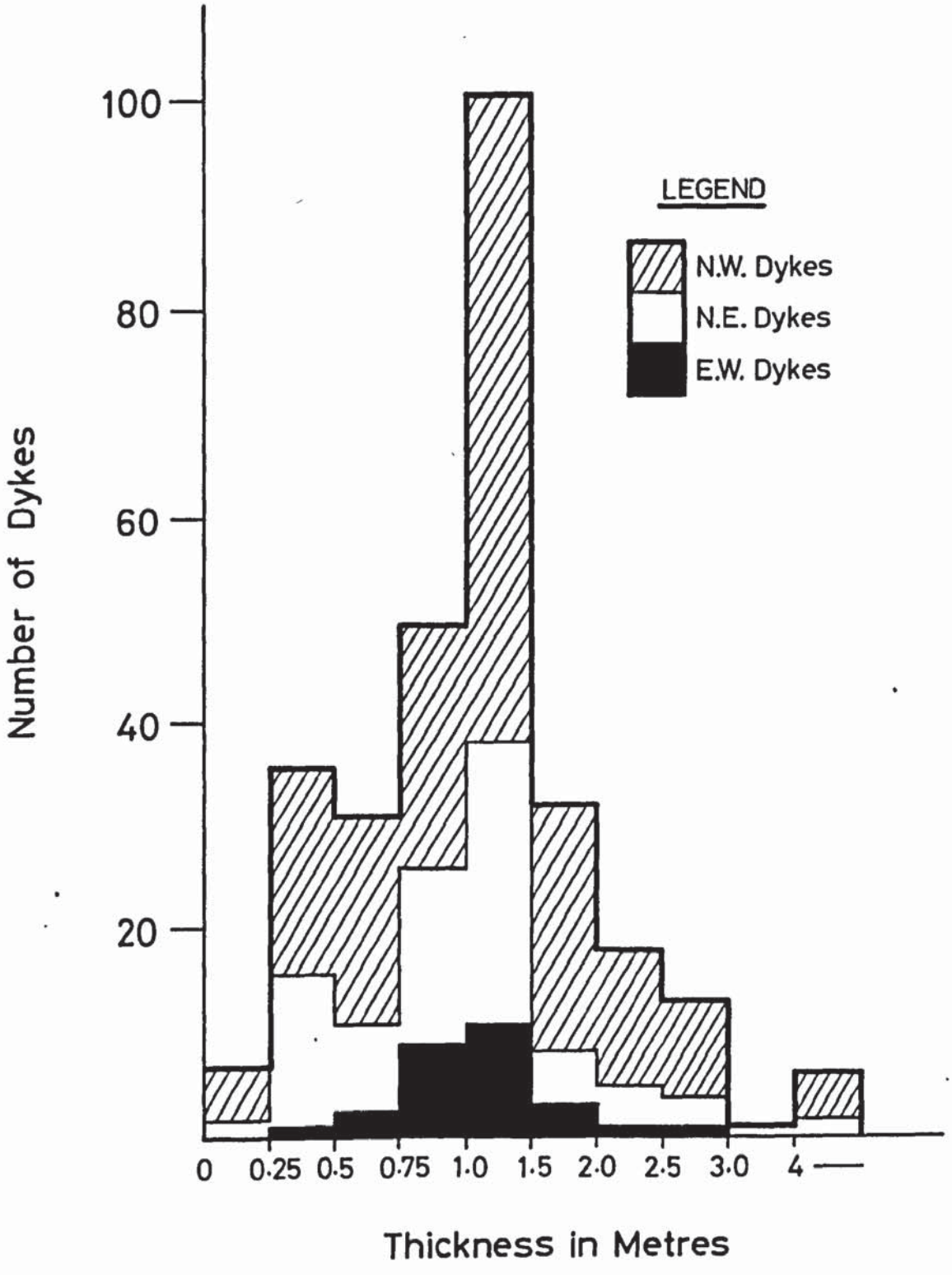

group except that a higher proportion of north east dykes exceed 3 metres in thickness. The variation of dyke thickness within individual swarms, cannot be shown to vary significantly as a function of the petrology or relative age of that swarm compared with those of other swarms or the dyke system of the complex as a whole . The mean thickness of the dykes in Figure 2.8 is 1.4 metres and the modal thickness 1 - 1.5 metres.

The numbers of dykes encountered in a series of traverses at right angles to the principal axes of dyke injection at localities with extensive exposure (see Fig. 2.9) are set out in Table 2.1. Five of these localities (A - E) are within 6 km of the geographical centre of the complex at Spellikanee, and are entirely within areas of sedimentary country rock, they are assumed to reflect dyke injections at its most intense. The traverses at Carnawaddy (F) and south west Slieve Foye (G) although nearer to the centre are within the area occupied by the gabbro or granophyre, as is that at Drumenagh Hill (H), and thus evidence of dykes of the earlier episodes have been obliterated in these areas. The beach traverse at Whitestown (I) is some 10 km south east of Spellikanee but almost astride the north west - south east axis of the complex. The intensity of dyke injection in limestone is apparently much higher than in the Silurian sediments, this may reflect differences in the physical properties of the country rocks or be a function of exposure.

The average total crustal dilation resulting from the injection of north west trending dykes in the area within 6 km of Spellikanee

Figure 2.9

Sketch map of the complex indicating localities of traverses listed in Tables 2.1 and 2.2.

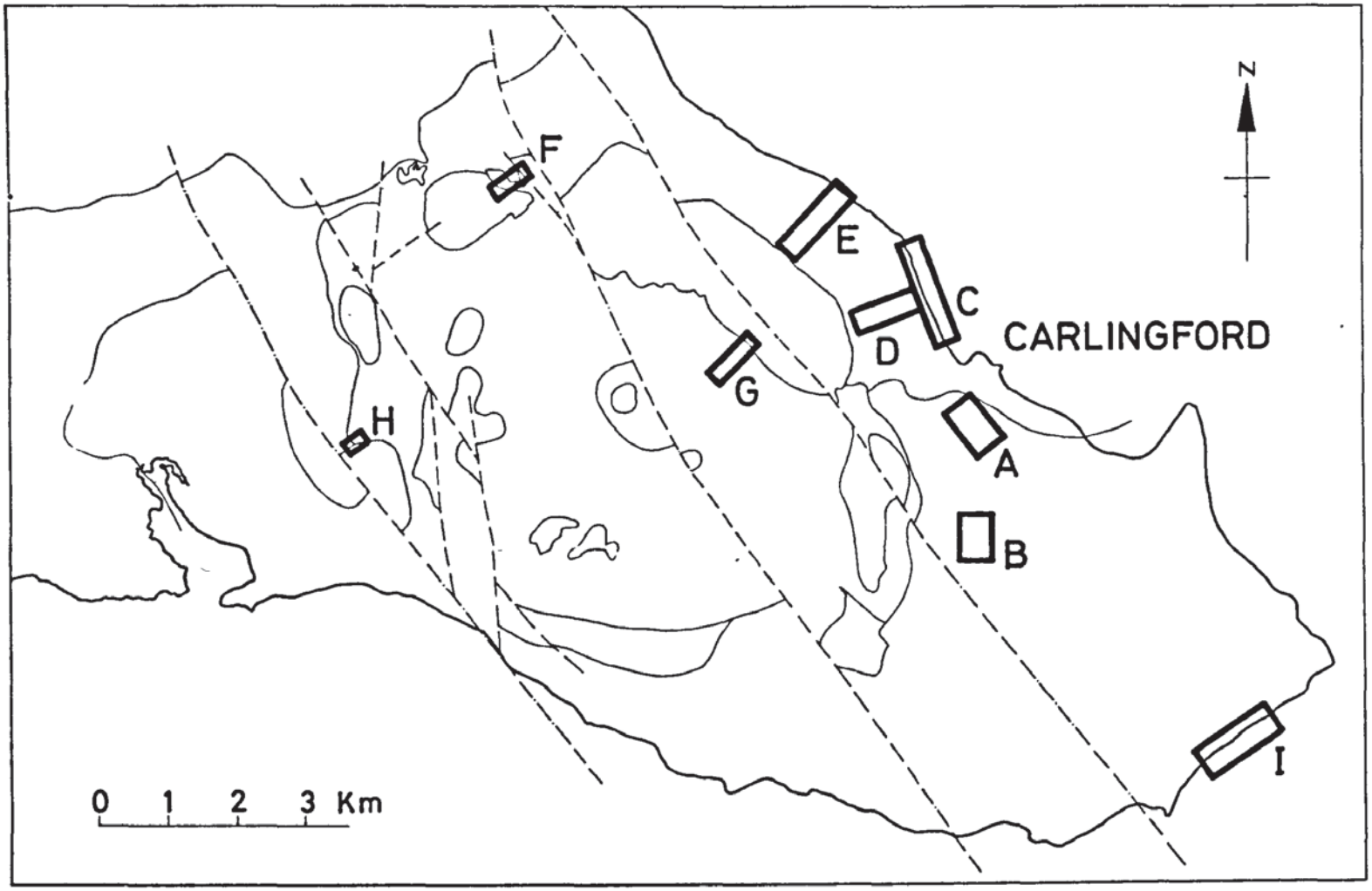

TABLE 2.1

Dyke injection at nine localities on the Carlingford Peninsula (see Fig. 2.9).

Locality	Dyke Trend	Traverse Length	Number of Dykes	Total Thickness	Mean Thickness	Modal Thickness	Percent Dilation	Country Rock
A. Carlingford Quarries	NW	200m.	17	25.1m.	1.5m.	1-1.5m.	12.6%	Limestone
	NE	500m.	6	3.5m.	0.5m.	0.5-0.75m.	0.7%	
	E-W	400m.	1	1.5m.	1.5m.	1.5m.	0.4%	
B. Rosemount Quarries	NW	150m.	18	19.6m.	1.1m.	1-1.5m.	13.1%	Limestone
	NE	400m.	0	-	-	-	-	
	E-W	300m.	6	5.9m.	1.0m.	1-1.5m.	2.0%	
C. Carlingford Shore	NW	750m.	5	7.8m.	1.6m.	1-1.5m.	1.0%	Silurian Sediments
	NE	1800m.	4	4.7m.	1.2m.	1-1.5m.	0.3%	
	E-W	2000m.	1	1.5m.	1.5m.	1.5m.	0.1%	
D. Golden River	NW	800m.	6	8.7m.	1.5m.	1-1.5m.	1.1%	Silurian Sediments
	NE	150m.	2	2.4m.	1.4m.	1-1.5m.	1.6%	
	E-W	200m.	0	-	-	-	-	
E. Two Mile River	NW	600m.	8	10.6m.	1.3m.	1-1.5m.	1.8%	Silurian Sediments
	NE	100m.	2	2m.	1.0m.	1.0m.	2%	
	E-W	500m.	0	-	-	-	-	

TABLE 2.1 Cont.

Locality	Dyke Trend	Traverse Length	Number of Dykes	Total Thickness	Mean Thickness	Modal Thickness	Percent Dilation	Country Rock
F. Carnawaddy	NW	500m.	7	13.6m.	1.9m.	1.5-2.0m.	2.7%	)
	NE	150m.	1	1.5m.	1.5m.	1.5m.	1.0%	) Gabbro/
	E-W	200m.	2	3.6m.	1.8m.	-	1.4%	) Granophyre
G. Alta William	NW	250m.	2	3.6m.	1.8m.	-	1.4%	)
	NE	300m.	1	1.2m.	1.2m.	1.2m.	0.4%	) Gabbro/
	E-W	250m.	0	-	-	-	-	) Granophyre
H. Drumenagh	NW	70m.	1	2.4m.	2.4m.	2.4m.	3.4%	)
Hill Quarry	NE	50m.	2	2.0m.	1.0m.	1.0m.	4.0%	) Gabbro/
	E-W	50m.	0	-	-	-	-	) Granophyre
I. Whitestown	NW	300m.	18	19.5m.	1.1m.	1-1.5m.	6.5%	)
	NE	150m.	0	-	-	-	-	) Limestone
	E-W	200m.	0	-	-	-	-	)

Traverses at rightangles to dyke trend. All distances measured in metres.
Mean thickness and dilation calculated to nearest first decimal place.

is approximately 3% assuming that the average frequency of injection (1 dyke every 46 metres) for the traverses A - E Table 2.1 reflects that for the area as a whole (wherever country rock is exposed dykes are always present), and taking the mean thickness of all dykes as 1.4 metres. Similar calculations yield figures of 0.7% and 0.3% for dilation at right angles to the north east and east west axes in that order, dyke frequency being 1 dyke every 204 metres and 475 metres respectively. These figures indicate that dyke injection in Carlingford is by no means as intense as that of Arran (Tyrrell 1928) but similar to that of Mull (Bailey et al. 1924). Unfortunately it has not proved possible to contour the intensity of dyke injection for the Carlingford Complex in the manner of Skelhorn et al (1971 p 98) due to the lack of exposure in extensive areas, moreover, the composite nature of the swarm renders such an exercise meaningless.

A variety of types of dyke swarm might be expected to occur within the complex, notably linear swarms, radial swarms and tangential or orthogonal conjugate swarms. Linear swarms are developed throughout the British Tertiary Province principally with a north west - south east trend, radial swarms are described from Rhum and Skye and a tangential swarm from Skye (Richey 1961).

The fractures occupied by elongate linear dyke swarms associated with intrusive igneous centres cannot be generated by magma pressure within those centres (Roberts 1970 p 314). Linear swarms are probably an expression of more deep seated processes, the intrusive centres acting as points of weakness through which the

swarms passed (Richey 1939). Recently the argument has been reversed by Skelhorn et al. who suggest that the intersection of deep seated structures giving rise to the north west dyke swarms of the Hebrides, with planes of weakness in the crust, would lead to the development of intrusive centres at those points (1971 p 98). In either case linear dyke swarms and intrusive centres are distinctly separate, though related, expressions of intrusive magmatic activity.

Radial and tangential dyke swarms on the other hand are directly related to, and the product of, magmatic activity within an intrusive centre. Radial swarms result from high magma pressure in a "magma chamber" subject to uniform horizontal tension (Roberts, 1970, p 314). Sherbon Hills suggests that updoming of country rocks by excess magma pressure would give rise to radial tension fractures that would be occupied by radial dykes (Sherbon Hills, 1963, p 377). Tangential or "paired" dyke swarms, as Roberts (1970) describes them, occupy shear fractures resulting from a directed horizontal tension applied across a "magma chamber" as shown in Fig 2.10. Orthogonal conjugate dyke swarms also occupy shear fractures resulting from directed horizontal tension (Spencer 1959) and are thus of the same nature as tangential dyke swarms. In tangential and conjugate swarms dyke sets are oblique to, and symmetrical about, the direction of minimum pressure, i.e. direction of relative tension.

The pattern of dyke injection associated with the Carlingford Complex or any other intrusive complex, at any moment in time, reflects the stress pattern acting on it at that time as a result

Figure 2.10

Stress patterns arising from directed stress across a magma chamber of simple shape after Roberts 1970 Fig. 5 p. 312.

a) The intrusion and fault patterns developed around a cavity of any shape under horizontal tension or horizontal compression (view from the right hand side of the figure in the latter case).

b) The additional intrusion and fault patterns developed around the elliptical cavities $M \lhd 0$ and $M \rhd 0$ (view from the right hand side of the figure in the latter case. If $M \lhd 0$, sills may be produced under horizontal compression whereas curved normal faults may be formed under horizontal tension. If $M \rhd 0$, paired (tangential) dyke swarms may be produced under horizontal compression, whereas curved thrust faults may be formed under horizontal tension.

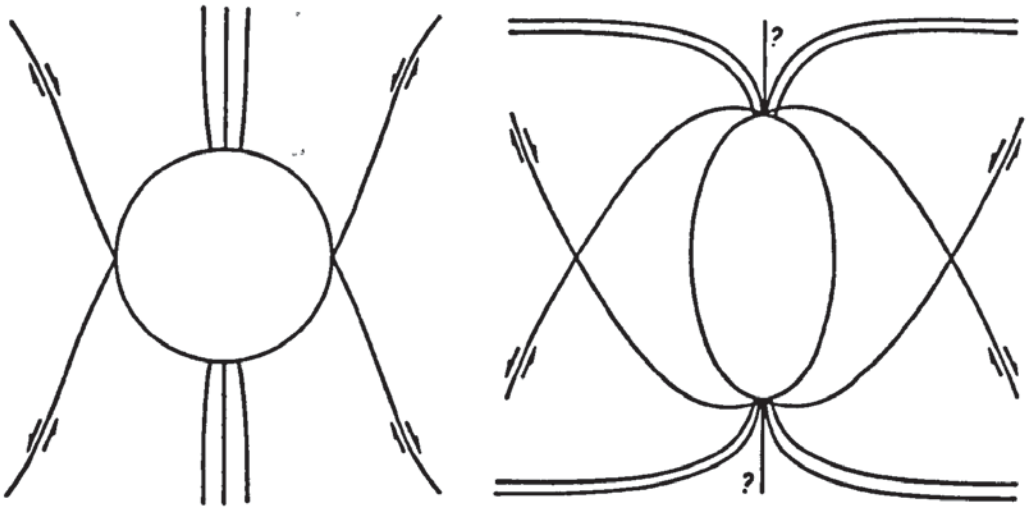

Note: The figure shows a vertical cross section through a horizontal cylindrical body (theoretical magma chamber) where M is a function of the axes x (horizontal) and z (vertical), of the elliptical cross section. $M = (x - z)/(x + z)$ thus if M is positive (greater than 0) the major axis of the ellipse is horizontal and if M is negative (less than 0) the major axis of the ellipse is vertical. If M = zero the radii are equal and the cylinder is circular in cross section as in a above (Roberts 1970 p. 306).

of magmatic activity within the complex and more deep seated magmatic activity or regional stress patterns, and in part distinguishes between the relative significance of these contributing factors.

It should be noted that the structural grain of the country rock into which igneous bodies are intruded inpart modifies the form of those intrusions (Ode 1957). The marked contrast in the physical properties and structure of the tightly folded Silurian sediments, the flat lying Carboniferous Limestones and the massive granophyre and gabbro, to some extent must result in a change in pattern of dyke injection across their mutual boundaries.

Cone Sheets and Related Intrusions.

The cone sheets associated with the Carlingford Complex show many features in common with those of Mull (Bailey et al. 1924), Ardnamurchan (Richey and Thomas et al 1930, Deer 1969), and Skye (Harker 1904). The angle of inclination shows a tendency to decrease as the distance from the centre increases, thus sheets cutting the granophyre on the south west flanks of Slieve Foye and within 1500 metres of Spellickanee, are frequently inclined at angles in excess of 60°, while those cutting the Silurian sediments north and east of Slieve Foye and some 4 km from Spellickanee, are inclined at angles between 30 - 45°. On the shores of Carlingford Lough dips in excess of 35° are rarely recorded while in the gently folded Carboniferous Limestones to the east, cone sheets have the form of transgressive sills largely conformable with the bedding but

Figure 2.11

Drawing of quarry face at the southern end of Carlingford limestone quarry facing northwards, showing dykes and cone sheets (appear as transgressive sills) cutting Carboniferous Limestone. Limestone is shown ornamented by faint hatching parallel to bedding, intrusions are unornamented. The section is approximately 50 metres long. Cone sheet intersections show that their emplacement involved both uplift and horizontal crustal extension.

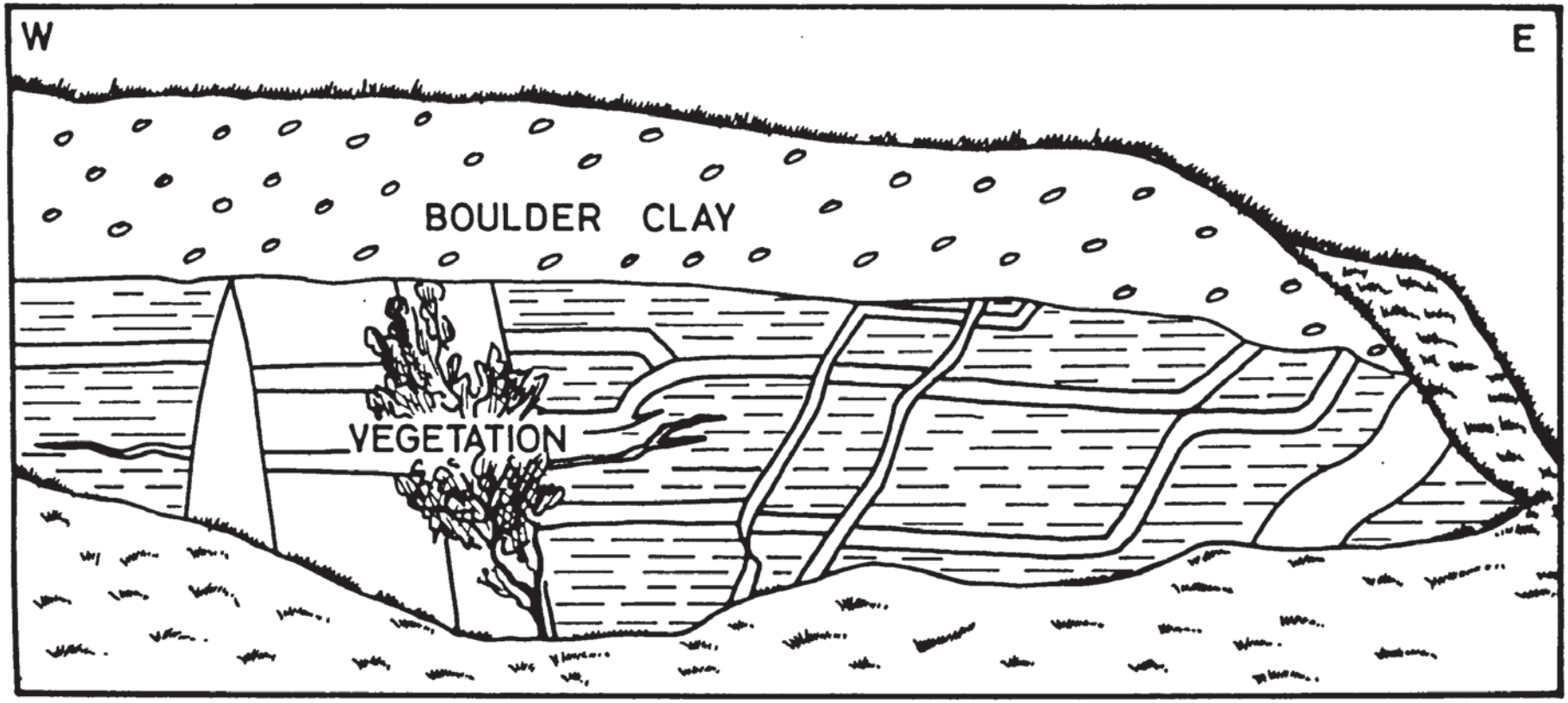

frequently breaking across it to maintain their inclined attitude. This latter phenomenon is well displayed in the limestone quarries south east of Carlingford (see Figure 2.11), the sill like form of the cone-sheets is also exhibited in the quarries at Mullattee to the east of Carlingford, and at Mountpleasant near Dundalk to the west of the complex.

As with the dykes, a series of superimposed cone sheet swarms are present (see Chapter 1 above), these are dealt with individually in detail below. The axes of the focii of the cone sheet swarms have been plotted on the reconstructed "defaulted" base map (see above) Fig. 2.12. by constructing down dip radii at right angles to the average strike of individual sheets within each swarm. This process shows that the majority of cone sheet swarms are roughly coaxial, focussing on an elliptical area about 1.5 km wide by 2.5 km long south of Spellikanee, and within close proximity to the vents of Slievenaglogh, Annaloughan and Spellickanee.

Attempts to determine the depth of focus of the individual cone sheet swarms proves more difficult, not only do the sheets within each swarm apparently focus at different depths, the form of the individual sheets controls the depth of their focus and is itself a function of the mechanics of cone sheet injection,for which a number of models have been proposed.

Durrances model of cone sheets within the Ardnamurchan Complex as a single series of logarithmic spirals (Durrance 1967) is rejected not only on the grounds that it is geologically unrealistic (Roberts 1970 p 317) but also that no such spiral arrangement of cone

Figure 2.12

Location of cone sheet focii for Cycle 1, Cycle 11 and Cycle 111 swarms indicated on the reconstructed base map of the Complex (see Fig. 2.7). Cone sheets are shown as heavy lines with down dip radii.

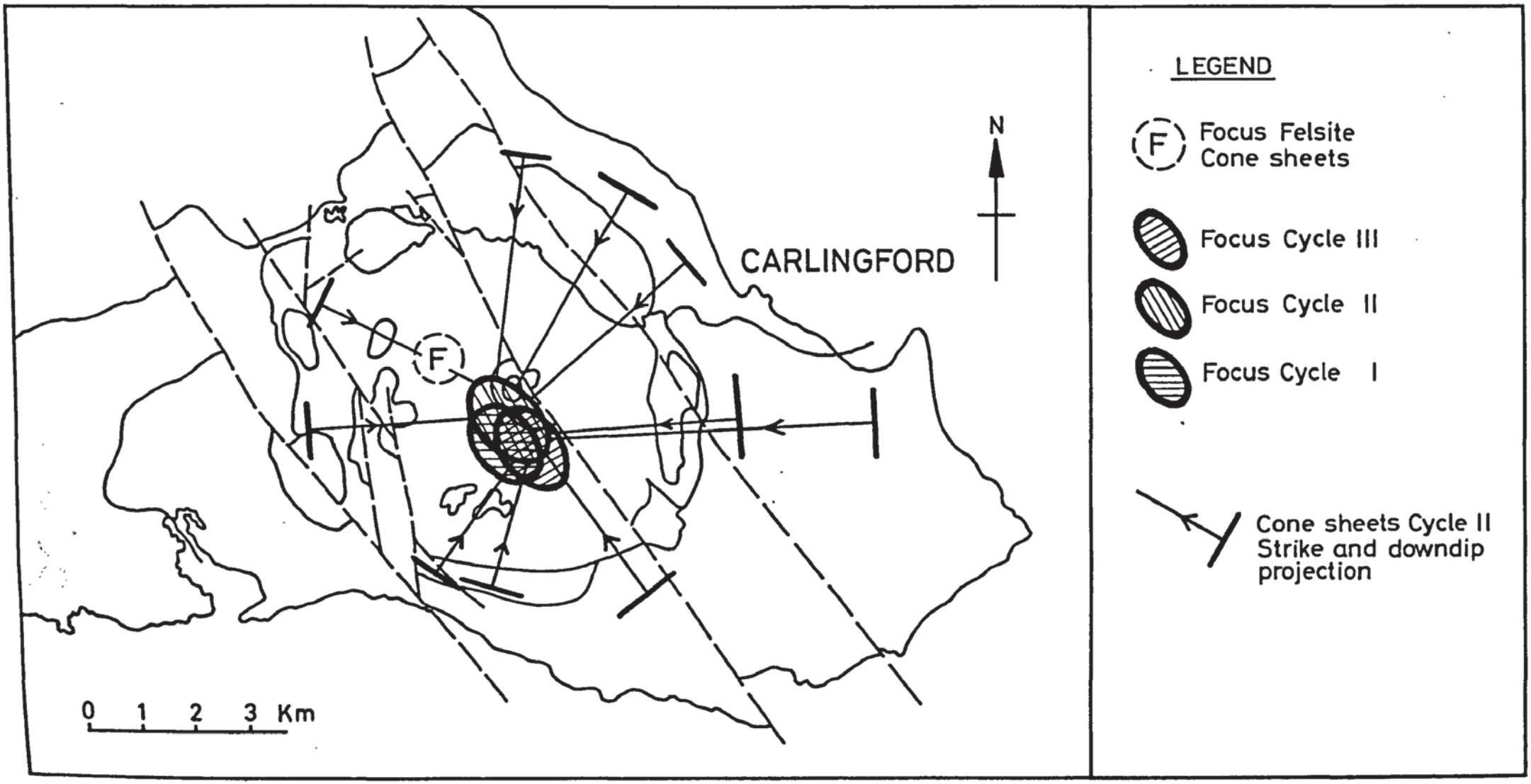

Figure 2.13

Cone sheet stress pattern models and the form of cone-sheets in vertical section.

a) Stress diagram after Anderson (Bailey et al. 1924 Fig. 1). Fine lines, cone-sheet fissures; heavy lines, ring dyke fissures; broken lines, lines of superimposed pressure (high magma pressure) or superimposed tension (low magma pressure).

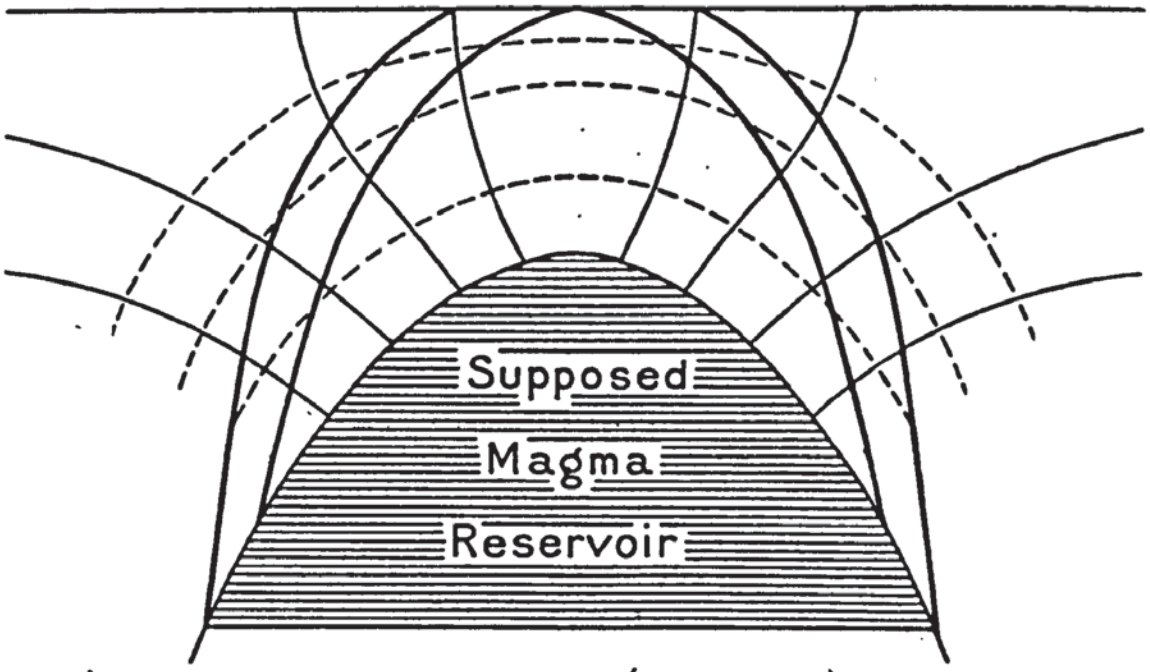

b) Stress diagram after Roberts (1970 Fig. 7). Approximate form of the stress trajectories around a circular cavity near the free edge of a semi-infinite plate. The upper diagram shows the principal stress trajectories and the lower diagram the maximum shear stress trajectories. The sectors marked C and S in the upper diagram represent the sectors where tangential stress at the surface of the cavity has a minimum value under the conditions which would form parallel to the directions of maximum principal stress under such conditions, cone-sheets developing from tensile failure in the sector C, sills resulting from tensile failure in the sector S.

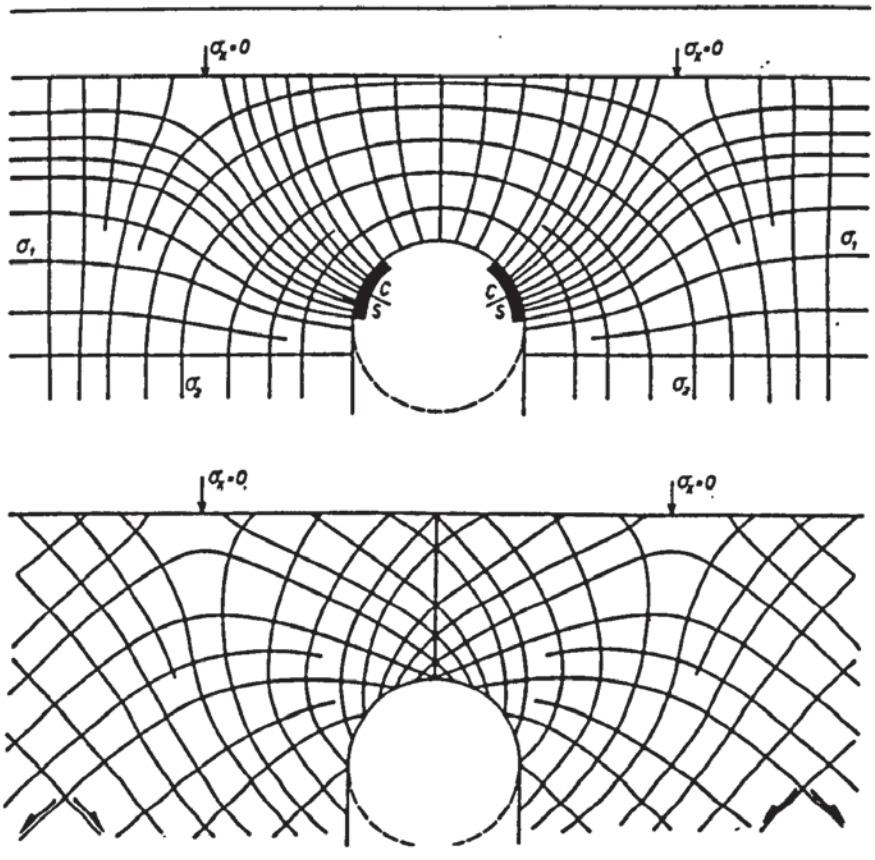

c) Block diagram showing cone sheets and ring dykes in section after Richey (1932 Fig. 2).

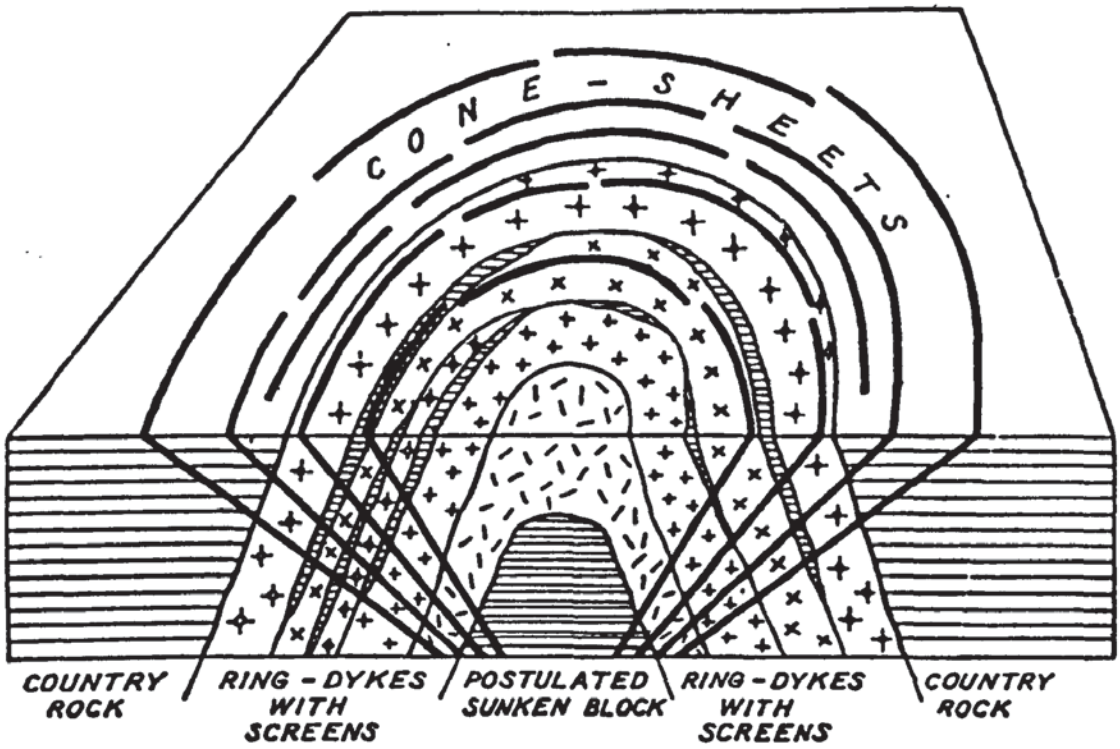

sheets can be demonstrated at Carlingford. Garson's model of inclined sheet injection in Malawi (Garson 1959, Garson and Smith 1958) is rejected as mathematically unsound by Roberts (1970 p 322). Leaving these models aside, two remain, Anderson's original point source model (Anderson 1936) recently modified by Robson and Barr (1964), and Roberts spherical source model (Roberts 1970). These give cone sheets and related intrusions of quite different form in vertical section - see Fig. 2.13. and set lower and upper limits respectively to the depth of cone sheet focii. Anderson 1936 Fig. 5 p 136) shows cone sheets in vertical section as curves which monotonically increase in inclination towards the focus, except near the surface immediately above the centre. Alternatively Roberts (1970 Fig. 7 p 320) shows a cone sheet-sill complex emerging from the surface of a sphere in section, and except that the sill complex flattens out at distance from the source, both cone sheets and sills monotonically decrease in inclination towards the source. Insufficient relief is present at Carlingford to provide conclusive evidence in favour of either of these alternatives. Plotting graphically the shapes of cone sheet traces in section for each of the models, using the angles of inclination and cone sheet distribution at Carlingford, the maximum and minimum depth limits for cone sheet focii in the complex are obtained (Fig. 2.14) - depths of 7.5 km and 3.5 km respectively for the deeper focussing sheets and at depths of 4 km and 1.5 km respectively for the shallower focussing sheets. As it is not possible to define the depths of focus more closely than within these limits all further calculations have been made by

Figure 2.14

Diagrammatic vertical section across the Carlingford Complex adopting 1 the Anderson Model (Bailey et al. 1924) and 2 the Roberts Model (Roberts 1970) the resulting alternative depths of focus are indicated.

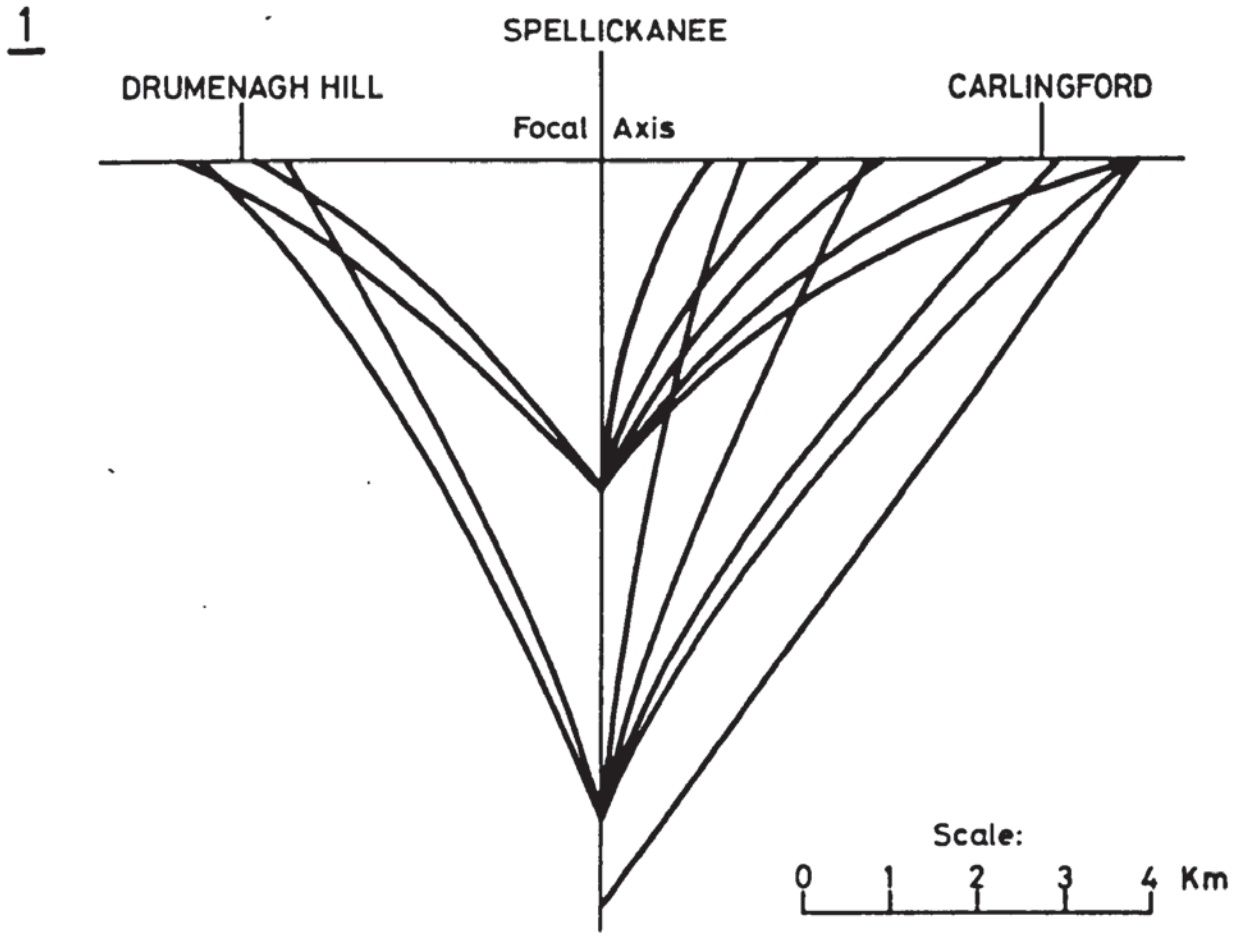

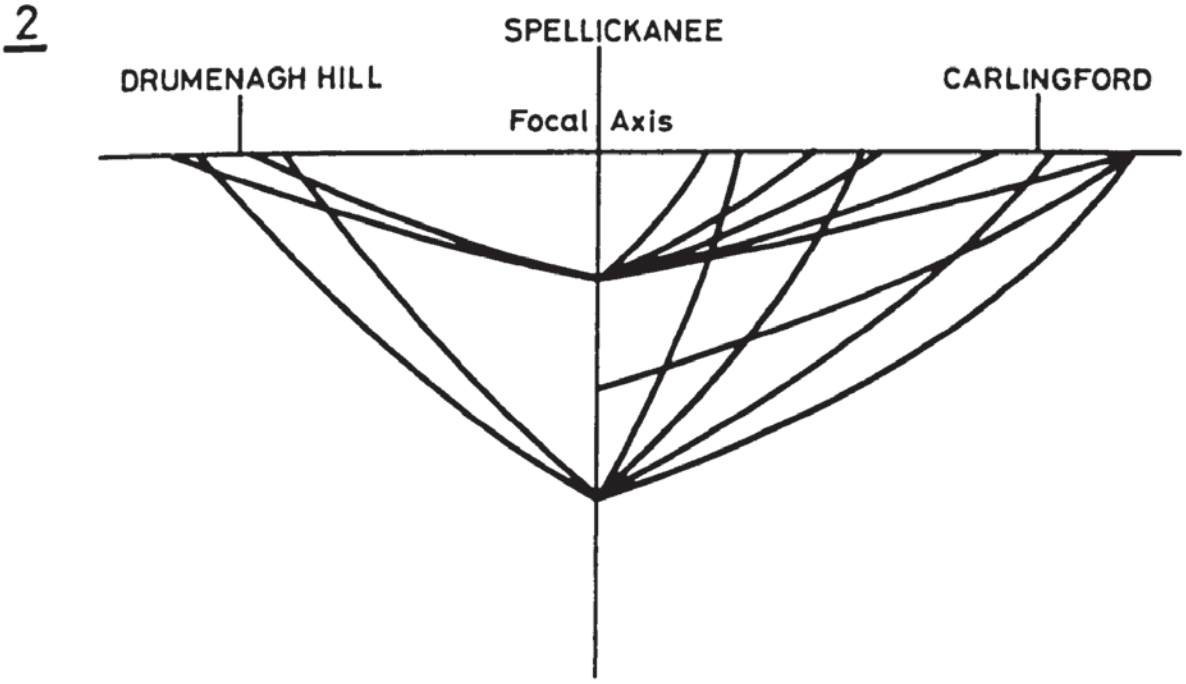

simply plotting the cone sheet traces as straight lines as in Richeys diagrams (Richey 1961 Fig. 23) a convention also adopted by Garson (Garson 1959, Garson and Smith 1958), this gives an approximate mean depth of focus for each swarm between the Anderson - Roberts limits.

In an attempt to define the approximate size and shape of the source magma body of one of the cone sheet swarms (the high-alumina gabbros and feldsparphyric dolerites) structure contours were drawn on the surface of the sheets (Badgley 1959 Chapter 4). The following assumptions must apply if this technique is to be successful:

1. That the majority of sheets emerge at approximately the same level on the surface of the magma body (see Roberts 1970 Fig. 7).
2. That no two sheets from the same swarm cross at depth.
3. That the form of the source body is simple and fairly regular - a hemisphere or hemiellipsoid.
4. That the cone sheets are linear in vertical section.

The construction (Fig. 2.15) was not entirely successful, for not only is assumption 4 an over simplification, many of the individual sheets are impersistant in the field and it is difficult to obtain sufficient data from any single cone sheet swarm. The results however appear reasonable, and indicate a magma body of elliptical plan 3 km by 2 km in diameter (north west - south east and north east - south west respectively) at a depth of 2 km below sea level, as the source of the swarm.

Figure 2.15

Construction of structure contours on cone-sheets of the episode 11e - 111a swarm on the reconstructed defaulted base map (see Fig. 2.7), indicating depth and approximate form of the parent magma body.

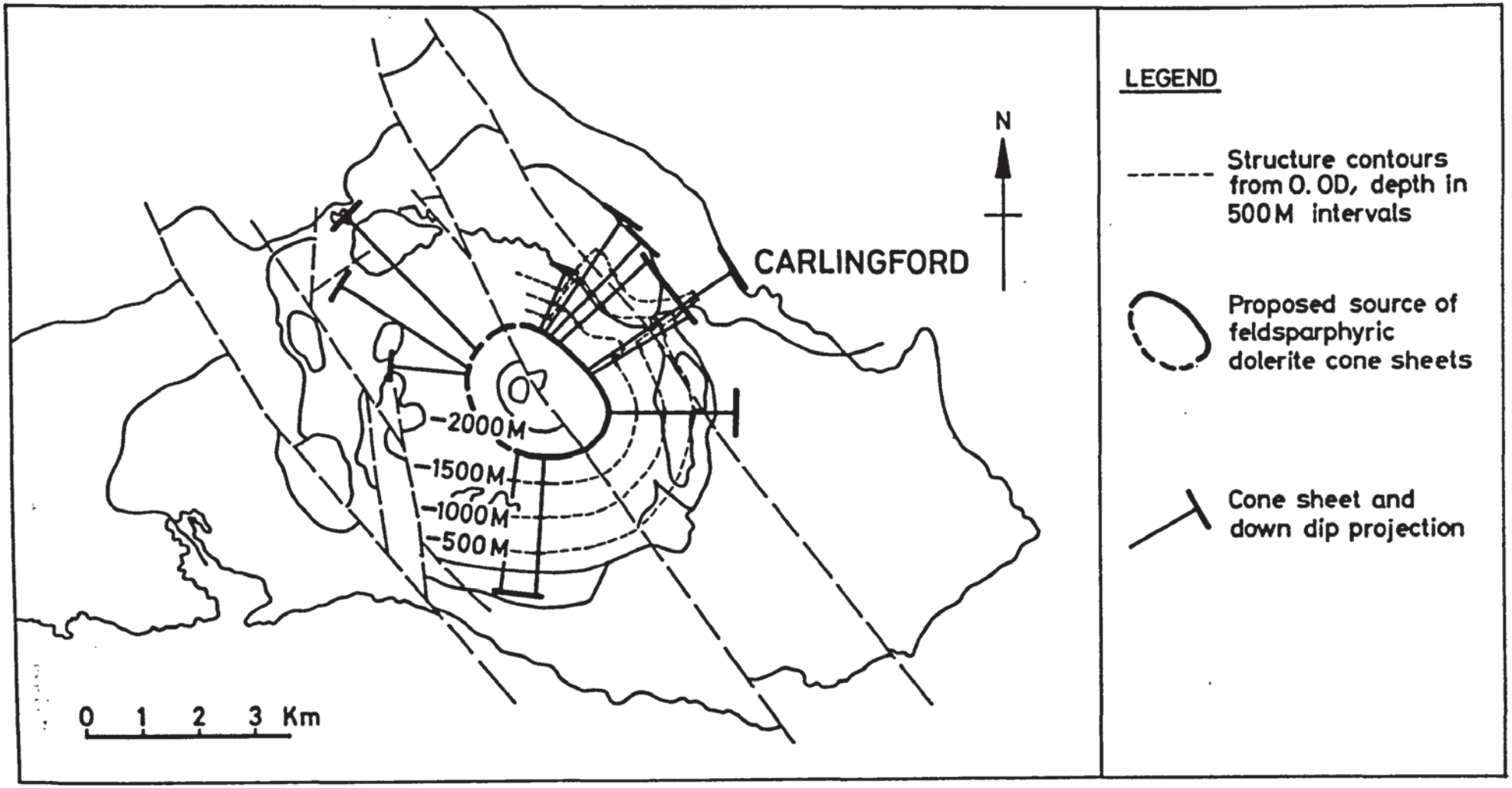

All the proposed models of cone-sheet injection (Anderson 1936, Garson 1959, Durrance 1967, Roberts 1970) assume increased magma pressure within the source body,in excess of the hydrostatic pressure of the overburden,as a prerequisite for the process. Robson and Barr (1964) predicted that cone-sheets occupy shear fractures, Roberts however supports Andersons view that cone sheets occupy tensional fractures (Anderson 1936), though rejecting his point source model as realistic only in exceptional conditions (Roberts 1970 p 317). Thus, assuming Roberts is correct, the injection of cone sheets, though largely resulting in uplift as suggested by Le Bas (1971), must also result in some lateral crustal extension, this is confirmed by Figure 2.11.

Figure 2.16 is a histogram of thickness frequency of some 610 measured cone sheets from the complex. This indicates that the majority of cone sheets fall within the range 0.25 metres to 1.5 metres in thickness. The calculated mean cone-sheet thickness is 1.5 m and the modal thickness 1. to 1.5 m. A few exceptional sheets exceed 3 metres in thickness but a large proportion of these are high-alumina gabbros and feldsparphyric dolerites which have a tendency to form thicker sheets as indicated by the diagram. With that exception no significant variation in the thickness frequency distribution of cone sheets can be recognised between rocks of different petrological suites or of different age.

Table 2.2 indicates the number and thickness of the cone sheets encountered in the traverses already discussed in relation to the dykes. The lengths of traverses D, E, F and G have been recalculated as if horizontal assuming the mean angle of inclination

Figure 2.16

Thickness frequency histrogram for 610 measured cone sheets. The cone sheets of episode 11e - 111a are ornamented separately. Peak height reflects the number of sheets within the thickness limits indicated.

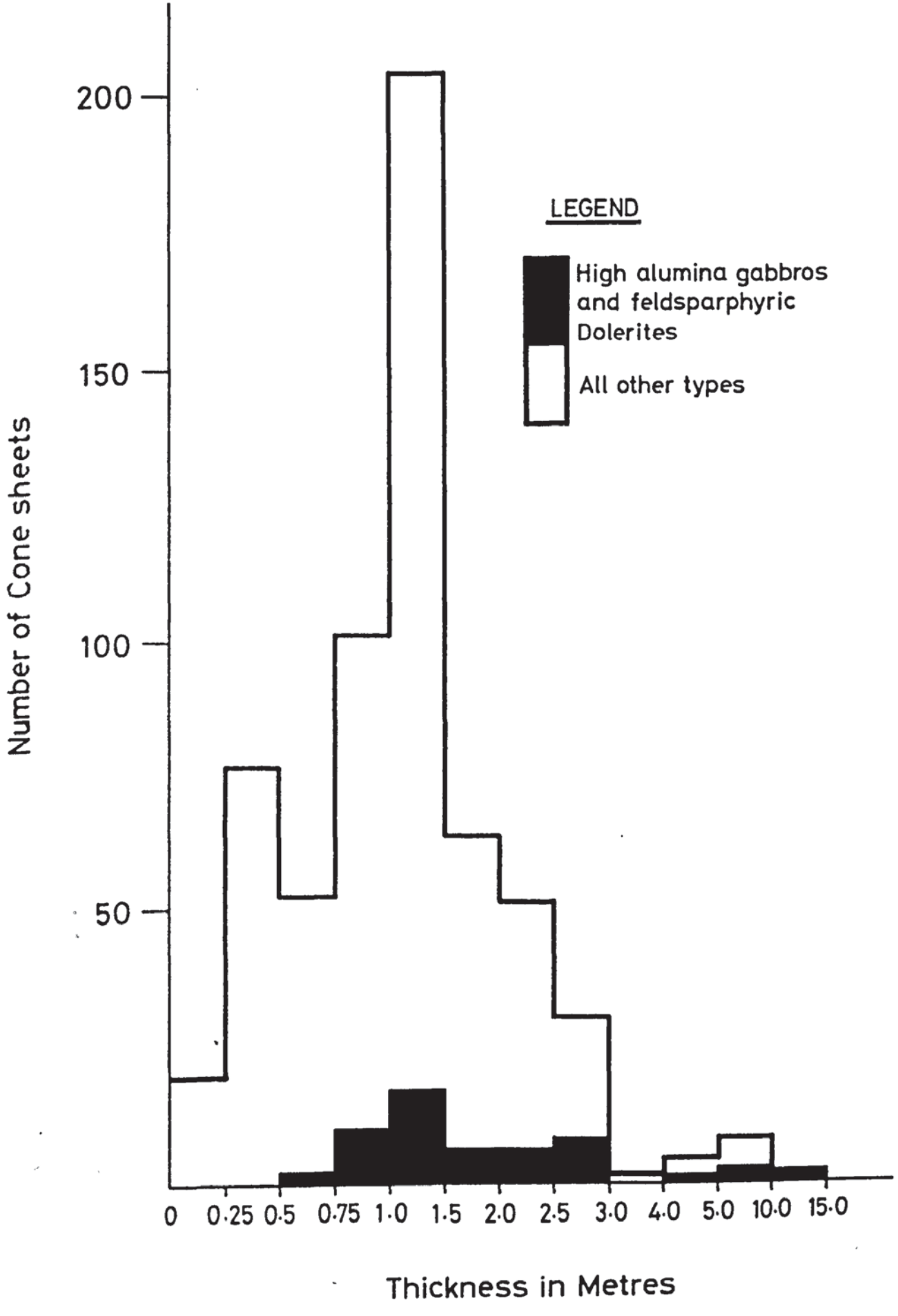

TABLE 2.2.

Cone sheet injection at nine localities on the Carlingford Peninsula (see Fig. 2.9).

Locality	Traverse length	Number of Conesheets	Total Thickness	Mean Thickness	Modal Thickness	Range Recorded Attitudes
A. Carlingford Quarries.	200m.	11	12.9m	1.2m	1-1.5m	0°-51°
B. Rosemount Quarries	100m.	12	15.2m	1.3m	1-1.5m	18°-61°
C. Carlingford Shore	750m.	45	54m	1.2m	1-1.5m	25°-53°
D. Golden River	1100m.*	25	43m	1.7m	1-1.5m	20°-60°
E. Two Mile River	725m.*	36	43.4m	1.2m	1-1.5m	25°-70°
F. Carnawaddy	360m.*	7	11.1m	1.6m	-	20°-70°
G. Alta William River	230m.*	3	5.7m	1.9m	1-1.5m	20°-70°
H. Drumenagh Hill Quarry	60m.	6	6.2m	1.0m	1-1.5m	23°-47°
I. Whitestown Shore.	300m.	1	1.5m	1.5m	1.5m	20°

* Traverse length corrected for change of altitude - see text. Thicknesses quoted are true thickness.

of the cone sheets to be 40°, using the equation:

$$\text{Calculated length of traverse} = X + Y \tan 40^{\circ}$$

(X = actual traverse length, Y = change in altitude, Y is positive when the ground slopes away from the cone sheet focii). These figures indicate that within the sedimentary rocks there is on average one cone sheet every 22 metres in the horizontal plane (the cone sheet frequency). Cutting the granophyre there is one cone sheet every 56 metres on average. Assuming for the purposes of calculation that displacement brought about by cone sheet injection in the area periferal to the focus is essentially vertical, the total uplift resulting from cone sheet injection within any given traverse is given by the equation:

$$\text{Total uplift} = \frac{\text{Distance} \times \text{Mean cone sheet thickness}}{\text{Cone sheet frequency} \times \cos 40^{\circ}}$$

Thus the total uplift between the shores of Carlingford Lough and the centre of the complex at Spellickanee some 5 km to the south west is of the order of 265 metres, calculated on the basis that there are 2 km of sediment and 3 km of granophyre along that line. This figure may be excessive for the consequence of Roberts model (1970) is that at least some displacement in cone-sheet injection takes place in the horizontal plane, the cone-sheets near the centre of the complex being steeply inclined would be emplaced almost entirely by horizontal dilation. By these calculations cone sheets could contribute about 85 metres of uplift to the updoming of the Carboniferous Limestone unconformity in the vicinity of Carlingford which Le Bas estimates to be updomed by some 200 m.in 1 km. (Le Bas 1971), the remaining 120 metres or so must be attributed to the emplacement of the Carlingford granophyre (see above).

Finally, it should be noted that many of the cone-sheets either branch and join to form a reticulate mesh, the high-alumina gabbros and feldsparphyric gabbro cone sheets on the slopes of Slieve Foye above Carlingford Town for example; (see Maps 1 and 2) or are interconnected by dykes, a phenomenon seen in many of the limestone quarries. Thus it is possible that at least some dykes are branches of cone sheets or perhaps feeders to cone sheets rather than independent fissures penetrating to great depth.

The Complementary Cone-Sheets

A series of intrusive sheets inclined at angles of 40° or less radially outwards from the cone-sheet focii and coaxial with them, crop out on the eastern and north eastern flanks of Carlingford Mountain and cut the limestones east of Barnavave. These sheets are referred to herein as 'complementary cone-sheets'. Cropping out as they do parallel to the hillside it is difficult to define their age relations as exposure is often concealed, however it is clear that complementary cone sheets accompany several of the cone sheet swarms (see below). They are regarded as being analogous to Garson's shear fracture dykes type B (Garson 1959 Fig. 5) which Roberts suggests are produced by fluctuations in magma pressure in the underlying source (Roberts 1970 p 322), shear failure taking place along fractures inclined radially outwards from the centre as magma pressure falls after an earlier high pressure episode involving cone sheet injection. Thus complementary cone sheets might be expected to occur in areas such as Carlingford where repeated cone-sheet injection has taken place

and where intervals of relatively low magma pressure must have intervened between episodes of cone sheet emplacement.

The Minor Intrusions of Cycle One

The minor intrusions of Cycle 1. were all injected prior to the intrusion of the layered gabbro (see Chapter 1 above). Some of this intrusive activity may have taken place at the same time as the extrusion of the basalt lavas, however it is not possible to establish the time relations of the lavas with any Cycle 1 intrusion. None of the Carlingford dykes can be demonstrated to have acted as lava feeders, such as those described from a number of localities in Ireland by Preston (1965, 1967a, 1967b, 1971), Patterson (1950) and Walker (1959).

The relative proportion of dykes and cone sheets (including complementary cone-sheets) associated with each cycle, to all such intrusions of known age, together with the relative abundance of each rock type within the intrusions of each cycle, are summarised in Table 2.3. These figures show that the number of intrusions firmly attributed to Cycle 1. is relatively small, however the proportion of the various rock types forming them, reflect the relative abundance of those rocks in the swarm as a whole. Provided the sample is unbiased, the proportion of each rock type attributed to each cycle may be assumed to reflect the availability of each magma type within it.

Figure 2.17 is a rose diagram showing the azimuth of the dyke trends of Cycle 1. peaks reflecting the number of dykes at the azimuth

TABLE 2.3.

Relative proportions of petrological types in 652 minor intrusions of known relative age.

A. Dykes.

Rock Types	Cycle I		Cycle II		Feldsparphyric dolerites		Cycle III		Total	
	1	2	3	4	5	6	7	8	9	10
	No.	Percent	No.	Percent	No.	Percent	No.	Percent	No.	Percent
Alkali dolerite	3	4.2	45	62.5	-	-	24	33.3	72	28.2
Olivine dolerite	15	14.6	64	62.1	-	-	24	23.3	103	40.4
Feldsparphyric dolerite	-	-	-	-	11	100	-	-	11	4.3
Quartz dolerite	6	16.7	16	44.4	-	-	14	38.9	36	14.1
Craignurite	3	12.5	14	58.3	-	-	7	29.2	24	9.4
Felsite	-	-	9	100	-	-	-	-	9	3.5
Total	27	10.6	148	58.0	11	4.3	69	27.1	255	-

Percentages in columns 2,4,6, and 8 are percentages of the totals in column 9. Percentages in column 10 are percentages of the overall total in column 9.

Alkali dolerite includes data for hawaiitic and mugearitic basalts, and trachy basalts.

Olivine dolerite includes data for transition dolerites and tholeiitic olivine dolerites.

Feldsparphyric dolerite includes data for high alumina gabbros.

Craignurite includes data for craignuritic felsites.

TABLE 2.3.
Relative proportions of petrological types in 652 minor intrusions of known relative age.

B. Cone-sheets and Complementary Cone-Sheets

Rock Types	Cycle I		Cycle II		Feldsparphyric dolerites		Cycle III		Total	
	1	2	3	4	5	6	7	8	9	10
	No.	Percent	No.	Percent	No.	Percent	No.	Percent	No.	Percent
Alkali dolerite	2	33.3	4	66.6	-	-	-	-	6	1.5
Olivine dolerite	40	22.9	117	66.9	-	-	18	10.3	175	44.1
Feldsparphyric dolerite	-	-	-	-	79	100	-	-	79	19.9
Quartz dolerite	10	11.1	69	76.7	-	-	11	12.2	90	22.7
Craignurite	1	2.4	34	82.9	-	-	6	14.6	41	10.3
Felsite	-	-	6	100	-	-	-	-	6	1.5
Total	53	13.4	230	57.9	79	19.9	35	8.8	397	-

Percentages in columns 2,4,6, and 8 are percentages of the totals in column 9. Percentages in column 10 are percentages of the overall total in column 9.
Alkali dolerite includes data for hawaiitic and mugearitic basalts, and trachy basalts.
Olivine dolerite includes data for transition dolerites and tholeiitic olivine dolerites.
Feldsparphyric dolerite includes data for high alumina gabbros.
Craignurite includes data for craignuritic felsites.

Figure 2.17

Rose diagram of dyke trend azimuths for 25 dykes of Cycle 1, where peak height from the base circle is proportional to the number of dykes per 10° arc (001° - 010° inc., 011° - 020° inc., etc., etc.). All azimuths are measured from True North.

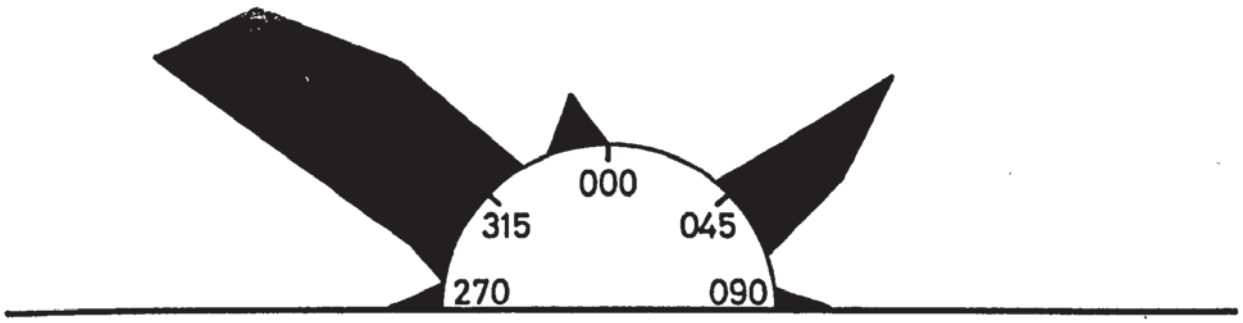

in question. This shows the dominant swarm has a north west south east trend at 300 - 310° True, this includes rocks of all types. A subsidiary swarm, almost orthogonal to the former, with a trend maximum at 050° True, is entirely comprised of transition dolerites and tholeiitic dolerites. On the basis of the figures in Table 2.3. it is calculated that the injection of the north west dykes of Cycle 1 would give rise to 0.3% crustal extension at right angles to that trend, and the north east trending dykes of Cycle 1., 0.1% dilation.

Cone sheets of all rock types in Cycle 1. focus at depths of the order of 1500 - 2000 metres on the focal axis. Total uplift resulting from the injection of Cycle 1. cone sheets is calculated to be 30 metres at the centre of the complex. Complementary cone-sheets are associated with this swarm.

Time relations suggest that the intrusion of the quartz dolerite and craignurite cone sheets and north west dykes preceded the injection of the transition and tholeiitic dolerite dykes within Cycle 1., and that the north east trending dolerite dykes postdate all other intrusions within the Cycle.

The Minor Intrusions of Cycle Two.

The injection of the dykes and cone sheets of Cycle II took place between the emplacement of the layered gabbros and the Carlingford granophyre (see Chapter 1). Minor intrusions associated with this cycle are the most numerous contributing some 58% of the cone sheets and also 58% of the dykes of known relative age. A number of separate episodes of intrusive activity are recognisable within this Cycle.

a) The first identifiable event in Cycle II was the emplacement of a series of dykes, cone-sheets and complementary cone-sheets, of relatively minor significance in terms of abundance (see "Felsite" Table 2.3). They consist of the rock types referred to as "biotite felsite"and "quartz feldspar porphyry " in Chapter 1. With so few cone-sheets it is difficult to plot the position of the swarm focus, there is evidence however that they focus about 1 km. north west of Spellickanee and therefore some distance to the north and west of the majority of cone-sheets (see Fig. 2.18), the depth of focus is uncertain.

Some "felsite" dykes have a radial distribution and may constitute a minor radial swarm focusing to the north west of Spellickanee on approximately the same axis as the cone-sheets.

The occurrence of this episode of felsite intrusion immediately following the emplacement of the layered gabbros suggests that they may be genetically associated. It is suggested by Le Bas that the granophyres of the Carlingford complex were formed by melting of Silurian sediments adjacent to a large reservoir of basic magma which fed the layered gabbro lopolith (Le Bas 1967 p 336). The time relations of the felsite dykes are in keeping with their formation by such a mechanism (further consideration is given to this problem in Chapter 8). If they were formed by the melting of sediments adjacent to the gabbro feeder then that feeder lies to the north and west of Spellickanee on the focal axis of the cone-sheet swarm and associated dyke swarm.

b). The intrusion of a swarm of alkali dolerite dykes has been

Figure 2.18.

Sketch map showing projection of dyke trends and location of cone-sheet focus for episode 11a (drawn on the reconstructed base map - see Fig. 2.7).

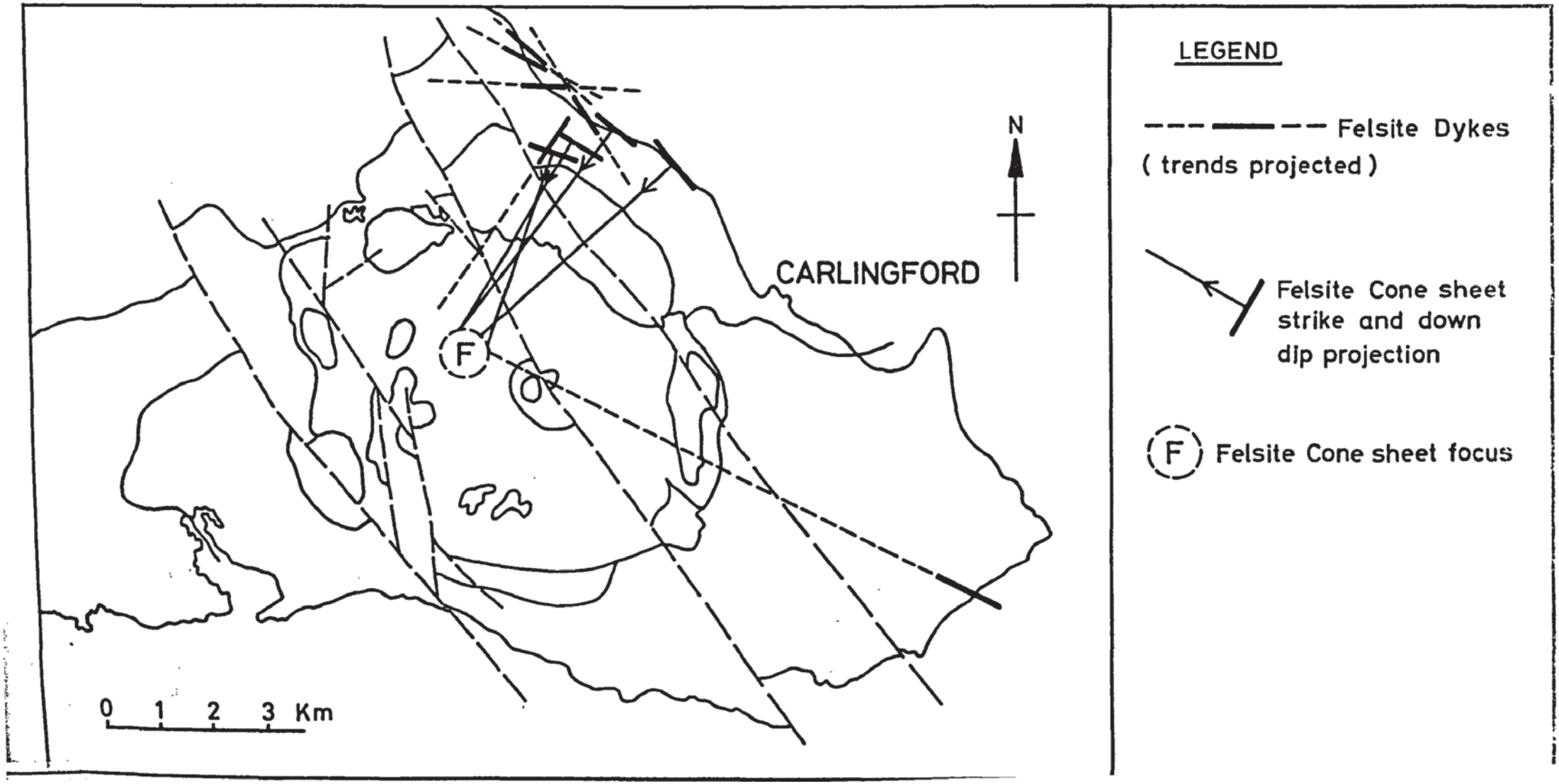

identified as the next episode in Cycle II. Rare alkali dolerite cone-sheets are associated with this swarm but it is dominated by a strong north west - south east dyke swarm (see Fig. 2.19) which is particularly well developed to the east of the complex at Whitestown and Mullatee, but has also identified on the shores of Carlingford Lough north west of Carlingford, and in the limestone quarries at Rosemount and Carlingford (Fig. 2.20). Minor north east - south west and east - west swarms are also associated with this episode, and may constitute a partially developed radial swarm, their time relations with the north west dykes are uncertain. A particularly prominant north east - south west dyke attributed to this episode and about 3 metres thick (spec 1351) traverses the shore of Carlingford Lough 1 km. south of Omeath. It is similar in petrology to others cropping out across the Lough on the flanks of the Mourne Mountains and may be an outlier of a Mourne swarm rather than a member of the Carlingford swarm under discussion, of course the swarms may be contemporaneous. In the light of the current research on the Carlingford minor intrusions, it may be possible, by a similar investigation of the Mourne dykes, to establish the degree of mutual independence of the two centres and the time relations of events within them.

The north west trending alkali dolerite dykes contribute about 0.7% dilation to crustal extension atright angles to their trend (calculated from the data in Table 2.1.). However, in the Carboniferous Limestone on the shores at Whitestown, north east - south west dilation resulting from the injection of dykes attributed to this episode is 4.3% which suggests that the Whitestown area is astride the

Figure 2.19

Rose diagram of dyke trend azimuths for 37 dykes of episode 11b (alkali dolerites), where peak height from the base circle is proportional to the number of dykes per 10° arc ($001^{\circ} - 010^{\circ}$ inc., $011^{\circ} - 020^{\circ}$ inc., etc., etc.). All azimuths are measured from True North.

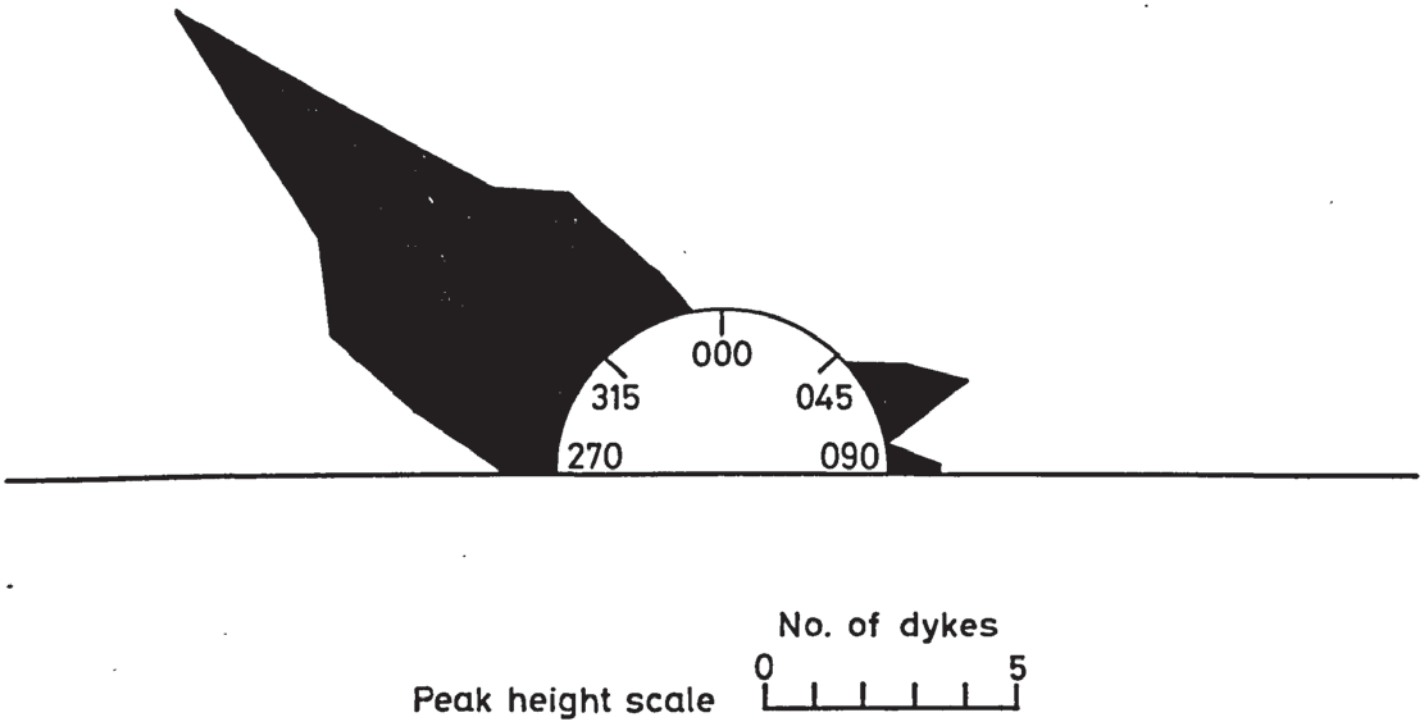

Figure 2.20

Sketch map showing projection of dyke trends for episode 11b (drawn on the reconstructed base map - see Fig. 2.7).

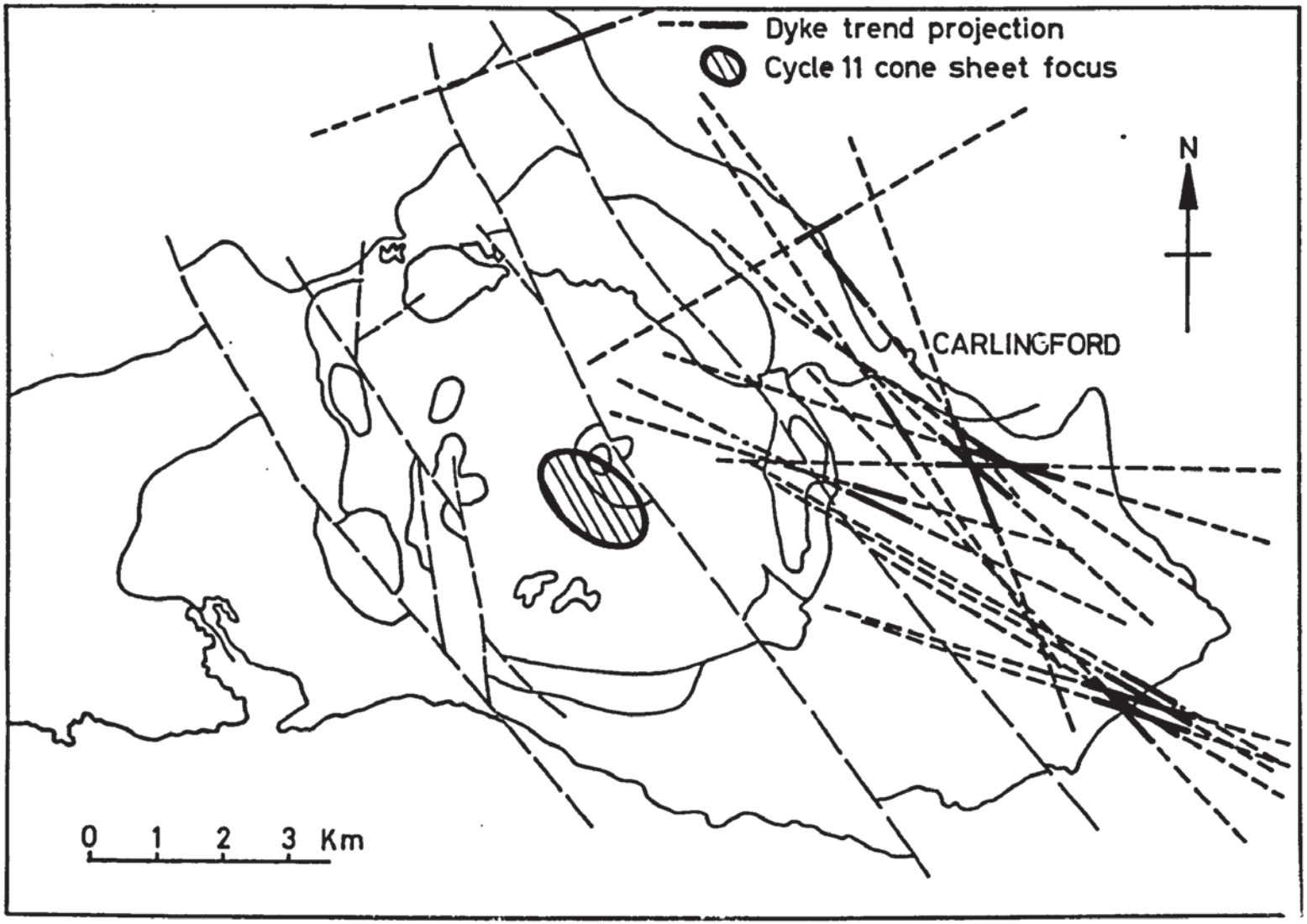

median axis of the swarm.

c). Following the emplacement of the alkali dolerite dyke swarm of Cycle II, a series of dykes and cone-sheets of quartz-dolerite and craignurite composition were emplaced.

Cone-sheets of this episode are particularly well displayed in the limestone quarries at Carlingford, Rosemount and Mullatee (see Maps 3, 4 and 5) where they appear in the form of transgressive sills; they account for 44% of all cone-sheets attributed to Cycle II, and contribute about 55 metres of uplift at the centre of the complex. The majority of these sheets focus at depths of 1500 to 2000 metres below sea level on the focal axis south of Spellickanee, however a few focus at greater depths of the order of 3000 - 4000 m. on that axis, it is therefore possible that two swarms are in fact present. There is evidence that the shallow focus swarm postdates the deep focus swarm. Complementary cone-sheets are associated with these cone-sheets.

Figure 2.21 is a rose diagram of the dyke trends of this episode. A major north west - south east axis trending 310° True is indicated but the width of the base of the peak suggests that two or more sub-swarms may be present. It is calculated that in total these dykes contribute some 0.6% dilation to crustal extension in a north east - south west sense. Two north east - south west trending axes of injection at 030° True and 050° True associated with this episode may be orthogonal subswarms of the north west trending dyke sets. Minor north - south and east - west peaks are also present in Figure 2.21 and may constitute a further orthogonal swarm. The distribution of dykes attributable to this episode do not suggest the presence of a

Figure 2.21

Rose diagram of dyke trend azimuths for 37 dykes of episode 11c, where peak height from the base circle is proportional to the number of dykes per 10° arc (001° - 010° inc., 011° - 020° inc., etc., etc.). All azimuths are measured from True North.

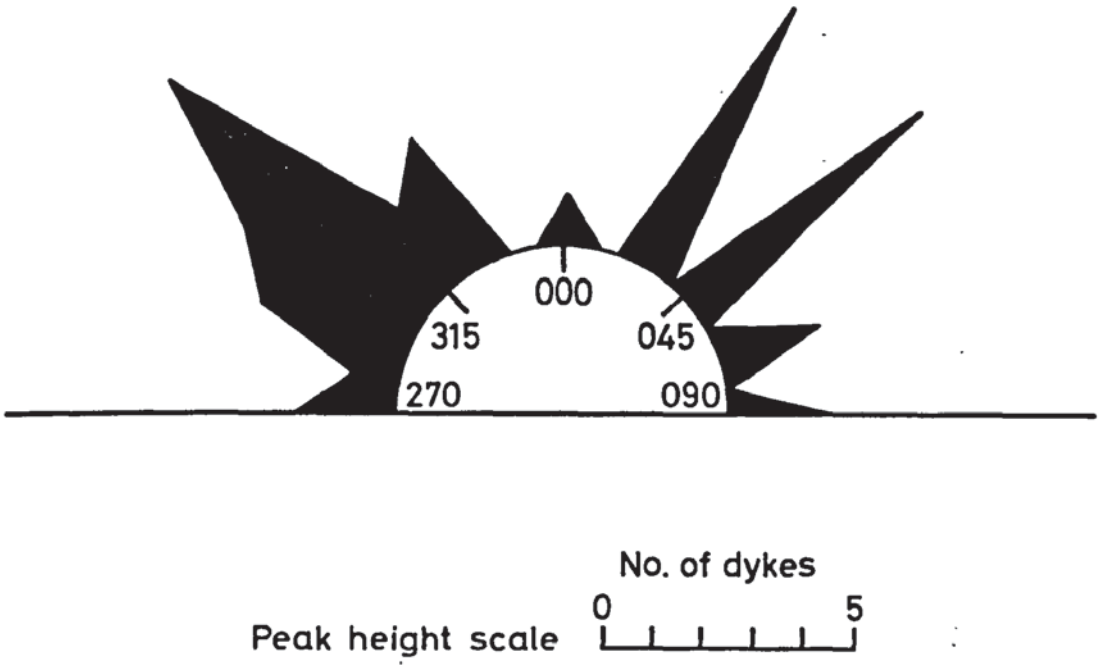

Figure 2.22

Rose diagram of dyke trend azimuths for 73 dykes of episode 11d, where peak height from the base circle is proportional to the number of dykes per 10° (001° - 010° inc., 011° - 020° inc., etc., etc.). All azimuths are measured from True North.

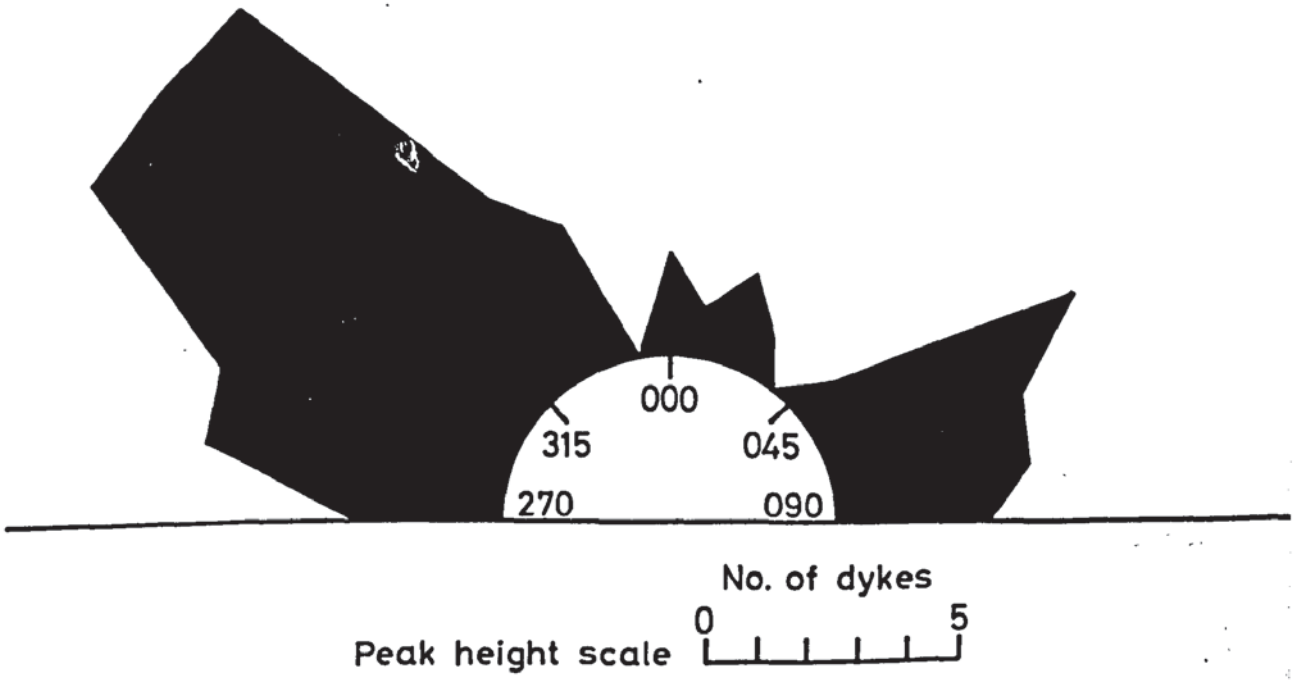

radial swarm in spite of the weak radial pattern of Figure 2.21 d). The transition dolerite and tholeiitic dolerite dykes and cone-sheets of Cycle II also show a complex pattern of injection. They clearly postdate the felsites and alkali dolerites of the cycle, and appear, at least in part, to be later than some of the quartz dolerites and craignurites. Probably there is considerable overlap between "episodes" IIc and IId and a close petrogenetic connection between them.

The cone-sheets of this episode focus at two levels on the focal axis, 1500 and 3000-4000 m. respectively, suggesting that two swarms are again present, the shallower focused swarm postdating the deeper focused swarm. The two swarms together contribute perhaps 65 metres of uplift at the centre of the complex.

Figure 2.22 demonstrates the complex nature of the transition dolerite - tholeiitic dolerite dyke system associated with Cycle II. There is the usual strongly developed north west - south east axis, the peak width suggests that it is composite and consists of two or more separate swarms. These north west dykes account for 0.80% crustal extension at right angles to their trend. There is a strong north east - south west axis trending 060° True, and minor north east - south west axis trending 020° True and 080° True, together with minor north-south and east-west dyke sets.

Close examination of the time relations of this episode indicates the following sequence of events:

1. Injection of north west dykes trending 310 - 330° True.
2. Injection of cone sheets focusing at 3000 - 4000 metres depth.

3. Injection of a second set of north west dykes trending 280° - 310°.
4. Injection of north east - south west dykes trending 240° - 260° True.
5. Injection of cone sheets focusing at 1500 metres depth.
6. Injection of an orthogonal north south - east west conjugate dyke swarm.

It is admitted that this sequence is based on relatively little data, however it does provide a framework.

e). The injection of high alumina gabbro and feldsparphyric dolerite cone sheets and dykes took place at the close of Cycle II. These intrusions are dealt with separately below.

The High Alumina Gabbro, Feldsparphyric Dolerite Cone Sheet Swarm.

The emplacement of high alumina gabbros and feldsparphyric dolerites as cone-sheets and dykes commenced at the close of Cycle II. (episode IIe). Some of the cone-sheets of the swarm are cut by offshoots of granophyre to the east of Slieve Foye. However, intrusive activity of this episode also continued after the injection of the granophyre which some cone-sheets of this type cut at Doolargy (see Map 1), though they are earlier than the other post granophyre intrusions of Cycle III. It is considered that the intrusion of these rocks both immediately preceding and subsequent to the emplacement of the granophyre, constitute a single episode related to the latter event.

Cone-sheet injection dominates this episode (see Table 2.3),

cone-sheets attributed to it constitute about 20% of all cone-sheets in the complex, they also tend to be the most persistant and massive of such intrusions (see Fig. 2.16) with a mean thickness of about 3 metres. It has already been shown that cone-sheets of this swarm focus on an elliptical area, coaxial with the focal axes of the majority of other cone-sheet swarms, at a depth of about 2 km. below sea level (see Fig. 2.15).

A few dykes attributed to this episode are present, plotting their trends as a rose diagram (Fig. 2.23) suggests a radial distribution, however the dykes are so few in number that the presence of a radial dyke swarm cannot be substantiated. A prominant north south dyke of this type (trend 000-010° True) traverses the northern slopes of Carlingford Mountain (see Map 2) and is seen to branch laterally into a series of cone-sheets of the same episode. This dyke is considered to be a radial fracture formed simultaneously with the cone-sheet swarm and acting as a feeder to some of its members.

The high-alumina gabbros are identical in composition and petrology with those of layered gabbros (see below), indeed Traill suggested that the cone sheets were offshoots of the gabbro (1878 p 22). The injection of the dykes and cone-sheets of this episode indicates the influx of a fresh batch of magma of the type which formed the layered gabbro, the coincidence of the incoming of this magma with the emplacement of the granophyre is significant. As noted above Le Bas attributes the forming of the Carlingford granophyre to melting of Silurian sediments by the layered gabbro magma (Le Bas 1967), however a number of intrusive episodes intervene between the

Figure 2.23

Rose diagram of dyke trend azimuths for 12 dykes of episode 11e - 111a, where peak height from the base circle is proportional to the number of dykes per 10° arc (001° - 010° inc., 011° - 020° inc., etc., etc.). All azimuths are measured from True North.

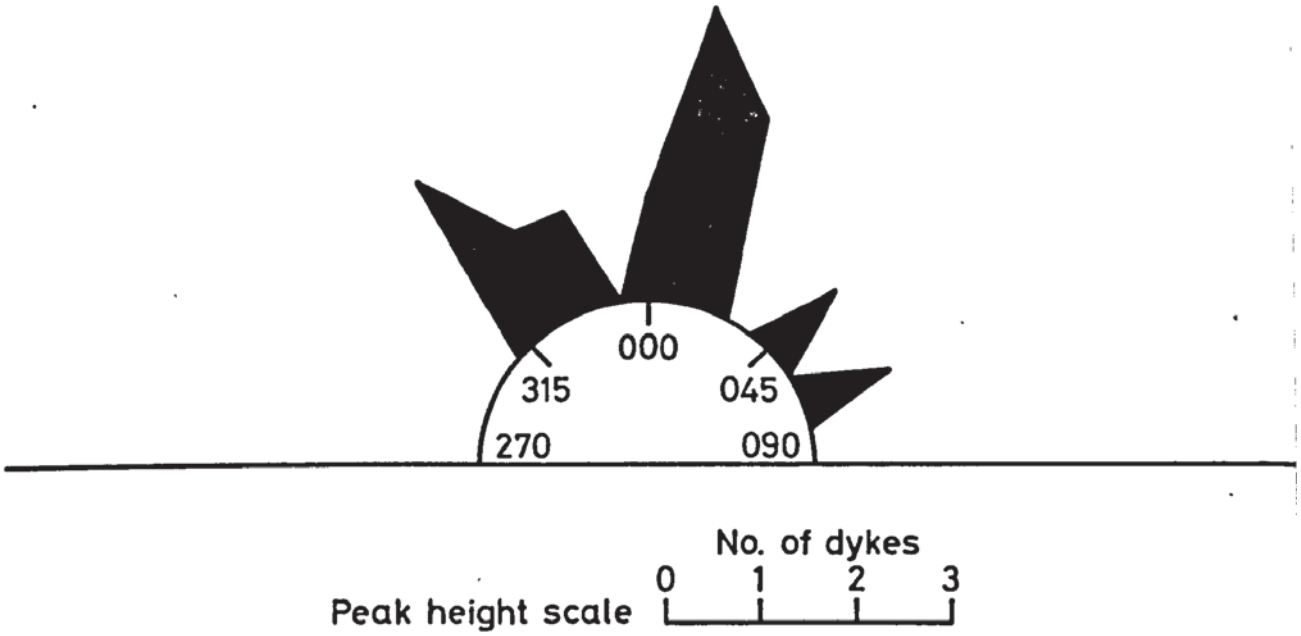

Figure 2.24

Rose diagram of dyke trend azimuths for 16 dykes of episode 111b, where peak height from the base circle is proportional to the number of dykes per 10° arc (001° - 010° inc., 011° - 020° inc., etc., etc.). All azimuths are measured from True North.

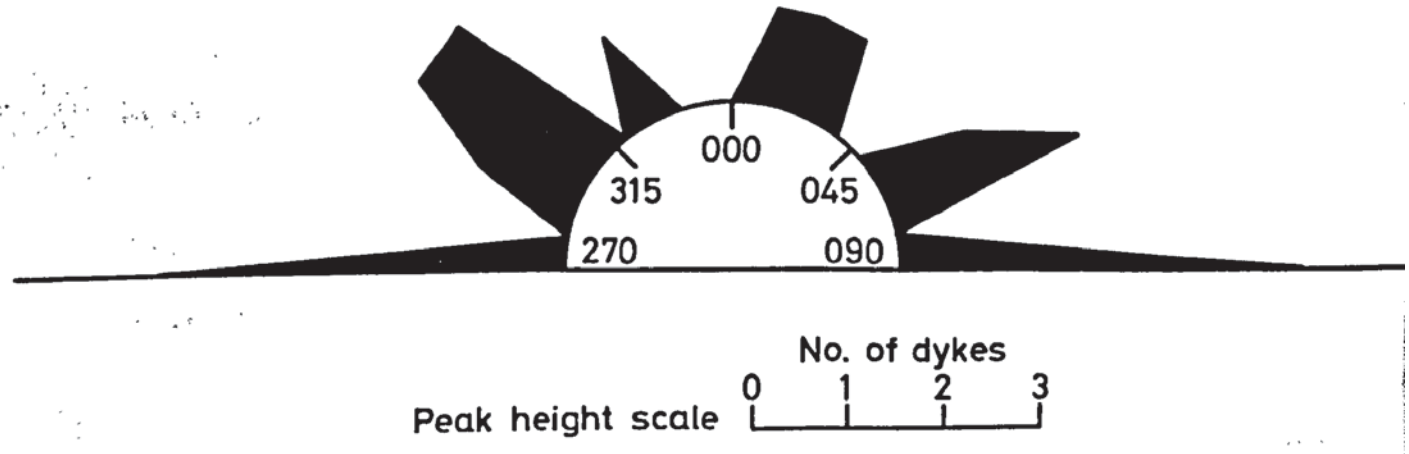

intrusion of the gabbros and the granophyre. It is possible that the emplacement of large masses of the high alumina basalt magma feeding the cone-sheet swarm in question, brought about the crustal melting which gave rise to the granophyre melts.

The Minor Intrusions of Cycle Three.

The minor intrusions of Cycle III were all injected after the emplacement of the Carlingford granophyre.

a). Intrusion of feldsparphyric dolerite cone-sheets (see above).

b). Emplacement of a series of craignurite and quartz-dolerite dykes and cone-sheets. The cone-sheets constitute about half those attributable to Cycle III (Table 2.3), they focus at depths of about 3000 metres below sea level on the focal axis and give about 10 metres total uplift at the centre of the complex.

The dykes of this episode have a radial distribution when their trends are plotted as a rose diagram (Fig. 2.24), a strong east - west trend is also evident. The presence of a radial swarm is confirmed by the distribution of the dykes on Figure 2.25 which shows that a superimposed north west - south east element is present too. The members of the radial dyke swarm focus on the focal axis south of Spellickanee, some of them are cut by cone-sheets of this episode and hence it appears that the radial swarm is somewhat earlier than the cone-sheet swarm, though within the same episode.

c). Following the intrusion of the quartz-dolerites and craignurites of Cycle III a series of transition dolerites and tholeiitic dolerite dykes and cone-sheets were emplaced.

Figure 2.25

Sketch map showing projection of dyke trends and location of cone-sheet focus for episode 111b, (drawn on the reconstructed base map - see Fig. 2.7).

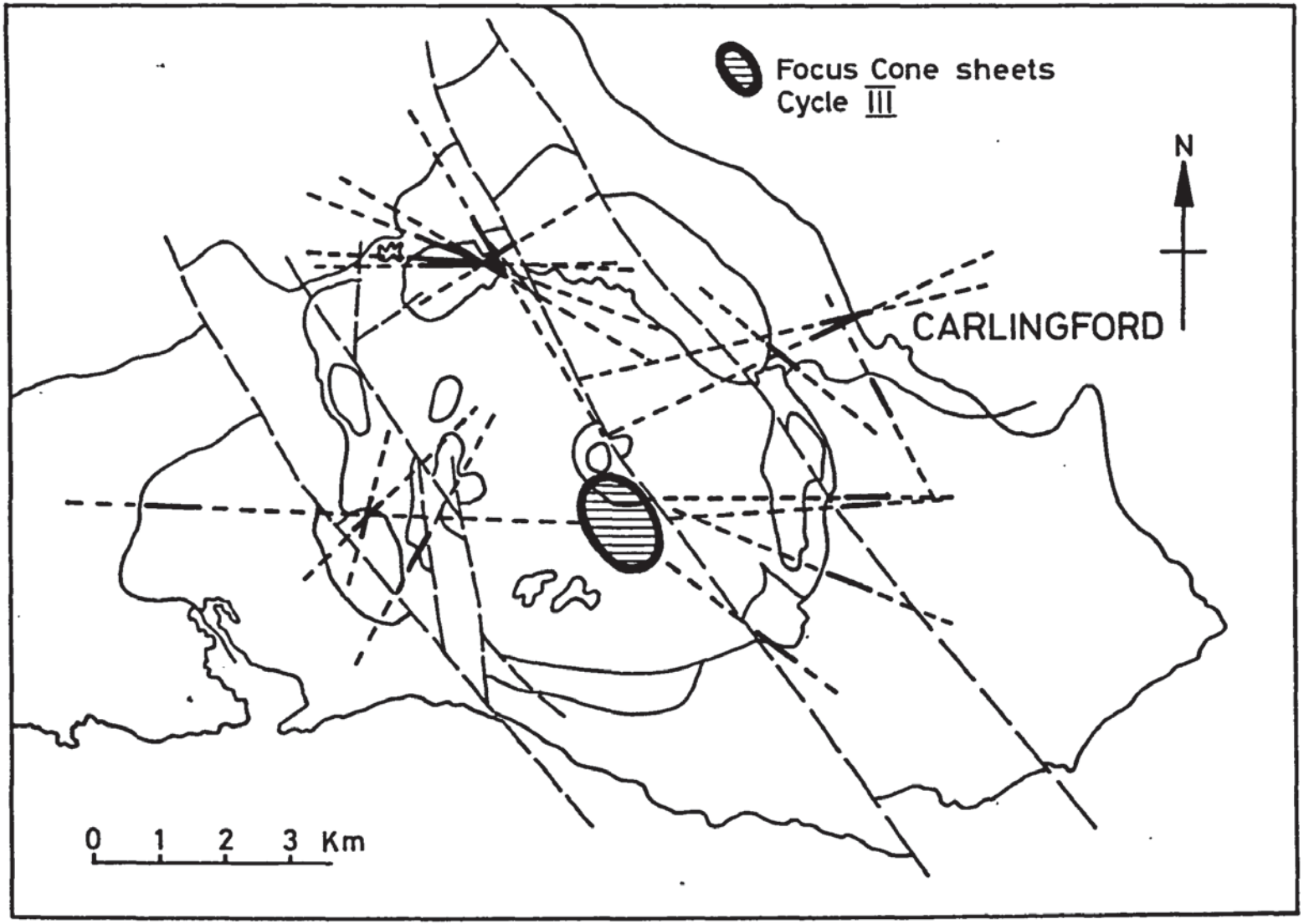

The cone-sheets of IIIC focus at depths of about 3000 metres on the focal axis. Uplift resulting from the injection of this cone-sheet swarm is of the order of 10 metres at the focal axis. Complementary cone-sheets are associated with the swarm.

The majority of tholeiitic dykes are earlier than the cone-sheets, while the transition dolerite dykes all post date them. A rose diagram of the dyke trends (Fig. 2.26) shows a dominant north west - south east axis (trend 320° True), and an orthogonal north east - south west axis (trend 050° True). Minor axes at 090°, 280°, and 300° are of uncertain significance. The north west - south east elements of this swarm are calculated to have contributed about 0.25% dilation to north east - south west crustal extension.

d). Postdating all other intrusions in the complex are a series of alkali olivine dolerite dykes readily identified by their marked spheroidal weathering in the field. They form an orthogonal conjugate swarm largely tangential to the complex (Fig. 2.27) but including an axial north west- south east element. The principal axes trend 300 - 330° True and 220 - 230° True (Fig. 2.28) and are thus coincident with those of episode IIIC above suggesting that the dykes of the two episodes were injected under a similar stress regime, a horizontal tension directed approximately north-south across the complex (see above).

The Occurrence of Xenoliths Within the Minor Intrusions.

Xenoliths occur in many of the Carlingford minor intrusions; they range in size from a few millimetres to more than a metre in

Figure 2.26

Rose diagram of dyke trend azimuths for 24 dykes of episode 111c, where peak height from the base circle is proportional to the number of dykes per 10° arc (001° - 010° inc., 001° - 020° inc., etc., etc.). All azimuths are measured from True North.

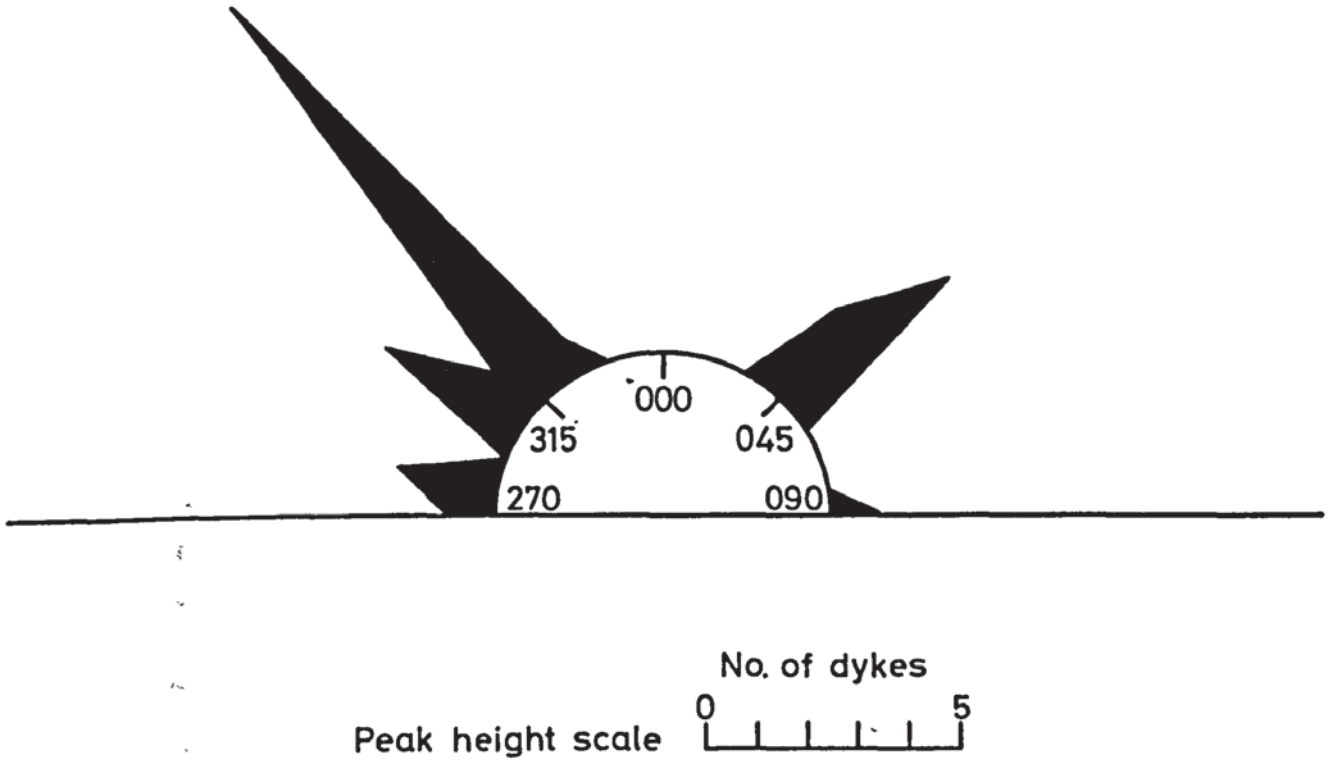

Figure 2.27

Sketch map showing projection of dyke trends for episode 111e (drawn on the reconstructed base map - Fig. 2.7).

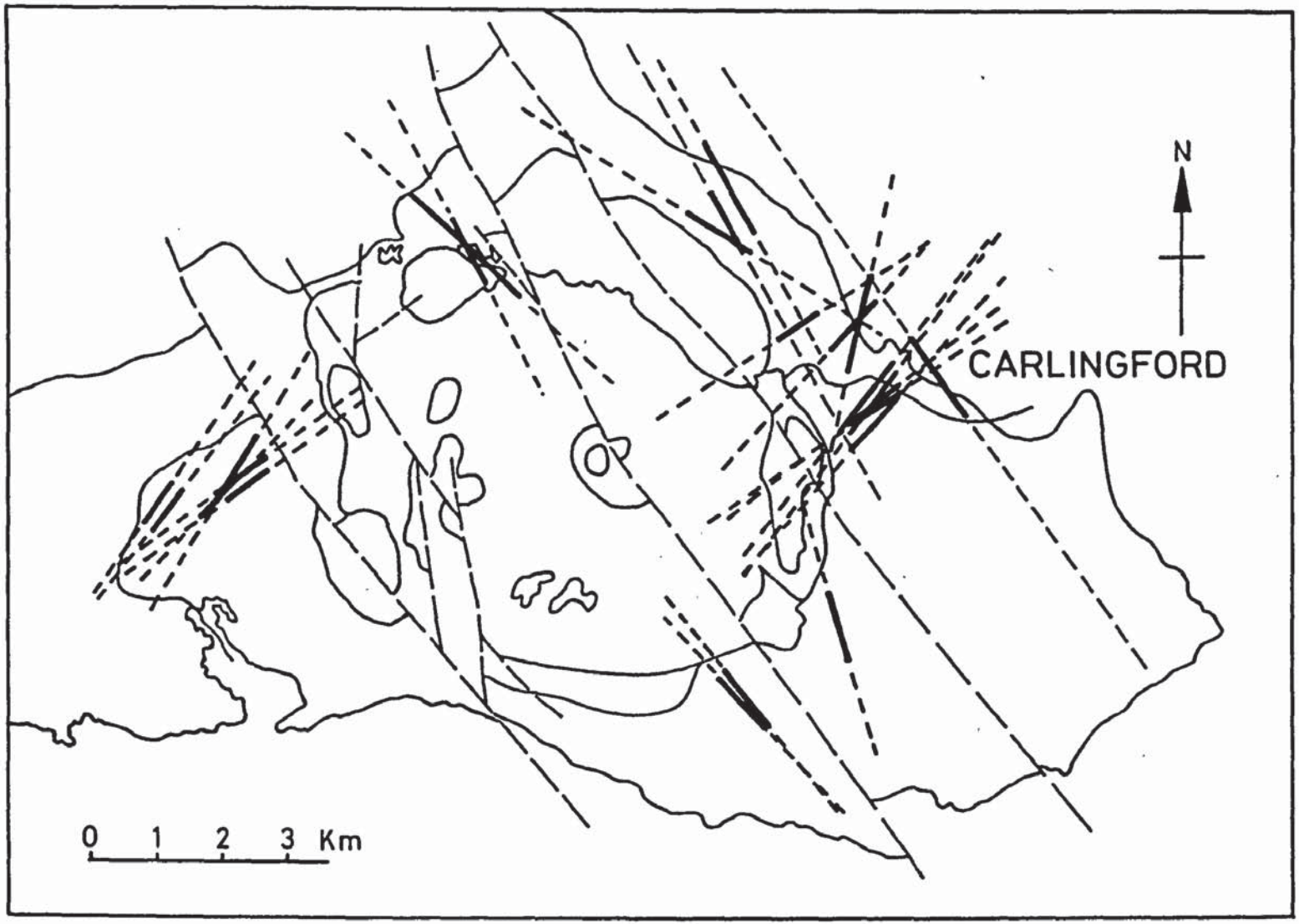

Figure 2.28

Rose diagram of dyke trend azimuths for 24 dykes of episode 111d, where peak height from the base circle is proportional to the number of dykes per 10° arc (001° - 010° inc., 011° - 020° inc., etc., etc.). All azimuths are measured from True North.

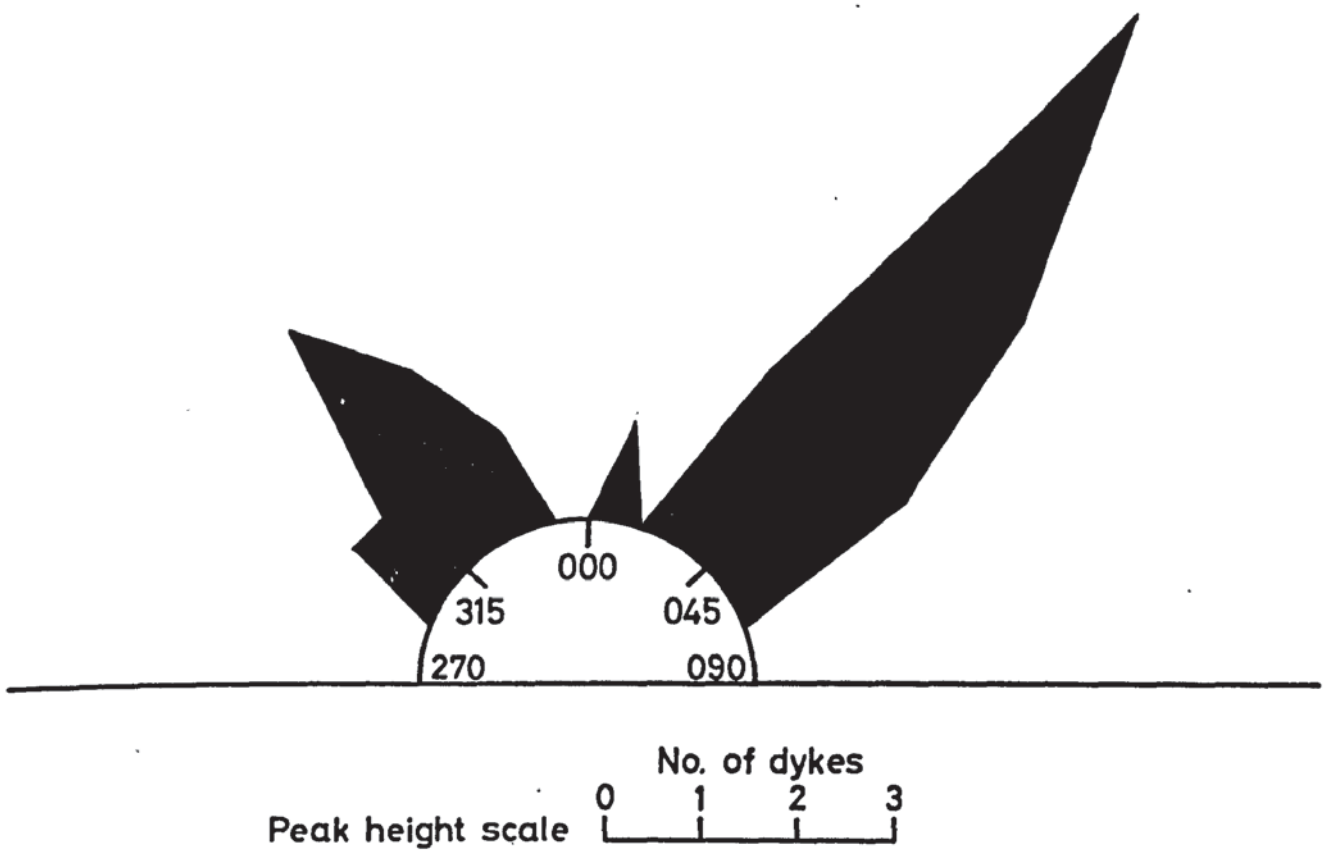

diameter. Gabbro of a type petrologically and petrochemically identical with the layered gabbro is the most abundant rock type occurring as such. A particularly large gabbro xenolith about 2 metres in diameter occurs in a craignurite cone-sheet cropping out in the railway cutting about 200 metres north west of Carlingford town. The larger masses are usually well rounded, and some show corrosion and assimilation by their host. Also present in both dykes and cone-sheets are fragments of olivine-dolerite, quartz-dolerite, craignurite and hornfelsed sediment together with occasional fragments of felsite and granophyre. Thus the same suite of rocks is present as xenoliths in minor intrusions, as occurs in the agglomerates of Annaloughan and Slievenaglogh (Le Bas 1955) though not in the same proportions. Such included xenoliths provide a random sample of the rock types occurring at depth within the complex. The abundance of gabbro fragments and particularly their occurrence in minor intrusions outside and below the present outcrop of the layered gabbros (Fig 2.29) indicates the presence of large buried masses of this rock type within the complex, as they could not be derived from the lopolith itself.

C. THE SUBSTRUCTURE OF THE COMPLEX

The intense system of minor intrusions at Carlingford consists, of a series of superimposed dyke and cone-sheet swarms reflecting the complex igneous substructure at depth within the centre. The type of minor intrusions injected at any moment in time within the complex reflected stress the patterns acting on it at that time.

A variety of magma types were available at different times within

Figure 2.29

Sketch map of the Carlingford Complex showing the distribution of xenoliths of gabbro and hornfelsed Silurian sediments. Sample numbers are indicated where collected.

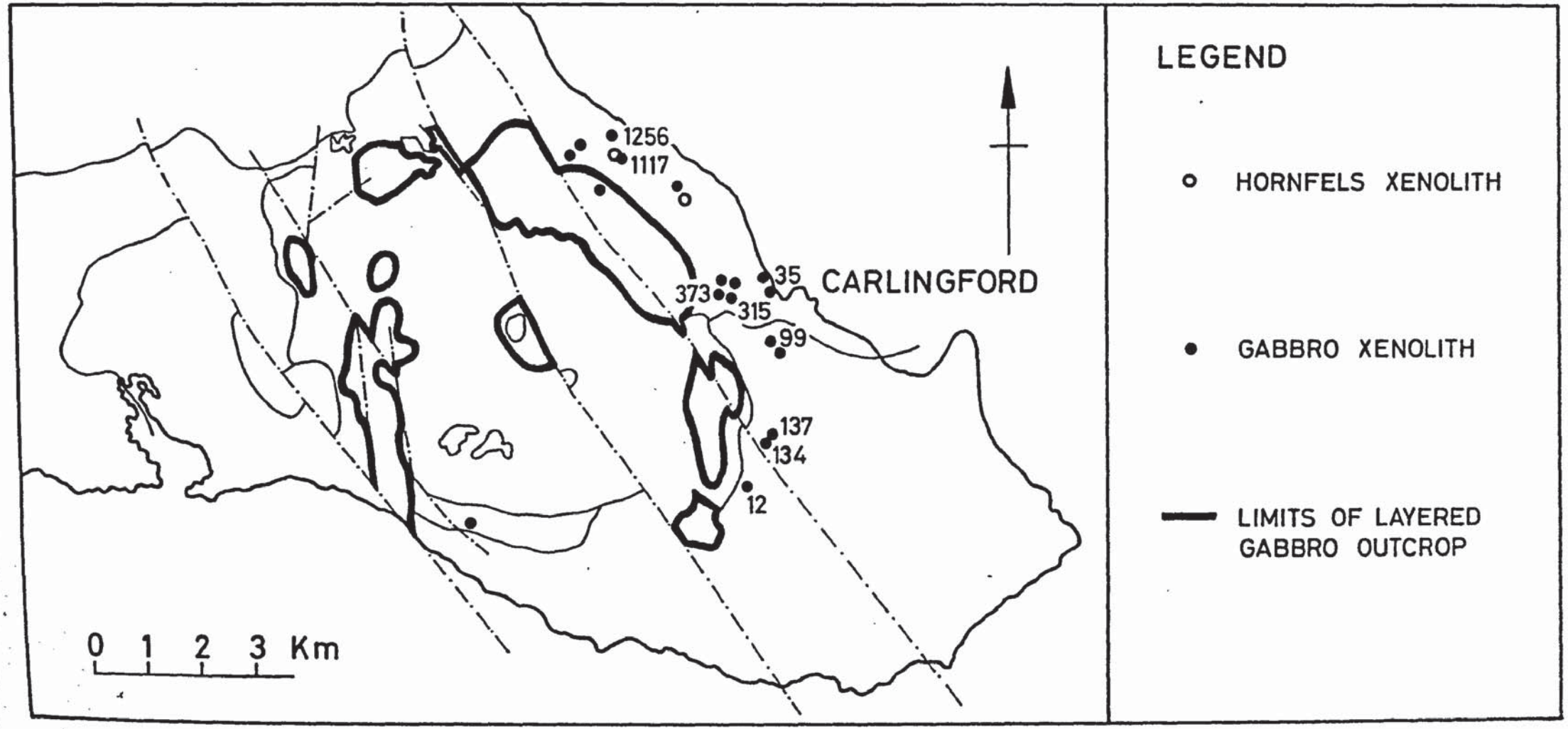

the complex, many appearing repeatedly in cycles. The majority of cone-sheet swarms focus coaxially on a focal axis about 1 km. south of Spellickanee, however they do not all focus at the same depth. It seems that magma was repeatedly injected into the complex from below, each new magma batches giving rise to a series of derivatives. The conventional hypothesis that a "magma chamber" was repeatedly replenished is unacceptable as such,as it is clear from the abundant xenoliths present in many of the minor intrusions that earlier magma batches had cooled by the arrival of succeeding pulses; and moreover,that the source-depth of cone-sheet swarms varied. It is proposed that each fresh batch of magma injected into the complex was emplaced diapirically and rose along similar pathways through earlier batches, then cooled, intruding them as well as the surrounding country rock. Thus the substructure of the complex would consist of a series of diapiric plugs of basaltic rock.

The sequence of intrusive events within the cycles, and particularly during "Cycle II", suggests that on the arrival of each magma batch, intrusive activity took place in the following order:

1) North west - south east dykes.
2) Cone sheets and/or radial dykes.
3) Complementary cone-sheets.
4) North east - south west dykes, or conjugate or tangential dyke swarms.

Thus emplacement commenced under a north east - south west regional tensional stress regime, subsequently the intrusive style became dominated by stresses generated by magma pressure within the centre

Figure 2.30

Geological map of the North of Ireland showing the distribution of pre Tertiary rocks, the Tertiary lavas, intrusive centres and dyke swarms (after Emeleus and Preston 1969, Fig. 1, ps. 36 - 37). Note particularly the strong Carlingford - Donegal dyke swarm.

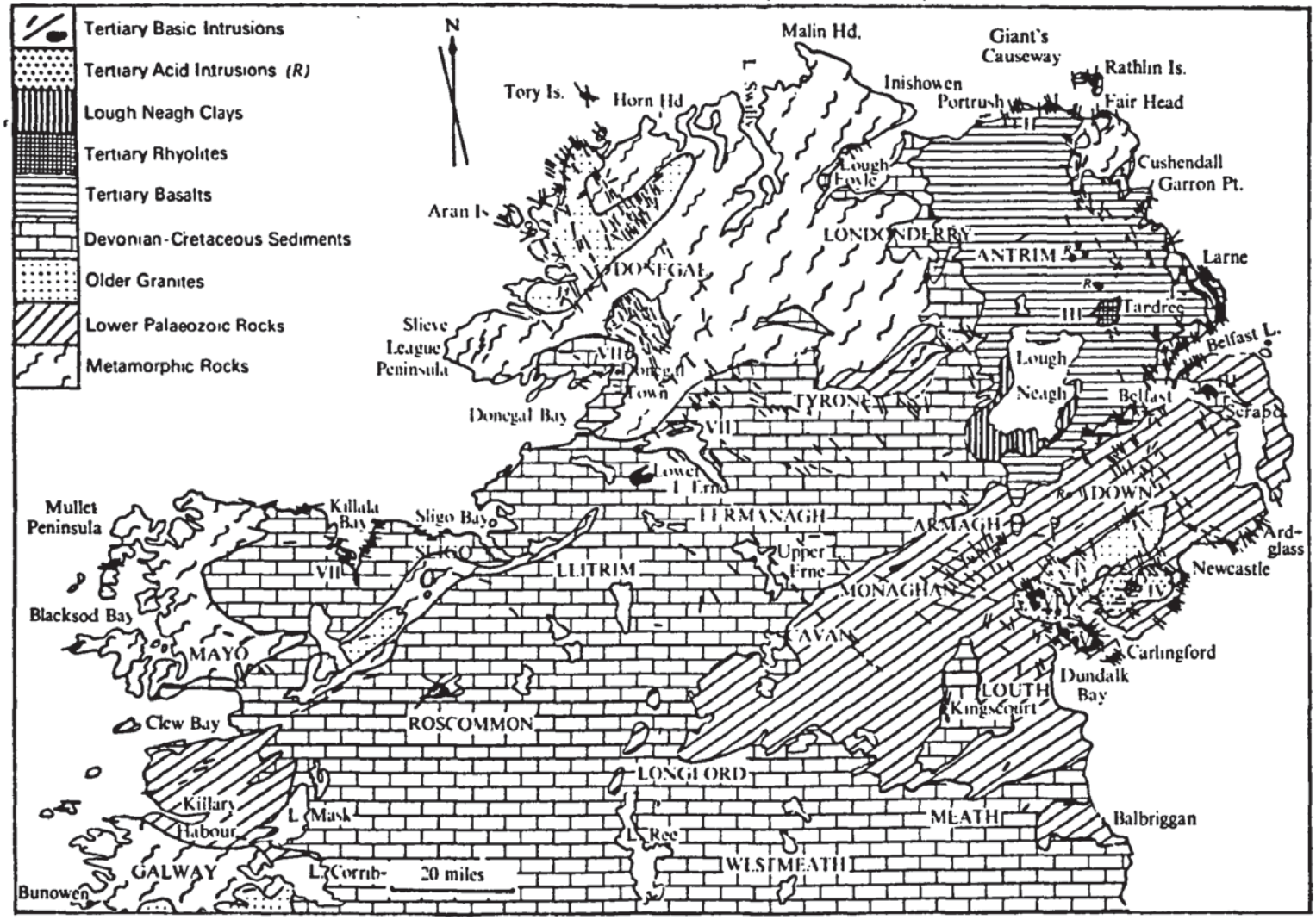

and finally by north - south or north west - south east tensional stress acting on the complex. It is significant that members of the craignuritic suite and the high alumina gabbro feldsparphyric dolerite suite occur most commonly in cone-sheets and radial dykes both of which types of structure focus on a restricted central magma source. Alkali dolerites occur almost exclusively in north west - south east dykes and conjugate north east - south west dykes or tangential swarms which were developed when the complex was subjected to directed stress, probably as a result of regional stress patterns. *

North west - south east trending dykes occur as intermittent swarms lying on the Carlingford - Slieve Gullion axis in Armagh, Tyrone and Donegal as shown in Fig. 2.30 (Emeleus and Preston 1969 Fig. 1 p36). Skelhorn et al. suggest that such regional dyke "swarms" arise from the crests of elongate ridges of magma at depth (1971). It is proposed that batches of magma rose along such north west - south east ridges running through Carlingford and Slieve Gullion where two coalescent culminations developed. Such ridges have the form of narrow elongate hogsbacks with steeply inclined flanks extending downwards as a wall to the mantle, and upwards through the crust as north west - south east dykes (see Fig. 2.31). The individual ridges combine to form a multiple mega-ridge structure. After the initial injection of a magma batch within a ridge, further intrusive activity became concentrated at culminations on the ridge crest forming cupolas which may have risen diapirically to higher levels in the crust. Within such cupolas the magma gave rise to derivative liquids by processes of fractionation, assimilation or partical melting.

* NOTE: SUGGESTS THAT THE ALKALI DOLERITE MAGMA ORIGINATES AT MORE FUNDAMENTAL DEPTHS THAN THE HIGH ALUMINA BASALT AND CRAIGNURITE MAGMAS.

Figure 2.31

Block diagram of the lithosphere beneath the North of Ireland, showing ridges of basaltic magma extending upwards from the Moho.

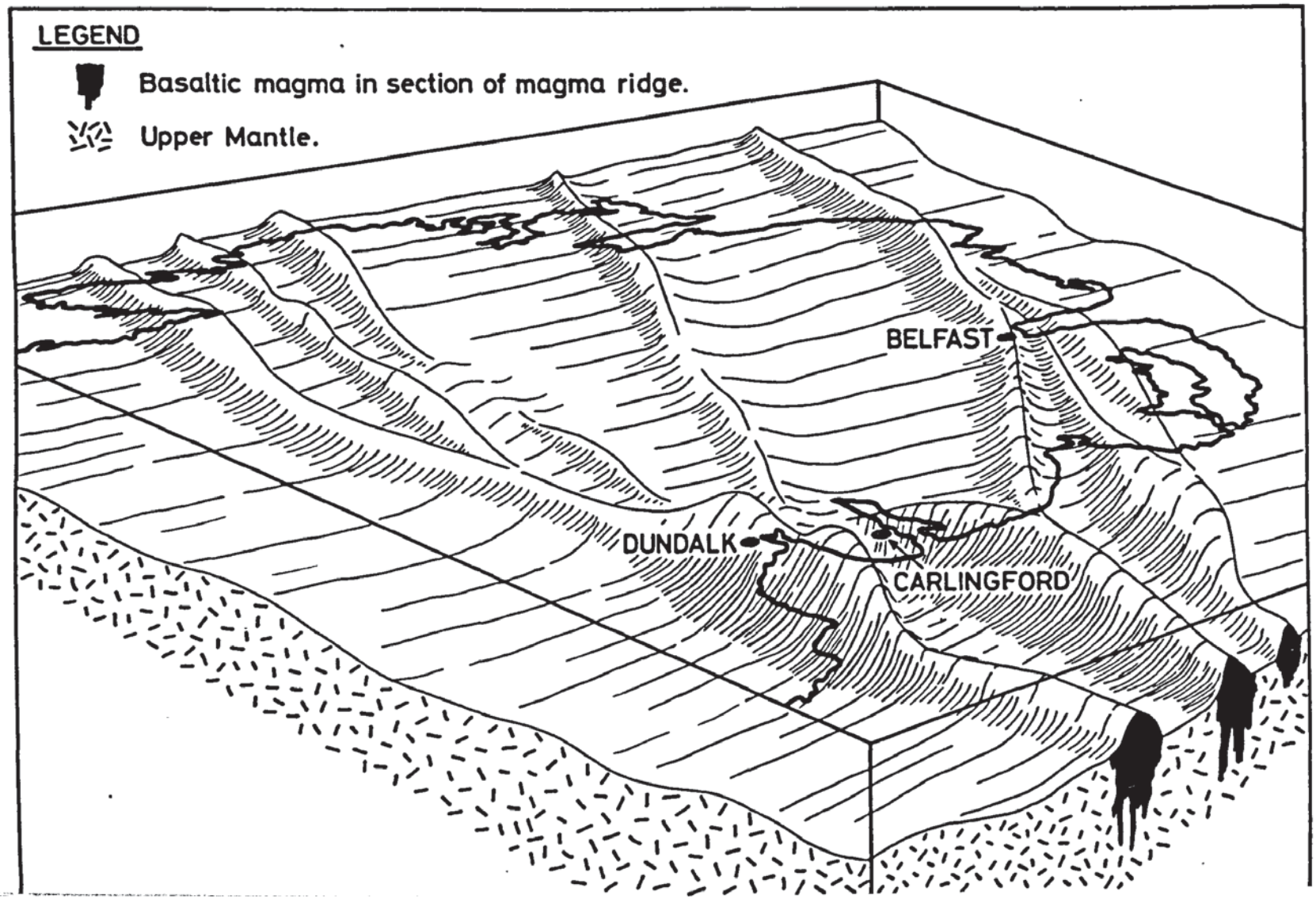

Cupolas rising to a few kilometres below present levels of erosion gave rise to cone-sheet and radial dyke swarms.

Domes rising to higher levels on finding suitable horizontal planes of weakness such as the Tertiary unconformity, gave rise to sills or lopoliths such as the layered gabbros of Carlingford and Slieve Gullion (note; Le Bas suggests that the gabbros of the north west belt of Slieve Gullion are remnants of a gabbro lopolith, possibly continuous with that of Carlingford rather than metamorphosed lavas as suggested by Reynolds (Le Bas 1960, Reynolds 1951)). Cupolas, or dykes emerging from them or direct from the parent ridge crest would act as lava feeders on reaching the surface; the Trumpet Hill, Drumenagh Hill plug may be a cupola which rose sufficiently high to become such a lava feeder. The build up of high volatile pressures within a cupola penetrating to high levelsgave rise to explosive volcanism at the surface.

It is envisaged that cupolas would be of the order of 1.5 to 3 km. in plan length by 1 to 2 km. in width (north west - south east and north east - south west respectively) at their summits. Sufficiently large batches of basic magma could give rise to acid magmas by crustal melting (Jaeger 1964) which in turn could be emplaced as cone-sheets and radial dykes focusing on the source plug, or granophyre diapirs if sufficiently voluminous.

The ridge - cupola/plug hypothesis proposed above predicts the presence of large masses of basaltic rock beneath the Carlingford Complex. A gravity survey by Cook and Murphy confirms the presence of such a basic mass running beneath both Carlingford and Slieve Gullion

and which, they propose, has the form of a horizontal cylinder or ridge running north west - south east (Cook and Murphy 1952). The dimensions of this mass - maximum width 8 km., depth of upper surface about 2.5 km. below sea level, length about 30km., are in keeping with the proportions of the culmination on a multiple magma ridge proposed above.

The presence of buried masses of basic rock with proportions of the order of those envisaged for the proposed structure is confirmed by the I.G.S. aeromagnetic survey of Great Britain and Northern Ireland (Bullerwell 1964), which shows an intense magnetic anomaly in the Carlingford - Slieve Gullion area. Peaks in excess of 350 gammas intensity at the centres of the complexes are separated by a low, suggesting that the form of this buried structure is a hogsback with steep flanks rising to two cupolas, one beneath each centre, as predicted.

The north west - south east trend of the parent magma ridges not only on the Carlingford Slieve Gullion axis,but throughout the British Tertiary Province, indicates that their emplacement was controlled by regional stress patterns operative throughout the area. The trend of the tear faults which traverse Carlingford is approximately coincident with that of the proposed magma ridges, suggesting a genetic relationship between them. It is possible that while basaltic magma was available, fracturing of the crust gave rise to the ridges, but subsequently,when the source of the magma dried up,that tear faulting developed in response to the continuing stress regime. The opening of the Atlantic, which is believed by some authors to have been

taking place at this time (Evans, Fitch and Miller 1973 p436) may have provided the necessary crustal stress.

SUMMARY

The development of the Carlingford Igneous Complex is illustrated by Figure 2.32 and may be summarized as follows:

1. Injection of a north west - south east ridge of magma giving rise to plug-like culminations and dykes, possibly feeding lava flows.

2. Development of centralized intrusive activity (cone-sheets) about culminations on the magma ridge, followed by injection of north east - south west dykes as a result of north west - south east tension (Cycle I).

3. Injection of large masses of high-alumina basalt magma feeding the layered gabbro lopolith at the base of the lava pile. Resulting melting of crustal sediments gave rise to acid magma intruded as radial dykes and cone-sheets (episode IIa).

4. Injection of alkali basalt magma as a north west - south east ridge feeding alkali dolerite dykes (episode IIb).

5. Injection of further batches of basaltic magma in ridges culminating in cupolas, giving rise to north west dykes and subsequently cone-sheets and other dyke swarms, together with explosive volcanism at the surface (the latter may alternatively be attributed to 3 above).

6. Injection of a large mass of high-alumina basalt magma which gave rise to a cone-sheet swarm. (episode IIe and IIIa).

7. Crustal melting resulting from 6 above gave rise to granitic melts which rose diapirically to form the Carlingford granophyre (note -

Figure 2.32

Diagrammatic vertical sections of the Carlingford Complex showing its development through time, see text for discussion.

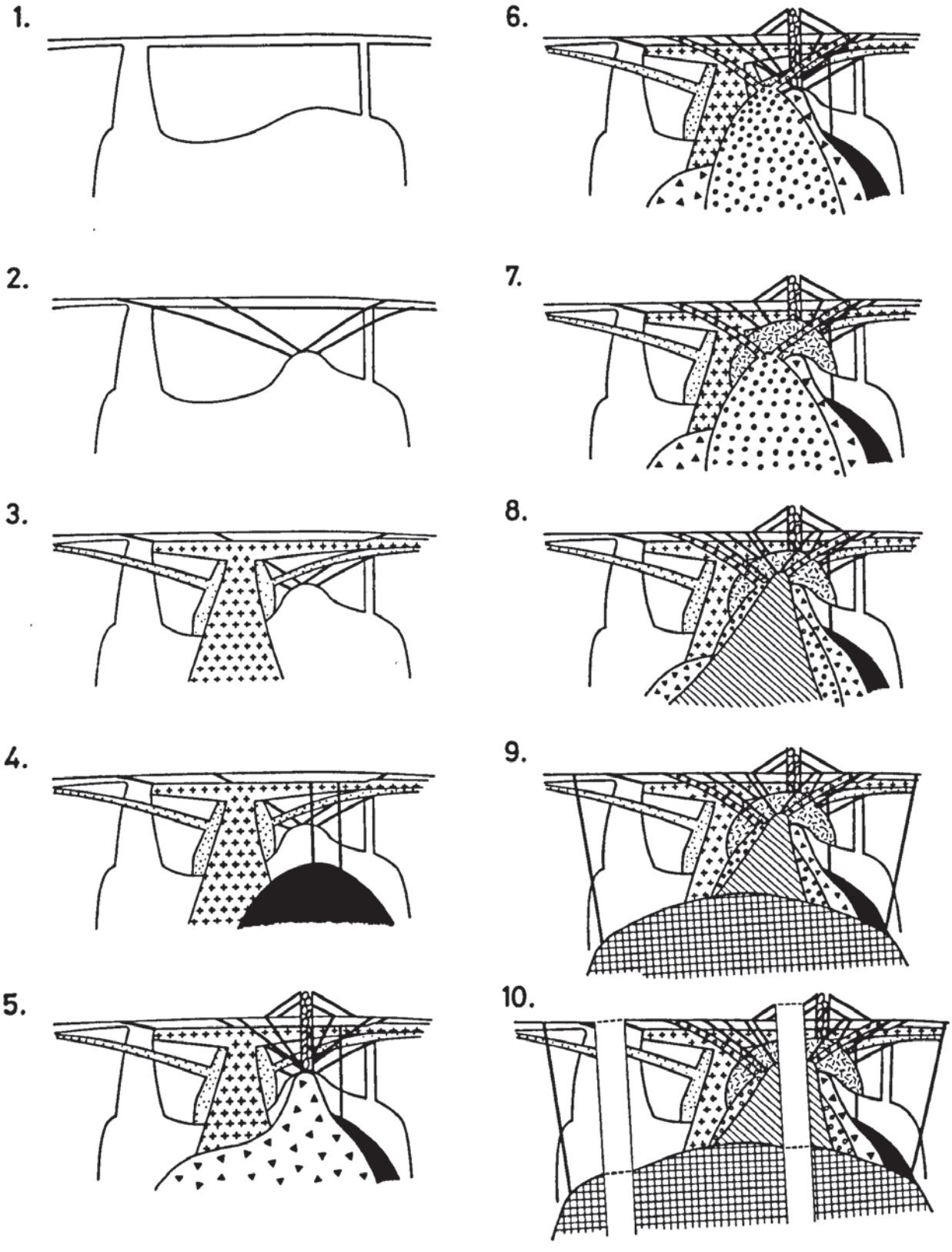

there is some overlap with 6).

8. Injection of a batch, or batches, of basaltic magma in ridges giving north west - south east dykes and culminating in cupolas from which cone-sheets and radial dykes emerged. Subsequently, as a result of north - south tension across the complex, a conjugate dyke swarm developed(episodes IIIb and c).

9. Injection of tangential dyke swarm of alkali dolerite (episode IIId).

10. North west - south east dextral tear faulting.

Intrusive activity within the complex was almost continuous, and took place against a background of frequent changes in the regional stress regime which was dominated by stress patterns giving rise to regional north west - south east trending structures. Repeated injection of large diapiric masses of basic magma beneath the centre, built up a complex composite substructure, with the overall form of a massive hogsback of basaltic rock. The form of individual intrusions and swarms was determined by the size and form of the feeding diapir and the nature of the regional stress pattern at the time of their intrusion.

CHAPTER 3.

THE CLASSIFICATION OF THE TERTIARY IGNEOUS ROCKS OF CARLINGFORD

Abstract.

The igneous rocks of the Carlingford Complex have been classified petrographically. A petrochemical classification is erected on the basis of the petrographic scheme. It shows that the majority of rocks in the complex can be attributed to one of three series, the alkali basalt series, the high alumina basalt series and the tholeiitic basalt - craignurite series. A number of acid rock types can only be identified on the basis of petrography without further petrochemical investigation. Members of the alkali basalt series may be identified most reliably by petrographic studies. The craignurites of Hebridean literature are established as an important rock group in their own right; they have low $Na_2O:K_2O$ ratios which distinguish them from the icelandites and similar rocks, and with the tholeiitic dolerites, form the tholeiitic basalt - craignurite series.

Introduction.

The rocks occurring in the minor intrusions of the Carlingford Complex have been classified on a petrological basis as outlined in Chapter 1, a scheme adopted in Chapter 2. This petrological classification is summarised below. It is based largely on the classic

studies of Hebridean petrology by Harker (1904, 1908), Anderson and Radley (1917), Bailey et al.(1924), Tyrrell (1928) and Richey and Thomas (1930) and on more recent investigations of Hawaiian petrology (Macdonald and Katsura 1964) and Japanese rocks (Kuno et al 1957, Kuno 1959). The petrology of basaltic rocks was reviewed recently by Wilkinson (1968) who cites the contributions of Holmes and Harwood (1929), Kennedy (1933), Tilley (1950), Wilkinson (1956) and Yoder and Tilley (1962) in addition to these quoted above.

In order to investigate the petrochemistry and petrochemical behaviour of rocks in the Carlingford suite it was necessary to establish a rigorous classification based on the petrographic scheme but defined in petrochemical terms. A number of classification schemes have appeared recently, noteably those of Streckeissen (1965, 1967), Irvine and Baragar (1971) and Middlemost (1972). The schemes presented by Irvine and Baragar and Middlemost draw upon many recent contributions to petrology and petrochemistry, including the classifications of basaltic rocks erected by Yoder and Tilley (1962), Poldevaart (1964) and Green (1969, 1970) and the work of Macdonald (1960, 1968), Baker et al (1964) and Carmichael (1964).

The classification scheme adopted herein is set out in detail below, it is based on the scheme proposed by Middlemost (1972) with contributions from that of Irvine and Baragar (1971) combined and amended in the light of Hebridean petrology and petrochemistry, and that of Carlingford in particular. It is unfortunate that both Middlemost and Irvine and Baragar largely ignore the earlier work on Hebridean intermediate rocks (Anderson and Radley 1917, Bailey

et al 1924, Richey and Thomas 1930, Tomkeieff and Marshall 1935) and as a result an important rock group, the craignuritic series, is omitted from their classifications, that omission is corrected below.

PETROLOGICAL CLASSIFICATION

The petrological classification on which the petrochemical classification is based is as follows:-

Alkali dolerite series.

Olivine is invariably present, usually in the groundmass, and shows no reaction relationship with pyroxene (Tilley 1950, Kuno et al. 1957). The only pyroxene present is a calcic clinopyroxene usually lilac/pink titanaugite (Bailey et al. 1924 p14, Macdonald and Katsura 1964 p 92). Interstitial phases are chlorite or feldspathoid (Bailey et al. 1924 p 14) or alkali feldspar (Macdonald and Katsura 1964 p 92). Alkaline rocks with groundmass plagioclase compositions more calcic than An_{50} are alkali dolerites, except when modal olivine exceeds 25%, when they are alkali picrites (Drever and Johnson 1958, Flett 1930, Wilkinson 1968 p 189). Alkaline rocks with andesine as the groundmass plagioclase are referred to as "hawaiitic" and those with oligoclase "mugearitic" (Harker 1904 p 264, Bailey et al. 1924 p 143, Macdonald 1957, 1960). Generally speaking the dolerites and picrites have basaltic textures while mugearitic and hawaiitic varieties are trachytic.

Tholeiitic dolerites and Quartz dolerites.

"Tholeiities", in general, are defined as consisting of augite

or subcalcic augite, plagioclase near An_{50} in composition and iron oxides (Yoder and Tilley 1962 p 353). Though orthopyroxene and pigeonite are often present in rocks of tholeiitic affinities elsewhere (Kuno 1950, Wilkinson 1968) they have not been recognised in the Carlingford "tholeiites" and are rare in similar rocks elsewhere in the Hebrides (Holland and Brown 1972 p 142).

Hebridean tholeiitic dolerites characteristically have brown glass, a quartzo feldspathic mesostasis or quartz as interstitial phases (Bailey et al. 1924 pp 280, 303). Two types of tholeiitic dolerites are recognised at Carlingford. Those containing modal olivine and only minor proportions of mesostasis or quartz are referred to as "Tholeiitic dolerites" in the text and are equivalent to the Salen Type of the Mull Memoir (Bailey et al. 1924 p 285). Dolerites containing no olivine and conspicuous free quartz or mesostasis are referred to as "Quartz dolerites", a term well established in Hebridean literature and equivalent to the Talaidh Type of Mull (Bailey et al. 1924 p 284). Basaltic and variolitic textures are typical of rocks in these categories, the pyroxenes of the tholeiitic dolerites tending to be subophitic, those of the quartz dolerites prismatic.

Transition dolerites and picrites.

The petrological characteristics of the transition dolerites and related picrites are intermediate between those of the alkali dolerites and those of the tholeiitic dolerites. Olivine is usually present in the groundmass and in the picrites exceeds 25%

in the mode, hypersthene and pigeonite are absent as are interstitial glass, quartz, quartzo feldspathic mesostasis, alkali feldspar or feldspathoid. The clinopyroxene is not apparently titaniferous, while groundmass plagioclase is relatively basic. Textures are typically ophitic. The transition dolerites grade into tholeiitic dolerites with the appearence of an interstitial siliceous phase.

High alumina gabbros and feldsparphyric dolerites.

Rocks in this group are characterised by abundant basic plagioclase in the mode (over 50%). In the feldsparphyric dolerites much of this plagioclase occurs as large equant phenocrysts, the remainder of the rock being composed of a doleritic matrix. The high alumina gabbros consist of plagioclase and subordinate clinopyroxene with a gabbroic texture. Olivine is often present, but ore is usually only a minor constituent. These rocks are petrologically identical to the Porphyritic Central Magma Type of Mull (Bailey et al. 1924 p 23-25) and the gabbros with those of the Carlingford lopolith (Le Bas 1960).

Craignurite - craignuritic felsite series.

Rocks of craignuritic affinity have been described in detail from Mull (Anderson and Radley 1917, Bailey et al. 1924) and elsewhere in the Hebridean Province (Richey and Thomas 1930, Tomkeieff and Marshall 1935). They are characterised by prismatic pyroxene and lathes of oligoclase or andesine (often skeletal) set in a quartzo feldspathic or glassy residuum (Bailey et al. 1924 p 227), they are thus tholeiitic in character and with increasing An content

in the plagioclases and decreasing proportions of the acid residuum grade into quartz dolerites. Craignurites, which are predominantly composed of a fine grained quartzo feldspathic or glassy matrix, are referred to as "craignuritic felsites", if aphyric they correspond to leidleites, and if porphyritic to inninmorites (Bailey et al. 1924 p 281 - 284). Rocks of this suite are referred to in general terms as "andesites" by Tomkeieff and Marshall(1935 p 262).

Rhyolites, felsites and quartz-porphyries.

Rocks consisting entirely of a groundmass of quartz and alkali feldspar are referred to as "rhyolites". With the incoming of plagioclase and pyroxene the rhyolites grade into the craignuritic felsites. Rhyolitic rocks with abundant quartz and feldspar phenocrysts are described as "quartz-feldspar-porphyries". Other acid rock types are referred to in general terms as "felsites", a group consisting of a matrix of feldspar quartz and mica, with phenocrysts of plagioclase and biotite, are identified as "biotite felsites".

Lamprophyres.

Other rock types, possibly of Tertiary age, include vogesitic and spessartitic lamprophyres consisting of hornblende phenocrysts embedded in a feldspathic matrix.

CHEMICAL CLASSIFICATION

Processing the analytical data.

Whole rock analyses of members of the Carlingford suite are

tabulated in Appendices II, III, IV and V according to type, additional analyses are presented in Apendix XV. CIPW norms of these rocks are utilised in this and subsequent chapters, they are tabulated in Appendices VI, VII, VIII and IX (analyses in Appendix XV have not been normed) and were calculated by using a routine incorporated in the computer programme "Petrographic Calculation Package" compiled at Reading University by Dr. G.A.R. Till.

The alkaline rocks of Carlingford exhibit variable and relatively high loss on ignition values, which include high CO_2 values where determined. As both CO_2 and loss on ignition levels are not consistant in rocks of the same type and CO_2 determinations are not available for all rocks in the alkaline suite, it was decided to recalculate all analyses to 100% without volatiles. These recalculated analyses are listed alongside the original determinations in Appendix II, they were used for all normative calculations. The resulting removal of CO_2 leaves excess CaO in the analyses, though much of the carbonate present is siderite (further reason for excluding CO_2 as $FeCO_3$ does not appear in the CIPW norm system), hence normative values for minerals bearing CaO must be considered artificially high.

Not only are the alkaline rocks of Carlingford hydrated and carbonated, they also have relatively high Fe_2O_3: FeO ratios indicating oxidation, a problem which has been noted in other alkaline suites (Kuno 1968 p 662, Irvine and Baragar 1971 p 531). To a lesser extent the same phenomenon is true of some of the tholeiitic rocks in the Carlingford series. As a result of oxidation

magnetite values in the norm are enhanced such that the rock appears more saturated than is appropriate (Muir and Tilley 1957 p 251). This phenomenon, together with hydration and serpentinization, can give rise to the appearance of quartz in the norm of an alkaline rock (Tilley and Muir 1962 p 210, Le Bas 1965a p 94). Coombs (1963) attempted to overcome this problem by reducing Fe_2O_3 values to an arbitrary 1.5% in all basaltic analyses and recalculating the remaining Fe_2O_3 (if any) as FeO, subsequently Chayes chose to select only those analyses with Fe_2O_3: FeO ratios less than 0.6, for incorporation in normative plots (Chayes 1966). Recently Irvine and Baragar, noting the similar behaviour of Fe_2O_3 and TiO_2 in fresh rocks, recalculated Fe_2O_3 in analyses in which it exceeded % TiO_2 + 1.5% to that level in order to obviate the problem (1971 p 526). The latter convention has been adopted herein for all Carlingford rocks in order to standardise treatment, the resulting magnetite values in the norms thus determined, compare favourably with modal concentrations allowing for the observed extent of ulvospinel solid solution (see below). As noted by Irvine and Baragar, this upper limit for Fe_2O_3 values may not be sufficiently severe in the case of some alkaline rocks (1971 p 531).

In summary, all analyses of rocks attributed to the alkaline series have been recalculated to 100% volatile free; and analyses of all rocks with Fe_2O_3 in excess of % TiO_2 + 1.5% have been adjusted such that the concentration of Fe_2O_3 equals that value, the excess being recalculated as FeO, prior to the calculation of norms. Analyses of a few tholeiitic rocks with loss on ignition in

excess of 5% have also been recalculated anhydrous (see Appendix IV).

Distinction between the alkaline and tholeiitic series.

Irvine and Baragar (1971) distinguished between alkaline and tholeiitic rocks using a revised version of the triangular plot normative quartz, olivine, nepheline, devised by Yoder and Tilley (1962) and subsequently modified by Poldevaart (1964). Attempts to use this sophisticated diagram with Carlingford analyses have not proved successful however, analyses of alkaline rocks listed in Appendix II fall in the hypersthene, olivine, plagioclase field or even the hypersthene,quartz,plagioclase field in the majority of cases (see Figure 3.1). This partly reflects the use of the CIPW norm rather than the molecular norm adopted by Irvine and Baragar which depresses slightly the quantity of normative ore and thus decreases the degree of saturation (1971 p 526). It is probably largely the result of alteration as indicated by the high'loss on ignition'values.

The fields of the alkali dolerites,transition dolerites and tholeiitic dolerites overlap extensively, the alkali and tholeiitic fields separate in rocks which show more advanced fractionation, the hawaiitic and mugearitic varieties on the one hand and the craignuritic varieties on the other.

Application of the limiting concentrations of $Na_2O + K_2O$ and SiO_2 for basaltic rocks proposed by Middlemost (1972 pp 394-5) to the Carlingford suite, shows that members of the alkali series are alkalic if the uncorrected analyses listed in Appendix II are used,

Figure 3.1

Compositions of Carlingford rocks in terms of normative, quartz, albite, hypersthene and olivine, plotted on the triangular diagram normative Quartz (Qz), Olivine (Ol), Nepheline (Ne), where En = Enstatite and Ab = Albite.

A. Alkali basalt series.
B. Tholeiitic basalt - craignurite series.
C. High alumina basalt series.
D. Miscellaneous rocks.

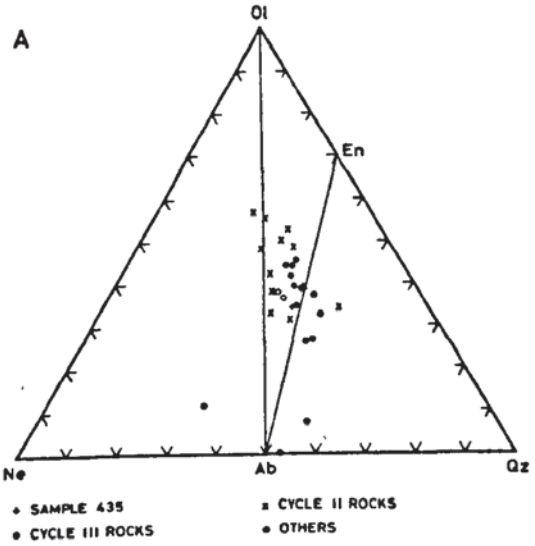

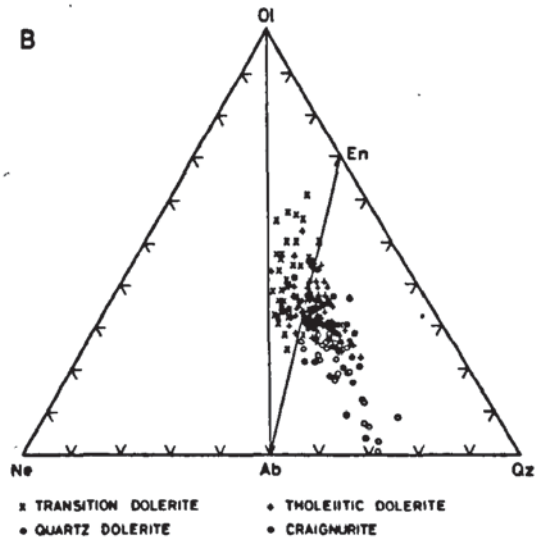

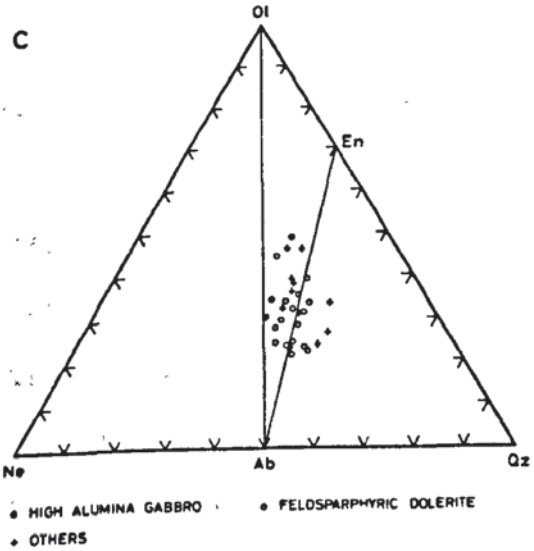

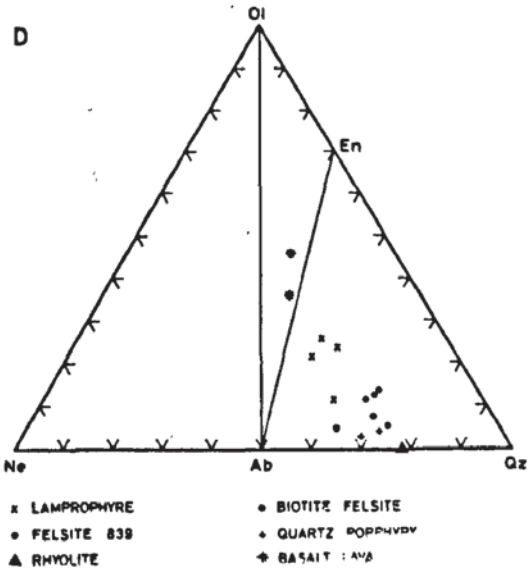

but that the majority have SiO_2 concentrations below the permitted limit of 45% for basaltic rocks. The corrected analyses have SiO_2 values which fall within the basalt range but alkali concentrations below the proposed limits for alkali basalts. The transition dolerites, tholeiitic dolerites, quartz dolerites, high alumina gabbros and feldsparphyric dolerites have compositions which fall in Middlemosts subalkalic category without the application of the volatile correction, indicating their truly tholeiitic character.

The alkali-silica limits quoted by Middlemost (1972) are largely derived from alkali-silica diagrams of the type used by Kuno (1968) and Macdonald (1968). Such diagrams were also used by Irvine and Baragar (1971 Fig. 3 p 532) to distinguish the alkaline and tholeiitic series, though not considered as reliable as the quartz, olivine, nepheline diagram by those authors in this context (p531). $Na_2O + K_2O$ are plotted against SiO_2 for the Carlingford suite in Figure 3.2, the alkaline rocks are plotted twice on Figure 3.2 using a the uncorrected analyses and b the corrected values. Macdonalds field divider for Hawaiian rocks is included in these diagrams, in 3.2b however a second line B-B' is drawn, it represents an adjustment of the original divider by 5.5% (the mean correction applied to the alkaline rocks for loss on ignition). These diagrams show that the Carlingford tholeiitic dolerites and quartz dolerites fall, as expected, in the tholeiitic field (Fig. 3.2c) as do the transition dolerites (Fig. 3.2d) and the high alumina gabbros and feldsparphyric dolerites (Fig. 3.2e). The alkali dolerites, on the other hand, fall astride the divider

Figure 3.2

Alkali v silica diagrams for rocks in the Carlingford suites. The oblique solid line in A - F is Macdonalds field divider for Hawaiian rocks (Macdonald 1968). The line B - B' in B represents Macdonalds divider adjusted by 5.5% (mean loss on ignition) to allow for recalculation of alkaline rock compositions to 100% volatile free. Line C - C' in C, D and F delineates rocks designated "transition dolerites", from other tholeiitic types.

A. Alkali basalt series; B. Alkali basalt series recalculated to 100% anhydrous; C. Petrographic tholeiitic dolerites and quartz dolerites (includes high iron transition dolerites), craignurites and craignuritic felsites; D. Petrographic transition dolerites; E. High alumina basalt series (includes feldsparphyric tholeiities); F. Felsites, quartz porphyries, lamprophyres and basalt lavas.

● Symbol refers to none specified varieties unless otherwise stated.

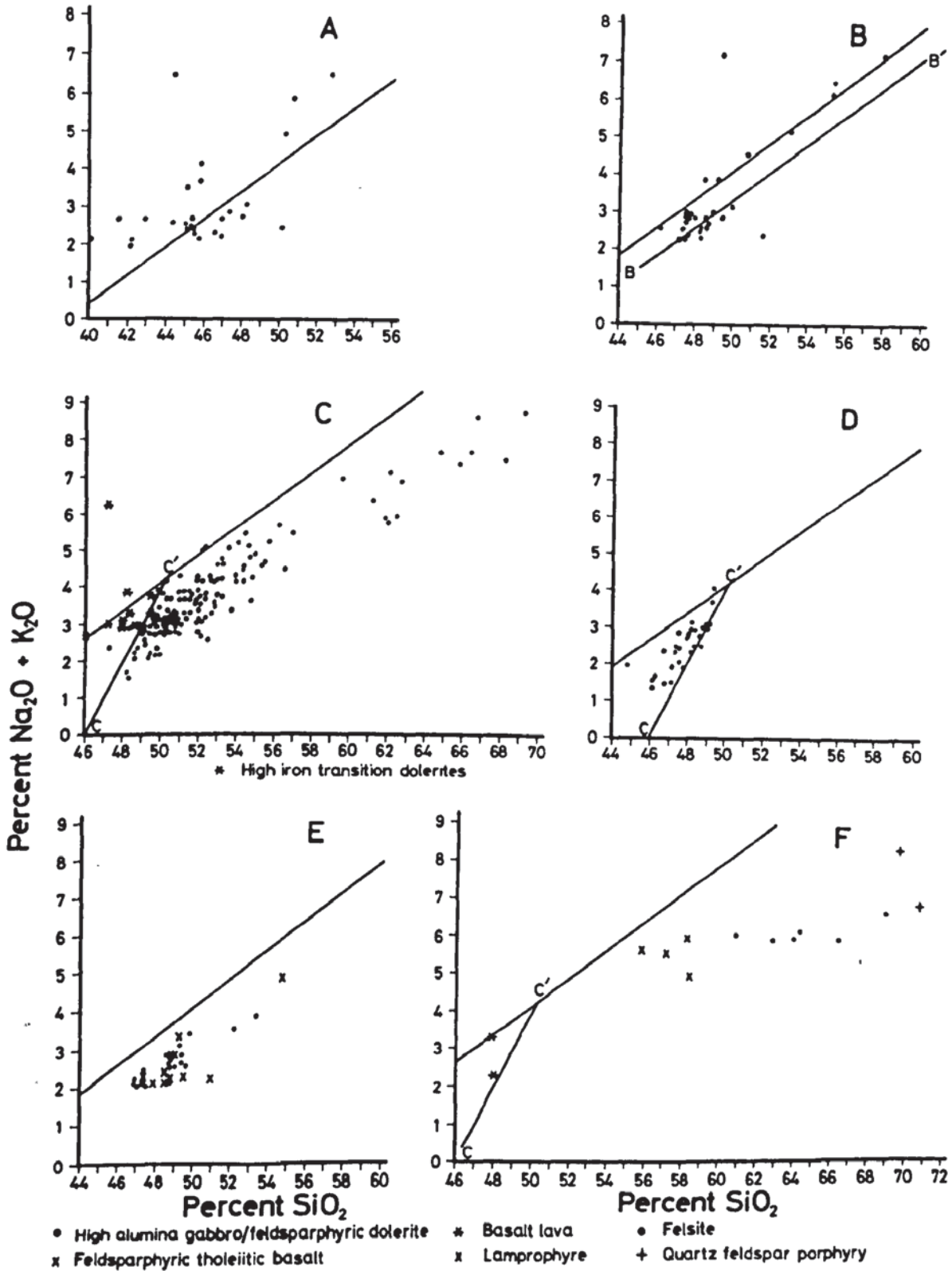

B-B' in Fig. 3.2b, the alkalic nature of the group is clearly demonstrated by the hawaiitic and mugearitic varieties which form a series falling inside the alkali fields in both 3.2a and 3.2b. Surprisingly, the trend of the majority of rocks in the Carlingford alkaline series is parallel to that of the Hawaiian alkali series, only a few fall on the more alkali enriched Hebridean trend (Fig. 3.3). The intermediate and acid members of the tholeiitic suite (the craignurites and craignuritic felsites) form a series which plots in the tholeiitic field, and has a distribution similar to that of a suite of related rocks in Ardnamurchan (Holland and Brown 1972) - see Fig. 3.4.

The transition dolerites.

Dolerites which are petrographically transitional between the alkali dolerites and the tholeiitic dolerites, fall almost entirely in the olivine, orthophyroxene, plagioclase field of the quartz, olivine, nepheline triangle (see Fig. 3.1). Strictly, they are olivine tholeiites as defined by Green (1970 p 35), that is, they are olivine, hypersthene normative, with hypersthene in excess of 3% (see Norm tables, Appendix VIII). When plotted on the alkali silica diagram (Fig. 3.2d) they fall, with few exceptions, in the tholeiitic field, most contain less than 49% SiO_2. Those with SiO_2 less than 47% have total alkali concentrations of less than 2%, the majority of those with SiO_2 in the range 47% to 49%, have Na_2O + K_2O in excess of 2%, they thus form a series which approaches the Macdonald field divider with increasing SiO_2 values, one specimen

Figure 3.3a

Alkali v silica diagram for rocks of the Carlingford alkali basalt series using raw analytical data. For explanation of symbols see Fig. 3.1., solid line is the Hawaiian alkali basalt - tholeiitic basalt field divider, dashed lines fractionation trends - A. Hebridean alkalic trend, B. Hawaiian alkalic trend, C. Hawaiian tholeiitic trend (after Holland and Brown, 1972, Fig. 9.), D. Carlingford tholeiitic trend (this investigation).

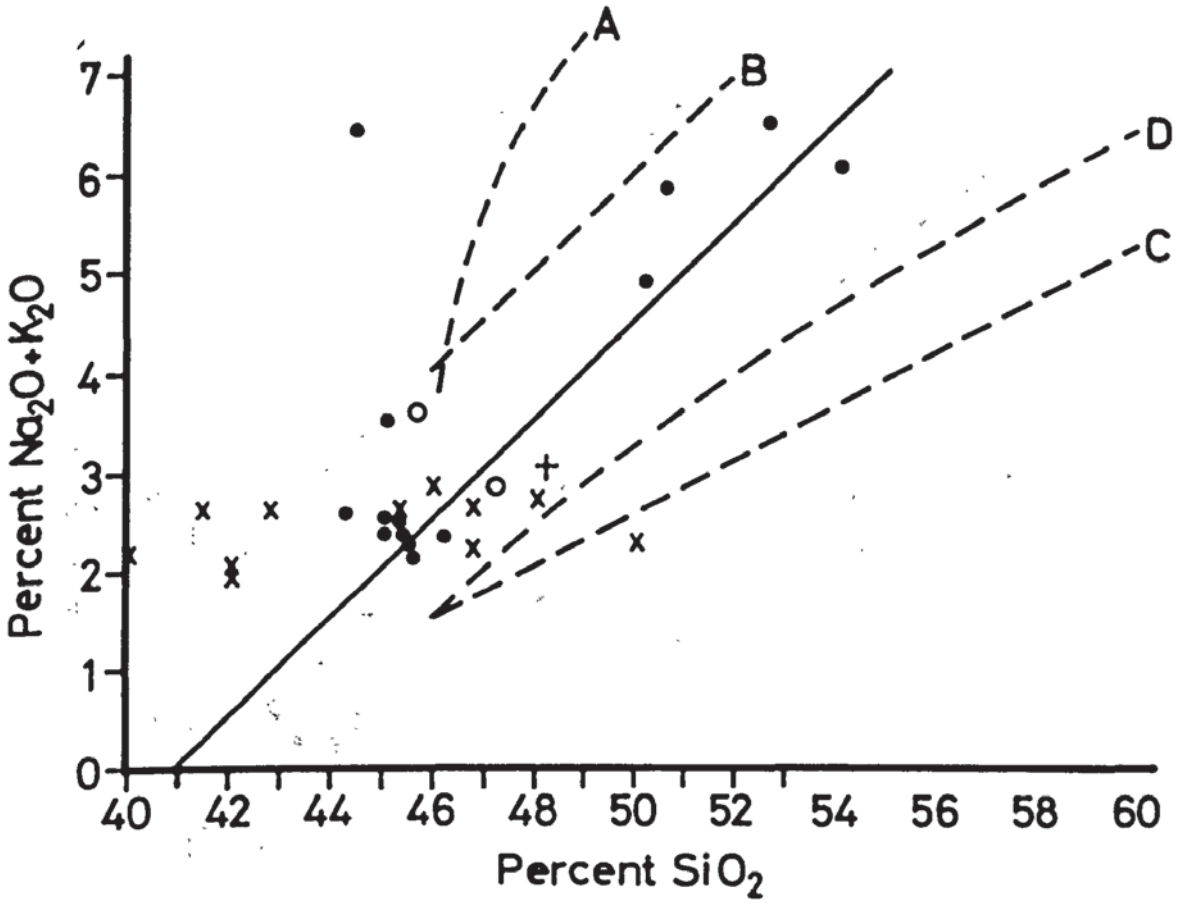

Figure 3.3b

Alkali v silica diagram for rocks of the Carlingford alkali basalt series using analysed compositions recalculated to 100% volatile free. For explanation of symbols see Fig. 3.1., solid line is the Hawaiian alkali basalt - tholeiitic basalt field divider, dashed lines fractionation trends - A. Hebridean alkalic trend, B. Hawaiian alkalic trend, C. Hawaiian tholeiitic trend (after Holland and Brown, 1972, Fig. 9.), D. Carlingford tholeiitic trend (this investigation).

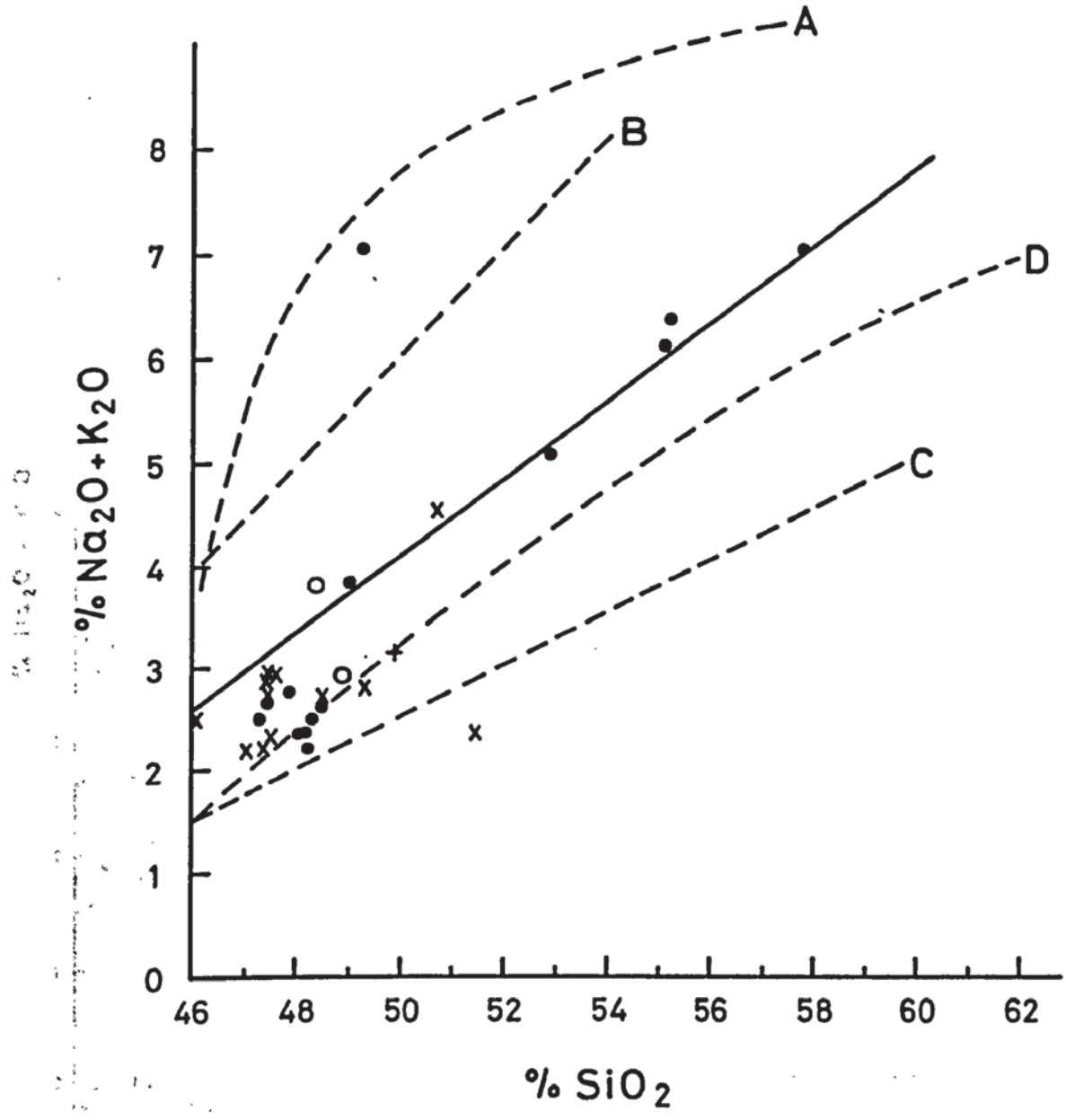

Figure 3.4

Alkali v silica diagram for the tholeiitic rocks (including craignuritic rocks) of Ardnamurchan. (After Holland and Brown, 1972, Fig. 9

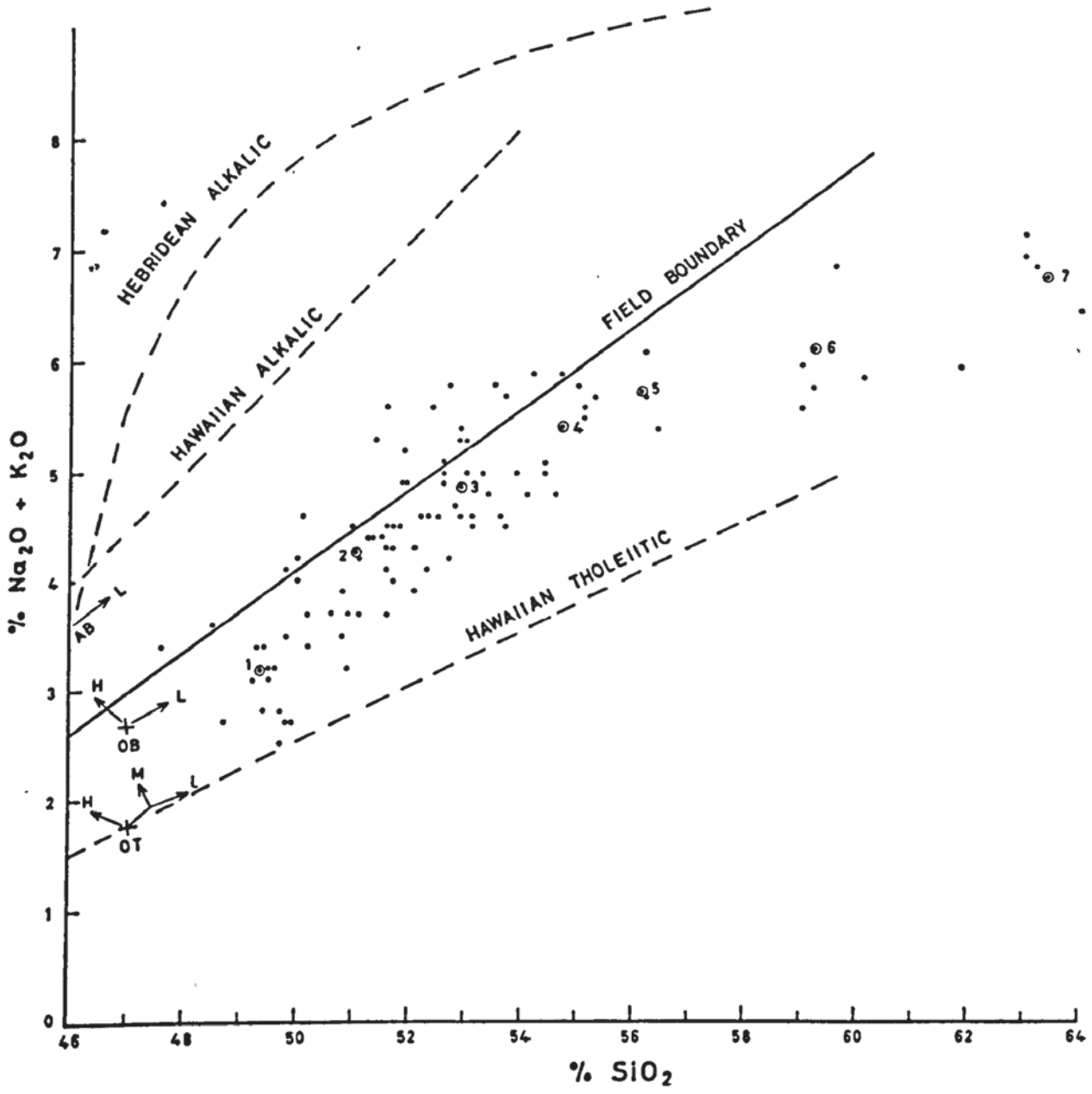

(130) actually falling in the alkaline field, reflecting the transitional nature of the group. The line C-C' in Figure 3.2d, taken in conjunction with Macdonalds divider, defines a field which encloses the compositions of the transition dolerites but few other rocks, and it is proposed that the transition dolerites be defined petrochemically on that basis.

The high iron transition dolerites.

A small group of rocks with alkali - silica ratios which fall in the field of the transition dolerites defined above, would otherwise be classified petrographically as tholeiitic dolerites and quartz dolerites. An examination of their composition shows that they all have FeO + Fe_2O_3, recalculated as total Fe_2O_3, in excess of 14% which is higher than in other transition dolerites, they are thus classified as "high iron transition dolerites".

The high alumina basalt series.

The feldsparphyric dolerites and high alumina gabbros plot astride the olivine, orthopyroxene, plagioclase - quartz,orthopyroxene, plagioclase field boundary in Figure 3.1, the high alumina gabbros tending to be somewhat less saturated than the feldsparphyric dolerites. On the alkali silica diagram 3.2c they form a series overlapping those of the transition dolerites and tholeiitic dolerites in the tholeiitic field.

Kuno distinguishes a high alumina basalt series on the occurrence of Al_2O_3 concentrations in excess of 16.5% in basaltic

rocks with alkali concentrations transitional between those of Japanese alkali dolerites and tholeiites (1968 p 625). Middlemost defines high alumina basalts simply as being subalkalic and with Al_2O_3 values in excess of 16% (1972 pp 394-5). Irvine and Baragar also place high alumina basalt with the subalkaline suite which alsc includes tholeiites (1971 Fig. 1 p 524).

The high alumina gabbros and feldsparphyric dolerites of the Carlingford suite have Al_2O_3 values in excess of 16.5%. For the purposes of the classification during the current investigation it has therefore been decided to attribute all Carlingford rocks which have tholeiitic affinities (fall in the tholeiitic field of the alkali silica diagram) and Al_2O_3 concentrations in excess of 16.5%, to the high alumina basalt series. The high alumina basalt series thus encompasses all high alumina gabbros and feldsparphyric dolerites, it also includes a few porphyritic members of the tholeiitic basalt series.

The tholeiitic basalt series.

Basaltic rocks which have alkali silica ratios which fall in the tholeiitic field of the alkali diagram (see Fig. 3.2c), and which cannot be classified as transition dolerites or members of the high alumina basalt series, and are too basic to be considered craignurites (see below), are described as members of the tholeiitic basalt series. This group incorporates the tholeiitic dolerite and quartz dolerite petrographic suites.

The basalt "andesite" boundary.

The definition of the basalt "andesite" boundary has been discussed by many authors, the literature pertaining to this topic being reviewed by Coats (1968 p 691). The convention of Williams, Turner and Gilbert (1954 p43) is adopted here; that is that basaltic rocks with SiO_2 in excess of 52%, and with normative plagioclase less basic than An_{50}, are "andesites" or in this case "andesitic". All rocks with SiO_2 values in excess of 55%, regardless of normative plagioclase composition, are attributed to intermediate or acidic categories accordingly (55% is the upper limit for SiO_2 concentrations in basalts set by Eyles and Simpson 1921 p 437, and adopted by Bailey et al.1924 p 280 and recently by Badham 1973 p 1321). Rocks with SiO_2 concentrations between 52% and 55%, but with normative plagioclase more calcic than An_{50}, are regarded as "basalts". Middlemost chooses the value 53.5% SiO_2 as an arbitrary basalt andesite boundary (1972 p 389), however the more flexible boundary incorporating normative plagioclase compositions adopted herein is considered more appropriate for Carlingford rocks on the basis of petrography. As so defined the majority of andesitic rocks at Carlingford have differentiation indices (Thornton and Tuttle 1960) in excess of 40, which has been adopted as the basalt andesite discriminator by Thompson (1972 p 107).

Subdivision of the alkali basalt series.

The basaltic rocks of the alkali basalt series can be subdivided into four types on the basis of normative plagioclase

and $Na_2O:K_2O$ ratios. Alkali basalts with $Na_2O:K_2O$ ratios less than 2:1 are trachy basalts (Baker et al 1964, Middlemost 1972 p 389). Alkali basalts with normative andesine are hawaiites (Macdonald 1960 p 175), those with normative oligoclase are mugearites (Macdonald 1957), the remaining rocks are alkali basalts sensu stricto. No attempt has been made to distinguish the alkali dolerites and picrites on chemical grounds, though rocks with D.I (differentiation index) values less than 20 are approximately equivalent to Middlemosts accumulative basalt group (1972 p 394). Other alkali basalts have D.I. values between 20 and 40 while the hawaiites, mugearites and trachy basalts have D.I. values between 40 and 50.

The andesitic rocks of the alkali dolerite series are defined as benmorites with $Na_2O:K_2O$ ratio greater than 1.5 and as tristanites with $Na_2O:K_2O$ less than 1.5 (Middlemost 1972 p 390). The tristanites and benmorites have D.I. values in excess of 50. More siliceous alkaline rocks, such as trachytes and phonolites, have not been recorded at Carlingford.

Craignurites and craignuritic felsites.

The craignurites are "andesites" of tholeiitic affinities (see Fig. 3.2c). Since the investigation of the Thingmuli volcanics by Carmichael (1964) "tholeiitic andesites" have been attributed to the tholeiitic basalt - icelandite series (Irvine and Baragar 1971, Middlemost 1972), such rocks usually have relatively high iron concentrations. The Carlingford craignurites also have high iron

concentrations and might, on that basis, be superficially classified as members of that series, however, together with others from the Hebridean Province variously described as leidleites and innin-morites (Bailey et al 1924), they form a petrographically distinct series. Examination of analyses of the Carlingford craignurites (see Appendices IV and XV) and of published analyses of similar rocks from the British Tertiary Province (Bailey et al 1924, Table III, p 19: Richey and Thomas 1930, Table III, p 84- Tomkeieff and Marshall 1935, Table II, p 261; Holland and Brown 1972, Table I, p 144) and comparison with those of Thingmuli (Carmichael 1964, Tables 3,4, and 5) indicate that the two series are chemically distinctive, somewhat in the manner of the trachy basalt - tristanite series and the alkali basalt - mugearite - benmorite series among the alkaline suite. Members of the craignurite series show progressive and rapid enrichment of K_2O relative to Na_2O with increasing SiO_2 values, the increase of K_2O in relation to Na_2O in the icelandites is much smaller, thus craignurites have Na_2O:K_2O ratios of less than 1.5 and generally approaching 1, while the icelandites have Na_2O: K_2O ratios in excess of 1.5 and often in excess of 2. This distinction is emphasised by Fig. 3.5, a triangular diagram of normative feldspar compositions for rocks of the two series.

The upper limit of the craignurite series is set at 70% SiO_2 which is the lower limit for rhyolite accepted by most authors (Middlemost 1972, p 391). The craignurites thus form a series with SiO_2 values ranging from 52% to 70%. The series is subdivided into the "basaltic craignurites" with SiO_2 less than 55% and recognised

Figure 3.5

Normative feldspar composition of Carlingford craignurites and quartz dolerites, and Icelandic tholeiitic basalts, basaltic andesites and icelandites (data from Carmichael 1964) plotted on the triangle normative Orthoclase (Or), Anorthite (An), Albite (Ab). The diagram emphasises the distinction between the craignurite and icelandite series.

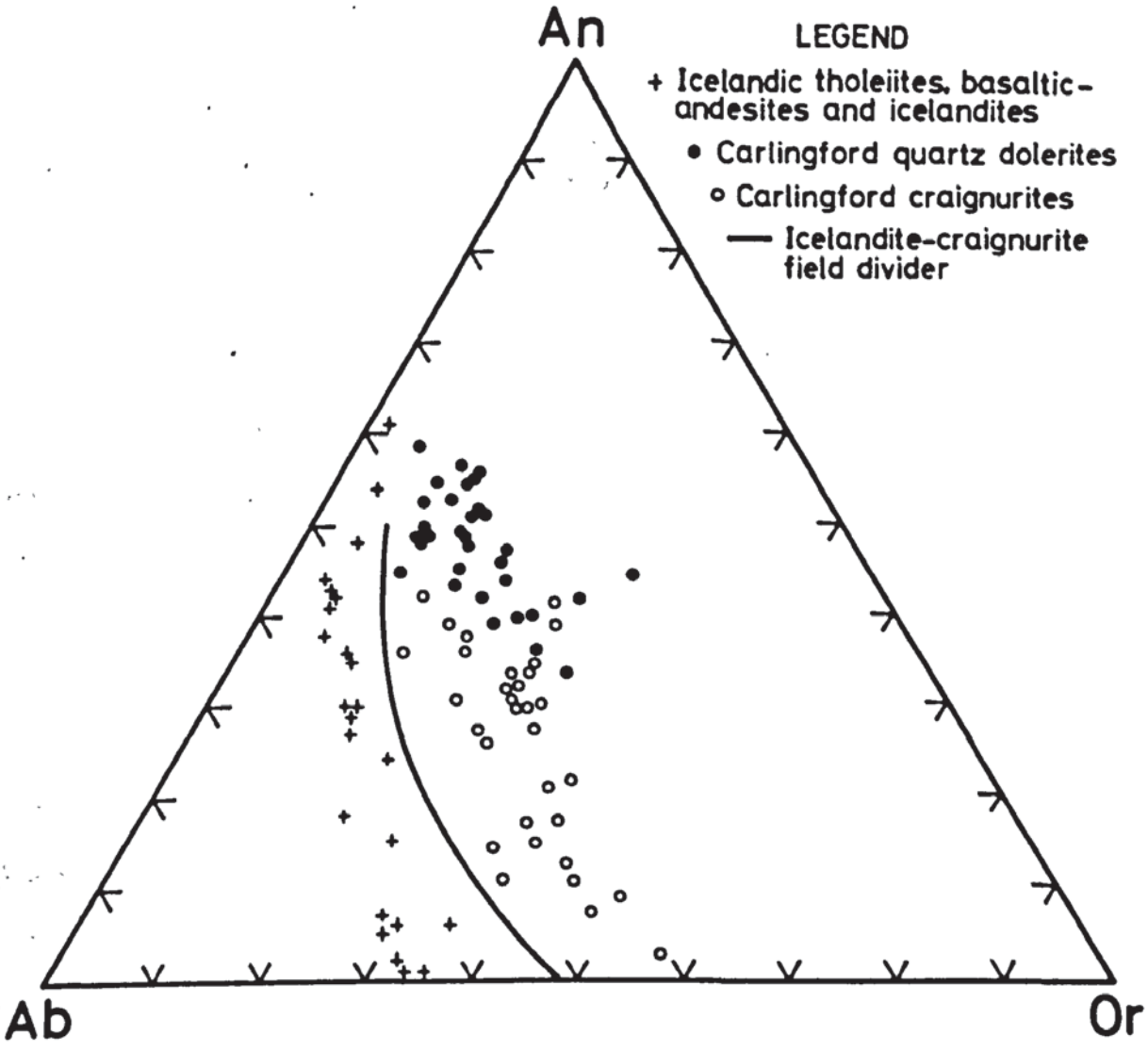

only by the low An content of their normative plagioclase, a group which incorporates rocks classified as tholeiitic basalts by Bailey et al (1924 p 281); the craignurites sensu stricto with SiO_2 in the range 55% to 60%; and the craignuritic felsites with SiO_2 concentrations between 60% and 70% and which includes the published compositions of most rocks referred to as leidleite, inninmorite or acid craignurite (Bailey et al. 1924, Richey and Thomas 1930). D.I. values in the group range from about 40 in the basaltic craignurites to values in excess of 80 in more acidic craignuritic felsites.

As demonstrated by Fig. 3.2, the craignurites form a continuous series with the tholeiitic basalts and transition dolerites, that series is referred to below as the "tholeiitic basalt craignurite series".

High alumina craignurites.

Rocks which qualify petrochemically as craignurites as defined above, but which have Al_2O_3 concentrations in excess of 16.5%, are referred to as "high alumina craignurites" as they thus fall in the andesitic field of the high alumina basalt series. Following Middlemosts scheme such rocks should be classified as andesites, however the use of terminology associated with the calc alkaline series is considered inappropriate for Hebridean rocks. Two such rocks have been analysed, specimens 446 and 447, the compositions of both are listed in Appendix XV.

Rhyolites and quartz-feldspar-porphyries.

Rocks with SiO_2 concentrations in excess of 70% are classified as rhyolites, one such rock, specimen 859, has been analysed. Some of the quartz feldspar porphyries are also classified as rhyolites on that basis (see 1203), while others with less than 70% silica should be regarded as craignuritic felsites if the only criteria considered are those set out above, the quartz-porphyries must therefore be distinguished petrographically; a detailed consideration of their petrochemistry in Chapter 8 outlines their chemical characteristics. The petrochemical affinities of the rhyolite 859, which is aphyric, are also discussed in Chapter 8.

The biotite felsites and lamprophyres.

The biotite felsites and lamprophyres cannot be distinguished from craignuritic rocks on the basis of the criteria set out to define the latter group above, except that the five analysed biotite felsites (see Appendix V) form a cluster which falls somewhat nearer the quartz apex of the triangle normative quartz, olivine, nepheline, than does the craignurite field (see Fig. 3.1). Further detailed consideration of the petrochemistry of these groups is reserved for Chapter 8.

SUMMARY

A. The rocks of the Carlingford suite can be classified as types belonging to one of the following series or groups on the basis of petrography:

1) Alkali dolerite series.

2) Transition dolerites

3) Tholeiitic dolerite, quartz dolerite, craignurite, craignuritic felsite series.

4) High alumina gabbro, feldsparphyric dolerite series.

5) Rhyolites

6) Quartz-feldspar-porphyries

7) Miscellaneous felsites

8) Lamprophyres.

B. The petrographic classification scheme forms the basis of a petrochemical classification which may be summarised as follows:

1) Rocks which are classified petrographically as members of the alkali dolerite series, generally have alkali silica ratios which fall in the alkaline field of the alkali silica diagram as defined by Macdonalds divider (Fig. 3.2a) or by the divider B-B' (Fig. 3.2b) in the case of analyses recalculated volatile free to 100%. The petrography of the alkaline rocks is the most reliable distinguishing characteristic however.

2) The alkali basalt series is subdivided into:

a) alkali basalt - SiO_2 less than 55%, normative plagioclase more calcic than An_{50}, $Na_2O:K_2O$ ratio in excess of 2.1.

b) hawaiite - SiO_2 less than 52%, $Na_2O:K_2O$ ratio in excess of 2.1, normative plagioclase An_{30} to An_{50}.

c) Mugearite - SiO_2 less than 52%, $Na_2O:K_2O$ ratio in excess of 2:1, normative plagioclase more sodic than An_{30}.

d) trachy basalt - SiO_2 less than 55%, normative plagioclase more basic than An_{50}, $Na_2O:K_2O$ ratio less than 2:1.

e) benmorite - SiO_2 in excess of 52%, normative plagioclase less calcic than An_{50}, $Na_2O:K_2O$ ratio in excess of 1.5:1.

f) tristanite - SiO_2 in excess of 52%, normative plagioclase less calcic than An_{50}, $Na_2O:K_2O$ ratio less than 1.5:1.

3) Members of the tholeitic basalt - craignurite series are defined as having alkali silica ratios which fall in the tholeiitic field of the alkali silica diagram (Fig. 3.2) and Al_2O_3 concentrations less than 16.5%.

4) The tholeiitic basalt craignurite series is subdivided into:

a) transition dolerite - falls in the transition dolerite field defined by the Macdonald divider and the line C - C' in Fig. 3.2d (alkali silica diagram), and with less than 14.0% total Fe_2O_3.

b) High iron transition dolerite - as with transition dolerite but with total Fe_2O_3 in excess of 14.0 (petrographically tholeiitic dolerites and quartz dolerites).

c) tholeiitic basalts - SiO_2 less than 52% and not attributable to the transition dolerite group, or SiO_2 less than 55% and more than 52% with normative plagioclase more calcic than An_{50}.

d) basaltic craignurite - SiO_2 in the range 52% to 55%, normative plagioclase more sodic than An_{50}.

e) Craignurite - SiO_2 in the range 55% to 60%.

f) Craignuritic felsite - SiO_2 in the range 60% - 70%.

5) Members of the high alumina basalt series are defined as having alkali:silica ratios which fall in the tholeiitic field of the alkali silica diagram (Fig. 3.2) and Al_2O_3 concentrations in excess of 16.5%.

6) The high alumina basalt series is subdivided into:

a) high alumina basalts - SiO_2 less than 52%, or less than 55% and normative plagioclase more calcic than An_{50}.

b) high alumina craignurites - SiO_2 in excess of 55%, or SiO_2 in excess of 52% and normative plagioclase more sodic than An_{50}.

7) All rocks with SiO_2 in excess of 70% are rhyolites, quartz feldspar porphyries which qualify on that basis can be distinguised from rhyolites sensu stricto on the basis of their characteristic petrography.

8) The biotite felsites, lamprophyres and some quartz feldspar porphyries cannot be distinguished from the craignurites and craignuritic felsites on the basis of

chemical characteristics described above, and thus can only be indentified by petrography. Further consideration of the petrochemistry of these rock types, together with that of the rhyolites, is given in Chapter 8.

C. The tholeiitic basalt - craignurite series exhibits markedly greater enrichment in K_2O relative to Na_2O with increasing SiO_2 concentrations than does the tholeiitic basalt - icelandite series, and is thus defined as a separate series in its own right.

CHAPTER 4

THE PETROLOGY AND PETROCHEMISTRY OF THE ALKALI DOLERITES AND RELATED ROCKS

Abstract

A suite of alkali dolerites and related rock types emplaced at Carlingford as dykes is subdivided on the basis of time relations into at least three subsuites. The petrology and petrochemistry of the suite are described. Mechanisms involving separation of olivine, or olivine plus plagioclase, and subsequent separation of titanomagnetite are proposed to explain the differentiation trends exhibited by it. Partitioning behaviour of TiO_2 between clinopyroxene and ore in these melts was dependant on the availability of oxygen. Trace element concentrations in these rocks confirm the proposed mechanisms of fractionation and the behaviour of TiO_2.

Introduction

Alkali dolerites and related rocks occur almost exclusively as dykes at Carlingford. Alkali dolerite dyke swarms of significance have been recognised twice in the sequence of intrusive activity established for the complex (see Fig. 1.11), episode IIb a north west - south east dyke swarm, and episode IIId an orthogonal tangential dyke swarm. A minor alkaline intrusive episode, is attributed to Cycle I (see Chapter 1). In the field, members of the alkali dolerite suite are recognised by their characteristic spheroidal weathering and ochrous weathering products, fresh surfaces are typically dark green in colour; the less basic varieties are pale brown or pink when

weathered. Amygdales are conspicuous in the majority of these rocks particularly near the contacts of dykes. The petrological range, and the mineralogical and petrochemical variation of the alkaline suite are discussed in the following paragraphs.

PETROLOGY

The members of the alkali dolerite suite have a number of petrological characteristics in common. Olivine is present in all, including the most silicic derivatives, in which it appears as a phenocryst phase only; clinopyroxene is typically pink or lilac in colour and titaniferous in composition, it occurs only in the ground mass; an interstitial phase, chlorite, alkali feldspar, or occasionally zeolite, is usually present though in small quantities.

Alteration is commonly intense in the alkaline rocks, olivine is invariably pseudomorphed by iddingsite, bowlingite or calcite; chlorite and other alteration products are generally abundant throughout the rock. Calcite and siderite are often present in the groundmass too. Amygdales consist of chlorite, calcite or siderite and, more rarely, natrolite. Textures in the alkaline rocks vary from basaltic to trachytic. Inspite of these similarities, rocks attributed to different intrusive episodes have petrological characteristics which distinguish them, each group is described separately below. The modal composition of nine alkaline rocks which represent the petrological range of the suite are listed in Table 4.1.

TABLE 4.1.

Modal compositions of nine selected alkaline rocks

Sample No.	435	135	783	1175	36	61	119	191	748
Rock Type	Alkali dolerite	Alkali dolerite	Alkali dolerite	Alkali picrite	Alkali dolerite	Alkali dolerite	Alkali dolerite	Trachy basalt	Mugearite
Relative Age	C. 1.	C. 11b	C. 11b	C. 11b	C. 111d	C. 111d	C. 111d	C. 111d	C. 111d
Plagioclase (phenocrysts)	-	tr	6	11	1	3	21	-	tr
Plagioclase (groundmass)	34	37	39	22	49	38	24	46	62
Clino-pyroxene	28	20	10	20	19	20	25	21	1
Ore	11	9	6	7	10	10	4	16	4
Olivine*	-	12	4	28	14	12	11	3	-
Chlorite (groundmass)	22	15	2	-	5	11	11	9	-
Chlorite (amygdales)	1	6	4	3	-	5	2	-	-
Carbonates	-	-	27	9	1	1	1	-	31
Natrolite	-	-	6	-	-	-	-	-	-
Epidote	3	-	-	-	-	-	-	-	-
Biotite	-	-	-	1	tr	-	-	4	tr

tr = trace
* Note olivine is largely pseudomorphed by secondary minerals in all these rocks.

Groundmass plagioclase constitutes from 24% to 49% of the modal composition of alkali dolerites, while there is as little as 22% modal groundmass plagioclase in the picrites. Over 60% of the modal

composition of mugearitic varieties consists of groundmass plagioclase. Clinopyroxene concentrations range from 10% to 28% in the dolerites but these figures may, in some cases, be artificially low due to alteration. Olivine in picritic varieties can comprise up to 28% of the mode while in mugearitic varieties it may be as little as 0.4%, in the dolerites it ranges from 3% to 12%.

a) The alkali dolerites of Cycle I.

Only a few isolated alkali dolerite dykes which crop out on the north eastern flanks of Carlingford Mountain are attributed to the igneous activity of Cycle I, no derivative types are associated with them. They are all altered and are represented by specimen 435 which is intensively chloritized and characteristic of the group as a whole.

Sample 435 consists of a doleritic mesh of plagioclase laths up to 1.2mm in length, subophitic lilac titanaugite up to 0.8mm in length, which has suffered chloritization and uralitization, and granular magnetite up to 0.1mm in diameter. The abundant chlorite constitutes over 20% of the rock replacing ferromagnesian minerals including olivine. Occasional flakes of red-brown biotite are present in the groundmass. The composition of the groundmass feldspar, as determined by measurement of symmetrical extinction (Deer Howie and Zussman 1966 p 329), approaches An_{67}. The matrix encloses dark subspherical patches up to 4mm in diameter which consists of plagioclase and elongate clinopyroxene with a poorly developed variolitic texture; also present are a series of amygdales, maximum

diameter 3mm, consisting of chlorite and epidote.

b). The alkaline rocks of Cycle II.

A swarm of north west - south east trending alkali dolerite dykes was emplaced early during Cycle II of the intrusive sequence at Carlingford. They are particularly well represented in the Carboniferous Limestone on the shore at Whitestown and in the quarries at Mullatee and Rosemount. Though a number of rock types are attributed to this episode no feldspathic fractionates have been recognised, only dolerites and picrites are present as represented by specimens 135 and 783, and 1175 respectively.

Specimen 135 consists of a groundmass of plagioclase laths, (composition An_{70}, up to 1mm in length), subophitic to ophitic titan-augite ranging from 0.2mm to 0.6mm in diameter, subhedral olivine pseudomorphed by chlorite, and granular ore including both titan-omagnetite and pyrrhotite. This matrix, which also has a high chlorite content, encloses a few equant euhedral phenocrysts of plagioclase showing zoned rims, and numerous amygdales of chlorite and secondary ore.

The alkali dolerite dykes cutting the limestones near Whitestown and Mullatee are of a distinctive type represented by specimen 783, they have a characteristically high carbonate content. In 783 zoned plagioclase phenocrysts are set in a groundmass of plagioclase laths (composition An_{70}, maximum length 0.7mm), subordinate subophitic titanaugite and subhedral bowlingitised olivine. The groundmass contains abundant carbonate rhombs, up to 0.4mm in diameter which

constitute about 20% of the mode; scattered magnetite octahedra; minor quantities of biotite and interstitial natrolite. Amygdales ranging from 0.8mm to 2.2mm in diameter are also present, they consist of an outer layer of euhedral siderite enclosing fibrous natrolite sometimes with a little chlorite, and sometimes enclosing a core of siderite in turn.

Also present in the Whitestown area are a series of picritic dykes exemplified by specimen 1175. This rock contains up to 28% modal olivine as euhedral or subhedral phenocrysts ranging from 0.5 to 2mm in diameter and now pseudomorphed by chlorite and calcite, together with subhedral plagioclase phenocrysts, compositon An_{80}. The groundmass is variable in grain size, coarser rock consisting of crystals up to 1mm in length is veined by much finer material of the same composition. Groundmass plagioclase has the composition An_{70}, also present are subophitic clinopyroxene and octahedral magnetite crystals. Subhedral and corroded xenocrysts of orange brown spinel occur in the rock together with numerous amygdales consisting of siderite and chlorite.

c). The alkaline rocks of Cycle III.

The emplacement of a series of alkali dolerites and related derivatives as orthogonal tangential dykes (episode 111d) was the final intrusive event in the Carlingford Complex. A wide variety of rock types is present in these dykes ranging from alkali dolerite to mugearite, benmorite and tristanite. The alkali dolerites themselves show a wide range of composition. Specimen 119 is among the

most basic, consisting of phenocrysts of serpentinised olivine and calcic plagioclase, set in a basaltic matrix of plagioclase laths and prismatic titanaugite. The phenocrysts often occur in clusters the plagioclase enclosing the olivine. Ore (titanomagnetite) is present in relatively small quantities occurringas skeletal octahedra up to 0.2mm in diameter, interstitial chlorite is also present.

Specimens 36 and 61 consist of a mesh of plagioclase laths, up to 1.5mm in length with cores of composition An_{55} (61) and An_{67} (36), and subophitic lilac titanaugite. The groundmass also includes olivine pseudomorphed by iddingsite and bowlingite, and skeletal grains of titanomagnetite. Plagioclase phenocrysts are uncommon in both rocks but when present are subhedral, equant and zoned. Interstitial chlorite and calcite and minor biotite are present in the groundmass. Specimen 61 has amygdales consisting of chlorite enclosing calcite cores.

Specimen 191 a trachy basalt consists of a groundmass of plagioclase laths (composition An_{45} and up to 0.5mm in length), pale pink prismatic titanaugite, titanomagnetic octahedra, flakes of biotite, and interstitial chlorite and alkali felspar. Subhedral phenocrysts of olivine pseudomorphed by calcite and bowlingite are present but not numerous. The texture is subtrachytic.

Calcite and siderite are particularly abundant in some of the more fractionated derivatives of episode IIIc as exemplified by specimen 748 a mugearite. The bulk of the rock consists of laths of alkali feldspar composition An_{10} the majority not exceeding 0.2mm in length. Also present in the groundmass are minor clinopyroxene

(largely altered), apatite needles up to 0.1mm in length, granular ore and interstitial alkali feldspar. A few phenocrysts of olivine now pseudomorphed by iddingsite, oxidised subhedral skeletal ore and plagioclase are also present, as are amygdales of calcite, chlorite and natrolite. The rock has a trachytic texture.

Mineralogy of the Cycle III alkali dolerites

A series of microprobe analyses of feldspars, pyroxenes, "olivines" and ores in samples 61 and 119 are set out in tables 4.2, 4.3, 4.4 and 4.5, the analytical methods adopted are described in Appendix 1. Both rocks are attributed to the Cycle III alkaline suite.

The plagioclase compositions listed in Table 4.2 are semiquantitative, the Na_2O values have been calculated as they are below the limits of detection of the A.E.I. probe used during this investigation. Two feldspar analyses are quoted for each specimen, the compositions of each pair are mutually consistant, and are believed to approximate to the actual feldspar compositions. As such they suggest a range of plagioclase compositions of at least An_{75} to An_{51} in the groundmass feldspar of doleritic rocks in this suite. Note the relatively high concentrations of iron which are a feature of Carlingford plagioclases in general (Le Bas 1970a p 69).

The pyroxene compositions quoted in Table 4.3 do not include Na_2O values which were not determined.

Calculation of the structural formulae on the basis of six oxygens shows that the analyses are not strictly stoichiometric and

Table 4.2

Compositions of groundmass plagioclase in alkali dolerites of Cycle III

		Sample 61		Sample 119	
		a	b	a	b
	SiO_2	58.10	57.29	52.82	50.79
	Al_2O_3	25.08	25.90	28.66	30.52
	Fe_2O_3	0.83	0.80	0.54	0.75
	CaO	9.84	10.21	15.12	15.01
	Na_2O*	5.34	5.45	2.71	2.82
	k_2O	0.81	0.35	0.14	0.11
	Total	100.0	100.0	99.99	100.0
Molecular	(Ab	47.1	48.1	24.3	25.2
Percent	(An	48.1	49.9	75.0	74.2
	(Or	4.7	2.0	0.8	0.6

* Na_2O percentages are derived by calculation using the formula:

$$Na_2O = 31 \times \left(\left[\frac{\frac{Al_2O_3}{51} + \frac{SiO_2}{60}}{4} \right] - \frac{CaO}{56} - \frac{k_2O}{47} \right)$$

Table 4.3

Compositions of clinopyroxenes in alkali dolerites of Cycle III

	Sample 61 a	Sample 61 b	Sample 119 a	Sample 119 b
SiO_2	52.40	52.20	46.82	47.62
TiO_2	2.79	2.76	3.27	2.71
Al_2O_3	4.22	2.13	5.26	3.56
Fe_2O_3	11.30	10.90	15.83	18.55
MgO	10.90	11.60	7.85	7.39
CaO	18.30	20.20	21.02	20.22
Na_2O	N.D.	N.D.	N.D.	N.D.
K_2O	0.15	0.17	N.D.	N.D.
Total	99.96	99.96	100.05	100.05
Molecular (Wo	44.4	46.1	48.8	46.4
Percent (En	36.6	36.7	25.5	23.8
(Fs	19.1	17.2	25.8	29.8

N.D. = Not determined.

must be treated as semiquantitative. They are markedly titaniferous with values in the range 2.7% to 3.3% TiO_2. Al_2O_3 concentrations range from 2.13% to 5.26%, the highest Al_2O_3 value being recorded from a pyroxene in specimen 119 which is the more basic of the two rocks. The overall compositions of the pyroxenes fall in the range Wo_{44}, En_{37}, Fs_{19} (specimen 61) to Wo_{49}, En_{25}, Fs_{26} (specimen 119).

Fresh olivine has not been identified in the alkali dolerite

suite at Carlingford. The results of analyses of two iddingsitised olivines from sample 61 are listed in Table 4.4 together with the composition of an olivine (Fo_{86}) from a Rhum allivalite quoted by Brown (1956), for comparison.

Table 4.4

Compositions of altered olivines in alkali dolerite of Cycle III (dolerite)

	61		
	a	b	Rhum
SiO_2	41.6	46.4	39.87
TiO_2	N.D.	N.D.	0.03
Al_2O_3	17.7	13.3	0.00
Fe_2O_3	22.1	23.3	0.86
FeO	N.D.	N.D.	13.20
MnO	N.D.	N.D.	0.22
MgO	17.2	14.7	45.38
CaO	1.15	1.97	0.25
Na_2O	N.D.	N.D.	0.04
K_2O	0.19	0.32	0.01
H_2O+	N.D.	N.D.	0.33
H_2O-	N.D.	N.D.	0.10
Total	99.94	99.99	100.30

N.D. = Not determined.

The analyses show that the replacement of olivine by iddingsite involves the massive introduction of Al_2O_3 and CaO, presumably

with substitution for MgO and FeO. According to Deer, Howie and Zussman (1966 p 5) iddingsite consists principally of goethite, haematite and silicates with an embryonic structure. The high SiO_2 and CaO values suggests that free quartz and calcite are also present in the altered olivine samples analysed. Considering the degree of alteration, the two analyses show a great degree of similarity, it is possible therefore that the relative proportions of FeO and MgO have remained unchanged. On that basis the primary olivine of Sample 61 would fall in the range Fo_{56} to Fo_{61} i.e. in the Hyalosidersite range (Deer, Howie and Zussman 1966).

Table 4.5

Composition of titanomagnetite in alkali dolerites of Cycle III

		61		119	
		a	b	a	b
	TiO_2	25.7	27.9	15.02	16.77
	Fe_2O_3	74.3	72.1	83.59	82.09
Molecular Percent	Ulvospinel	77.0	83.7	45.7	51.0
	Magnetite	23.0	16.3	54.3	49.0

The relative significance of TiO_2 solid solution in titanomagnetite in two alkali dolerites has been determined by reference to the partial analyses of opaque phases listed in Table 4.5. The high TiO_2 concentrations are self evident and the ores range in composition from $Ulvospinel_{84}\ Magnetite_{16}$ to $Ulvospinel_{46}\ Magnetite_{54}$ in 61 and 119 respectively.

The partitioning of CaO between coexisting plagioclase and clinopyroxene is sympathetic such that plagioclase An_{75} coexists with titanaugite Wo_{49} in specimen 119, and An_{50} with Wo_{44} in specimen 61, reflecting the decreasing availability of CaO in the melt as a whole with increasing fractionation (see below). The partitioning of TiO_2 between coexisting pyroxenes and ores such that TiO_2 increases in titanomagnetite as it decreases in the pyroxene, is of particular significance and probably reflects varying availability of oxygen in the melt, TiO_2 entering the titanomagnetite lattice preferentially in conditions of relatively high oxygen fugacity (Le Bas 1970b p 223). The high titania ores of specimen 61 appear to coexist with high iron olivine.

PETROCHEMISTRY

Composition in terms of major elements.

Whole rock analyses of selected members of the alkaline suite are listed in Table 4.6, all analyses of rocks of this group are tabulated in Appendix II. It is unfortunate that the Carlingford alkaline rocks all show alteration, often intense, the olivine being particularly susceptable. This alteration is reflected by the high volatile content of the rocks listed and as a result analyses of members of the alkaline suite must be treated with caution. The majority of rocks in the suite contain relatively large modal concentrations of carbonate phases either calcite or siderite, and have relatively high CO_2 concentrations even in the case of fresh samples. High carbonate concentrations have been reported

recently from a basic dyke of similar type in Ardnamurchan, and are considered of primary origin (Wells and Smith 1973).* In view of the relatively intense and variable degree of alteration exhibited by the analysed members of the suite, the high and variable level of CO_2 concentrations, and the incomplete coverage of CO_2 determinations, it has been considered advisable to recalculate all analyses to 100%, excluding water and CO_2, for the purpose of calculating norms and for use in the various plots of oxide percent which follow, (see also Chapter 3) a listing of these recalculated analyses is included in Appendix II. This expedient has the advantage that modal siderite is not recorded as normative calcite in the CIPW norm, however CaO and FeO from modal carbonates are included in normative silicate percentages as a result.

A series of conventional Harker variation diagrams of recalculated oxide percent versus silica for rocks of the alkaline suite are set out in Fig. 4.1 indicating the range of compositions of this group of rocks.

TiO_2 values from a scatter when plotted against SiO_2. Rocks with recalculated SiO_2 values of less than 50% have TiO_2 concentrations falling into the range 1.15% to 3.3% TiO_2 and show some evidence of TiO_2 enrichment with increasing SiO_2, more fractionated rocks with SiO_2 in excess of 50% show a tendency towards progressive TiO_2 depletion. There is little difference in the range of TiO_2 values in rocks of different age and the same SiO_2 concentration.

Recalculated concentrations of Al_2O_3 range from 14.4% to 18.4%. The majority of Cycle III rocks show a progressive increase

* NOTE: ABSTRACT ONLY. SINCE THE TIME OF WRITING, THIS PAPER HAS BEEN PUBLISHED IN FULL (WELLS, SMITH AND BOWLES, 1974).

Figure 4.1

Compositions of rocks in the Carlingford alkali basalt series, recalculated to 100% volatile free, depicted graphically as a series of silica variation diagrams.

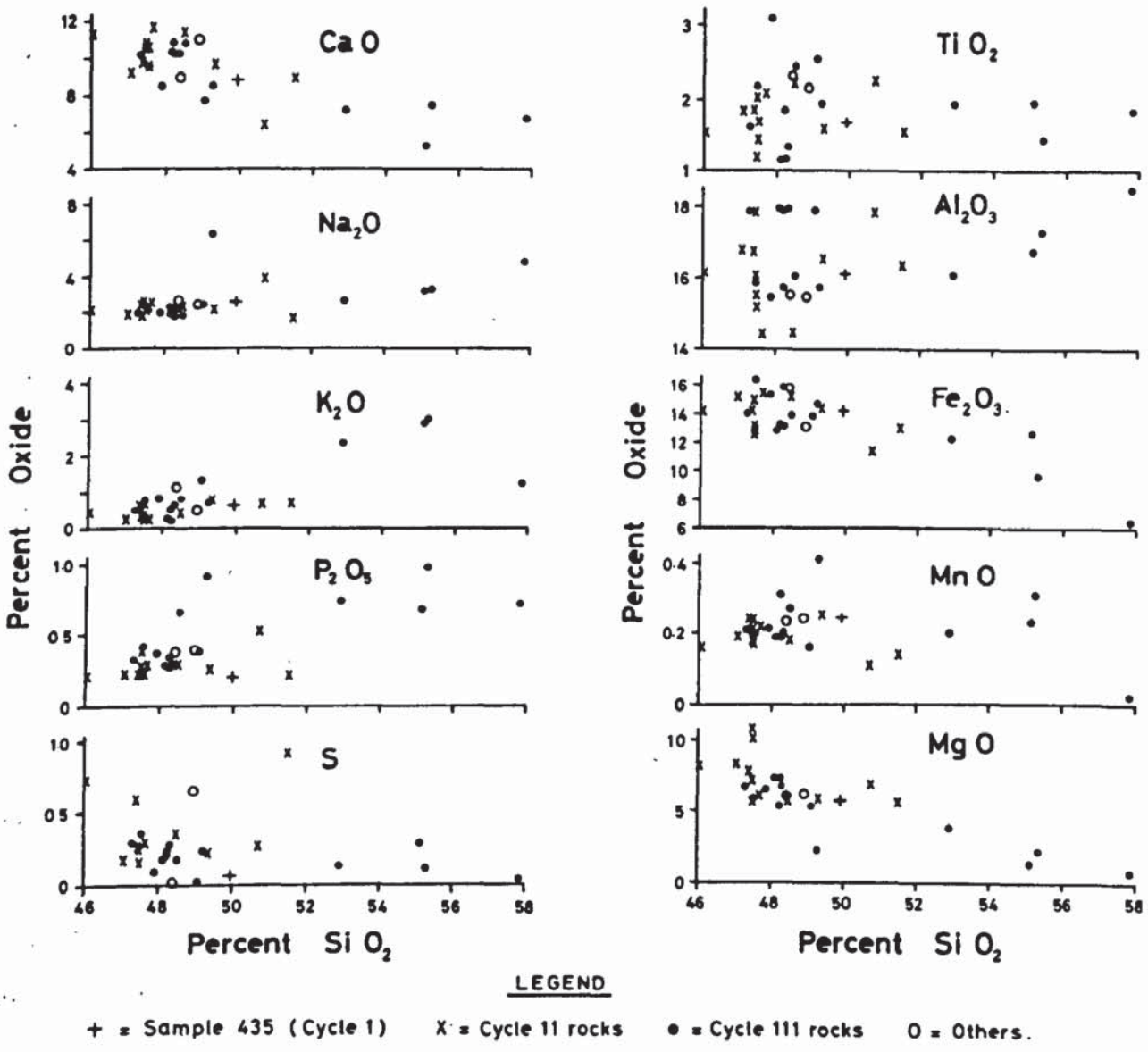

Table 4.6

Compositions of nine selected alkaline rocks

Sample No.	36	61	119	135	191	435	748	783	1175
SiO_2	45.09	44.39	46.26	46.82	50.34	48.24	44.41	42.07	41.53
TiO_2	2.09	3.02	1.14	1.84	1.86	1.60	1.74	1.64	1.48
Al_2O_3	15.06	14.36	17.20	16.55	15.37	15.56	14.19	15.01	13.29
Fe_2O_3	7.90	7.16	3.38	1.96	4.60	4.12	3.60	1.67	0.53
FeO	6.37	6.81	8.16	10.92	6.42	8.67	8.73	10.74	9.79
MnO	0.19	0.20	0.18	0.24	0.19	0.23	0.37	0.17	0.16
MgO	5.64	6.09	7.04	7.67	3.73	5.41	1.98	7.51	9.04
CaO	9.19	7.91	9.95	9.79	7.03	9.53	7.75	8.29	8.46
Na_2O	2.20	1.85	2.07	1.89	2.62	2.46	5.74	1.78	2.00
K_2O	0.36	0.74	0.26	0.31	2.28	0.60	0.68	0.20	0.62
P_2O_5	0.38	0.35	0.26	0.21	0.69	0.19	0.82	0.19	0.34
CO_2	0.39	0.31	0.89	0.22	0.22	N.D.	9.69	9.11	9.52
S	0.33	0.07	0.17	0.58	0.12	0.06	0.22	0.15	0.21
$H_2O^{\pm}$	3.78	5.98	2.30	0.75	2.77	2.79	0.57	1.39	1.21
Total	99.47	99.17	99.26	99.75	98.24	99.46	100.49	99.92	98.18

N.D. Not determined.

of Al_2O_3 with increasing SiO_2. A group of Cycle III dolerites have relatively high Al_2O_3 concentrations approaching 18% (recalculated), the majority of this group, including specimen 119, contain plagioclase phenocrysts suggesting early separation and accumulation of plagioclase during fractionation.

The concentration of iron (plotted as Fe_2O_3) in the alkaline rocks with less than 50% SiO_2 (recalculated)forms a cluster falling in the range 12.6% to 16.4% Fe_2O_3. Rocks with more than 50% SiO_2 (mainly attributable to Cycle III) show progressive depletion in Fe_2O_3 with increasing SiO_2 values.

There is a complete scatter of points for MnO concentrations versus SiO_2 and no meaningful trends are discernable.

Both MgO and CaO show progressive depletion with increasing SiO_2 in rocks of the alkaline suite. There is considerable overlap between the concentrations of these oxides in the Cycle II and Cycle III dolerites. With few exceptions, recalculated MgO values fall in the range 5% to 8%, and CaO values in the range 9% to 11%, in rocks with less than 50% SiO_2 (recalculated).

Alkaline rocks with less than 50% SiO_2 (recalculated) have Na_2O concentrations in the range 1.8% to 2.6% with the exception of sample 748 which has anomalously high Na_2O. Cycle III rocks with more than 50% SiO_2 show a progressive increase in Na_2O concentrations with increasing SiO_2 values. K_2O enrichment is more marked than that of Na_2O in rocks with more than 50% SiO_2, though specimen 745 has relatively low K_2O. There is complete overlap of K_2O concentrations in rocks of Cycle II and Cycle III with less than 50% SiO_2 (recalculated). It must be noted that some of the more basic members of the suite plot in the tholeiitic field of the alkali silica diagram (see Chapter 3 Fig. 3.2) but that derivative types lie clearly within the alkaline field.

P_2O_5 values plotted against SiO_2 form a scatter but, in general,

the underlying trend is towards increased P_2O_5 concentrations with increased SiO_2. The dolerites and picrites of Cycles II and III with less than 50% SiO_2 (recalculated) have less than 0.4% P_2O_5 with the exception of samples 102 and 748 which are anomalous. In varieties with recalculated SiO_2 in excess of 50%, values of up to 0.98% P_2O_5 have been recorded (specimen 1320).

Sulphur was originally treated as a trace element during analysis but was found to have a very variable range of values within the alkaline suite, concentrations as low as 100 ppm and up to 9000 ppm being recorded. As many of the rocks have S in excess of 1000 ppm (0.1%) it is treated here as a major constituent. Recalculated sulphur concentrations plotted against SiO_2 form a scatter, there is some evidence of lower S concentrations in rocks with SiO_2 in excess of 50%, however this is not clear. The range of S concentrations in the rocks with less than 50% SiO_2 is considerable and there is complete overlap of the ranges of S values in Cycle II and Cycle III dolerites. It is proposed that levels of S concentration are, at least in part, secondary, reflecting overprinting of original concentrations by post magmatic mineralization. S is normally present as pyrite, however in Sample 135 (Cycle III) it is largely in the form of disseminated pyrrhotite which may be a primary phase in this rock. There is no evidence of primary immiscible sulphide liquids such as those reported in Icelandic volcanics by Jakobsson et al.(1973).

CIPW norms of selected alkaline rocks, calculated on the basis of the recalculated oxide percentages are set out in Table 4.7.

TABLE 4.7

C.I.P.W. Norms of nine selected alkaline rocks

Sample No.	36	61	119	135	191	435	748	783	1175
Quartz	0.71	3.83	-	-	5.72	1.47	-	-	-
Orthoclase	2.25	4.73	1.60	1.83	14.18	3.66	4.43	1.30	4.14
Albite	19.63	16.92	18.28	16.16	23.27	21.49	35.47	16.84	19.38
Anorthite	31.77	30.95	38.41	36.22	24.66	30.73	12.16	36.23	29.13
Nepheline	-	-	-	-	-	-	9.94	-	-
Clinopyroxene									
Wo	5.72	3.76	4.69	4.83	3.02	7.07	10.24	3.50	6.81
En	2.88	2.27	2.64	2.64	1.56	3.54	3.16	1.85	3.91
Fs	2.71	1.29	1.85	2.02	1.39	3.38	7.47	1.55	2.60
Hypersthene									
En	11.91	14.14	13.05	13.83	8.21	10.40	-	12.30	4.53
Fs	11.21	8.02	9.15	10.60	7.31	9.92	-	10.28	3.02
Forsterite	-	-	1.80	2.00	-	-	1.62	4.74	12.11
Fayalite	-	-	1.39	1.69	-	-	4.22	4.37	8.88
Magnetite	5.36	6.90	3.90	2.87	5.02	4.58	4.97	2.71	0.87
Ilmenite	4.18	6.19	2.26	3.53	3.72	3.15	3.67	3.48	3.23
Apatite	0.95	0.88	0.64	0.50	1.73	0.47	2.16	0.50	0.92
Pyrite	0.65	0.15	0.34	1.10	0.24	0.11	0.45	0.32	0.43
Sum.	99.93	100.03	99.98	99.84	100.03	99.99	99.96	99.97	99.95

Figure 4.2

Compositions of rocks in the Carlingford alkali basalt series in terms of normative, quartz, albite, hypersthene and olivine, plotted on the triangular diagram normative Quartz (Qz), Olivine (Ol), Nepheline (Ne), where En = Enstatite and Ab = Albite.

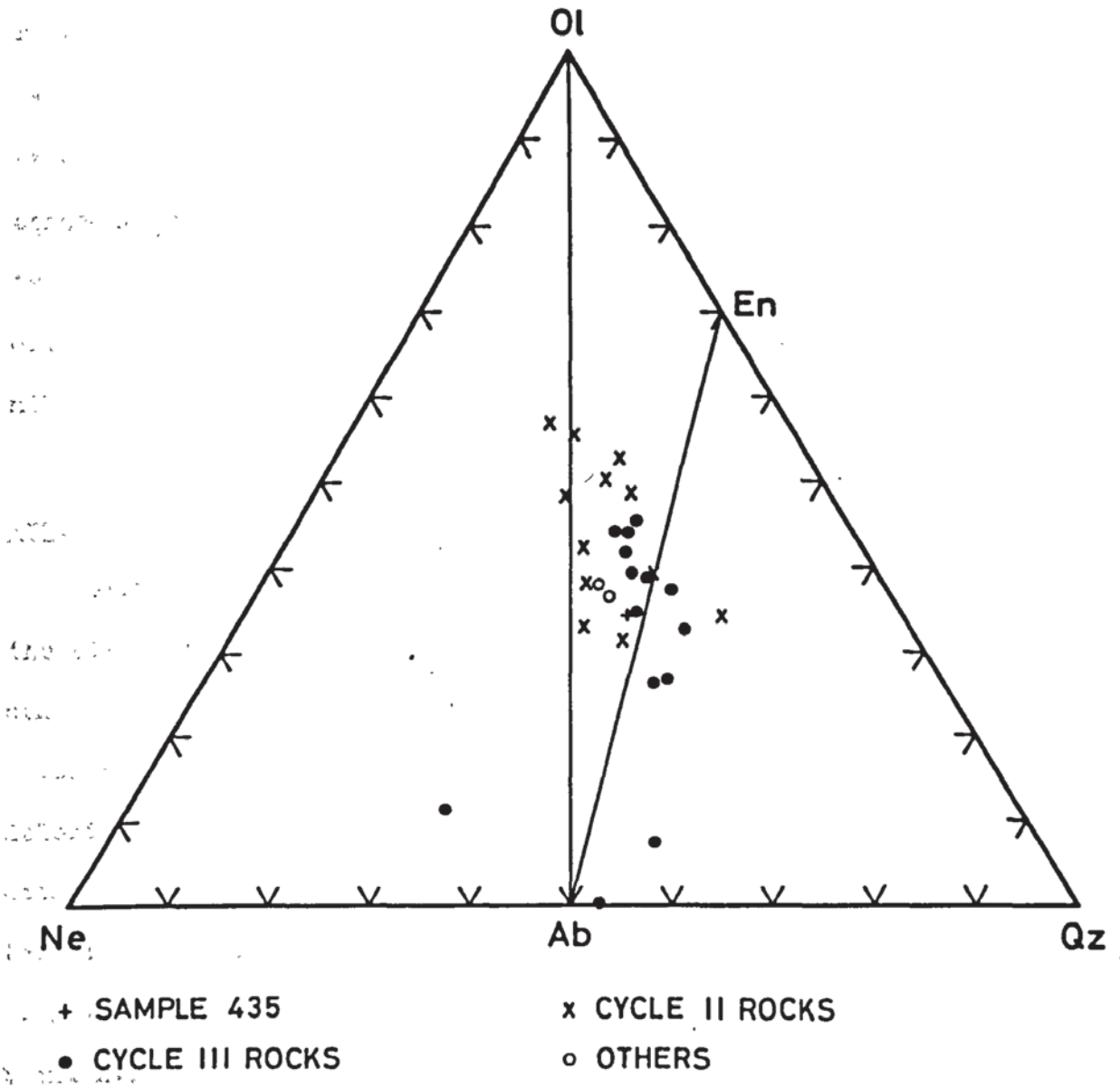

norms of other members of the alkaline suite are listed in Appendix VI. As discussed under Chapter 3 above the majority of rocks in the alkaline suite are hypersthene normative, a feature which may in part be due to alteration. The majority of Cycle II rocks are olivine, hypersthene normative, while the majority of Cycle III rocks are mildly quartz normative with the peculiar exception of 748 which, as a result of its exceptionally high concentration of Na_2O, is markedly nepheline normative. Thus the two suites tend to fall in two distinct clusters on the Nepheline, Olivine, Quartz triangle, (see Fig. 4.2). Specimen 435 (Cycle I) is mildly quartz normative.

Trace Elements

Histograms of the concentration of fourteen trace elements in the alkali dolerite suite are set out in Figure 4.3. This data is summarised and discussed below, together with the concentration of seven other trace elements which have been determined for the alkali dolerite suite. The latter group of elements (Ga,Ge,Nb,Sn,La,Th,U) either have concentrations near the detection limits of the analytical technique (see Appendix I) or incomplete coverage of the suite is available. Trace element concentrations are listed in Appendices X and XV.

The behaviour of trace elements during fractionation is summarised by Figure 4.4, in which trace element concentrations are plotted against the differentiation index (D.I.) (Thornton and

Figure 4.3

Histogram of trace element abundance frequencies in rocks of the alkali basalt series. A few exceptional values lying outside the range depicted have been excluded. (See text for details).

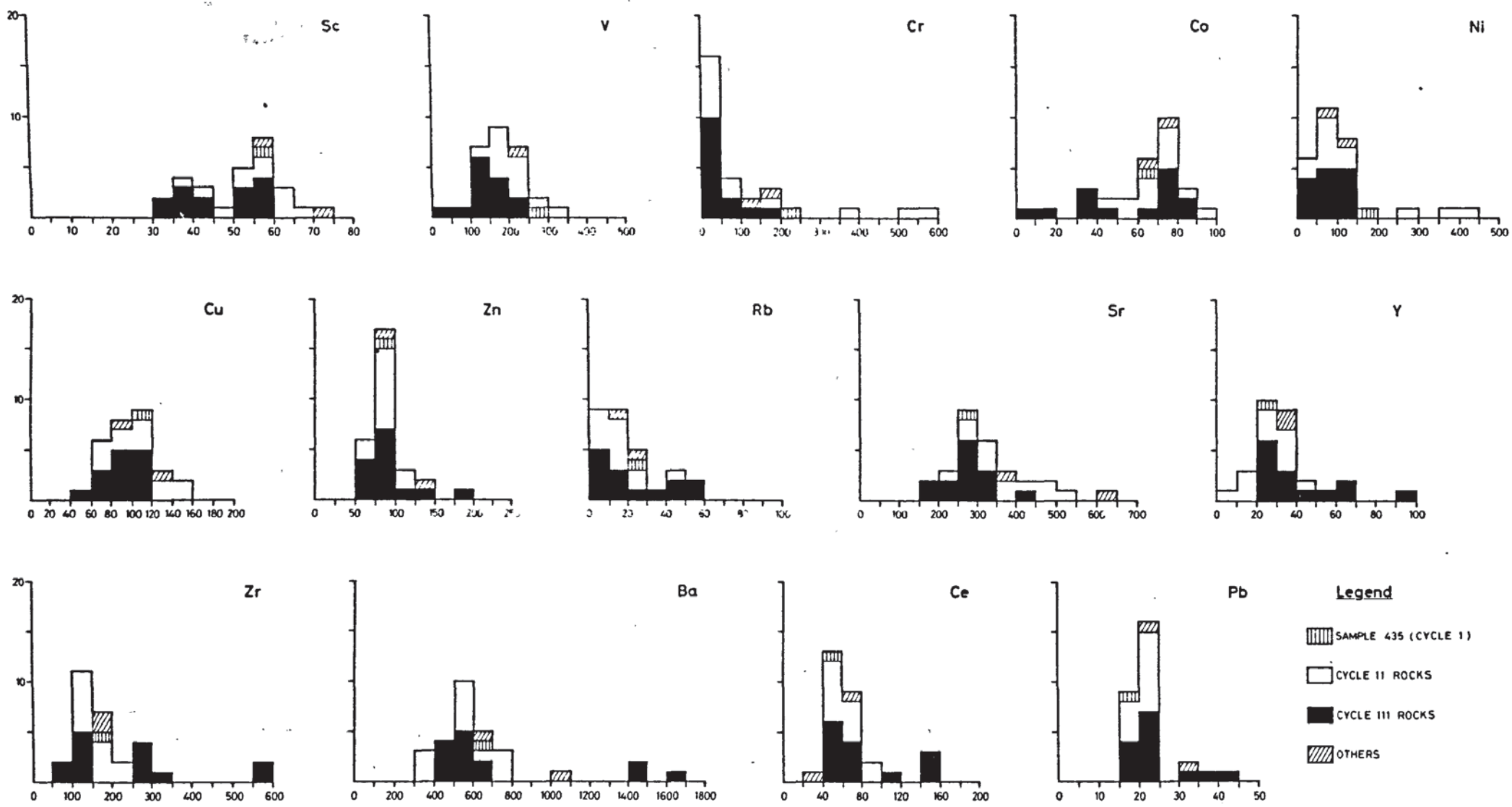

Figure 4.4

Behaviour of trace elements during fractionation in the Carlingford alkali basalt series depicted as a series of variation diagrams of concentration versus Differentiation Index (D.I.).

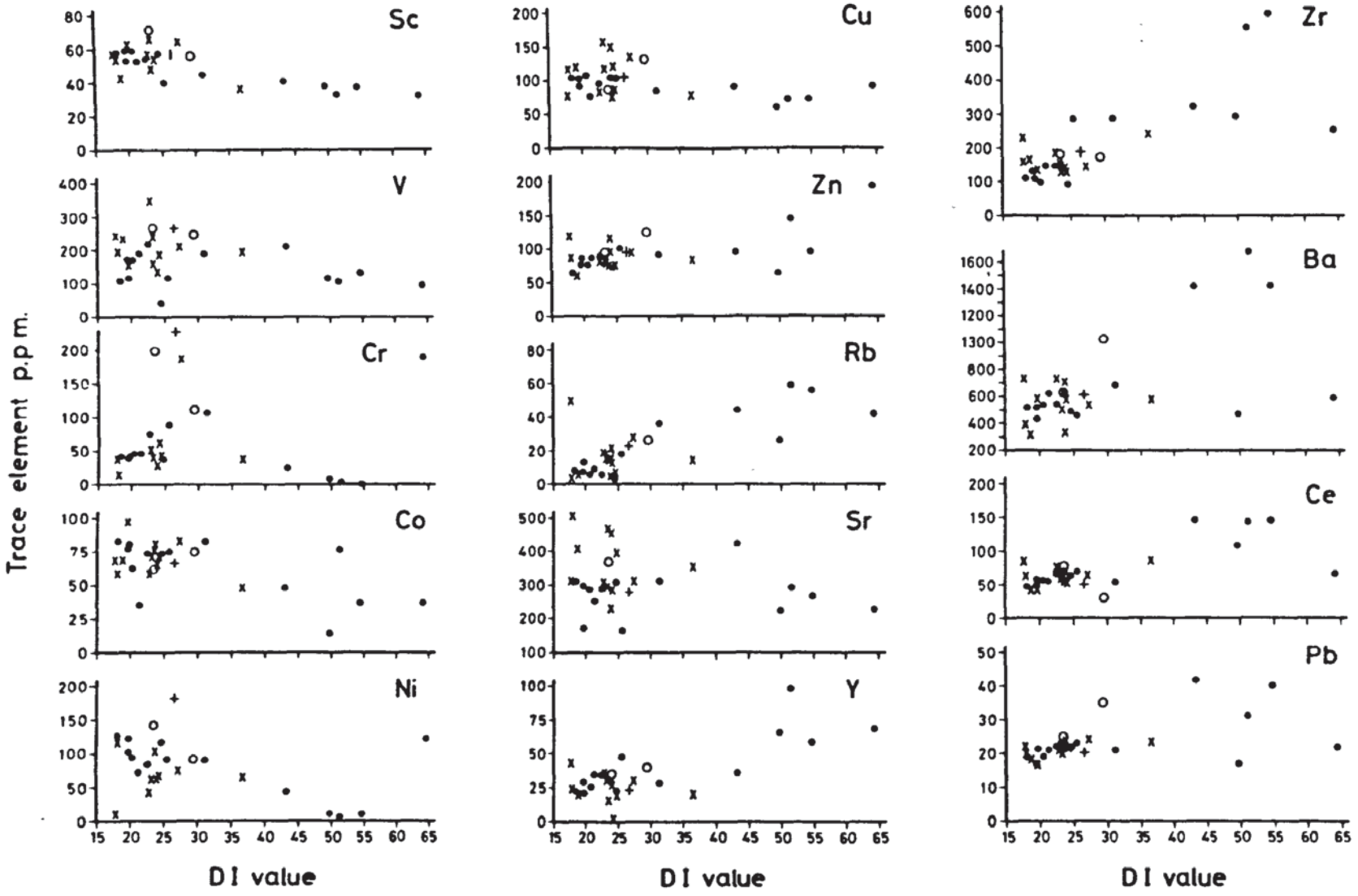

Tuttle 1960) of the rock in question.

Scandium:

Scandium concentrations fall within the range 30 to 80 ppm in the suite as a whole, with a mode at 51 to 60 ppm. The bimodality of concentrations in the Cycle III rocks reflects a chemical discontinuity discernable in the range of major element concentrations in those rocks (see below), they have Sc values between 30 and 60 ppm. The concentrations of Sc in the Cycle II rocks scatter throughout the range. Sample 435 (Cycle I) has 67 ppm Sc.

A plot of Sc versus D.I. shows that this element is depleted in the more fractionated rocks of Cycle III (Fig. 4.4). The petrochemical behaviour of Sc is not fully understood (Norman and Haskin 1968), Fryklund and Fleischer (1963) suggest that it is captured by clinopyroxene, substituting for Fe^{2+} and possibly Mg^{2+} according to Prinz (1968 p 309). The lack of Sc in olivine (Leibenburg 1960) explains the relatively low concentration of this element in the picritic varieties of Cycle II, such as 1175.

Vanadium:

Vanadium values quoted are semiquantative (see Appendix I), they range from less than 40 ppm in specimen 745 (a mugearite of Cycle III) to 344 ppm in specimen 107 (a dolerite of Cycle II), with a modal range of 150-250 ppm. Specimen 435 has a V concentration of 264 ppm. The Cycle II dolerites and picrites have concentrations in the range 100 to 350 ppm, while the alkali dolerites and related

rocks of Cycle III have vanadium concentrations ranging from 30 to 250 ppm.

Figure 4.4 includes a plot of V concentrations in Cycle III alkaline rocks against D.I. which indicates there is an increase in V values during the early stages of fractionation as reported by Wager and Mitchell (1951) and Wilkinson (1959). During the later stages of fractionation V shows progressive depletion. Prinz (1968) indicates that Vanadium is diadochic with Fe^{3+} and is most abundant in magnetite, Hafner (1960) suggests that V may also substitute for the Ti in the ore phases. This substitution of V for Ti in the Carlingford alkaline rocks is confirmed by the covariance of these elements.

Chromium:

Chromium concentrations fall in the range 0 to 600 ppm in the alkali dolerite suite, the highest Cr values being recorded for the picritic varieties of Cycle II (specimen 807 and 1175). The majority of the dolerites in the suite have Cr values between 0 and 100 ppm, the most fractionated rocks having very low concentrations. The high concentration of Cr in the picritic rocks of Cycle II as reflected by the bimodality shown in Fig 4.3, may be explained by the presence of inclusions of chrome-spinel in cumulate olivine (Prinz 1968) as olivine itself discriminates against Cr (Turekian 1963), specimen 1175 also contains xenocrysts of spinel. Removal of olivine with included spinel from the melt would leave derivative liquids depleted in Cr (see Fig.4.4). The alkali dolerites of

Cycle III also show Cr depletion with fractionation (see Fig 4.4), the high Cr value for sample 745 is considered anomalous.

Cobalt:

Cobalt values for the alkali dolerite suite fall in the range 0 to 100 ppm with concentrations in the range 71 to 80 ppm forming the mode. The Cycle II rocks have Co concentrations in the range 40 to 100 ppm while rocks of the Cycle III suite have Cr values spanning virtually the whole range, reflecting the greater degree of fractionation among them. The bimodality of the Cycle III values (Fig.4.3) reflects the chemical discontinuity in this suite discussed under "Fraction Trends" below. As with Cr, Co shows depletion with increasing fractionation, and complementary enrichment in picritic rocks bearing cumulus olivine such as those of Cycle II (See Fig. 4.4). Olivine and pyroxene provide the majority of sites for Co (Prinz 1968 p 299).

Nickel:

The behaviour of Ni also mirrors that of Cr (see Fig. 4.4). The majority of rocks in both the Cycle II and Cycle III suites have Ni concentrations in the range 0 to 150 ppm, with those rocks which have undergone more advanced fractionation showing Ni depletion. The picritic rocks of Cycle II show enrichment in Ni with concentrations up to 432 ppm (sample 1175) being recorded. In general the rocks of Cycle II have Cr:Ni rations in excess of 1, while the majority of those attributed to Cycle III have Cr:Ni

ratios less than 1, presumably reflecting intitial concentrations in the parent magmas. Specimen 435 (Cycle I) has a relatively high Ni value (182 ppm) and a Cr:Ni ratio of 1.25. Nickel concentrations have a modal range between 50 and 100 ppm in Fig. 4.3.

Copper:

Copper concentrations fall in the range 40 to 160 ppm, the rocks of Cycle II ranging from 60 to 160 ppm Cu and those of Cycle III 40 to 140 ppm. 435 has a copper content of 107 ppm which falls in the modal range of 101 to 120 ppm. Copper shows depletion with advanced fractionation in the Cycle III rocks.

Zinc:

All but one of the alkaline rocks (specimen 745) have Zn values between 50 and 150 ppm. Specimen 745, a Cycle III benmorite has a Zn value of 195 ppm. The range of Zn concentrations in dolerites of Cycles II and III are essentially similar with a modal range of 75 to 100 ppm. The Cycle I dolerite 435 has a Zn concentration of 95 ppm (within the modal range). As indicated by sample 745, the Cycle III rocks shown Zn enrichment in the later stages of fractionation.

Rubidium:

Rubidium is concentrated in feldspars and feldspathoids (Prinz 1968) and is thus enriched in the later stages of fraction-

ation, this is particularly true of the alkaline rocks of Cycle III (see Fig. 4.4). Rb values for the suite as a whole fall in the range 0 to 60 ppm, only the more fractionated members of Cycle III suite have Rb values in excess of 30, with the exception of sample 135 (Cycle II) which is considered anomalous.

Strontium:

The range of Sr concentrations displayed by the alkali dolerite suites of Cycle II and Cycle III are contrasting (see Fig. 4.3). The Cycle II rocks have Sr values between 250 and 650 ppm while the majority of Cycle III rocks have Sr concentrations in the range 150 to 350 ppm, the exception is 191 with 425 ppm Sr. The modal concentration range of Sr in the suite as a whole is 251 to 300 ppm. Specimen 435 (Cycle I) has a Sr value of 280 ppm. Prinz indicates that Sr is most concentrated in the feldspars (1968 p 311) where it is admitted by Ca (Le Bas 1970a).

Figure 4.4 suggest that Sr is first enriched, as reported by Turekian and Kulp (1956) and Wager and Mitchel (1951), then depleted with advancing fractionation in the Cycle III rocks, however such an interpretation is dependant on the accuracy of one determination (191) and is therefore tenuous. Specimens 64 and 61 apparently have anomalously low Sr values, possibly reflecting degrees of alteration. Rb:Sr ratios show progressive increase with advancing fractionation in the rocks of Cycle III.

Yttrium:

Yttrium values for the Carlingford alkaline dolerite suite fall in the range 0 to 100 ppm. Alkali dolerites attributed to Cycle II have Y concentrations between 0 and 50 ppm. Cycle III rocks have Y values ranging from 20 to 80 ppm, the slight bimodality of Y concentrations in Cycle III rocks apparent in Fig. 4.3 is not considered significant. Specimen 435 has a Y value of 24 ppm which falls in the modal range of 20 to 40 ppm for Y concentrations in the suite as a whole.

As Y values in Cycle II rocks are generally lower than in members of the Cycle III suite while Sr concentrations are higher, Sr:Y ratios are greater in the majority of Cycle II rocks. A plot of Sr:Y ratios versus Cr:N: ratios for the two suites discrimates them with a high degree of success (Figure 4.5).

Y is concentrated in apatite and, to a lesser extent, in pyroxenes (Wilkinson 1959) and opaque phases (Cornwall and Rose 1957). In the alkaline dolerite suite of Carlingford it shows enrichment in more fractionated varieties (see Fig. 4.4) suggesting an increased quantity of modal apatite in these rocks as reflected by relatively high P_2O_5 concentrations.

Zirconium:

The majority of rocks have Zr values between 50 and 350 ppm. Specimens 1320 and 1382, both attributed to Cycle III, have Zr concentrations in excess of 550 ppm. Figure 4.4 shows progressive Zr enrichment with advancing fractionation in Cycle III rocks,

Figure 4.5

Sr : Y values plotted against Cr : N values for rocks of the Carlingford alkali basalt series. (See Fig. 4.1 for explanation of symbols). The diagonal line separates the majority of Cycle 11 rocks from those of Cycle 111, and is adopted as a means of establishing the relative age of alkaline rocks occurring within the complex, where uncertain.

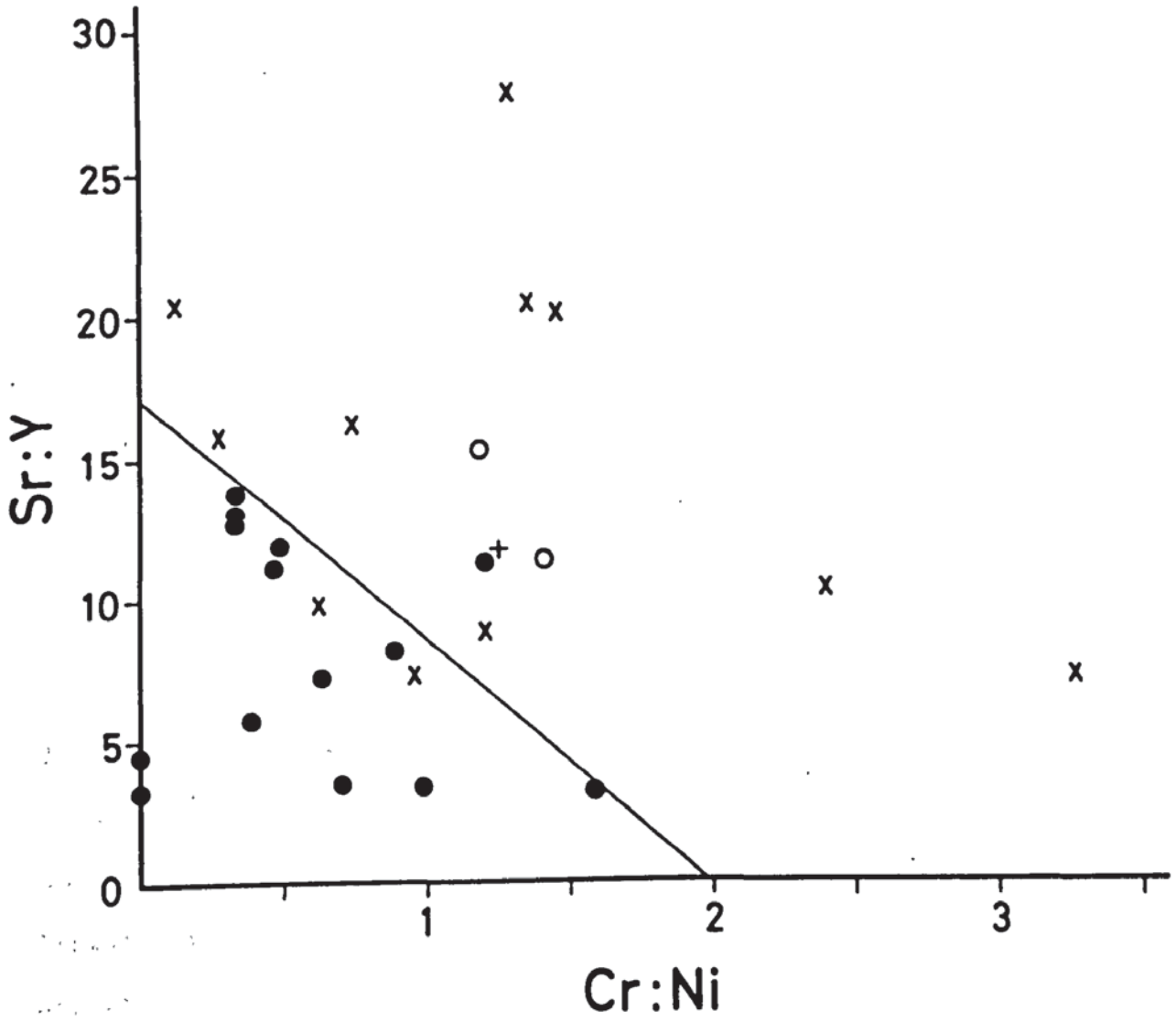

however Fig. 4.3 shows that Zr concentrations in rocks, other than 1320 and 1382, form two distinct clusters. This bimodality reflects the distribution of K_2O in the Cycle III rocks, those with less than 0.5 K_2O also having low Zr concentrations, and is emphasized by the chemical discontinuity apparent in the suite (see below). The modal concentration of Zr in the alkaline suite as a whole is in the range 100 to 150 ppm. The Cycle II members of the suite form a coherent group with Zr values between 100 and 250 ppm reflecting the limited degree of fractionation in these rocks. Specimen 435 (Cycle I) has a Zr concentration of 191 ppm.

Barium:

Ba values range from 314 to 1675 ppm, with concentrations between 500 and 600 ppm forming the mode. Specimen 435 has a Ba value of 603 ppm. The Cycle II dolerites fall in the range 300 to 800 ppm Ba in three families, this is not considered significant and is attributed to sampling bias and/or alteration.

The majority of Cycle III rocks have Ba values in the range 400 to 700 ppm. Only those rocks at a more advanced state of fractionation and with K_2O in excess of 2% show marked Ba enrichment, again the bimodality of Ba in part reflects a true or apparent chemical discontinuity. The covariance of Ba with K is well known (Prinz 1968), Barium substituting for Potassium in the feldspars and feldspathoids. Le Bas has suggested that Ba may be admitted by Ca in the plagioclases in the Carlingford layered gabbros (1970a p 72),as indicated by the work of Sen (1960), however the

covariance of Ba with K indicates that this is not the case in the alkaline rocks. Nockolds and Allen (1953) predict constant or increasing K:Ba ratios with increased fractionation. The alkali dolerites of Cycle III show increasing K:Ba with increasing differentiation indesces.

Cerium:

Cerium shows a similar distribution to that of Ba in the rocks of the alkaline suite, exhibiting increasing concentration of Ce with advancing fractionation in the Cycle III suite, and covariance with K_2O. Concentrations for the suite as a whole fall in the range 20 to 160 ppm. The Cycle II rocks have Ce values between 40 and 100 ppm, while the more fractionated potash rich Cycle III rocks have up to 150 ppm Ce. The modal concentration range of Ce for the suite as a whole is 41 to 60 ppm, specimen 435, with a Ce value of 50 ppm, falls within that range.

Lead:

The majority of the rocks in the alkaline suite have lead values in the range 15 to 25 ppm, all the Cycle II rocks and specimen 435 (Cycle I) fall within this range as do the majority of Cycle III rocks. However as with Zr, Ba and Ce, Cycle III rocks showing K_2O enrichment also show Pb enrichment with advancing fractionation (the maximum recorded Pb concentration for a rock in this suite is 42 ppm - specimen 191). This indicates that Pb is admitted by K in the feldspars as suggested by Ringwood (1955)

and Wedepohl (1959). In the Carlingford layered gabbros it is captured by Ca (Le Bas 1970a p 71).

Gallium:

Most rocks in the alkaline suite have Ga values between 15 and 21 ppm. the fractionated rocks of Cycle III, which show potash enrichment, have Ga values as high as 25 ppm.

Germanium:

Germanium concentrations in the alkaline suite are at the limits of detection, the highest recorded value being 3 ppm.

Niobium:

Niobium values in the majority of alkaline dolerites and associated picritic rocks are at the limits of detection, values of 10 ppm or less being recorded. Nb shows enrichment in the fractionated rocks of Cycle III, with a value of 98 ppm being recorded for specimen 748 which is Na_2O rich (see Appendix XV).

Tin:

Sn values in the alkaline suite are low and at the limits of detection, the highest values, up to 8 ppm, being recorded from the K_2O rich fractionates of Cycle III.

Lanthanum:

Lanthanum enrichment occurs in the K_2O rich fractionates of

Cycle III, 53 ppm La being recorded for specimen 191. Other rocks in the alkaline suite have La values at the limits of detection - less than 10 ppm.

Thorium:

Thorium values for the majority of rocks in the alkaline suite rarely exceed 10 ppm and are at the limits of detection. Rocks of the Cycle III suite rich in K_2O have Th values up to, and including, 14 ppm.

Uranium:

Uranium values for the suite as a whole are at the limits of detection, the highest concentrations, 3 ppm, being recorded for the more fractionated rocks of Cycle III.

Fractionation trends

Figure 4.6 is a plot of a series of oxide concentrations versus differentiation index (D.I) for suite as a whole. MgO shows progressive depletion in rocks with increasing D.I. (increasing fractionation). CaO also shows depletion with increasing D.I. but due to scatter the trend is not so clear. Total Fe, calculated as Fe_2O_3, remains relatively constant between about 13% and 16% in rocks with D.I. less than 40, in rocks with D.I. greater than 40 Fe shows progressive and rapid depletion. TiO_2 shows depletion in rocks with D.I. higher than 30, Figure 4.6 also indicates however, that there is an increase in TiO_2 concentrations with fractionation

Figure 4.6

Changes of composition within the Carlingford alkali basalt series during fractionation, depicted by a series of variation diagrams of major element oxides (analyses recalculated to 100% volatile free), versus Differentiation Index (D.I.).

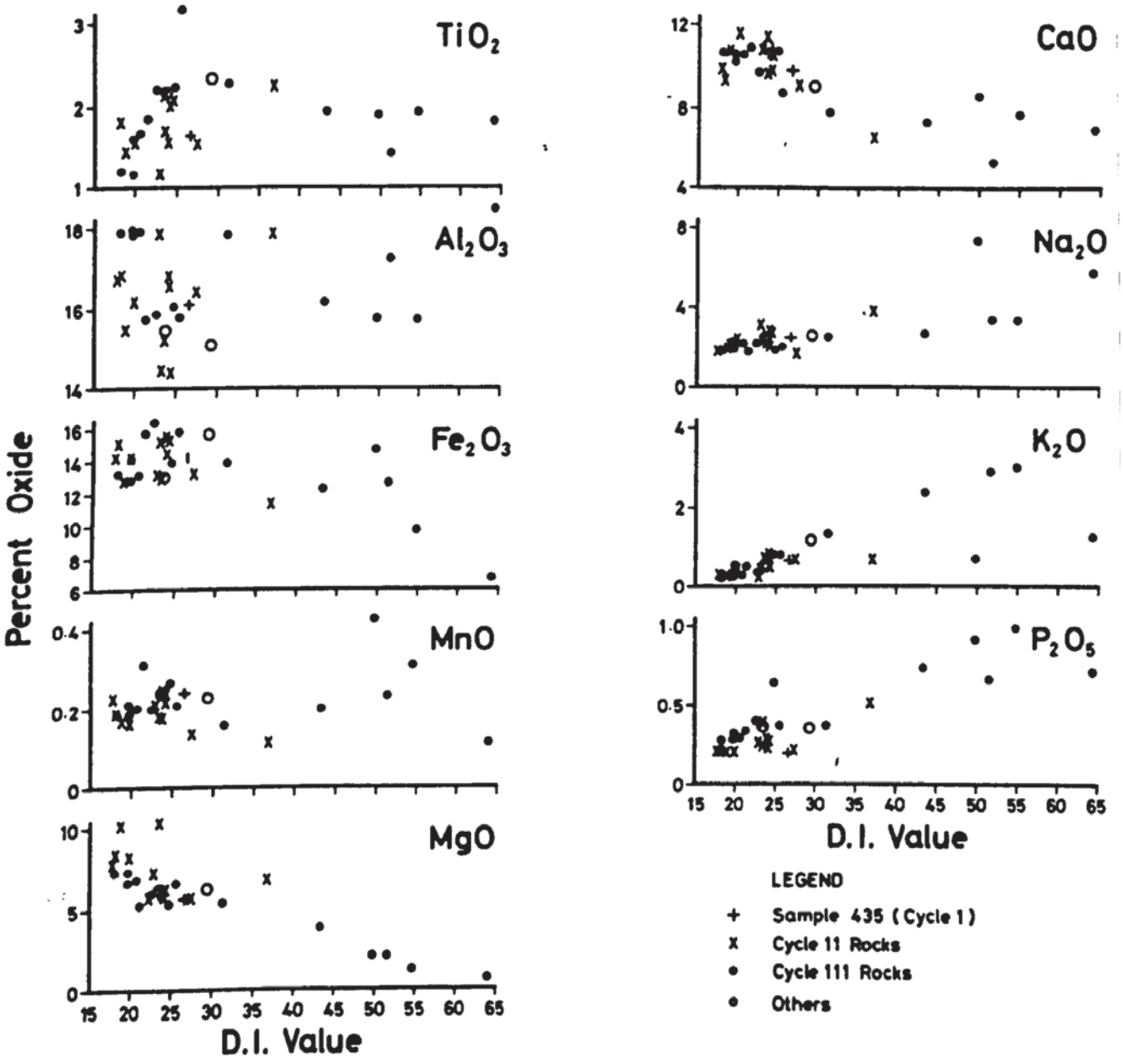

in rocks with D.I. less than 30. By comparison the alkalies K_2O and Na_2O, together with P_2O_5, show progressive enrichment with increasing D.I. throughout the range.

Plotted on an A.F.M. diagram,

$$A = \frac{(Na_2O + K_2O) \times 100}{FeO + 0.9\ Fe_2O_3 + MgO + K_2O + Na_2O}$$

$$F = \frac{(FeO + 0.9\ Fe_2O_3) \times 100}{FeO + 0.9\ Fe_2O_3 + MgO + K_2O + Na_2O} \quad \text{and}$$

$$M = \frac{MgO \times 100}{FeO + 0.9\ Fe_2O_3 + MgO + K_2O + Na_2O},$$

(Coats 1968 p 693), all rocks in the Carlingford alkaline suite show high iron concentrations relative to MgO (see Fig. 4.7).

The alkaline rocks of Cycle I have not been identified in sufficient number to enable proper investigation of petrochemical processes within that group. Only one has been analysed at Nottingham, specimen 435, it proves to be an alkaline dolerite, fairly typical among the doleritic members of the suite in terms of composition, it has relatively high Cr and Ni values, a similar rock 434 has been analysed at Reading (see Appendix XV).

The alkaline rocks of Cycle II do not display advanced fractionation. No analysed member of the group has D.I. in excess of 40. The dolerites are Fe rich and are accompanied by more Mg rich picritic varieties with abundant phenocryst olivine. The trend, albeit slight, towards further Fe enrichment exhibited by this group on the A.F.M. diagram suggest olivine fractionation from a magma approaching specimen 783 in composition, giving rise to the picritic accumulates and MgO depleted derivatives.

Figure 4.7

Composition of rocks in the Carlingford alkali basalt series in terms of $Na_2O + K_2O$, Fe as FeO and MgO plotted on the triangle A.F.M. For explanation of symbols see Fig. 4.1.

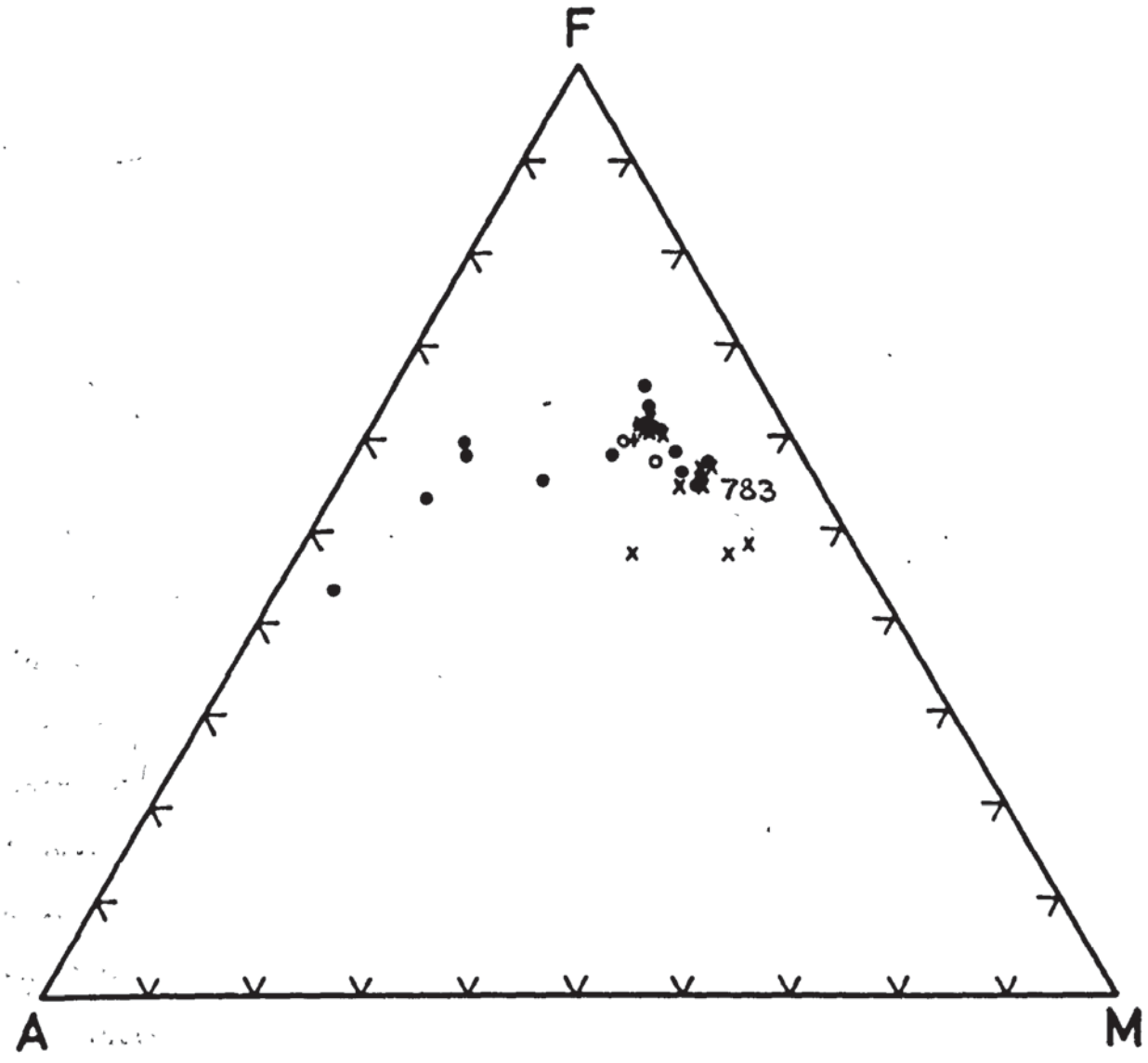

Olivine fractionation is also indicated by the behaviour of Cr, Co and Ni which show depletion in more fractionated derivatives and marked enrichment in the picrites.

The rocks of Cycle III also show an initially high iron content, followed by relative enrichment of Fe during the early stages of fractionation (see Fig. 4.7), with further fractionation Fe decreases. Cr, Co and Ni show depletion with fractionation in these rocks too but picritic accumulates with relatively high concentrations of those elements have not been recognised. Olivine is present as a phenocryst phase in some of the dolerites attributed to this group (specimen 119 for example), and olivine fractionation is therefore assumed to play an important role within it. Consideration of the relative concentrations of Na_2O and K_2O in rocks showing more advanced fractionation shows that two divergent fractionation trends are present (see Fig. 4.8), one giving rise to derivatives enriched in Na_2O and of mugearite/benmorite affinities, and a second, more well developed, trend showing K_2O enrichment relative to Na_2O and attributed to the trachy basalt/tristanite series. Olivine fractionation accompanied later by titanomagnetite separation could have given rise to the mugearite benmorite series, however enrichment of K_2O relative to Na_2O in the trachy basalt - tristanite series required the removal of a soda bearing phase from the parent melt. Plagioclase accompanies olivine as a phenocryst phase in many of the dolerites of this group, and as CaO shows progressive depletion with fractionation in these

Figure 4.8

Variation diagram of K_2O versus Na_2O (analyses recalculated to 100% volatile free) for rocks in the Carlingford alkali basalt series. The Cycle 111 suite shows two divergent trends, A. showing potash enrichment, the trachy basalt - tristanite series, and B, soda enrichment, the hawaiite - mugearite - benmorite series. For explanation of symbols see Fig. 4.1.

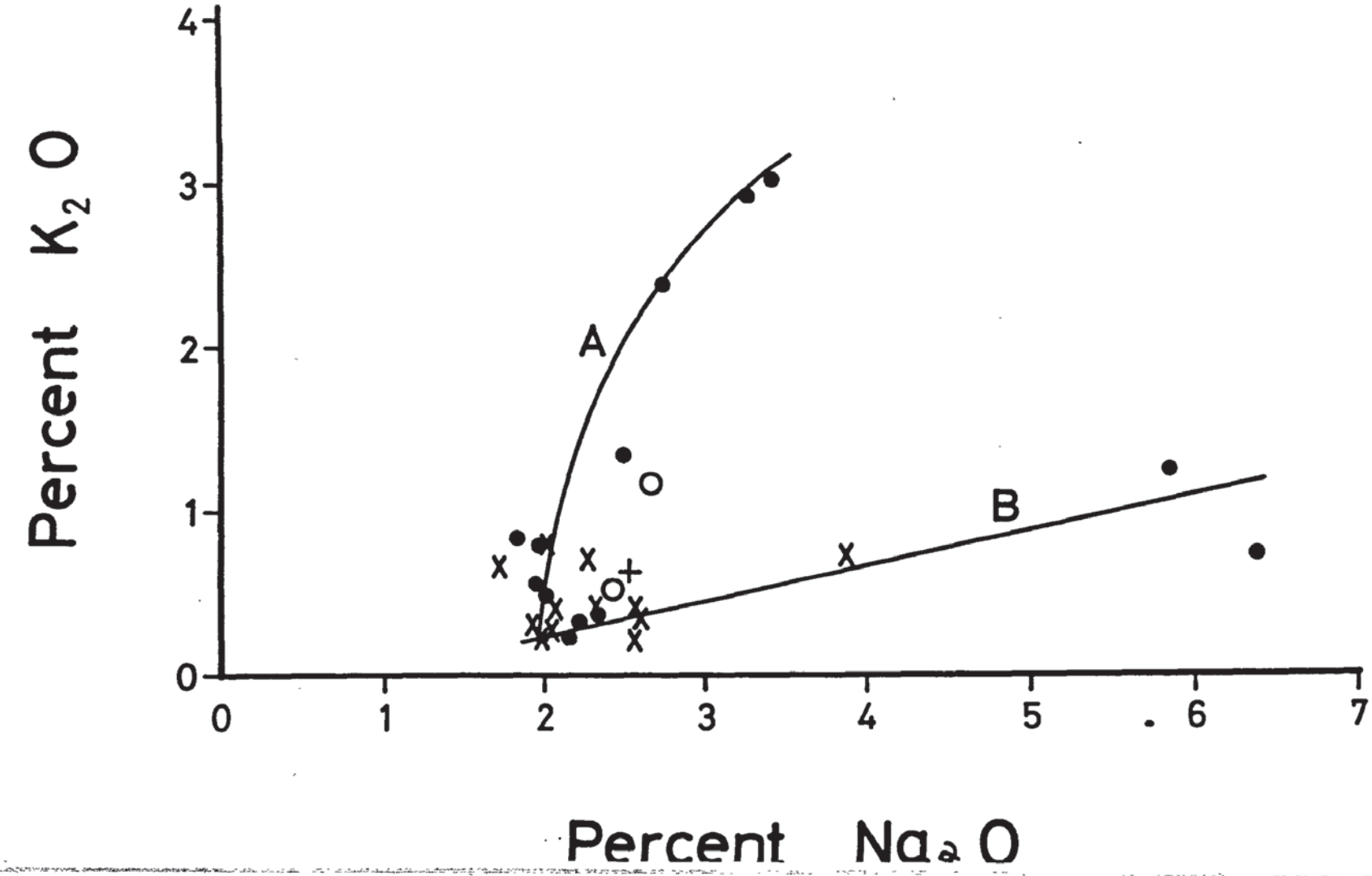

rocks, it is considered that simultaneous separation of olivine and plagioclase, and later fractionation of titanomagnetite, gave rise to the series in question. Fractionation involving the separation of plagioclase and olivine is suggested as having taken place in the alkali basalts of the Small Isles by Ridley (1971a p 265).

Plots of K_2O, Na_2O and MgO against CaO (Fig. 4.9) show that the alkalies are enriched in rocks with low CaO while MgO is depleted as expected. Also that K_2O is more rapidly enriched in the rocks of the high potash series than in those of the sodic series but that Na_2O concentrations in the high potash series increases only gradually with decreasing CaO, reflecting the extraction of Na_2O in fractionating plagioclase. MgO shows significantly greater depletion in soda rich fractionates than in the potassic varieties with the same CaO concentrations. Plotting K_2O and Na_2O against MgO shows that the K_2O and Na_2O concentrations of the sodic mugearite-benmorite series fall near to olivine control lines passing through the dolerite field, indicating that such derivatives may be formed by simple olivine fractionation. The trachy basalt tristanite series on the other hand, show K_2O concentrations that are higher, and Na_2O concentrations that are lower, than can be explained by simple removal of olivine alone (see olivine control lines). As olivine fractionation plays an important role in the development of both series, the recorded depletion of Cr, Co and Ni in more fractionated derivatives is explained. The behaviour of other trace

Figure 4.9

Variation diagrams of K_2O, Na_2O and MgO versus CaO (analyses recalculated to 100% volatile free) for rocks in the Carlingford alkali basalt series. The Cycle 111 trachy basalt - tristanite trend A, and the hawaiite - mugearite - benmorite trend B, are indicated. For explanation of symbols see Fig. 4.1.

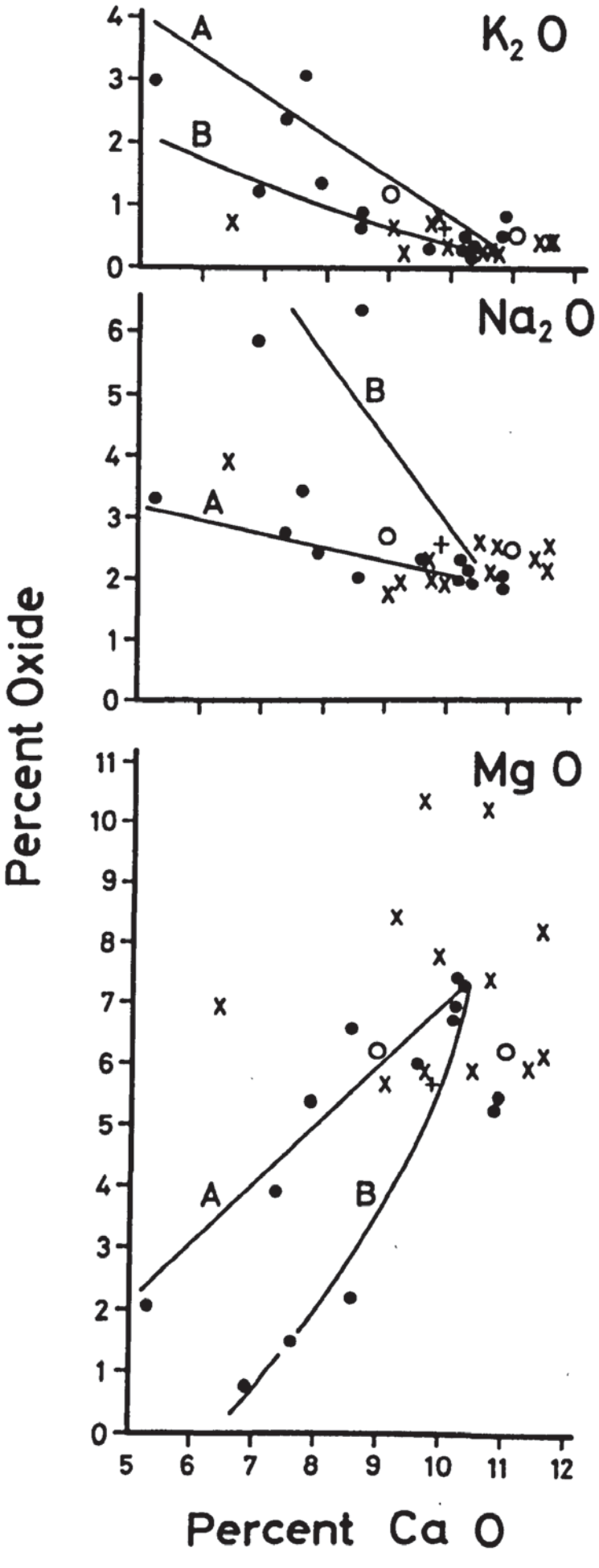

Figure 4.10

Variation diagrams of K_2O and Na_2O versus MgO (analyses recalculated to 100% volatile free) for rocks in the Carlingford alkali basalt series. The Cycle 111 trachy basalt - tristanite trend A, and the hawaiite - mugearite - benmorite trend B, are indicated, as are the olivine (Fo_{60}) control lines O - O'. For the explanation of symbols see Fig. 4.1.

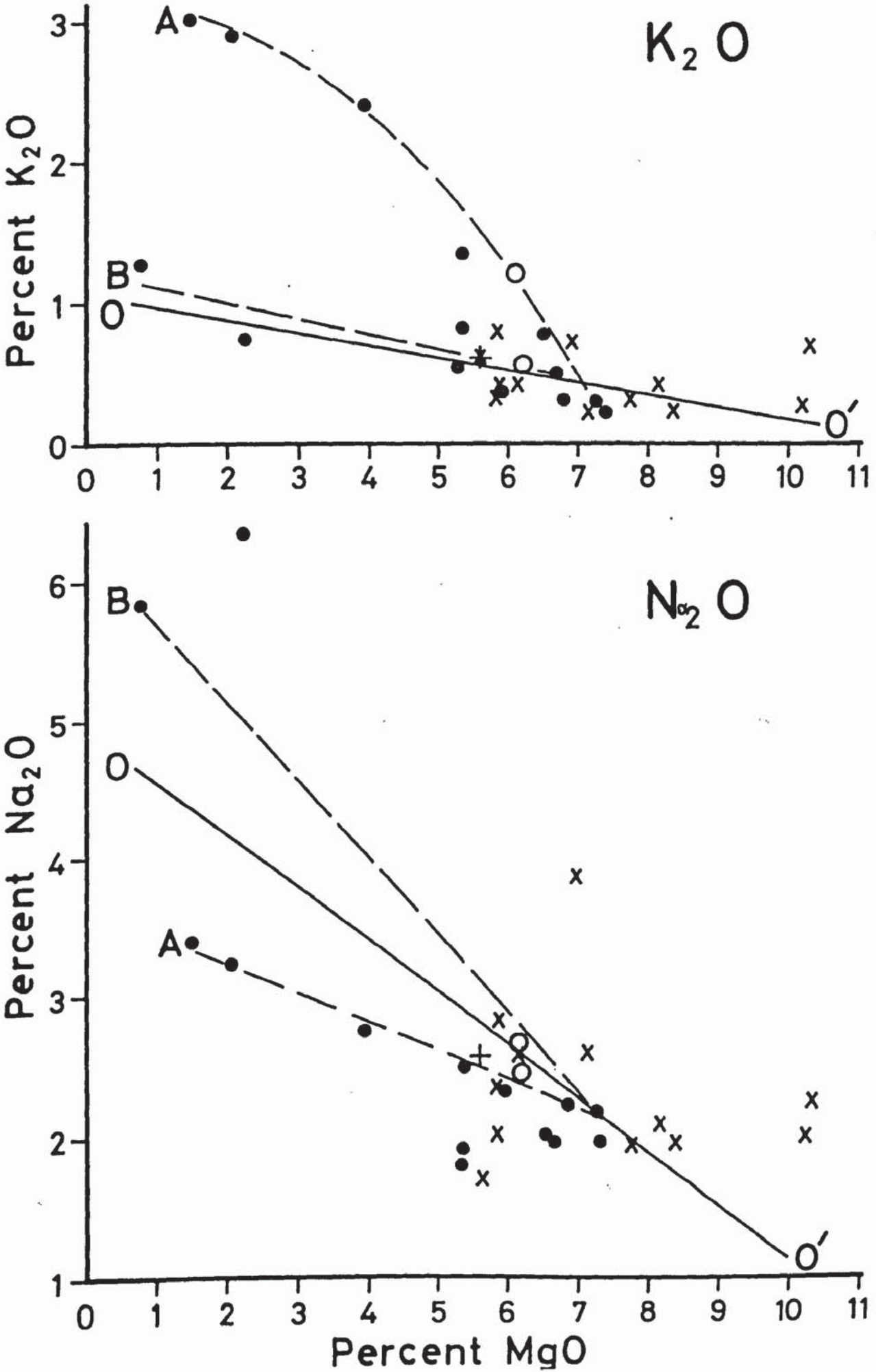

elements largely reflects the major element chemistry. Sc is depleted with fractionation, Rb and Y become more concentrated in the rocks with higher concentrations of alkalies and P_2O_5, ie in more fractionated derivatives. Zr, Ba and Ce also show enrichment with fractionation particularly in the high potash series, for like Pb they show covariance with K_2O. Sr appears to show enrichment in the middle stages of fractionation, probably entering the plagioclases at these compositions most readily, leaving later fractionates to be depleted in this element.

The depletion of Fe during the later stages of fractionation indicates the appearance of significant quantities of ore on the liquidus in both the sodic and the potassic series, this is reflected by the marked increase in modal titanomagnetite at this stage (see samples 61 and 191). In specimens 36 and 119 ore concentrations in the mode are relatively low, indicating a low oxygen fugacity at this stage of fractionation, as a result Ti entered the pyroxenes in preference to the ore phases. Olivine or olivine plus plagioclase separation in these conditions gave rise to iron-enrichment in the early stages of fractionation as observed. Olivine separating from iron-enriched melts was itself iron-rich with compositions such as that of the"olivine" occurring in sample 61. A subsequent increase in the availability of oxygen in the middle and later stages of fractionation led to separation of significant quantities of titanomagnetite and Fe depletion (Ridley 1971a p 281). With increased oxygen fugacity,

titanium entered the ores in preference to the pyroxenes as indicated by the increase of ulvospinel solid solution in the ores of specimen 61. Thus the depletion of Fe and TiO_2, and the increase in modal ore during middle and late stages of differentiation, and, the recorded variation in the partitioning behaviour of TiO_2 in coexisting pyroxenes and titanomagnetite can be accounted for by this mechanism. The behaviour of V reflects that of TiO_2 showing initial enrichment followed by subsequent depletion, V follows Ti into the ores.

Finally it should be noted that there is an apparent gap in the range of compositions exhibited by both the sodic and potassic series of Cycle III (see Figs. 4.4 and 4.6) and also in trace element concentrations in those rocks. This gap may be attributable to sampling bias, it may alternatively reflect a real chemical discontinuity at the basalt - andesite transition i.e. in rocks with D.I. values approaching 40 as discussed by Thompson (1972). Thompson proposes fractionation involving separation of interstitial liquids from a partly crystallised rigid magma, as a mechanism which could give rise to such a petrochemical discontinuity, and the possibility that such a mechanism operated at Carlingford during the fractionation of the alkali basalts of Episode IIId is not ruled out.

Summary

a) Three episodes of intrusion of alkaline dolerite dykes have been recognised, the earliest of which is currently only

represented by two analysed samples. The Cycle II (north west - south east dykes) and Cycle III (orthogonal tangential dykes), rocks can be distinguished on petrological grounds, they also show petrochemical differences most noteably in Cr:Ni and Sr:Y ratios which when used in conjunction provide a highly successful means of discrimination.

b) All the alkaline dolerites show initial iron-enrichment, subsequent fractionation lead to further iron-enrichment then depletion in iron. Rocks of the Cycle II series underwent olivine fractionation giving rise to accumulative picritic derivatives. Only the Cycle III suite has highly fractionated derivatives, these show fractionation giving rise to a sodic series and a potassic series, the former by separation of olivine and the latter by separation of olivine and plagioclase together.

c) During the middle and later stages of fractionation in the Cycle III rocks oxygen fugacity increased, enabling separation of significant quantities of ore which was relatively TiO_2 rich.

d) The progressive depletion of Sc, Cr, Co and Ni, the enrichment of Rb, Y, Zr, Ba, Ce and Pb and the initial enrichment and subsequent depletion of V and Sr in the Cycle III suite, confirm the operation of the fractionation processes described.

e) The possible operation of a "filter press" mechanism during fractionation such that highly fractionated liquids were expelled from a semi crystallised rigid magma as described by Thompson (1972) is indicated by a petrochemical discontinuity

and bimodal distribution of trace element concentrations in the alkali dolerites of Cycle III.

CHAPTER 5

THE PETROLOGY AND PETROCHEMISTRY OF THE HIGH ALUMINA BASALT SERIES

Abstract

A number of rocks in the minor intrusions of the Carlingford Complex can be attributed to the high alumina basalt series, only those described as high alumina gabbros and feldsparphyric dolerites are true representatives of a high alumina magma series, others are plagioclase-phyric tholeiitic dolerites. The petrology, mineralogy and petrochemistry of the series as a whole are discussed. The petrochemical data leads to the conclusion that the high alumina gabbros and feldsparphyric dolerites which were injected during a single intrusive episode, were derived by fractionation of calcic plagioclase accompagnied by other phases in minor quantities, from a high alumina basalt magma.

Introduction

A number of rocks attributed to the high alumina basalt series have been identified at Carlingford (see Chapter 3, above). All tholeiitic basaltic rocks with Al_2O_3 in excess of 16.5% are classified chemically as high alumina basalts (Kuno 1968 p 625). Kuno's distinction that the alkali concentrations of high alumina basalts lie between those of tholeiitic basalts and alkali basalts (Kuno 1960) is not appropriate at Carlingford.

Rocks characterised petrographically as feldsparphyric dolerites and

high alumina gabbros are all members of the high alumina basalt series, together they constitute a single intrusive episode dominated by cone-sheet injection which took place at the end of Cycle II and at the beginning of Cycle III (episodes IIe and IIIa) in the Carlingford sequence (see Chapter 1, above). Other rocks which may be defined as high alumina basalts are also present, however they do not form a coherent suite which can be defined in petrographic terms; they are all attributable to the tholeiitic basalt series on the basis of petrography but have relatively high concentrations of plagioclase phenocrysts, hence the high Al_2O_3 values. These miscellaneous high alumina basalts occur among the tholeiitic rocks of episodes IId and IIIb and do not represent separate intrusive episodes, they are thus not considered in detail herein and are referred to again elsewhere (Chapter 6). Discussion is largely restricted to the petrology and petrochemistry of the high alumina gabbro - feldsparphyric dolerite suite, in the succeeding paragraphs.

PETROGRAPHY

The high alumina gabbros and feldsparphyric dolerites of Carlingford are identified as a suite by their time relations and their characteristic petrology. Modal compositions of selected representative members of this suite are set out in Table 5.1. The majority of rocks in the suite contain 65 to 75 percent modal plagioclase; in most feldsparphyric dolerites (samples 40, 124, 137) plagioclase phenocrysts constitute over 45% of the rock. Specimen 269 is exceptional containing only 52% modal plagioclase with phenocrysts comprising about

TABLE 5.1

Modal composition of selected high alumina basalts.

Sample Number	40	124	137	177	269	437	A
Rock Type	Feldsparphyric dolerite	Feldsparphyric dolerite	Feldsparphyric dolerite	High Alumina Gabbro	Feldsparphyric dolerite	High Alumina Gabbro	Feldsparphyric dolerite
Plagioclase (Phenocryst)	50	53	48	-	30	-	57
Plagioclase (Groundmass)	18	16	24	73	22	74	12
Clynopyroxene (Phenocryst)	-	1	3	-	1	-	-
Clinopyroxene (Groundmass)	21	16	16	16	33	12	13
Olivine (Phenocryst)	-	1	-	-	-	-	-
Olivine (Groundmass)	tr	3	3	4	-	-	-
Titano-magnetite	4	4	5	1	2	2	2
Pyrite	1	tr	-	-	-	-	-
Chlorite and uralite	3	5	1	4	8	12	16
Quartz	tr	-	-	tr	3	-	-
Calcite	1	1	-	-	tr	tr	-
Epidote	-	-	-	1	1	-	-
Interstitial material	2	1	-	tr	-	-	-
Biotite	-	-	-	-	tr	tr	-

A, Modal analysis of Feldsparphyric Dolerite by M.J. Le Bas (specimen 72 (Le Bas 1955)- sample 172 in the current investigation.)

tr = trace

30% of the rock. In the high alumina gabbros (samples 177 and 437) the majority of plagioclase occurs as large, equant, subhedral crystals up to 5mm in maximum dimension; a minor second generation of plagioclase is present as laths up to 1mm long embedded in coarse ophitic

augite which makes up the bulk of the rest of the rock. A small quantity of alkali feldspar is present as an interstitial phase in 177. In both the high alumina gabbros and feldsparphyric dolerites a basic plagioclase (compositions calculated to fall in the range An_{65} to An_{70} in specimens 40, 124 and 269,on the basis of symmetrical extinction (Deer, Howie and Zussman 1966 p 329)) formed early during crystallization. The two rock types grade into each other, the later formed ophitic clinopyroxene and a more abundant second generation plagioclase forming a continuous groundmass in the feldsparphyric dolerites. Plagioclase phenocrysts occurring in rocks of the later type have zoned rims about 0.05mm in width, they also tend to occur in interlocking aggregates up to 10mm in diameter. Occasional anhedral phenocrysts of augite also occur in some feldsparphyric dolerites (see specimens 124, 137 and 269).

Olivine, pseudomorphed by iddingsite or bowlingite, is present in the high alumina gabbros and some feldsparphyric dolerites, it occurs as large corroded phenocrysts in specimen 124 and as subhedral crystals up to 0.5mm long in the groundmass of samples 40, 124, and 137. Olivine has not yet been recognised in 437 though it is probably represented by secondary alteration products which are present throughout the rock.

In all members of the suite, ore is a relatively minor constituent, primary titanomagnetite constituting less than 5 percent of the rock. In the feldsparphyric dolerites (40, 124, 137, 269) it occurs as skeletal octahedra up to 0.5mm in diameter, 437 (high alumina gabbro) however contains large subhedral skeletal crystals of titanomagnetite

showing ex-solution of ilmenite and its subsequent alteration to leucoxene. Secondary pyrite is present in 40 and 124, and a little free quartz is present as irregular interstitial crystals in samples 40, 177 and 269. Specimens 124 and 269 contain amygdales consisting of chlorite and calcite; and quartz, chlorite, calcite and epidote respectively. Subspherical patches consisting of plagioclase laths, rod like crystals of ore, uralitized clinopyroxene, quartz and a paste of chlorite and calcite occur in the groundmass of sample 40.

The majority of rocks attributed to the suite show some degree of alteration, most prominent being the uralitization of pyroxene and replacement of olivine. Epidote (specimens 177, 269) and biotite (specimens 269 and 437) are also present in some rocks.

MINERALOGY OF THE FELDSPARPHYRIC DOLERITES

Semi quantitative probe analyses of the composition of the groundmass and phenocryst plagioclase in two feldsparphyric dolerites are listed in Table 5.2 (Na_2O concentrations are calculated). Plagioclase phenocrysts in both rocks are considerably more basic than coexisting groundmass plagioclase, An_{70} (phenocryst) with An_{50} in 124 and An_{80} (phenocryst) with An_{64} in 137. Analysis of the rim of a zoned phenocryst in 124 shows the marked change of composition of the plagioclase (approaching An_{40}) with advancing crystallization. Le Bas reports that over 50 percent of the plagioclase in his sample 72 (feldsparphyric dolerite 172 in current investigation) is more basic than An_{80} (Le Bas 1955 Table XVII). As with the alkali dolerites (see Chapter 4 above) and the layered gabbro (Sollas 1894, Le Bas

1970a) the plagioclases in the feldsparphyric dolerites are relatively iron rich with Fe_2O_3 in excess of 0.5 percent.

TABLE 5.2

Composition of plagioclases in feldsparphyric dolerites.

	124				137			
	Pheno-cryst Core	Pheno-cryst Rim	Ground mass a	Ground mass b	Pheno-cryst a	Pheno-cryst b	Ground mass a	Ground mass b
SiO_2	58.27	58.88	61.72	58.17	50.72	51.09	55.01	54.62
Al_2O_3	23.46	24.79	21.49	24.92	30.51	29.87	27.11	27.45
Fe_2O_3	0.77	0.93	0.91	0.94	0.51	0.56	0.83	0.79
CaO	14.06	8.52	9.85	10.04	15.85	16.33	12.81	13.14
Na_2O *	3.06	6.09	5.31	5.38	2.32	2.01	3.93	3.80
K_2O	0.37	0.85	0.72	0.54	0.15	0.14	0.31	0.24
Total	99.99	100.06	100.0	99.99	100.06	100.0	100.0	100.04
Molecular Percent (Ab	27.6	53.6	47.3	47.6	20.7	18.0	35.0	33.8
Molecular Percent (An	70.2	41.5	48.5	49.2	78.4	81.2	63.2	64.8
Molecular Percent (Or	2.2	4.9	4.2	3.2	0.9	0.8	1.8	1.4

* Na_2O calculated.

The composition of analysed groundmass clinopyroxenes in the two feldsparphyric dolerites ranges from $Wo_{35}\ En_{48}\ Fs_{18}$ to $Wo_{39}\ En_{49}\ Fs_{12}$ (see Table 5.3), a coexisting clinopyroxene phenocryst in specimen 124 is less calcic, having the composition $Wo_{34}\ En_{48}\ Fs_{17}$ Calculation of the structural formulae on the basis of six oxygens shows that these analyses are not strictly stoichiometric and must be treated as semi quantitative.

Compositions of pyroxenes in both rocks fall in the augite range (Poldervaart and Hess 1951) but are less calcic than those of the alkali basalt series (see Chapter 4 above). The compositions are consistant with the compositional behaviour of pyroxenes in basaltic rocks discussed by Le Bas (1962) in being relatively poor in Al_2O_3 and TiO_2, and rich in SiO_2, by comparison with those of the alkali basalt series. This behaviour is attributed to the availability of SiO_2 (degree of silica saturation) in the parent melt (Kushiro 1960, Le Bas 1962).

TABLE 5.3

Composition of pyroxenes in feldsparphyric dolerites.

	124			137	
	a	b	c*	a	b
SiO_2	55.8	53.4	54.9	52.15	51.13
TiO_2	0.47	0.72	0.69	0.79	0.42
Al_2O_3	1.34	4.28	3.06	1.74	3.19
Fe_2O_3	11.3	8.8	11.2	8.92	8.62
MgO	15.5	15.4	15.7	18.09	17.23
CaO	15.5	17.3	14.2	18.41	19.40
K_2O	0.13	0.08	1.15	N.D.	N.D.
	100.04	99.98	99.9	100.1	99.99
Molecular Percent (Wo	35.0	38.6	34.3	36.8	39.1
(En	47.5	47.8	48.4	50.6	48.7
(Fs	17.5	13.6	17.3	12.5	12.2

* Pyroxene 124c is a phenocryst.

N.D. Not Determined.

Fresh olivine has not been identified in the feldsparphyric dolerites of Carlingford, the compositions of two altered olivines from sample 124 are listed in Table 5.4. Alteration has led to enrichment of Al_2O_3 and K_2O in a, and of SiO_2 in b, and it is doubtful that further consideration of their composition in relation to that of the original olivine is of value. If it is assumed that alteration has not altered the Mg:Fe ratio in these minerals, the parent olivines would have compositions approaching Fo_{50} in both cases.

Table 5.4

Composition of altered olivines in sample 124 (Feldsparphyric dolerite)

	124 a	124 b
SiO_2	37.7	56.1
TiO_2	0.17	0.04
Al_2O_3	15.9	0.82
Fe_2O_3	29.7	27.3
MgO	14.1	15.4
CaO	0.15	0.25
K_2O	2.24	0.15
Total	99.96	100.06

The degree of ulvospinel solid solution in the titanomagnetites of the feldsparphyric dolerites as reflected by partial analyses of four listed in Table 5.5 is somewhat variable, those of sample 137 are less titaniferous than those of 124.

Table 5.5

Composition of titanomagnetite in feldsparphyric dolerites.

		124		137	
		a	b	a	b
	TiO_2	23.3	23.6	11.01	20.08
	Fe_2O_3	76.7	76.4	88.99	79.92
	Total	100.0	100.0	100.0	100.0
Molecular Percent	(Ulvospinel	69.9	70.8	33.1	60.2
	(Magnetite	30.1	29.2	66.9	39.8

The early separation of calcic plagioclase from the parental magma of the high alumina gabbro - feldsparphyric dolerite suite is indicated by the compositions of coexisting plagioclase and pyroxenes in the feldsparphyric dolerites; early separation of basic plagioclase phenocrysts left the melt somewhat depleted in CaO, thus coprecipitating plagioclase and clinopyroxene of the groundmass have relatively high proportions of Ab and En respectively. TiO_2 concentrations in coexisting clinopyroxene and titanomagnetite favours the latter in the feldsparphyric dolerites.

PETROCHEMISTRY.

Analyses of high alumina gabbros, feldsparphyric dolerites and other members of the high alumina basalt series are listed in Appendix III (major elements) and Appendix XI (trace elements) with additional analyses in Appendix XV. CIPW norms of these rocks are set out in Appendix VII. This data is discussed in the following section.

Composition in terms of major elements.

The degree of alteration exhibited by members of the high alumina basalt series is generally not excessive, though some individual specimens do exhibit extensive uralitization and chloritization. Loss on ignition and, where determined, CO_2 values are at acceptable levels and it was therefore not considered necessary to process analyses prior to petrochemical examination, other than to limit Fe_2O_3 to % TiO_2 + 1.5% in the manner of Irvine and Baragar (1971 p 526) for the purpose of normative calculations.

The compositional range exhibited by members of high alumina basalt series is summarised graphically by a series of conventional Harker variation diagrams (Fig. 5.1) SiO_2 concentrations in all analysed high alumina gabbros are less than 48 percent, while in other high alumina types including the feldsparphyric dolerites SiO_2 values in most rocks are in excess of 48 percent.

TiO_2 concentrations in the suite as a whole, and within the high alumina gabbros and feldsparphyric dolerites in particular, show little variation. All rocks have TiO_2 values within the range 0.5 percent to 1.5 percent, there is no apparent systematic decrease or increase in TiO_2 concentrations with increasing SiO_2 values.

Al_2O_3 concentrations for the suite as a whole fall in the range 16.5 percent to 23.5 percent though as a general rule members of the high alumina gabbro-feldsparphyric dolerite series have higher values than other members of the suite with the same concentrations of SiO_2. There is evidence of negative covariance of Al_2O_3 with SiO_2 in the high alumina gabbro - feldsparphyric dolerite series.

Figure 5.1

Compositions of rocks in the Carlingford high alumina basalt series, depicted graphically as a series of silica variation diagrams.

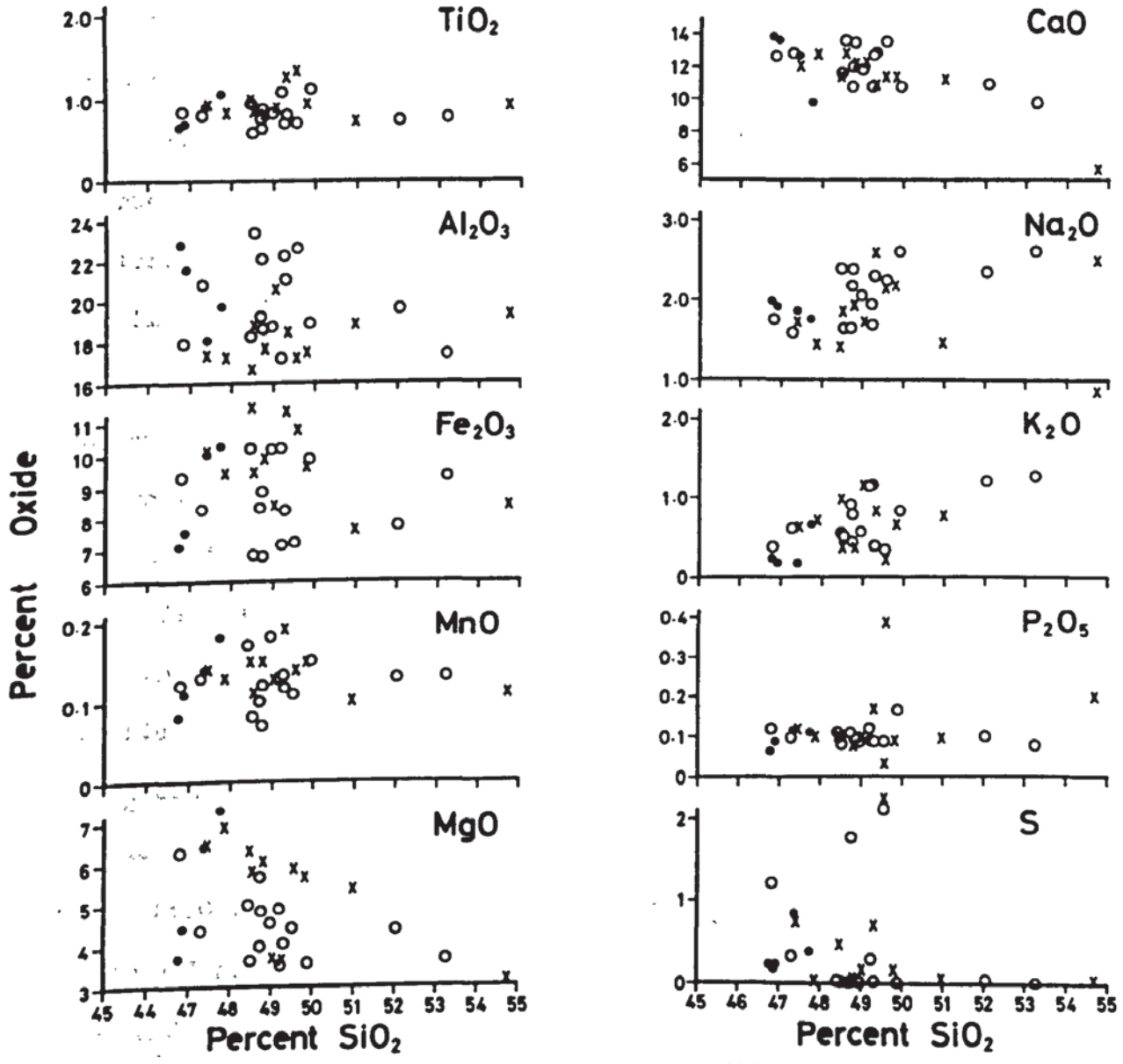

Total iron (as Fe_2O_3) and MnO concentrations form scatters showing no systematic variation with SiO_2, and which fall in the ranges 6.5 to 11.5 percent and 0.07 to 0.20 percent respectively. The majority of the high alumina gabbro-feldsparphyric dolerite group have total iron values less than 9 percent, which is low compared with Fe concentrations in other Carlingford rocks. The opposite is true of the other high alumina types considered to be plagioclase phyric tholeiitic basalts.

MgO values for the suite as a whole fall in the range 3 to 8 percent, though the majority of high alumina gabbros and feldsparphyric dolerites have lower MgO values than other high alumina types with similar concentrations of SiO_2. The diagram indicates that there is a general decline in MgO concentrations with rising SiO_2 values, however in the high alumina gabbro - feldsparphyric dolerite series there is evidence of an initial increase in MgO concentrations with rising SiO_2 values.

CaO concentrations also show negative co-variance with SiO_2 both for the suite as a whole and in the high alumina gabbro feldsparphyric dolerite group in particular. More than half the rocks with SiO_2 concentrations less than 50 percent have CaO values in excess of 12 percent.

Na_2O values range from 1.4 percent to 2.6 percent, K_2O values from 0.3 percent to 1.3 percent with the exception of sample 443, which has K_2O in excess of 2.0 percent but in which SiO_2 exceeds 54 percent. There is a progressive increase in Na_2O and K_2O concentrations with increasing SiO_2 values, Na_2O values being almost doubled and K_2O

TABLE 5.6

Composition of high alumina basaltic rocks from Carlingford, Skaergaard and the Hebrides

Sample	137	450	A	B	C
SiO_2	48.76	46.80	51.02	48.13	48.34
TiO_2	0.87	0.66	0.29	0.25	0.95
Al_2O_3	18.61	22.61	21.06	27.51	20.10
Fe_2O_3	1.76	0.77	1.27	0.88	1.97
FeO	6.35	5.64	5.62	1.91	6.62
MnO	0.12	0.08	0.12	0.02	0.32
MgO	4.81	3.71	8.04	3.21	5.49
CaO	12.09	13.99	9.74	15.49	13.16
Na_2O	2.37	1.99	2.32	1.97	1.66
K_2O	0.39	0.24	0.28	0.25	0.98
P_2O_5	0.11	0.07	0.01	0.02	0.04
S	1.76	0.22	-	-	-
Cr_2O_3	-	-	-	-	-
BaO	-	-	-	-	0.10
CO_2	)	)	-	-	0.11
H_2O+	) 2.46	) 1.35	0.61	0.65	0.44
H_2O^-	)	)	0.12	0.09	0.02
Total	100.46	98.38	100.50	100.38	100.30

137 feldsparphyric dolerite (current investigation); 450 high alumina gabbro (current investigation); A. chilled hypersthene gabbro, Carlingford (Le Bas 1960, p 188, No 99A); B. Feldsparphyric gabbro, Carlingford (Le Bas 1960, p 188, No 1071); C. Olivine gabbro, Mull (Bailey et al.1924, p 24, No II);

TABLE 5.6 cont.

Composition of high alumina basaltic rocks from Carlingford, Skaergaard and the Hebrides

Sample	D	E	F	G
SiO_2	47.28	47.26	47.33	48.08
TiO_2	0.28	0.38	0.15	1.17
Al_2O_3	21.11	22.80	20.08	17.22
Fe_2O_3	3.52	2.21	0.55	1.32
FeO	3.91	5.41	3.24	8.44
MnO	0.15	0.31	0.28	0.16
MgO	8.06	7.76	12.53	8.62
CaO	13.42	10.93	14.47	11.38
Na_2O	1.52	1.72	1.34	2.37
K_2O	0.29	0.29	0.07	0.25
P_2O_5	trace	0.06	trace	0.10
S	-	-	-	-
Cr_2O_3	-	-	0.18	-
BaO	-	-	-	-
CO_2)	-	0.10	-	-
H_2O+)	0.53	0.90	0.21	1.01
H_2O-)	0.13	0.11	0.14	0.05
Total	100.20	100.24	100.37	100.17

D. olivine gabbro, Skye (Harker 1904, p 103, No II); E. Biotite eucrite, Ardnamurchan (Richey and Thomas 1930, p 85, No I); F. Allivalite, Rhum (Brown 1957, p 47, No 2); G. chilled gabbro, Skaergaard (Wager and Brown 1968, p 152).

values quadrupled in the SiO_2 range 47 to 53 percent.

The majority of rocks in the suite have P_2O_5 values in the narrow range 0.07 to 0.12 percent, only specimens 443, 563 and 1399 being exceptional with P_2O_5 concentrations not less than 0.18 percent. There is little covariance of P_2O_5 with SiO_2 either in the suite as a whole or in the high alumina gabbro-feldsparphyric dolerite series in particular.

Concentrations of S within the suite are variable falling in the range of 0.2 percent to 2 percent, thus meriting major element status. There is some degree of negative covariance with SiO_2 but it is uncertain to what extent S concentrations in this suite reflect primary concentrations, or, are the product of secondary pyritization.

It is notable that the composition of the high alumina gabbros and more basic feldsparphyric dolerites is very similar to that of the Carlingford layered gabbros (see Table 5.6 for comparision), though TiO_2, K_2O and P_2O_5 values are generally somewhat higher. Magmas of similar composition - tholeiitic high alumina basalt - are considered to be parental to the Skaerguard and Rhum layered intrusions (Wager and Brown 1968 ps151 and 291) - see Table 5.6.

Generally speaking, those members of the high alumina basalt suite not attributed to the high alumina gabbro - feldsparphyric dolerites series, have higher concentrations of Fe, TiO_2 and MgO and lower concentrations of Al_2O_3. Both groups of rocks are either olivine, orthopyroxene normative or quartz, othopyroxene normative, reflecting the tholeiitic affinities of the high alumina basalt series as a whole. All analysed high alumina gabbros are olivine, ortho-

Table 5.7

C.I.P.W. norms of selected high alumina basalts

Sample Number		40	124	137	269	437
Quartz		0.62	-	2.65	4.76	-
Orthoclase		6.91	2.01	2.30	7.21	1.06
Albite		14.30	19.04	20.06	19.80	16.16
Anorthite		49.73	50.43	38.99	39.54	50.00
Clino-- pyroxene	(Wo	5.47	7.00	8.46	5.82	7.29
	(En	2.50	4.03	5.45	2.84	3.88
	(Fs	2.92	2.65	2.45	2.87	3.18
Ortho- pyroxene	(En	6.32	6.65	6.52	5.58	4.97
	(Fs	7.40	4.37	2.93	5.64	4.07
Forsterite		-	0.25	-	-	1.63
Fayalite		-	0.18	-	-	1.47
Magnetite		-	1.84	2.55	1.83	1.10
Ilmenite		1.33	1.33	1.65	1.42	1.33
Apatite		0.21	0.21	0.26	0.24	0.21
Pyrite		0.51	0.41	3.29	0.07	0.37
Calcite		-	-	-	-	0.11
Sum		98.21	100.40	97.57	97.62	98.86

pyroxene normative. The majority of feldsparphyric dolerites are quartz , orthopyroxene normative (see Table 5.7 for norms of selected members of the high alumina basalt series). When plotted on the Quartz, Nepheline, Olivine triangle, the high alumina gabbros and feldsparphyric dolerites form a field astride the line orthopyroxene - plagioclase which overlaps that of the Carlingford alkali basalt series (see Fig. 3.1). All rocks with analyses listed in Appendix III, with the exception

of 443, have differentiation indices (Thornton and Tuttle 1960) not exceeding 36, and the majority have D.I. values less than 30, no analysed high alumina gabbro has D.I. in excess of 20, this reflects the relatively high proportion of anorthite in the norm of members of the latter group .

Trace Elements

The range of concentration of fourteen trace elements in the high alumina basalt suite are set out in histogram form in Figure 5.2. That data, together with the concentrations of Ga, Ge, Nb, Sn, La, Th, U are discussed in the following section. The latter seven elements are not considered in detail, for the reasons stated in Chapter 4 above. The geochemical behaviour of Sc, V, Cr, Co, Ni, Cu, Zn, Rb, Sr, Y, Zn, Ba, Ce and Pb in basaltic rocks is discussed in some detail in relation to the alkali basalt suite in Chapter 4, further detailed consideration is given only where differences in behaviour are observed in the high alumina basalt series. The behaviour of the latter fourteen elements in the latter series is summarized in Figure 5.3 in which their concentrations are plotted against the differentiation indices (D.I.) of the rocks in question.

Scandium:

Members of the high alumina basalt series have Sc concentrations between 45 and 85 ppm, a range which largely overlaps that of the alkali basalt series, the somewhat higher upper limit of the range reflects the tendency for tholeiitic types to have higher Sc values

Figure 5.2

Histograms of trace element abundance frequencies in rocks of the Carlingford high alumina basalt series.

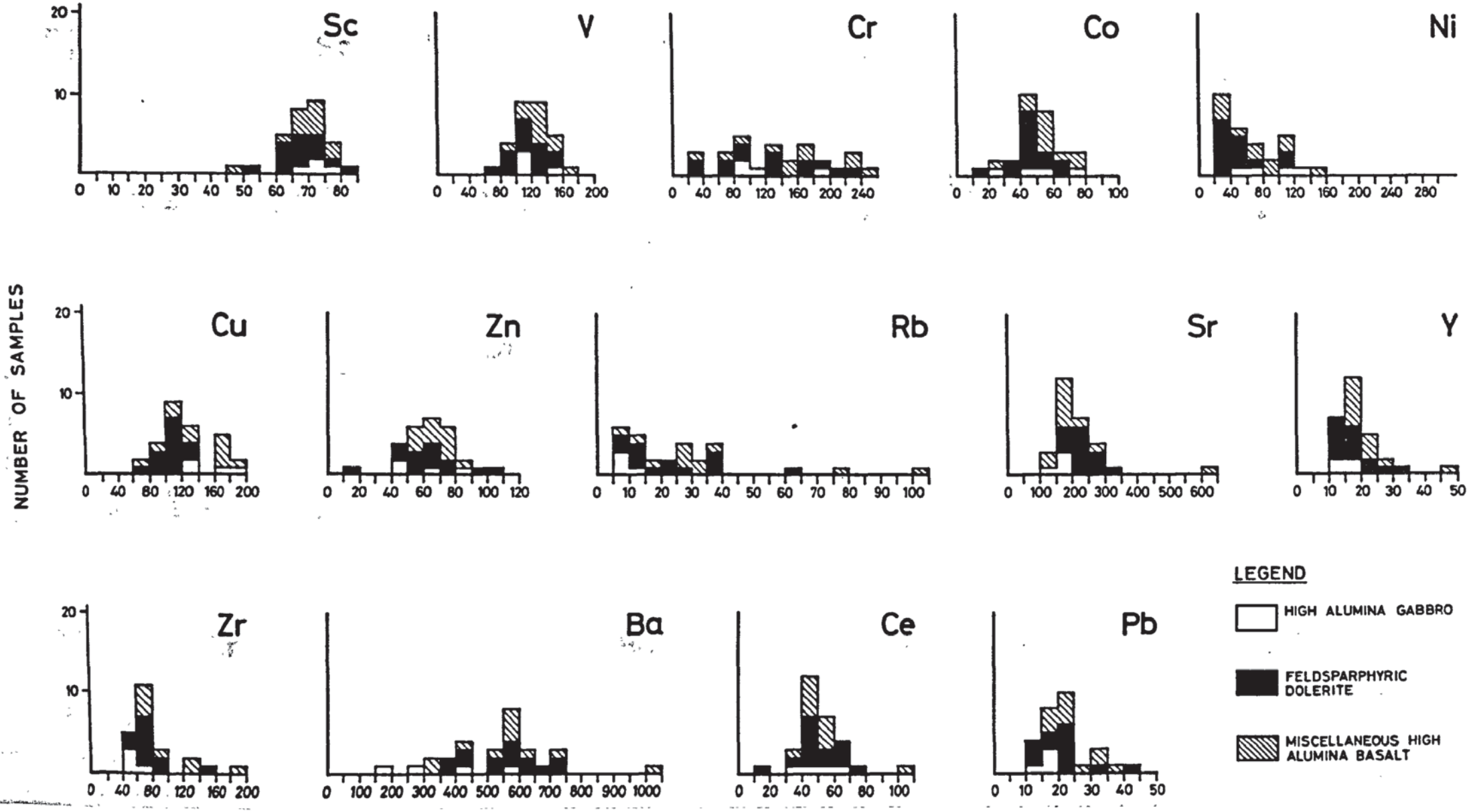

Figure 5.3

Behaviour of trace elements during fractionation in the Carlingford high alumina basalt, series depicted as a series of variation diagrams of concentration versus Differentiation Index (D.I.).

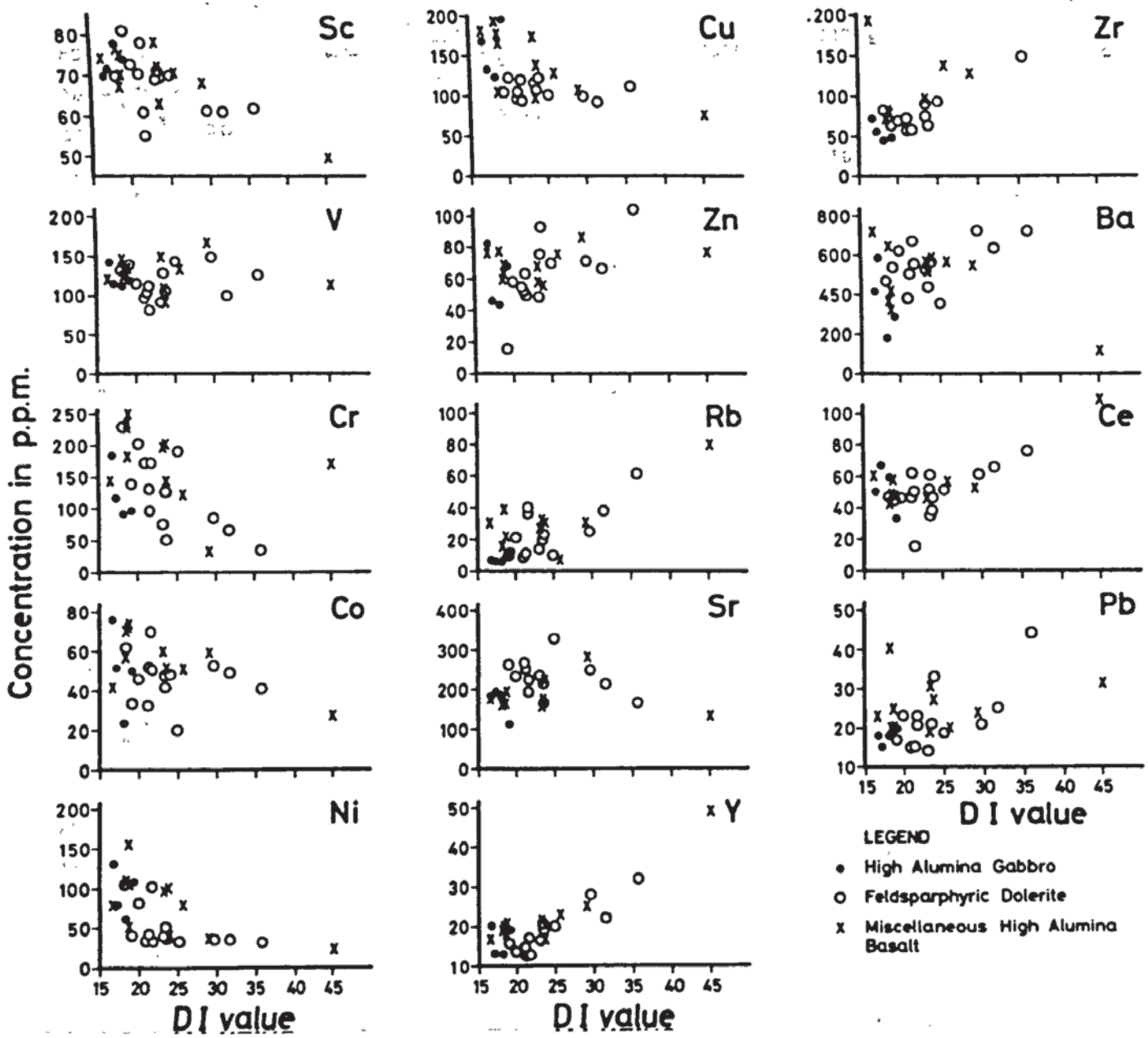

than alkali basalts (Prinz 1968 p 309). Concentrations in the range 70 to 75 ppm from the mode.

Figure 5.3 shows that Sc exhibits depletion with advancing fractionation in the high alumina gabbro-feldsparphyric dolerite series. As basic plagioclase was the dominant phase separating from such melts during the early stages of fractionation (see above) it is considered probable that Sc was removed in the feldspar. Norman and Haskin (1968) discuss the possible substitution of Sc for Ca^{2+}, however no substitution of Sc occurs in the Skaergaard plagioclase, (Wager and Mitchell 1951), the underlying cause of the behaviour of Scandium in the high alumina series is therefore uncertain.

Vanadium:

Quoted Vanadium concentrations are semiquantitative. They form a coherent none skewed cluster falling in the range 60 to 180 ppm, the feldsparphyric dolerites spanning nearly the whole range (Figure 5.2). The majority of high alumina gabbros have values between 100 and 120 ppm. Concentrations in the range 100 to 140 ppm form the mode for the suite as a whole. A plot of V versus D.I. (Fig. 5.3) suggests depletion with advancing fractionation, however the evidence is inconclusive.

Chromium:

Chromium shows a wide range of concentrations in feldsparphyric dolerites and other rock types in the high alumina basalt series. There is no significant modal range of concentrations for the suite. When plotted against D.I. Cr values for the high alumina gabbros and

feldsparphyric dolerites form a scatter showing a tendency towards Cr depletion with increasing D.I. values (Fig. 5.3).

Cobalt:

Cobalt values range from 10 to 80 ppm in the high alumina basalt series, values for the high alumina gabbro-feldsparphyric dolerite group spanning the whole range which has a none skewed distribution. Values in the range of 40 to 50 ppm form the mode.

Figure 5.3 suggest that concentrations remained constant or increased slightly during the initial stages of fractionation if the anomalous high Co value for sample 74 is ignored, with subsequent depletion during the later stages.

Nickel:

Ni values show a distinctly skewed distribution in Figure 5.2, with values falling in the range 20 to 160 ppm, but with values in the range 20 to 40 ppm forming the mode. All high alumina gabbros have Ni in excess of 40 ppm.

When plotted against D.I., Ni shows rapid depletion in the early stages of fractionation (Fig. 5.3) followed by a subsequent more gradual decrease in Ni concentrations. As nickel is most concentrated in olivine during the early stages of fractionation (Prinz 1968 p 306) the behaviour of this element suggests separation of olivine during differentiation of the high alumina gabbro - feldsparphyric dolerite series.

The combined behaviour of Co and Ni in rocks of the high alumina

suite ensured that the Co:Ni ratio increased during the early stages of fractionation. Similar behaviour of Ni and Co in the Carlingford layered gabbro enable Le Bas to use the Co:Ni ratio as an index of fractionation (Le Bas 1970b).

Copper:

Copper values fall in the range 60 to 200 ppm in the high alumina basalt series, with values between 100 and 120 ppm forming the mode. The high alumina gabbros and feldsparphyric dolerites form a coherent group with a skewed distribution, the high alumina gabbros having higher Cu values than the feldsparphyric dolerites (not less than 120 ppm). The bimodality apparent in the copper values of other high alumina basalts is not considered significant as those rocks do not form a single coherent suite.

Copper shows progressive depletion with increasing D.I. values in the high alumina gabbros and feldsparphyric dolerites when plotted against differentiation index (Fig. 5.3).Copper occurs in primary copper sulphides phases in the Skaergaard layered gabbro (Wager, Vincent and Smales 1957), which are interpreted to have separated as immiscible sulphide liquids on the basis of textural considerations (Wager and Brown 1968 p 56). In the Carlingford high alumina basalt series there is no evidence of covariance of Cu with S and the presence of copper sulphides has not been detected. Prinz notes that Cu has been recorded in the olivines, pyroxenes, plagioclase and iron ore of basaltic magmas (1968 p 300), and McDougall and Lovering (1963 p 336) have shown increasing Cu values in some silicates with

advancing fractionation. It is probable therefore that copper was depleted by removal in such non-sulphide phases in high alumina basalt magmas at Carlingford.

Zinc:

The majority of analysed high alumina basalts have Zn concentrations in the range 40 to 110 ppm, with values in the range 60 to 70 ppm forming the mode, 399 has an anomalously low Zn value. Zn shows a tendency towards enrichment with increasing fractionation, i.e. it increases in sympathy with D.I. values. It has been suggested that Zn is concentrated in the magnetites of the Skaergaard gabbros (Woode 1961, Wager and Brown 1968 p 200). There is no evidence to support that view in the case of the Carlingford suite.

Rubidium:

Rubidium values in Figure 5.2 fall in the range 0 to 80 ppm, the majority of rocks having values less than 40 ppm. The high alumina gabbros have concentrations of less than 15 ppm Rb. When plotted against D.I. Rubidium shows progressive enrichment with advancing fractionation in the feldsparphyric dolerites (Fig. 5.3).

Strontium:

The majority of rocks in the high alumina basalt series have Sr concentrations within the range 100 to 350 ppm, sample 141 has an anomalously high Sr value. The high alumina gabbros tend to have

lower Sr values than the feldsparphyric dolerites. Rocks with D.I. values less than 25 have variable Sr values. The feldsparphyric dolerites with D.I. in excess of 25 show evidence of progressive depletion of Sr with increasing fractionation indicating the removal of Sr, perhaps by substitution in plagioclase, during the middle and later stages of that process.

Yttrium:

Yttrium like Rubidium, shows progressive enrichment with increasing fractionation in the high alumina gabbro-feldsparphyric dolerite series, as reflected by a plot of Y concentrations versus D.I. (Fig. 5.3). All analysed rocks in the high alumina basalt series have Y concentrations between 10 and 35 ppm with the exception of 443 (49 ppm). Rocks with Y values between 10 and 15 ppm form the mode for the high alumina gabbro feldsparphyric dolerite suite, while for the suite as a whole concentrations of 15 to 20 ppm form the mode.

Zirconium:

Zirconium values are not available for all rocks in the suite. Those that have been determined fall in the range 40 to 200 ppm, with concentrations in the range 60 to 80 ppm forming the mode. The high alumina gabbros in each case have Zr concentrations less than 80 ppm.

Zr concentrations in the high alumina gabbro-feldsparphyric dolerite series show a progressive increase with advancing fractionation when plotted against D.I. (Fig. 5.3).

Barium:

Barium has a relatively wide range of concentrations in the Carlingford high alumina basalts, ranging from 188 ppm in sample 450 to 1050 ppm in 443. Values in the range 550 to 600 ppm form the mode. Barium shows enrichment with advancing fractionation. (Fig. 5.3)

Cerium:

Cerium also shows enrichment with advancing fractionation, Ce values for the feldsparphyric dolerites falling close to a line when plotted against D.I. (Fig. 5.3). Ce concentrations range from 16 ppm (40) to 107 ppm (443) in the suite as a whole, values in the range 40 to 45 ppm form the mode. The bimodality apparent for the feldsparphyric dolerites in Fig. 5.2 is not considered significant.

Lead:

Lead values fall in the range 10 to 45 ppm with a modal range of 20 to 25 ppm, the high alumina gabbros have Pb values not exceeding 20 ppm. Lead shows a tendency towards enrichment with advancing fractionation in rocks with D.I. values in excess of 25.

Gallium:

Gallium ranges in concentration from 14 to 20 ppm in the suite as a whole. In the high alumina gabbro-feldsparphyric dolerite series the gabbros tend to have lower Ga values (none of the four analysed samples have Ga in excess of 16 ppm), which suggests that Ga is enriched by progressive fractionation.

Germanium:

Germanium concentrations are at the limits of detection in the high alumina basalt series, no analysed rock has a Ge value in excess of 3 ppm.

Niobium:

Niobium values have been determined for nine members of the high alumina basalt suite (Appendix XV). None of those defined as basalts (see Chapter 3) have Nb concentrations in excess of 10 ppm. Samples 446 and 447, which are high alumina craignurites attributed to the high alumina gabbro-feldsparphyric dolerite series, have Nb concentration of 15 and 18 ppm respectively, indicating Nb enrichment with progressive fractionation. Nb values are, in general, lower in the high alumina series than in the alkali basalt series.

Tin:

Tin concentrations are at the limits of detection in the high alumina basalt series, 5 ppm is the highest Sn value recorded for any member of the suite (sample 563).

Lanthanum:

Four rocks analysed for La all have concentrations less than 10 ppm (Appendix XV).

Thorium:

Thorium shows progressive enrichment with increasing fractionation

in the high alumina basalts. In many feldsparphyric dolerites and other high alumina basalts Th is at the limits of detection, values of less than 5 ppm being recorded. In more fractionated feldsparphyric dolerites up to 11 ppm Th has been recorded (1166). Sample 443 has 16 ppm Th.

Uranium:

Uranium concentrations in the high alumina basalt series are at the limits of detection of the analytical techniques used during the current investigation. The highest recorded value of U in any member of the suite being 3 ppm for sample 443.

PETROGENESIS

The true nature of the high alumina gabbros and feldsparphyric dolerites

The petrography and petrochemistry of the high alumina gabbros and feldsparphyric dolerites have been described in the preceding paragraphs. These rocks form a continous spectrum and can be shown to be genetically related as they were injected contemporaneously and even occur within the same intrusive body in some instances. It has been implicit in the preceding petrochemical discussion that high alumina gabbros and feldsparphyric dolerites are members of a high alumina basalt fractionation series. Other high alumina basalts have been described herein as tholeiitic basalts with accumulated plagioclase phenocrysts, Le Bas attributes a similar origin to the feldsparphyric dolerites (1955 p 239). These conflicting interpretations must be reconciled before further consideration may be given to the operation of fractionation mechanisms

within the suite .

The high alumina gabbros are more basic than the feldsparphyric dolerites and in many respects similar to the gabbros of the layered lopolith; while discussing the layered gabbros Le Bas (1960, p 179) implies that they are the product of a high alumina basalt parent, citing the views of Richey (1958), Tilley (1950) and Yoder and Tilley (1957). In a later publication Le Bas unequivocally attributes the gabbros to the "high alumina tholeiitic basalt type" (1970b p 217). It is inconsistant to consider the layered gabbros to be true high alumina basalts in the sense of Tilley (1950) and Kuno (1960) while dismissing members of the petrographically and petrochemically similar high alumina gabbro-feldsparphyric dolerite series as feldsparphyric tholeiites.

Le Bas has shown that subtraction of 37% plagioclase composition An_{85} from a feldsparphyric dolerite leaves a composition which is similar to that of a tholeiitic basalt (1955 p 238). Quite different conclusions are reached if a similar exercise is attempted with a high alumina gabbro such as sample 450. Table 5.8 shows the results of subtracting progressively 30% and 50% plagioclase, composition An_{81} (phenocryst b in sample 137 - see Table 5.2 above - the most basic of plagioclase compositions determined in the current investigation), from 450.

Removal of 30% plagioclase leaves a basaltic composition which is still high alumina in character. To produce a composition with Al_2O_3 less than 16.5% (the upper limit set in Chapter 3 for tholeiitic basalts) removal of almost 50% of the rock as plagioclase is required, by which point the resulting SiO_2 value is less than 44% such that the

TABLE 5.8.

	Sample 450	Phenocryst b 137	450-30% plagioclase	450-50% plagioclase
SiO_2	46.80	51.09	45.61	43.39
TiO_2	0.66	-	0.96	1.35
Al_2O_3	22.86	29.87	20.14	16.17
Fe_2O_3)) FeO)	7.03	0.56	9.94	13.78
MnO	0.08	-	0.12	0.16
MgO	3.71	-	5.38	7.57
CaO	13.99	16.33	13.17	11.88
Na_2O	1.99	2.01	2.01	2.00
K_2O	0.24	0.14	0.29	0.35
P_2O_5	0.07	-	0.10	0.14
S	0.22	-	0.32	0.45
H_2O^+	1.35	-	1.96	2.76
Total	99.00	100.0	100.00	100.00

calculated composition is no longer basaltic.

The high alumina gabbros in general have lower concentrations of MgO and iron and higher concentrations of Al_2O_3 than the feldsparphyric dolerites, thus to have been produced by the addition of accumulated feldspar to tholeiitic basalt melts considerably greater quantities of plagioclase would have to be added to the high alumina gabbros which should thus be richer in SiO_2 by comparison with the feldsparphyric dolerites, which is not the case in reality. Further more

trace element concentrations in the high alumina gabbros are relatively more primitive than in the feldsparphyric dolerites, that is they have higher Sc, V, Cr, Ni and Cu values and lower Zn, Rb, Y, Zr, Ba and Ce values; Le Bas has pointed out that concentrations of V, Cr and Ni are low in plagioclase in basic rocks (1970a p 73), thus the high alumina gabbros if formed by the addition of large quantities of plagioclase would have diluted and not the observed enhanced concentrations of those elements. These considerations demonstrate that the high alumina gabbros cannot be considered to be plagioclase-phyric tholeiites, and their association and petrochemical affinity for the feldsparphyric dolerites suggests that the same is true of the latter group. It is therefore suggested that the high alumina gabbros and feldsparphyric dolerites are derivatives of a high alumina basalt magma and form a true fractionation series, for as King (1962 p 621) comments while writing on the problem of high alumina basalts in relation to the Hebridean Province in general: "it is surely more plausible that the high alumina is the cause rather than the result of early crystallization of plagioclase".

Fractionation trends

Highly evolved members of the high alumina basalt series, such as high alumina craignurites, are not abundant at Carlingford, analyses of two such rocks attributed to episode IIe-IIIa are listed in Appendix XV. An investigation of the fractionation processes which the high alumina gabbro-feldsparphyric dolerite suite has undergone is undertaken in the following paragraphs on the basis of the data in

Appendices III and XI (excludes samples 172, 177, 446 and 447 listed in Appendix XV). No further consideration is given herein to other rocks defined as high alumina basalts on the basis of chemical considerations set out in Chapter 3 but which are more appropriately attributed to the tholeiitic basalt - craignurite series, as has been discussed above.

The degree of evolution exhibited by individual members of the high alumina gabbro - feldsparphyric dolerite suite is indicated by their differentiation indices which fall in the range 16 to 36. Concentrations of nine oxides are plotted against D.I. in Figure 5.4. Al_2O_3 forms a scatter but does show a general trend towards depletion in rocks with high D.I. values. CaO shows progressive depletion with increasing D.I. The behaviour of MgO is unclear the majority of rocks with D.I. less than 26, shows a tendency towards enrichment in MgO with increasing D.I.; those with D.I. values greater than 26 show depletion in MgO. Similar behaviour is observed for TiO_2, total iron, MnO and P_2O_5 reflecting that of Co among the trace elements (Figure 5.3). Na_2O and K_2O show progressive enrichment with increasing D.I. values. In all these plots sample 450, a high alumina gabbro which has a particularly low D.I. value (18.26), lies near the average trend of the majority and is thus a suitable parent for the suite as a whole samples 74, 426 and 665 show anomalous values for several oxides by comparision with those of the majority, they have particularly high values for MgO and Fe, and are considered atypical.

The behaviour of CaO reflects the progressive separation of calcic plagioclase from the melt with advancing fractionation, indicated

Figure 5.4a

Changes of composition within the Carlingford high alumina gabbro-feldsparphyric dolerite series during fractionation, depicted by a series of variation diagrams of major element oxides versus Differentiation Index (D. I.).

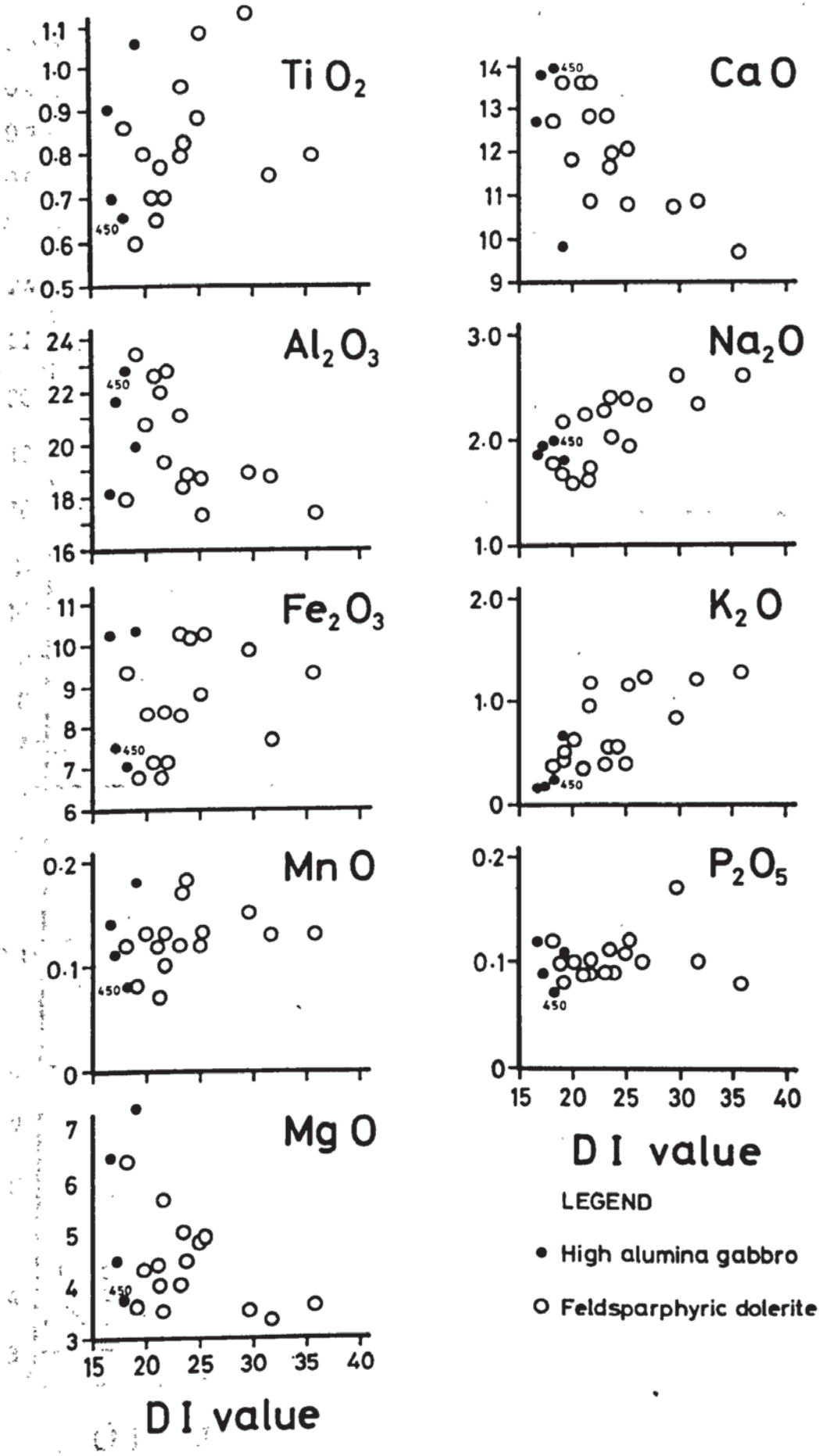

Figure 5.4b

As Fig. 5.4a except that sample numbers 74, 426 and 665 are excluded in order to clarify the trends.

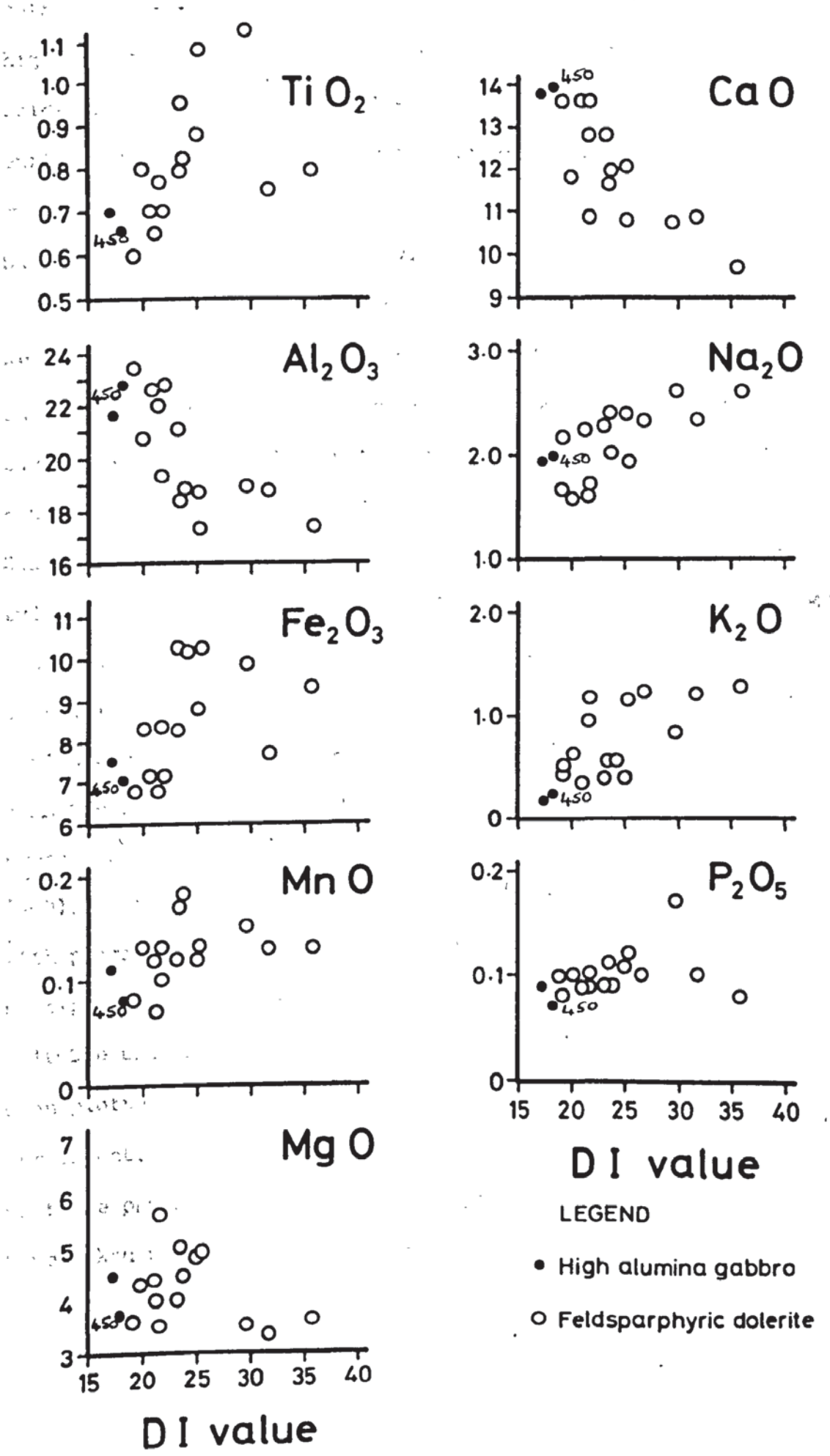

petrographically by the early crystallization of the latter in the high alumina gabbros and its occurrence as phenocrysts in the feldsparphyric dolerites. K_2O shows almost double the degree of enrichment exhibited by Na_2O with increasing D.I. as it occurs in much lower concentrations in the plagioclase. The behaviour of Rb, Ba, Ce and Pb follow that of K_2O.

SiO_2 concentrations in the basic plagioclase of the early stages of crystallization are higher than those of suitable parental types such as the high alumina gabbro 450 (see above), thus separation of such phases in isolation must lead to depletion in SiO_2 (Kuno 1968 p 658, Wager and Brown 1968 p 168), a phenomenon observed in the Skaergaard gabbro (Wager and Deer 1939 p 297). However, there is no evidence of SiO_2 depletion at Carlingford, Na_2O and K_2O show progressive positive covariance with SiO_2,and CaO progressive negative covariance, a behaviour which could not be expected if SiO_2 depletion had accompagnied removal of basic plagioclase. Separation of calcic augite cannot explain this phenomenon as SiO_2 concentrations in analysed pyroxenes are also higher than that of the proposed parental melt (450). A phase or phases relatively poor in SiO_2 must have separated with plagioclase if the range of variation exhibited by the suite is to be explained by crystal liquid fractionation. Olivine and iron ore are suitable phases from the point of view of SiO_2 concentrations, however when plotted against D.I. MgO, Fe and TiO_2 show evidence of initial enrichment, which though slight, indicates that substantial removal of those phases during the early stages of fractionation could not have taken place. The early separation of at least some olivine is

indicated by progressive depletion of Ni concentrations with increasing D.I. values (see above), Ni preferentially enters the olivine lattice (Prinz 1968 p 306). Olivine also occurs as a phenocryst of minor importance in some feldsparphyric dolerites (see 124). Ore occurs only in relatively minor quantities in the high alumina gabbros. It is considered that coprecipitation of plagioclase and minor olivine perhaps accompagnied by the separation of a little ore from a parental high alumina basalt magma can account for the observed behaviour of both major components and trace elements in the high alumina basalt - feldsparphyric dolerite fractionation series. There is no evidence of the operation of other fractionation mechanisms.

In view of the significance of plagioclase as the dominant phase separating during fractionation, and the uncertain behaviour of SiO_2 during such a process, it is considered that CaO concentration is the most appropriate index of fractionation in the high alumina gabbro - feldsparphyric dolerite suite. Plots of TiO_2, Al_2O_3, total iron, MnO, MgO, Na_2O, K_2O and P_2O_5 versus CaO have been prepared (Figure 5.5). These diagrams indicate progressive covariant depletion of Al_2O_3 with CaO, and negative covariant enrichment of TiO_2, Total Fe, MnO and K_2O with CaO. There is some evidence of negative covariance of MgO with CaO. At higher CaO concentrations Na_2O values form a scatter. P_2O_5 values show little variation with CaO. The suitability of 450 as a parental type is confirmed by its position in these plots.

Kuno recognises two fractionation trends in high alumina basalts, the Skaergaard trend showing high iron enrichment, and a trend showing moderate iron enrichment (Kuno 1968). The high alumina basalt series

Figure 5.5

Variation diagrams of major oxides versus CaO for rocks in the Carlingford high alumina gabbro - feldsparphyric dolerite series.

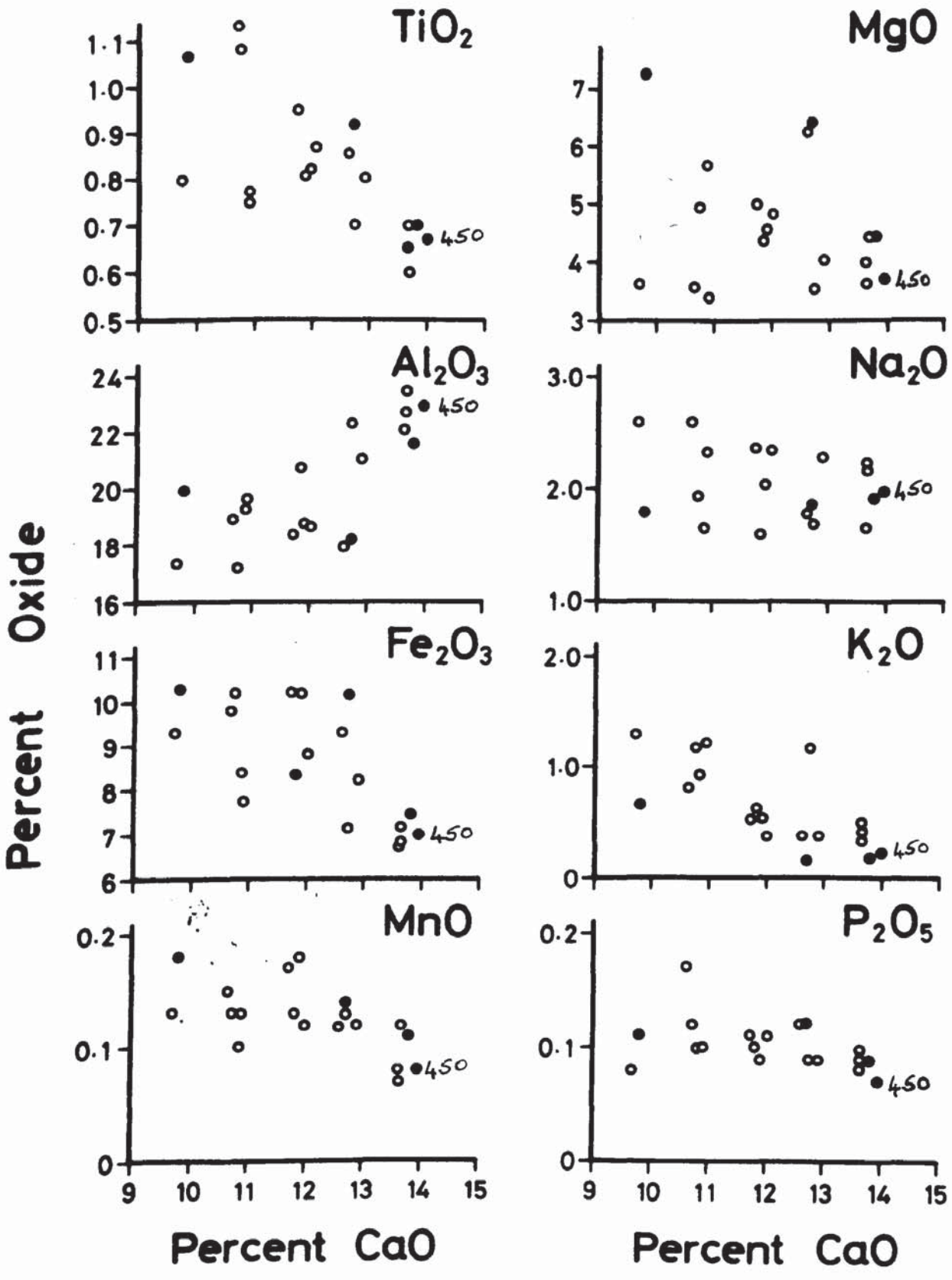

at Carlingford shows only moderate iron enrichment, with initial iron concentrations being relatively low by comparison with other Carlingford rocks. The lack of marked Fe enrichment in rocks of the high alumina basalt-feldsparphyric dolerite series, is shown by the AFM diagram, Figure 5.6. Moderate iron enrichment suggests that the partial pressure of oxygen was sufficiently high to enable some separation of ore during the early stages of fractionation, but not high enough to suppress a mild increase of Fe. The low initial concentrations of iron limited the modal abundance of ore in the suite. Ti, MnO and Co mimic the behaviour of iron.

It is proposed that the high alumina gabbro feldsparphyric dolerite suite was derived by fractionation from a parent high alumina magma approaching sample 450 in composition. Separation of basic plagioclase was the principal factor controlling the variation of major element concentrations within the suite, this was accompanied by separation of minor quantities of olivine and ore, thus preventing SiO_2 depletion. The removal of olivine and ore during the early stages was insufficient to prevent enrichment in Fe, Ti, Mn and Mg. The relatively high, but variable, concentrations of Fe and Mg in some of the more basic members of the suite, such as 426, reflect higher concentrations of accumulated olivine and ore in those rocks. Enrichment of residual elements such as Y and Zr took place progressively with increasing fractionation, but the behaviour of P_2O_5 indicates that it was removed continuously from the parent melt, maintaining initial levels of concentration.

Figure 5.6

Composition of rocks in the Carlingford high alumina gabbro - feldsparphyric dolerite series in terms of $Na_2O + K_2O$, Fe as FeO and MgO plotted on the triangle A.F.M.

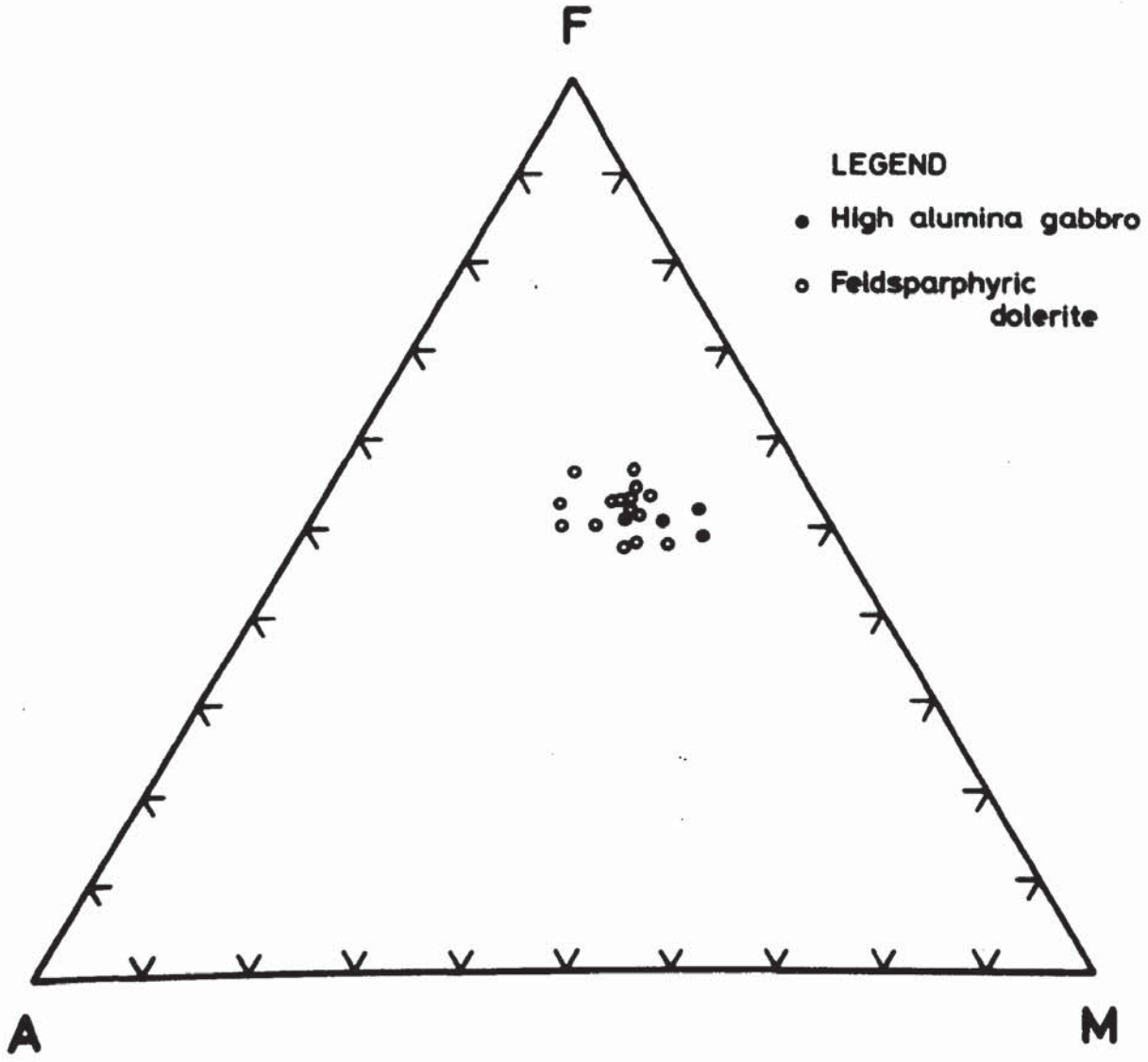

Summary.

1. The high alumina gabbros and feldsparphyric dolerites form a coherent suite in terms of their time relations, petrography and petrochemistry. Other rocks attributed to the high alumina basalt series, on the basis of the chemical classification of Chapter 3, do not form a coherent suite in terms of their time relations and petrography. The latter rocks have higher Fe, TiO_2 and MgO concentrations than the high alumina gabbros and feldsparphyric dolerites, and are considered to be members of the tholeiitic basalt - craignurite series with accumulated plagioclase phenocrysts. The high alumina gabbros cannot be considered to be tholeiitic basalts which have been enriched in Al_2O_3 by the addition of accumulated plagioclase, they are thus believed to form a true high alumina basalt magma series with the feldsparphyric dolerites.

2. The composition of sample 450 approaches that of melts parental to the high alumina gabbro-feldsparphyric dolerite series.

3. Fractionation of the parent high alumina melt proceeded by separation of calcic plagioclase with minor olivine and minor ore, leading to enrichment in SiO_2, Total Fe, TiO_2, Na_2O, K_2O, Zn, Rb, Y, Zr, Ba, Ce and Pb.

In conclusion it must be remarked that, the significance of the high alumina basalt magma type in the Carlingford complex, and in the British Tertiary Province in general as the Porphyritic Central Magma type of Bailey et al (1924), shows that it merits equal status with the alkali basalt series and tholeiitic basalt - craignurite series.

CHAPTER 6

THE PETROLOGY, MINERALOGY AND PETROCHEMISTRY OF THE THOLEIITIC BASALT - CRAIGNURITE SERIES

Abstract.

The abundant tholeiitic-basalt craignurite series is the dominant rock group in thethree intrusive cycles at Carlingford. The petrology and petrochemistry of the suite are described and shown to form a continuous series from basic to acid compositions. The continuity of the series, and relative proportions of the constituent rock types, indicates that the exhibited range of compositions has arisen by petrogenetic processes such as crystal liquid fractionation from basaltic parental melts approaching the more basic members of the transition dolerite group in composition.

The observed behaviour of the major elements, and trace elements alike, indicates that the series evolved from such parental melts by simultaneous separation of olivine and plagioclase in the early stages of fractionation followed by the separation of clinopyroxene, plagioclase and ore during later stages.

Introduction

Members of the tholeiitic basalt - craignurite series form numerically the most abundant group of rocks in the minor intrusions of the Carlingford Complex, constituting about 65 percent of those exposed (see Chapter 2 above). They dominate intrusive activity in all three intrusive cycles, and occur in both dykes and cone-sheets.

The series is subdivided into transition dolerites, tholeiitic

dolerites and quartz dolerites, craignurites and craignuritic felsites on the basis of petrography and petrochemistry (see Chapter 3 above), and forms a continuous coherent spectrum of rock types indicating a fundamental genetic relationship between acid and basic members of the series. The series is characterised as a separate entity to that of the tholeiitic basalt - icelandite series described by Carmichael (1964) and defined geochemically by Irvine and Baragar (1971) and Middlemost (1972), as it exhibits enrichment of K_2O relative to Na_2O, particularly in the craignuritic members of the suite (see Chapter 3).

PETROGRAPHY

The tholeiitic basalt-craignurite series forms a complete petrographic series, with a continuous spectrum of rock types between the two petrographic end members (the transition dolerites and craignuritic felsites). There are no petrographic distinctions between rocks of the same type of different age . Modal analyses of seventeen selected samples are set out in Tables 6.1. and 6.2.

The transition dolerites are represented by samples 53, 54, 76, 111 and 297, they consist of a groundmass of plagioclase lathes, subophitic or ophitic, pinkish brown clinopyroxene, skeletal titanomagnetite and olivine. Interstitial chlorite is present in 53, 54 and 76, in sample 297 there is interstitial feldspar, and in 111 the intersteces are occupied by plagioclase, chlorite and rod shaped ore crystals, occasionally accompanied by quartz. Specimen 53 incorporates rare crystals of green spinel not more than 0.05mm. in diameter. Subequant plagioclase phenocrysts, up to 2mm. long, occur in minor quantities in

TABLE 6.1

Modal composition of transition dolerites and tholeiitic dolerites

Sample No.	3	38	53	54	76	99	111	297	330
Plagioclase (phenocryst)	5	tr	tr	1	-	21	tr	-	7
Plagioclase (groundmass)	35	36	41	33	45	21	43	40	33
Clinopyroxene (xenocryst)	-	-	-	-	-	4	-	-	-
Clinopyroxene (groundmass)	26	37	32	33	19	23	38	38	22
Olivine *	-	7	11	22	29	12	5	1	4
Titanomagnetite	15	5	6	4	3	3	6	6	3
Iron sulphide	4	-	tr	-	tr	-	tr	-	tr
Chlorite	3	4	6	7	5	16	9	-	27
Quartz	1	1	-	-	-	-	-	-	-
Miscellaneous interstitial phases	10	10	5	-	-	-	-	14	4
Biotite	tr	-	-	-	-	-	-	tr	tr
Calcite	-	tr	-	tr	-	-	-	-	-
Spinel	-	-	tr	-	-	tr	-	-	-

tr = Trace
* olivine is largely represented by alteration products.

samples 53, 54, 76 and 297; measurement of symmetrical extinction (Deer, Howie and Zussman 1966 p 329) indicates that these have compositions approaching An_{70}. Olivine occurs as abundant subhedral phenocrysts up to 3mm long in 54 and 76; in 76 it exceeds 25% in the mode and hence the latter is picritic (see Chapter 3). In all rocks the olivine shows alteration to chlorite, bowlingite and ore, or iddingsite. The clinopyroxene in samples 53 and 76 shows some uralitization while secondary pyrite occurs as subhedral cubic crystals in 53, 54 and 111, in 76 it is present in veins cutting the rock. Calcite and secondary brown biotite are also present in some rocks. Specimen 297 shows the development of finely divided magnetite at pyroxene grain boundaries as the result of hornfelsing.

It has been noted that a number of rocks classified as transition dolerites on the basis of petrochemistry have relatively high iron concentrations and petrographic affinities with the quartz dolerites (see Chapter 3). These high iron transition dolerites are represented by sample 3 in Table 6.1, it consists of a groundmass of plagioclase laths composition An_{50} (maximum recorded symmetrical extinction 28°), subophitic augite and skeletal titanomagnetite, with interstitial feldspar, quartz and ore, including iron sulphide, enclosing scattered subhedral plagioclase phenocrysts up to 2mm in length. Secondary minerals include chlorite and brown biotite.

Samples 38, 99 and 330 are tholeiitic dolerites as defined in Chapter 3. Specimen 38 is aphyric, while 330 contains phenocrysts of plagioclase, composition An_{80}, and olivine, which compromise about 7.0 and 3.5 percent of the rock respectively. 99 incorporates large

crystals of plagioclase up to 5mm long, clinopyroxene up to 2.5mm in diameter and olivine, the latter are embayed and up to 3mm in length, also present are embayed subhedral crystals of brown spinel. Some of the olivine, pyroxene and plagioclase occur in gabbroic aggregates with which the spinel is associated, indicating that these phases are xenolithic in origin. The groundmass of specimen 38 consists of subophitic clinopyroxene and an interlocking mesh of plagioclase laths, composition An_{65} (maximum recorded symmetrical extinction 34^{o}), in almost equal proportions, and abundant skeletal octahedra of titanomagnetite. Subhedral olivine comprises nearly 7.0 percent of the rock but is replaced by bowlingite and ore. Interstitial material consists of a brownish paste of chlorite and calcite with quartz and ore. In specimen 99 the groundmass is similar to that of many transition dolerites, consisting of ophitic clinopyroxene and plagioclase (An_{65}), with relatively abundant skeletal titanomagnetite; olive green chlorite and rod shaped crystals of ore occur in the interstices. The ophitic groundmass of specimen 330 is relatively coarse grained, individual clinopyroxene crystals are up to 1.5mm in diameter and plagioclase laths up to 1mm in length. The subhedral skeletal crystals of ore show exsolved ilmenite lamellae which are replaced by leucoxene due to alteration. Chlorite and feldspar are present in the interstices. Subhedral pyrite is present in 38 and 330, it is somewhat hematised in the latter, the pyroxenes in both rocks are partly altered.

The modal composition of the quartz dolerites 11, 71 and 72 are listed in Table 6.2. Plagioclase in the groundmass constitutes from 27 to 45 percent in the mode and ranges in composition between An_{45}

TABLE 6.2

Modal composition of quartz dolerites and craignurites

Sample No.	5	6	11	22	23	35	71	72
Plagioclase (phenocrysts)	20	10	tr	tr	3	-	-	-
Plagioclase (groundmass)	-	38	27	-	-	-	45	28
Clinopyroxene (phenocrysts)	12	2	tr	tr	1	-	-	-
Clinopyroxene (groundmass)	12	36	56	32	25	28	31	34
Titanomagnetite	4	9	12	-	1	2	9	5
Iron Sulphide	8	3	2	-	1	5	4	2
Chlorite	-	2	1	8	4	4	7	7
Quartz	1	tr	1	2	1	3	2	tr
Miscellaneous interstitial phases or groundmass	42	-	-	55	62	55	-	8
Biotite	tr	1	1	-	tr	2	1	-
Calcite	-	-	tr	tr	-	1	1	tr
Epidote	-	-	-	2	3	-	-	-

tr = Trace

(sample 11) and An_{65} (sample 72), clinopyroxene constitutes the larger part of the remainder, comprising about 56 percent of sample 11. Ore is an important constituent in all three samples, but in 11 and 71 it exceeds 13 percent in the mode; the dominant ore phase is titanomagnetite occurring as subhedral skeletal octahedra, rod like crystals and anhedral grains, but iron sulphide is also a primary phase in the quartz dolerites present as disseminated anhedral crystals throughout the groundmass. Interstitial quartz is present in sample 11, interstitial material in 71 and 72 includes chlorite, calcite and quartz. Specimen 71 is aphyric, but both 11 and 72 incorporate a small quantity of clinopyroxene and plagioclase phenocrysts, the former are typically anhedral. Amygdales of chlorite and quartz or calcite occur in samples 71 and 72. Biotite and chlorite are the principal secondary minerals in the quartz dolerites, though chlorite is largely absent in 11, veins of chlorite and calcite cut 72. Secondary pyrite as subhedral cubic crystals or irregular "porphyroblastic" patches is present in 71 and 72. Textures vary from basaltic to variolitic, sample 11 exhibiting a well developed variolitic texture.

Sample 6 is a basaltic craignurite (Chapter 3), the groundmass consists of a mesh of plagioclase laths composition An_{45} (symmetrical extinction 25°), prismatic clinopyroxene, skeletal titanomagnetite and subhedral iron sulphide, interstitial quartz, and a little secondary chlorite and biotite. It encloses phenocrysts of plagioclase and clinopyroxene, the former, comprising nearly 10 percent in the mode, are subequant in form and approach An_{80} in composition (maximum

recorded symmetrical extinction 38°). Some phenocrysts occur in interlocking gabbroic aggregates and may be xenolithic in origin.

The craignurites and craignuritic felsites are represented in Table 6.2 by samples 22 and 35, and 5 and 23 respectively. They are largely composed of a fine grained feldspathic matrix enclosing prismatic crystals of pyroxene which are frequently altered, and interstitial patches of quartz. This feldspathic material is similar to that which occur in the interstices of some quartz dolerites as remarked on Mull by Bailey et al. (1924 p 280). Ore is largely absent from the groundmass of specimen 22, a minor quantity of titanomagnetite is present in 23, in 35 however, primary iron sulphide in the groundmass is the dominant ore phase present, while in sample 5 it is the only groundmass ore phase and constitutes nearly 8 percent of the rock. Sample 35 is aphyric, 5, 22 and 23 are all porphyritic enclosing phenocrysts of plagioclase, clinopyroxene and, in the case of 5, titanomagnetite. In 22 and 23 phenocryst phases are not abundant; in sample 5 however, they occur in clusters, thus the modal composition of 5 set out in Table 6.2 cannot be considered entirely representative and may include a disproportionate quantity of phenocryst material. The phenocryst plagioclase and pyroxene in specimen 5 are euhedral, the plagioclase attaining up to 7mm in maximum dimension, the titanomagnetite is subhedral and embayed. Xenoliths of chloritised basalt and gabbro occur in sample 22, while fragments of granophyre are present in sample 5. Secondary minerals in these rocks include chlorite, biotite, epidote and uralite. Secondary pyrite, occurring as subhedral cubic crystals, is present in samples 23 and 35. Specimen 22 is cut

by veins of chlorite, calcite and epidote, while 35 encloses amygdales, up to 3mm in diameter, consisting of calcite and euhedral quartz crystals.

Many of the rock types described above are represented by tachylites when chilled, specimen 9 is a tachylitic transition dolerite, specimen 67 a high iron transition tachylite, 852 is a tachylitic quartz dolerite,and 1336 a tachylite with the composition of basaltic craignurite. The variolitic texture is also frequently developed, particularly in chilled quartz dolerites, a phenomenon noted elsewhere in the Hebridean Tertiary Province (Bailey et al.1924, Tomkeieff and Marshall 1935).

The presence of spinel in some of the more basic members of the suite is significant; corroded xenocrysts of brown spinel other than those described have also been noted in samples 809 and 1381. Resorbed relicts of green spinel, similar to those in sample 53, are enclosed by a plagioclase phenocryst with which they have reacted in specimen 1352 (a porphyritic tholeiite described as a high alumina basalt in terms of composition - see Chapter 5). Also of significance is the appearance of iron sulphide as a primary ore phase in the quartz dolerites and craignurites.

MINERALOGY

The composition of constituent plagioclase, pyroxene, olivine (altered) and ore have been determined by microprobe analysis for a number of rocks in the tholeiitic basalt - craignurite series (Tables 6.3, 6.4, 6.5, 6.6). No attempt has been made to distinguish variations in composition of mineral phases in rocks of the same type but of

TABLE 6.3

Composition of plagioclase in members of the tholeiitic basalt-craignurite series

Sample	5		6		11			54		71		76			330	
Analysis	a	b	a	b	a	b	c	a	b	a	b	a	b	c	a	b
SiO_2	57.26	57.81	51.84	50.23	57.26	56.12	57.97	50.03	49.64	56.2	56.96	59.92	50.93	50.01	52.51	52.86
TiO_2	ND	ND	BLD	BLD	0.13	BLD	BLD	BLD	BLD	BLD	BLD	ND	ND	ND	BLD	BLD
Al_2O_3	26.66	25.65	29.47	30.76	25.61	26.01	24.69	28.62	30.40	26.33	25.5	20.65	30.23	31.27	28.74	28.70
Fe_2O_3	0.54	0.67	0.75	0.67	1.17	1.52	0.96	4.01	0.47	0.91	1.02	2.77	1.03	0.88	0.82	0.72
CaO	8.61	9.52	14.94	16.03	9.73	10.96	10.96	14.5	14.57	11.75	11.81	12.64	14.39	14.66	14.90	14.35
MgO	ND	BLD	BLD	BLD	BLD	BLD	BLD	BLD	1.92	BLD	BLD	ND	ND	ND	BLD	BLD
Na_2O *	6.19	5.58	2.75	2.46	5.50	4.64	4.70	2.67	2.89	4.47	4.47	3.60	2.77	2.90	2.78	3.12
K_2O	0.75	0.77	0.22	0.26	0.60	0.75	0.71	0.18	0.10	0.43	0.34	0.43	0.66	0.28	0.19	0.19
Total	100.01	100.00	99.97	100.07	100.0	100.0	99.99	100.01	99.99	100.09	100.1	99.91	100.01	100.00	99.94	99.94
Molecular Percent (Ab	54.0	49.2	24.7	19.0	48.7	41.5	41.9	24.7	26.3	39.7	39.8	33.1	24.8	25.9	24.9	27.9
(An	41.6	46.4	74.0	79.5	47.7	54.1	54.0	74.3	73.1	57.8	58.2	64.3	71.3	72.4	74.0	71.0
(Or	4.3	4.4	1.3	1.5	3.5	4.4	4.1	1.1	0.6	2.5	2.0	2.6	3.9	1.7	1.1	1.1

* Na_2O values derived by calculation (see Chapter 4)

Note 5a, 5b, 6a, 6b, 11b, 11c, 76b and 76c are phenocrysts

BLD BELOW DETECTION LIMITS ND NOT DETERMINED

different age.

The plagioclase analyses listed in Table 6.3 are semiquantative, Na_2O values are calculated (see Chapter 4), they show that plagioclase phenocrysts are more basic than coexisting groundmass plagioclase in rocks of all types. Specimen 76, a picritic transition dolerite, has phenocrysts of composition An_{70-75} while the groundmass plagioclase has the composition An_{64}. Plagioclase composition An_{74} occurs in the groundmass of specimen 54 (a transition dolerite). Plagioclase phenocrysts in the tholeiitic dolerites and craignurites range from An_{80} (sample 6) to An_{54} (sample 11), while analysed groundmass compositions fall in the range An_{74} (sample 330) to An_{48} (sample 11). Phenocrysts in the craignuritic felsite, sample 5, have compositions in the range An_{41} to An_{47}, the groundmass consists of a fine grained feldspathic matrix in which it is not possible to determine individual feldspar compositions. All analysed plagioclases show relatively high Fe_2O_3 concentrations, as do those in the alkali dolerites, high alumina basalts and layered gabbro at Carlingford (see Chapters 4 and 5 above, also Le Bas 1970a), similar high iron concentrations are reported from Japan by Iida (1961). Brown suggests that Fe replaces Si^{4+} or Al^{3+} as Fe^{3+} in the plagioclase lattice (1968 p 111). TiO_2 concentrations are below the limits of detection in all plagioclases for which data are available, with the exception of 11a, MgO is also below the limits of detection except in the case of 54b.

Pyroxene compositions in the tholeiitic basalt - craignurite series (see Table 6.4) fall in the range salite, augite, ferroaugite, with some varieties relatively low in CaO approaching subcalcic augite

TABLE 6.4

Composition of clinopyroxene in members of the tholeiitic basalt-craignurite series

Sample	5			6		11		54		71		76	330	
Analysis	a	b	c	a	b	a	b	a	b	a	b	a	a	b
SiO_2	51.3	51.8	44.7	52.91	49.82	48.8	54.1	52.4	51.6	49.92	49.39	50.0	53.26	51.68
TiO_2	ND	ND	ND	0.97	0.69	1.70	1.46	1.46	1.36	1.58	1.54	2.02	0.78	0.95
Al_2O_3	2.20	1.47	5.0	1.95	3.94	4.84	3.84	4.80	4.53	3.91	4.45	4.42	1.90	3.01
Fe_2O_3	20.5	18.1	28.1	17.97	16.02	21.5	15.5	7.57	8.11	14.09	13.31	11.4	9.55	9.91
CaO	15.0	18.8	17.6	13.16	15.23	13.5	11.2	20.2	19.7	15.62	18.48	21.6	19.71	20.07
MgO	10.9	9.79	4.61	13.00	14.35	8.65	13.8	13.6	14.6	14.94	12.87	10.6	14.90	14.38
K_2O	ND	ND	ND	0.15	BLD	1.02	0.14	BLD	BLD	BLD	BLD	ND	BLD	BLD
Total	99.9	99.96	100.01	100.11	100.05	100.01	100.04	100.03	99.9	100.06	100.04	100.04	100.10	100.00
Molecular (Wo	36.6	41.6	40.2	30.2	32.7	35.2	27.4	45.4	43.0	33.7	40.3	48.6	41.7	42.5
Percent (En	34.3	30.4	14.7	41.2	43.2	28.9	46.5	42.7	44.6	45.1	39.4	33.4	44.2	42.8
(Fs	32.1	28.0	45.1	28.6	24.1	36.0	26.1	11.9	12.3	21.2	20.3	18.0	14.1	14.7

Note 5a, 5b, 11b are phenocrysts.

N D Not determined

BLD Below detection limits.

in composition (Poldevaart and Hess 1951 p 472). Orthopyroxene and pigeonite have not been identified in the Carlingford tholeiitic series; Holland and Brown report that orthopyroxene is absent and pigeonite rare in the tholeiitic rocks of Ardnamurchan (1972 p 142). Clinopyroxene occurs mainly in the groundmass though it is also present as phenocrysts in some rocks particularly in porphyritic craignuritic felsites (inninmorite) such as specimen 5. Pyroxenesin the transition dolerites and tholeiitic dolerites are calcic and relatively iron poor compared with those of other rocks in the suite, (those in the more basic alkali dolerites and in the high alumina basalts are generally less iron rich), they range from Wo_{49} En_{33} Fs_{18} in sample 76 to Wo_{42} En_{44} Fs_{14} in 330. Pyroxenes in quartz dolerites and craignurites show progressive iron enrichment with increasing acidity, which is reflected by the composition of coexisting phenocrysts and groundmass crystals, phenocrysts being less Fe rich. Pyroxenes in the quartz dolerites show depletion in CaO compared with those in transition dolerites (see Figure 6.1). Phenocrysts in samples 5 show higher SiO_2 and lower Al_2O_3 concentrations than coexisting groundmass pyroxenes and there is a general decrease in Al_2O_3 concentrations between pyroxenes in the transition dolerites and those in the quartz dolerites and craignurites. TiO_2 concentrations are considerably lower than those of pyroxenes in the alkaline suite in the majority of cases, though an analysed groundmass pyroxene in 76 (picritic transition dolerite) does contain more than 2.0 percent TiO_2. Several pyroxenes from rocks in the tholeiitic suite have TiO_2 values much in excess of those recorded from the high alumina basalt series.

Figure 6.1

Pyroxene compositions in rocks of the Carlingford tholeiitic basalt - craignurite series.

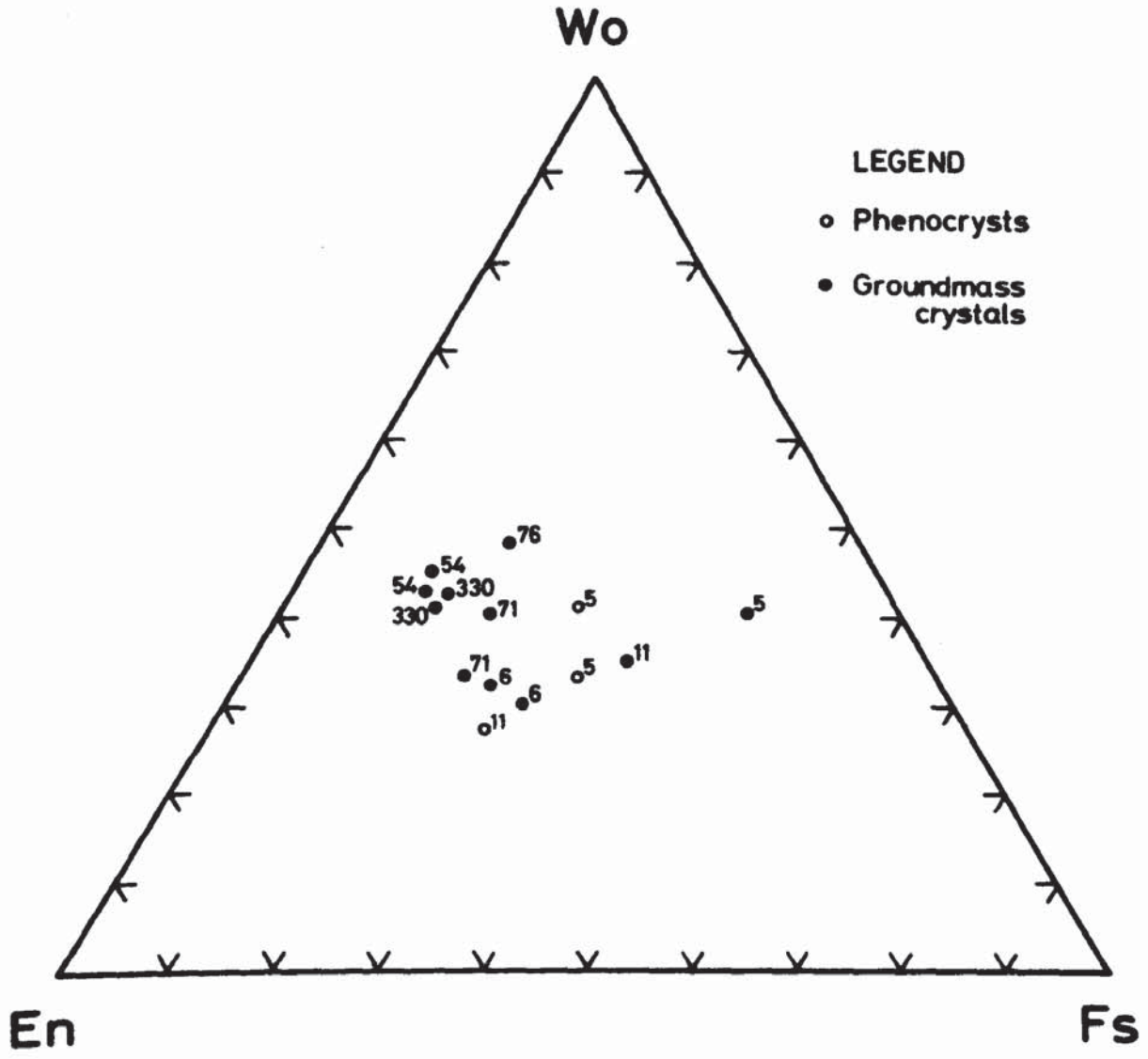

TABLE 6.5

Composition of altered olivine in transition dolerites

	54		76	
	a	b	a	b
SiO_2	56.4	59.1	57.2	51.8
TiO_2	BLD	ND	BLD	BLD
Al_2O_3	3.03	2.55	5.40	4.98
Fe_2O_3	11.5	9.69	8.28	7.19
CaO	0.18	0.47	4.97	4.32
MgO	28.7	28.1	24.2	31.7
K_2O	0.26	0.15	ND	ND
Total	100.07	100.06	100.05	99.99

ND Not determined
BLD Below detection limits

TABLE 6.6

Composition of titanomagnetite in a craignuritic felsite and a tholeiitic dolerite

	5		71		
	a	b	a	b	
TiO_2	25.4	31.4	30.41	29.51	
Fe_2O_3	74.6	68.6	67.85	68.48	
MnO	ND	ND	1.79	1.99	
Total	100.0	100.0	100.05	99.98	
Molecular)	23.8	5.8	7.1	9.6	Magnetite
Percent)	76.2	94.2	92.9	90.4	Ulvospinel

Note 5a and 5b are phenocrysts
ND Not determined.

Olivines in the transition dolerites and tholeiitic dolerites of Carlingford are invariably altered as they are in other rock types (see Chapters 4 and 5 above). The four analyses listed in Table 6.5 are those of altered olivines as witnessed by their relatively high SiO_2 and Al_2O_3 concentrations, (and high CaO values in the case of those in 76); which occur in two transition dolerites. The two pairs of analyses are mutually consistant within reasonable limits and assuming on that basis that alteration has not greatly affected the Mg:Fe ratios, they suggest that the primary olivine compositions fell in the range Fo_{83} to Fo_{85} and Fo_{85} to Fo_{90} in 54 and 76 respectively. Such high proportions of forsterite suggest that the olivines separated early during the crystallization of the parent magmas (Brown 1968 p 141).

Partial analyses of titanomagnetites occurring in two members of the tholeiitic basalt - craignurite series are listed in Table 6.6, those present in specimen 5 occur as phenocrysts only. TiO_2 solid solution is extensive in the ores of both samples, such that ulvospinel comprises between 76 and 94 percent. Titanomagnetite in sample 330 shows exsolution of ilmenite as lamellae and its subsequent alteration to leucoxene.

The partitioning of CaO in coexisting plagioclase and clinopyroxene is sympathetic. Plagioclase An_{74} coexisting with clinopyroxene Wo_{45} in the groundmass of sample 54, and An_{48} with Wo_{33} in sample 11, the trend exhibited by these pairs suggests a decreasing availability of CaO in quartz dolerites compared with transition dolerites. MgO entered olivine and pyroxene in the transition dolerites and pyroxene in the quartz dolerites in relative abundance, the craignuritic rocks

however show Fe enrichment at the expense of Mg in the pyroxenes.

PETROCHEMISTRY

Appendix IV lists the analysed compositions of members of the tholeiitic basalt-craignurite series in terms of major element concentrations, trace element concentrations for the same rocks are listed in Appendix XII. Compositions calculated in terms of the CIPW norm for those rocks are set out in Appendix VIII, additional analyses are listed in Appendix XV.

It was not considered necessary to amend these analyses prior to further investigation, other than to recalculate analyses with loss on ignition in excess of 5%,as anhydrous,and Fe_2O_3 so not to exceed % TiO_2 + 1.5%, for the purpose of normative calculations (Irvine and Baragar 1971 p 526).

Composition in terms of major elements.

The composition of rocks of all three intrusive cycles attributed to the tholeiitic basalt - craignurite series are summarised in Figure 6.2 by a series of silica variation diagrams. There is no distinction in terms of major element chemistry between the rocks of the three cycles as far as can be ascertained,and when plotted in this manner the majority of rocks fall in coherent fields with trends common to all three age series. There is also no distinction between the composition of rocks occurring as dykes and those in cone-sheets. The compositional continuity of the suite throughout its petrographic range indicates its underlying petrogenetic coherence and suggests that

Figure 6.2

Compositions of rocks in the Carlingford tholeiitic basalt - craignurite series, depicted graphically as a series of silica variation diagrams.

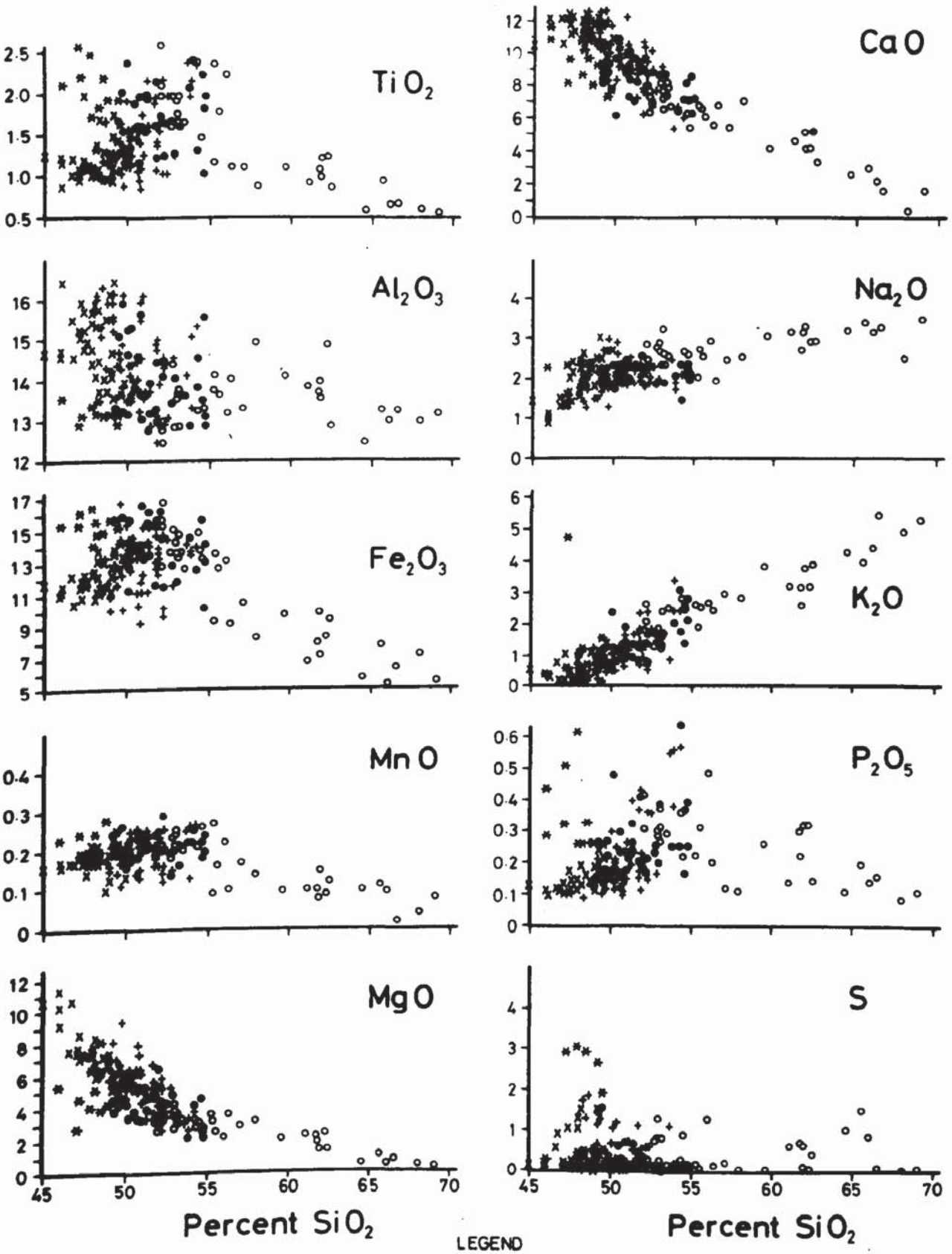

the chemical variation shown is the product of a simple petrogenetic process or processes such as crystal fractionation. Similar coherent series have been described from Ardnamurchan, where it also proved impractical to distinguish rocks of different age on chemical grounds (Holland and Brown 1972), and Mull (Bailey et al. 1924). The high iron transition dolerites are an exception to the continuity exhibited by the suite as a whole and form distinct clusters separate from those of the other transition dolerites on several of the plots in Figure 6.2.

The behaviour of TiO_2 in Figure 6.2 is very similar to that of Fe, the majority of rocks form a field with concentrations of both components increasing in value with increasing SiO_2 concentrations up to the 52 percent SiO_2 level, there then follows progressive depletion in TiO_2 and Fe with increasing SiO_2 values. The high iron transition dolerites are exceptional in having higher values for both TiO_2 and Fe than other rocks with the same SiO_2 concentrations, that is values in excess of 1.5 percent and 14 percent respectively. The majority of transition dolerites have TiO_2 values between 0.75 and 1.25 percent and Fe concentrations between 11 and 14 percent. TiO_2 and Fe concentrations in the majority of tholeiitic dolerites and quartz dolerites fall in the range 1 to 2.5 percent and 11 to 16 percent respectively; they range from 0.5 to 2.5 percent and 5 to 16 percent respectively in the craignuritic rocks of the series. Those rocks classified chemically as high alumina basalts but regarded as feldsparphyric members of the tholeiitic series show a similar range of TiO_2 and Fe concentrations (see Chapter 5 Fig. 5.1 above).

The covariance of TiO_2 with iron suggests that its behaviour is

largely controlled by the separation of ore phases.

Al_2O_3 concentrations show progressive depletion with increasing SiO_2 values for the suite as a whole with theexception of the high iron transition dolerites, though this is somewhat obscured by the wide range of values exhibited. The high iron transition dolerites all contain less than 14.0 percent Al_2O_3, while Al_2O_3 concentrations in the majority of other transition dolerites fall in the range 14 to 16.5 percent. The tholeiitic dolerites and quartz dolerites have Al_2O_3 values between 16.5 and 12.5 percent, in the craignuritic rocks they range from 15.7 to 12.4 percent.

MnO behaves in the same manner as TiO_2 being covariant with iron, it shows initial enrichment with increasing SiO_2 values up to about 52 percent, followed by subsequent depletion. The high iron transition dolerites have higher values than the majority of other transition dolerites. Almost all dolerites in the suite have MnO values in the range 0.1 to 0.3 percent, MnO in the craignuritic rocks ranges from 0.02 to 0.27 percent.

Both MgO and CaO show progressive negative covariance with SiO_2, values in the high iron transition dolerites are lower for both oxides than other dolerites with the same SiO_2 concentrations, otherwise MgO falls from 7 to 9 percent in the transition dolerites to less than 2 percent in the craignuritic felsites, and CaO from values in excess of 10 percent to between 0.2 and 5 percent. The majority of porphyritic tholeiitic dolerites in the high alumina basalt series have MgO and CaO values consistant with those of the tholeiitic dolerites of the tholeiitic basalt-craignurite series.

Na_2O and K_2O both show progressive enrichment with increasing SiO_2 values, Na_2O concentrations ranging from about 1 percent in the most basic transition dolerites to 3.5 percent in the craignuritic felsites, while K_2O concentrations increase from 0.1 to 5.5 percent. The more marked enrichment of K_2O in the Hebridean tholeiitic dolerite-craignurite series contrasts with that of the tholeiite - icelandite series of Iceland (Carmichael 1964) and is diagnostic of the former (see Chapter 3). The concentrations of alkalies in the high iron transition dolerites are similar to those of the majority of other transition dolerites though higher than some, the exceptionally high concentration of K_2O in 1293 which occurs as a dyke, is attributed to contamination by the Carlingford granophyre which it cuts.

P_2O_5 shows enrichment with increasing SiO_2 values in rocks with up to 54 percent SiO_2, at which point the majority have concentrations in excess of 0.25 percent, values fall progressively to 0.1 to 0.2 percent in the craignuritic felsites. The high iron transition dolerites have P_2O_5 in the range 0.2 to 0.35 percent while other transition dolerites have P_2O_5 between 0.1 and 0.2 percent. Concentrations of P_2O_5 in those high alumina basalts considered to be porphyritic tholeiitic dolerites approach 0.1 percent in the majority of cases.

As in the alkali basalts and high alumina basalts sulphur attains major element status in the tholeiitic basalt - craignurite series. The behaviour of S is somewhat obscure, the majority of rocks have S values not exceeding 0.5 percent. Those with S in excess of 0.5 percent contain secondary pyrite in the majority of cases, however there is some evidence of enrichment of S in rocks with SiO_2 concent-

rations in the range 50 to 54 percent, which is reflected by the appearance of iron sulphide as a primary ore phase (see above). The majority of craignuritic felsites have low S concentrations and contain almost no primary ore, sample 5 is unusual however in having 1.5 percent S and retaining iron sulphide as a primary ore phase.

Comparison of compositions of rocks in the Carlingford tholeiitic basalt-craignurite series, with those of similar suites in the Hebridean province listed in Table 6.7, indicates its widespread occurrence throughout the area, and thus its significance as a petrogenetic series.

The high iron transition dolerites are somewhat atypical, and are characterised by high concentrations of Fe, TiO_2 and P_2O_5 and low MgO, CaO and Al_2O_3 values. As a result the ratio FeO + Fe_2O_3 : FeO + Fe_2O_3 + MgO exceeds 0.7 for these rocks which is higher than that for other rock types with similar SiO_2 values. The feldsparphyric tholeiitic dolerites attributed to the high alumina basalt series have compositions which are comparable to those of members of the tholeiitic dolerite-craignurite series with the exception of high Al_2O_3 concentrations.

The majority of rocks in the series are quartz, orthopyroxene normative though some transition dolerites are olivine, orthopyroxene normative - see Appendix VIII (the majority of high iron transition dolerites are quartz normative). When plotted on the triangle normative quartz, nepheline, olivine they form a field astride the line enstatite albite, trending towards the quartz nepheline boundary on which it impinges somewhat nearer the quartz apex than either the alkali basalt series or high alumina basalt series (see Fig. 3.1).

A differentiation index (D.I.) has been calculated for each rock

TABLE 6.7

Composition of members of the tholeiitic basalt-craignurite series in the British Tertiary Province

	A	B	C	D	E	F
SiO_2	64.3	50.10	54.00	69.26	55.00	60.20
TiO_2	0.75	2.98	2.83	0.45	2.40	1.05
Al_2O_3	14.18	12.08	13.09	11.60	16.48	14.82
Fe_2O_3	1.09	4.35	3.53	1.31	1.50	1.90
FeO	4.44	11.18	8.45	2.57	9.85	7.93
MnO	0.26	0.25	0.37	0.45	0.45	0.26
MgO	1.47	3.93	3.49	1.10	2.82	1.34
CaO	2.87	8.85	5.55	2.61	5.40	4.25
Na_2O	4.30	3.06	3.27	2.08	1.92	2.40
K_2O	2.83	0.96	1.80	3.88	2.60	4.15
P_2O_5	0.17	0.17	0.31	0.10	0.18	0.73
S	-	-	-	-	tr	-
FeS_2	-	0.28	0.14	-	-	-
Fe_7S_8	-	0.02	-	-	-	-
(Co, Ni)O	-	-	-	-	-	-
BaO	0.16	0.05	0.02	-	-	-
CO_2	0.0	tr	0.25	1.76	-	-
H_2O+)	3.02	1.01	1.71	1.67	1.20	0.60
H_2O^-)		0.53	1.26	1.61	0.10	0.50
Total	99.84	99.8	100.07	100.45	99.90	100.13

A. Inninmorite-pitchstone, lava, Ardnamurchan (Richey and Thomas 1930, p84, Table III, No 1); B. Quartz dolerite, cone-sheet, Ardnamurchan (Richey and Thomas 1930, p82, Table II, No 1); C. Quartz dolerite, sill, Arran (Tyrrell 1928, p 147, Table II, No 4); D. Felsite, dyke, Arran (Tyrrell 1928, p 147, Table II, No 6); E. Andesite, dyke, Mournes (Tomkeieff and Marshall 1935, p 261, Table II, No 2); F. Variolite, dyke, Mournes (Tomkeieff and Marshall 1935, p 261, Table II, No 3).

TABLE 6.7 cont.

Composition of members of the tholeiitic basalt-craignurite series in the British Tertiary Province

	G	H	I	J	K	L
SiO_2	55.82	64.13	66.27	47.35	52.16	66.48
TiO_2	1.62	1.19	0.87	1.75	3.25	0.62
Al_2O_3	11.47	13.15	11.92	13.90	11.95	14.01
Fe_2O_3	3.68	1.08	3.09	5.87	4.86	0.60
FeO	7.66	6.31	3.18	8.96	9.92	4.55
MnO	0.40	0.27	0.31	0.23	0.18	0.12
MgO	4.08	1.08	1.44	5.97	3.77	1.32
CaO	7.88	3.62	3.30	10.65	7.14	1.88
Na_2O	2.58	3.64	2.89	2.73	2.36	3.58
K_2O	2.00	2.32	4.03	0.54	1.74	3.55
P_2O_5	0.23	0.31	0.17	0.24	0.24	0.09
S	-	-	-	0.23	0.18	-
FeS_2	0.09	-	-	-	-	-
Fe_7S_8	-	-	-	-	-	-
(Co,Ni)O	0.04	-	-	-	-	-
BaO	0.03	0.09	-	-	-	-
CO_2	0.08	-	0.53	0.32	0.18	1.56
H_2O+)	1.88	2.71	1.51	1.16	1.95	1.41
H_2O^-	0.66	0.36	0.78	1.04	0.56	0.44
Total	100.18	100.26	100.29	100.94	100.44	100.21

G. Basic craignurite, cone-sheet, Mull (Bailey et al. 1924, p 19, Table III, No 1); H. Inninmorite pitchstone, sheet, Mull (Bailey et al. 1924, p 19, Table III, No V); I. Acid craignurite, cone-sheet, Mull (Bailey et al. 1924, p 19, Table III No VI); J. Salen tholeiite, dyke, Mull (Bailey et al. 1924, p 17, Table II, No 1); K. Quartz dolerite, cone-sheet, Mull (Bailey et al. 1924, p 17, Table II, No VIII); L. Felsite, sill, Skye (Buist 1959, p 248, Table 1, No 2).

from its CIPW norm in the manner of Thornton and Tuttle (1960), they are assumed to reflect the degree of evolution exhibited by the rock in question. The high iron transition dolerites have D.I. values in excess of 25 while other transition dolerites have D.I. values less than 25 and as low as 12 in some cases. The majority of tholeiitic dolerites and quartz dolerites have differentiation indices in the range 20 to 40, while craignuritic rocks have values between 36 and 90.

Trace Elements.

Figure 6.3 consists of a series of histograms of the concentrations of fourteen trace elements listed in Appendix XII plotted separately for rocks in each of the three intrusive cycles. These values are discussed below, together with the concentration of seven other trace elements, including some listed only in Appendix XV.

The behaviour of Sc, V, Cr, Co, Ni, Cu, Zn, Rb, Sr, Y, Zr, Ba, Ce and Pb in the tholeiitic basalt - craignurite series is summarised graphically in Figure 6.4.

Scandium:

Rocks in all three intrusive cycles have similar ranges of Sc values which fall between 10 and 90 ppm for the suite as a whole. Values in the range 60 to 70 ppm form the mode, which is also the mode for transition dolerites in Cycles I and II and the tholeiitic dolerites and quartz dolerites of Cycles II and III. The majority of transition dolerites, including the high iron transition dolerites, have Sc values in excess of 60 ppm while almost all craignuritic rocks have Sc values

Figure 6.3

Histograms of trace element abundance frequencies in rocks of the Carlingford tholeiitic basalt - craignurite series. A few exceptional values lying outside the range depicted have been excluded (see text for details).

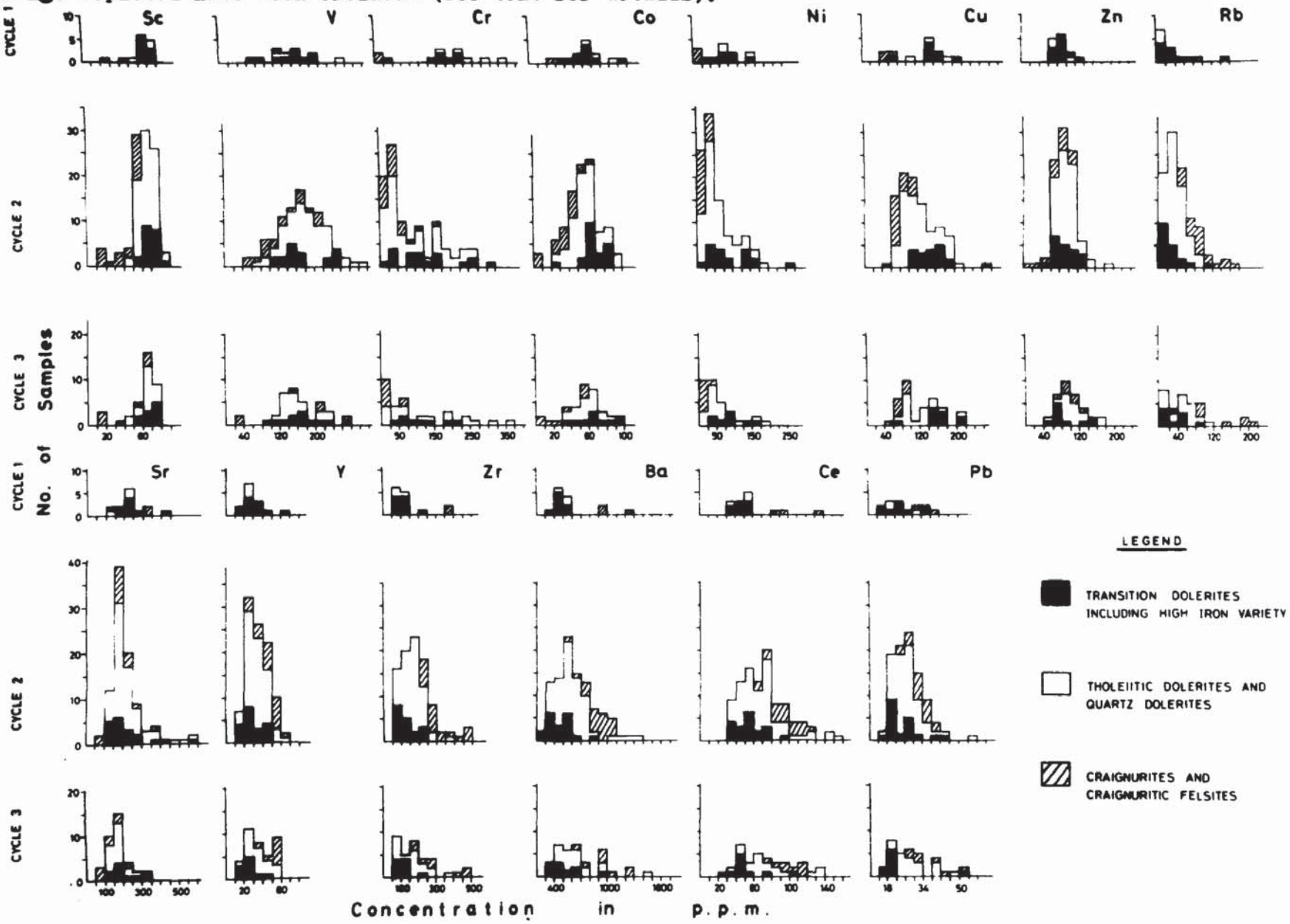

Figure 6.4

Behaviour of trace elements during fractionation in the Carlingford tholeiitic basalt - craignurite series depicted as a series of variation diagrams of concentration versus Differentiation Index (D.I.).

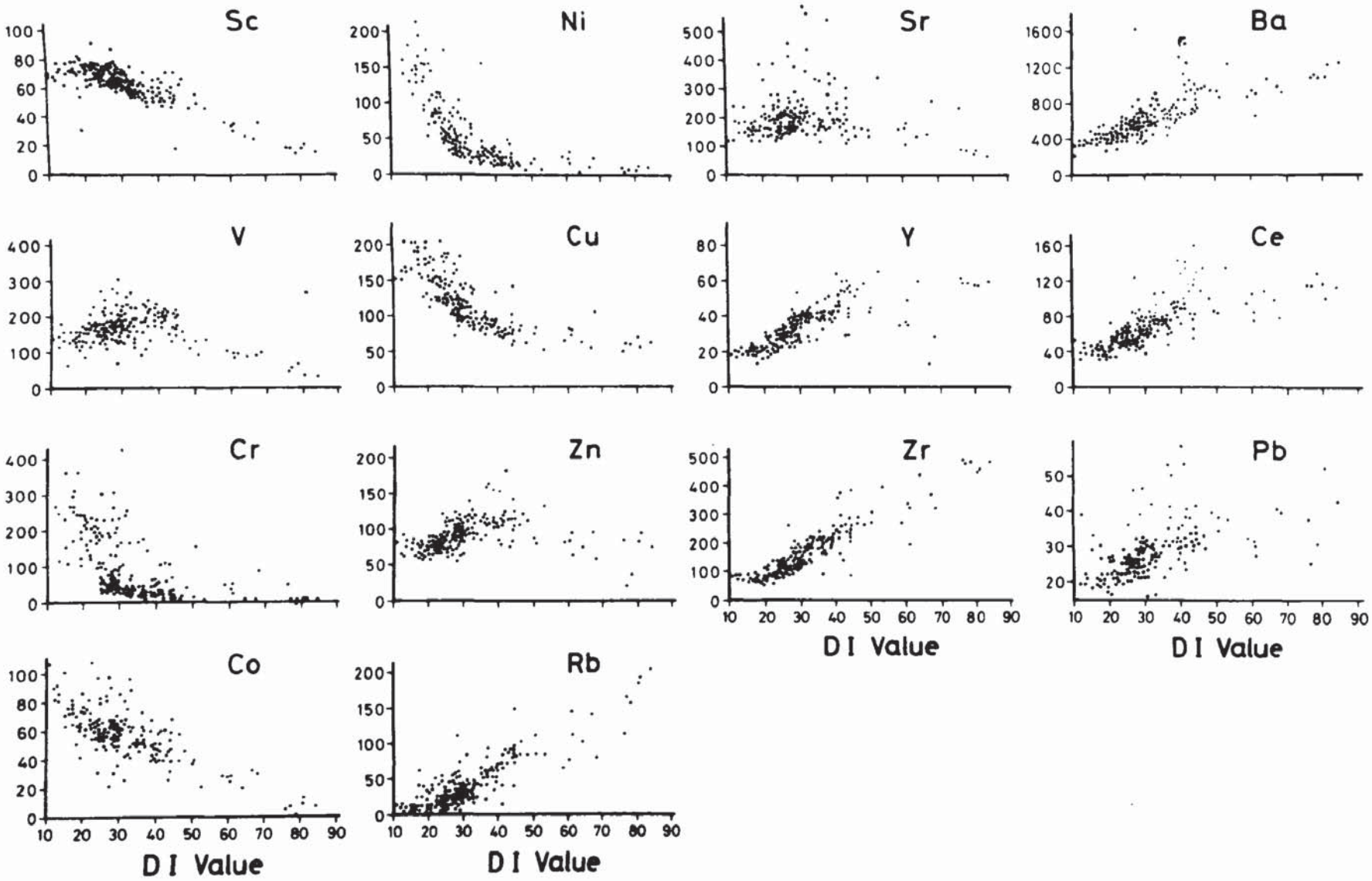

less than 60 ppm indicating depletion with increasing acidity. This behaviour is confirmed when Sc is plotted against D.I. in Figure 6.4, suggesting that Sc is removed in early formed plagioclase (see also Chapter 5). Sc may also have been removed in pyroxenes, for which it has an affinity (Prinz 1968 p 309), during the later stages of fractionation.

Vanadium:

Vanadium values fall in the range 20 to 320 ppm for the suite as a whole. The Cycle II transition dolerites show a distinct bimodality reflecting their subdivision into high iron transition dolerites and normal transition dolerites. All high iron transition dolerites have V values in excess of 160 ppm, all Cycle II transition dolerites with V in excess of 200 ppm are of that type. There is no such clear distinction in the V values of the transition dolerites of Cycle III. The range of V values exhibited by the tholeiitic dolerites and quartz dolerites is similar to that of the transition dolerites for the suite as a whole, values in the range 180 to 200 ppm form the mode in Cycle II, while in Cycle III values in the range 120 to 140 form the mode. V concentrations in the majority of craignuritic rocks are lower than 180 ppm, some of the more acidic varieties having values in the range 40 to 60 ppm in Cycle II, and 20 to 40 ppm in Cycle III, suggesting V depletion in the acid members of the series. When plotted against D. I. V concentrations show initial enrichment with increasing

D.I. up to D.I. 40 followed by a subsequent depletion in rocks with higher D.I. values (see Fig. 6.4).

Chromium:

The majority of rocks in the tholeiitic basalt - craignurite series have Cr values in the range 0 to 400 ppm. The majority of high iron transition dolerites have Cr values less than 100 ppm, nearly all other transition dolerites have Cr in excess of 100 ppm, two olivine rich samples attributed to Cycle III and not included on Figure 6.3, have chrome values in excess of 600 ppm (samples 54 and 84). Values in the range 25 to 50 ppm and 0 to 25 ppm form the mode for the Cycle II and Cycle III suites as a whole respectively, as a large proportion of the tholeiitic dolerites, quartz dolerites and craignurites have Cr values less than 50 ppm. The bimodality apparent in the Cycle II suite is of uncertain significance. When plotted against D.I. Cr values show progressive depletion with increasing D.I. values up to D.I. 40; concentrations of Cr are low in the majority of rocks with D.I. in excess of 40 hence further depletion is not readily apparent.

Cobalt:

Cobalt values fall in the range 0 to 110 ppm. The majority of transition dolerites have Co values in excess of 50 ppm, with concentrations in the range 60 to 70 ppm forming the mode for all three age groups, concentrations in the high iron varieties span the range. Values in the range 50 to 60 ppm form the mode for the quartz dolerites and tholeiitic dolerites of Cycles II and III, while the majority of

craignuritic rocks have Co concentrations less than 50 ppm indicating Co depletion with increasing acidity. The latter phenomenon is confirmed when Co is plotted against D.I. (Fig. 6.4).

Nickel:

The majority of rocks in the series have Ni values in the range 0 to 200 ppm, a few transition dolerites, including 54 and 84, have Ni values in excess of 250 ppm and are not included in Fig. 6.3. The majority of transition dolerites with the exception of the high iron varieties have Ni values in excess of 50 ppm the latter have less than 50 ppm Ni. Values in the range 25 to 50 ppm form the mode in the tholeiitic dolerites and quartz dolerites of Cycle II and III. The majority of craignurites have Ni values not exceeding 50 ppm. When plotted against D.I. (Fig. 6.4) Ni concentrations show a behaviour similar to that of Cr (see above).

Copper:

Most rocks attributed to the series have Cu values in the range 40 to 220 ppm, the significance of the bimodality of distribution apparent in the Cycle II and Cycle III suites is uncertain. The majority of transition dolerites have Cu values in excess of 100 ppm, the majority of the high iron transition dolerites of Cycle II having values between 100 and 160 ppm, other types having higher concentrations. The range of concentrations exhibited by the tholeiitic dolerites and quartz dolerites overlaps that of the transition dolerites but with modal values in the range 80 to 100 ppm. The majority of craignurites

have Cu values less than 80 ppm. Figure 6.4 shows that Cu values are progressively depleted as D.I. values increase, the rate of depletion being greatest in rocks with D.I. less than 40.

Zinc:

The majority of rocks in the tholeiitic basalt - craignurite series have Zn concentrations in the range 40 to 200 ppm, with values in the range 80 to 100 ppm forming the mode in Cycles II and III. The high iron transition dolerites tend to have higher Zn values than other transition dolerites, otherwise the range of concentrations in the various rock types attributed to the suite overlap to such an extent that no trends are apparent from the histogram (Fig. 6.3). When plotted against D.I. however, Zn shows initial enrichment with increasing D.I. values in rocks with D.I. less than 40, and depletion with increasing D.I. in the craignuritic members of the series (see Fig. 6.4).

Two rocks (851 a quartz dolerite and 911b a basaltic craignurite) from a composite cone-sheet have exceptionally high Zn values in excess of 300 ppm (see Chapter 7 below).

Rubidium:

Rb values in the range 0 to 20 ppm form the mode in the transition dolerites of all three Cycles, higher concentrations of rubidium occur in the high iron transition dolerites than other transition dolerites, for example 1293 (Cycle III) has an Rb values of 349 ppm which is exceptional (not included in Fig. 6.3). The tholeiitic dolerites and quartz dolerites have Rb concentrations in the range 0 to

120 ppm, with concentrations in the range 20 to 40 ppm and 60 to 80 ppm forming the mode in Cycle II and Cycle III respectively. The majority of craignuritic rocks have Rb values in the range 40 to 180 ppm, some craignurites and craignuritic felsites of Cycle III have Rb values in excess of 180 ppm. When plotted against D.I. (Figure 6.4) Rb shows progressive enrichment with increasing fractionation.

Strontium:

The majority of rocks in the series have Sr values in the range 50 to 400 ppm, sample 75 (Cycle III) has a Sr value of 763 ppm (not included in Fig. 6.3) which is exceptional. Sr concentrations in the transition dolerites, tholeiitic dolerites and quartz dolerites show a similar range, though the high iron transition dolerites of Cycle II show higher Sr values than other transition dolerites. Sr values in craignuritic rocks do not exceed 400 ppm and several have less than 100 ppm. Sr values form a scatter when plotted against D.I. (Fig.6.4) however the underlying trend is towards Sr enrichment with increasing D.I. values up to D.I. 40 and depletion in rocks with higher values, it was probably removed by substitution in the intermediate plagioclases (Prinz 1968 p 311).

Yttrium:

Concentrations of Y fall in the range 10 to 70 ppm. Values in the range 20 to 30 ppm form the mode in the transition dolerites of Cycles II and III, and in which only the high iron transition dolerites have Y values in excess of 30 ppm. Y concentrations in the tholeiitic

dolerites and quartz dolerites span the range for the suite as a whole, with values in the range 20 to 30 and 20 to 40 forming the modes in Cycle II and III respectively. The majority of craignuritic rocks have Y values in excess of 40 ppm indicating enrichment of Y in the acidic members of the series. Progressive enrichment of Y with increasing D.I. values is demonstrated by Figure 6.4.

Zirconium:

Zirconium concentrations are not available for all rocks in the series, however all determined values are included in Figure 6.3, they fall in the range 50 to 500 ppm for the suite as a whole. Concentrations in the transition dolerites range from 50 to 250 ppm, but only the high iron transition dolerites have Zr values in excess of 150 ppm. Values of up to 400 ppm have been recorded in the tholeiitic dolerite-quartz dolerite group, with values in the range 150 to 200 ppm forming the mode. The majority of craignuritic rocks have Zr values in excess of 200 ppm and, when plotted against D.I. Zr shows progressive enrichment with increasing fractionation (Figure 6.4).

Barium:

Barium, like Zr, exhibits enrichment with increasing fractionation when plotted against D.I. (Figure 6.4). Concentrations in the majority of transition dolerites fall in the range 200 to 700 ppm, the high iron variety exhibiting a tendency to have higher Ba values than other transition dolerites. Ba concentrations in the range 500 to 600 ppm form the mode in the tholeiitic dolerite-quartz dolerite group of

Cycle II, a similar modal range is exhibited by equivalent rocks of Cycle III. Ba concentrations in the majority of craignuritic rocks exceed 800 ppm.

Cerium:

Cerium concentrations fall in the range 20 to 160 ppm. As with Sr, Y, Rb and Ba, Ce concentrations in the high iron transition dolerites tend to be higher than in other transition dolerites, the majority of transition dolerites have Ce values between 20 and 80 ppm. The tholeiitic dolerite-quartz dolerite group have Ce concentrations up to 150 ppm, values in the range 70 to 80 ppm and 60 to 70 ppm forming the modes in Cycles II and III respectively. As Ce shows progressive enrichment with increasing fractionation in the manner of Ba etc (see plot of Ce versus D.I. in Figure 6.4), concentrations in the craignuritic varieties tend to be higher than in the majority of basaltic rocks.

Lead:

The majority of rocks in the series have lead values in the range 15 to 50 ppm, a few have higher concentrations. Pb values in the high iron transition dolerites tend to be higher than in the other transition dolerites though there is considerable overlap in the range of values exhibited. Members of the tholeiitic dolerite-quartz dolerite group in turn tend to have higher Pb concentrations than the transition dolerites as a whole but again there is considerable overlap of the two ranges. Concentrations in the majority of craignuritic rocks exceed 30 ppm, though values as low as 24 ppm are recorded in some. The

overall trend is thus for enrichment in Pb with increasing acidity.

Gallium:

Ga values in the majority of transition dolerites fall in the range 15 to 20 ppm. The high iron transition dolerites have Ga values of 18ppm or more, other rocks in the series have Ga values in the range 15 to 24 ppm with few exceptions. There is some evidence of Ga enrichment with increasing fractionation.

Germanium:

Germanium concentrations are at the limits of detection in the tholeiitic basalt-craignurite series. Recorded values, for all rock types, fall in the range 0 to 4 ppm.

Niobium:

Niobium values listed in Appendix XV include concentrations of less than 10 ppm in the majority of rocks with SiO_2 concentrations less than 50 percent. Values rise progressively in rocks with SiO_2 in excess of 50 percent such that recorded concentrations in the craignuritic felsites approach 50 ppm.

Tin:

Tin concentrations are near the limits of detection. In the transition dolerites they range from 0 to 6 ppm, values up to 10 ppm have been recorded in tholeiitic dolerites, quartz dolerites and craignurites suggesting enrichment in Sn with advancing fractionation.

Lanthanum:

Lanthanum concentrations listed in Appendix XV show a similar behaviour to those of niobium, rocks with SiO_2 concentrations less than 50 percent have recorded La values of less than 10 ppm. La values rise progressively with increasing SiO_2 values in rocks with SiO_2 in excess of 50 percent, values up to 80 ppm being recorded in the craignuritic felsites. Specimen 24, a tachylitic basaltic craignurite has a recorded La value of 148 ppm which is exceptional.

Thorium:

Thorium concentrations do not exceed 10 ppm in the tholeiitic dolerites, transition dolerites and quartz dolerites with the exception of samples 1393 and 889. Th values rise progressively with increasing SiO_2 concentrations in the craignuritic rocks, with concentrations in excess of 30 ppm being recorded in some craignuritic felsites.

Uranium:

Uranium concentrations are at the limits of detection. Recorded values in the transition dolerites, tholeiitic dolerites and quartz dolerites do not exceed 2 ppm. Concentrations of up to 6 ppm U have been recorded in craignuritic rocks indicating enrichment with fractionation.

In summary, trace element concentrations in the tholeiitic basalt-craignurite series form a continuous coherent spectrum, no clear distinction is apparent for concentrations of individual trace elements in rocks of the same type attributed to different intrusive episodes.

Concentrations of Sc, Cr, Co, Ni and Cu show progressive depletion with increasing fractionation while Rb, Y, Zr, Ba, Ce, Pb, Nb, La and Th show progressive enrichment. There is also evidence of progressive enrichment of Ga, Sn and U with increasing fractionation. V, Zn and Sr show initial enrichment in the early stages of fractionation but subsequent depletion in the craignuritic rocks reflecting the behaviour of Fe, TiO_2, MnO and P_2O_5 among the major elements. Concentrations of those elements showing progressive enrichment with fractionation, includingV Zn and Sr, are higher in the high iron transition dolerites than in other transition dolerites, while the former have lower values of Cr, Co. Ni and Cu. This behaviour indicates that the high iron transition dolerites are more evolved than other transition dolerites, which is also suggested by their higher D.I. values. The range of individual trace element concentrations exhibited by those tholeiitic basalts attributed to the high alumina basalt series as a result of their high Al_2O_3 values (see Chapter 5 above) fall within the ranges exhibited by the majority of rocks in the tholeiitic basalt-craignurite series proper, confirming their close affinity to the latter.

Fractionation trends

The petrographic continuity and petrochemical continuity of the Carlingford tholeiitic basalt-craignurite series has been demonstrated in the preceding sections, phenomena which suggest that intermediate and acid members of the series have been derived from parental melts similar in composition to basic rocks in the suite, by processes such as crystal liquid fractionation. The relative abundance of the various

rock types within the suite as reflected by the number of their recorded occurrences in minor intrusions within the complex (see Chapter 2 above) are consistant with such a petrogenetic model. The most abundant rock types in the suite are the tholeiitic dolerites and quartz dolerites, the majority of which have SiO_2 concentrations in the range 48 to 52 percent, and together constitute about 55 percent of all rocks in the series. The high iron transition dolerites make up about 5 percent of the total while other transition dolerites constitute about 20 percent. The craignurites and craignuritic felsites together make up the remaining 20 percent. Thus the volume of acid and intermediate end products is relatively small compared with the volume of basaltic material as required by models involving fractional crystallization.

Considering fractional crystallization to be the mechanism most likely to have made an important contribution to the chemical variation exhibited within the suite, and that the Thornton Tuttle differentiation index is a more appropriate measure of the degree of fractionation exhibited by a rock than its SiO_2 concentration, a series of major element oxides have been plotted against D.I. (Fig. 6.5) for the suite as a whole (as the petrochemical behaviour of rocks in the three intrusive Cycles is identical they are not plotted separately). Al_2O_3 values form a scatter showing a general decrease in concentrations with increasing D.I.. TiO_2, MnO and Total Fe show progressive enrichment with increasing D.I. up to D.I. 40, then progressive depletion in rocks with higher D.I. values, that behaviour is reflected by V and Zn among the trace elements. CaO and MgO are strongly covariant both showing progressive depletion with increasing D.I. throughout the suite, though the rate of MgO

Figure 6.5

Changes of composition within the Carlingford tholeiitic basalt - craignurite series during fractionation, depicted by a series of variation diagrams of major oxides versus Differentiation Index (D. I.). For explanation of symbols see Fig. 6.2.

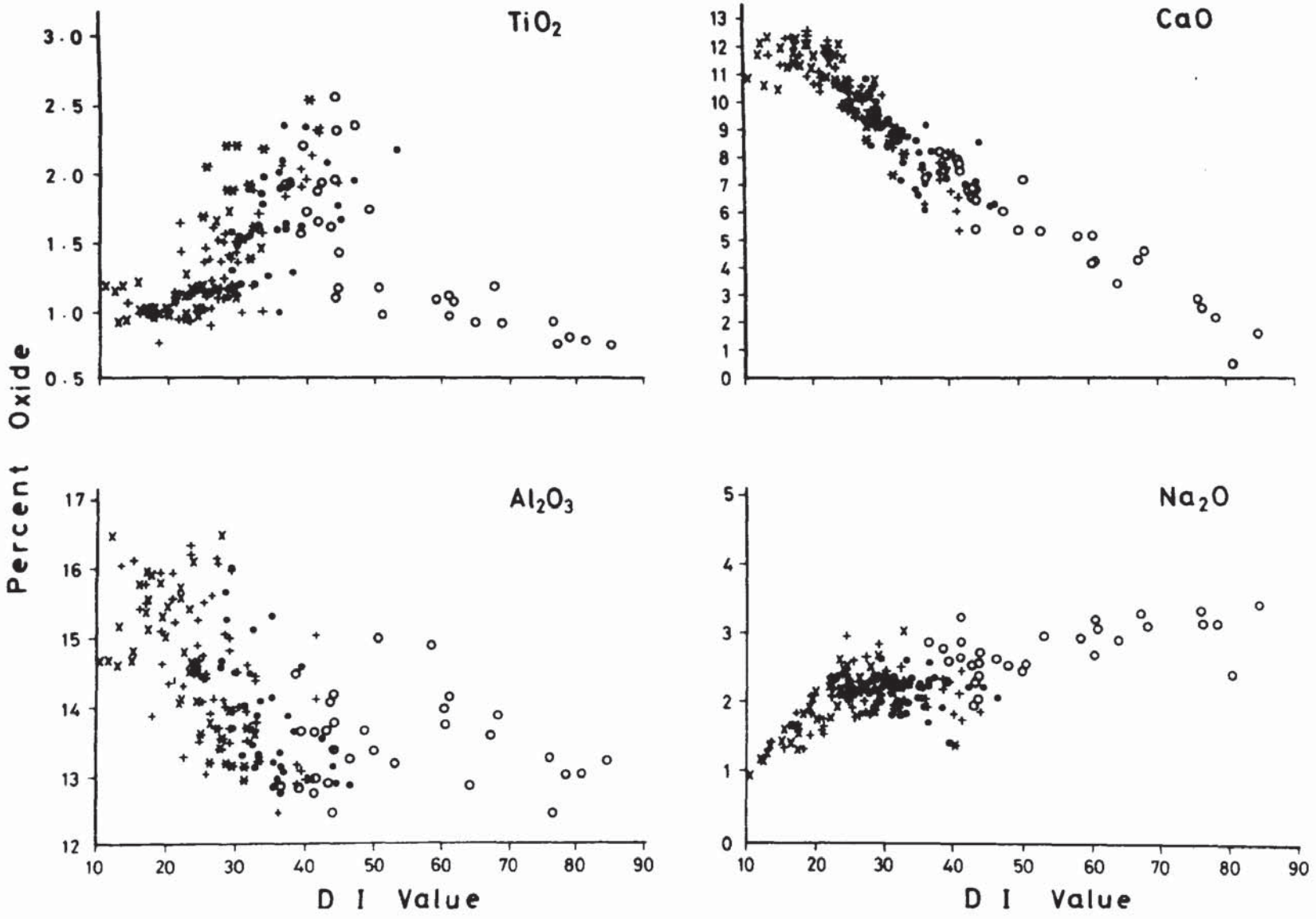

Figure 6.5 contd.

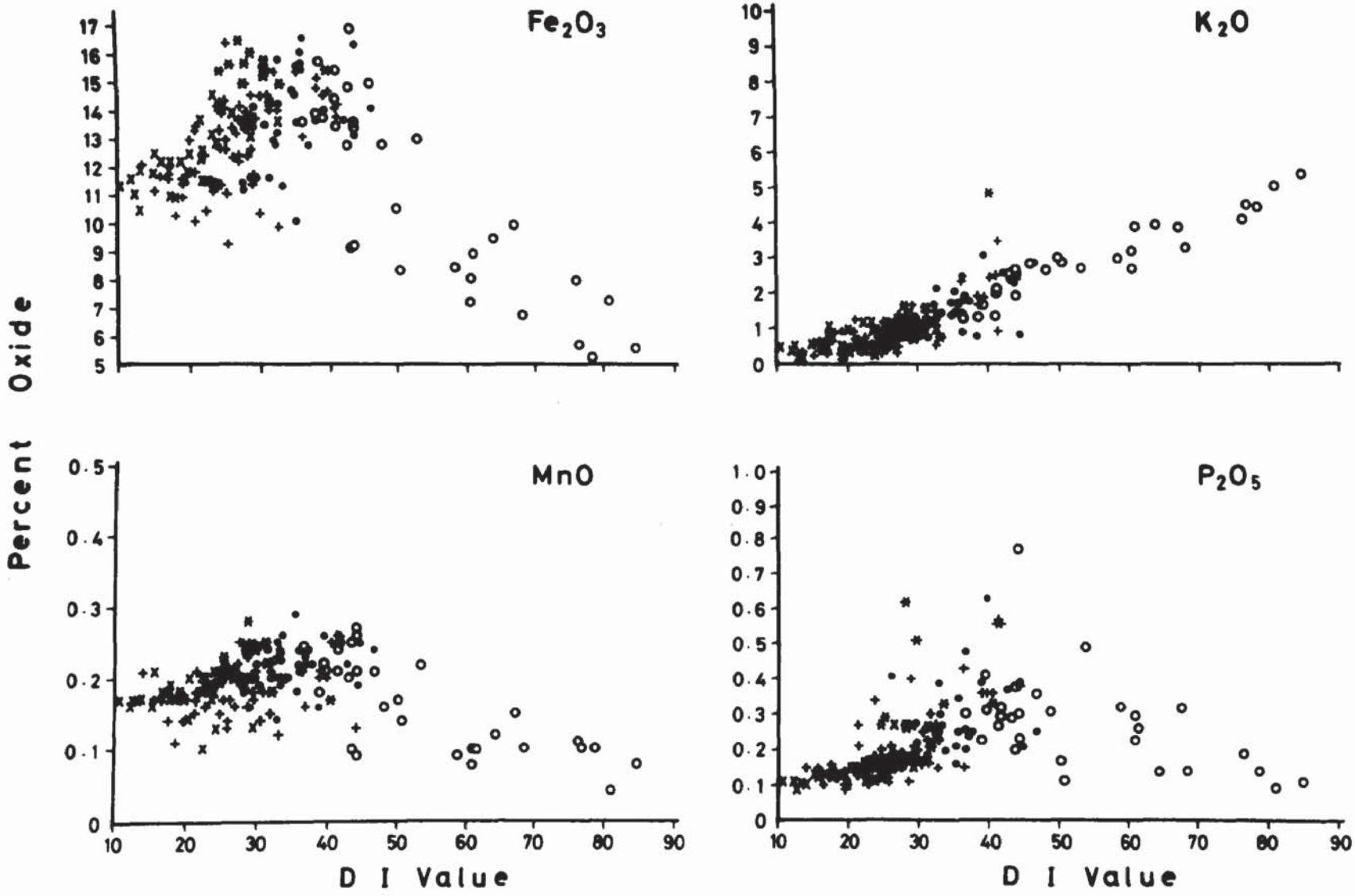

Figure 6.5 contd.

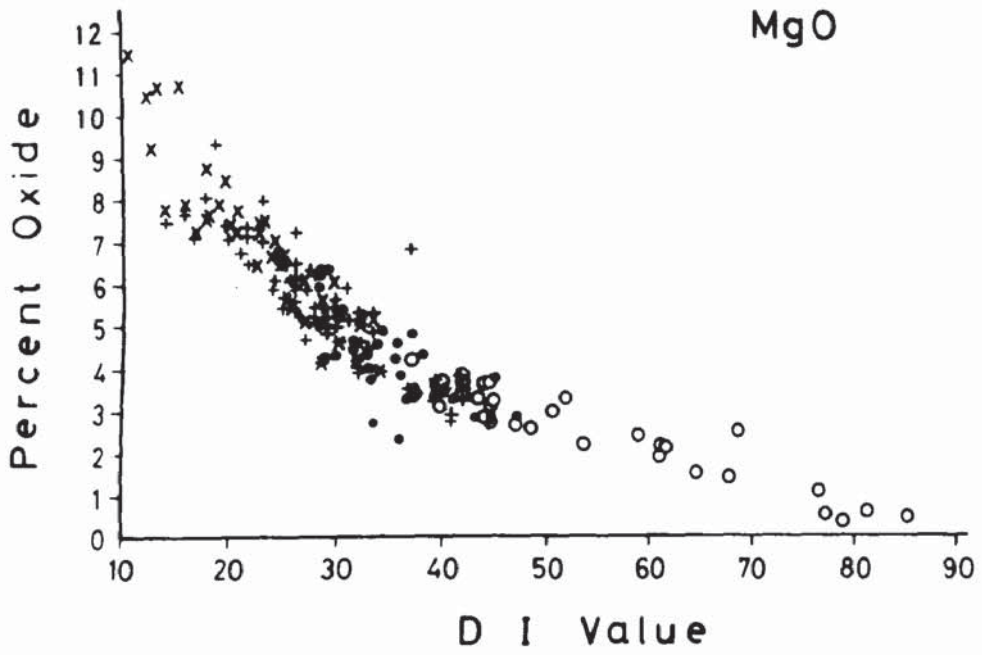

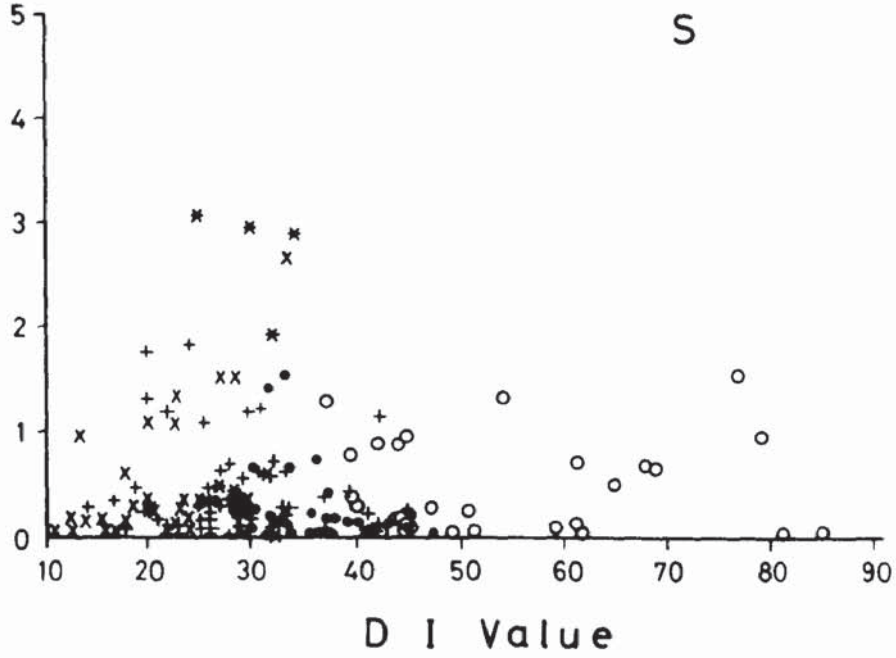

depletion decreases slightly in rocks with D.I. greater than 40. Na_2O and K_2O show progressive enrichment with increasing D.I. values, Na_2O increasing by a factor of three and K_2O by a factor of thirty between the more basic transition dolerites (D.I. < 15) and the acid craignuritic felsites (D.I. > 80), thus Na_2O:K_2O ratios fall from values of about 6 to approximately 0.6, emphasising the marked relative enrichment of K_2O in the suite. The behaviour of P_2O_5 is somewhat obscured by its wide scatter in Figure 6.5. however, the general trend towards enrichment with increasing D.I. in rocks with D.I. less than 40, followed by depletion in rocks with higher D.I. values, is apparent. The behaviour of S appears to be similar to that of P_2O_5, the degree of scatter is probably the result of overprinting of primary S concentrations by secondary pyritization.

The progressive depletion of MgO, CaO and Al_2O_3 indicates simultaneous early separation of olivine and basic plagioclase, plagioclase occurs as phenocrysts throughout the series, olivine occurs in the transition dolerites and tholeiitic dolerites only, calcium poor clinopyroxene is significant as a phenocryst phase in rocks with SiO_2 concentrations in excess of 50 percent (D.I. 30) and probably took over from olivine as the main Mg bearing phase separating from such melts. Further evidence for the early separation of olivine is provided by the behaviour of Cr and Ni concentrations, while the depletion of Sc may be attributed to the removal of plagioclase and subsequently clinopyroxene (see above). The separation of a silica poor phase (olivine) and a silica rich phase (basic plagioclase) led to the observed behaviour of MgO, CaO and Al_2O_3, while SiO_2 concentrations rose

relatively slowly enabling enrichment of K_2O and trace elements such as Rb, Y, Zr, Ba, Ce, Pb, Nb, La and Th, Na_2O showing less rapid enrichment due to removal in plagioclase. Thus contrary to the arguments of Jamieson and Clarke (1970) low pressure fractionation can give rise to the observed enrichment of incompatable elements in tholeiitic basalts. Holland and Brown (1972 p 58) have proposed a similar mechanism to explain the compositional range of the tholeiitic rocks of Ardnamurchan.

Concentrations of iron in the basaltic members of the series are high when compared with average values for basaltic rocks quoted by Manson (1968) suggesting that initial concentrations of iron in the primitive parents were unusually high. Further enrichment of Fe, TiO_2 and MnO indicates the suppression of iron rich phases in the early stages of crystallization (olivine compositions in transition dolerite have been shown to be forsteritic- see above), suggesting crystallization under conditions of relatively low oxygen partial pressure (Osborn 1959,1962). Titanomagnetite appears in abundance in tholeiitic dolerites and quartz dolerites with SiO_2 values greater than 50 percent, it is frequently accompanied by iron sulphide due to an enrichment in S parallel to that of Fe. The removal of such iron rich phases led to Fe depletion in the craignuritic members of the series. The behaviour of V indicates that it is largely present in the ore phases as predicted by Prinz (1968 p 312). The similar behaviour of Zn suggests that it also entered the ore phases as is suggested to be the case in the Skaergaard layered gabbro (Woode 1961, Wager and Brown 1968 p 200).

The high iron transition dolerites are anomalous, the concentration

of Al_2O_3, CaO, MgO, Na_2O, K_2O, P_2O_5 and the trace elements, coupled with high D.I. values and iron enrichment exhibited by these rocks indicates that they are more highly evolved than other transition dolerites, while their relatively low SiO_2 concentrations leads to their inclusion in the transition dolerite group. It is suggested that these rocks evolved by separation of olivine and plagioclase from a basic parent in the manner of other members of the series but that plagioclase was dominant over olivine hence enrichment in SiO_2 could not proceed.

The general trend of iron enrichment in the series is well shown by the A.F.M. diagram Figure 6.6. which enables comparison of the Carlingford trend with those of Thingmuli (Carmichael 1964) and Skaergaard (Wager and Brown 1968). Iron enrichment is also reflected by increasing Fe concentrations in the pyroxenes of more fractionated rocks in the series (see above).

As olivine and plagioclase were the principal phases separating during the early stages of fractionation, CaO and MgO are suitable indices of differentiation for rocks in this series, however it is not considered necessary to include variation diagrams using these components as the abscissa, with the exception of those in Figures 6.7 and 6.8, as such diagrams merely confirm the trends exhibited in Figures 6.2 and 6.5. Figure 6.7 indicates the covariance of MgO and CaO and the negative covariance of K_2O with CaO, while Figure 6.8 (K_2O versus MgO) demonstrates that separation of forsteritic olivine alone could not give rise to the degree of potassium enrichment exhibited by the series, and enables comparison with fractionation trends in other tholeiitic

Figure 6.6

Composition of rocks in the Carlingford tholeiitic basalt - craignurite series in terms of $Na_2O + K_2O$, Fe as FeO and MgO plotted on the triangle A.F.M. The Skaergaard and Thingmuli trends are included for comparison (taken from Carmichael, 1964, Fig. 3.).

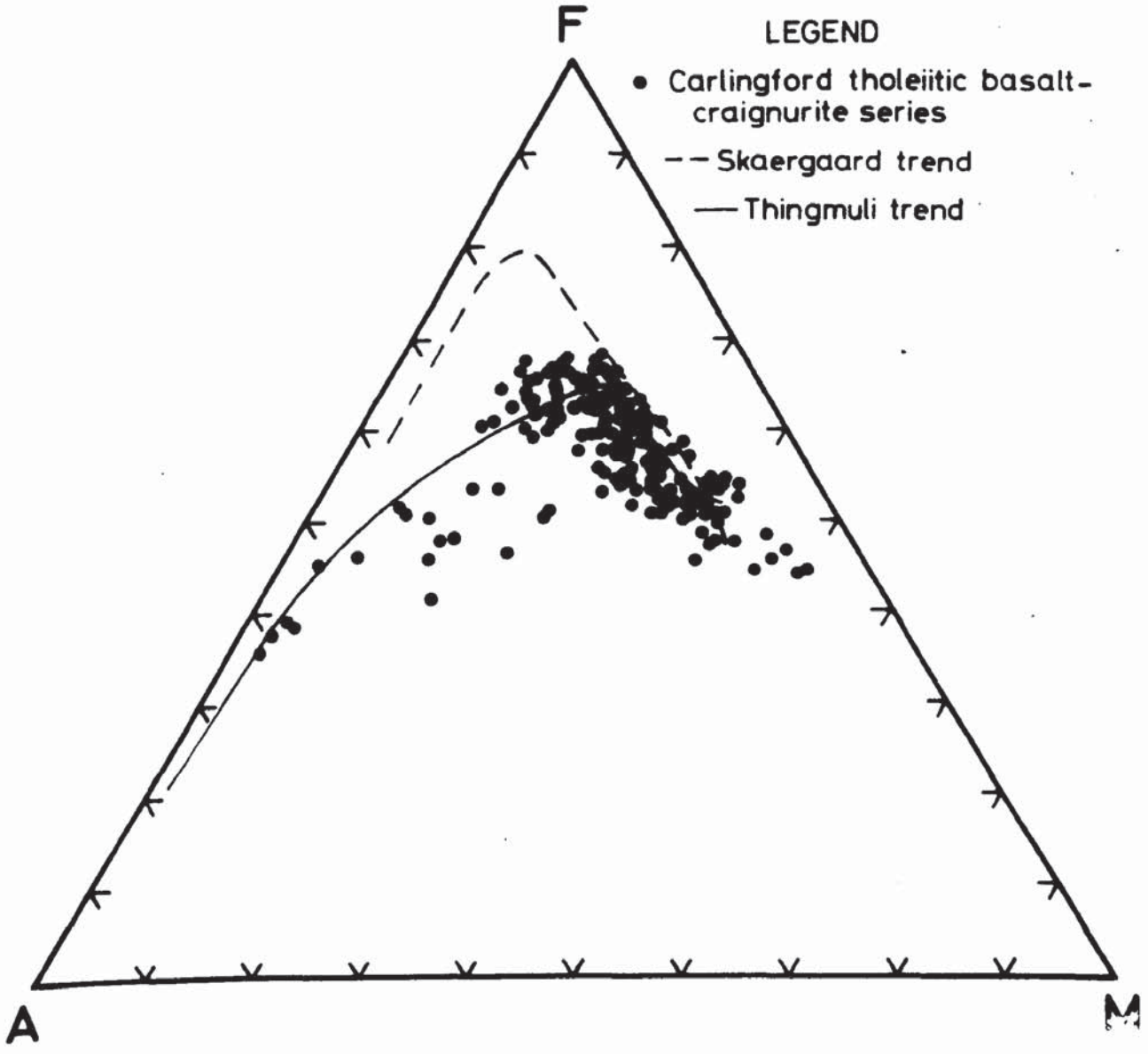

Figure 6.7

Variation diagrams of MgO and K_2O versus CaO for the Carlingford tholeiitic basalt - craignurite series, note the strong covariance of MgO with CaO and negative covariance of K_2O with CaO.

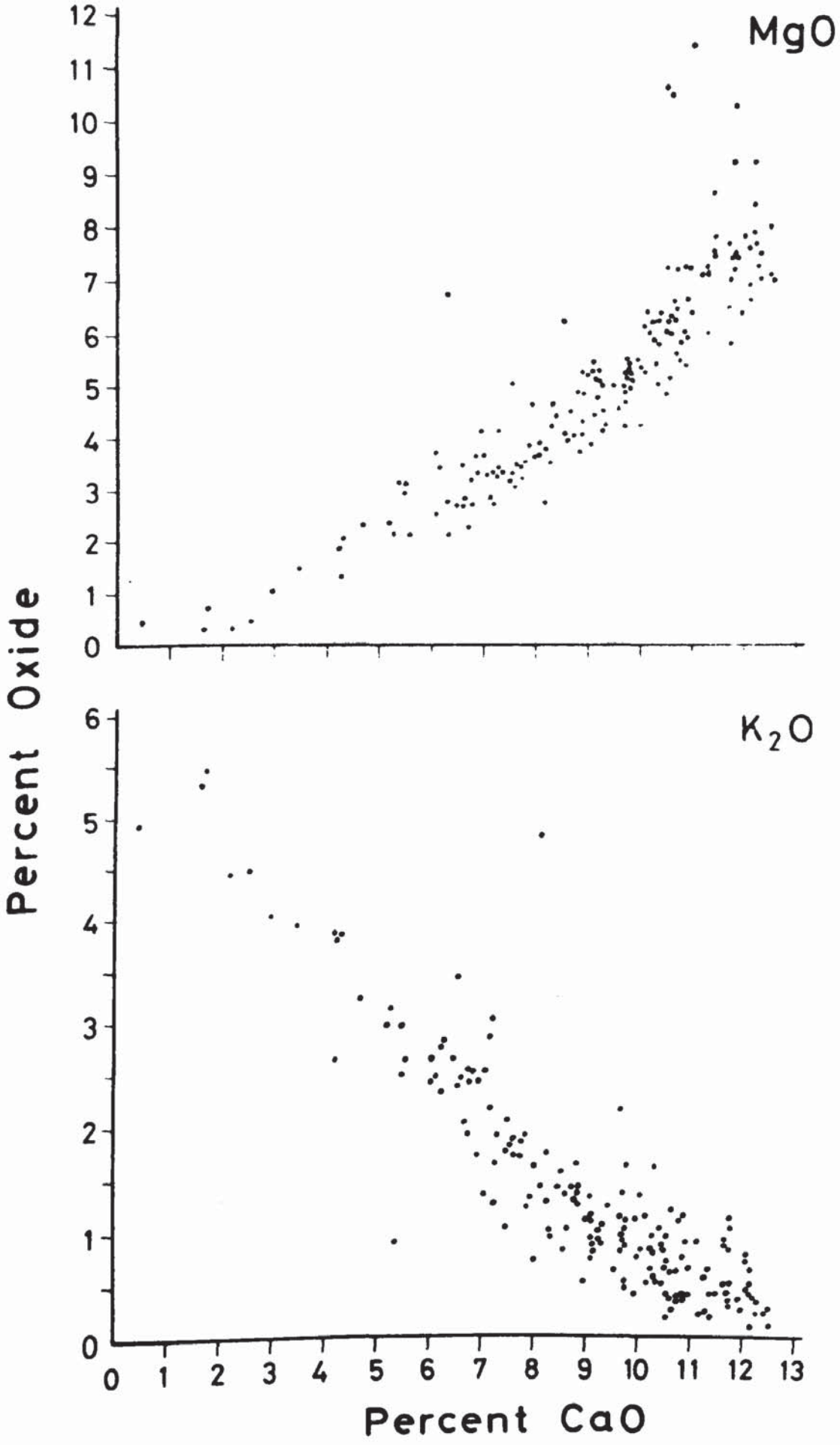

Figure 6.8

Variation diagram of K_2O versus MgO for the Carlingford tholeiitic basalt - craignurite series. The Skaergaard, Thingmuli and Kilauea trends are included for comparison (taken from Wager and Brown 1968, Carmichael 1964, Jamieson and Clarke 1970). The olivine (Fo_{85}) control line is indicated.

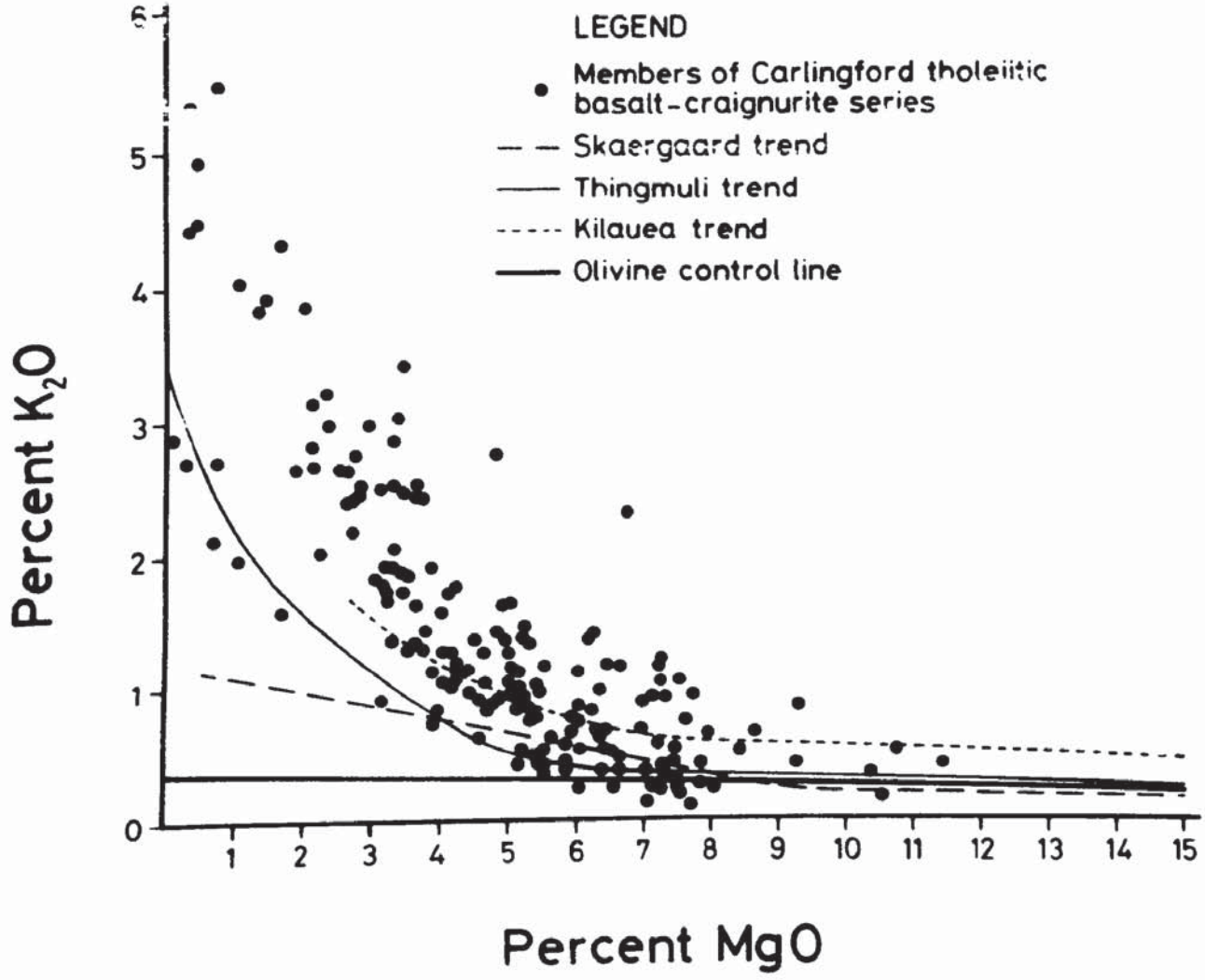

series as plotted by Jamieson and Clarke (1970 p 191). The triangular diagram Na_2O, K_2O, CaO (Figure 6.9) clearly shows the trend towards enrichment in K_2O rather than Na_2O in rocks with depleted CaO concentrations.

CaO values, when plotted against the ratio (FeO + Fe_2O_3): (MgO + FeO + Fe_2O3) in the manner of Thompson (1972) form a continuum with no evident gaps (Figure 6.10). The same result is obtained when rocks of Cycles II and III are plotted independently, (the Cycle I suite is too poorly represented to enable proper assessment). The chemical continuity of the series in other plots has already been noted on occasions. Thus it is not necessary to call upon the elegant fractionation mechanism proposed by Thompson (1972 p 109) to explain the chemical variation of the Carlingford tholeiitic series, simple gravity setting of early formed crystals is adequate. Holland and Brown do suggest the presence of a chemical discontinuity in the tholeiitic basalt - craignurite series of Ardnamurchan (1972 p 158), thus Thompsons fractionation mechanism is not inappropriate to Hebridean igneous activity and its operation at Carlingford is not ruled out.

The transition dolerites are the most basic rocks in the series with D.I. values as low as 12 in some cases, they also have higher concentrations of CaO and MgO than other rocks, and K_2O values which approach "primitive" levels as defined by Jamieson and Clarke (1970). The compositions of such rocks therefore are appropriate as those of parental magmas for the series as a whole. Samples 54, 76 and 84 are among the most suitable in that sense, all three show high concentrations of Ni and Cu, though both 76 and 84 have somewhat higher K_2O values than 54.

Figure 6.9

Composition of rocks in the Carlingford tholeiitic basalt - craignurite series in terms of Na_2O, K_2O and CaO plotted as a triangular diagram.

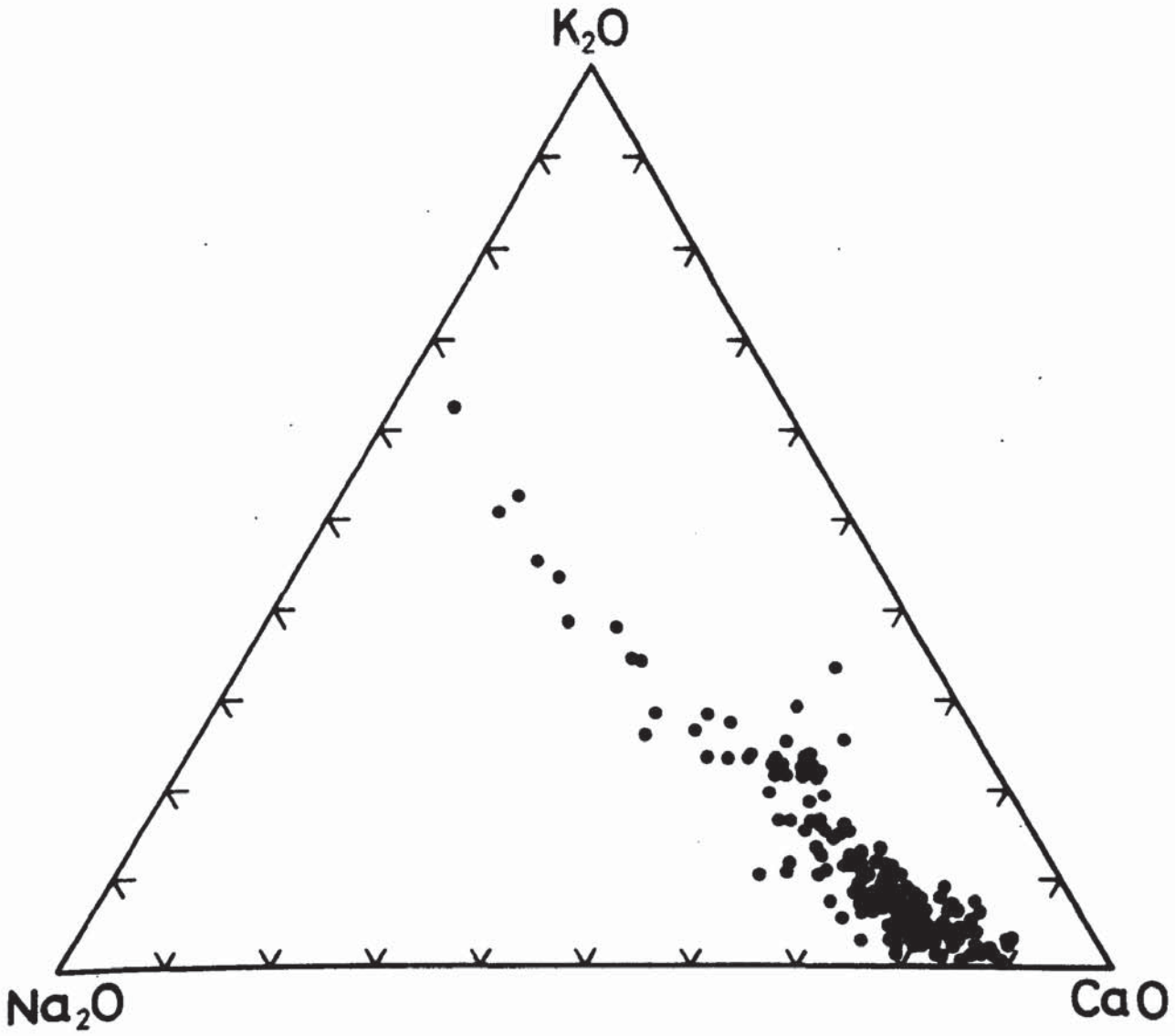

Figure 6.10

Variation diagram of CaO versus FeO + Fe_2O_3 : FeO + Fe_2O_3 + MgO, for rocks in the Carlingford tholeiitic basalt - craignurite series, showing the continuity of the suite.

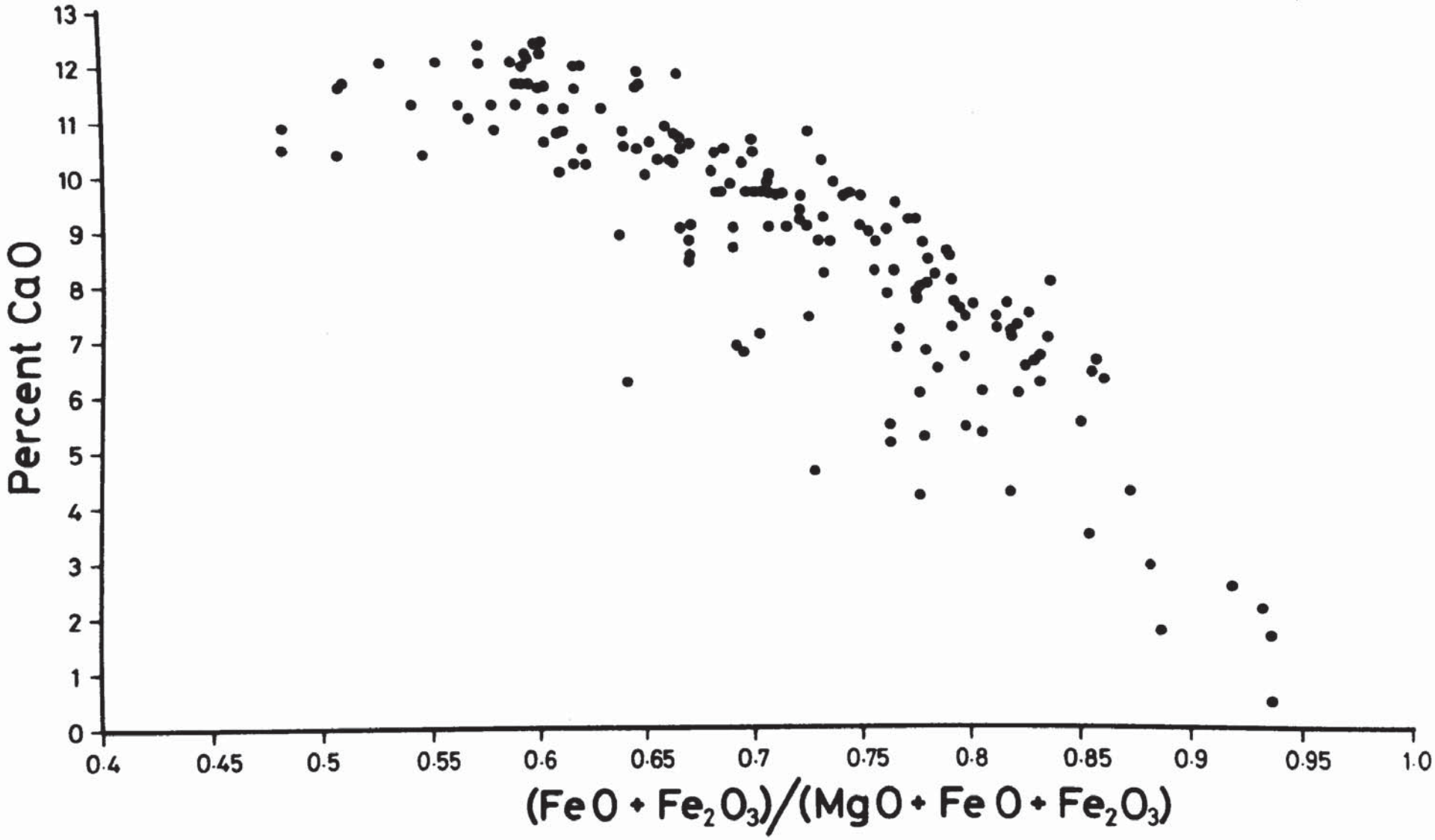

Summary.

a) The tholeiitic basalt- craignurite series is the dominant suite among the minor intrusions of Carlingford.

b) The suite forms a continuous petrographic series grading from basic transition dolerites to acid craignuritic felsites.

c) The petrographic continuity of the series is reflected by the chemical continuity it exhibits both in the case of trace elements and of major elements.

d) No clearly defined distinguishing petrographic or petrochemical characteristics can be recognised in rocks of different intrusive events.

e) The dominant petrochemical trends are towards depletion in MgO and CaO, progressive enrichment in Na_2O and K_2O, together with initial enrichment of Fe, TiO_2 MnO and P_2O_5 followed by their depletion in the craignuritic rocks. This behaviour is reflected in the high MgO content of olivines and CaO content of plagioclases in the transition dolerites, and increasing Fe enrichment in the pyroxenes occurring in the quartz dolerites and craignurites.

f) Sc, Cr, Co, Ni, and Cu show progressive depletion with fractionation, while Rb, Y, Zr, Ba, Ce, Pb, Ga, Nb, La and Th show progressive enrichment. V, Zn and Sr show initial enrichment and subsequent depletion.

g) The behaviour of both major and trace element concentrations suggest that the series was formed by fractionation of basaltic parental melts, involving separation of olivine and calcic plagioclase under conditions of low partial pressures of oxygen in the early stages ,

followed by the separation of calcium poor clinopyroxene and plagioclase accompanied by ore phases, including iron sulphides, in the latter stages.

h) The high iron transition dolerites are more highly evolved than other transition dolerites and were produced by the same fractionation mechanism but with plagioclase dominant over olivine preventing enrichment in SiO_2.

i) The relative abundances of the various rock types in the series are consistant with the fractionation model proposed, about 80% of the sample are basaltic and only 20% intermediate or acid in composition.

j) The compositions of those members of the high alumina basalt series, which have been considered to be feldsparphyric tholeiitic dolerites, are consistant with that interpretation.

k) The series exhibits marked enrichment of K_2O relative to Na_2O which distinguishes it from the tholeiitic basalt-icelandite series.

l) Concentrations of iron in the basaltic members of the series are unusually high, indicating high initial iron concentrations in the parent melts.

m) The absence of chemical discontinuities in the series does not provide support to the view that the fractionation mechanism recently described by Thompson, involving filter pressing of residual liquids from a semi rigid magma, operated at Carlingford, however its operation is not ruled out.

n) The composition of parental melts probably approached those of some of the more basic transition dolerites such as 54, 76 and 84 which exhibit relatively primative concentrations of K_2O and trace elements.

CHAPTER 7

THE PETROCHEMISTRY AND PETROGENESIS OF A QUARTZ DOLERITE-CRAIGNURITIC FELSITE COMPOSITE CONE-SHEET AT CARLINGFORD

Abstract.

Composite intrusions are abundant in the British Tertiary Province in general, but rare at Carlingford. The petrochemistry and petrogenesis of one such intrusion in the Carlingford Complex, a quartz dolerite-craignuritic felsite cone-sheet, is described and shown to be somewhat atypical of such bodies. Its development included the hybridization of quartz dolerite and craignuritic felsite magmas produced by fractionation of tholeiitic liquids. The quartz dolerite involved in this process forms the upper margin of the cone-sheet, it had been contaminated by material rich in Pb and Zn prior to its emplacement as such. The lower margin of the cone-sheet consists of a second layer of quartz dolerite which is considered to have been intruded independently of the upper layer, after the emplacement of the central felsite.

Introduction

Acid-basic composite intrusions are well known throughout the British Tertiary Province and a number of such bodies have been described, including the Glasdrumman cone-sheet of the Mourne (Cole 1894, Tomkeieff and Marshall 1935, Akiman 1973); the Rudh' an Eireannaich Sill (Buist 1959) and the other composite sheets of Skye (Harker 1904, Skelhorn 1959); the composite intrusions of Mull (Bailey

et al. 1924, Skelhorn 1959) including the Rudh'an Chromain Sill (Buist 1961); the composite intrusions of Arran (Judd 1893, Tyrrell 1928); and the South Bute composite Sill (Smellie 1913, Buist 1952). The general characteristics of such intrusions have been briefly summarised by Richey (1961 p 59) and in more detail by King (1964, 1965a) who discussed the uncertainties surrounding the mechanism of their emplacement and weighs the merits of the various hypotheses put forward in explanation.

Composite intrusions are rare at Carlingford though multiple basic intrusions are relatively abundant. One such composite body crops out in a railway cutting and on the shores of Carlingford Lough about 500 metres north west of Carlingford Harbour. This mass, which has the form of a cone-sheet dipping south west at about 40°, is described in the following paragraphs, its emplacement is attributed to episode IIc of the Carlingford intrusive sequence (see Chapter 1 above).

Description

The cone-sheet is well displayed in vertical section in the railway cutting. It consists of an upper margin of quartz dolerite 0.25 m thick, a lower margin of quartz dolerite some 0.3 m thick and a buff coloured central layer of craignuritic felsite (leidleite) about 1.5 m thick. The contacts between the basic margins and the felsite are sharp and smooth but, as all three members are relatively fine grained, internal chilling of one against another is not readily apparent, the lower basic unit does have the appearence of being

chilled against the felsite on close inspection however.

The sheet crops out again on the shore of the Lough a few metres to the south east where the central craignuritic felsite encloses xenoliths of basic material similar to that of the basaltic margins. The xenoliths have rounded outlines, some exhibit sharp contacts with the enclosing felsite while others, with diffuse margins, are in part digested by their host. The craignuritic felsite shows varying degrees of basicification by assimilation of this basic material and varies in colour from buff or pink where relatively uncontaminated, to light grey with dark streaks.

Petrographically the rock types occurring within the sheet, including the basic xenoliths, are normal members of the tholeiitic basalt - craignurite series (see Chapter 6 above).

Petrochemistry

Six analyses of rocks from this intrusion have been carried out during the current investigation (listed in Appendices IV and XII). Sample 850 is an uncontaminated craignuritic felsite from the railway cutting exposure, 851 and 852 are from the upper and lower quartz dolerite margins respectively. 911B is of a basic xenolith, with the composition of basaltic craignurite, enclosed by relatively uncontaminated felsite 911A (both samples derived from specimen 911). 912 is basified craignuritic felsite; both 911 and 912 were collected from the shore line outcrop.

The major element concentrations of these rocks are tabulated for comparison in Table 7.1, which shows that their compositions are

consistant with those of members of the tholeiitic basalt-craignurite series.

TABLE 7.1.

Composition of samples from a composite cone-sheet.

Sample	850	851	852	911A	911B	912
SiO_2	66.29	52.25	50.99	64.56	54.53	62.51
TiO_2	0.68	1.63	1.60	0.59	1.47	0.86
Al_2O_3	12.99	14.09	15.63	12.45	13.32	12.84
Fe_2O_3	1.45	2.00	1.50	2.09	0.00	0.00
FeO	3.39	11.43	11.04	3.20	12.09	8.55
MnO	0.10	0.29	0.24	0.10	0.26	0.12
MgO	0.36	4.16	6.26	0.48	3.13	1.48
CaO	2.18	6.91	8.44	2.58	5.44	3.47
Na_2O	3.19	2.07	2.40	3.17	2.60	2.93
K_2O	4.44	1.73	1.42	4.47	2.50	3.94
P_2O_5	0.14	0.21	0.17	0.11	0.23	0.14
S	0.95	0.21	0.23	0.01	0.94	0.49
$H_2O\pm$	3.53	2.17	1.77	3.19	3.69	2.26
Total	99.69	99.16	101.69	98.02	100.20	99.59

See text for sample descriptions and localities.

Concentrations of selected trace elements in the six analysed rocks are listed in Table 7.2. These are again consistant, in the main, with those of quartz dolerites, craignurites and craignuritic felsites with similar SiO_2 values, however, as noted in Chapter 6 above, samples

851 and 911B have high Zn and Pb values. The hybrid 912 also has relatively high concentrations of these elements even for a rock with SiO_2 in excess of 60%.

TABLE 7.2.

Trace element concentrations in samples from a composite cone-sheet.

Sample	850	851	852	911A	911B	912
Sc	15	62	72	19	18	27
V	65	186	208	52	174	87
Cr	BLD	43	48	1	18	8
Co	BLD	50	69	9	40	21
Ni	8	23	27	3	16	4
Cu	61	98	89	61	64	65
Zn	39	321	92	20	338	79
Rb	157	68	57	167	150	102
Sr	81	174	167	84	150	129
Y	59	39	39	58	40	60
Zr	493	208	185	482	249	447
Ba	1080	703	704	1099	746	1052
Ce	128	72	78	113	66	108
Pb	30	103	46	25	160	87
Th	26	9	5	27	11	25

BLD Below limits of detection.

See text for sample description and localities.

Petrogenesis

The major element compositions listed in Table 7.1 have been recalculated to 100% volatile free with FeO and Fe_2O_3 as Fe_2O_3. The results, with the exception of MnO and P_2O_5 values, have been plotted as a variation diagram against the resulting SiO_2 values in the manner of Buist (1952, Fig. 3, p 64), see Figure 7.1. The trace element concentrations listed in Table 7.2 have also been plotted against the recalculated SiO_2 values in Figure 7.2.

The behaviour exhibited by the major constituents of these rocks in Figure 7.1 is to a large extent consistant with the intermediate members of the series (samples 911B and 912) having been produced by a process of hybridization involving the acid and basic end members, though none of the components show the straight line relationship demonstrated by Buist (1952) in rocks from the south Bute Sill, and which Harker considered would result from the operation of such hybridization processes (1904, p 231). The inconsistancies exhibited by concentrations of some components in 850 and 911A may be the result of analytical error as may the deviation of S values from a covariant rectilinear relationship with SiO_2. S does show a general overall increase in concentration with increasing SiO_2 values, however, S levels must be treated with caution, as there is evidence that they have been modified in a number of Carlingford rocks by post magmatic mineralization (see Chapters 1,4 and 5). It is noteable that concentrations of TiO_2, Na_2O and Fe_2O_3 in sample 852, the most basic rock of the series, are not consistant with it having participated in the hybridization process.

Figure 7.1

Variation in composition within a composite cone-sheet at Carlingford, (analyses recalculated to 100%, volatile free). Numbers refer to sample numbers, see text for discussion.

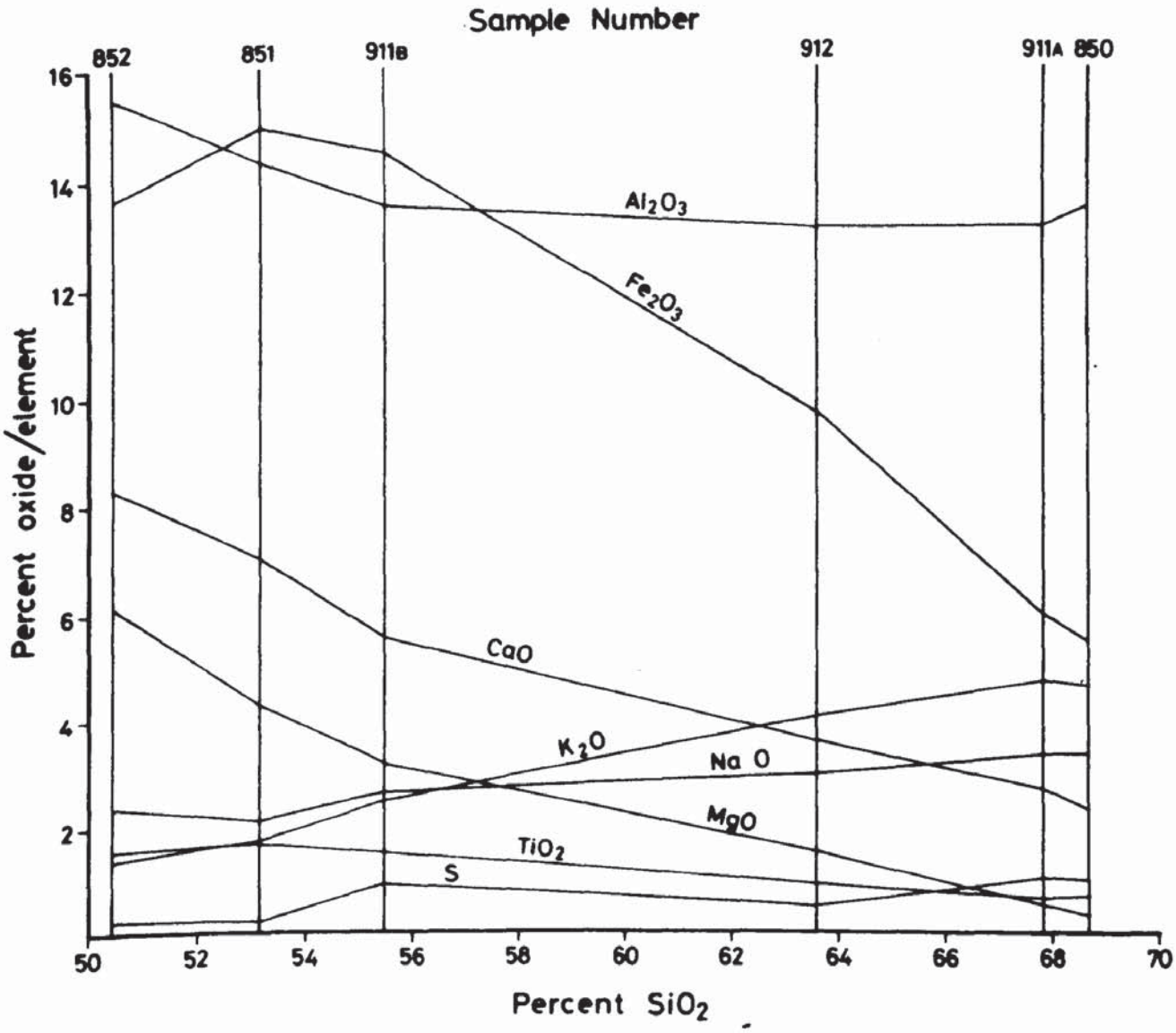

Figure 7.2

Variation of trace element concentrations within a composite cone-sheet at Carlingford (SiO_2 values from analyses recalculated to 100% volatile free). Numbers refer to sample numbers, see text for discussion.

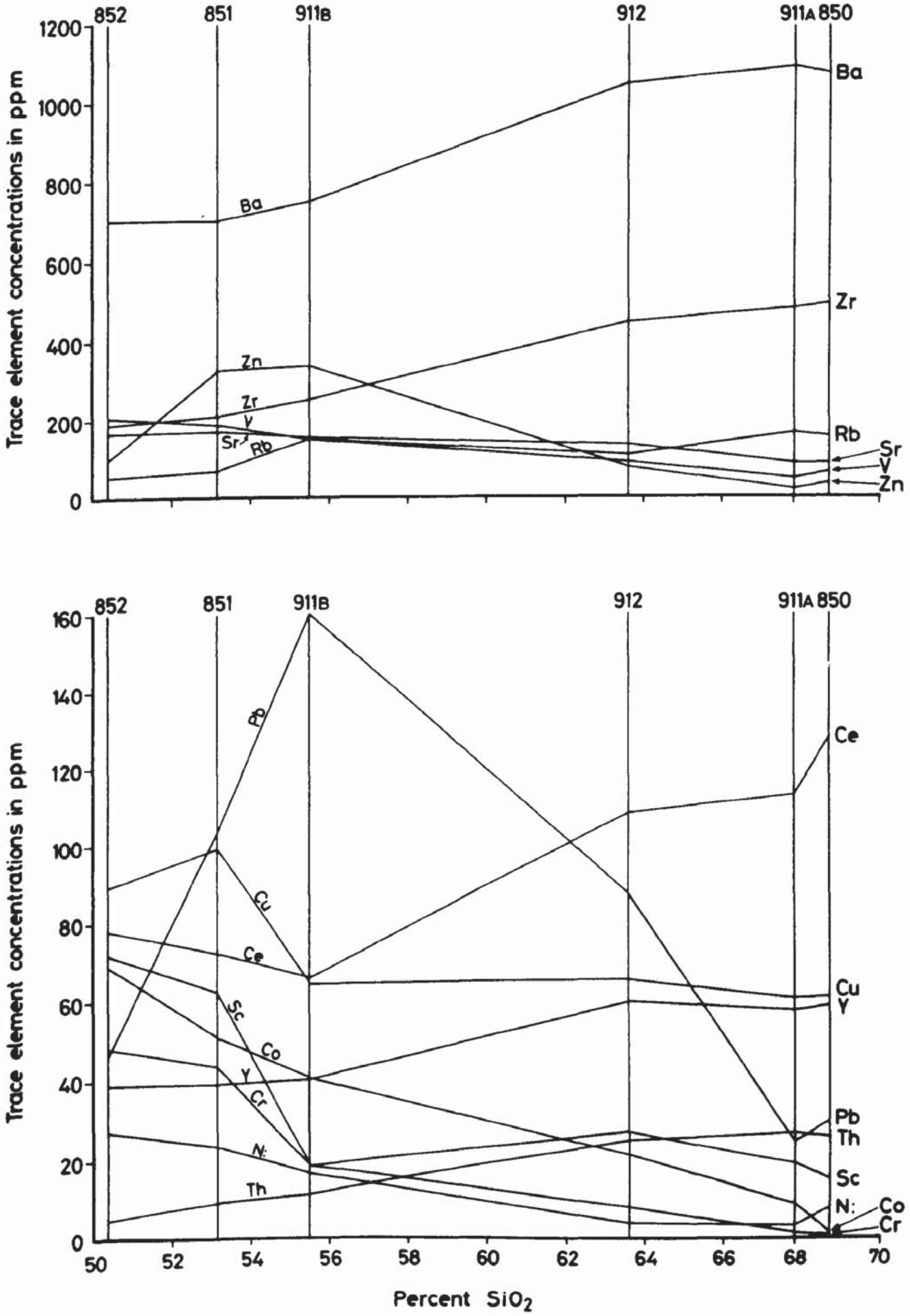

Figure 7.2 indicates that the behaviour of many trace elements in the six analysed samples is consistant with the process of hybridization indicated by the major element chemistry, none however exhibit perfect linear relationships, concentrations of Sc, Cu, Zn, Rb and Pb are most anomalous in that respect. It is probable that fractionation of the hybridized magma, or selective diffusion of constituents in the melt, may account for at least some of the deviations from the predicted linear behaviour of those elements (King 1964 p 291). The low concentrations of Pb and Zn in 852 indicate that hybridization of that rock with the craignuritic felsite magma could not have given rise to the intermediate types 911B and 912, which have high concentrations of those elements (see above).

The concentrations of both major elements and trace elements thus indicate that the lower marginal layer of basic rock represented by sample 852 took no part in the hybridization process, the material assimilated by the central layer which thus gave rise to rocks with compositions represented by sample 912, and the basic xenoliths represented by sample 911B were derived from the upper basic layer which has appropriate concentrations of major components and trace elements. This phenomenon is somewhat atypical of composite sheets, King (1964 p 286) notes that basic xenoliths are commonly concentrated in the lower parts of such intrusions and implies that they are frequently derived from their lower basic members, though he does qualify the statement with the remark that this, "does not preclude the possibility that contributions have also been made from the upper parts of the sills." In the same paper, King also points out that acidification is usually

more marked in the lower basic members of such intrusions (1964 p 289).

Having arrived at the conclusion that the lower basic margin took no part in the process of hybridization, it is necessary to explain that phenomenon. In the first place, the petrochemistry of the upper and lower layers are somewhat distinct as shown by Figures 7.1 and 7.2, in particular, concentrations of Fe_2O_3 (FeO + Fe_2O_3), Zn and Pb are noteably higher in the upper basic margin, which suggests that the two layers were not produced directly from the same quartz dolerite magma and were thus not coeval. It is therefore considered that the lower sheet was either intruded before the upper margin, and was already completely solid before the injection of the felsite centre; or that it was emplaced after the injection of both the upper basic margin and the felsite. In view of some evidence of chilling of the lower layer against the acid centre (see above) it is concluded that the latter interpretation is correct. Such asymmetry of the intrusive sequence is also atypical of composite intrusions (King 1964 p 283).

It is evident from the inclusion of xenoliths from the upper basic layer in the craignuritic felsite of the central layer that the intrusion of the former predated the emplacement of the latter, though it (the upper basic layer) may not have been completely crystalline and solid before it was, in part, disrupted by the felsite, a possibility considered by Bailey and McCallien with reference to the Glasdrumman composite cone-sheet (1956 p 472). The role of immiscibility of the acid and basic magmas in the hybridization process is uncertain.

The composition, and trace element concentrations of the uncontaminated craignuritic felsite of the central layer, indicates that it could have been produced by fractionation from a tholeiitic magma (tholeiitic basalt - craignurite fractionation series). Such a fractionation process has been established as the source of craignuritic rocks in the Carlingford Complex, though some authors would prefer to interpret similar rocks occurring elsewhere in the Hebridean Province as the products of hybridization processes involving acid and basic magmas such as that observed in the composite sheet itself (Srirama Rao 1959). Only the upper basic layer, and material derived from it as xenoliths or contaminated by it through assimilation, exhibit abnormally high concentrations of Pb and Zn. The rock itself is a typical iron rich quartz dolerite with a composition similar to those of others prcduced by fractionation of tholeiitic magma (see Chapter 6), no fractionation processes have been observed which give rise to such enrichment in Pb and Zn however. It is therfore concluded that the high Pb and Zn values exhibited by this rock were attained by assimilation of materials rich in those elements prior to its intrusion. Traill noted the presence of minor lead mineralization at Whitestown (1878 p 42) and it is assumed that similar mineralization or rocks with high Pb and Zn values are present at depth beneath the complex.

Conclusions.

It is concluded from the above observations that the development of the composite cone-sheet in question was the result of the

following sequence of events. The process was initiated by the fractionation of tholeiitic liquids which thus gave rise to the quartz dolerite magma of the upper basic layer, that magma was then injected as a cone-sheet. During the fractionation, or subsequent injection of the quartz dolerite melt, it became contaminated by material rich in Pb and Zn. Further fractionation of the tholeiitic parent magma, following the tholeiitic basalt - craignurite fractionation trend, gave rise to craignuritic felsite melts with normal trace element abundances. The craignuritic felsite was then emplaced immediately beneath the upper basic layer, possibly before it was completely solid. Incorporation of xenoliths, which were partially assimilated by the felsite, gave rise to hybrid derivatives of craignuritic affinity with high Pb and Zn values. Injection of a second pulse of quartz dolerite magma possibly derived from the same source magma body as both the upper basic layer and the central felsite, took place along the base of the felsite layer. This batch of magma did not suffer contamination by Pb and Zn rich rocks, and on being emplaced was chilled against the felsite.

Summary.

The following points have arisen from the preceding discussion:

a) Composite intrusions of the type numerous elsewhere in the British Tertiary Province are not abundant at Carlingford, though one such does occur on the shores of Carlingford Lough.

b) That body, a composite cone-sheet, consists of an upper layer of quartz dolerite, a central layer of craignuritic felsite,

which incorporates xenoliths of quartz dolerite and has in part been contaminated by assimilation of basic material, and a lower layer of quartz dolerite.

c) The composition of the quartz dolerites and craignuritic felsite are consistant with those of members of the tholeiitic basalt-craignurite series.

d) The upper basic layer is exceptionally rich in Pb and Zn, such that it must have been contaminated by material with high concentrations of those elements prior to intrusion.

e) The lower basic margin does not exhibit high Pb and Zn values and is thus considered to have formed from a body of magma injected into the sheet independently of the upper quartz dolerite.

f) The composition of the basified (contaminated) felsite of the central layer indicates that it was produced by a process of hybridization involving the upper basic layer and the craignuritic felsite only. This hybridization process may have been modified by fractionation or selective diffusion.

g) The composition of a basic xenolith enclosed by the central craignuritic felsite suggests that it was derived from the upper basic layer.

h) The sequence of events during the development of the composite cone-sheet was as follows:

i. Genesis of quartz dolerite magma by fractionation from tholeiitic liquids.

ii. Contamination of quartz dolerite magma by Pb, Zn rich material, and its subsequent injection as a cone-sheet.

iii. Further fractionation of tholeiitic magma gave rise to a craignuritic felsite melt, which was injected beneath the upper basic layer.

iv. Assimilation of material from the upper basic layer by the central felsite during emplacement gave rise to craignuritic hybrids. Xenoliths of the upper quartz dolerite were also incorporated by the felsite.

v. Injection of a second batch of quartz dolerite as the lower basic margin.

i) These conclusions are not altogether typical of those put forward to explain the development of other such composite bodies in the British Tertiary Province.

CHAPTER 8

THE PETROCHEMISTRY OF THE COUNTRY ROCKS, GABBRO XENOLITHS, LAMPROPHYRES AND ACID ROCKS IN THE CARLINGFORD COMPLEX.

Abstract.

The petrochemistry of a number of rock types, including sediments lamprophyres, felsites, rhyolites, and gabbro xenoliths, occurring within the Carlingford Complex are discussed. Consideration of the petrogenesis of Tertiary magmas included in this group, leads to the conclusion that the majority of acid melts were produced by partial fusion of argillaceous sediments, and that a group of lamprophyric rocks tenuously attributed to the Tertiary on the basis of structural, petrographic and petrochemical considerations, were formed by assimilation of basic material rich in Sr and Ba by such acid liquids during that partial melting process or their subsequent injection.

Introduction.

A number of igneous rock types occurring at Carlingford are not attributable to the three main magma series, and as such have not been considered in the preceding discussions of petrology and petrochemistry (Chapters 4,5 and 6). Felsite and quartz feldspar porphyry dykes and cone-sheets were intruded at the beginning of Cycle II. The age of a group of lamprophyres (vogesites and spessartites) is uncertain, but they may be related to the felsites. The Carlingford granophyre was emplaced at the beginning of Cycle III and it has been suggested that it was derived by partial melting of crustal rocks (Le Bas 1967), a similar interpretation has been placed on the origin of other acid

intrusions in the British Tertiary Province (Brown 1963). The petrochemistry of the felsites, granophyre and lamprophyres are described in the following paragraphs as are the compositions of the Silurian sediments, a Caledonian minette dyke, Carboniferous Limestone and Tertiary basalts, which together comprise the country rocks into which they were intruded. The composition of the layered gabbro and gabbro xenoliths occurring in minor intrusions are also discussed. Analyses of the rocks in question are listed in Appendix V (major elements), Appendix IX (CIPW norms where appropriate) and Appendix XIII (trace elements), their petrography is not discussed in detail, an outline having been given in Chapter 1 above.

The Composition of the Sedimentary Country rocks.

Two samples of Silurian sediment have been analysed during the current investigation, specimen 31 from a railway cutting near Dundalk has a calcite cement, while 945, from Carlingford Mountain, has been hornfelsed by the adjacent layered gabbro. Analyses of other Silurian rocks are listed by Le Bas (1960 Table IV (major element composition), 1970b Table 9 (trace element concentrations)), these analyses, with selected trace element concentrations, are tabulated below for comparison (Table 8.1). The composition of a limestone (746) from the Carboniferous Limestones exposed at Big River Bridge has also been determined by the current author.

The Composition of the Silurian rocks listed in Table 8.1 shows considerable variation, the proportion of iron in Samples 31, A and E is considerably lower than in 945, B,C and D, while CaO concentrations

TABLE 8.1.

Composition of Silurian Sediments and Hornfelses.

	31	945	A	B	C	D	E
SiO_2	57.14	57.94	65.44	58.0	54.0	54.0	49.22
TiO_2	0.69	0.92	-	1.0	1.0	1.1	0.26
Al_2O_3	10.87	18.55	13.48	16.0	17.0	18.0	18.63
Fe_2O_3	0.85	1.36	2.16)	7.9	8.1	9.5	0.46
FeO	3.00	6.84	2.85)				5.50
MnO	0.04	0.01	0.40	0.08	0.10	0.09	0.15
MgO	3.53	4.14	3.08	5.8	6.1	6.3	9.52
CaO	8.91	0.79	8.08	4.1	3.5	2.9	14.87
Na_2O	1.89	1.15	1.94	2.5	1.2	2.6	0.68
K_2O	1.51	4.61	1.74	4.1	4.0	4.4	0.21
P_2O_5	0.15	0.11	-	-	-	-	-
S	0.02	0.25	-	-	-	-	-
H_2O^+	9.57	1.52	0.40	-	-	-	0.62
H_2O^-				-	-	-	0.18
Total	98.17	98.19	99.57	99.5	95.0	98.9	100.30
Sc	37	18	-	22	22	15	-
Cr	113	107	-	150	230	160	-
Ni	77	136	-	100	100	125	-
Rb	53	190	-	250	250	350	-
Sr	196	40	-	250	40	100	-
Y	19	19	-	30	30	30	-
Zr	189	217	-	200	200	200	-
Ba	358	781	-	350	350	600	-

31 and 945 see text for description. A. "Slate"(Hull 1875 p 86).
B. Le Bas sample 1218. C. Le Bas sample 1216. D. Le Bas sample 1307.
E. Hornfels (Harry 1952 p 413).

are much higher. Al_2O_3 and K_2O values are also very variable. Comparison of trace element concentrations listed indicates that Cr, Rb, Sr and Ba values exhibit considerable variation, while Sc and Y values are relatively low throughout. The variation in composition may in part be due to varying degrees of hornfelsing (sample 31 is unmetamorphosed while 945 has suffered high grade contact metamorphism at sanidinite facies), but probably in large part reflects initial compositional variation at the time of deposition.

The composition of the limestone 746 is somewhat siliceous, Al_2O_3, iron, Na_2O and K_2O are also relatively abundant and are probably present in the turbid clay fraction. Concentrations of Ga, Rb, Y, Zr and Ba are relatively low, while the Sr value is high and the Sc value exceptionally high compared with those of igneous rocks in the complex.

The Composition of a Caledonian Minette Dyke.

A minette dyke of Caledonian age (sample 32) which cuts the Silurian argillaceous sandstone sample 31, is among the analysed rocks with compositions listed in Appendices V and XIII. Table 8.2 lists the composition of the rock in terms of major element oxides together with those of minettes from the Ards Peninsula (Reynolds 1931 p 156) and Arizona (Williams 1936 p 166) for comparison. All three have relatively high concentrations of ($FeO+Fe_2O_3+MgO$), (Na_2O+K_2O) and volatiles typical of lamprophyres in general (Turner and Veerhoogen 1960 p 251).

TABLE 8.2

Composition of Minette Dykes.

	32	A	B
SiO_2	49.68	48.80	51.50
TiO_2	0.80	1.10	1.85
Al_2O_3	11.79	12.80	11.55
Fe_2O_3	3.49	1.64	2.38
FeO	4.65	5.98	4.72
MnO	0.09	0.28	0.10
MgO	10.74	10.35	7.90
CaO	7.97	7.65	9.10
Na_2O	1.43	2.73	2.55
K_2O	2.30	2.74	5.65
P_2O_5	0.45	0.49	0.96
S	0.32	0.12	-
H_2O^+	))	3.00	1.10
H_2O^-	6.99)	0.50	0.45
CO_2	)	1.70	-
Total.	100.68	99.88	99.81

32 Carlingford

A. Ards Peninsula (Reynolds 1931 p 156)

B. Arizona (Williams 1936 p 166 No9)

Sample 32 exhibits high Cr and Ni values, and high concentrations of Sr and Ba which is typical of lamprophyres (Williams, Turner and Gilbert 1954 p 85), but concentrations of Y and Ce are relatively low.

The CIPW norm for sample 32, listed in Appendix IX has been calculated from the analysis set out in Table 8.2 recalculated to 100 percent volatile free, and with Fe_2O_3 reduced to TiO_2% + 1.5%, excess Fe_2O_3 being recalculated as FeO, (Irvine and Baragar 1971 p 526). The rock is quartz, orthopyroxene normative, the high anorthite content results from the presence of calcite which is not included in the norm.

The Composition of the Basalt Lavas.

Two lavas from the Rockmarshall outcrop have been analysed during the current investigation, sample 19 (400 metres southwest of Rockmarshall House) and sample 21 (300 metres east south east of Donalds Rock). Le Bas (1965a) lists an analysis of an hawaiitic lava from the same area. When plotted on the alkali silica diagram samples 19 and 21 fall in the transition dolerite field of the tholeiitic basalt - craignurite series (see Chapter 3), sample 21 plotting near the alkali basalt/tholeiitic basalt field divider; Le Bas' hawaiite falls in the alkali basalt field. Both 19 and 21 are olivine, orthopyroxene normative (see Appendix IX). Sample 19 has Al_2O_3 in excess of 16.5% and is therefore attributable to the high alumina basalt series, however the relatively high concentrations of iron, TiO_2 and MgO are more in keeping with those of rocks in the tholeiitic basalt - craignurite series (see Chapters 5 and 6).

Concentrations of S, Sc, V, Cu, Zn, Ga, Y and Pb are similar in the two rocks, Cr, Co and Ni values are higher in sample 19 while Rb, Sr, Zr and Ba are more abundant in sample 21. Trace element concent-

rations in both rocks fall in the range exhibited by the transition dolerites of the tholeiitic basalt - craignurite series emphasising their chemical affinity with rocks of that category and suggesting that they may have been derived from a magma similar to that which fed the tholeiitic minor intrusions of Cycle I. The lavas may be coeval with the latter, at least in part, and it is tempting to suggest that some of the tholeiitic dykes of Cycle I were thus lava feeders. The alkali basalt lavas in the Rockmarshall outcrop can be shown to postdate the tholeiitic lavas on the basis of field relations (the alkali basalts occupy the core of a syncline flanked by tholeiitic basalt (Le Bas 1965a)) and thus it may be suggested that the alkali basalt intrusions of Cycle I are younger than the intrusions of the tholeiitic basalt - craignurite series attributed to that event.

The Origin of the Gabbro Xenoliths.

It has been noted in Chapters 1 and 2 that gabbro xenoliths occur in many of the minor intrusions of the complex, though they are almost entirely restricted to rocks of the tholeiitic basalt - craignurite series (it is difficult to recognise them in rocks of the high alumina basalt series, even when present, as their petrology is almost identical). Three such xenoliths have been analysed, samples 12, 34, 373, they are similar in composition to rocks in the layered gabbro sequence (see Table 8.3). Comparison of trace element concentrations in these three rocks with those of four gabbros from the layered gabbro, numbers 1, 396, 636 and 1082 listed in Appendix XIII (further determinations of trace element concentrations in the layered gabbro

are listed by Le Bas 1970b, Tables 5, 7, 8 and 10), emphasises the similarity. Specimen 34 is somewhat atypical in that it has partly reacted with its host (sample 33, a quartz dolerite).

TABLE 8.3.

Composition of a gabbro xenolith and the layered gabbro.

	12	396	A	B	C	D
SiO_2	49.83	49.38	51.02	46.76	48.13	49.32
TiO_2	0.75	0.79	0.29	0.75	0.25	0.45
Al_2O_3	20.99	15.11	21.06	16.59	27.51	22.64
Fe_2O_3	2.06	2.19	1.27	3.43	0.88	0.70
FeO	6.27	8.59	5.62	7.35	1.91	3.33
MnO	0.10	0.17	0.12	0.16	0.02	0.07
MgO	3.99	7.24	8.04	9.28	3.21	3.47
CaO	11.98	12.63	9.74	12.74	15.49	17.25
Na_2O	2.08	1.57	2.32	1.76	1.97	2.02
K_2O	0.54	0.15	0.28	0.20	0.25	0.39
P_2O_5	0.10	0.01	0.01	0.01	0.02	0.01
S	0.22	0.16	-	-	-	-
H_2O^+	) 0.70	) 0.22	0.61	1.23	0.65	0.57
H_2O^-	)	)	0.12	0.12	0.09	0.10
Total	99.61	98.25	100.50	100.38	100.38	100.32

12 Gabbro xenolith, Grange Irish.
396 Layered gabbro, near base of sequence on Carlingford Mountain.

A. Chilled gabbro (Le Bas 1960 Table III, 99a)
B. Granulitic gabbro (Le Bas 1960 Table III, 100).
C. Feldsparphyric gabbro (Le Bas 1960 Table III, 1071).
D. Leucocratic gabbro (Le Bas 1960 Table III, 512).

The petrochemical similarity of the gabbro xenoliths and layered gabbro lends support to the suggestion put forward in Chapter I that the xenoliths have been derived from a hidden mass of gabbroic high alumina basalt which fed the layered gabbro lopolith , and through which the host dykes and cone-sheets passed.

The composition of the quartz-feldspar-porphyries.

Quartz feldspar porphyries are relatively uncommon in the Carlingford Complex, and only a few dykes of this rock type have been recognized, two have been analysed, 1203 and 1212 (trace element concentrations have not been determined for 1203). The concentration of SiO_2 in these rocks falls either side of the 70% SiO_2 divider proposed to distinguish the craignuritic felsites from rhyolites in Chapter 3. The petrography of the quartz-feldspar-porphyries is not appropriate for members of the tholeiitic basalt - craignurite series however, and comparison of their chemistry with the trends exhibited by the latter suite, shows that concentrations of Fe (Fe_2O_3 and FeO as Fe_2O_3), MnO and K_2O are lower, and Al_2O_3 values higher, than in craignuritic felsites with similar differentiation indices (see Figure 8.1). The concentrations of Y, Sr and Ce in 1212 are also anomalous when compared with those in the craignuritic felsites, the Y and Ce values being exceptionally low for such rocks, while Sr is relatively high. Low Y concentrations are characteristic of the biotite felsites (see below) which also have relatively high Sr values.

Figure 8.1

Compositions of Carlingford felsites, granophyres, quartz-feldspar-porphyries, rhyolites and lamprophyres depicted as a series of variation diagrams of major element oxide concentrations versus Differentiation Index (D. I.). The tholeiitic basalt - craignurite trend is included for comparison.

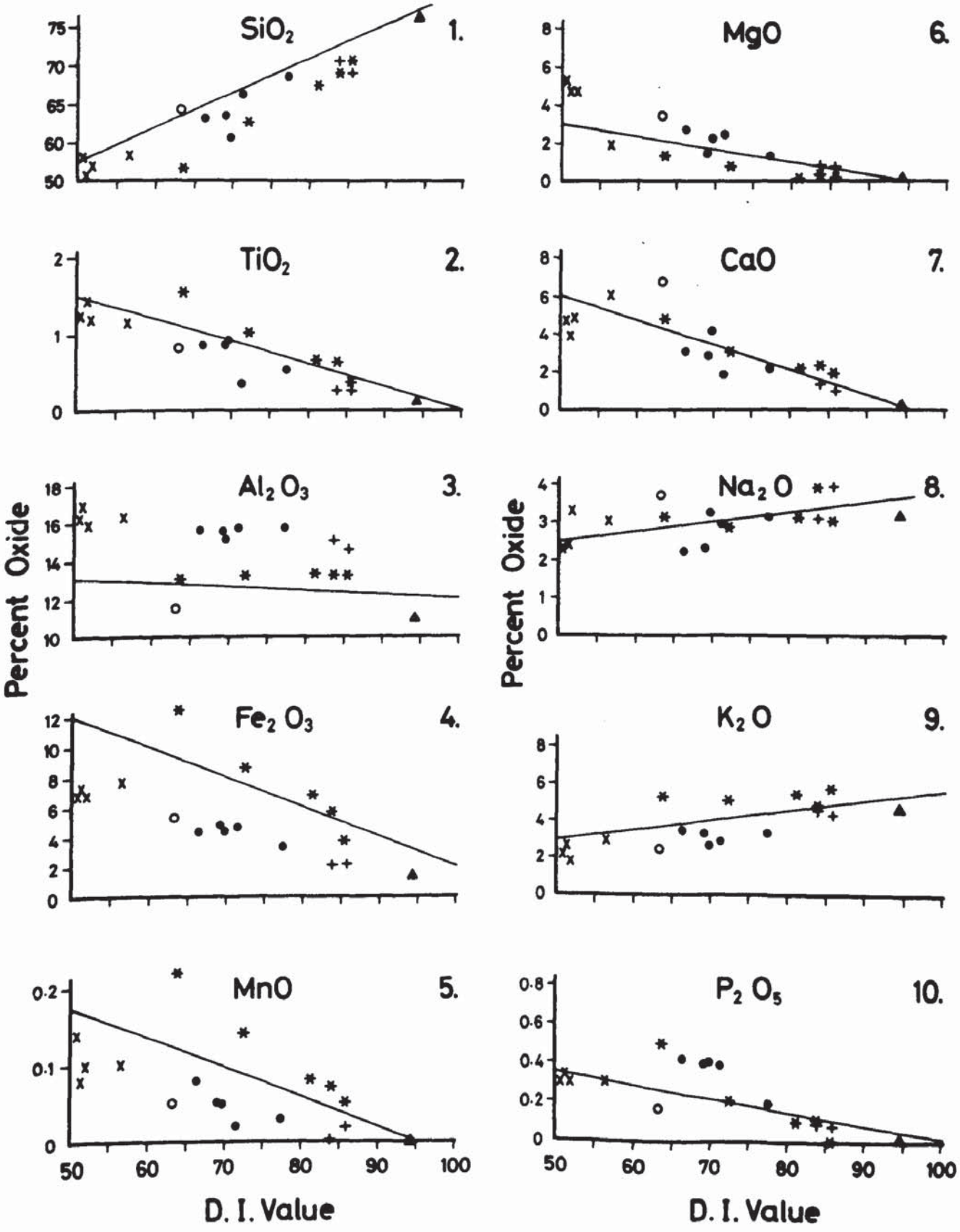

The composition of the biotite felsites

The group of rocks referred to as biotite felsites in Chapters 1 and 3 above are petrographically distinct from the craignuritic felsites. Five such felsites have been analysed, samples 593, 885, 897, 1180 and 1250, their compositions are represented in terms of major element oxides plotted against D.I. in Figure 8.1, which emphasises their similarity with the quartz feldspar porphyries. Comparison of the biotite felsite compositions with the tholeiitic basalt - craignurite trend indicated in Figure 8.1, shows that the felsites exhibit lower concentrations of K_2O and MnO, and considerably lower concentrations of Fe (Fe_2O_3 and FeO as Fe_2O_3), than the craignuritic felsites, and have higher concentrations of Al_2O_3 and P_2O_5. CaO and Na_2O values are similar in both series. Trace element concentrations in the biotite felsites (see Appendix XIII) are also distinct from those in craignuritic rocks with similar D.I. values. Sc values tend to be lower in the felsites while Sr values are relatively high; most noteable are the exceptionally low Y values recorded in the felsites relative to those of other acidic rocks in the complex.

Specimen 1250 is intermediate between the other biotite felsites and the quartz feldspar porphyries both in petrography and petrochemistry, it has the highest differentiation index of the five analysed felsites and contains corroded quartz phenocrysts similar to those in the porphyries. In view of the petrochemical similarities exhibited by the biotite felsites and quartz feldspar porphyries it is concluded that they are members of the same magma series.

The composition of a rhyolite.

Two rocks have been identified that can be classified as rhyolites on the basis of the petrochemical criteria set out in Chapter 3, one of those, sample 1203, is petrographically a quartz feldspar porphyry (see above); the other, sample 859, occurs as a cone-sheet attributed to Cycle II which crops out on the shores of Carlingford Lough, 800 metres north west of Carlingford. Figure 8.1. shows that in composition 859 plots near to the projected trend of the tholeiitic basalt - craignurite series, trace element concentrations listed in Appendix XIII are also appropriate for a highly fractionated rock in that suite. Rb, Y, Ce, Pb and Th values recorded for 859 are relatively high, while concentrations of Sc, V and Sr are low. The low Ba value (489 ppm) is atypical and suggests that depletion of that element takes place in the later stages of fractionation in the tholeiitic basalt-craignurite series probably as a result of the separation of feldspar.

The composition of the felsite sample 839.

Sample 839 is petrographically unique among the Carlingford suite. The rock is a felsite consisting of a fine grained feldspathic matrix in which abundant subhedral phenocrysts of clinopyroxene are embedded. It forms the upper part of a composite cone-sheet which cuts the Carboniferous Limestone near Mullatee. The composition of the rock is represented graphically in Figure 8.1, which shows that it exhibits some similarities with those of the biotite felsites except that it has much lower Al_2O_3 and P_2O_5 values and more abundant CaO. The rock exhibits little petrochemical compatability with the tholeiitic

basalt - craignurite trend. Cr, Ni and Sr values in 839 are relatively high for a rock with a differentiation index in excess of 60, while the concentration of Y present is low (see Appendix XIII); the abundances of the trace elements in general are similar to those of the lamprophyres (see below) though the Ba value is lower.

The high CaO content of 839 and high Sr value may partly be the result of assimilation of Carboniferous Limestone and certainly calcite is present in the groundmass; however, the high concentration of Sc in 746 suggests that assimilation of limestone on a large scale would result in a much higher Sc value while Cr and Ni concentrations would be diluted.

The composition of the Carlingford granophyre.

Analyses of a number of samples of the Carlingford granophyre carried out during the current investigation are listed in Appendices V and XIII. The majority are contaminated by assimilation of basic material, sample 13 is a gabbro from the Cooley mass which has been acidified by the granophyre. Eight analyses, including three selected from the literature are set out for comparison in Table 8.4.

The compositions of the granophyres listed in Appendix V are plotted against D.I. in Figure 8.1, enabling direct comparison with the biotite felsites, quartz feldspar porphyries and the tholeiitic basalt - craignurite trend. Concentrations of TiO_2, Fe (Fe_2O_3 and FeO as Fe_2O_3), MnO and K_2O are higher in the granophyre than in other rocks with similar D.I. values; the high TiO_2, Fe and MnO values may partly be the result of contamination by gabbro. Al_2O_3 values in the

TABLE 8.4

Composition of the Carlingford granophyre and related rocks.

	2	13	15	29a	29b	29c	X	Y	Z
SiO_2	69.02	49.82	70.41	67.68	56.78	62.82	75.00	74.60	70.48
TiO_2	0.61	0.91	0.36	0.69	1.56	1.01	0.22	0.25	-
Al_2O_3	13.21	14.68	13.45	13.55	13.14	13.25	12.29	12.30	14.24
Fe_2O_3	2.11	2.19	1.37	2.19	3.06	2.51	1.42	0.70	3.72
FeO	3.20	8.49	2.07	4.25	8.44	5.57	1.17	1.75	-
MnO	0.07	0.15	0.05	0.08	0.22	0.14	tr	-	-
MgO	0.54	6.70	0.26	0.09	1.46	0.87	0.11	tr	0.40
CaO	2.15	10.96	1.97	2.12	4.79	3.05	0.52	0.80	1.48
Na_2O	3.90	2.07	3.02	3.10	3.29	2.92	3.78	3.68	3.66
K_2O	4.76	0.85	5.70	5.38	5.23	5.10	5.10	5.47	4.26
P_2O_5	0.13	0.11	0.03	0.11	0.50	0.21	0.05	tr	-
S	0.01	0.01	0.01	0.01	0.01	0.01	-	-	-
H_2O^+	)						0.30	0.35	)
	)0.01	1.26	1.16	0.37	0.69	0.62			) 1.59
H_2O^-	)						0.22	0.20	)
Total	99.72	98.20	99.86	99.77	99.32	98.21	100.18	100.10	99.83

2. Contaminated granophyre, Barnavave.
13. Acidified gabbro, Cooley.
15. Granophyre vein, Cooley.
29a. Granophyre, Drumenagh Hill.
29b. Acidified gabbro xenolith, Drumenagh Hill.
29c. Contaminated granophyre, Drumenagh Hill.
X. Granophyre, Barnavave (Nockolds 1935 p 304 No VII).
Y. Granophyre, Barnavave (Nockolds 1935 p 304 No VIII)
Z. Granophyre, Slievenaglogh (Sollas 1894 p 491).
tr.= Trace.

granophyres are similar to those of craignuritic felsites but lower than those of the other rock types depicted.

Trace element concentrations in the granophyre are typical of those of acid rocks determined during the current investigation. S, Sc, V, Cr, Co, Ni, Cu and Sr values are relatively low while Rb, Y, Zr, Sn, Ba, Ce, Pb and Th values are high. U values of 3 or 4 ppm have been recorded in several of the granophyres analysed.

Analyses 29a, 29b and 29c (see Table 8.4) are of samples selected from various parts of a single specimen of granophyre collected in a quarry on Drumenagh Hill where the granophyre cuts the "early gabbro". The analyses reflect progressive assimilation of gabbroic xenoliths by the granophyre, 29a is of a relatively uncontaminated granophyre, 29b is a gabbro xenolith somewhat acidified but still coherent and 29c is of a patch of melanocratic granophyre representing a digested xenolith. The assimilation process in question involves simple mixing of the two end members, the acid magma and the basic material incorporated in it, as is demonstrated by these analyses. The product of the mixing process are not comparable in composition to the biotite felsites, or members of the tholeiitic basalt - craignurite series, as shown by Figure 8.1, thus it is inferred that such rock types have not been produced by assimilation, or by mixing of acid and basic magmas, which mechanisms have been suggested by some workers to have produced intermediate - acid rock types in the Hebridean Province (Harker 1904 Ch. XI, Tomkeieff and Marshall 1935, Skelhorn 1959 Srirama Rao 1959).

The composition of the lamprophyres.

It has been noted in Chapter 1 above that a number of intrusive masses of lamprophyre of doubtful age have been recorded in the northern part of the area under consideration (see Map 1). These rocks have been attributed petrographically to the vogesite - spessartite clan, four samples have been analysed. Specimens 1235 and 1236 were collected from a sheet like mass, possibly a complementary cone-sheet, which crops out in a quarry and on the hill slopes near Ballyonan; 1350 occurs as a dyke cutting the Silurian sediments on the shores of Carlingford Lough near Greers Quay; and 1366 collected from a two metre thick north west - south east trending dyke which traverses the shore in the vicinity of Ballinteskin. Specimen 1366 is somewhat more feldspathic in composition than the others, it has granophyric patches in the matrix and is petrographically intermediate between the other lamprophyres and the biotite felsites.

The compositions of the four analysed rocks together with those of a "hornblende porphyrite", a vogesite and a spessartite of Caledonian age from the Ards Peninsula (Reynolds 1931) are listed in Table 8.5 for comparison. This data shows that the concentrations of SiO_2, K_2O and P_2O_5 are generally higher in the Carlingford rocks while MgO, CaO and Na_2O are lower than in the Ards Peninsula lamprophyres.

The compositions of the four Carlingford rocks are plotted in Figure 8.1 for comparison with those of the felsites, craignurites, granophyres and quartz feldspar porphyries; they are generally more basic than the other rock types plotted, all having differentiation indices between 50 and 57, 1366 having the highest D.I. value.

TABLE 8.5

Composition of some lamprophyric rocks

	1235	1236	1350	1366	A	B	C
SiO_2	57.05	58.40	55.75	58.27	55.40	50.40	54.30
TiO_2	1.20	1.25	1.45	1.17	0.42	1.24	0.90
Al_2O_3	15.94	16.26	16.89	16.35	16.22	17.05	15.46
Fe_2O_3	1.48	1.82	0.95	2.68	1.71	1.32	1.86
FeO	4.70	4.63	5.85	4.56	3.72	6.15	5.20
MnO	0.10	0.14	0.08	0.10	tr	tr	0.22
MgO	4.75	5.26	4.74	1.97	5.45	5.30	5.61
CaO	4.85	4.80	3.95	6.08	5.40	5.65	5.50
Na_2O	3.71	2.70	2.89	3.02	4.20	3.94	4.30
K_2O	1.88	2.27	2.74	2.92	2.15	1.80	1.94
P_2O_5	0.30	0.30	0.33	0.31	0.24	0.18	0.22
S	0.01	0.01	0.09	0.01	0.22	tr	tr
H_2O^+)	)	)	)		2.40	3.60	2.80
H_2O^-)	)2.47	)1.97	)3.86	2.51	0.30	0.50	0.44
CO_2)	)	)	)		2.00	2.80	1.35
Total	99.44	99.80	99.57	99.95	99.83	99.93	100.10

1235, 1236, 1350, 1366 Current investigation. (see text for description and localities).

A. "Hornblende porphyrite", Ards Peninsula (Reynolds 1931 p 109)

B. Vogesite, Ards Peninsula (Reynolds 1931 p 146)

C. Spessartite, Ards Peninsula (Reynolds 1931 p 151)

tr.=Traces

Though having noteably higher concentrations of MgO and CaO than the biotite felsites, the compositions of the lamprophyres show many similarities with those of the latter group, with 1366 falling in an intermediate position between the two suites as suggested by its petrography. Like the biotite felsites the lamprophyres are petrographically and petrochemically distinct from members of the tholeiitic basalt - craignurite series, and in particular have much higher concentrations of Al_2O_3 and MgO and lower concentrations of Fe (FeO and Fe_2O_3 as Fe_2O_3) than the latter suite.

Members of the Carlingford vogesite-spessartite suite exhibit high concentrations of Sr and Ba (see Appendix XIII) as is typical of lamprophyres in general (Williams, Turner and Gilbert 1954 p 85, Turner and Veerhoogen 1960 p 251). Cr and Ni values are also relatively high in these rocks, while concentrations of Y on the other hand do not exceed 15 ppm, which is low for rocks with D.I. values in excess of 50 (see Chapters 4 and 6), low Y values are a feature of the biotite felsites (see above).

The petrochemical affinity of the lamprophyres for the biotite felsites is considered of significance.

The Origin of the Acid Magmas

The considerable volume of intrusive acid magmas in the central complexes of the British Tertiary Province has led to the suggestion that they have been produced by processes other than fractionation of basaltic melts as invisaged by Bowen (1928), involving mechanisms of assimilation and partial melting of crustal rocks by basic magmas

(Skelhorn 1959, Brown 1963). The problem has been reviewed by King (1962, 1963a, 1963b, 1964, 1965a, 1965b).

Le Bas attributes the petrogenesis of the Carlingford granophyre to melting of argillaceous Silurian sediments by masses of basaltic magma at a depth of a few kilometres below the surface (Le Bas 1967). Brown (1963) considers the melting of basement Lewisian gneisses and in some cases of Torridonian Sandstone as the source of some Hebridean acid magmas. Crustal melting as a petrogenetic mechanism has recently been challenged in the case of the Irish acid intrusions by Meighan and Gamble (1973) who have produced evidence of differentiation in the granophyres of Carlingford and the Mournes, however their data does not preclude those magmas, though fractionated, having been produced by partial melting in the first place.

Le Bas (1967 p 332) notes the appearance of corundum in the norms of the granophyres and granites of Carlingford and the Mournes, and considers that phenomenon to be evidence favouring argillaceous sediments as the source of those melts, as suggested by Luth, Jahns, and Tuttle (1964). It must be admitted that the norms of the samples of granophyre analysed during the current investigation are corundum free (see Appendix IX), however its absence is probably the result of contamination by basic rocks and thus in isolation does not throw doubt on Le Bas' hypothesis. In view of the considerable volume of granophyre exposed at Carlingford and the absence of suitable intermediate types indicating fractionation from a basaltic parent, the melting of argillaceous sediments is accepted, with reservations, as the most probable source of that magma. The partial melting is

considered by the current author to have been brought about by the intrusion of the large masses of basic magma which fed the dykes and cone-sheets of Cycle II, and the high alumina gabbros and feldspar-phyric dolerites of IIe - IIIa in particular (see Chapters 1 and 2 above). Further consideration of the petrogenesis of the Carlingford granophyre is beyond the scope of the current investigation.

Turning to the biotite felsites and quartz-porphyries the volume problem does not arise as they are relatively uncommon rocks occurring as isolated dykes and sheets. However, as has been discussed above, the compositions of these types do not fall on the line of descent of tholeiitic magma described in Chapter 6 (see Figure 8.1); further, the fractionation processes described in Chapters 4,5 and 6 have been shown to give rise to Y enrichment, while the biotite felsites have exceptionally low Y values. In the absence of evidence suggesting that fractionation of basaltic magma has given rise to these acid melts, crustal melting is again inferred. Brown (1963) considered the behaviour of acid melts in terms of the ternary system Quartz, Albite, Orthoclase in the presence of water, investigated experimentally by Tuttle and Bowen (1958). Those phases, the principle components of "petrogenys residua system" (Bowen 1937), are not as abundant in the biotite felsites as in the granitic rocks investigated by Brown, however they exceed 65% in the norms of those samples analysed (CO_2 in excess of normative calcite was excluded from the norm calculations for sample 885), anorthite (except in 885), corundum and orthopyroxene make up the majority of the remainder of the norm in each case. Schairer (1957) has shown that the addition of small quantities of

anorthite or pyroxene to the systems Ab - SiO_2 and Or - SiO_2 have little effect on the position of the alkali feldspar - quartz field boundaries, it is therefore considered that the system Quartz, Albite, Orthoclase reflects the behaviour of the felsite melts quite closely. Normative Quartz, Albite and Orthoclase for the biotite felsites have been recalculated to 100 percent and plotted on the triangle Qu, Ab, Or (Figure 8.2), it is noteable that the majority of rocks in the suite fall near the low melting point on the quartz-alkali feldspar cotectic at 1000 bars p H_2O; specimen 593 falls inside the quartz field, as does the normative composition of the Coire Uaigneich granophyre when plotted in a similar manner (Brown 1963), the latter is considered to represent melted Torridonian arkose (Wager et al 1953, Brown 1963), no such source rock is known to be available at Carlingford however. Wyllie and Tuttle (1961) have shown that partial melting of pelitic sediments gives rise to liquids in the quartz field, thus such a process could have given rise to liquids with the composition of sample 593, subsequent fractionation then having produced the other felsite compositions. As has been noted above the norms of the rocks in biotite felsite suite include corundum, a phenomenon which Luth et al (1964) and Le Bas (1967) consider as evidence that such rocks have been produced by a process involving the partial melting of argillaceous sediment.

The normative compositions of the two analysed Silurian sediments fall near the alkali feldspar-quartz cotectic when plotted on the Quartz, Albite, Orthoclase triangle (see Figure 8.2), however those components comprise less than 60% of the norm in both cases. Sample 31

Figure 8.2

Composition of acid igneous rocks and Silurian sediments of the Carlingford suite in terms of normative albite, orthoclase and quartz, plotted on the Albite (Ab), Orthoclase (Or), Quartz (Qu) triangle. The quartz - feldspar cotectics at 500 and 1000 Kg/cm^2 water vapour pressure are included.

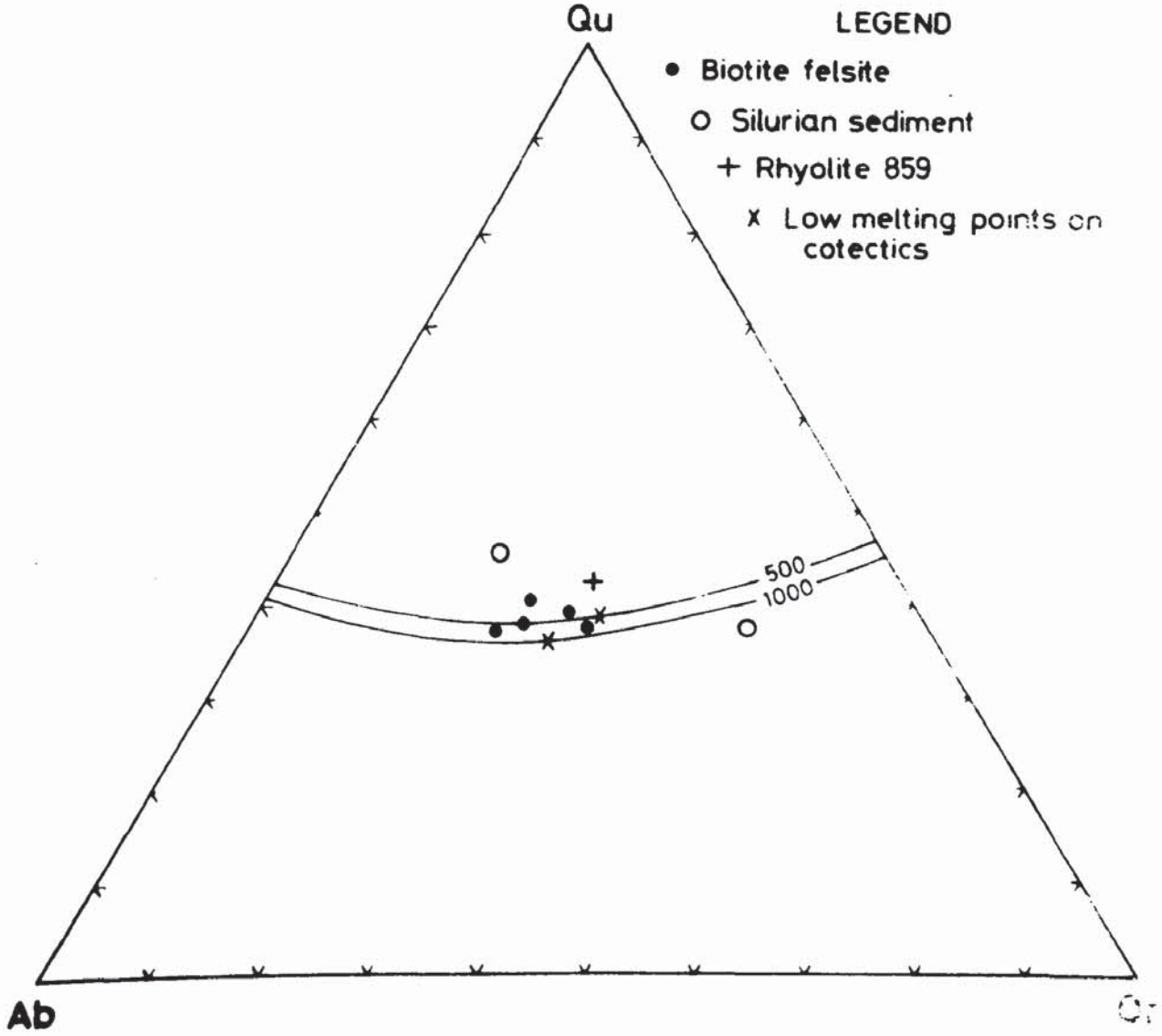

falls in the quartz field and thus its composition may approach those of rocks parental to the felsite melts. The degree of compositional variation exhibited by the Silurian rocks (see above) indicates that sediments of a suitable parental composition are likely to be present in the area even though they may not yet have been identified.

The low concentrations of Y in the felsites introduces a problem. Le Bas has noted the relatively low concentrations of Y in the granophyres and Silurian sediments at Carlingford (Le Bas 1967 p 334), however Y values in the felsites are even lower, not exceeding 10 ppm. The behaviour of Y during the fractionation of the alkali basalt series, the high alumina basalt series and the tholeiitic basalt series shows that it becomes enriched with progressive differentiation (see Chapters 4, 5 and 6 above). This residual behaviour suggests that Y would preferentially enter the acid products of partial melting, thus becoming enriched in such melts relative to concentrations in the parent sediment. The depletion of Y in the hornfelses adjacent to the layered gabbros (see Table 8.6) lends support to that interpretation. Thus the source rock which gave rise to the felsite melts must have been depleted in Y prior to that process.

Le Bas reports the presence of a granophyre predating the main granophyre mass at Carlingford and represented by xenolithic fragments in the vents of Slievenaglogh,which he refers to as the "early" granophyre (Le Bas 1967 p 325). Microxenoliths of granophyre have been recognised in some of the minor intrusions of the tholeiitic basalt-craignurite series and quartz-porphyries of Cycle II, during the current investigation, confirming the presence of such a granophyre

TABLE 8.6

Variation of Y concentration in hornfels with proximity to the gabbro contact.

	1218	1216	1307	1186	1185	1184	1183	1182	851	850
Y value	30	30	30	30	40	25	20	10	15	BLD
Vertical distance to contact in metres	104	73	45	37	23	15	45	0.6	0.6	0.15

BLD - below limits of detection (10 ppm)

Sample numbers refer to Le Bas' localities

Numbers 1218, 1216, 1307, 1186, 1185 and 1184 - hornfelsed Silurian sediments.

Numbers 1183, 1182, 851 and 850 - hornfelsed basalt lavas.

Data (Le Bas 1970b, Table 9).

Sample locations and descriptions (Le Bas 1970b, p 236).

body below the surface prior to the emplacement of the Carlingford granophyre itself. A xenolith of this granophyre contains 50 ppm Y (Le Bas 1967 Table 2 p 333) which is more concentrated than in the Silurian sediments (see above). It is suggested herein that the sediments which gave rise to the felsites, initially yielded the early granophyre melt in which Y was enriched thus depleting its concentration in the parent rock, subsequent partial melting of the residue gave rise to the somewhat less acid felsite melts with low Y values. It is probable that volatiles including H_2O were concentrated in the products of the early stages of partial fusion (the early granophyre), while the later felsite melts were correspondingly less volatile rich. The wet granophyre

would be unable to migrate far before crystallizing (Brown 1963 p 532, King 1963 p 619, Cann 1970 p 337), while the drier felsites were able to rise to higher levels as dykes and cone-sheets such that they are now exposed at present levels of erosion. As has been noted in Chapter 2 above it is considered that the magma body, which fed the layered gabbro lopolith, supplied the heat which brought about this melting process. It is of significance that similar masses of high alumina basalt are believed to have contributed to the petrogenesis of the Carlingford granophyre (see above).

The petrochemical similarities exhibited by the quartz-prophyries and biotite felsites have been noted above, including the low concentration of Y in members of both suites. Figure 8.1 shows that they form a series when major element concentrations are plotted against the differentiation indices of the rocks in question, the quartz-porphyries having higher D.I. values than the felsites. In the field the two suites have a similar distribution, the majority of intrusions of both types occurring in the northern part of the area near Two Mile River and Ballyonan; a quartz-porphyry dyke which traverses the shore at Whitestown in the south east is an exception. The petrochemical data and the field relations thus indicate that the quartz-porphyries are petrogenetically related to the biotite felsites and it is therefore suggested that the former were derived from the felsite magma by fractionation, an interpretation which is supported by petrography of sample 1250, (see above).

It has been shown above that the composition of the rhyolite 859 falls near the tholeiitic basalt - craignurite trend, it is therefore

considered to be a fractionated derivative of that suite, an interpretation which is in keeping with trace element concentrations in the rock (concentrations of Y are too high for the rock to have been produced by fractionation from the felsite magma). Carmichael considers that it is impossible to derive such silica rich melts (the normative composition of 859 plots in the quartz field of the Qu, Ab, Or triangle - Figure 8.2) by direct fractional crystallization of tholeiitic magmas (Carmichael 1963), which is in conflict with the above conclusions. It is considered possible that assimilation of siliceous crustal rocks by the fractionating parent craignuritic melts in question may have given rise to the rhyolite magma, a mechanism which overcomes Carmichaels objections, however as noted by King, such conclusions must be treated with caution (King 1963 p 626).

The petrogenesis of the felsite 839, is considered below.

The origin of the Lamprophyres.

The origin of lamprophyric rocks remains a petrogenetic problem. Turner and Veerhoogen have reviewed a number of hypothesis put forward to explain their petrogenesis (1960 pp 254-6), none can be applied satisfactorily to all types of lamprophyres. Many authors consider that the ferromagnesian phenocryst phases, and alkaline feldspathic matrix, which characterise the lamprophyre group, originate independently (Bowen 1928 Chapter XIII, Williams Turner and Gilbert 1954 p 85). Reynolds (1931), discussing the petrogenesis of the lamprophyres of the Ards Peninsula, invisages a complex process involving the reaction of hornblende separating from the fractionating Newry granite, with

underlying basaltic magmas, as having given rise to the lamprophyric magma, a mechanism suggested by Bowen (1928 Chapters XIII and XIV), followed by subsequent fractionation of that magma to produce the variety of lamprophyre types exhibited.

The problem at Carlingford is exacerbated by the uncertain age of the lamprophyres with the exception of the minettes which are accepted as being Caledonian in age. It is therefore appropriate to establish the age of vogesites and spessartites before proceeding to further discussion of their petrogenesis. The following points are relevant to that problem:

a) The occurrence of dykes of similar type and of Caledonian age in the Ards Peninsula, where they invariably have a north east - south west trend (Reynolds 1931 p 164).

b) The Carlingford lamprophyres occur as dykes with a north west - south east trend, or as sheets inclined radially to the centre of the complex in the manner of Tertiary cone-sheets or complementary cone-sheets.

c) The Carlingford lamprophyres show petrographic and petrochemical similarities with the biotite felsites of known Tertiary age (see above) and which have a similar spacial distribution in the field.

d) Concentrations of trace elements in sample 839, a unique Tertiary felsite, show similarities with those of the lamprophyres with which it has some affinity in terms of composition, suggesting a possible petrogenetic relationship.

The weight of evidence structural, petrographic and petrochemical, albeit tenuous, is thus in favour of attributing a Tertiary age to the

Carlingford lamprophyres (it is worth noting that Bailey et al. attribute a Tertiary age to other such lamprophyres in the Hebrides (1924 p 379)). That view is accepted, with reservation, by the current author, inspite of the doubts raised by the age of the Ards dykes.

Assuming that the lamprophyres are Tertiary in age, their petrogenesis can be considered in the light of other Tertiary processes. There is no evidence that they have been derived by processes involving the fractional crystallization of basaltic magma; the analysed lamprophyres in the Carlingford suite are strongly quartz-normative (see Appendix IX), thus the petrogenetic scheme put forward by Bowen (1928), whereby hornblende crystals react with alkali olivine basalt magma to produce a strongly alkalic lamprophyre melt is inappropriate. It has been noted above that the petrochemical affinity of the lamprophyres for the biotite felsites is considered of significance, it suggests that the two suites are petrogenetically related. The lamprophyres have higher concentrations of Fe (Fe_2O_3 and FeO as Fe_2O_3), TiO_2, Al_2O_3, MgO and CaO than the felsites, and assuming that the former have been formed by processes of partial melting involving argillaceous sediments in the same manner, addition of material rich in those components to the resulting felsite melts must have taken place to produce the lamprophyric magma. The addition of such basic material may either have taken place during the partial melting process itself, by incorporation of suitable parental rock, or by assimilation during the subsequent intrusion of the melt. The following basic rock types are known to have been available at the beginning of Cycle II when the felsite magma was produced:

a) Caledonian minette dykes.

b) The tholeiitic rocks of Cycle I, including feeders for the tholeiitic lavas.

c) Alkali dolerite intrusions of Cycle I, including feeders for the alkali basalt lavas.

d) The early gabbro.

e) The high alumina basalt mass which fed the layered gabbro.

Though the Caledonian minette has appropriate concentrations of trace elements (high Cr, Ni, Sc and Ba values, low Y and Rb values) and of SiO_2, MgO and CaO, it exhibits TiO_2 and Al_2O_3 values which are too low and a P_2O_5 content too high for it to have been a suitable additive. The tholeiitic rocks of Cycle I, including the lavas, are not considered appropriate as additives even though Cr and Ni values are relatively high in the more basic members of the suite, for concentrations of Al_2O_3 Sr and Ba are not high enough in the majority of rocks therein; Y values, on the other hand, are too high in all but the transition dolerites. Members of the high alumina basalt series have low TiO_2 concentrations too and are thus not ideal additives, which is also true of the acidified gabbro. Concentrations of Sr and Ba in the layered gabbros are too low. The composition of the early gabbros are not sufficiently well known for them to be considered further in this context.

Members of the alkali basalt suite generally have higher concentrations of Sr and somewhat higher concentrations of Ba than rocks in the high alumina basalt and tholeiitic basalt series (see Chapters 4, 5 and 6). They also exhibit relatively high Cr and Ni values and high

concentrations of TiO_2 and Al_2O_3. Rb and Y values in the more basic members of the alkaline series are appropriately low.

Thus, of the various rock types known to have been available, the alkali basalts of Cycle I are the most suitable in composition to have acted as additives to the partial melt products of argillaceous sediments at Carlingford during the process which gave rise to the lamprophyric magmas. The petrogenesis of the Carlingford lamprophyres is thus tentatively ascribed to the partial melting of argillaceous Silurian sediment in the presence of alkali basalt which participated in that partial melting, or was subsequently assimilated by the product melts. Being considered to be coeval with the biotite felsites, the lamprophyres are attributed to episode 11a of the Carlingford sequence (see Chapter 1).

The composition of sample 839, together with its trace element concentrations, indicates that it cannot have been produced by fractional crystallization of tholeiitic magma or of the felsite magma, or by processes involving assimilation of limestone by those melts (see above) It does show underlying petrochemical affinities with the lamprophyres however, and it is considered probable that this rock was derived by fractionation from the lamprophyre magma involving the separation of plagioclase as indicated by the low Al_2O_3 value exhibited by the rock.

Summary.

The compositions of a number of rock types occurring in the Carlingford Complex, including those of the country rocks, have been considered and the following conclusions have been drawn:

1. The composition of the Silurian sediments is variable, though Y and Sc are relatively low in all samples analysed. High Sc and Sr values have been recorded in a sample of Carboniferous Limestone.

2. A Caledonian minette, exhibits high concentrations of Sr and Ba, which is typical of lamprophyres, together with high Cr and Ni values.

3. Two analysed basalt lavas of Tertiary age are similar in composition to the transition dolerites of the tholeiitic basalt - craignurite series. It is considered that the intrusion of dykes of similar composition attributed to Cycle I may have been, in part, coeval with the extrusion of the basalt lavas and that some may have acted as feeders. The alkali lavas of Rock Marshall postdate the tholeiitic basalts in that locality and it is considered probable that the alkali dolerite dykes of Cycle I also post date the tholeiitic dolerite dykes of that event.

4. The composition of the gabbro xenoliths indicates that they were derived from the magma body which fed the layered gabbro lopolith, as has been suggested in previous Chapters.

5. The assumption that the Carlingford granophyre was derived by partial melting of argillaceous sediments is accepted. The large masses of basic magma which fed the minor intrusions of Cycle II, and the high alumina basalt cone-sheets of episodes IIe and IIIa in particular, induced the partial melting which gave rise to the granophyre magma.

6. The biotite felsites are characterized by low Y concentrations. Their petrochemistry is inconsistant with their derivation from tholeiitic magma by fractionation, and indicates that they were produced by partial melting of parental argillaceous sediment already depleted

in Y and volatiles as a result of the partial melting which had previously given rise to the "early" granophyre. These processes were brought about by the emplacement of the high alumina basalt magmas which fed the layered gabbro lopolith.

7. The petrochemistry of the quartz-feldspar-porphyries suggests that they were derived by fractionation of the felsite magma.

8. The rhyolite 859 was derived by fractionation of craignuritic magma, and is thus a member of the tholeiitic basalt - craignurite series as indicated by its petrochemistry. It is possible that assimilation of siliceous crustal rocks contributed to the high concentration of SiO_2 exhibited by this rock.

9. Inspite of the occurrence of Caledonian lamprophyre dykes in the Ards Peninsula, similar rocks at Carlingford are considered to be of Tertiary age. The petrogenesis of these lamprophyres is tentatively attributed to the incorporation of basic material rich in Ni, Cr, Sc and Ba, (e.g. alkali basalts of Cycle I) by biotite felsite melts, either while being produced by partial melting of argillaceous sediments, or by subsequent assimilation. The lamprophyres are thus coeval with the felsites in the Carlingford sequence (episode IIa).

10. The felsite 839 is petrographically and petrochemically atypical. It is considered to have been produced by fractionation of plagioclase from the lamprophyre magma.

It must be admitted in conclusion that the volume of data on which many of the above arguments have been based is limited and only sufficient to outline the processes described, thus many of the conclusions put forward are tenuous. These reservations are particularly

applicable to the petrogenesis of the lamprophyres, which are a poorly understood group of rocks at best, and above all, to the petrogenesis of the felsite, sample 839.

CHAPTER 9

THE ORIGIN OF BASALTIC MAGMAS OCCURRING WITHIN THE CARLINGFORD COMPLEX.

Abstract

The three basaltic magma series described in previous chapters are shown to have fractionated at relatively low pressure (10 kb or less). Investigation of the petrochemistry of rocks approaching primitive parental melts in composition, and reconsideration of the Carlingford time sequence indicates that parental alkali basalt, high alumina basalt and tholeiitic basalt magmas were derived from an olivine tholeiite primary magma by processes of crystal liquid fractionation at depth. The primary olivine tholeiite magma was derived by up to 20% partial melting of parental peridotite at depths in excess of 60 km. The role of PO_2 in differentiation at Carlingford is examined in the light of the scheme of magma genesis put forward.

Introduction

The petrogenesis of the wide spectrum of basaltic magma types occurring in nature is a problem which has exercised many authors over a period of several years, with noteable contributions to the literature by Bowen (1928), Kennedy (1933), Daly (1933), Tilley (1950), Harris (1957), Kuno (1959), Kushiro (1961,1968), Yoder and Tilley (1962), Kushiro and Kuno (1963), O'Hara and Yoder (1963, 1967), O'Hara (1965, 1968a), Green and Ringwood (1967), Green, Green and Ringwood (1967), Gast (1968), Green (1968, 1969 a, b, 1970), Jamieson and Clark (1970). The work of the experimental petrologists among these authors has been

of particular significance in this area of research but as yet has served to introduce further controversy. Recent petrochemical investigations of Hawaiian alkali basalts, nephelinites and tholeiites (Macdonald 1968), Hebridean alkali basalts (Ridley 1971 a,b) and tholeiitic basalts (Holland and Brown 1972) have given rise to the suggestion that all are derived from parental olivine tholeiite magmas in the manner proposed by Green and Ringwood (1967).

Three basaltic magma series have been recognised at Carlingford and are described in preceding chapters, namely the alkali basalt series (Chapter 4), the high alumina basalt series, (Chapter 5) and the tholeiitic basalt-craignurite series (Chapter 6). Ridley (1971a) and Holland and Brown (1972) emphasised the transitional nature of the Hebridean alkali and tholeiitic series compared with those of Hawaii, a characteristic applicable to the basaltic rocks of Carlingford(see Chapters 4 and 6). The origin of the basaltic magmas of the complex and their significance in relation to the petrogenesis of basaltic magmas in general are discussed in the following paragraphs.

Summary of Carlingford fractionation trends

The fractionation trends of the alkali basalt, high alumina basalt and tholeiitic basalt-craignurite series at Carlingford are summarised in Figures 9.1 (major elements v D.I.) and 9.2 (trace elements v D.I). It has been shown in Chapter 4 that the members of the alkali basalt series have been derived from alkali basalt parents by fractionation of olivine giving rise to picritic accumulative basalts in the Cycle II suite and the Mugearite-benmorite series in Cycle III; or of olivine

Figure 9.1

Diagrammatic summary of the fractionation trends exhibited by rocks in the alkali basalt series, (broken lines - the trachy basalt - tristanite trend, A. and hawaiite - mugearite - benmorite trend B. are shown separately where appropriate), high alumina basalt series (dotted lines), and, tholeiitic basalt - craignurite series (solid lines), described in Chapters 4, 5 and 6 respectively, in terms of major element concentrations plotted against differentiation indices.

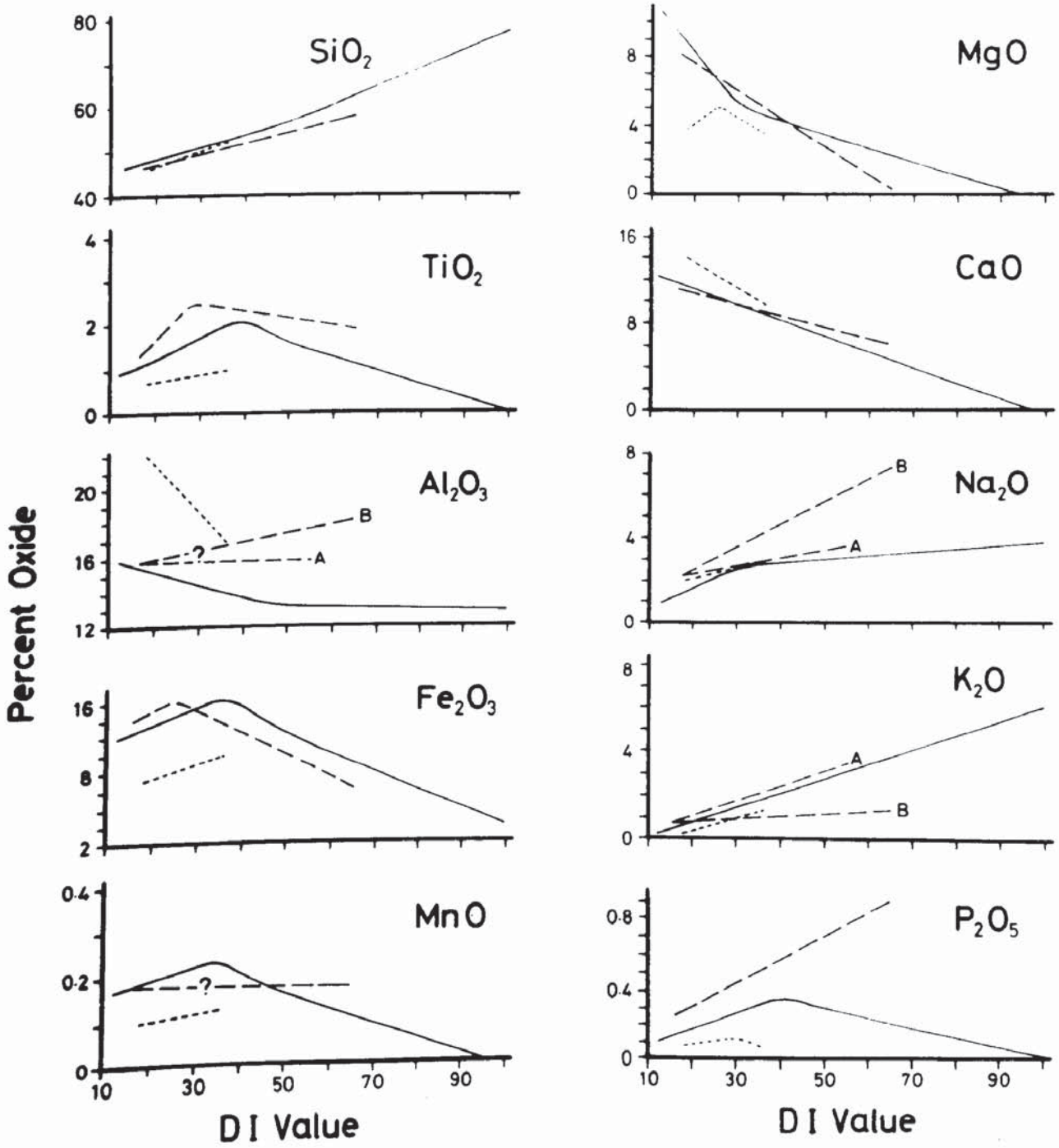

Figure 9.2

Diagrammatic summary of the behaviour of trace element concentrations during fractionation exhibited by rocks in the high alumina basalt series, (broken lines - the trachy basalt - tristanite trend, A. and hawaiite - mugearite - benmorite trend, B. are shown separately where appropriate), high alumina basalt series (dotted lines) and, tholeiitic basalt - craigmurite series (solid lines), and described in Chapters 4, 5 and 6 respectively, in terms of concentration plotted against differentiation indices.

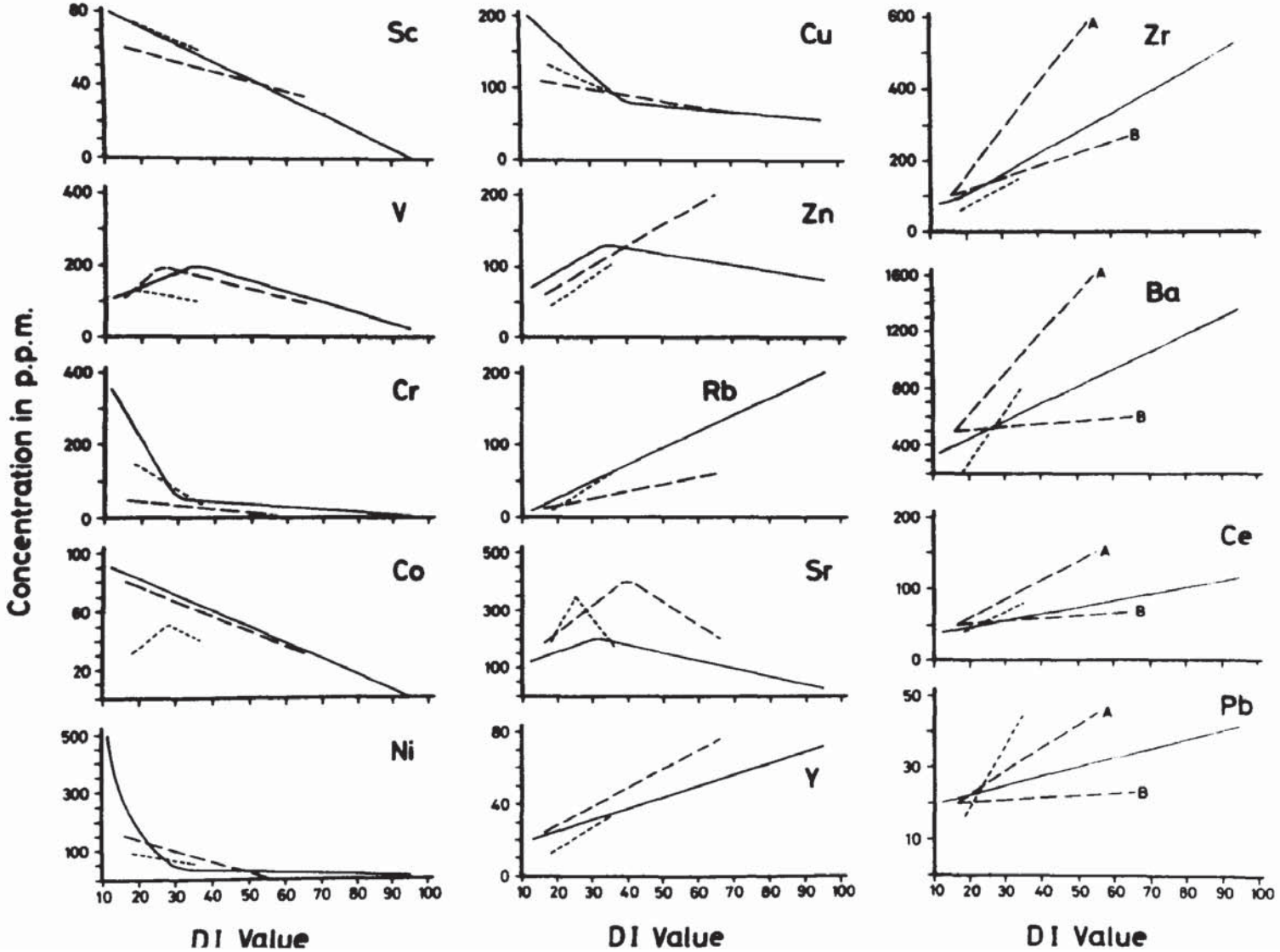

with plagioclase which gave rise to the trachy basalt - tristanite series of Cycle III. Separation of titanomagnetite played an important role in the late stages of fractionation in the alkali basalt series. The high alumina basalt series was derived by fractionation of plagioclase and minor olivine and ore from a high alumina basalt parent (Chapter 5), while the tholeiitic basalt - craignurite series was derived from olivine tholeiite (transition dolerite) parental melts by fractionation of olivine and plagioclase as described in Chapter 6. Thus fractionation of olivine and plagioclase together in varying proportions played an important role in the petrogenesis of derivative liquids in all three series.

Green and Ringwood (1967) have shown experimentally that plagioclase separates from alkali olivine basalt and olivine tholeiite melts, only at low pressures (10 Kb or less - see their Figures 4 and 6). Similar results were obtained in more aluminous olivine tholeiite melts, equivalent to the high alumina basalts of the current investigation, investigated by Green, Green and Ringwood (1967 Fig. 2) and Cohen, Ito and Kennedy (1967 Fig. 3), plagioclase separating at up to 12 Kb in the experiments of the latter group of workers. Furthermore, according to Green, Green and Ringwood (1967 p. 46), it is only possible for olivine tholeiite melts to give rise to quartz normative derivative liquids at pressures of 4.5 Kb or less, though such melts may approach the quartz normative condition by fractionation of olivine at slightly higher pressures. Thus the fractionation series exhibited by the Carlingford suites are the products of low to moderate pressure differentiation which took place at depths not

exceeding 35 Km, and at least in the case of the quartz normative derivatives not exceeding 15 Km, i.e. within the continental crust.

The dominant fractionation of olivine in the alkali basalts and picrites of Cycle II,and the alkali basalt - mugearite - benmorite series of Cycle III probably took place at somewhat greater depth than the fractionation of plagioclase and olivine which gave rise to the trachy basalt - tristanite series,i.e. at pressures of 9 Kb or more (see Green and Ringwood 1967 Fig. 6 p 140). As fractionation of all three series took place at similar pressures the parental magmas must already have acquired their alkaline, tholeiitic or high alumina characteristics before that fractionation took place, presumably at greater depths as indicated by experimental results. (Green and Ringwood 1967, O'Hara 1968a).

Reconsideration of the Carlingford Time Sequence

The sequence of intrusive activity at Carlingford has been discussed in Chapter 1 and outlined in Figure 1.11. The sequence was subdivided into three cycles, though "Cycle II" may in fact represent two or more such cycles (see Chapter 2). For convenience Cycle I was considered to be terminated by the intrusion of the layered gabbro, and Cycle II separated from Cycle III by the emplacement of the Carlingford granophyre. The high alumina basalt magmas of the layered gabbro and the cone-sheets of episode IIe and IIIa have been shown to be tholeiitic in character but to represent a magma series in their own right (Chapter 5), meriting equal status with the alkali basalt and tholeiitic basalt-craignurite series. The high alumina basalts

are thus considered to be normal members of the Carlingford cyclic sequence and reconsideration of that sequence is therefore felt necessary.

Ignoring the felsites of episode IIa, the alkali dolerite of Cycle I, the lavas and the granophyre, the sequence of intrusive events may be summarised as:-

Craignurite and quartz dolerite	(Ia)
Tholeiitic basalt and transition dolerite	(Ib)
High alumina basalt (layered gabbro)	
Alkali basalt	(IIb)
Craignurite and quartz dolerite	(IIc)
Tholeiitic basalt and transition dolerite	(IId)
High alumina basalt	(IIe - IIIa)
Craignurite and quartz dolerite	(IIIb)
Tholeiitic basalt and transition dolerite	(IIIc)
Alkali basalt	(IIId)

Thus complete individual cyclic sequences may more reasonably be considered to be:- craignurite - quartz dolerite; tholeiitic basalt - transition dolerite; high alumina basalt; alkali basalt, in that order with Cycle II in the strict sense beginning after episode IIb ,and Cycle III after episode IIIa. To some extent individual cycles may be incomplete for instance alkali basalts do not appear in Cycle II or high alumina basalts in Cycle III, as thus defined. This redefinition of individual cycles, which becomes apparent on reconsideration of Fig. 1.11, has significance in the interpretation of petrogenetic processes in the complex.

"Primitive" and "Primary" Magmas

Rocks, other than accumulative picrites, with low differentiation indices are considered "primitive" in the sense of Jamieson (1966), or at least more primitive than others in the same series with higher D.I. values, and are assumed to approach parental melts in terms of composition. In spite of their underlying distinctive characteristics and markedly different fractionation products, primative tholeiitic basalts ("transition dolerites") primitive alkali basalts and primitive high alumina basalts, ("high alumina gabbro"), have somewhat similar compositions as reflected in Figures 9.1 and 9.2, and there is a tendancy for the trends of most components, including trace elements, to converge at the primitive end of the spectrum. Al_2O_3 concentrations are of course much higher in the high alumina gabbros than in the transition dolerites or primitive alkali basalts, while Fe_2O_3, MgO and Co values are lower; The alkali basalts have higher concentrations of Fe_2O_3 than the transition dolerites which is reflected by their high V values, they also have relatively high Na_2O and TiO_2 concentrations and low Cu values, but underlying similarities are clear. * Thus it may be concluded that the primitive melts were derived from similar parental material, either directly from a peridotite source by varying degrees of partial melting (O'Hara 1968a), or by crystal fractionation from a parental primary magma derived from such a source (Green and Ringwood 1967).

It is noteable that the so called "incompatable elements" (Ringwood 1966) are not strongly enriched in the alkali basalts of Carlingford which is reported to frequently be the case in such rocks

*NOTE IT HAS BEEN POINTED OUT THAT THE RIGOROUS CHEMICAL SUBDIVISION OF BASALTS INTO ALKALINE AND THOLEIITIC STEMS EMPHASISED BY THE WORK OF CHAYES (1972) IS LARGELY ARBITRARY AS BASALTS FORM A CONTINUOUS SPECTRUM (COX 1972).

TABLE 9.1

Composition of the Upper Mantle

A. Major Elements

	A	B	C	D	E	F
SiO_2	44.5	44.2	44.9	44.22	45.85	45.16
TiO_2	0.15	0.1	0.08	0.11	0.41	0.71
Al_2O_3	2.55	2.7	3.15	2.55	2.05	3.54
Fe_2O_3	1.5	1.1	1.28	0.81	-	0.46
FeO	7.3	7.3	6.69	7.41	7.14	8.04
MnO	0.14	0.15	0.11	0.14	0.15	0.14
MgO	41.7	41.3	39.7	41.69	41.63	37.49
CaO	2.25	2.4	3.14	2.18	1.76	3.08
Na_2O	0.25	0.25	0.24	0.24	0.15	0.57
k_2O	0.015	0.015	0.042	0.05	0.08	0.13
P_2O_5				0.03	0.03	0.06
Cr_2O_3		0.30	0.43	0.29	0.48	0.43
NiO		0.20	0.24	0.28	0.26	0.20
CoO						0.01

TABLE 9.1

Composition of the Upper Mantle

B. Trace Elements

(concentrations in p.p.m.)

	V	W	X	Y	Z
Rb	1	1	1.04		
Sr	20	10	27.2		
Zr		30			
Th	0.06	0.02			
U	0.02	0.05		0.12	0.04

A. Predicted mantle composition (White 1967, No 1, Table 1, p16)

B. Predicted mantle composition (Harris et al. 1967, No 3, Table 2, p 6366)

C. Average 20 spinel lherzolite xenoliths (19 for Na_2O), Monistrol d' Allier, France (Harris et al. 1972, No 1, Table 1, p 319)

D. Average 8 peridotite xenoliths in basalt (Green 1968b, No 2, Table 1, p 841)

E. Garnet lherzolite xenolith in kimberlite recalculated anhydrous (Ito and Kennedy 1967, No 2, Table 1, p 521)

F. Pyrolite (Ringwood 1969, Table 1, p 7)

V. Estimate of trace element concentrations in "average" ultramafic rock (Goles 1967, Table II. 1, p 354)

W. Estimate of trace element concentrations in the mantle (Harris 1972, Table 1, p 282)

X. Rb and Sr concentrations in peridotite, Bulfontein (Griffin and Murthy 1968, Table 3, p 499)

Y. Average U concentrations in the mantle (Varne 1970, p 50)

Z. Average U concentration in the upper mantle (Gast 1968, p 25)

in other provinces (Engel and Engel 1964 p 1330 , Engel, Fisher and Engel 1965 p 606, Green and Ringwood 1967 p 174). C'Hara (1968a p 117) suggests that varying degrees of partial melting of peridotite and subsequent fractionation of the resulting parental magmas in the mantle yields overall enrichment factors between 5 and 33 for the incompatable elements. Comparison of the concentrations of TiO_2, K_2O, P_2O_5, Rb, Sr and Zr in primitive melts of the three Carlingford magma series exhibited in Figures 9.1 and 9.2 with those of assumed mantle compositions in Table 9.1 shows that enrichment by the order of a factor of 10 in the primitive alkali basalts, and by factors of 5 to 8 in the primitive tholeiitic basalts and high alumina basalts, could have given rise to the recorded concentrations of the components in question in those rocks. Thus the concentrations of the incompatable elements in primitive Carlingford melts are consistant with such liquids having been produced by limited partial melting of mantle material and/or crystal fractionation in the mantle, and can be explained without recourse to such mechanisms as "wall rock reaction" (Green and Ringwood 1967 p 174). Subsequent enrichment of incompatable elements in derivative magmas can be explained by low pressure fractionation of olivine and plagioclase (Chapters 4,5 and 6).

Engel, Engel and Havens (1965) consider low potash "oceanic" tholeiites to be parental to alkali basalt magmas by processes of crystal liquid fractionation, alkali transfer and crustal contamination, at low pressure; it has been shown that tholeiitic liquids cannot give rise to alkali basalt derivatives at low pressure by crystal liquid fractionation alone (Green and Ringwood 1964 p 1276). Green

and Ringwood (1967) Green, Green and Ringwood (1967) and Green (1969a, b, 1970) consider olivine tholeiite to be parental to alkali basalts, high alumina basalts and quartz tholeiites by fractionation at different pressures. O'Hara and Yoder (1967) and O'Hara (1968a) consider picritic olivine tholeiite to be the direct product of mantle partial melting at pressures in excess of 20 Kb. Macdonald (1968) adopts the argument of Green and Ringwood (1967), and suggests that olivine tholeiite magmas are parental to the Hawaiian magma series both alkaline and tholeiitic. Both Ridley (1971a, p 264,b) and Holland and Brown (1972) consider olivine basalts to be parental to the Hebridean magma series. Thus there is a considerable body of opinion based on experimental evidence in favour of regarding olivine tholeiite or olivine basalt to be parental to other magma stems, and the use of such a model has been extended to the British Tertiary Province.

Comparison of the average composition of primitive tholeiitic magmas at Carlingford as depicted in Figure 9.1 and of actual analyses in Table 9.2., with the average composition of 282 oceanic tholeiites reported by Manson (1968 Table IV p 223) - see Table 9.2-demonstrates the underlying similarities between Carlingford "transition dolerites" and tholeiitic oceanic basalts. Using the bulk distribution coefficients of Gast (1968) and adopting the relatively low figures for K_2O concentrations in the mantle proposed by Hurley (1968a, b), Jamieson and Clarke predict that primary magmas as defined by Jamieson (1966) i.e. direct products of mantle partial melting, should have K_2O concentrations ir the range 0.06% to 0.22% (1970 p 192). Some of the

TABLE 9.2

Composition of tholeiitic basalts from Carlingford and the oceans

A. Major Elements

	53	54	84	664	A	B	C	D	E	F	G
SiO_2	47.54	46.71	46.01	47.16	49.3	49.4	49.34	49.20	49.21	49.41	50.65
TiO_2	1.12	1.20	1.17	0.90	2.4	2.5	1.49	2.03	1.39	1.12	1.36
Al_2O_3	14.98	14.57	14.65	15.22	14.6	13.9	17.04	16.09	15.81	16.31	17.09
Fe_2O_3	3.59	2.29	2.52	3.07	3.2	3.0	1.99	2.72	2.21	1.80	1.66
FeO	7.38	7.35	8.10	7.88	8.5	8.5	6.82	7.77	7.19	6.92	7.00
MnO	0.14	0.17	0.16	0.17	0.17	0.2	0.17	0.18	0.16	0.16	0.15
MgO	7.24	10.58	10.39	7.71	7.4	8.4	7.19	6.44	8.53	8.00	7.49
CaO	11.25	10.54	11.74	12.15	10.6	10.3	11.72	10.46	11.14	11.85	11.52
Na_2O	2.16	1.28	1.18	1.38	2.2	2.2	2.73	3.01	2.71	2.61	2.82
K_2O	0.24	0.18	0.37	0.10	0.53	0.4	0.16	0.14	0.26	0.06	0.18
P_2O_5	0.14	0.11	0.11	0.10	0.26	0.3	0.16	0.70		0.15	0.08
S	0.28	0.94	0.15	0.11							
H_2O+	)	)	)	)	0.79		0.69	0.95		1.33	
	)3.10	)2.92	)2.37	)							
H_2O^-	)	)	)	)2.83			0.58	0.23		0.55	
CO_2	0.45	0.38	0.53	)							
	99.61	99.22	99.45	98.83				99.92		100.27	

TABLE 9.2

Composition of tholeiitic basalts from Carlingford and the oceans

	B Trace Elements *						
	53	54	84	664	C	D	X
Sc	76	78	67	73	61	44	29
V	154	180	144	133	292	280	183
Cr	218	696	630	119	297	220	218
Co	76	92	91	86	32	32	43
Ni	175	535	394	163	97	87	130
Cu	177	205	152	168	77	66	75
Ga	17	15	15	16	17	20	17
Rb	10	9	13	12	10	10	18
Sr	330	189	235	145	130	190	350
Y	22	20	20	19	43	60	32
Zr	78	87	84	61	95	160	91
Ba	478	311	342	372	14	5	215

53, 54, 84, 664 Current investigation.

A. Average 282 oceanic tholeiites (Manson 1968, p 223)

B. Average 200 tholeiites, Hawaii (Macdonald 1968, Table 8, p 503)

C. Average 10 oceanic tholeiites (Engel et al.1965, Table 2, p 721)

D. Tholeiitic basalt, Atlantic (Engel et al.1965, No AD2, Table I, p 720)

E. Average 33 oceanic tholeiites (Melson, et al.1968, A, Table 4, p 5930)

F. Tholeiitic basalt (Melson et al. 1968, No. 3, Table 4, p 5930)

G. Average 4 oceanic tholeiites, Indian Ocean (Engel, Fisher and Engel, 1965, No. I, Table 3, p 608)

X. Average value for olivine tholeiite (Prinz 1968, No. 2, Table II, p 278)

* CONCENTRATIONS IN PPM.

Carlingford transition dolerites (olivine tholeiites) have low K_2O values of that order, see Table 9.2, and as noted above primitive trace element concentrations, they are thus suitable for consideration as primitive parental magmas. The composition of primitive magmas in all three series is consistant with the interpretation that the alkali basalts and high alumina basalts as well as the quartz dolerites and craignurites have been derived from such an olivine tholeiite parent, though the possibility that the parental melts of each series have been derived independently by partial melting of peridotite of similar composition at different depths as predicted by Kuno et al (1957) and Yoder and Tilley (1962), or by varying degrees of partial melting at similar depths as suggested by O'Hara (1968a), are not ruled out. It is with reference to the O'Hara model (1968 ps 98-9) that the relative order of appearence of the various magma types at Carlingford has particular significance; in that scheme alkali basalt liquids are produced by a smaller degree of partial melting than tholeiitic magmas and it would thus seem likely that they would appear earlier in the cyclic sequence than the latter. That is contrary to the observed order of events which suggests that the alkali basalts are a residue rather than a precursor of tholeiitic activity. Further in the O'Hara scheme high alumina basalts are produced by partial melting under a limited range of temperature pressure conditions and would thus be unlikely to appear regularly in the intrusive sequence unless those specific conditions pertained, during each cycle, at the same stage during its development.

The primitive and the transitional nature of the parental magmas

in both the alkali basalt and tholeiitic basalt -craignurite series renders it unnecessary, in the case of such rocks in the British Tertiary Province, to recourse to varying degrees of incorporation of hydrous phases such as phlogopite during partial melting to account for their chemistry, as has been suggested by some authors (Flower 1971, Allen et al. 1972). Thus the weight of evidence is in favour of olivine tholeiite being parental to the other basaltic magmas stems at Carlingford.

It must be pointed out that O'Hara (1968a, b) questions the likelihood of "primary magmas" as such appearing at high levels considering that all must suffer some fractionation of olivine during their ascent. It is not suggested herein that the transition dolerites are primary magmas in the strict sense, but rather that they are primitive and approach most closely parental melts in terms of composition.

The origin of parental alkali basalt magmas

Having assumed that primitive alkali basalt melts at Carlingford were derived from parental olivine tholeiite magmas by crystal fractionation at depth, consideration of the composition of those derivative liquids indicates that the process involved enrichment of Na_2O, K_2O, TiO_2 and P_2O_5 by a factor of 1.5 - 2, and of iron by a smaller proportion, but that otherwise the major element chemistry and normative mineralogy was not markedly altered (Figure 9.1). This cannot be the result of olivine fractionation which leads to SiO_2 enrichment.

A number of authors have suggested that excess separation of

aluminous orthopyroxene from olivine tholeiite would produce alkali basalts melts (Powers 1935, Macdonald 1949, Tilley 1950), O'Hara argues however that such a mechanism is implausable unless the parent magma descends to greater depths after its formation (1968a p 93). Here to some extent the experimental results are in conflict, Green and Ringwood, have shown that orthopyroxene will separate in abundance from olivine tholeiite melts in the 12 to 20 Kb pressure range (1964, 1967). Such a mechanism would lead to a marked degree of silica undersaturation if it proceededto more than a limited extent; the Carlingford alkaline suite like other Hebridean suites is only mildly alkaline and transitional in nature, few members are nepheline normative while several are quartz normative, though that may in part be the result of alteration (Chapter 4). Moreover separation of orthopyroxene leads to depletion in MgO, concentrations of MgO are not much lower in the primitive alkali basalts than they are in primitive tholeiitic basalts at Carlingford (Fig. 9.1). Green (1970) assumes the composition of the primary olivine tholeiite produced by partial melting to be considerably more picritic in composition than the Carlingford transition dolerites and it is indeed probable that the latter have suffered some olivine fractionation since they were first generated i.e. they are not true primary melts (see above), however such olivine fractionation cannot have been extensive as many retain primitive K_2O concentrations and are not enriched in SiO_2. Thus extensive separation of orthopyroxene from parental olivine tholeiite melts of the type represented by the "transition dolerites" of Carlingford cannot have taken place during the generation of the alkali

basalts observed in the complex.

Cohen, Ito and Kennedy (1967) identified calcic clinopyroxene separating early and in some abundance from an olivine tholeiite melt at pressures in the range 12 to 20 Kb. CaO concentrations in the primitive alkali basalts are generally slightly lower than in the primitive olivine tholeiite of the complex (Fig. 9.1) and it is thus possible that separation of calcic clinopyroxene may have taken place during their derivation from the latter. Separation of aluminous calcic clinopyroxene would lead to enrichment in alkalies, P_2O_5 and iron, however the degree of CaO depletion exhibited by the primitive alkali basalts relative to the transition dolerites severely limits the permissable extent of such a process and it is doubtful that it could have given rise to the enrichment factors observed.

The separation of orthopyroxene and clinopyroxene together at 10 to 20 Kb, the "pyroxenite stage" of Yoder and Tilley (1962) and Tilley and Yoder (1964), or of olivine, orthopyroxene and clinopyroxene (O'Hara 1968a p 102) might yield the observed enrichment factors, if in the appropriate proportions. Such a process is still subject to the limitations set by the concentrations of MgO, CaO and SiO_2 in both parent and daughter melts, though not so severely as the separation of orthopyroxene or clinopyroxene in isolation.

O'Hara and Yoder (1967) have discussed the possibility that eclogite fractionation (separation of clinopyroxene and garnet), at pressures in excess of 20 Kb, could yield alkalic derivatives from olivine tholeiite parent melts. O'Hara argues that up to 50% of such a melt may crystallize as ecologite thus doubling enrichment factors of

TiO_2 and P_2O_5 without greatly modifying the normative mineralogy of the product, indeed without it becoming nepheline normative (1968a p 118). It has been suggested by some workers that separation of ec logite compositions may lead to Na_2O depletion (Harris and Rowell 1960; Hough in discussion of O'Hara 1972), O'Hara has pointed out however that ec logite with high solidus temperatures might have Na_2O values of less than 1% (O'Hara 1972 in discussion). Separation of such low soda ec logite from primitive olivine tholeiite melts could have led to the observed enrichment of Na_2O in the alkali basalts of Carlingford.

In summary orthopyroxene, clinopyroxene and pyroxenite fractionation at intermediate pressures or ec logite fractionation at high pressure are all mechanisms by which alkali basalt magmas may plausably be derived from olivine tholeiite melts. In the case of the Carlingford alkaline suite however, it is doubtful that either orthopyroxene or clinopyroxene fractionation could have given rise to the degree of enrichment of Na_2O, TiO_2 and P_2O_5 observed in even the most primitive alkali basalts, without modifying the concentrations of MgO or CaO to an unacceptable extent. A similar conclusion may be drawn in the case of alkaline magmas elsewhere in the Hebridean Province (see compositions quoted by Bailey et al. 1924, Tilley and Muir 1962), contrary to the hypothesis of Holland and Brown (1972), unless the primary olivine tholeiite magmas involved in the process were considerably richer in MgO than seems to have been the case. The extensive orthopyroxene fractionation required to give rise to the observed enrichment factors of Na_2O, TiO_2 and P_2O_5 in alkali basalts both at

Carlingford and in the Hebrides in general, would have generated strongly nepheline normative melts (Green and Ringwood 1967), which is contrary to the transitional nature of the rocks in question (above and Ridley 1971a, Holland and Brown 1972). Pyroxenite fractionation may have been capable of producing the observed enrichment factors in the daughter melts without modifying their composition too drastically, but eclogite fractionation appears to be the most acceptable processes in the generation of the Carlingford alkali basalts provided the eclogite separated had a low Na_2O concentration. It is possible of course that liquids which were derived by eclogite fractionation at pressures in excess of 20 Kb may have subsequently undergone limited pyroxene fractionation in the intermediate pressure regime, the strongly nepheline normative mugearite 748 is a case in question. The problem with such considerations of processes at depth is that Hebridean suites are dominated by low pressure fractionation trends, thus there is no direct evidence to support the operation of any of these processes at Carlingford. Phenocrysts or xenocrysts of orthopyroxene are absent and those phenocrysts and xenocrysts of clinopyroxene present can be attributed to crystallization at low pressure. Eclogite, pyroxenite or peridotite nodules have not been identified in any of the Carlingford rocks and moreover the ultimate prcduct of eclogite fractionation, kimberlites and carbonatites (O'Hara and Yoder 1967), are absent in the British Tertiary Province.

The generation of high alumina basalt magmas

Green and Ringwood (1967), and Green, Green and Ringwood (1967)

have shown experimentally that olivine and alumina poor pyroxene fractionate from olivine tholeiite melts at pressures of the order of 9 Kb giving rise to high alumina basalt derivatives. They conclude that high alumina basalts are thus generated by fractional crystallization at depths of 15 to 35 km. O'Hara (1968a) also considers that high alumina basalts may be generated in the low-moderate pressure regime but suggests that they may be formed at greater depths too, in each case under a limited range of temperature pressure conditions by direct partial melting. The petrochemistry and time relations of the Carlingford high alumina basalts are consistant with the Green and Ringwood model which is adopted herein.

Role of PO_2 in Carlingford fractionation trends

It has been suggested in Chapters 4, 5 and 6 that variation in the partial pressure of oxygen to some extent modified and controlled the fractionation paths adopted by Carlingford magmas during differentiation. Experimental studies of the behaviour of the synthetic system MgO-FeO-Fe_2O_3-SiO_2 undergoing fractional crystallization under varying partial pressures of oxygen, have been described by Muan and Osborn (1956) and Osborn (1959, 1962). Addition of CaO or $CaAl_2Si_2O_8$ to these synthetic systems such that they more nearly approach natural basaltic melts in composition has been shown not to markedly modify the results obtained (Presnall 1963, 1966; Osborn and Roeder 1960; Roeder and Osborn 1966) which may thus be considered applicable to consideration of the behaviour of such melts. It has been suggested by Osborn (1959, 1962), on the basis of these studies, that two

distinct fractionation paths are available to basaltic magmas; fractionation with constant composition leading to decreasing PO_2 with advancing crystallization of the melt, giving rise to the progressive iron enrichment of the latter, the "Fenner Trend"; and fractionation under constant PO_2 giving rise to SiO_2 enrichment of derivative liquids with advancing differentiation - the "Bowen Trend" (Hamilton and Anderson 1968 p 465). Thus iron enrichment in basaltic melts is the result of fractionation under relatively low PO_2 as at Skaergaard (Wager and Brown 1968 p 242), and silica enrichment fractionation under more oxidising conditions (Walker 1953 p 57). Carmichael and Nicholls (1967 p 4674) point out that the two fractionation paths are produced by the operation of a single controlling factor, PO_2, and are thus extreme members of a spectrum of fractionation trends.

The majority of rocks in the alkali basalt series at Carlingford have a much higher Fe_2O_3:FeO ratio than basalts attributed to the tholeiitic basalt-craignurite series and high alumina basalt series, a phenomenon which may in part be due to alteration (see Chapter 4), however other alkali basalts have similar high oxidation states which in the case of those occurring on oceanic islands have been interpreted to be the result of fractionation under more oxidising conditions than those which pertained during the crystallization of oceanic tholeiites (Engel et al 1965 p 726). Furthermore alkali basalts of the early stages of fractionation of the alkali basalt series (D.I. less than 40) show hardly any iron enrichment at Carlingford (see Chapter 4) and may therefore considered to have fractionated under higher PO_2

conditions than the tholeiitic basalt-craignurite series or high alumina basalt series. The marked increase of modal concentrations of titanomagnetite in members of the alkali basalt series in the middle stages of fractionation (D.I. values approaching 40) is attributed to an increase in oxygen fugacityat that stage, a similar argument having been put forward by Ridley in the case of the Small Isles basalts (1971a p 261). It has been shown in preceding sections that alkali basalt magmas were generated at depth within the mantle by fractionation from olivine tholeiite melts, and that they subsequently underwent low pressure fractionation at higher levels. O'Hara (1968a) considers that magmas undergo continous fractionation of at least olivine during their ascent, and it is possible that the early stages of fractionation of the alkali basalts of Carlingford took place as the parent magmas rose from their source through the upper mantle and lower crust, more advanced fractionation subsequently having taken place at low pressures in the upper crust where the PO_2 of the melts had risen.

The coincidence of high volatile concentrations with high oxidation states in the rocks of the alkali basalt series is perhaps significant, though it is partly the result of alteration. The separation of anhydrous phases such as orthopyroxene, clinopyroxene and garnet from an olivine tholeiite melt would by necessity increase the proportions of volatiles in the derivative magma, H_2O and CO_2 in the parent peridotite already having been concentrated in the primary magma during partial melting (O'Hara and Yoder 1967 p 110). Alkali basalt magmas derived by ec logite fractionation must be more

volatile rich than associated tholeiites such that the high H_2O and CO_2 concentrations in the Carlingford alkali basalt magmas may in part be primary. Hamilton and Anderson discuss the possible role of disassociation of water in controlling the PO_2 of fractionating basaltic melts (1968 ps 470-475), and conclude with reference to such a process that "there is every reason to suppose, however, that the diffusion of hydrogen away from basalt could be an important factor in determining the PO_2 of the basalt". It is tentatively proposed that the PO_2 of hydrous alkali basalt magmas formed at a depth beneath the Carlingford complex increased markedly during low pressure fractionation in the crust, as a result of disassociation of water accompanied by H_2 diffusion, and that the presence of higher concentrations of volatiles ensured that the alkali basalt magmas were at all times more oxidised than associated tholeiites. It must be pointed out that the concentration of alkalies in alkali basalt magmas may also control their oxidation state to some extent (Carmichael and Nicholls 1967 ps 4666-4667).

Both the tholeiitic basalt-craignurite series and the high alumina basalt series show iron enrichment in the early stages of fractionation, (see Chapters 5 and 6), the phenomenon is most markedly expressed by the high iron transition dolerites. However iron enrichment did not proceed in rocks of either suite with D.I. values in excess of 40, thus the extreme iron enrichment of the Skaergaard complex (Wager and Deer 1939) was not achieved, and though more reduced and less hydrous than the alkali basalt magmas, tholeiitic and high alumina basalt magmas did not fractionate at Carlingford under such low PO_2

conditions as those of Skaergaard. Le Bas comes to a similar conclusion with reference to the Carlingford layered gabbro (Le Bas 1960 p 186).

No attempt has been made during the current investigation, to use the composition of opaque oxide phases as a geothermometer in the manner suggested by Buddington, Fahey and Vlisidis (1955); or, except in qualitate terms, as an oxygen barometer as discussed by Buddington and Lindsley (1964), Carmichael (1967) and Carmichael and Nicholls (1967), which in view of the reservations expressed by the later authors (p 4684) are left for future investigation.

The occurrence of spinel xenocrysts

The absence of spinel in Carlingford rocks derived by low pressure fractionation e.g. the quartz dolerites, craignurites and tristanites, and their occurrence only as corroded "xenocrysts" in alkali picrites and tholeiitic basalts suggests that they were formed by crystallization at depths in excess of 20km. The latter interpretation is supported by the experiments of Green and Ringwood (1967) during which spinel crystallized at pressures of the order of 9 Kb in alkali basalt melts, and 13 Kb in olivine tholeiite and olivine basalt melts but did not appear at lower pressures. The occurrence of spinel "xenocrysts" in intrusive rocks indicates that the latter must have originated at depth and that they have not suffered extensive fractionation since they incorporated the spinel. The former conclusion is in keeping with the depth of origin inferred for the rock types in which they occur.

Conclusions

On the basis of the arguments set out in the preceding sections it is proposed that magma genesis in the case of the Carlingford Complex and of the British Tertiary Province in general, which it represents, followed the scheme summarized in Figure 9.3. That is that olivine tholeiite magmas were generated by partial melting at depths in excess of 60Km, (enrichment factors of incompatable elements of the order of 5:1 in some of the transition dolerites indicating that up to 20% partial melting of mantle peridotite took place during this process). Up to 50% ecologite fractionation at pressures in excess of 20 Kb increased enrichment of Na_2O, TiO_2, K_2O and P_2O_5 by a factor of 2 and generated parental alkali basalt melts, while fractionation of olivine and perhaps alumina poor pyroxene from the primitive olivine tholeiite parent at depths of the order of 20 to 30km, gave rise to high alumina basalt magmas. Fractionation of olivine and plagioclase in varying proportions at depths of the order of 30km or less from the parental alkali basalt, high alumina basalt and olivine tholeiite magmas, gave rise to the alkali basalt-trachy-basalt-tristanite series, the high alumina basalt series, and tholeiitic basalt - craignurite series respectively (the later series fractionated at depths not exceeding 15 km), while fractionation of olivine at depths of 30km or more, or perhaps in some cases of orthopyroxene, at pressures in the 10 to 20 Kb range, gave rise to the alkali basalt-mugearite-benmorite series.

The Carlingford time sequence discussed above is thus a sequence in terms of increasing depth of fractionation of the magmas involved,

Figure 9.3

Diagrammatic summary of the petrogenetic processes whereby magmas of the tholeiitic basalt - craignurite series, high alumina basalt series, and alkali basalt series occurring at Carlingford were derived from parental peridotite in the mantle, during the early Tertiary.

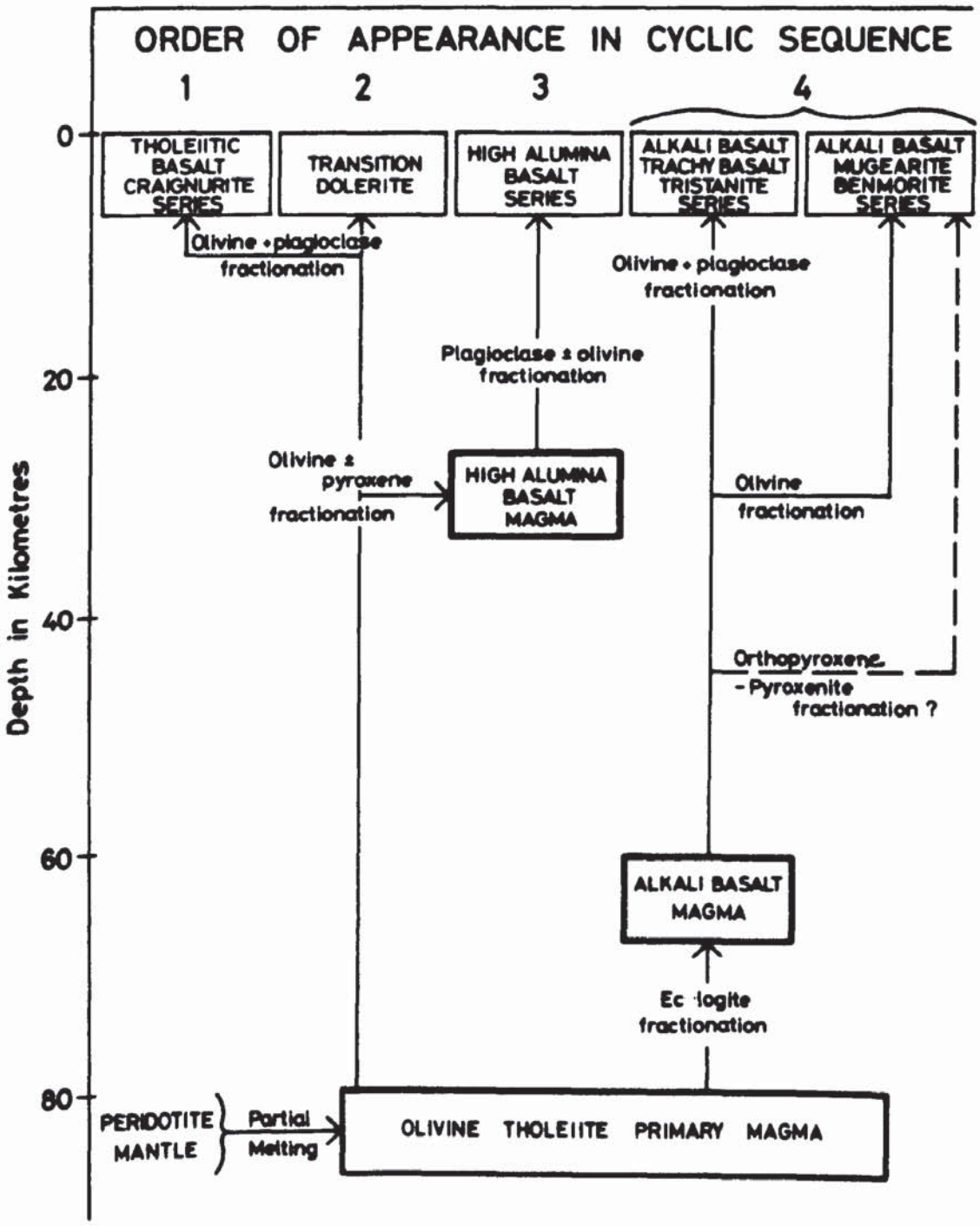

the craignurites, quartz dolerites and tholeiitic dolerites fractionated at high levels, and the largely unfractionated transition dolerites , appearing early in the sequence; the high alumina basalts with parental magmas generated by fractionation at moderate depth appearing next, and the alkali basalts derived by ec logite fractionation at depths of the order of 60km being intruded last in each cycle.

The alkali basalt stem having been rendered more volatile rich by extensive fractionation of anhydrous phases at depth underwent differentiation under higher PO_2 conditions than the other magmas series at high levels due to the disassociation of water. Extremely low PO_2 conditions did not pertain during the evolution of any of the Carlingford magmas at low pressure such that the extreme Skaergaard iron enrichment trend was never attained.

Summary

1. The three Carlingford basaltic magma series are dominated by fractionation of olivine and plagioclase at relatively low pressures.
2. The Carlingford cyclic sequence may be considered to be: craignurite - quartz dolerite; tholeiitic dolerite - transition dolerite; high alumina basalt; alkali basalt.
3. On the basis of petrochemistry and time relations it is considered that olivine tholeiite magmas were parental to both alkali basalt and high alumina basalt derivatives by fractionation of ecologite, and olivine and alumina poor pyroxene ,respectively.
4. Low pressure fractionation of members of the alkali basalt series

took place under relatively high PO_2 conditions perhaps as a result of disassociation of H_2O. Though fractionated under somewhat lower PO_2 conditions neither the high alumina basalt series or tholeiitic basalt-craignurite series exhibit marked iron enrichment.

5. Spinel "xenocrysts" only occur in rocks which have not undergone excessive fractionation at pressures of less than 9 Kb or there - abouts.

6. Magma genesis in the Carlingford Complex followed the paths outlined in Figure 9.3.

CHAPTER 10

A SUMMARY AND SYNTHESIS OF THE MAGMATIC PROCESSES WHICH TOOK PLACE IN THE CARLINGFORD COMPLEX.

Abstract

Conclusions based on structural and petrochemical investigations of igneous rocks in the Carlingford Complex are synthesised into a unified model of magmatic activity therein during the early Tertiary.

Introduction

The structural development of the Carlingford Complex has been discussed (Chapter 2) and the petrography, petrochemistry and petrochronology of its constituent intrusions described (Chapters 1,3,4, 5,6,7 and 8). Consideration of processes of magma genesis in the light of that work has enabled the erection of a petrogenetic scheme to explain the derivation of the various basaltic and derivative rock types present and the origin of the three parental magma stems (Chapter 9). The aim of this concluding chapter is to synthesise these previous discussions into a brief account of the development of the complex.

Processes within the Mantle

Generation of parental olivine tholeiite magmas took place generally beneath the British Tertiary Province at the beginning of the Tertiary, about 70 m.y. b.p., or soon afterwards. The lithospheric movements which gave rise to the North Atlantic were taking place at about that time (Scrutton et al. 1971) and it is tempting to infer that the two events were causally related. Consideration of the

possible diapiric upward movement of peridotite and accompanying partial melt products in the upper mantle discussed by Green and Ringwood (1967) and O'Hara (1972), or of convective systems and thermal plumes within the mantle (Elder 1966, Morgan 1971, Gass 1972, Middlemost 1973, Schilling 1973a,b) is beyond the scope of the present investigation.

Once generated the parental magmas rose upwards through the overlying upper mantle and crust along north west-south east trending lines of weakness perhaps initiated by shearing of the lithosphere during Atlantic opening. The existance of such lines of weakness is indicated by the primitive nature of some of the rock types intruded at Carlingford, which further suggests that mechanisms such as mantle stoping leading to 'zone refining' (Harris 1957, 1972) or 'wall rock reaction' (Green and Ringwood 1967) did not take place. One such line of weakness ran beneath the Carlingford complex on the Carlingford-Slieve Gullion axis.

Olivine tholeiite rising to crustal levels in the Carlingford Peninsula fractionated to give rise to the high alumina basalt and tholeiitic basalt-craignurite series (see below). Ec logite fractionation of the primary olivine tholeiite melts at depths in excess of 60 km., and thus within the upper mantle, gave rise to alkali basalt magmas which rose to the crust in the wake of unfractionated olivine tholeiite. The primitive alkali basalt melts may, in some cases, have undergone subsequent orthopyroxene or pyroxenite fractionation in the intermediate pressure regime at depths in the range 30 to 60 km.

Magmas arrived at crustal levels in the sequence olivine tholeiite,

alkali basalt. That sequence was initiated at least three times at Carlingford.

Processes within the crust

Olivine tholeiite magmas arriving at the base of the crust either fractionated at depths of the order of 30 km. to give parental high alumina basalt magmas; or, continued to higher levels and with fractionation at depths of less than 15 km., gave rise to the tholeiitic basalt-craignurite series, extreme fractionation generated rhyolite (see Chapter 8). Fractionation of olivine and plagioclase in varying proportions from parental alkali basalt and high alumina basalt magmas at similar low pressures within the crust generated the alkali basalt series and high alumina basalt series respectively. The order of intrusion of magmas at high crustal levels thus followed the sequence:

1. Craignurite - quartz dolerite (fractionation of olivine tholeiite at pressures of less than 5 Kb).
2. Tholeiitic dolerite - transition dolerite (largely unfractionated parental olivine tholeiite).
3. High alumina basalt (parental melts derived by fractionation at depths of about 30km).
4. Alkali basalt (generated by fractionation within the upper mantle).

There was some overlap between 1 and 2 in this sequence.

Each injection of olivine tholeiite magma within the upper crust took the form of a ridge, elongated north west - south east, from which north west - south east dyke swarms emerged, some of the dykes perhaps

feeding lava flows in Cycle I. Subsequently magmatic activity became concentrated about diapiric cupolas rising directly beneath the complex and which fed cone-sheet and radial dyke swarms.

Bodies of high alumina basalt magma were emplaced at high levels in the crust as diapiric cupolas rather than ridges, perhaps a function of their having been generated at relatively shallow depths. The first of these domes penetrated to the base of the Tertiary lava pile and fed the layered gabbro lopolith, a subsequent injection of high alumina basalt fed an extensive cone-sheet swarm (episodes IIe and IIIa).

The form of bodies of alkali basalt magma rising from the mantle was again that of elongate ridges running north west - south east which is the trend of the extensive alkali basalt dyke swarm episode IIb. In the case of the alkali basalt magmas of Cycle III, the ridge rose to a dome like culmination enabling the development of an orthogonal - tangential dyke swarm in response to north-south tension across the complex at the time of its emplacement (Chapter 2).

The explosive volcanism of which there is evidence at Carlingford may have been the product of diapiric bodies of volatile rich magma rising from parent ridges. Other plugs may have reached the surface and acted as lava feeders.

The injection of high alumina basalt magmas during the closing stages of Cycles I and II, as redefined in Chapter 9, was accompanied by crustal melting which gave rise to acid magmas in each case. The diapir feeding the layered gabbro lopolith melted argillaceous Silurian sediments leading to the development of the "early granophyre"

and biotite felsite melts. When the latter incorporated basic material during partial melting or by subsequent assimilation, lamprophyre magmas were produced. The biotite felsites and lamprophyres were emplaced as dykes, cone-sheets and complementary cone-sheets - episode IIa (Chapters 2 and 8), while quartz feldspar porphyries derived by fractionation of the biotite felsites were injected as dykes with a radial distribution. The Carlingford granophyre magma was generated by partial melting of Silurian sediments (Le Bas 1967) accompanying the injection of the cone-sheets of episodes IIe and IIIa; it was emplaced diapirically as a dome.

The generation of basaltic magmas beneath the Carlingford complex and the majority of igneous activity throughout the British Tertiary Province as a whole came to an end soon after 58 m.y. b.p. (Evans, Fitch and Miller 1973). Subsequent movement along the planes of weakness which had acted as pathways for rising magmas, led to the development of major tear faults which now traverse both Carlingford and Slieve Gullion.

Conclusion

In conclusion it must be stated that magmatic activity within the Carlingford Complex during the Tertiary was dominated by basaltic magmatism. Intermediate and acid rock types were produced by fractionation of parental basalts at low pressures, though acid magmas in their own right were generated by crustal melting resulting from the emplacement of those basalts. Mixing of acid and basic magmas or the contamination of basic melts by crustal material did

not play an important role in processes of magma genesis at Carlingford, and can be demonstrated only in the case of isolated intrusive bodies (see Chapter 7).

The dominant process in basalt fractionation in the British Tertiary Province was the separation at low pressures of olivine and plagioclase in varying proportions from the parent magmas produced at greater depth. Separation of olivine and plagioclase from alkali basalt and olivine tholeiite parents led to the generation of potash rich derivatures, trachy basalts and tristanites, and craignurites respectively; the craignurites and related types have not previously been defined as such. During these fractionation processes volatiles and PO_2 played a significant role in controlling the petrogenetic pathways adopted.

APPENDIX I

Analytical Techniques

Introduction

During the current investigation 262 analyses of Carlingford rocks were carried out by the author using XRF techniques in the Department of Geology, Nottingham University, several analyses were duplicated. A further 58 samples have been analysed at Reading by Dr. A. Parker using XRF including 29 duplicates of samples analysed at Nottingham. One rock, 748, a mugearite, has also been analysed by XRF at Durham. Some 17 samples have been analysed by wet methods in the Department of Geology, Reading University, by analysts S.A. Malik and D.A. Bungard, 3 of which had previously been analysed wet by the author at Leicester. A number of CO_2 determinations were made by the same workers on rocks analysed by XRF only. FeO determinations used in conjunction with XRF analyses were carried out by the author in the Department of Geology, Leicester University.

Analyses determined by XRF at Nottingham are listed in Appendices II, III, IV, V, (major elements) and X, XI, XII, XIII (trace elements). The Reading XRF results are listed in Appendix XV. XRF and wet determinations are listed for comparison in Appendix XIV there is reasonable agreement between results determined by different workers and techniques, though generally the Reading wet analyses agree more closely with those of Nottingham XRF. The Nottingham XRF results are used almost exclusively in preceeding chapters in order to achieve internal consistency.

Electron microprobe analyses were carried out in the Department of Geology, Leicester University, by R.L. Wilson.

Sample Preparation

Samples were prepared for analysis by the author at Leicester. Approximately 100 gms of sample was selected and trimmed to remove weathered surfaces, it was then broken into chips using a rock splitter and the chips crushed using a jaw crusher. The crushed sample

was passed through an agate Tema Mill for one minute and the resulting powder stored, without sieving, in glass bottles.

XRF Nottingham

a) Major Elements

Major elements with the exception of Na_2O were determined using the technique described by Harvey et al (1972) based on the method of Norrish and Hutton (1969) and involving the use of fusion beads.

b) Trace Elements

Trace element values and Na_2O were determined using powder pellet preparations by methods modified after Leake et al (1968) and described by Taylor (1972). The powder pellets were prepared by thoroughly mixing 6 gm of rock powder with 1 gm of phenolformaldehyde resin in a plastic phial containing plastic balls. The balls were removed and the mixture placed in a $1\frac{1}{4}$ in. die between two tungsten carbide platens and pressed under vacuum, at 30 tons p.s.i. for 5 minutes using a hydraulic press. The resulting pellet was baked for 35 minutes at $80^{\circ}C.$, and then stored between tissues in a cardboard pill box.

c) Standards

Major elements were run against a machine standard, Nottingham internal standard 1005 (an Andesite) prepared by D.M. Taylor and calibrated using international U.S.G.S. standards. Na_2O and trace elements, with the exception of S, V, Sc and Sn, were run against the powder pellet standard 1005 prepared by D.M. Taylor; S, V, Sc and Sn were compared with the Nottingham internal standard 1000, a gabbro prepared by Dr. D. Field. In each case the standards were calibrated against "spiked" preparations of the same material.

While analysing batches of samples U.S.G.S. standards were run and the results compared with recommended values (Flanagan 1972) observed and recommended values for AGV1, BCR1 and GSP1 are listed for

Table A1.1a U.S.G.S. Standards Major Elements

	AGV1		BCR1		GSP1	
	Obs	Rec	Obs	Rec	Obs	Rec
SiO_2	58.83	59.00	53.86	54.50	67.16	67.38
TiO_2	1.08	1.04	2.26	2.20	0.69	0.66
Al_2O_3	16.95	17.25	12.92	13.61	15.09	15.25
Fe_2O_3	4.50	4.51	3.70	3.68	1.80	1.77
FeO	2.00	2.05	8.82	8.80	2.30	2.31
MnO	0.09	0.10	0.20	0.18	0.10	0.04
MgO	1.54	1.53	3.54	3.46	0.94	0.96
CaO	4.97	4.90	7.03	6.92	2.03	2.02
Na_2O	4.33	4.26	3.39	3.27	2.77	2.80
K_2O	2.89	2.89	1.71	1.70	5.47	5.53
P_2O_5	0.46	0.49	0.35	0.36	0.28	0.28
CO	1.34	0.06	1.70	0.03	0.79	0.15
H_2O+		0.81		0.77		0.57
H_2O-		0.16		0.80		0.12
Total	98.98	99.91	99.48	100.28	99.42	99.84
Fe_2O_3 Total	6.72	6.76	13.50	13.40	4.36	4.33

Obs = Observed

Rec = Recommended

Table A1.1b U.S.G.S. Standards Trace Elements

	AGV1		BCR1		GSP1	
	Obs	Rec	Obs	Rec	Obs	Rec
S	133	<10	711	392	470	162
Sc	13	13	27	33	9	7
V	119	125	279	399	74	53
Cr	13	12	25	18	17	13
Co	10	14	22	38	6	6
Ni	21	19	11	16	14	13
Cu	103	60	49	18	79	33
Zn	83	84	116	120	100	98
Ga	20	21	21	20	21	22
Ge	1	1	2	2	1	1
Rb	64	67	45	47	239	254
Sr	647	657	323	330	230	233
Y	12	21	28	37	13	30
Zr	282	225	228	190	620	500
Sn	5	4	7	3	8	6
Ba	1557	1208	990	675	1582	1300
Ce	76	63	63	54	323	394
Pb	69	35	44	18	118	51
Th	8	6	49	6	133	104
U	3	2	1	2	3	2

Obs = Observed

Rec = Recommended

comparison in Table A1.1 showing reasonable agreement between the results. V values were determined by the semiquantitative method described by Cooper (1971), but the results were found to be consistantly high by a factor of 4, all values have thus been reduced accordingly but cannot be considered more than semiquantitative. Pb values are also excessive and recent investigations have shown that they should be reduced by a factor of about 2.0 (D. Field private communication), the values quoted have not been corrected as this information was not available at the time of writing, however, though they may not be taken as absolute, they are internally consistent.

d) Operating Conditions

Operating conditions for the Philips P.W.1212 automatic X-ray fluorescence spectrometer used during this investigation are listed in Harvey et al (1972 Table 2) for major element determinations. Trace element determinations were carried out under the instrument conditions set out in Table A1.2.

XRF Reading

XRF analyses at Reading were carried out by Dr. A. Parker using Philips P.W.1410 X-ray fluorescence spectrometer following standard procedures described by Parker (1973).

Wet Analysis Leicester

a) Complete analyses of three rocks including FeO determinations were carried out by the author using the method of Shapiro and Brannock (1952, 1956) as modified and improved by Riley (1958).

b) FeO values for use with XRF analyses were determined by Wilsons method (Wilson 1955, 1960) as described in modified form by Jeffery (1970). Some difficulty was encountered in achieving complete solution of ore during this process and in some cases the FeO value quoted may be considered low as a result. FeO values for international standards determined during the analysis of the Carlingford rocks by the same method give reasonable agreement with recommended values (see Table A1.1).

Table A1.2 Operating Conditions for Trace Element Determination using Philips P.W.1212 Automatic Xray Fluorescence Spectrometer

Element	S	Sc	V	Cr	Co	Ni	Cu	Zn	Ga	Ge	Rb
Standard	1000	1000	1000	1005	1005	1005	1005	1005	1005	1005	1005
Tube	Cr	Cr	Cr	W	W	W	Mo	Mo	Mo	Mo	Mo
Line	Ka	Ka	Ka	Ka	Ka	Ka	Ka	Ka	Ka	Ka	Ka
2θ peak	75.85	97.69	79.95	69.30	77.79	71.19	65.56	60.60	56.18	52.34	37.99
2θ Bk. 1	73.35	94.65	82.12	67.38	77.26	72.07	66.56	61.25	55.32	53.32	36.95
2θ Bk. 2	-	-	-	-	78.51	-	-	-	57.46	-	38.82
Factor	-	-	-	-	0.57	-	-	-	0.60	-	0.44
Kv.	60	60	60	60	60	60	100	100	100	100	100
MA.	24	24	24	32	32	32	20	20	20	20	20
Collimator	Course	Fine	Fine	Fine	Fine	Fine	Fine	Fine	Fine	Fine	Fine
Crystal	P.E.	LiF_{200}	LiF_{200}	LiF_{200}	LiF_{220}	LiF_{220}	LiF_{220}	LiF_{220}	LiF_{220}	LiF_{200}	LiF_{220}
Counter	F	F	F	F	S	F+S	F+S	F+S	F+S	F+S	S
Time (Secs.)	20	20	20	20	20	20	20	20	20	20	20
Slope	1627.58	76.38	-	122.85	186.90	172.08	188.47	181.69	125.53	104.68	130.11
Detection Limit	30	4	-	2	10	3	2	4	2	4	1

Table A1.2 Cont.

Element	Sr	Y	Zr	Sn	Ba	Ce	Pb	Th	U
Standard	1005	1005	1005	1000	1005	1005	1005	1005	1005
Tube	Mo	Mo	W	Cr	W	W	Mo	Mo	Mo
Line	Kα	Kα	Kα	Lα	Lβ	Lβ	Lβ	Lβ	Lα
2θ peak	35.87	33.93	31.97	126.73	128.85	111.70	40.34	39.23	37.31
2θ Bk. 1	34.97	32.93	30.97	127.91	131.85	109.70	39.85	38.82	36.95
2θ Bk. 2	36.95	34.97	32.97	-	-	-	40.81	39.85	38.82
Factor	0.54	0.51	0.50	-	-	-	0.48	0.57	0.78
Kv.	100	100	100	60	50	60	100	100	100
MA.	20	20	16	24	40	32	20	20	20
Collimator	Fine	Fine	Fine	Fine	Course	Course	Fine	Fine	Fine
Crystal	LiF_{220}	LiF_{220}	LiF_{220}	LiF_{200}	LiF_{220}	LiF_{220}	LiF_{220}	LiF_{220}	LiF_{220}
Counter	S	S	S	F	F+S	F+S	F	F	F
Time (Secs.)	20	20	20	20	20	20	20	20	20
Slope	998.50	132.32	454.57	49.20	1872.78	435.29	221.60	158.77	152.20
Detection Limit	1	3	5	3	9	8	7	4	3

P.E. Penta erythriol crystal
F: Gas flow proportional counter
S: Scintillation counter
Vacuum path throughout

Wet Analysis Reading

a) Sample splitting

Powder samples were homogenised in a Turbula shaker-mixer, Type T2A (Bachofen Limited, Switzerland), for 20-30 minutes. Sample aliquots were selected for analysis by 'coning and quartering' except in cases where the quantity of powder was small.

b) Sample decomposition

i. A 100 mg. sample of rock powder (undried) was fused with NaOH in a nickel crucible, acidified with 2.5N sulphuric acid and made to 1 litre with deionised water. Silica and alumina were determined on aliquots of this solution (Riley 1958).

ii. A 500 mg. sample of rock powder (undried) was digested with hydrofluoric and perchloric acids in a platinum crucible. Silicon, as SiF_4, was removed by evaporation. The residue was taken up in perchloric acid and the solution made to 500 ml with deionised water (Riley, 1958). Total iron as Fe_2O_3, TiO_2, MnO, P_2O_5, CaO, MgO, Na_2O and K_2O were determined using aliquots of this solution.

c) Analytical methods

i. SiO_2 - Colorimetric. A silicomolybdate complex was reduced to molybdenum blue using 1-amino-2-naphthol-4-sulphuric acid (Shapiro and Brannock, 1962).

ii. Al_2O_3 - Colorimetric. An orange complex was formed with eriochrome cyanine R. Ascorbic acid was used to suppress iron interference (Hill 1959).

iii. Total iron as Fe_2O_3 - Colorimetric. 2,2-dipyridyl method (Riley, 1958).

iv. TiO_2 - Colorimetric. Tiron (1,2 dihydroxybenzene, 3,5 - disulphonic acid, disodium salt) method. (Rigg and Wagenbauer, 1961).

v. MnO - Colorimetric. Permanganate method with ammonium persulphate as oxidant and silver nitrate as catalyst (Shapiro and Brannock, 1956).

Table A1.3 Operating Conditions for A.E.I. SEM 2 Microprobe

Element	Si	Ti	Al	Fe	Mn	Mg	Ca	K
Line	Kα	Kα	Kα	Kα	Kα	Kα	Kα	Kα
Reflection Order	1st	1st	1st	1st	1st	1st	3rd	3rd
Crystal	Mica	LiF	Mica	LiF	LiF	Mica	Mica	Mica
KV	20	20	20	20	20	20	20	20
Aperture Current (10^{-7} Amps)	100	100	100	100	100	100	100	100
Pulse Height Analysis								
a) Pulse height	30v	30v	30v	30v	30v	30v	30v	30v
b) Threshold	20v	20v	20v	20v	20v	20v	20v	20v
c) Window	20v	20v	20v	20v	20v	20v	20v	20v
Angle	20.92°θ	43.07°θ	24.70°θ	28.76°θ	31.49°θ	29.81θ°	30.33°θ	34.23°θ
Counter	Flow	Flow	Flow	Flow	Flow	Flow	Flow	Flow
Standard	Mel.	P.Met.	Mel.	Mel.	P.Met.	Mel.	Mel.	K.Tant.

Standard Abbreviations: Mel = Synthetic Melilite glass (see Table A1.4);
P. Met = Pure Metal (Ti Metals Research 99.9% pure,
Mn Koch-Light 99.995% pure);
K. Tant = Potassium Tantalate (Imperial College)

vi. P_2O_5 - Colorimetric. Molybdi-vanado-phosphoric acid complex method. (Shapiro and Brannock, 1956).

vii. CaO and MgO - Atomic absorption spectroscopy. Lanthanum chloride solution was added to sample and standard solutions to suppress interference from aluminium and phosphorous.

viii. Na_2O and K_2O - Atomic absorption spectroscopy. Excess alkali was added to eliminate ionisation interferences.

ix. FeO - Titrimetric, using Wilson's method (Wilson, 1955, 1960), as described in modified form by Jeffery (1970). Difficulties encountered with magnetite digestion (see above).

x. H_2O^+ - Gravimetric. Modified Penfield method.

xi. H_2O- - Gravimetric. Determined on separate sample aliquots by drying at 110°C for 3 hrs.

xii. CO_2 - Gravimetric. Groves' (1951) method was modified to include cupric orthophosphate as an absorbant to remove H_2S evolved by sulphide phases and otherwise included with CO_2.

Microprobe Analysis

Microprobe analyses of Plagioclase, Pyroxene, Olivine and Ore in a number of Carlingford rocks were carried out at Leicester by R.L. Wilson on an A.E.I. machine. Na_2O values in these phases were below the limits of detection, Na_2O concentrations in plagioclases were calculated (see text). The results in general are considered only semiquantitive, olivine showed considerable alteration in the samples and only partial analyses of ore phases were carried out. A planned programme of scans to investigate zoning in plagioclase and pyroxene was shelved due to pressure of time and machine failure.

The rock specimens were cut and mounted on microscope slides, ground down to 30 microns thickness and polished using diamond paste. Prior to analysis the polished sections were coated with gold.

Probe operating conditions and standards are listed in Table A1.3, composition of the Melilite glass standard used for some elements is set out in Table A1.4.

Table A1.4

Composition of Melilite Glass Standard

(Prepared by J.A. Dixon, Dept. Geology, Leicester University)

SiO_2	37.4
Al_2O_3	9.4
Fe_2O_3	9.3
MgO	9.3
CaO	34.6
Total	100.0

APPENDIX II

Composition of Carlingford Alkaline Rocks

a. Analysed composition.

b. Analysis reclaculated to 100% without Volatiles and where $Fe_2O_3 = \%TiO_2 + 1.5\%$ if greater than that value.

c. Fe_2O_3 Total $= \frac{FeO}{0.9} + Fe_2O_3$

Specimen No.	36		61		64		66		96		102	
	a	b	a	b	a	b	a	b	a	b	a	b
SiO_2	45.09	47.53	44.39	47.90	45.12	47.30	45.14	49.05	45.49	48.34	45.36	48.52
TiO_2	2.09	2.20	3.02	3.26	1.53	1.60	2.31	2.51	1.23	1.31	2.28	2.44
Al_2O_3	15.06	15.87	14.36	15.5	17.00	17.82	16.40	17.82	16.90	17.96	15.02	16.07
Fe_2O_3	7.90	3.70	7.16	4.76	4.04	3.10	7.07	4.01	4.28	2.81	6.41	3.94
FeO	6.87	11.41	6.81	10.02	8.46	9.90	5.19	8.95	7.20	9.23	5.94	9.03
MnO	0.19	0.20	0.20	0.21	0.20	0.21	0.15	0.16	0.19	0.20	0.25	0.27
MgO	5.64	5.94	6.09	6.57	6.36	6.67	4.92	5.35	6.42	6.82	5.03	5.38
CaO	9.19	9.69	7.91	8.54	9.79	10.26	7.26	7.89	9.63	10.23	10.16	10.87
Na_2O	2.20	2.32	1.85	2.00	1.90	1.99	2.30	2.50	2.09	2.22	1.70	1.81
K_2O	0.36	0.38	0.74	0.80	0.50	0.52	1.24	1.35	0.30	0.32	0.78	0.83
P_2O_5	0.38	0.40	0.35	0.37	0.31	0.32	0.34	0.37	0.27	0.29	0.61	0.65
CO_2	0.39	-	0.31	-	4.09	-	1.52	-	0.47	-	N.D.	-
S	0.33	0.35	0.07	0.08	0.28	0.29	0.03	0.04	0.25	0.27	0.17	0.18
H_2O^+	3.78	-	5.98	-	-	-	5.65	-	3.62	-	5.80	-
Total	99.47	99.99	99.17	100.01	99.58	99.98	99.49	100.0	98.34	100.0	99.51	99.99
Fe_2O_3 Total	15.53	16.38	14.73	15.89	13.44	14.09	12.84	13.95	12.28	13.06	13.01	13.97

Specimen No.	107		115		119		135		140		143	
	a	b	a	b	a	b	a	b	a	b	a	b
SiO_2	45.40	47.47	45.65	48.22	46.26	48.19	46.82	47.40	46.10	47.67	46.82	48.50
TiO_2	1.15	1.20	1.13	1.19	1.14	1.19	1.84	1.86	2.02	2.09	2.05	2.12
Al_2O_3	17.03	17.81	16.94	17.89	17.20	17.92	16.55	16.75	13.96	14.43	13.95	14.45
Fe_2O_3	5.24	2.70	4.88	2.69	3.38	2.69	1.96	1.98	4.94	3.59	4.70	3.62
FeO	6.54	9.35	6.79	9.40	8.16	9.26	10.92	11.05	8.97	10.65	9.03	10.49
MnO	0.20	0.21	0.18	0.19	0.18	0.19	0.24	0.24	0.21	0.22	0.17	0.18
MgO	6.85	7.16	6.98	7.37	7.04	7.33	7.67	7.76	5.92	6.12	5.64	5.84
CaO	10.33	10.80	9.79	10.34	9.95	10.36	9.79	9.91	11.30	11.68	11.03	11.43
Na_2O	2.45	2.56	1.88	1.99	2.07	2.16	1.89	1.91	2.49	2.57	2.25	2.33
K_2O	0.20	0.21	0.24	0.25	0.26	0.27	0.31	0.31	0.41	0.42	0.40	0.41
P_2O_5	N.D.	-	0.62	-	0.26	0.27	0.21	0.21	0.27	0.28	0.27	0.25
CO_2	0.25	0.26	0.19	0.20	0.89	-	0.22	-	N.D.	-	1.88	-
S	0.25	0.26	0.19	0.20	0.17	0.18	0.58	0.59	0.28	0.29	0.34	0.35
H_2O^+	3.88	-	3.79	-	2.30	-	0.75	-	2.89	-	0.56	-
Total	99.77	99.99	99.32	100.0	99.26	100.01	99.75	99.97	99.76	100.01	100.1	100.0
Fe_2O_3 Total	12.51	13.08	12.42	13.13	12.45	12.97	14.09	14.26	14.91	15.42	14.74	15.28

Specimen No.	191		379		435		745		748		783	
	a	b	a	b	a	b	a	b	a	b	a	b
SiO_2	50.34	52.92	47.29	48.91	48.24	49.95	52.77	57.85	44.41	49.24	42.07	47.05
TiO_2	1.86	1.96	2.10	2.17	1.60	1.66	1.67	1.83	1.74	1.93	1.64	1.83
Al_2O_3	5.37	16.16	14.93	15.44	15.56	16.11	16.81	18.42	14.19	15.73	15.01	16.79
Fe_2O_3	4.60	3.46	1.38	1.43	4.12	3.16	3.96	3.33	3.60	3.43	1.67	1.87
FeO	6.42	8.00	10.26	10.61	8.67	9.98	1.84	2.93	8.73	10.18	10.74	12.01
MnO	0.19	0.20	0.23	0.24	0.23	0.24	0.10	0.11	0.37	0.41	0.17	0.19
MgO	3.73	3.92	5.96	6.16	5.41	5.60	0.68	0.75	1.98	2.20	7.51	8.40
CaO	7.03	7.39	10.68	11.05	9.53	9.87	6.31	6.92	7.75	8.59	8.29	9.27
Na_2O	2.62	2.75	2.36	2.44	2.46	2.54	5.34	5.85	5.74	6.36	1.78	1.99
K_2O	2.28	2.40	0.49	0.51	0.60	0.62	1.16	1.27	0.68	0.75	0.20	0.22
P_2O_5	0.69	0.73	0.37	0.38	0.19	0.20	0.64	0.71	0.82	0.91	0.19	0.21
CO_2	0.22	-	N.D.	-	N.D.	-	4.67	-	9.69	-	9.11	-
S	0.12	0.13	0.63	0.65	0.06	0.06	0.02	0.03	0.22	0.24	0.15	0.17
H_2O^+	2.77	-	3.71	-	2.79	-	3.89	-	0.57	-	1.39	-
Total	98.24	100.02	100.39	99.99	99.46	99.99	99.86	100.0	100.49	99.97	99.92	100.0
Fe_2O_3 Total	11.73	12.35	12.78	13.22	13.75	14.25	6.00	6.59	13.30	14.74	13.60	15.2

Specimen No.	799		802		807		831		840		1175	
	a	b	a	b	a	b	a	b	a	b	a	b
SiO_2	42.05	47.51	45.74	50.73	40.05	46.02	50.03	51.52	45.79	48.40	41.53	47.50
TiO_2	1.30	1.47	2.03	2.25	1.34	1.54	1.50	1.54	2.20	2.33	1.48	1.70
Al_2O_3	13.70	15.48	16.09	17.84	14.06	16.15	15.93	16.40	14.26	15.07	13.29	15.20
Fe_2O_3	2.48	2.80	0.13	0.14	0.0	0.0	3.31	3.04	3.43	3.62	0.53	0.60
FeO	7.94	8.97	9.21	10.21	11.46	12.86	8.52	9.11	10.41	11.00	9.79	11.19
MnO	0.15	0.17	0.10	0.11	0.14	0.16	0.14	0.14	0.22	0.23	0.16	0.18
MgO	9.03	10.20	6.26	6.94	7.11	8.17	5.45	5.61	5.79	6.12	9.04	10.33
CaO	9.48	10.71	5.78	6.41	10.14	11.65	8.85	9.11	8.53	9.02	8.46	9.67
Na_2O	1.81	2.04	3.49	3.87	1.82	2.09	1.66	1.71	2.51	2.65	2.00	2.29
K_2O	0.25	0.28	0.64	0.71	0.36	0.42	0.64	0.66	1.12	1.18	0.62	0.70
P_2O_5	0.19	0.21	0.47	0.52	0.18	0.20	0.21	0.22	0.34	0.36	0.34	0.39
CO_2	8.27	-	4.84	-	10.30	-	N.D.	-	0.17	-	9.52	-
S	0.13	0.15	0.23	0.26	0.66	0.74	0.90	0.93	0.01	0.01	0.21	0.23
H_2O^+	2.52	-	4.46	-	0.48	-	3.30	-	3.19	-	1.21	-
Total	99.27	99.99	99.47	99.99	98.1	100.1	100.44	99.99	97.97	99.99	98.18	99.98
Fe_2O_3 Total	11.30	12.77	10.36	11.48	12.73	14.29	12.78	13.16	15.00	15.84	11.41	13.03

Specimen No.	1319		1320		1351		1382		9556	
	a	b	a	b	a	b	a	b	a	b
SiO_2	45.50	48.21	50.69	55.24	48.06	49.36	54.15	55.14	42.88	47.47
TiO_2	1.74	1.84	1.82	1.98	1.54	1.58	1.39	1.42	1.83	2.03
Al_2O_3	14.83	15.71	15.38	16.76	16.14	16.58	16.95	17.26	15.18	16.80
Fe_2O_3	6.28	3.34	4.71	3.48	3.82	3.08	1.94	1.98	0.00	0.00
FeO	7.89	11.35	3.78	5.61	9.27	10.28	9.39	9.56	12.60	13.95
MnO	0.29	0.31	0.28	0.31	0.24	0.25	0.23	0.23	0.22	0.24
MgO	5.03	5.33	1.37	1.49	5.66	5.81	1.97	2.01	5.26	5.82
CaO	10.27	10.88	6.99	7.62	9.51	9.78	5.17	5.26	9.52	10.54
Na_2O	1.83	1.94	3.12	3.40	1.98	2.03	3.19	3.25	2.35	2.60
K_2O	0.48	0.51	2.76	3.01	0.78	0.80	2.89	2.94	0.30	0.33
P_2O_5	0.32	0.34	0.90	0.98	0.24	0.25	0.65	0.66	0.20	0.22
CO_2	1.74	-	3.31	-	N.D.	-	2.35	-	8.34	-
S	0.22	0.23	0.11	0.12	0.21	0.29	0.28	0.29	N.D.	-
H_2O^+	2.41	-	3.43	-	1.91	-	0.15	-	0.52	-
Total	98.83	99.99	98.65	100.0	99.36	100.02	100.70	100.0	99.20	100.0
Fe_2O_3 Total	15.05	15.95	8.91	9.71	13.83	14.50	12.37	12.60	14.00	15.50

APPENDIX III

Composition of Carlingford High Alumina Basalts

$$Fe_2O_3 \text{ Total} = \frac{FeO}{0.9} + Fe_2O_3$$

Sample Number	40	45	74	114	124	137	141	190	269	273	399
SiO_2	49.21	49.20	46.82	47.43	49.54	48.76	49.57	49.30	52.04	48.49	48.52
TiO_2	0.70	1.08	0.86	0.94	0.70	0.87	1.33	0.80	0.75	0.95	0.60
Al_2O_3	22.27	17.22	17.97	17.41	22.55	18.61	17.14	21.04	19.66	18.30	23.53
Fe_2O_3	0.00	1.40	2.71	2.05	1.27	1.76	3.16	2.44	1.26	2.83	1.64
FeO	6.42	7.92	5.94	7.26	5.28	6.35	6.81	5.25	5.79	6.66	4.65
MnO	0.13	0.13	0.12	0.14	0.12	0.12	0.14	0.12	0.13	0.17	0.08
MgO	3.54	4.93	6.27	6.45	4.43	4.81	5.85	4.02	3.38	5.00	3.62
CaO	12.78	10.78	12.61	12.02	13.66	12.09	11.28	12.92	10.91	11.73	13.64
Na_2O	1.69	1.94	1.76	1.73	2.25	2.37	2.15	2.27	2.34	2.36	1.66
K_2O	1.17	1.17	0.38	0.63	0.34	0.39	0.21	0.38	1.22	0.54	0.50
P_2O_5	0.09	0.12	0.12	0.12	0.09	0.11	0.38	0.09	0.10	0.11	0.08
CO_2	N.D.	N.D.	N.D.	N.D.	N.D.	N.D.	N.D.	N.D.	N.D.	N.D.	N.D.
S	0.27	N.D.	1.22	0.72	0.22	1.76	2.24	0.03	0.04	0.03	0.02
H_2O^+	1.59	2.16	1.85	1.90	1.02	2.46	1.70	0.72	1.45	1.20	0.96
Total	99.86	98.05	98.63	98.80	101.47	100.46	101.96	99.38	99.07	98.37	99.50
Fe_2O_3 Total	7.13	10.20	9.31	10.12	7.14	8.82	10.73	8.27	7.70	10.23	6.81

Sample Number	426	437	442	443	444	450	452	458	563	658	665
SiO_2	47.41	46.90	48.79	54.68	49.80	46.80	47.33	48.70	49.89	50.99	47.77
TiO_2	0.92	0.70	0.82	0.94	0.97	0.66	0.80	0.77	1.13	0.74	1.06
Al_2O_3	18.07	21.66	17.76	19.26	17.49	22.86	20.75	19.25	18.94	18.86	19.97
Fe_2O_3	0.00	0.76	1.13	0.99	0.93	0.77	1.84	1.38	2.18	1.25	1.24
FeO	9.21	6.07	7.92	6.63	7.88	5.64	5.82	6.27	6.90	5.73	8.17
MnO	0.14	0.11	0.15	0.11	0.15	0.08	0.13	0.10	0.15	0.10	0.18
MgO	6.45	4.49	6.01	3.11	5.62	3.71	4.38	5.66	3.55	5.35	7.32
CaO	12.72	13.78	12.07	5.84	11.36	13.99	11.85	10.88	10.72	11.30	9.80
Na_2O	1.87	1.91	1.91	2.48	2.19	1.99	1.57	1.65	2.60	1.48	1.79
K_2O	0.16	0.18	0.37	2.36	0.68	0.24	0.62	0.91	0.82	0.79	0.67
P_2O_5	0.12	0.09	0.08	0.20	0.09	0.07	0.10	0.10	0.17	0.10	0.11
CO_2	1.50	1.38	N.D.	N.D.	N.D.	N.D.	N.D.	N.D.	N.D.	N.D.	N.D.
S	0.82	0.20	0.07	0.05	0.18	0.22	0.32	0.02	0.03	0.05	0.39
H_2O^+	1.50	1.38	1.54	2.88	1.94	1.35	2.96	2.87	1.38	2.30	1.53
Total	99.39	98.27	98.62	99.53	99.28	98.38	98.47	98.54	98.46	99.04	100.00
Fe_2O_3 Total	10.23	7.50	9.93	8.36	9.69	7.04	8.31	8.35	9.85	7.62	10.32

Sample Number	718	1001	1119	1162	1166	1352	1387	1399
SiO_2	47.86	48.75	48.56	48.99	53.25	48.47	49.07	49.32
TiO_2	0.83	0.65	0.82	0.82	0.79	1.00	0.90	1.28
Al_2O_3	17.29	22.05	18.59	18.74	17.38	16,63	20.60	18.35
Fe_2O_3	1.08	1.44	1.73	2.32	1.73	0.71	1.10	2.37
FeO	7.56	4.83	6.97	7.07	6.81	9.42	6.48	7.89
MnO	0.13	0.07	0.11	0.18	0.13	0.15	0.13	0.19
MgO	6.91	4.00	5.82	4.52	3.63	6.32	3.70	3.62
CaO	12.83	13.64	12.72	11.97	9.72	11.31	12.26	10.84
Na_2O	1.46	2.16	1.83	2.03	2.60	1.43	1.71	2.57
K_2O	0.71	0.45	0.36	0.55	1.28	0.99	1.15	0.82
P_2O_5	0.10	0.10	0.10	0.09	0.08	0.10	0.10	0.17
CO_2	N.D.	N.D.	N.D.	0.70	N.D.	N.D.	N.D.	N.D.
S	0.03	0.05	0.02	0.01	0.01	0.48	0.15	0.70
H_2O^+	2.57	1.18	1.85	1.45	2.12	2.67	2.17	1.14
Total	99.36	99.37	99.48	99.44	99.53	99.68	99.52	99.26
Fe_2O_3 Total	9.48	6.81	9.47	10.18	9.30	11.18	8.30	11.14

APPENDIX IV

Composition of Carlingford Tholeiitic Basalts and Craignurites

$$Fe_2O_3 \text{ Total} = \frac{FeO}{0.9} + Fe_2O_3$$

* Recalculated to 100% volatile free (loss on ignition greater than 5%).

Sample Number	3	5	6	9	11	18	22	23	24	25	27
SiO_2	48.59	65.69	52.69	49.80	51.80	52.03	59.55	66.60	52.28	69.15	54.83
TiO_2	2.20	0.89	1.60	1.24	1.64	1.71	1.10	0.68	2.58	0.55	1.98
Al_2O_3	13.19	13.22	14.46	13.93	13.30	12.87	14.10	13.26	12.45	13.18	12.85
Fe_2O_3	3.27	2.31	3.31	1.97	2.89	3.73	1.97	3.18	4.44	2.87	2.96
FeO	10.53	5.01	9.45	9.93	11.28	11.31	7.11	2.88	11.18	2.37	10.02
MnO	0.20	0.11	0.18	0.13	0.24	0.25	0.10	0.02	0.21	0.08	0.24
MgO	3.90	1.01	3.54	6.06	4.79	3.99	2.02	0.75	2.66	0.36	2.12
CaO	8.07	2.95	8.22	10.80	9.12	8.59	4.23	1.76	6.46	1.65	6.30
Na_2O	2.26	3.36	2.80	2.70	2.57	2.23	3.09	3.14	2.41	3.46	2.06
K_2O	0.72	4.02	1.30	1.11	0.89	0.83	3.86	5.48	2.64	5.31	2.81
P_2O_5	0.33	0.19	0.23	0.15	0.20	0.21	0.26	0.16	0.30	0.11	0.25
CO_2	N.D.	0.61	N.D.	N.D.	N.D.	N.D.	N.D.	N.D.	N.D.	N.D.	N.D.
S	2.89	1.52	0.77	0.35	0.40	0.20	0.01	0.01	0.03	0.01	0.04
$H_2O \pm$	4.34	0.30	0.68	0.43	0.38	1.15	1.96	1.90	1.40	0.69	2.64
Total	100.49	101.19	99.23	98.60	99.50	99.10	99.43	99.82	99.04	99.79	99.10
Fe_2O_3 Total	14.97	7.88	13.82	13.01	15.42	16.30	9.87	6.38	16.86	5.50	14.09

Sample Number	28	30	33	35	37	38	46*	53	54	58	59
SiO_2	49.09	53.81	52.78	57.14	54.36	49.33	62.32	47.54	46.71	61.9	53.53
TiO_2	0.94	2.06	1.66	1.20	2.38	1.32	1.22	1.12	1.20	0.99	1.65
Al_2O_3	14.63	12.84	13.44	13.33	13.21	14.37	14.86	14.98	14.57	13.94	13.62
Fe_2O_3	2.13	2.43	2.84	0.67	2.48	2.72	0.54	3.59	2.29	0.13	1.56
FeO	9.03	10.95	9.09	8.85	11.19	9.24	7.09	7.38	7.35	6.30	10.08
MnO	0.18	0.22	0.14	0.17	0.21	0.21	0.09	0.14	0.17	0.08	0.20
MgO	7.00	2.24	4.31	2.98	2.79	6.06	2.38	7.24	10.58	1.87	3.33
CaO	11.61	6.69	8.83	5.45	6.27	10.54	5.19	11.25	10.54	4.2	6.84
Na_2O	2.20	2.08	1.92	2.48	2.65	2.17	2.94	2.16	1.28	3.13	2.54
K_2O	0.90	2.04	1.66	2.97	2.77	0.74	2.98	0.24	0.18	2.63	2.52
P_2O_5	0.11	0.25	0.25	0.17	0.36	0.16	0.32	0.14	0.11	0.23	0.29
CO_2	N.D.	1.72	N.D.	N.D.	N.D.	0.63	N.D.	0.45	0.38	N.D.	N.D.
S	0.05	0.04	0.15	0.22	0.26	0.19	0.08	0.28	0.94	0.11	0.15
H_2O^+	1.74	1.65	2.53	2.48	0.28	0.96	0.0	3.10	2.92	4.1	1.93
Total	99.61	99.02	99.60	98.11	99.31	98.64	100.01	99.61	99.22	99.61	98.24
Fe_2O_3 Total	12.17	14.60	12.94	10.50	14.91	12.99	8.42	11.80	10.46	7.13	12.76

Sample Number	63*	67	68	71	72	73	75	76	78	80	84
SiO_2	54.54	47.97	50.87	49.26	50.73	51.40	53.65	44.78	50.45	50.97	46.01
TiO_2	2.21	2.47	1.39	1.93	1.13	2.14	2.36	1.23	1.55	1.57	1.17
Al_2O_3	13.50	13.37	15.95	13.28	14.54	12.87	14.09	14.63	13.98	13.66	14.65
Fe_2O_3	2.18	2.73	0.98	4.82	1.44	3.78	2.17	3.21	3.11	2.81	2.52
FeO	12.15	12.39	9.69	9.63	8.77	10.23	10.86	7.71	10.29	10.23	8.10
MnO	0.22	0.20	0.21	0.24	0.19	0.21	0.25	0.16	0.18	0.22	0.16
MgO	2.83	4.05	4.95	4.42	6.27	3.23	3.17	10.73	5.11	5.06	10.39
CaO	7.09	8.64	9.78	8.32	10.21	7.22	5.37	10.44	9.16	9.24	11.74
Na_2O	2.24	1.88	2.20	1.81	2.15	2.20	2.48	1.45	2.31	2.02	1.18
K_2O	2.54	1.05	1.63	0.96	0.83	1.67	0.90	0.51	0.82	0.95	0.37
P_2O_5	0.37	0.62	0.17	0.27	0.17	0.40	0.55	0.13	0.25	0.24	0.11
CO_2	N.D.	N.D.	N.D.	0.69	1.22	N.D.	N.D.	N.D.	N.D.	N.D.	0.53
S	0.13	0.43	0.16	1.41	0.32	0.53	1.13	0.13	1.20	0.65	0.15
$H_2O^{\pm}$	0.0	3.51	1.30	1.98	0.87	2.19	3.48	3.13	1.94	2.09	2.37
Total	100.0	99.31	99.28	99.02	98.84	98.07	100.46	98.24	100.41	99.71	99.45
Fe_2O_3 Total	15.68	16.5	11.75	15.52	11.19	15.15	14.24	11.77	14.54	14.18	11.52

Sample Number	93	97	99	111	113	122	123	125	127	130	131
SiO_2	61.14	46.06	49.87	48.59	47.49	50.02	52.98	47.45	53.13	49.30	47.26
TiO_2	0.87	2.14	0.79	1.29	1.19	1.19	1.28	0.98	1.75	1.49	2.21
Al_2O_3	13.85	13.59	13.83	14.05	14.76	14.61	14.08	15.26	13.62	13.58	13.11
Fe_2O_3	1.78	4.07	2.52	4.1	2.01	2.31	1.19	2.48	2.50	1.74	4.90
FeO	4.50	10.62	6.96	8.64	8.58	8.17	9.57	8.16	10.14	10.62	10.05
MnO	0.10	0.23	0.11	0.20	0.19	0.18	0.20	0.17	0.21	0.23	0.24
MgO	2.37	5.43	9.26	6.40	7.48	5.99	4.87	7.30	3.65	5.15	4.57
CaO	4.64	10.82	11.72	11.90	11.39	10.85	8.75	12.20	8.04	9.10	9.58
Na_2O	3.14	2.27	1.32	2.32	2.40	2.32	2.34	2.05	2.61	3.06	2.38
K_2O	3.22	0.42	0.87	0.39	0.43	0.79	1.42	0.40	1.63	0.95	0.63
P_2O_5	0.14	0.29	0.12	0.16	0.17	0.17	0.20	0.10	0.31	0.24	0.51
CO_2	2.60	2.05	N.D.	0.28	N.D.	1.13	N.D.	N.D.	0.29	N.D.	N.D.
S	0.66	0.30	0.45	0.32	0.24	0.25	0.10	1.08	0.28	2.65	2.95
H_2O^+	1.37	1.59	2.24	0.67	3.03	0.80	2.45	1.50	1.16	2.37	1.67
Total	100.38	99.49	100.06	99.31	99.36	98.78	99.43	99.17	99.32	100.48	100.06
Fe_2O_3 Total	6.78	15.44	10.25	13.7	11.55	11.39	11.82	11.55	13.77	13.54	16.07

Sample Number	133	142	145	147	151	155	156	158	160	162	166
SiO_2	51.37	48.52	49.46	49.59	61.97	52.96	47.93	56.16	50.84	49.24	55.60
TiO_2	1.91	1.18	1.09	1.06	1.22	1.91	1.71	2.21	0.84	1.74	1.77
Al_2O_3	13.19	16.30	14.58	14.62	13.53	13.59	14.44	13.14	15.47	16.45	13.61
Fe_2O_3	3.41	3.25	1.27	2.18	3.16	3.81	1.60	2.08	2.16	0.64	2.60
FeO	11.00	6.99	9.27	9.36	6.15	9.48	11.28	9.90	6.39	11.64	9.15
MnO	0.24	0.18	0.14	0.20	0.15	0.24	0.19	0.22	0.13	0.19	0.16
MgO	3.80	6.05	7.04	6.38	1.35	3.87	6.37	2.15	7.23	5.54	2.55
CaO	8.16	11.25	12.52	10.55	4.27	7.83	10.62	5.52	10.42	9.08	6.06
Na_2O	2.22	2.12	2.08	2.24	3.32	2.67	2.42	2.99	1.90	2.51	2.55
K_2O	1.45	0.23	0.12	0.98	3.84	1.91	0.62	2.67	1.06	1.17	2.65
P_2O_5	0.32	0.34	0.10	0.12	0.32	0.29	0.27	0.49	0.11	0.26	0.31
CO_2	N.D.	N.D.	N.D.	N.D.	N.D.	N.D.	N.D.	N.D.	N.D.	N.D.	N.D.
S	0.72	1.83	1.30	0.13	0.69	0.87	3.05	1.33	0.15	1.50	0.01
H_2O^+	1.50	1.77	1.34	1.21	0.19	1.83	N.D.	0.41	2.92	0.94	1.36
Total	99.29	100.01	100.31	98.62	100.16	101.26	100.50	99.27	99.62	100.90	98.38
Fe_2O_3 Total	15.63	11.19	11.57	12.58	9.99	14.34	14.13	13.08	9.26	13.58	12.77

Sample Number	173	174	175	176	181	192	235	236	253	292	297
SiO_2	52.80	52.29	54.31	51.80	49.81	48.39	48.08	57.96	46.02	48.99	49.04
TiO_2	1.21	1.22	1.30	1.22	1.51	1.68	1.00	0.78	1.20	1.21	1.22
Al_2O_3	14.56	14.47	13.83	14.49	15.96	13.73	15.89	14.96	14.63	16.08	14.04
Fe_2O_3	1.47	0.93	1.07	0.00	1.13	3.25	1.39	1.98	2.45	2.71	3.54
FeO	9.21	9.60	10.32	10.47	10.75	9.54	8.55	5.73	7.98	7.86	8.34
MnO	0.15	0.20	0.22	0.19	0.20	0.20	0.17	0.14	0.17	0.13	0.19
MgO	5.27	5.25	4.22	5.31	4.25	6.04	7.82	3.31	11.44	6.61	6.57
CaO	9.16	8.82	8.22	9.09	9.95	10.17	11.38	7.18	10.92	12.03	11.64
Na_2O	1.99	2.27	2.37	2.29	2.69	2.37	1.86	2.57	0.96	2.50	2.51
K_2O	1.48	1.39	1.78	1.34	1.14	0.53	0.42	2.87	0.41	0.49	0.51
P_2O_5	0.16	0.17	0.25	0.17	0.22	0.27	0.13	0.11	0.11	0.19	0.16
CO_2	N.D.	N.D.	N.D.	N.D.	N.D.	N.D.	N.D.	0.29	N.D.	N.D.	N.D.
S	0.09	0.14	0.18	0.25	0.08	1.50	0.26	0.03	0.02	0.02	0.34
H_2O^+	1.57	1.45	1.08	1.47	0.99	1.11	1.86	1.56	2.93	N.D.	0.37
Total	99.12	98.20	99.15	98.09	98.68	98.78	98.81	99.47	99.24	98.82	98.47
Fe_2O_3 Total	11.70	11.59	12.54	11.63	13.08	13.85	10.90	8.35	11.32	11.44	12.81

Sample Number	298	300	305	314	330	369	371	400	421	424	425
SiO_2	46.09	49.80	47.96	49.34	51.75	49.84	51.04	47.84	47.22	49.02	47.95
TiO_2	0.87	1.37	1.12	1.45	1.87	1.25	1.73	1.09	0.96	0.97	1.04
Al_2O_3	16.42	14.82	15.43	15.20	12.44	16.10	13.64	14.79	15.91	15.92	15.69
Fe_2O_3	2.18	2.47	2.13	1.76	3.35	2.73	3.25	2.90	1.82	1.43	0.81
FeO	7.95	9.72	9.30	10.41	8.73	8.52	10.85	8.60	8.22	8.52	10.53
MnO	0.17	0.21	0.20	0.21	0.16	0.19	0.23	0.21	0.18	0.18	0.20
MgO	9.23	5.56	7.72	6.45	6.79	5.17	4.43	7.86	8.68	7.33	7.31
CaO	12.11	9.92	11.62	10.36	6.27	10.52	9.07	11.95	11.36	10.90	10.86
Na_2O	1.17	2.99	1.75	1.64	1.95	2.69	2.52	1.60	1.64	1.51	2.37
K_2O	0.44	0.41	0.95	0.52	2.32	0.43	1.14	0.29	0.67	0.93	0.37
P_2O_5	0.09	0.18	0.15	0.21	0.15	0.16	0.27	0.12	0.14	0.14	0.11
CO_2	N.D.	N.D.	N.D.	N.D.	0.05	N.D.	N.D.	N.D.	N.D.	N.D.	N.D.
S	0.02	0.29	0.20	1.16	0.07	0.32	0.19	0.01	0.11	0.21	1.06
H_2O^+	2.52	1.21	0.76	1.58	2.86	1.04	0.79	1.95	2.12	2.38	2.12
Total	99.26	98.95	99.29	100.29	98.76	98.96	99.15	99.21	99.03	99.46	100.42
Fe_2O_3 Total	11.01	13.27	12.46	13.33	13.05	12.20	15.31	12.46	10.95	10.92	12.51

Sample Number	429	438	439	441	445	451	457	461	499	500	536
SiO_2	52.25	49.06	50.61	49.33	50.87	50.26	48.61	51.86	48.17	48.27	50.74
TiO_2	1.01	1.13	1.09	1.01	1.09	1.45	1.67	1.14	1.13	1.37	0.89
Al_2O_3	14.49	14.27	14.43	15.47	14.59	13.66	14.33	14.89	14.07	14.48	13.23
Fe_2O_3	1.61	0.58	0.68	2.74	1.20	3.00	2.50	2.94	2.00	3.54	2.54
FeO	7.81	10.71	9.33	7.92	9.12	9.69	9.87	7.54	9.24	8.61	7.11
MnO	0.14	0.16	0.14	0.14	0.15	0.17	0.18	0.18	0.18	0.21	0.19
MgO	5.93	6.99	6.48	8.02	6.37	5.43	6.44	5.62	7.46	6.54	7.96
CaO	10.24	12.06	10.12	12.41	10.51	9.73	10.95	10.63	11.71	10.63	12.16
Na_2O	2.48	2.21	2.09	1.86	2.09	2.36	1.79	2.14	2.25	2.64	2.10
K_2O	0.67	0.70	1.18	0.24	0.67	1.01	0.68	0.63	0.54	0.25	0.65
P_2O_5	0.16	0.15	0.12	0.16	0.12	0.18	0.27	0.17	0.15	0.19	0.10
CO_2	N.D.	N.D.	N.D.	N.D.	N.D.	N.D.	N.D.	N.D.	N.D.	N.D.	N.D.
S	0.60	0.10	0.04	0.05	0.05	0.18	0.08	1.19	1.32	0.17	0.02
H_2O^+	1.39	0.98	2.18	0.56	1.50	1.83	1.66	1.69	1.32	1.64	1.59
Total	98.78	99.10	98.49	99.91	98.33	98.95	99.03	100.62	99.77	98.54	99.28
Fe_2O_3 Total	10.29	12.48	11.05	11.55	11.33	13.77	13.47	11.32	12.27	13.11	10.44

Sample Number	557	559	562	565	568	589	603	605	619	625	629
SiO_2	50.32	50.30	51.91	51.47	51.96	51.47	48.15	51.98	61.78	52.22	50.06
TiO_2	1.53	1.24	1.53	1.57	1.35	1.60	1.08	1.61	1.14	2.16	1.33
Al_2O_3	13.47	14.39	13.90	13.98	15.00	13.72	16.00	13.90	13.71	12.91	15.22
Fe_2O_3	1.49	1.88	2.33	2.15	1.73	2.57	0.00	0.45	1.35	2.52	1.11
FeO	11.73	9.66	10.26	10.21	9.51	10.29	10.88	12.18	6.00	10.98	10.46
MnO	0.25	0.21	0.24	0.22	0.16	0.24	0.21	0.22	0.10	0.25	0.20
MgO	5.32	5.86	5.18	4.59	4.83	4.82	7.48	4.09	2.11	2.73	5.40
CaO	9.10	10.74	9.70	9.28	10.47	8.82	11.74	8.81	5.22	6.77	9.78
Na_2O	2.88	2.63	2.13	2.37	2.20	2.33	1.41	2.22	2.72	1.86	2.17
K_2O	0.75	0.39	0.99	0.91	0.90	1.44	0.31	1.29	3.14	2.42	0.49
P_2O_5	0.21	0.14	0.20	0.24	0.11	0.23	0.15	0.23	0.30	0.36	0.20
CO_2	N.D.	N.D.	N.D.	N.D.	N.D.	N.D.	N.D.	0.25	N.D.	N.D.	N.D.
S	0.21	0.04	0.15	0.03	0.01	0.24	0.24	0.56	0.72	0.20	0.29
H_2O^+	1.63	1.13	1.24	1.94	0.91	1.34	1.96	1.77	2.01	3.82	2.58
Total	99.09	98.61	99.76	98.96	99.14	99.11	99.61	99.56	100.30	99.20	99.29
Fe_2O_3 Total	14.53	12.61	13.74	13.50	12.30	14.00	12.09	13.99	8.02	14.72	12.74

Sample Number	630*	659	663	664	682	684	719	744	747	759	762
SiO_2	51.08	48.99	50.14	47.16	48.16	48.49	48.26	53.14	48.31	51.81	48.43
TiO_2	1.24	1.15	1.48	0.90	1.09	0.97	1.02	1.99	1.36	1.39	1.00
Al_2O_3	16.06	15.54	13.48	15.22	15.38	15.04	16.08	12.88	13.15	14.79	15.38
Fe_2O_3	1.57	2.36	0.47	3.07	1.76	2.74	2.04	2.55	4.89	0.96	0.57
FeO	9.81	8.55	12.42	7.88	8.61	7.86	8.17	11.10	9.63	10.45	9.95
MnO	0.20	0.17	0.20	0.17	0.17	0.17	0.17	0.25	0.21	0.20	0.17
MgO	6.20	7.28	5.40	7.71	6.69	7.13	7.56	2.81	5.01	4.99	7.06
CaO	10.02	10.64	9.99	12.15	10.83	12.47	11.38	6.61	9.65	9.74	12.29
Na_2O	2.29	1.53	2.07	1.38	1.96	1.85	1.36	2.30	2.17	2.01	1.69
K_2O	1.38	1.22	0.77	0.10	1.16	0.26	0.20	2.47	1.15	1.38	0.36
P_2O_5	0.15	0.13	0.17	0.10	0.15	0.09	0.14	0.38	0.16	0.19	0.10
CO_2	N.D.	N.D.	N.D.	N.D.	N.D.	N.D.	N.D.	N.D.	N.D.	N.D.	N.D.
S	0.01	0.03	1.08	0.11	0.27	1.75	0.02	0.86	0.46	0.17	0.31
$H_2O^{\pm}$	0.0	1.97	1.92	2.83	2.17	1.99	2.13	1.58	1.96	1.06	1.29
Total	100.01	99.56	99.59	98.83	98.40	100.81	98.53	98.92	98.11	99.14	98.60
Fe_2O_3 Total	12.47	11.86	14.27	11.82	11.33	11.48	11.12	14.88	15.60	12.57	11.63

Sample Number	765	766	767	768	769	770	771	772	775	780	827
SiO_2	51.83	52.04	50.01	47.49	46.62	47.17	49.23	47.18	51.87	51.75	50.03
TiO_2	2.19	2.23	2.38	1.10	1.01	1.10	1.24	1.03	2.21	1.94	1.90
Al_2O_3	12.87	12.80	13.14	15.74	15.51	15.09	15.56	15.33	12.92	13.14	13.49
Fe_2O_3	1.92	3.18	2.49	2.32	0.00	2.46	4.03	1.83	2.23	5.19	4.61
FeO	12.06	11.28	11.85	8.91	10.98	8.46	7.44	8.82	12.06	8.61	9.79
MnO	0.21	0.22	0.22	0.18	0.17	0.19	0.20	0.19	0.21	0.20	0.21
MgO	3.47	3.04	3.49	7.21	7.62	7.55	5.86	7.52	3.21	3.57	4.64
CaO	7.67	7.56	6.11	11.29	12.07	12.26	10.33	11.76	7.71	7.78	8.30
Na_2O	2.08	2.30	1.71	1.42	1.56	1.65	2.31	1.32	1.96	2.35	1.92
K_2O	1.73	1.84	2.48	0.59	0.75	0.24	0.59	1.06	1.72	1.86	1.04
P_2O_5	0.43	0.42	0.48	0.13	0.12	0.11	0.15	0.13	0.41	0.36	0.30
CO_2	N.D.	N.D.	N.D.	N.D.	N.D.	1.65	0.97	N.D.	N.D.	N.D.	N.D.
S	0.38	0.37	0.03	0.06	0.59	0.15	0.62	0.08	0.33	0.43	0.70
H_2O^+	1.31	1.78	4.53	2.77	1.89	1.22	0.24	1.82	1.57	2.46	2.40
Total	98.15	99.06	98.92	99.21	98.89	99.35	98.77	98.07	98.41	99.64	99.33
Fe_2O_3 Total	15.32	15.72	15.66	12.22	12.2	11.86	12.30	11.63	15.63	14.76	15.49

Sample Number	830	841	842	850	851	852	856	864	876*	877*	878*
SiO_2	53.82	49.64	52.38	66.29	52.26	50.99	50.23	51.11	53.99	54.31	55.40
TiO_2	1.96	1.62	1.03	0.68	1.63	1.60	1.38	1.55	2.33	2.34	2.35
Al_2O_3	13.37	13.65	14.38	12.99	14.09	15.63	14.09	13.65	15.06	15.30	14.15
Fe_2O_3	3.46	4.16	2.41	1.45	2.00	1.50	3.59	2.38	0.81	1.85	1.55
FeO	9.10	9.09	6.66	3.39	11.43	11.04	8.67	9.96	11.67	11.00	10.87
MnO	0.13	0.18	0.12	0.10	0.29	0.24	0.22	0.20	0.26	0.26	0.27
MgO	2.66	5.01	5.21	0.36	4.16	6.26	6.26	5.24	3.47	3.75	3.20
CaO	6.59	7.46	8.98	2.18	6.91	8.44	10.28	9.76	6.55	6.02	6.72
Na_2O	1.89	1.95	2.02	3.19	2.07	2.40	2.01	2.38	1.78	2.12	2.72
K_2O	2.40	1.06	0.52	4.44	1.73	1.42	0.82	0.89	3.42	2.44	1.94
P_2O_5	0.38	0.21	0.15	0.14	0.21	0.17	0.17	0.21	0.56	0.56	0.77
CO_2	N.D.	N.D.	0.73	N.D.	N.D.	N.D.	0.99	N.D.	N.D.	N.D.	N.D.
S	0.23	1.90	0.61	0.95	0.21	0.23	0.30	0.06	0.10	0.04	0.05
$H_2O^{\pm}$	2.72	3.17	3.44	3.53	2.17	1.77	0.98	1.71	0.0	0.0	0.0
Total	98.71	99.10	98.64	99.69	99.16	101.69	99.99	99.1	100.0	99.99	99.99
Fe_2O_3 Total	13.57	14.26	9.81	5.22	14.7	13.77	13.23	13.45	13.78	14.07	13.63

Sample Number	879	884*	889	891	911A	911B	912	916	944	948	976
SiO_2	55.30	54.27	49.05	56.41	64.56	54.53	62.51	49.19	48.28	54.70	49.79
TiO_2	1.18	2.38	0.93	1.12	0.59	1.47	0.86	1.20	1.08	1.03	2.00
Al_2O_3	13.71	14.53	15.90	14.03	12.45	13.32	12.84	16.17	15.75	15.54	13.21
Fe_2O_3	1.02	1.39	2.11	0.39	2.09	0.00	0.00	2.70	1.80	0.76	4.32
FeO	7.32	11.35	7.13	7.86	3.20	12.09	8.55	7.92	9.33	8.34	10.38
MnO	0.09	0.26	0.15	0.10	0.10	0.26	0.12	0.19	0.18	0.26	0.21
MgO	3.68	3.40	7.14	3.67	0.48	3.13	1.48	5.83	8.41	4.53	4.63
CaO	6.80	7.22	11.13	6.98	2.58	5.44	3.47	11.70	12.12	8.60	7.88
Na_2O	2.04	1.42	1.59	1.97	3.17	2.60	2.93	2.40	1.93	2.21	2.61
K_2O	2.53	3.03	0.93	2.44	4.47	2.50	3.94	0.44	0.52	1.39	1.27
P_2O_5	0.23	0.63	0.15	0.20	0.11	0.23	0.14	0.18	0.13	0.16	0.27
CO_2	N.D.	N.D.	N.D.	N.D.	N.D.	N.D.	N.D.	N.D.	N.D.	N.D.	N.D.
S	0.10	0.12	0.05	0.16	1.01	0.94	0.49	0.06	0.35	0.02	0.02
H_2O^+	4.09	0.0	2.43	4.08	3.19	3.69	2.26	0.27	0.33	2.08	1.83
Total	98.09	100.0	98.69	99.41	98.02	100.20	99.59	98.29	100.21	99.54	98.47
Fe_2O_3 Total	9.15	14.00	10.04	9.12	5.65	13.43	9.50	11.50	12.17	10.03	15.86

Sample Number	980	991	1002	1066	1067	1095	1118	1168	1171	1192	1193
SiO_2	53.20	49.69	48.80	50.44	52.15	50.34	52.00	50.15	51.34	51.34	49.52
TiO_2	1.68	1.30	0.94	1.15	1.97	1.13	1.54	1.34	1.94	1.59	1.40
Al_2O_3	13.74	14.30	15.54	14.03	12.92	14.40	13.88	15.22	12.72	13.67	14.70
Fe_2O_3	2.85	1.41	1.22	3.51	4.14	4.08	0.07	4.59	4.35	0.41	3.32
FeO	9.54	10.41	9.27	9.54	10.20	8.91	12.02	8.19	10.56	12.40	9.99
MnO	0.21	N.D.	0.10	0.23	0.25	0.17	0.16	0.16	0.23	0.25	0.21
MgO	3.61	6.63	7.24	6.07	3.34	5.54	4.68	4.22	3.30	5.00	5.51
CaO	7.97	10.60	11.75	10.49	7.50	10.74	9.69	9.69	7.07	9.41	9.73
Na_2O	3.25	1.78	1.79	2.15	2.92	2.38	1.82	1.92	2.25	1.88	2.15
K_2O	1.35	0.39	1.18	0.86	2.07	0.36	0.83	1.17	1.36	1.27	0.53
P_2O_5	0.27	0.15	0.13	0.15	0.32	0.12	0.19	0.18	0.26	0.19	0.17
CO_2	N.D.	N.D.	N.D.	N.D.	N.D.	N.D.	N.D.	N.D.	N.D.	N.D.	N.D.
S	0.02	0.14	0.10	0.09	0.01	0.01	0.29	0.01	0.15	0.69	0.45
$H_2O^{\pm}$	1.48	1.86	2.75	0.88	1.27	0.98	2.10	1.78	2.92	1.41	1.82
Total	99.17	98.66	100.81	99.59	99.06	99.16	99.27	98.62	98.45	99.51	99.48
Fe_2O_3 Total	13.45	12.98	11.52	14.11	15.47	13.98	13.43	13.69	16.09	14.19	14.42

Sample Number	1197	1234	1255	1289	1293	1303	1317	1318	1341	1390	1392
SiO_2	50.80	50.25	49.62	53.17	47.16	49.46	50.82	68.05	48.20	50.58	54.74
TiO_2	1.53	1.42	1.64	1.65	2.56	1.40	1.95	0.62	1.81	1.44	1.80
Al_2O_3	13.68	13.54	13.00	13.61	12.90	12.90	13.05	12.99	13.51	14.05	13.10
Fe_2O_3	2.07	3.14	3.94	2.91	6.12	2.90	6.41	6.10	2.33	2.60	3.60
FeO	10.68	9.75	11.13	9.72	8.40	11.57	9.09	0.99	11.34	9.72	8.61
MnO	0.25	0.25	0.17	0.16	0.17	0.22	0.24	0.04	0.24	0.23	0.19
MgO	5.33	5.23	5.15	3.20	2.76	4.09	3.30	0.46	5.06	5.46	2.71
CaO	10.08	9.71	9.77	7.47	8.13	8.51	7.32	0.44	10.31	10.27	7.18
Na_2O	2.21	2.21	1.80	1.95	1.40	2.14	2.33	2.48	2.20	2.31	2.04
K_2O	0.84	0.92	1.11	1.77	4.83	1.59	1.92	4.93	1.63	0.99	2.18
P_2O_5	0.17	0.17	0.21	0.38	0.33	0.18	0.24	0.09	0.27	0.16	0.39
CO_2	N.D.	N.D.	N.D.	N.D.	N.D.	N.D.	N.D.	N.D.	N.D.	N.D.	N.D.
S	0.18	0.08	N.D.	0.12	0.02	0.03	0.01	0.01	0.35	0.16	0.19
H_2O^+	1.49	1.78	1.63	3.27	4.64	3.50	2.13	2.02	2.12	1.22	1.91
Total	99.31	98.45	99.17	99.38	99.42	98.49	98.81	99.22	99.37	99.19	98.64
Fe_2O_3 Total	13.94	13.98	16.31	13.71	15.45	15.76	16.51	7.20	14.93	13.40	13.16

Sample Number	1393	1397	1398	1401	1407	9554
SiO_2	50.53	49.50	48.93	52.90	49.53	52.50
TiO_2	1.88	1.92	1.91	1.94	1.65	1.98
Al_2O_3	13.82	13.09	13.17	12.82	15.08	13.05
Fe_2O_3	3.29	5.62	5.63	0.00	5.51	5.00
FeO	9.85	8.67	9.03	13.60	6.54	8.58
MnO	0.23	0.25	0.28	0.24	0.20	0.20
MgO	3.77	4.18	4.23	4.16	3.90	3.49
CaO	8.80	9.25	9.27	7.25	9.04	7.60
Na_2O	1.93	2.28	1.89	2.89	2.00	2.30
K_2O	1.30	1.02	1.06	1.29	1.12	1.87
P_2O_5	0.30	0.26	0.27	0.30	0.26	0.36
CO_2	N.D.	N.D.	N.D.	N.D.	0.40	N.D.
S	0.63	0.57	0.57	1.29	1.51	N.D.
$H_2O^{\pm}$	2.23	2.04	1.97	2.80	1.38	2.31
Total	98.56	98.65	98.21	101.48	98.12	99.24
Fe_2O_3 Total	14.23	15.25	15.67	15.11	12.78	14.53

APPENDIX V

Composition of Miscellaneous Carlingford Rocks

$$Fe_2O_3 \text{ Total} = \frac{FeO}{0.9} + Fe_2O_3$$

Suffixes to sample numbers indicate rock type

B.	Basalt lavas
C.	Carboniferous Limestone
E.	Gabbro
E.G.	Acidified gabbro
F.	Biotite Felsite
F'.	Miscellaneous felsite
G.	Granophyre
L.	Lamprophyre (vogesite, Spessartite)
M.	Minette
Q.	Quartz feldspar porphyry
R.	Rhyolite
S.	Silurian sediment
X.	Gabbro xenolith

Sample Number	1.X.	2.G.	12.X.	13E.G.	15.G.	19.B.	21.B.	29a.G	29b.G	29c.G	31.S.
SiO_2	51.15	69.02	49.83	49.82	70.41	48.09	47.97	67.68	56.78	62.82	57.14
TiO_2	2.46	0.61	0.75	0.91	0.36	1.38	1.73	0.69	1.56	1.01	0.69
Al_2O_3	12.09	13.21	20.99	14.68	13.45	16.52	15.72	13.55	13.14	13.25	10.87
Fe_2O_3	4.11	2.11	2.06	2.19	1.37	4.45	1.89	2.19	3.06	2.51	0.85
FeO	11.67	3.20	6.27	8.49	2.07	7.31	8.46	4.25	8.44	5.57	3.00
MnO	0.22	0.07	0.10	0.15	0.05	0.14	0.15	0.08	0.22	0.14	0.04
MgO	4.11	0.54	3.99	6.70	0.26	8.54	5.88	0.09	1.46	0.87	3.53
CaO	7.96	2.15	11.98	10.96	1.97	9.84	9.37	2.12	4.79	3.05	8.91
Na_2O	3.01	3.90	2.08	2.07	3.02	1.99	2.34	3.10	3.29	2.92	1.89
K_2O	1.46	4.76	0.54	0.85	5.70	0.36	0.95	5.38	5.23	5.10	1.51
P_2O_5	0.27	0.13	0.10	0.11	0.03	0.12	0.33	0.11	0.50	0.21	0.15
S	0.19	0.01	0.22	0.01	0.01	0.01	0.02	0.01	0.01	0.01	0.02
CO_2, $H_2O^{\pm}$	0.02	0.01	0.70	1.26	1.16	0.58	3.59	0.37	0.69	0.62	9.57
Total	98.72	99.72	99.61	98.20	99.86	99.33	98.40	99.77	99.32	98.21	98.17
Fe_2O_3 Total	17.08	5.67	9.03	11.62	3.67	12.57	11.29	6.91	12.44	8.70	4.18

Sample Number	32.M.	34.X.	373.X	396.E	593.F	636.E	746.C	839.F	859.R	885.F	897.F
SiO_2	49.68	47.30	48.80	49.38	66.25	47.39	12.97	64.10	76.52	60.74	63.82
TiO_2	0.80	0.43	0.40	0.79	0.38	0.61	0.07	0.81	0.15	0.91	0.88
Al_2O_3	11.79	23.48	26.70	15.11	15.78	22.84	1.47	11.57	11.11	15.12	15.69
Fe_2O_3	3.49	0.25	1.63	2.19	0.85	1.13	0.00	1.09	1.37	0.52	3.06
FeO	4.65	4.68	2.55	8.59	3.39	4.77	0.84	3.75	0.09	3.51	1.56
MnO	0.09	0.05	0.04	0.17	0.02	0.10	0.00	0.05	0.00	0.05	0.05
MgO	10.74	4.31	1.99	7.24	2.41	3.80	0.68	3.49	0.20	2.16	1.48
CaO	7.97	11.92	13.72	12.63	1.93	12.84	46.62	6.77	0.16	4.10	2.81
Na_2O	1.43	0.95	2.06	1.57	2.94	2.26	0.22	3.71	3.23	3.28	2.58
K_2O	2.30	1.98	1.04	0.15	2.97	0.50	0.77	2.48	4.53	2.73	3.37
P_2O_5	0.45	0.05	0.07	0.01	0.40	0.08	0.02	0.17	0.01	0.41	0.40
S	0.32	0.16	0.04	0.16	0.02	0.03	0.09	0.01	0.02	0.06	0.04
CO_2	6.99	3.27	1.18	0.22	2.43	3.22	37.14	1.43	0.05	4.18	4.17
H_2O^+									1.25	1.97	
Total	100.68	98.83	100.22	98.25	99.77	99.57	100.89	99.43	98.96	99.68	99.91
Fe_2O_3 Total	8.66	5.45	4.46	11.73	4.62	6.43	0.93	5.26	1.47	4.42	4.79

Sample Number	945.S	1082.E	1180.F	1203.Q	1212.Q	1235.L	1236.L	1250.F	1350.L	1366.L
SiO_2	57.94	45.84	63.63	70.44	69.51	57.05	58.40	68.69	55.75	58.27
TiO_2	0.92	2.75	0.87	0.28	0.27	1.20	1.25	0.51	1.45	1.17
Al_2O_3	18.55	13.40	15.65	15.08	14.71	15.94	16.26	15.83	16.89	16.35
Fe_2O_3	1.36	5.37	0.72	0.53	0.97	1.48	1.82	0.52	0.95	2.68
FeO	6.84	12.81	3.30	1.35	1.01	4.70	4.63	2.55	5.85	4.56
MnO	0.01	0.30	0.08	0.00	0.02	0.10	0.14	0.03	0.08	0.10
MgO	4.14	4.89	2.61	0.80	0.80	4.75	5.26	1.27	4.74	1.97
CaO	0.79	8.94	3.10	1.37	0.98	4.85	4.80	2.07	3.95	6.08
Na_2O	1.15	1.92	2.42	3.19	3.93	3.71	2.70	3.33	2.89	3.02
K_2O	4.61	0.69	3.52	4.62	4.38	1.88	2.27	3.30	2.74	2.92
P_2O_5	0.11	0.10	0.42	0.10	0.09	0.30	0.30	0.20	0.33	0.31
S	0.25	0.01	0.02	N.D.	0.01	0.01	0.01	0.01	0.09	0.01
CO_2, H_2O^+	1.52	1.17	2.30	1.82	1.43	2.47	1.97	1.51	3.86	2.51
Total	98.19	98.19	98.99	99.58	98.11	99.44	99.80	99.82	99.57	99.95
Fe_2O_3 Total	8.96	19.60	4.39	2.03	2.09	6.70	6.96	3.35	7.45	7.75

APPENDIX VI

C.I.P.W. Norms of Carlingford Alkaline Rocks

Qz	Quartz
Or	Orthoclase
Ab	Albite
An	Anorthite
Ne	Nepheline
Co	Corundum
Wo	Wollastonite
Di (Wo, En, Fs)	Clinopyroxene
Hy (En, Fs)	Hypersthene
Fo	Forsterite
Fa	Fayalite
Mt	Magnetite
He	Hematite
Il	Ilmenite
Ap	Apatite
Pr	Pyrite
D.I.	Differentiation Index

Qz′	Quartz	Quartz, Albite, Nepheline, Hypersthene, Forsterite and Fayalite recalculated to 100% as these components.
Ol′	Olivine	
Ne′	Nepheline	

Specimen Number	36	61	64	66	96	102	107	115
Qz	0.71	3.83	-	2.03	-	4.58	-	-
Or	2.25	4.73	3.07	7.98	1.89	4.91	1.24	1.48
Ab	19.63	16.92	16.84	21.16	18.79	15.32	21.66	16.84
An	31.77	30.95	38.16	33.42	38.10	33.27	36.49	39.15
Ne	-	-	-	-	-	-	-	-
Co	-	-	-	-	-	-	-	-
Wo	-	-	-	-	-	-	-	-
Di Wo	5.72	3.76	4.37	1.38	4.49	6.85	6.43	4.34
Di En	2.88	2.27	2.43	0.78	2.51	3.86	3.59	2.44
Di Fs	2.71	1.29	1.83	0.54	1.81	2.71	2.58	1.73
Hy En	11.91	14.14	12.96	12.54	13.75	9.54	5.99	15.10
Hy Fs	11.21	8.02	9.74	8.65	9.94	6.71	4.30	10.71
Fo	-	-	0.92	-	0.51	-	5.78	0.57
Fa	-	-	0.75	-	0.41	-	4.58	0.45
Mt	5.36	6.90	4.49	5.81	4.07	5.71	3.91	3.90
He	-	-	-	-	-	-	-	-
Il	4.18	6.19	3.04	4.77	2.49	4.63	2.28	2.26
Ap	0.95	0.88	0.76	0.88	0.69	1.54	0.62	0.62
Pr	0.65	0.15	0.54	0.07	0.51	0.34	0.49	0.37
Sum	99.93	100.03	99.90	100.01	99.95	99.98	99.94	99.97
D.I.	22.59	25.48	19.91	31.17	20.68	24.81	22.90	18.32
Qz′	36.41	41.11	33.51	39.32	34.54	44.22	30.01	33.61
Ol′	39.11	37.51	44.33	34.84	42.00	32.82	42.25	45.49
Ne′	24.48	21.37	22.15	25.84	23.46	22.96	27.75	20.90

Specimen Number	119	135	140	143	191	379	435	745
Qz	-	-	-	1.18	5.72	-	1.47	7.05
Or	1.60	1.83	2.48	2.42	14.18	3.01	3.66	7.51
Ab	18.28	16.16	21.75	19.72	23.27	20.65	21.49	49.50
An	38.41	36.22	26.60	27.76	24.66	29.67	30.73	20.25
Ne	-	-	-	-	-	-	-	-
Co	-	-	-	-	-	-	-	-
Wo	-	-	-	-	-	-	-	-
Di Wo	4.69	4.83	12.33	11.32	3.02	9.46	7.07	2.16
Di En	2.64	2.64	6.47	5.94	1.56	4.85	3.54	1.87
Di Fs	1.85	2.02	5.50	5.06	1.39	4.37	3.38	-
Hy En	13.05	13.83	5.17	8.61	8.21	9.64	10.40	-
Hy Fs	9.15	10.60	4.40	7.33	7.31	8.69	9.92	-
Fo	1.80	2.00	2.52	-	-	0.59	-	-
Fa	1.39	1.69	2.36	-	-	0.59	-	-
Mt	3.90	2.87	5.21	5.25	5.02	2.07	4.58	4.39
He	-	-	-	-	-	-	-	0.30
Il	2.26	3.53	3.97	4.03	3.72	4.12	3.15	3.48
Ap	0.64	0.50	0.66	0.66	1.73	0.90	0.47	1.68
Pr	0.34	1.10	0.54	0.65	0.24	1.22	0.11	0.06
Sum	99.98	99.84	99.96	99.93	100.03	99.85	99.99	100.03
D.I.	19.98	17.99	24.23	23.32	43.17	23.66	26.62	64.06
Qz′	32.90	31.52	34.56	39.26	46.06	35.67	38.56	52.56
Ol′	44.41	48.70	32.88	31.73	25.60	36.47	34.53	0.00
Ne′	22.69	19.78	32.56	29.01	28.34	27.86	26.91	47.44

Specimen Number	748	783	799	802	807	831	840	1175
Qz	-	-	-	-	-	9.08	-	-
Or	4.43	1.30	1.65	4.20	2.48	3.90	6.97	4.14
Ab	35.47	16.84	17.26	32.75	17.10	14.47	22.42	19.38
An	12.16	36.23	32.26	28.41	33.45	35.13	25.74	29.13
Ne	9.94	-	-	-	0.31	-	-	-
Co	-	-	-	0.29	-	-	-	-
Wo	-	-	-	-	-	-	-	-
Di (Wo)	10.24	3.50	8.15	-	9.62	3.61	6.96	6.81
Di (En)	3.16	1.85	5.21	-	4.77	2.02	3.56	3.91
Di (Fs)	7.47	1.55	2.41	-	4.66	1.45	3.22	2.60
Hy (En)	-	12.30	10.00	9.64	-	11.95	8.43	4.53
Hy (Fs)	-	10.28	4.62	8.14	-	8.58	7.62	3.02
Fo	1.62	4.74	7.14	5.36	10.91	-	2.28	12.11
Fa	4.22	4.37	3.64	4.98	11.73	-	2.27	8.88
Mt	4.97	2.71	4.06	0.20	-	4.41	5.25	0.87
He	-	-	-	-	-	-	-	-
Il	3.67	3.48	2.79	4.27	2.92	2.92	4.43	3.23
Ap	3.16	0.50	0.50	1.23	0.47	0.52	0.85	0.92
Pr	0.45	0.32	0.28	0.49	1.38	1.74	0.02	0.43
Sum	99.96	99.97	99.97	99.95	99.83	99.77	100.01	99.95
D.I.	49.84	18.14	18.91	36.95	19.89	27.45	29.39	23.52
Qz/	31.69	28.31	28.02	32.43	19.55	48.20	33.78	22.79
Ol/	11.41	52.89	50.05	38.40	56.52	34.01	37.96	55.29
Ne/	56.90	18.80	21.93	29.16	23.92	17.79	28.26	21.92

Specimen Number	1319	1320	1351	1382	9556
Qz	1.90	8.23	2.15	6.47	-
Or	3.01	17.79	4.73	17.37	1.95
Ab	16.42	28.77	17.18	27.50	22.00
An	32.65	21.58	33.77	21.79	33.20
Ne	-	-	-	-	-
Co	-	-	-	0.75	-
Wo	-	-	-	-	-
Di (Wo)	7.98	4.10	5.48	-	7.37
Di (En)	3.69	1.85	2.75	-	2.91
Di (Fs)	4.21	2.23	2.61	-	4.55
Hy (En)	9.58	1.86	11.72	5.01	2.31
Hy (Fs)	10.94	2.25	11.31	13.41	3.62
Fo	-	-	-	-	6.50
Fa	-	-	-	-	11.23
Mt	4.84	5.05	4.47	2.87	-
He	-	-	-	-	-
Il	3.49	3.76	3.00	2.70	3.86
Ap	0.81	2.32	0.59	1.56	0.52
Pr	0.43	0.22	0.41	0.54	-
Sum	99.95	100.01	99.98	99.97	100.02
D.I.	21.33	54.79	24.06	51.34	23.95
Qz′	38.06	54.67	38.09	45.08	25.39
Ol′	39.03	7.41	39.83	26.46	48.50
Ne′	22.91	37.92	22.07	28.46	26.12

APPENDIX VII

C.I.P.W. Norms of Carlingford High Alumina Basalts

Qz	Quartz	
Or	Orthoclase	
Ab	Albite	
An	Anorthite	
Co	Corundum	
Di (Wo (En (Fs	Clinoprroxene	
Hy (En (Fs	Hypersthene	
Fo	Forsterite	
Fa	Fayalite	
Mt	Magnetite	
Il	Ilmenite	
Ap	Apatite	
Pr	Pyrite	
Cc	Calcite	
D.I.	Differentiation Index	
Qz′	Quartz	) Quartz, Albite, Hypersthene
Ol′	Olivine	) Forsterite and
Ne′	Nepheline	) Fayalite recalculated to 100% as these components.

Sample Number	40	45	74	114	124	137	141	190
Qz	0.62	1.79	1.14	0.41	-	2.65	6.21	1.88
Or	6.91	6.91	2.25	3.72	2.01	2.30	1.24	2.25
Ab	14.30	16.42	14.89	14.64	19.04	20.06	18.19	19.21
An	49.73	38.82	40.01	37.88	50.43	38.99	36.50	46.10
Co	-	-	-	-	-	-	-	-
Di Wo	5.47	7.46	9.09	8.76	7.00	8.46	7.09	7.27
Di En	2.50	3.72	6.11	5.33	4.03	5.45	5.03	4.14
Di Fs	2.92	3.59	2.29	2.94	2.65	2.45	1.44	2.81
Hy En	6.32	8.56	9.50	10.73	6.65	6.52	9.54	5.87
Hy Fs	7.40	8.26	3.55	5.92	4.37	2.93	2.73	3.99
Fo	-	-	-	-	0.25	-	-	-
Fa	-	-	-	-	0.18	-	-	-
Mt	-	2.03	3.42	2.97	1.84	2.55	4.10	3.33
Il	1.33	2.05	1.63	1.79	1.33	1.65	2.53	1.52
Ap	0.21	0.28	0.28	0.28	0.21	0.26	0.90	0.21
Pr	0.51	-	2.28	1.35	0.41	3.29	4.19	0.06
Cc	-	-	-	-	-	-	-	-
Sum	98.21	95.90	96.45	96.73	100.40	97.57	99.69	98.64
D.I.	21.83	25.12	18.28	18.77	21.05	25.01	25.64	23.34
Qz′	37.53	39.27	39.95	36.85	38.40	44.95	49.15	43.12
Ol′	35.40	35.32	32.30	38.13	27.76	21.24	23.96	23.23
Ne′	27.07	25.40	27.75	25.02	33.84	33.81	26.89	33.64

Sample Number	269	273	399	426	437	442	443	444
Qz	4.76	0.34	2.24	-	-	0.46	10.12	0.82
Or	7.21	3.19	2.95	0.95	1.06	2.19	13.95	4.02
Ab	19.80	19.97	14.05	15.82	16.16	16.16	20.99	18.53
An	39.54	37.75	55.28	40.44	50.00	38.80	27.67	35.89
Co	-	-	-	-	-	-	2.49	-
Di Wo	5.82	8.24	4.96	9.14	7.29	8.59	-	8.30
Di En	2.84	4.50	2.80	4.75	3.88	4.55	-	4.34
Di Fs	2.87	3.44	1.95	4.13	3.18	3.77	-	3.73
Hy En	5.58	7.95	6.22	6.79	4.97	10.41	7.74	9.65
Hy Fs	5.64	6.08	4.35	5.90	4.07	8.62	9.91	8.28
Fo	-	-	-	3.17	1.63	-	-	-
Fa	-	-	-	3.04	1.47	-	-	-
Mt	1.83	3.55	2.38	-	1.10	1.64	1.44	1.35
Il	1.42	1.80	1.14	1.75	1.33	1.56	1.79	1.84
Ap	0.24	0.26	0.19	0.28	0.21	0.19	0.47	0.21
Pr	0.07	0.06	0.04	1.53	0.37	0.13	0.09	0.34
Cc	-	-	-	-	0.11	-	-	-
Sum	97.62	97.13	98.54	97.69	98.86	97.07	96.65	97.30
D.I.	31.77	23.50	19.24	16.77	17.22	18.81	45.06	23.37
Qz′	46.91	38.60	42.94	30.60	34.69	36.31	49.86	37.77
Ol′	23.09	29.88	28.72	44.70	34.37	39.12	26.82	35.29
Ne′	30.00	31.52	28.35	24.70	30.94	24.56	23.33	26.94

Sample Number	450	452	458	563	658	665	718	1001
Qz	-	3.05	2.29	5.77	6.44	-	-	0.39
Or	1.42	3.66	5.38	4.85	4.67	3.96	4.20	2.66
Ab	16.84	13.29	13.96	22.00	12.52	15.15	12.35	18.28
An	52.74	47.74	42.43	37.59	42.49	44.48	38.53	49.14
Co	-	-	-	-	-	-	-	-
Di Wo	6.77	4.34	4.55	6.05	5.40	1.43	10.22	7.46
Di En	3.47	2.47	2.62	2.91	3.16	0.83	5.75	4.28
Di Fs	3.13	1.68	1.71	3.04	1.98	0.53	4.05	2.85
Hy En	3.20	8.44	11.47	5.93	10.17	14.21	9.07	5.68
Hy Fs	2.88	5.75	7.53	6.18	6.37	9.17	6.39	3.78
Fo	1.80	-	-	-	-	2.24	1.68	-
Fa	1.79	-	-	-	-	1.59	1.30	-
Mt	1.12	2.67	2.00	3.16	1.81	1.80	1.57	2.09
Il	1.25	1.52	1.46	2.15	1.41	2.01	1.20	1.23
Ap	0.17	0.24	0.24	0.40	0.24	0.26	0.24	0.24
Pr	0.41	0.60	0.04	0.06	0.09	0.73	0.06	0.09
Cc	-	-	-	-	-	-	-	-
Sum	96.98	95.44	95.69	97.08	96.73	98.38	96.59	98.18
D.I.	18.26	20.00	21.63	29.62	23.63	19.11	16.55	21.33
Qz/	35.18	42.50	39.25	43.47	46.96	31.37	31.93	40.26
Ol/	30.39	33.91	39.28	24.20	33.92	49.25	46.33	24.52
Ne/	34.43	23.60	21.47	32.33	19.12	19.39	21.75	35.21

Sample Number		1119	1162	1166	1352	1387	1399
Qz		0.79	3.31	6.06	0.65	2.16	2.41
Or		2.13	3.25	7.56	5.85	6.80	4.85
Ab		15.49	17.18	22.00	12.10	14.47	21.75
An		41.45	40.40	31.97	36.04	45.14	36.11
Co		-	-	-	-	-	-
Di	Wo	8.77	5.83	6.57	8.11	6.28	6.91
	En	4.94	3.01	3.08	4.14	3.05	3.34
	Fs	3.47	2.68	3.41	3.77	3.12	3.46
Hy	En	9.55	8.25	5.96	11.60	6.17	5.67
	Fs	6.71	7.35	6.59	10.58	6.32	5.87
Fo		-	-	-	-	-	-
Fa		-	-	-	-	-	-
Mt		2.51	3.36	2.51	1.03	1.59	3.44
Il		1.56	1.56	1.50	1.90	1.71	2.43
Ap		0.24	0.21	0.19	0.24	0.24	0.40
Pr		0.04	0.02	0.02	0.90	0.28	1.31
Cc		-	1.59	-	-	-	-
Sum		97.63	97.99	97.41	96.90	97.32	97.96
D.I.		18.41	23.74	35.62	18.60	23.43	29.01
Qz′		37.71	42.45	47.83	34.57	41.48	33.01
Ol′		36.49	31.74	22.80	46.65	31.58	23.83
Ne′		25.80	25.80	29.37	18.78	26.94	43.16

APPENDIX VIII

C.I.P.W. Norms. of rocks in the Tholeiitic Basalt - Craignurite Series

Qz	Quartz	
Or	Orthoclase	
Ab	Albite	
An	Anorthite	
Co	Corundum	
Di (Wo, En, Fs)	Clinopyroxene	
Hy (En, Fs)	Hypersthene	
Fo	Forsterite	
Fa	Fayalite	
Mt	Magnetite	
Il	Ilmenite	
Ap	Apatite	
Pr	Pyrite	
Cc	Calcite	
D.I.	Differentiation Index	
Qz′	Quartz	Quartz, Orthoclase, Albite, Hypersthene, Forsterite and Fayalite recalculated to 100% as these components.
Ol′	Olivine	
Ne′	Nepheline	

Sample Number	3	5	6	9	11	18	22	23
Qz	10.19	23.90	7.56	-	9.57	8.75	12.42	21.47
Or	4.26	23.76	7.68	6.56	5.26	4.91	22.81	32.39
Ab	19.12	28.43	23.69	22.85	21.75	18.87	26.15	26.57
An	23.72	9.12	23.05	22.61	22.13	22.66	13.20	5.90
Co	-	-	-	-	-	-	-	-
Di (Wo)	5.91	0.18	6.78	12.52	9.11	7.76	2.36	0.75
Di (En)	3.23	0.08	2.97	6.33	2.19	2.99	0.82	0.24
Di (Fs)	2.47	0.09	3.80	5.91	7.47	4.88	1.60	0.53
Hy (En)	6.48	2.43	5.85	5.16	2.27	6.94	4.21	1.62
Hy (Fs)	4.96	2.81	7.47	4.81	7.77	11.33	8.18	3.51
Fo	-	-	-	2.52	-	-	-	-
Fa	-	-	-	2.60	-	-	-	-
Mt	4.74	3.35	4.49	2.86	4.19	4.65	2.86	3.16
Il	4.18	1.69	3.04	2.36	3.11	3.25	2.09	1.29
Ap	0.78	0.45	0.54	0.36	0.47	0.50	0.62	0.38
Pr	5.41	2.84	1.44	0.65	0.75	0.37	0.02	0.02
Cc	-	1.39	-	-	-	-	0.16	-
Sum	95.45	100.52	98.36	98.09	96.03	97.86	97.48	97.83
D.I.	33.57	76.09	38.93	29.41	36.58	32.53	61.38	80.43
Qz′	54.03	66.51	49.05	34.56	53.14	48.05	54.00	65.68
Ol′	20.53	6.72	22.14	32.81	18.36	29.66	18.19	7.24
Ne′	25.44	26.76	28.81	32.63	28.50	22.29	27.81	27.08

Sample Number	24	25	27	28	30	33	35	37
Qz	8.08	24.05	12.81	-	15.00	9.46	11.56	7.96
Or	15.60	31.38	16.61	5.32	12.06	9.81	17.55	16.37
Ab	20.39	29.28	17.43	18.62	17.60	16.25	20.99	22.42
An	15.36	4.75	17.52	27.39	19.67	23.15	16.47	15.97
Co	-	-	-	-	-	-	-	-
Di (Wo)	6.15	1.13	5.05	12.31	0.42	7.94	3.95	5.34
Di (En)	2.06	0.26	1.52	6.70	0.12	3.77	1.43	1.79
Di (Fs)	4.29	0.95	3.75	5.19	0.32	4.06	2.61	3.71
Hy (En)	4.57	0.63	3.76	6.67	5.46	6.06	5.99	5.16
Hy (Fs)	9.53	2.29	9.30	5.17	14.70	7.49	10.97	10.71
Fo	-	-	-	2.85	-	-	-	-
Fa	-	-	-	2.43	-	-	-	-
Mt	5.92	2.97	4.29	3.09	3.52	4.12	0.97	3.60
Il	4.90	1.04	3.76	1.79	3.91	3.15	2.28	4.52
Ap	0.71	0.26	0.59	0.26	0.59	0.59	0.40	0.85
Pr	0.06	0.02	0.07	0.09	0.07	0.28	0.41	0.49
Cc	-	-	-	-	3.91	-	-	-
Sum	97.61	99.02	96.47	97.87	97.38	97.05	95.59	98.89
D.I.	44.07	84.71	46.85	23.94	44.66	35.52	50.10	46.75
Qz′	49.24	67.85	55.50	32.75	53.15	51.53	51.43	48.02
Ol′	24.81	3.94	22.68	39.02	28.77	26.55	25.59	25.70
Ne′	25.96	28.21	21.82	28.24	18.08	21.93	22.97	26.28

Sample Number	38	46	53	54	58	59	63	67
Qz	3.06	16.34	0.47	1.31	18.72	6.64	8.75	5.96
Or	4.37	17.61	1.48	1.06	15.54	14.89	15.01	6.21
Ab	18.36	24.88	18.28	10.83	26.49	21.49	18.85	15.91
An	27.29	18.55	30.44	33.48	16.22	18.32	19.17	24.94
Co	-	-	-	-	-	-	-	-
Di Wo	8.29	2.13	9.02	6.55	1.30	5.73	5.57	5.79
Di En	4.39	0.78	5.35	4.60	0.43	2.12	1.69	2.28
Di Fs	3.65	1.39	3.22	1.40	0.91	3.72	4.08	3.59
Hy En	10.70	5.14	12.68	21.75	4.22	6.17	5.39	7.81
Hy Fs	8.89	9.17	7.62	6.61	8.84	10.84	12.79	12.32
Fo	-	-	-	-	-	-	-	-
Fa	-	-	-	-	-	-	-	-
Mt	3.94	0.78	3.80	3.32	0.19	2.26	3.25	3.96
Il	2.51	2.32	2.13	2.28	1.88	3.13	4.26	4.69
Ap	0.38	0.76	0.33	0.26	0.54	0.69	1.01	1.47
Pr	0.36	0.15	0.52	1.76	0.21	0.28	0.23	0.80
Cc	1.48	-	1.02	0.86	-	-	-	-
Sum	97.66	100.01	96.37	96.07	95.50	96.29	100.07	95.73
D.I.	25.79	58.83	20.23	13.20	60.75	43.02	42.62	28.08
Qz′	40.72	56.48	36.83	35.31	58.57	46.07	47.87	43.79
Ol′	35.02	19.24	37.81	50.20	16.80	28.12	29.81	35.69
Ne′	24.26	24.28	25.37	14.50	24.64	25.80	22.32	20.52

Sample Number	68	71	72	73	75	76	78	80
Qz	1.27	10.18	4.91	10.47	15.45	-	5.67	7.10
Or	9.63	5.67	4.91	9.87	5.32	3.01	4.85	5.61
Ab	18.62	15.32	18.19	18.62	20.99	12.27	20.06	17.09
An	28.83	25.28	27.57	20.31	23.05	31.91	25.09	25.40
Co	-	-	-	-	0.59	-	-	-
Di (Wo)	7.76	4.12	5.95	5.39	-	7.95	7.82	7.88
Di (En)	3.51	1.99	3.17	2.20	-	5.27	3.97	3.82
Di (Fs)	4.20	2.07	2.59	3.22	-	2.11	3.67	3.93
Hy (En)	8.82	9.02	12.44	5.84	7.89	10.28	8.76	8.78
Hy (Fs)	10.55	9.43	10.15	8.56	12.39	4.11	8.10	9.02
Fo	-	-	-	-	-	7.83	-	-
Fa	-	-	-	-	-	3.45	-	-
Mt	1.42	4.97	2.09	5.28	3.15	3.96	4.42	4.07
Il	2.64	3.67	2.15	4.06	4.48	2.34	2.94	2.98
Ap	0.40	0.64	0.40	0.95	1.30	0.31	0.59	0.57
Pr	0.30	2.64	0.60	0.99	2.11	0.24	2.25	1.22
Cc	-	1.57	2.77	-	-	-	-	-
Sum	97.95	96.57	97.90	95.76	96.73	95.04	98.18	97.47
D.I.	29.52	31.17	28.01	38.96	41.76	15.28	30.58	29.80
Qz′	37.81	50.16	42.19	52.19	53.33	25.40	45.37	46.71
Ol′	36.49	30.95	36.23	24.61	26.62	57.07	29.10	31.23
Ne′	25.70	18.89	21.58	23.20	20.05	17.53	25.52	22.06

Sample Number	84	93	97	99	111	113	122	123
Qz	-	22.66	3.41	2.15	0.08	-	3.72	5.79
Or	2.19	19.03	2.48	5.14	2.30	2.54	4.67	8.39
Ab	9.99	26.57	19.21	11.17	19.63	20.31	19.63	19.80
An	33.59	5.67	25.65	29.24	26.77	28.23	27.12	23.72
Co	-	3.12	-	-	-	-	-	-
Di (Wo)	8.60	-	5.50	11.74	12.30	11.34	8.02	7.68
Di (En)	5.63	-	2.77	7.78	6.50	6.58	4.45	3.46
Di (Fs)	2.36	-	2.61	3.11	5.43	4.24	3.27	4.17
Hy (En)	16.06	5.90	10.76	15.28	9.44	5.79	10.47	8.67
Hy (Fs)	6.73	4.18	10.16	6.12	7.88	3.73	7.68	10.47
Fo	2.93	-	-	-	-	4.38	-	-
Fa	1.35	-	-	-	-	3.11	-	-
Mt	3.65	2.58	5.28	3.32	4.05	2.91	3.35	1.73
Il	2.22	1.65	4.06	1.50	2.85	2.26	2.26	2.43
Ap	0.26	0.33	0.69	0.28	0.38	0.40	0.40	0.47
Pr	0.28	1.23	0.56	0.84	0.60	0.45	0.47	0.19
Cc	1.21	5.91	4.66	-	0.64	-	2.30	-
Sum	97.05	98.85	97.80	97.69	98.44	96.28	97.81	96.97
D.I.	12.18	68.26	25.10	18.46	22.01	22.85	28.02	33.98
Qz′	29.47	63.31	40.77	38.14	36.97	31.85	42.41	44.35
Ol′	55.93	12.41	35.32	44.42	34.29	38.66	31.96	31.65
Ne′	14.60	24.28	23.91	17.44	28.73	29.49	25.64	23.99

Sample Number	125	127	130	131	133	142	145	147
Qz		7.89	1.53	5.95	8.25	4.49	1.28	0.09
Or	2.36	9.63	5.61	3.72	8.57	1.36	0.71	5.79
Ab	17.35	22.09	25.89	20.14	18.79	17.94	17.60	18.96
An	31.26	20.63	20.51	23.23	21.74	34.28	30.09	26.94
Co	-	-	-	-	-	-	-	-
Di Wo	11.95	6.43	9.63	8.76	6.95	8.06	13.10	10.28
Di En	7.41	2.61	5.11	4.91	2.92	5.31	7.49	5.36
Di Fs	3.84	3.87	4.22	3.49	4.06	2.18	5.03	4.63
Hy En	8.72	6.48	7.71	6.47	6.55	9.76	10.04	10.53
Hy Fs	4.52	9.61	6.36	4.59	9.13	4.01	6.73	9.11
Fo	1.43	-	-	-	-	-	-	-
Fa	0.82	-	-	-	-	-	-	-
Mt	3.60	3.62	2.52	5.38	4.94	3.89	1.84	3.16
Il	1.86	3.32	2.83	4.20	3.63	2.24	2.07	2.01
Ap	0.24	0.73	0.57	1.21	0.76	0.81	0.24	0.28
Pr	2.02	0.52	4.96	5.52	1.35	3.42	2.43	0.24
Cc	-	0.66	-	-	-	-	-	-
Sum	97.37	98.11	97.46	97.56	97.63	97.75	98.65	97.39
D.I.	19.71	39.61	33.03	29.81	35.61	23.79	19.59	24.84
Qz/	35.29	48.05	41.32	48.88	48.91	45.72	38.94	36.19
Ol/	36.08	25.96	24.85	21.74	27.25	27.43	34.30	37.25
Ne/	28.63	25.99	33.82	29.38	23.84	26.85	26.76	26.56

Sample Number	151	155	156	158	160	162	166	173
Qz	16.51	7.27	0.37	12.20	3.48	-	11.44	6.13
Or	22.69	11.29	3.66	15.78	6.26	6.91	15.66	8.75
Ab	28.09	22.59	20.48	25.30	16.08	21.24	21.58	16.84
An	10.68	19.46	26.71	14.55	30.55	30.16	17.86	26.43
Co	-	-	-	-	-	-	-	-
Di Wo	3.52	7.31	10.11	4.02	8.53	5.51	4.25	7.50
Di En	1.22	3.41	5.79	1.40	5.42	2.59	1.51	3.60
Di Fs	2.39	3.81	3.88	2.74	2.56	2.86	2.85	3.79
Hy En	2.14	6.22	10.08	3.96	12.58	9.55	4.84	9.52
Hy Fs	4.21	6.94	6.76	7.75	5.94	10.55	9.16	10.01
Fo	-	-	-	-	-	1.16	-	-
Fa	-	-	-	-	-	1.42	-	-
Mt	3.94	4.94	2.32	3.02	3.13	0.93	3.77	2.13
Il	2.32	3.63	3.25	4.20	1.60	3.30	3.36	2.30
Ap	0.76	0.69	0.64	1.16	0.26	0.62	0.73	0.38
Pr	1.29	1.63	5.71	2.49	0.28	2.81	0.02	0.17
Cc	-	-	-	-	-	-	-	-
Sum	99.77	99.19	99.76	98.56	96.67	99.60	97.04	97.54
D.I.	67.29	41.15	24.51	53.28	25.82	28.15	48.68	31.72
Qz′	60.79	48.95	37.97	54.34	41.93	34.13	52.86	44.64
Ol′	9.33	22.59	32.58	17.80	35.18	39.66	22.27	33.88
Ne′	29.88	28.46	29.45	27.87	22.89	26.21	24.87	21.48

Sample Number	174	175	176	181	192	235	236	253
Qz	4.49	6.98	2.71	-	3.48	-	11.90	-
Or	8.21	10.52	7.92	6.74	3.13	2.48	16.96	2.42
Ab	19.21	20.06	19.38	22.76	20.06	15.74	21.75	8.12
An	25.19	21.84	25.30	28.11	24.28	33.77	20.81	34.40
Co	-	-	-	-	-	-	-	-
Di (Wo)	7.29	7.23	7.80	8.28	10.19	9.12	5.12	7.96
Di (En)	3.37	2.90	3.40	3.27	5.95	5.27	2.57	5.32
Di (Fs)	3.85	4.40	4.39	5.10	3.76	3.43	2.43	2.04
Hy (En)	9.70	7.61	9.82	6.58	9.09	11.79	5.67	17.65
Hy (Fs)	11.08	11.56	12.66	10.27	5.75	7.68	5.36	6.77
Fo	-	-	-	0.52	-	1.69	-	3.87
Fa	-	-	-	0.89	-	1.22	-	1.63
Mt	1.35	1.55	-	1.64	4.61	2.02	2.87	3.55
Il	2.32	2.47	2.32	2.87	3.19	1.90	1.48	2.28
Ap	0.40	0.59	0.40	0.52	0.64	0.31	0.26	0.26
Pr	0.26	0.34	0.47	0.15	2.81	0.49	0.06	0.04
Cc	-	-	-	-	-	-	0.66	-
Sum	96.73	98.04	96.57	97.68	96.94	96.89	97.91	96.31
D.I.	31.91	37.56	30.01	29.50	26.67	18.22	50.61	10.54
Qz/	42.08	45.61	39.05	35.92	43.52	32.77	55.47	27.74
Ol/	34.52	30.86	37.38	34.00	28.16	44.85	18.16	60.68
Ne/	23.40	23.52	23.57	30.08	28.32	22.38	26.38	11.50

Sample Number	292	297	298	300	305	314	330	369
Qz	-	0.37	-	5.37	-	4.31	6.30	2.17
Or	2.90	3.01	2.60	2.42	5.61	3.07	13.71	2.54
Ab	21.16	21.24	9.90	16.84	14.81	13.88	16.50	22.76
An	31.21	25.54	38.25	30.30	31.44	32.58	18.34	30.59
Co	-	-	-	-	-	-	-	-
Di Wo	11.37	13.01	8.87	7.41	10.53	7.29	4.79	8.58
Di En	6.64	7.67	5.53	3.69	5.94	3.87	2.83	4.49
Di Fs	4.19	4.70	2.80	3.56	4.15	3.19	1.73	3.85
Hy En	6.71	8.69	11.26	10.15	7.81	12.20	14.08	8.38
Hy Fs	4.24	5.33	5.70	9.78	5.45	10.08	8.60	7.17
Fo	2.18	-	4.34	-	3.83	-	-	-
Fa	1.52	-	2.42	-	2.95	-	-	-
Mt	3.93	5.13	3.16	3.58	3.09	2.55	4.86	3.96
Il	2.30	2.32	1.65	2.60	2.13	2.75	3.55	2.37
Ap	0.45	0.38	0.21	0.43	0.36	0.50	0.36	0.38
Pr	0.04	0.64	0.04	0.54	0.37	2.17	0.13	0.60
Cc	-	-	-	-	-	-	0.11	-
Sum	98.83	98.03	96.74	96.68	98.49	98.43	95.89	97.85
D.I.	24.06	24.62	12.50	24.63	20.42	21.26	36.51	27.47
Qz′	35.38	39.05	27.39	43.55	29.73	41.07	44.06	41.35
Ol′	32.60	28.64	56.65	34.79	47.24	40.34	36.28	28.18
Ne′	32.02	32.31	15.96	21.66	23.02	18.59	19.66	30.47

Sample Number	371	400	421	424	425	429	438	439
Qz	4.62	0.25	-	1.12	-	5.24	-	1.07
Or	6.74	1.71	3.96	5.50	2.19	3.96	4.14	6.97
Ab	21.32	13.54	13.88	12.78	20.06	20.99	18.70	17.69
An	22.54	32.32	34.07	33.92	31.08	26.43	26.95	26.51
Co	-	-	-	-	-	-	-	-
Di Wo	8.64	10.93	8.92	8.04	9.22	9.74	13.32	9.57
Di En	3.74	6.33	5.41	4.53	4.88	5.49	6.54	4.85
Di Fs	4.90	4.10	3.03	3.18	4.06	3.85	6.54	4.49
Hy En	7.29	13.32	9.95	13.73	6.70	9.28	4.51	11.29
Hy Fs	9.57	8.63	5.58	9.63	5.57	6.52	4.51	10.46
Fo	-	-	4.39	-	4.64	-	4.46	-
Fa	-	-	2.71	-	4.26	-	4.92	-
Mt	4.68	3.76	2.64	2.07	1.17	2.33	0.84	0.99
Il	3.29	2.07	1.82	1.84	1.98	1.92	2.15	2.07
Ap	0.64	0.28	0.33	0.33	0.26	0.38	0.36	0.28
Pr	0.36	0.08	0.21	0.39	1.98	1.12	0.19	0.07
Cc	-	-	-	-	-	-	-	-
Sum	98.33	97.27	96.89	97.04	98.04	97.25	98.11	96.31
D.I.	32.68	15.50	17.84	19.40	22.25	30.19	22.84	25.73
Qz′	43.80	34.71	29.06	35.64	30.23	45.50	29.50	36.87
Ol′	29.20	44.76	50.33	45.77	43.41	27.44	43.18	39.46
Ne′	27.00	20.53	20.61	18.59	26.37	27.06	27.33	23.67

Sample Number	441	445	451	457	461	499	500	536
Qz	0.23	2.98	3.36	2.23	7.46	-	-	1.30
Or	1.42	3.96	5.97	4.02	3.72	3.19	1.48	3.84
Ab	15.74	17.69	19.97	15.15	18.11	19.04	22.34	17.77
An	33.16	28.45	23.70	29.06	29.16	27.70	26.92	24.75
Co	-	-	-	-	-	-	-	-
Di (Wo)	11.43	9.56	9.77	9.81	9.38	12.70	10.26	14.58
Di (En)	6.89	4.93	4.88	5.17	5.61	7.55	5.63	9.06
Di (Fs)	3.92	4.39	4.69	4.35	3.28	4.50	4.26	4.65
Hy (En)	13.08	10.94	8.65	10.86	8.38	8.16	9.93	10.76
Hy (Fs)	7.44	9.74	8.31	9.13	4.89	4.86	7.52	5.53
Fo	-	-	-	-	-	2.01	0.52	-
Fa	-	-	-	-	-	1.32	0.43	-
Mt	3.64	1.74	4.28	3.62	3.83	2.90	4.16	3.47
Il	1.92	2.07	2.75	3.17	2.17	2.15	2.60	1.69
Ap	0.38	0.28	0.43	0.64	0.40	0.36	0.45	0.24
Pr	0.09	0.09	0.34	0.15	2.23	2.47	0.32	0.04
Cc	-	-	-	-	-	-	-	-
Sum	99.34	96.83	97.09	97.37	98.61	97.90	96.81	97.68
D.I.	17.39	24.63	29.30	21.40	29.29	22.23	23.82	22.91
Qz/	35.78	40.09	42.17	38.81	49.89	34.68	36.63	39.38
Ol/	40.85	36.72	30.96	39.22	24.83	36.16	33.65	33.38
Ne/	23.38	23.18	26.86	21.97	25.27	29.16	29.73	27.24

Sample Number	557	559	562	565	568	589	603	605
Qz	0.53	1.20	5.79	5.69	4.91	4.79	-	5.57
Or	4.43	2.30	5.85	5.38	5.32	8.34	1.83	7.62
Ab	24.37	22.26	18.02	20.06	18.62	19.90	11.93	18.79
An	21.61	26.31	25.44	24.82	28.40	22.79	36.41	24.15
Co	-	-	-	-	-	-	-	-
Di Wo	9.25	10.88	8.92	8.21	9.53	8.00	8.71	6.88
Di En	3.95	5.36	4.15	3.58	4.36	3.70	4.33	2.49
Di Fs	5.32	5.31	4.68	4.61	5.10	4.22	4.20	4.54
Hy En	9.30	9.23	8.75	7.85	7.67	8.39	12.65	7.70
Hy Fs	12.50	9.14	9.85	10.11	8.98	9.77	12.29	14.05
Fo	-	-	-	-	-	-	1.16	-
Fa	-	-	-	-	-	-	1.24	-
Mt	2.16	2.73	3.38	3.12	2.51	3.71	-	0.65
Il	2.91	2.36	2.91	2.98	2.56	3.04	2.05	3.06
Ap	0.50	0.33	0.47	0.57	0.26	0.67	0.36	0.54
Pr	0.39	0.07	0.28	0.06	0.02	0.48	0.45	1.05
Cc	-	-	-	-	-	-	-	0.57
Sum	97.22	97.48	98.50	97.03	98.24	97.80	97.60	97.67
D.I.	29.33	25.76	29.66	31.13	28.85	33.03	13.76	31.98
Qz/	37.10	38.83	44.58	44.68	44.25	43.50	30.70	42.68
Ol/	34.62	32.33	32.38	30.45	30.64	31.32	52.83	35.23
Ne/	28.29	28.84	23.04	24.87	25.11	25.18	16.47	22.08

Sample Number	619	625	629	630	659	663	664	682
Qz	19.12	10.43	3.54	-	0.94	2.94	1.26	-
Or	18.56	14.30	2.90	8.16	7.21	4.55	0.59	6.86
Ab	23.02	15.74	18.36	19.38	12.95	17.52	11.68	16.59
An	15.93	19.73	30.34	29.47	31.93	25.22	35.04	29.74
Co	-	-	-	-	-	-	-	-
Di Wo	3.35	4.80	7.04	8.04	8.35	9.70	10.26	9.61
Di En	1.46	1.58	3.21	3.99	4.79	4.14	5.98	5.31
Di Fs	1.87	3.38	3.79	3.89	3.20	5.58	3.80	3.93
Hy En	3.79	5.22	10.24	10.50	13.34	9.31	13.22	9.04
Hy Fs	4.85	11.19	12.08	10.21	8.91	12.55	8.39	6.68
Fo	-	-	-	0.66	-	-	-	1.62
Fa	-	-	-	0.71	-	-	-	1.32
Mt	1.96	3.65	1.61	2.28	3.42	0.68	3.48	2.55
Il	2.17	4.10	2.53	2.36	2.18	2.81	1.71	2.07
Ap	0.71	0.85	0.47	0.36	0.31	0.40	0.24	0.36
Pr	1.35	0.37	0.54	0.02	0.06	2.02	0.21	0.51
Cc	-	-	-	-	-	-	-	-
Sum	98.13	95.35	96.65	100.02	97.59	97.41	95.86	96.17
D.I.	60.70	40.47	24.80	27.54	21.10	25.01	13.53	23.45
Qz′	62.83	51.08	40.17	34.60	35.69	39.25	36.13	33.56
Ol′	12.60	28.89	37.32	40.07	44.89	38.31	45.55	40.93
Ne′	24.57	20.04	22.51	25.33	19.42	22.44	18.32	25.51

Sample Number	684	719	744	747	759	762	765	766
Qz	2.34	2.87	9.55	1.55	4.00	-	8.32	9.04
Or	1.54	1.18	14.60	6.80	8.16	2.13	10.22	10.87
Ab	15.65	11.51	19.46	18.36	17.01	14.30	17.60	19.46
An	31.97	37.18	17.53	22.75	27.26	34.55	20.67	19.17
Co	-	-	-	-	-	-	-	-
Di Wo	12.24	7.67	5.34	10.06	8.28	10.76	6.08	6.51
Di En	7.89	4.47	1.85	4.41	3.60	5.52	2.14	2.33
Di Fs	3.54	2.83	3.63	5.62	4.67	4.97	4.10	4.33
Hy En	9.87	14.35	5.14	8.06	8.83	10.08	6.50	5.24
Hy Fs	4.43	9.08	10.06	10.27	11.45	9.08	12.45	9.72
Fo	-	-	-	-	-	1.39	-	-
Fa	-	-	-	-	-	1.38	-	-
Mt	3.58	2.96	3.70	4.15	1.39	0.83	2.78	4.61
Il	1.84	1.94	3.78	2.58	2.64	1.90	4.16	4.24
Ap	0.21	0.33	0.90	0.38	0.45	0.24	1.02	0.99
Pr	3.27	0.04	1.61	0.86	0.32	0.58	0.71	0.69
Cc	-	-	-	-	-	-	-	-
Sum	98.37	96.40	97.15	95.86	98.05	97.69	96.77	97.21
D.I.	19.53	15.56	43.61	26.71	29.17	16.43	36.14	39.37
Qz/	41.74	38.37	50.43	38.47	41.27	32.13	47.16	50.01
Ol/	31.99	45.13	25.72	35.51	36.40	46.47	31.58	25.72
Ne/	26.27	16.50	23.86	26.02	22.33	21.40	21.26	24.27

Sample Number	767	768	769	770	771	772	775	780
Qz	7.65	0.94	-	2.21	3.90	-	9.35	8.00
Or	14.66	3.49	4.43	1.42	3.49	6.26	10.16	10.99
Ab	14.47	12.02	13.20	13.96	19.55	11.17	16.59	19.89
An	20.85	34.83	33.10	32.95	30.35	32.78	21.38	19.81
Co	-	-	-	-	-	-	-	-
Di (Wo)	2.64	8.49	10.85	6.98	5.76	10.32	5.93	6.86
Di (En)	0.95	4.75	5.50	4.09	3.21	5.81	2.00	2.91
Di (Fs)	1.76	3.40	5.10	2.55	2.32	4.09	4.10	3.97
Hy (En)	7.74	13.20	4.45	14.71	11.39	10.18	5.99	5.98
Hy (Fs)	14.36	9.44	4.12	9.18	8.25	7.16	12.27	8.18
Fo	-	-	6.33	-	-	1.92	-	-
Fa	-	-	6.47	-	-	1.49	-	-
Mt	3.61	3.36	-	3.57	3.97	2.65	3.23	4.99
Il	4.52	2.09	1.92	2.09	2.36	1.96	4.20	3.68
Ap	1.14	0.31	0.28	0.26	0.36	0.31	0.97	0.85
Pr	0.06	0.11	1.10	0.28	1.16	0.15	0.62	0.80
Cc	-	-	-	3.75	2.21	-	-	-
Sum	94.41	96.43	96.86	98.01	98.26	96.24	96.78	96.92
D.I.	36.78	16.45	17.63	17.59	26.94	17.43	36.10	38.88
Qz′	44.92	35.26	24.06	37.71	42.11	30.70	48.72	49.37
Ol′	37.35	46.45	55.24	43.40	33.30	50.34	30.94	24.99
Ne′	17.73	18.29	20.70	18.89	24.59	18.95	20.34	25.63

Sample Number	827	830	841	842	850	851	852	856
Qz	9.52	13.90	9.23	12.86	25.36	7.47	0.03	5.24
Or	6.15	14.18	6.26	3.07	26.24	10.22	8.39	4.85
Ab	16.25	15.99	16.50	17.09	26.99	17.52	20.31	17.01
An	25.12	20.91	25.36	28.64	8.01	24.05	27.68	27.00
Co	-	-	-	-	-	-	-	-
Di (Wo)	5.89	3.88	4.29	4.31	0.79	3.70	5.46	6.94
Di (En)	3.07	1.53	2.34	2.59	0.24	1.43	2.62	3.76
Di (Fs)	2.65	2.40	1.80	1.50	0.58	2.32	2.75	2.95
Hy (En)	8.48	5.09	10.14	10.39	0.65	8.93	12.97	11.83
Hy (Fs)	7.33	7.98	7.79	6.01	1.56	14.43	13.61	9.30
Fo	-	-	-	-	-	-	-	-
Fa	-	-	-	-	-	-	-	-
Mt	6.68	5.02	4.52	3.49	2.10	2.90	2.17	4.18
Il	3.61	3.72	3.08	1.96	1.29	3.10	3.04	2.62
Ap	0.71	0.90	0.50	0.36	0.33	0.50	0.40	0.40
Pr	1.31	0.43	3.55	1.14	1.78	0.39	0.43	0.56
Cc	-	-	-	1.66	-	-	-	2.25
Sum	96.77	95.95	95.37	95.06	95.93	96.95	99.87	98.89
D.I.	31.92	44.07	31.99	33.02	78.59	35.21	28.73	27.10
Qz/	50.92	57.18	49.47	54.30	70.14	44.37	34.76	43.09
Ol/	27.90	22.65	30.04	25.71	3.05	36.00	41.77	35.66
Ne/	21.18	20.16	20.48	19.99	26.81	19.64	23.47	21.25

Sample Number	864	876	877	878	879	884	889	891
Qz	4.34	6.35	9.05	9.88	11.98	9.96	2.10	12.62
Or	5.26	20.21	14.42	11.46	14.95	17.91	5.50	14.42
Ab	20.14	15.06	17.94	23.02	17.26	12.02	13.45	16.67
An	23.93	23.00	25.03	20.67	20.78	24.32	33.50	22.23
Co	-	-	-	-	-	-	-	-
Di Wo	9.65	2.44	0.49	3.19	4.78	3.08	8.66	4.63
Di En	4.59	0.84	0.19	1.12	2.20	1.09	5.24	1.99
Di Fs	4.93	1.67	0.31	2.15	2.54	2.07	2.95	2.64
Hy En	8.46	7.80	9.15	6.84	6.97	7.37	12.54	7.15
Hy Fs	9.08	15.52	14.90	13.05	8.07	13.94	7.04	9.48
Fo	-	-	-	-	-	-	-	-
Fa	-	-	-	-	-	-	-	-
Mt	3.45	1.17	2.68	2.25	1.48	2.02	3.06	0.57
Il	2.94	4.43	4.44	4.46	2.24	4.52	1.77	2.13
Ap	0.50	1.33	1.33	1.82	0.54	1.49	0.36	0.47
Pr	0.11	0.19	0.07	0.09	0.19	0.22	0.09	0.30
Cc	-	-	-	-	-	-	-	-
Sum	97.39	100.01	100.00	100.02	93.99	100.01	96.26	95.30
D.I.	29.74	41.62	41.41	44.36	44.19	39.89	21.05	43.71
Qz′	43.23	42.73	45.84	48.19	53.78	48.15	38.78	53.48
Ol′	30.80	39.02	35.11	28.17	25.09	36.81	40.47	26.84
Ne′	25.98	18.25	19.05	23.64	21.13	15.05	20.75	19.68

Sample Number	911A	911B	912	916	944	948	976	980
Qz	23.69	7.59	16.30	0.84	-	8.61	3.66	5.70
Or	26.42	14.77	23.28	2.60	3.07	8.21	7.51	7.98
Ab	26.82	22.00	24.79	20.31	16.33	18.70	22.09	27.50
An	6.54	17.29	10.25	32.05	32.78	28.38	20.58	18.92
Co	-	-	-	-	-	-	-	-
Di Wo	2.31	3.42	2.53	10.36	11.07	5.53	6.99	7.88
Di En	1.10	1.06	0.58	5.77	6.42	2.52	3.07	3.28
Di Fs	1.18	2.49	2.11	4.19	4.13	2.97	3.91	4.64
Hy En	0.09	6.73	3.11	8.75	6.69	8.76	8.46	5.71
Hy Fs	0.10	15.83	11.38	6.37	4.31	10.31	10.76	8.10
Fo	-	-	-	-	5.49	-	-	-
Fa	-	-	-	-	3.89	-	-	-
Mt	3.03	-	-	3.91	2.61	1.10	5.07	4.13
Il	1.12	2.79	1.63	2.28	2.05	1.96	3.80	3.19
Ap	0.26	0.54	0.33	0.43	0.31	0.38	0.64	0.64
Pr	1.89	1.76	0.92	0.11	0.65	0.04	0.04	0.04
Cc	-	-	-	-	-	-	-	-
Sum	94.57	96.29	97.22	97.98	99.80	97.47	96.57	97.70
D.I.	76.93	44.36	64.37	23.75	19.40	35.52	33.26	41.18
Qz/	71.04	44.64	56.09	39.19	28.51	47.74	41.72	46.48
Ol/	0.29	32.49	19.74	30.46	47.38	30.40	31.66	21.82
Ne/	28.67	22.86	24.18	30.35	24.11	21.85	26.62	31.70

Sample Number	991	1002	1066	1067	1095	118	1168	1171
Qz	3.30	-	2.06	4.77	2.73	6.31	5.50	9.65
Or	2.30	6.97	5.08	12.23	2.13	4.91	6.91	8.04
Ab	15.06	15.15	18.19	24.71	20.14	15.40	16.25	19.04
An	29.88	30.88	26.09	16.03	27.55	27.25	29.46	20.59
Co	-	-	-	-	-	-	-	-
Di Wo	9.07	11.09	10.43	7.97	10.42	8.59	7.28	5.34
Di En	4.57	5.96	5.12	3.00	4.92	3.30	3.16	1.93
Di Fs	4.30	4.77	5.11	5.11	5.36	5.42	4.11	3.52
Hy En	11.94	6.73	9.99	5.32	8.87	8.36	7.34	6.29
Hy Fs	11.22	5.39	9.98	9.05	9.66	13.75	9.55	11.46
Fo	-	3.75	-	-	-	-	-	-
Fa	-	3.31	-	-	-	-	-	-
Mt	2.04	1.77	3.84	5.03	3.81	0.10	4.12	4.99
Il	2.47	1.79	2.18	3.74	2.15	2.92	2.54	3.68
Ap	0.36	0.31	0.36	0.76	0.28	0.45	0.43	0.62
Pr	0.26	0.19	0.17	0.02	0.02	0.54	0.02	0.28
Cc	-	-	-	-	-	-	-	-
Sum	96.77	98.04	98.61	97.74	98.05	97.31	96.68	95.43
D.I.	20.66	22.12	25.33	41.71	25.00	26.62	28.66	36.73
Qz/	39.32	29.67	38.93	45.02	40.61	43.34	44.82	49.22
Ol/	41.01	46.41	36.56	24.44	33.03	37.59	32.40	28.55
Ne/	19.66	23.92	24.51	30.55	26.36	19.05	22.79	22.22

Sample Number	1192	1193	1197	1234	1255	1289	1293	1303
Qz	4.27	4.06	3.80	4.37	4.21	12.00	-	3.76
Or	7.51	3.13	4.96	5.44	6.56	10.46	28.54	9.40
Ab	15.91	18.19	18.70	18.70	15.23	16.50	11.85	18.11
An	25.11	28.90	24.93	24.31	24.11	23.16	14.65	20.90
Co	-	-	-	-	-	-	-	-
Di (Wo	3.49	7.63	10.01	9.50	9.60	4.77	9.82	8.41
Di (En	3.41	3.73	4.58	4.54	4.16	1.86	3.73	3.21
Di (Fs	5.16	3.76	5.34	4.82	5.44	2.98	6.25	5.33
Hy (En	9.04	9.99	8.69	8.48	8.67	6.11	2.79	6.97
Hy (Fs	13.69	10.04	10.13	8.99	11.34	9.79	4.68	11.56
Fo	-	-	-	-	-	-	0.25	-
Fa	-	-	-	-	-	-	0.45	-
Mt	0.59	4.20	3.00	4.23	4.55	4.22	5.89	4.20
Il	3.02	2.66	2.91	2.70	3.11	3.13	4.86	2.66
Ap	0.45	0.40	0.40	0.40	0.50	0.90	0.78	0.43
Pr	1.29	0.84	0.34	0.15	-	0.22	0.04	0.06
Cc	-	-	-	-	-	-	-	-
Sum	97.94	97.54	97.79	96.64	97.47	96.10	94.58	94.99
D.I.	27.69	25.38	27.46	28.51	26.00	38.96	40.39	31.27
Qz/	40.50	41.79	41.80	43.22	41.48	53.18	36.61	41.52
Ol/	39.40	34.89	33.66	31.78	37.59	26.68	31.31	34.18
Ne/	20.10	23.32	24.53	25.00	20.93	20.14	32.09	24.30

Sample Number	1317	1318	1341	1390	1392	1393	1397	1398
Qz	6.03	30.80	-	2.92	14.19	9.07	5.91	6.56
Or	11.35	29.14	9.63	5.85	12.88	7.68	6.03	6.26
Ab	19.72	20.99	18.62	19.55	17.26	16.33	19.29	15.99
An	19.48	1.60	22.18	25.05	20.15	25.21	22.47	24.32
Co	-	2.99	-	-	-	-	-	-
Di Wo	6.38	-	11.36	10.38	5.40	6.89	9.07	8.31
Di En	2.23	-	5.05	5.12	2.31	3.09	4.02	3.62
Di Fs	4.32	-	6.27	5.06	3.33	3.76	5.02	4.68
Hy En	5.99	1.15	5.91	8.47	4.62	6.29	6.29	6.91
Hy Fs	11.62	5.67	7.33	8.36	7.22	7.64	7.84	8.95
Fo	-	-	1.15	-	-	-	-	-
Fa	-	-	1.57	-	-	-	-	-
Mt	5.00	3.07	3.38	3.77	4.78	4.77	4.96	4.94
Il	3.70	1.18	3.44	2.73	3.42	3.57	3.65	3.63
Ap	0.57	0.21	0.64	0.38	0.92	0.71	0.62	0.64
Pr	0.02	0.02	0.65	0.30	0.36	1.18	1.07	1.07
Cc	-	-	-	-	-	-	-	-
Sum	96.39	96.80	97.18	97.94	96.67	96.19	96.22	95.90
D.I.	37.10	80.93	28.25	28.32	44.33	33.08	31.23	28.81
Qz/	44.97	71.74	34.60	41.50	58.03	51.28	46.82	46.84
Ol/	30.38	8.85	36.22	31.54	20.36	26.21	26.59	30.60
Ne/	24.65	19.41	29.18	26.96	21.61	22.50	26.59	22.56

Sample Number	1401	1407	9554
Qz	4.77	9.21	9.17
Or	7.62	6.62	11.05
Ab	24.46	16.92	19.46
An	18.20	28.86	19.76
Co	-	-	-
Di(Wo	6.60	4.91	6.51
Di(En	2.34	2.63	2.69
Di(Fs	4.42	2.13	3.86
Hy(En	8.02	7.09	6.00
Hy(Fs	15.14	5.73	8.63
Fo	-	-	-
Fa	-	-	-
Mt	-	4.57	5.05
Il	3.68	3.13	3.76
Ap	0.71	0.62	0.85
Pr	2.41	2.83	-
Cc	-	0.91	-
Sum	98.38	96.40	96.80
D.I.	36.85	32.75	39.68
Qz/	41.64	52.35	50.49
Ol/	33.05	24.11	25.13
Ne/	25.30	23.55	24.39

APPENDIX IX

C.I.P.W. Norms of Miscellaneous Carlingford Rocks.

Suffix to sample number indicates rock type.

(see Appendix V)

Qz		Quartz
Or		Orthoclase
Ab		Albite
An		Anorthite
Co		Corundum
Di	Wo, En, Fs	Clinopyroxene
Hy	En, Fs	Hypersthene
Fo		Forsterite
Fa		Fayalite
Mt		Magnetite
He		Hematite
Il		Ilmenite
Ru		Rutile
Ap		Apatite
Pr		Pyrite
Cc		Calcite
D.I.		Differentiation Index
Qz′	Quartz	Quartz, albite, hypersthene, forsterite, fayalite recalculated to 100% as these components.
Ol′	Olivine	
Ne′	Nepheline	

* CO_2 in excess of normative Calcite not included in norm.

Sample Number		1.X.	2.G.	12.X.	13.E.G	15.G.	19.B
Qz		3.96	22.75	3.23	1.14	26.23	-
Or		8.63	28.13	3.19	5.02	33.69	2.13
Ab		25.47	33.00	17.60	17.52	25.56	16.84
An		15.17	4.48	46.34	28.26	6.31	35.08
Co		-	-	-	-	-	-
Di	Wo	9.42	2.23	5.19	10.61	1.36	5.41
	En	3.94	0.68	2.74	5.83	0.33	3.30
	Fs	5.53	1.64	2.29	4.38	1.11	1.80
Hy	En	6.30	0.66	7.19	10.85	0.31	16.02
	Fs	8.84	1.60	6.01	8.15	1.04	8.73
Fo		-	-	-	-	-	1.36
Fa		-	-	-	-	-	-
Mt		5.74	3.06	2.99	3.18	1.99	4.18
He		-	-	-	-	-	-
Il		4.67	1.16	1.42	1.73	0.68	2.62
Ru		-	-	-	-	-	-
Ap		0.64	0.31	0.24	0.26	0.07	0.28
Pr		0.36	0.02	0.41	0.02	0.02	0.02
Cc		-	-	-	-	-	-
Sum		98.66	99.72	98.86	96.95	98.70	98.60
D.I.		38.06	83.13	24.02	23.68	85.48	18.97
Qz′		43.80	66.24	43.53	37.89	72.01	33.13
Ol′		25.23	2.93	28.45	36.90	1.92	46.02
Ne′		30.97	30.83	28.03	25.21	26.07	20.85

Sample Number		21.B	29a.G.	29b.G.	29c.G.	31.S	32.M
Qz		0.79	22.99	4.89	17.27	20.47	
Or		5.61	31.79	30.91	30.14	8.92	
Ab		19.80	26.23	27.84	24.71	15.99	
An		29.59	7.17	5.64	7.99	16.72	
Co		-	-	-	-	-	
Di	Wo	6.16	1.10	6.20	2.39	11.07	
	En	3.35	0.05	1.65	0.61	7.25	
	Fs	2.60	1.18	4.88	1.90	3.05	
Hy	En	11.30	0.17	1.99	1.55	1.55	
	Fs	8.76	3.81	5.90	4.82	0.65	
Fo		-	-	-	-	-	
Fa		-	-	-	-	-	
Mt		2.74	3.18	4.44	3.64	1.23	
He		-	-	-	-	-	
Il		3.29	1.31	2.96	1.92	1.31	
Ru		-	-	-	-	-	
Ap		0.78	0.26	1.18	0.50	0.36	
Pr		0.04	0.02	0.02	0.02	0.04	
Cc		-	-	-	-	-	
Sum		94.79	99.25	98.51	97.46	88.60	
D.I.		26.20	81.01	63.64	72.12	45.38	
Qz/		37.50	67.52	48.20	62.35	73.48	
Ol/		36.10	5.75	14.65	9.96	4.10	
Ne/		26.40	26.73	37.15	27.69	22.42	

NOT CALCULATED

Sample Number		34.X.	373.X.	396.E.	593.F.	636.E.	746.C.
Qz		0.03	0.95	2.19	28.95	-	
Or		11.70	6.12	1.12	17.55	2.95	
Ab		8.04	17.40	13.29	24.88	19.12	
An		53.96	60.55	33.62	6.96	50.70	
Co		-	-	-	-	-	
Di	Wo	2.03	2.98	12.10	-	5.21	
	En	1.15	1.82	6.82	-	2.89	
	Fs	0.79	0.99	4.78	-	2.12	
Hy	En	9.59	3.12	11.21	6.00	4.23	
	Fs	6.65	1.69	7.87	4.89	3.11	
Fo		-	-	-	-	1.64	
Fa		-	-	-	-	1.33	
Mt		0.36	2.37	3.18	1.23	1.64	
He		-	-	-	-	-	
Il		0.82	0.76	1.50	0.72	1.16	
Ru		-	-	-	-	-	
Ap		0.12	0.17	0.02	0.95	0.19	
Pr		0.30	0.07	0.30	0.04	0.06	
Cc		-	-	-	-	-	
Sum		95.52	98.99	97.99	97.36	96.35	
D.I.		19.77	24.47	16.60	71.38	22.07	
Qz/		33.32	44.21	38.86	66.84	36.48	
Ol/		48.75	15.07	40.31	12.33	28.30	
Ne/		17.93	40.72	20.84	20.83	35.22	

NOT CALCULATED

Sample Number		839.F./	859.R.	885.F*	897.F.	945.S.	1082.E
Qz		17.02	39.92	25.92	28.55	21.76	1.57
Or		14.66	26.77	16.12	19.92	27.24	4.08
Ab		31.39	27.33	27.27	21.83	9.73	16.25
An		7.59	0.41	-	11.33	3.20	25.91
Co		-	0.74	6.73	3.65	10.50	-
Di	Wo	10.39	-	-	-	-	7.43
	En	6.35	-	-	-	-	3.03
	Fs	3.45	-	-	-	-	4.43
Hy	En	2.34	0.50	5.40	3.69	10.31	9.14
	Fs	1.27	-	4.49	0.58	9.42	13.41
Fo		-	-	-	-	-	-
Fa		-	-	-	-	-	-
Mt		1.58	-	0.75	3.45	1.97	6.16
He		-	1.37	-	-	-	-
Il		1.54	0.19	1.67	1.67	1.75	5.22
Ru		-	0.05	-	-	-	-
Ap		0.40	0.02	1.01	0.95	0.26	0.24
Pr		0.02	0.04	0.11	0.07	0.47	0.02
Cc		-	0.11	6.35*	-	-	-
Sum		98.01	97.45	95.82	95.68	96.61	96.92
D.I.		63.07	94.02	69.81	70.30	58.73	21.90
Qz/		62.26	77.62	65.08	72.81	61.40	36.67
Ol/		5.03	0.51	11.49	5.54	28.30	41.52
Ne/		32.71	21.87	23.43	21.65	10.30	21.81

Sample Number		1180.F	1203.Q	1212.Q	1235.L	1236.L	1250.F
Qz		24.85	29.64	26.56	9.28	14.37	29.35
Or		20.80	27.30	25.88	11.11	13.42	19.50
Ab		20.48	26.99	33.26	31.39	22.85	28.18
An		12.64	6.14	4.27	21.29	21.86	8.96
Co		3.23	2.58	1.94	-	1.35	3.50
Di	Wo	-	-	-	0.34	-	-
	En	-	-	-	0.22	-	-
	Fs	-	-	-	0.10	-	-
Hy	En	6.50	1.99	1.99	11.61	13.10	3.16
	Fs	4.14	1.58	0.62	5.49	5.17	3.45
Fo		-	-	-	-	-	-
Fa		-	-	-	-	-	-
Mt		1.04	0.77	1.41	2.15	2.64	0.75
He		-	-	-	-	-	-
Il		1.65	0.53	0.51	2.28	2.37	0.97
Ru		-	-	-	-	-	-
Ap		0.99	0.24	0.21	0.71	0.71	0.47
Pr		0.04	-	0.02	0.02	0.02	0.02
Cc		-	-	-	-	-	-
Sum		96.36	97.77	96.68	95.98	97.86	98.32
D.I.		66.13	83.93	85.70	51.78	50.64	77.03
Qz/		66.33	71.35	68.12	49.13	53.95	68.59
Ol/		13.84	4.34	3.01	21.41	23.73	7.60
Ne/		19.83	24.30	28.87	29.45	22.32	23.81

Sample Number		1350.L	1366.L
Qz		10.43	13.65
Or		16.19	17.26
Ab		24.46	25.56
An		17.44	22.43
Co		2.78	-
Di	Wo	-	2.38
	En	-	1.22
	Fs	-	1.10
Hy	En	11.80	3.68
	Fs	7.53	3.32
Fo		-	-
Fa		-	-
Mt		1.38	3.87
He		-	-
Il		2.75	2.22
Ru		-	-
Ap		0.78	0.73
Pr		0.17	0.02
Cc		-	-
Sum		95.71	97.46
D.I.		51.00	56.47
Qz/		49.58	58.90
Ol/		25.97	11.13
Ne/		24.45	29.97

APPENDIX X

Trace Element Concentrations in
Rocks of the Alkali Basalt Series

Values in P.P.M.

N.D. Not Determined

BLD Below Limits of Detection

Sample Number	36	61	64	66	96	102	107	115
Sc	55	41	54	45	59	58	57	59
V	217	118	167	187	171	43	344	103
Cr	75	89	41	108	44	40	51	43
Co	74	75	77	83	63	74	58	84
Ni	85	91	104	90	95	117	42	126
Cu	94	105	90	86	107	105	90	102
Zn	90	101	87	92	78	71	81	63
Ga	18	20	19	19	17	15	19	15
Ge	1	3	2	1	2	2	2	3
Rb	7	19	13	36	7	4	19	8
Sr	288	164	172	316	289	306	306	309
Y	35	48	30	28	26	24	35	24
Zr	145	287	134	290	99	96	184	106
Sn	4	2	3	1	5	BLD	BLD	3
Ba	555	477	515	689	540	480	739	507
Ce	66	70	57	53	56	65	78	49
Pb	22	23	21	21	19	22	21	19
Th	4	2	4	5	3	2	4	3
U	BLD	BLD	1	BLD	BLD	BLD	BLD	1

Sample Number	119	135	140	143	191	379	435	745
Sc	58	57	63	67	40	72	57	33
V	115	243	181	239	204	265	264	97
G	42	36	40	38	22	199	228	190
Co	80	69	71	72	49	62	67	37
Ni	123	11	68	61	45	141	182	121
Cu	102	79	150	158	93	92	107	92
Zn	69	117	74	80	96	94	95	195
Ga	15	20	20	18	19	19	18	25
Ge	2	1	BLD	BLD	2	2	1	2
Rb	8	50	13	15	44	16	24	42
Sr	299	312	284	300	425	371	280	231
Y	22	44	2	31	36	33	24	69
Zr	106	231	133	155	322	184	191	258
Sn	3	7	BLD	BLD	7	3	3	4
Ba	440	734	580	504	1419	625	603	599
Ce	50	86	54	57	147	78	50	66
Pb	17	22	22	20	42	25	20	22
Th	3	8	3	1	11	3	2	10
U	BLD	BLD	BLD	BLD	2	BLD	BLD	1

Sample Number	748	783	799	802	807	831	840	1175
Sc	38	54	44	37	63	65	56	49
V	119	198	234	182	156	203	245	158
Cr	7	14	395	39	524	187	109	558
Co	14	59	70	48	97	82	74	74
Ni	10	119	292	53	362	78	92	432
Cu	60	118	120	78	122	134	132	118
Zn	64	86	61	84	77	97	126	80
Ga	22	17	15	19	15	21	19	15
Ge	1	2	1	1	2	3	2	2
Rb	27	4	6	15	9	28	26	17
Sr	229	507	406	356	399	315	604	471
Y	66	25	20	22	20	31	40	17
Zr	294	158	162	241	136	141	172	145
Sn	7	2	4	6	2	4	6	3
Ba	461	383	314	567	575	534	1041	614
Ce	108	63	42	88	43	65	31	59
Pb	17	20	18	23	17	24	35	22
Th	7	3	5	7	2	3	6	3
U	1	BLD	BLD	4	1	BLD	BLD	BLD

Sample Number	1319	1320	1351	1382	9556
Sc	53	37	54	32	N.D
V	189	135	129	104	N.D
Cr	47	BLD	61	BLD	28
Co	35	36	65	6	78
Ni	73	10	64	5	104
Cu	76	71	80	71	89
Zn	89	98	95	147	117
Ga	20	19	18	25	17
Ge	2	1	2	3	1
Rb	11	56	21	59	5
Sr	254	271	229	299	457
Y	35	60	32	91	29
Zr	145	599	140	553	133
Sn	2	8	3	4	N.D
Ba	631	1426	701	1675	335
Ce	53	144	71	144	53
Pb	21	40	21	31	23
Th	4	14	4	10	2
U	2	3	1	1	BLD

APPENDIX XI

Trace element concentration in rocks of the High Alumina Basalt Series.

Values in P.P.M.

N.D. Not Determined

BLD Below limits of detection

Sample Number	40	45	74	114	124	137	141	190	269	273	399	426	437
Sc	55	ND	70	75	72	70	71	68	62	72	81	70	72
V	80	ND	133	130	97	143	133	94	100	127	137	141	115
Cr	92	ND	230	240	171	183	123	74	64	126	138	184	115
Co	50	ND	62	74	32	20	52	48	49	42	33	76	51
Ni	35	ND	105	107	34	31	79	42	34	52	41	130	79
Cu	94	ND	ND	166	99	101	126	117	91	109	105	169	131
Zn	48	ND	ND	64	55	70	75	49	66	75	16	81	46
Ga	15	ND	ND	17	18	18	18	17	16	19	17	16	16
Ge	2	ND	ND	3	3	2	2	1	1	2	1	1	1
Rb	39	ND	ND	22	9	10	7	14	37	19	12	7	6
Sr	192	ND	ND	199	266	329	638	235	212	213	264	186	191
Y	13	ND	ND	16	15	20	26	17	24	21	12	20	13
Zr	59	ND	80	77	72	92	139	75	ND	90	63	73	55
Sn	4	ND	2	2	1	3	3	3	1	3	2	1	3
Ba	577	ND	453	317	383	353	566	532	634	438	551	417	593
Ce	16	ND	47	48	46	51	57	46	66	60	44	50	67
Pb	23	ND	ND	20	15	17	20	14	25	22	17	16	15
Th	4	ND	ND	2	2	1	6	3	7	3	2	1	BLD
U	BLD	ND	ND	BLD	BLD	BLD	BLD	BLD	2	BLD	BLD	1	2

Sample Number	442	443	444	450	452	458	563	658	665	718	1001	1119	1162
Sc	70	49	78	78	73	61	61	63	74	74	78	76	69
V	123	115	149	112	115	111	148	91	120	121	102	144	106
Cr	180	171	94	94	204	173	86	144	97	148	134	233	40
Co	70	28	60	23	46	70	52	53	50	41	51	56	49
Ni	51	23	99	60	80	104	35	100	108	76	43	112	37
Cu	106	78	173	122	122	120	100	135	190	180	106	191	121
Zn	69	77	66	44	59	64	71	57	67	76	53	76	94
Ga	17	17	17	14	16	15	17	16	14	15	17	16	18
Ge	1	3	BLD	2	2	2	BLD	2	1	2	2	1	2
Rb	11	80	27	6	22	37	26	30	11	32	15	16	23
Sr	161	134	157	193	236	226	249	225	113	172	251	184	167
Y	21	49	22	13	14	17	28	17	19	17	13	19	19
Zr	80	ND	98	45	69	ND	ND	ND	48	191	58	78	63
Sn	2	6	6	BLD	BLD	2	5	1	1	2	4	2	4
Ba	411	1050	575	188	612	652	711	591	286	713	509	349	566
Ce	48	107	36	59	46	49	61	50	33	59	62	43	39
Pb	25	31	32	16	23	21	21	27	20	23	15	40	33
Th	3	16	5	BLD	2	4	4	6	1	2	1	2	3
U	BLD	3	BLD	BLD	BLD	BLD	BLD	1	BLD	BLD	BLD	BLD	BLD

Sample Number	1166	1352	1387	1399
Sc	63	67	73	68
V	126	133	104	167
Cr	32	248	80	37
Co	41	71	46	59
Ni	33	155	40	35
Cu	111	175	97	108
Zn	104	58	56	86
Ga	17	15	18	18
Ge	2	2	2	2
Rb	61	39	34	30
Sr	163	133	176	282
Y	32	20	19	25
Zr	148	70	ND	128
Sn	1	2	1	4
Ba	719	643	525	551
Ce	76	57	46	52
Pb	44	21	19	24
Th	11	3	3	6
U	1	1	BLD	2

APPENDIX XII

Trace element concentrations in rocks of the Tholeiitic Basalt Craignurite Series.

Values in P.P.M.

N.D. Not determined

BLD Below limits of detection

Sample Number	3	5	6	9	11	18	22	23	24	25	27	28	30
Sc	56	19	66	77	72	75	35	19	61	16	67	75	72
V	250	43	189	192	198	173	89	37	206	35	136	273	149
Cr	35	50	61	128	36	21	53	1	11	1	16	99	17
Co	88	7	60	62	64	64	30	10	60	8	57	68	49
Ni	24	9	18	54	39	19	32	7	15	10	12	91	14
Cu	106	52	88	118	378	105	80	71	93	63	87	207	147
Zn	120	86	111	108	277	126	97	85	144	78	121	123	129
Ga	20	22	19	18	20	21	19	18	20	20	21	18	19
Ge	2	1	2	3	3	4	2	2	3	3	2	3	4
Rb	28	124	37	77	23	21	146	183	93	204	104	59	74
Sr	443	232	237	166	153	144	109	71	113	69	136	125	125
Y	41	62	38	29	39	43	49	57	56	60	55	27	54
Zr	201	496	188	101	152	162	196	450	202	488	288	91	256
Sn	2	8	3	6	4	3	6	3	3	9	6	3	6
Ba	598	1086	759	400	542	615	666	1091	908	1254	968	393	944
Ce	92	115	89	67	59	71	74	115	120	112	135	48	128
Pb	27	37	32	24	56	27	27	52	41	44	29	19	34
Th	6	26	7	3	5	3	21	29	15	32	20	7	16
U	1	5	BLD	BLD	BLD	BLD	4	6	1	6	2	1	2

Sample Number	33	35	37	38	46	53	54	58	59	63	67	68	71
Sc	58	56	64	73	38	76	78	35	59	71	76	62	71
V	152	131	153	138	105	154	180	99	150	214	175	149	235
Cr	23	20	15	64	50	218	696	36	60	18	42	207	25
Co	54	38	40	57	30	76	92	30	61	40	64	58	61
Ni	27	19	15	60	28	175	535	22	23	16	45	89	26
Cu	81	77	82	127	68	177	205	66	78	75	133	186	120
Zn	112	90	107	72	81	60	64	84	115	184	128	64	119
Ga	19	19	20	19	19	17	15	18	22	24	20	18	18
Ge	1	3	2	2	3	2	2	3	3	2	2	2	1
Rb	44	111	87	21	68	10	9	79	90	72	46	9	29
Sr	215	152	170	168	157	330	189	166	144	189	251	151	201
Y	27	42	52	31	35	22	20	36	54	60	44	26	42
Zr	177	275	274	128	270	78	87	346	267	134	207	124	166
Sn	2	3	6	2	4	BLD	4	3	3	3	3	1	2
Ba	647	910	977	563	888	478	311	942	911	1022	821	516	581
Ce	78	86	107	47	95	33	50	104	107	114	76	79	61
Pb	30	38	33	25	32	16	19	32	33	38	21	23	25
Th	9	16	18	6	18	BLD	2	21	16	14	8	3	5
U	1	4	1	1	3	1	BLD	6	2	1	1	BLD	1

Sample Number	72	73	75	76	78	80	84	93	97	99	111	113	122
Sc	88	61	65	62	74	74	67	37	68	60	76	76	76
V	262	222	214	65	188	202	144	100	248	108	223	161	160
Cr	261	43	29	360	426	60	630	86	28	366	134	197	228
Co	91	68	40	103	86	50	91	31	83	72	69	55	55
Ni	93	30	32	407	386	25	394	22	44	197	81	88	81
Cu	174	87	73	166	111	119	152	109	148	129	180	158	161
Zn	88	118	109	72	95	95	69	60	118	59	73	80	74
Ga	20	19	18	15	19	19	15	17	18	13	19	17	18
Ge	3	3	2	1	4	4	1	3	1	2	1	4	2
Rb	36	65	19	18	31	34	13	80	16	41	17	48	30
Sr	464	276	763	239	257	298	235	252	262	154	138	276	267
Y	29	42	52	20	33	35	20	28	30	13	29	20	25
Zr	167	214	375	87	137	163	84	324	140	66	133	132	129
Sn	7	4	6	3	2	2	3	6	4	BLD	BLD	BLD	4
Ba	687	599	1480	472	378	669	342	911	466	449	456	541	511
Ce	55	84	133	46	38	64	30	77	56	35	49	43	47
Pb	26	29	23	18	23	29	19	39	20	19	19	22	24
Th	7	8	15	1	5	4	1	20	4	3	4	3	5
U	1	2	BLD	BLD	1	2	1	4	BLD	BLD	2	1	BLD

Sample Number	123	125	127	130	131	133	142	145	147	151	155	156	158
Sc	66	81	55	60	64	64	68	82	70	25	66	68	46
V	159	158	205	116	231	235	127	170	138	97	206	217	136
Cr	41	124	49	69	91	17	165	199	302	7	31	172	1
Co	53	67	49	50	55	46	55	64	69	34	59	62	21
Ni	25	99	12	67	45	16	116	136	59	10	22	88	8
Cu	100	180	77	134	137	82	126	175	124	59	79	142	54
Zn	97	72	109	98	100	118	70	64	95	99	115	97	132
Ga	20	17	21	19	20	23	17	17	18	21	21	17	22
Ge	1	2	2	2	2	BLD	2	3	2	3	2	2	3
Rb	46	17	57	27	19	55	8	6	35	143	71	19	86
Sr	203	153	354	363	378	339	393	389	152	143	337	282	345
Y	39	21	42	28	37	47	23	23	30	13	43	32	66
Zr	220	78	254	134	160	243	109	107	93	372	214	131	396
Sn	4	BLD	4	1	BLD	BLD	2	5	9	3	6	4	7
Ba	798	249	829	915	654	729	460	332	478	958	993	454	1227
Ce	65	31	96	107	69	77	48	39	62	99	88	51	136
Pb	28	18	35	16	31	31	22	22	25	40	32	36	37
Th	10	4	11	4	7	10	5	2	7	21	11	1	17
U	1	BLD	3	1	1	BLD	1	1	1	4	2	1	2

Sample Number	160	162	166	173	174	175	176	181	192	235	236	253	292
Sc	62	63	46	69	66	59	71	66	65	69	50	69	77
V	110	182	118	145	159	130	165	222	171	116	92	144	166
Cr	233	307	48	247	254	144	235	85	92	234	156	674	208
Co	54	52	47	43	81	50	36	47	62	51	40	106	48
Ni	176	49	9	45	52	33	43	36	57	168	22	453	114
Cu	116	72	64	100	94	88	95	99	144	155	85	153	148
Zn	61	92	111	100	97	110	98	89	84	65	80	82	75
Ga	16	20	21	18	18	19	19	19	17	15	17	13	16
Ge	1	4	1	2	2	BLD	1	2	1	2	2	1	2
Rb	29	54	86	50	47	64	46	41	17	14	88	18	26
Sr	216	419	156	148	151	167	155	229	218	193	132	118	183
Y	17	34	59	41	40	50	40	35	29	20	44	19	23
Zr	98	95	268	175	175	205	180	142	142	ND	301	80	91
Sn	2	1	11	5	1	8	6	4	3	5	5	2	BLD
Ba	501	441	942	577	653	763	575	551	518	546	884	360	423
Ce	44	41	96	69	85	93	74	66	55	44	85	56	46
Pb	22	24	39	42	30	31	31	26	46	20	34	97	29
Th	6	6	16	9	9	13	10	5	4	4	19	1	3
U	3	1	2	1	2	1	2	1	BLD	BLD	3	BLD	BLD

Sample Number	297	298	300	305	314	330	369	371	400	421	424	425	429
Sc	69	66	68	76	61	63	74	66	79	71	53	63	59
V	158	118	205	159	171	107	278	223	155	147	84	160	125
Cr	182	268	183	245	170	176	181	18	155	314	180	172	167
Co	67	82	60	87	57	74	98	77	72	65	42	65	62
Ni	72	271	66	157	70	157	86	28	130	217	133	85	79
Cu	179	164	123	158	124	100	119	100	278	160	131	128	140
Zn	88	94	88	81	84	91	102	118	89	84	76	74	84
Ga	16	15	17	16	20	20	19	20	17	15	14	15	16
Ge	3	1	1	1	BLD	2	3	2	2	3	1	1	3
Rb	19	16	15	32	16	55	10	31	8	28	36	17	33
Sr	230	124	207	204	244	196	232	219	150	168	168	187	201
Y	24	16	28	21	29	38	25	41	20	19	16	21	25
Zr	110	79	95	61	117	92	101	178	63	80	62	52	139
Sn	6	4	4	4	5	4	3	2	BLD	2	BLD	3	3
Ba	474	341	616	331	500	435	557	862	394	436	445	278	475
Ce	51	38	65	45	42	47	56	70	34	42	33	59	63
Pb	25	39	25	25	27	30	32	29	29	22	17	20	15
Th	6	2	3	3	3	10	3	8	1	2	2	2	6
U	1	BLD	1	1	1	BLD	BLD	BLD	BLD	1	BLD	BLD	BLD

Sample Number	438	439	441	445	451	457	461	499	500	536	557	559	562
Sc	76	70	78	65	66	73	71	75	70	91	58	74	63
V	165	154	121	172	188	208	153	180	178	148	131	181	174
Cr	203	102	255	110	160	159	55	235	183	484	47	102	84
Co	63	59	77	97	59	76	50	74	64	108	59	58	72
Ni	72	102	151	111	102	102	53	111	80	90	35	53	31
Cu	148	182	190	184	145	150	120	156	145	127	118	119	112
Zn	76	75	69	86	86	88	68	82	91	71	114	97	103
Ga	16	16	15	17	16	18	15	16	19	14	19	18	18
Ge	2	2	4	BLD	3	BLD	1	3	2	3	3	4	1
Rb	28	49	10	26	40	41	22	21	8	27	28	11	28
Sr	130	133	121	127	206	212	201	201	228	155	186	183	164
Y	24	30	22	29	29	29	25	24	31	23	39	28	53
Zr	81	124	66	124	113	ND	131	83	119	84	145	98	190
Sn	3	3	2	4	BLD	5	1	4	1	1	4	4	6
Ba	369	575	432	560	321	469	471	531	516	397	658	492	686
Ce	60	44	33	61	47	53	52	33	58	54	60	64	78
Pb	22	26	20	32	24	23	28	22	25	22	31	20	23
Th	2	8	3	8	6	6	9	3	5	4	6	20	8
U	BLD	2	BLD	2	BLD	1	BLD	BLD	1	BLD	1	1	BLD

Sample Number	565	568	589	603	605	619	625	629	630	659	663	664	682
Sc	71	70	58	72	58	32	58	66	73	74	65	73	68
V	205	69	135	152	184	95	172	169	164	171	229	133	146
Cr	27	88	24	250	25	25	28	101	134	207	29	119	208
Co	57	31	64	81	68	26	45	32	22	62	81	86	60
Ni	26	41	24	142	27	19	15	64	68	117	63	163	110
Cu	99	112	93	163	86	79	82	128	122	181	186	168	157
Zn	98	58	97	86	141	65	89	94	92	78	107	78	88
Ga	18	18	20	17	20	19	22	20	17	16	19	16	18
Ge	1	3	3	2	2	BLD	2	3	3	2	2	2	2
Rb	29	15	50	14	45	113	74	18	49	6	31	13	49
Sr	186	225	222	186	190	184	194	200	213	200	138	145	196
Y	38	23	38	22	38	35	65	30	23	20	29	19	21
Zr	159	167	189	ND	178	322	362	ND	ND	82	ND	61	83
Sn	2	2	6	3	2	5	5	3	3	BLD	3	3	3
Ba	675	535	823	382	760	912	1110	560	632	465	456	372	613
Ce	76	42	81	46	78	82	127	69	122	58	51	37	65
Pb	30	21	26	22	27	30	36	26	26	21	26	21	25
Th	10	5	7	1	8	20	14	5	2	3	5	2	4
U	BLD	BLD	2	BLD	BLD	5	1	BLD	BLD	BLD	6	BLD	BLD

Sample Number	684	719	744	747	759	762	765	766	767	768	769	770	771
Sc	31	70	58	63	66	71	52	54	49	72	73	79	65
V	130	126	171	183	145	136	231	203	216	160	131	141	139
Cr	103	234	29	26	195	111	45	21	21	268	306	170	193
Co	64	64	46	85	55	76	58	44	51	74	83	78	83
Ni	94	181	14	53	44	113	50	29	26	149	150	130	71
Cu	197	204	85	149	97	204	89	90	75	192	180	195	126
Zn	65	85	118	114	99	64	123	108	118	80	78	62	67
Ga	18	16	22	20	20	16	21	20	21	18	18	17	18
Ge	3	3	2	2	2	3	1	2	1	2	2	3	3
Rb	10	12	82	58	47	12	ND	65	84	27	42	12	19
Sr	123	196	208	210	154	139	ND	159	116	156	176	147	221
Y	22	20	60	30	38	22	ND	43	32	22	21	21	24
Zr	56	72	285	103	167	ND	184	216	ND	67	92	77	92
Sn	BLD	3	4	BLD	4	2	5	4	9	BLD	4	3	BLD
Ba	407	358	975	490	705	456	685	670	709	321	507	406	593
Ce	40	38	117	53	66	42	76	91	66	54	51	41	53
Pb	22	33	29	25	28	21	ND	29	23	19	30	19	22
Th	1	3	13	1	6	3	ND	10	12	2	2	BLD	5
U	BLD	2	2	BLD	BLD	2	ND	2	3	BLD	1	2	1

Sample Number	772	775	780	827	830	841	842	850	851	852	856	864	876
Sc	74	56	56	60	48	66	59	15	62	72	76	74	54
V	155	196	235	265	214	179	133	65	186	208	150	192	208
Cr	260	22	27	25	12	43	168	BLD	43	48	73	45	23
Co	73	53	40	67	26	26	41	BLD	50	69	57	66	47
Ni	141	33	36	33	24	32	68	8	23	27	65	42	24
Cu	172	89	89	113	78	141	140	61	98	89	127	123	73
Zn	79	114	111	121	100	125	88	39	321	92	71	112	112
Ga	38	45	20	20	20	19	16	19	19	18	17	17	19
Ge	3	4	2	2	1	3	2	2	1	3	2	4	2
Rb	63	63	56	34	87	25	26	157	68	57	27	36	88
Sr	157	157	537	261	272	584	567	81	174	167	163	154	252
Y	18	43	42	40	41	38	25	59	39	39	30	34	48
Zr	ND	216	196	185	230	210	224	493	208	185	117	162	299
Sn	BLD	4	5	5	5	5	5	8	5	4	BLD	6	3
Ba	385	632	596	590	706	562	599	1080	703	704	549	559	1243
Ce	33	79	91	69	55	76	58	128	72	78	31	50	142
Pb	26	35	31	26	30	30	24	30	103	46	22	32	38
Th	2	10	10	7	14	8	10	26	9	5	4	5	11
U	BLD	2	2	1	2	BLD	1	6	BLD	2	BLD	BLD	BLD

Sample Number	877	878	879	884	889	891	911A	911B	912	916	944	948	976
Sc	49	51	52	55	65	54	19	18	27	77	72	55	54
V	199	209	162	200	117	131	52	174	87	152	135	99	196
Cr	107	10	73	20	231	109	1	18	8	231	247	171	71
Co	52	33	55	42	75	45	9	40	21	67	62	53	61
Ni	20	10	41	19	157	50	3	16	4	87	159	29	58
Cu	77	68	105	96	152	101	61	64	65	151	206	93	81
Zn	120	106	83	107	69	78	20	338	79	74	73	88	113
Ga	19	18	16	19	17	17	19	19	18	18	16	17	21
Ge	4	1	2	3	2	1	3	3	1	2	3	3	3
Rb	58	41	98	48	40	92	167	150	102	15	24	60	44
Sr	231	237	196	222	160	179	84	150	129	247	164	146	181
Y	47	56	29	37	17	29	58	40	60	23	21	42	45
Zr	166	378	228	ND	91	240	482	249	447	98	65	215	191
Sn	7	5	7	5	BLD	5	6	6	7	5	3	1	6
Ba	665	838	790	1305	473	706	1099	746	1052	556	388	648	722
Ce	100	160	78	141	52	82	113	66	108	60	40	107	72
Pb	40	35	32	26	26	31	25	160	87	22	18	21	32
Th	12	14	13	6	ND	ND	27	11	25	3	BLD	12	6
U	3	1	3	2	BLD	3	9	1	5	BLD	1	BLD	1

Sample Number	980	991	1002	1066	1067	1095	1118	1168	1171	1192	1193	1197
Sc	51	71	67	71	53	68	75	63	48	64	63	62
V	186	178	130	146	214	137	216	127	179	193	134	152
Cr	52	239	121	69	10	55	50	28	13	35	35	51
Co	47	75	83	56	60	66	48	66	63	60	60	69
Ni	29	52	148	53	14	50	34	29	20	29	79	33
Cu	89	112	168	162	80	151	103	127	100	108	187	104
Zn	80	89	77	115	128	91	88	119	161	107	73	99
Ga	21	17	15	19	21	20	19	19	20	19	20	19
Ge	1	1	3	3	4	BLD	1	3	1	3	1	2
Rb	41	10	53	40	93	15	27	62	65	60	19	28
Sr	199	136	165	141	168	204	148	156	176	147	156	156
Y	46	31	18	30	53	29	38	33	40	39	34	36
Zr	240	109	ND	96	251	87	258	123	168	179	111	154
Sn	2	4	4	2	5	3	4	1	10	2	3	2
Ba	838	378	447	460	917	505	769	508	646	500	362	1619
Ce	88	72	46	47	94	60	83	71	67	81	71	65
Pb	25	26	22	23	30	23	24	39	41	22	27	29
Th	10	8	4	4	15	7	10	9	10	7	6	8
U	BLD	BLD	BLD	BLD	BLD	BLD	2	2	BLD	BLD	1	2

Sample Number	1234	1255	1289	1293	1303	1317	1318	1341	1390	1392	1393	1397
Sc	68	ND	52	61	55	50	20	79	68	55	57	62
V	176	ND	179	208	168	222	266	236	134	203	221	254
Cr	53	55	23	56	27	24	4	76	65	34	33	110
Co	67	50	50	40	68	55	14	66	69	69	97	61
Ni	36	48	34	29	39	26	12	64	58	30	28	79
Cu	108	132	96	80	147	96	59	167	129	80	86	113
Zn	106	114	158	156	258	163	98	95	78	117	114	111
Ga	19	19	17	20	20	22	20	18	18	17	20	18
Ge	2	2	3	2	2	3	2	2	2	2	1	1
Rb	31	34	67	349	87	97	194	113	31	84	50	29
Sr	165	139	154	180	178	178	83	154	173	303	231	205
Y	35	35	51	37	42	39	57	34	32	44	38	41
Zr	151	107	216	245	143	163	454	107	129	77	191	130
Sn	1	ND	4	4	3	7	10	1	6	5	3	3
Ba	466	434	729	681	614	602	1241	336	572	727	557	527
Ce	87	48	95	71	60	60	99	49	52	82	73	56
Pb	29	24	32	53	83	50	63	28	24	30	28	21
Th	6	4	9	9	5	7	27	6	7	9	21	5
U	2	BLD	1	1	BLD	2	7	BLD	1	3	2	BLD

Sample Number	1398	1401	1407	9554
Sc	65	54	62	ND
V	309	246	195	ND
Cr	24	31	35	63
Co	63	52	43	51
Ni	27	35	28	39
Cu	116	108	99	136
Zn	122	110	102	105
Ga	20	19	18	18
Ge	1	2	2	1
Rb	28	45	39	68
Sr	204	326	215	324
Y	42	43	37	39
Zr	154	206	146	231
Sn	4	5	4	ND
Ba	463	508	445	653
Ce	74	74	73	78
Pb	21	38	27	28
Th	7	8	7	9
U	1	1	1	3

APPENDIX XIII

Trace element concentrations in Miscellaneous Carlingford Rocks.

Suffixes to sample numbers indicate rock type (see Appendix V).

Values in P.P.M.

N.D. Not Determined

BLD Below limits of detection

Sample Number	1.X.	2.G.	12.X.	13 E.G.	15.G.	19.B.	21.B.
Sc	69	35	55	69	9	64	59
V	114	4	101	122	35	158	156
Cr	35	BLD	38	101	3	341	202
Co	50	4	38	64	BLD	73	46
Ni	24	5	64	90	7	142	100
Cu	69	53	125	212	44	83	78
Zn	134	76	65	91	54	82	80
Ga	22	20	20	19	18	19	18
Ge	3	2	1	3	3	3	3
Rb	39	164	12	37	168	7	23
Sr	169	100	213	149	76	195	346
Y	45	58	16	26	66	25	23
Zr	123	536	82	93	520	106	165
Sn	4	6	BLD	3	7	3	3
Ba	707	1128	496	465	869	548	823
Ce	74	132	40	90	149	41	64
Pb	31	47	23	25	36	24	25
Th	7	20	3	4	41	4	4
U	1	3	BLD	BLD	4	BLD	BLD

Sample Number	29a.G.	29b.G.	29c.G.	31.S.	32.M.	34.X.	373.X.
Sc	38	27	33	37	39	46	63
V	131	32	37	75	110	67	58
Cr	7	6	1	113	589	108	102
Co	8	25	32	27	67	44	19
Ni	3	9	7	77	501	69	21
Cu	59	91	69	62	91	298	112
Zn	76	168	124	66	66	38	34
Ga	21	23	21	13	11	16	15
Ge	3	2	2	2	BLD	1	2
Rb	202	168	186	53	53	74	31
Sr	98	129	109	196	741	189	297
Y	67	75	72	19	9	4	6
Zr	522	505	295	189	194	126	65
Sn	11	9	9	3	6	2	4
Ba	1332	1454	1575	358	8261	918	587
Ce	157	155	155	66	29	83	39
Pb	38	40	41	28	40	18	18
Th	31	23	27	12	7	2	2
U	4	3	4	1	1	2	BLD

Sample Number	396.E.	593.F.	636.E.	746.C.	839.F.	859.R.	885.F.
Sc	70	12	66	199	32	2	22
V	140	120	86	22	96	24	86
Cr	57	79	98	17	145	3	64
Co	94	28	36	2	13	1	16
Ni	67	57	40	15	71	10	49
Cu	125	56	101	46	66	55	79
Zn	69	61	53	27	54	93	67
Ga	16	15	15	3	13	20	18
Ge	1	1	3	2	2	2	1
Rb	1	106	16	12	56	182	75
Sr	274	159	373	548	591	25	179
Y	8	9	12	4	20	73	9
Zr	23	238	72	34	282	N.D.	233
Sn	1	3	BLD	BLD	BLD	10	6
Ba	440	776	540	270	693	489	728
Ce	24	109	37	95	94	229	105
Pb	21	20	18	33	24	84	27
Th	1	15	1	1	12	36	17
U	7	4	1	BLD	3	8	7

Sample Number	897.F.	945.S.	1082.E	1180.F	1203.Q	1212.Q	1235.L
Sc	18	18	86	17	N.D.	6	28
V	77	101	183	78	N.D.	32	101
Cr	89	107	60	90	N.D.	11	148
Co	33	50	78	20	N.D.	5	39
Ni	53	136	31	64	N.D.	8	105
Cu	74	132	74	65	N.D.	62	61
Zn	69	94	109	69	N.D.	44	62
Ga	17	23	21	18	N.D.	19	16
Ge	1	3	3	2	N.D.	1	2
Rb	107	190	27	126	N.D.	164	52
Sr	232	40	217	214	N.D.	211	559
Y	9	9	29	10	N.D.	4	12
Zr	232	217	98	N.D.	N.D.	149	231
Sn	6	1	3	5	N.D.	6	BLD
Ba	642	781	644	710	N.D.	1344	1421
Ce	83	95	69	114	N.D.	54	51
Pb	22	25	37	32	N.D.	59	26
Th	18	16	1	16	N.D.	31	10
U	3	4	BLD	2	N.D.	5	BLD

Sample Number	1236.L	1250.F	1350.L	1366.L
Sc	29	10	29	37
V	88	48	139	95
Cr	175	28	163	292
Co	44	17	35	48
Ni	99	17	90	244
Cu	72	71	74	104
Zn	75	67	70	70
Ga	18	11	17	15
Ge	2	1	1	1
Rb	56	100	63	60
Sr	586	225	529	602
Y	14	7	15	12
Zr	276	227	278	193
Sn	4	3	7	3
Ba	971	1074	1071	1306
Ce	77	52	68	86
Pb	33	31	23	22
Th	8	17	7	9
U	3	5	2	1

APPENDIX XIV

Duplicate XRF and Wet Analyses of Carlingford Rocks

Analysts: TJH = Author

A.P. = Dr. A. Parker

S.M. = S. Malik

Fe_2O_3 Total = $\frac{FeO}{0.9}$ + Fe_2O_3

5i, 5ii } Separate powder preparations of Sample 5.

* Cr and Ni contamination during grinding

† Recalculated volatile free

Sample Number	5ai	5bii	5cii	5dii	5eii
Analyst	TJH	TJH	TJH	TJH	A.P.
Technique	XRF	XRF	XRF	Wet	XRF
Laboratory	Nottingham	Nottingham	Nottingham	Leicester	Reading
SiO_2	65.69	64.52	65.90	66.18	66.45
TiO_2	0.89	0.89	0.68	0.72	0.74
Al_2O_3	13.22	12.91	13.13	13.63	13.36
Fe_2O_3	2.31	1.86	0.49	0.83	6.47
FeO	5.01	5.06	5.06	5.09	-
MnO	0.11	0.12	0.12	0.14	0.17
MgO	1.01	0.97	0.97	0.86	0.80
CaO	2.95	2.99	2.34	2.70	2.55
Na_2O	3.36	3.30	3.30	3.42	3.23
K_2O	4.02	3.99	4.53	4.50	4.49
P_2O_5	0.19	0.18	0.18	0.15	0.19
CO_2	0.91	1.90	1.90	N.D.	1.90
H_2O+				1.41	
H_2O-				0.14	
Total	99.67	98.69	98.60	99.77	100.35
Fe_2O_3 Total	7.88	7.48	6.11	6.49	6.47
Sc	19	20	20	-	11
V	43	42	68	-	233
Cr	50	118*	99*	-	287*
Co	7	11	18	-	15
Ni	9	311*	264*	-	307*
Cu	52	53	50	-	19
Zn	86	86	82	-	79
Rb	124	125	119	-	149
Sr	232	234	224	-	204
Y	62	63	60	-	94
Zr	496	439	459	-	446
Ba	1086	1022	1088	-	805
[illegible]	115	110	123		95

Sample Number	5fii	22a	22b	22c	36a
Analyst	S.M.	TJH	A.P.	S.M.	TJH
Technique	Wet	XRF	XRF	Wet	XRF
Laboratory	Reading	Nottingham	Reading	Reading	Nottingham
SiO_2	66.70	59.55	57.09	58.90	45.09
TiO_2	0.69	1.10	1.19	1.07	2.09
Al_2O_3	13.32	14.10	13.87	14.41	15.06
Fe_2O_3	2.39	1.97	9.65	1.45	7.90
FeO	3.44	7.11	-	7.25	6.87
MnO	0.23	0.10	0.18	0.14	0.19
MgO	0.74	2.02	2.42	2.18	5.64
CaO	2.32	4.23	4.64	4.17	9.19
Na_2O	3.35	3.09	3.41	3.38	2.20
K_2O	4.50	3.86	3.91	3.81	0.36
P_2O_5	0.16	0.26	0.33	0.27	0.38
CO_2	0.61	1.96	2.03	0.07	4.17
H_2O+	1.04			2.15	
H_2O-	0.21			0.50	
Total	99.70	99.35	98.72	99.75	99.14
Fe_2O_3 Total	6.21	9.87	9.65	9.51	15.53
Sc	-	35	21	-	55
V	-	89	104	-	217
Cr	-	53	140	-	75
Co	-	30	14	-	74
Ni	-	32	47	-	85
Cu	-	80	64	-	94
Zn	-	97	110	-	90
Rb	-	146	133	-	7
Sr	-	109	118	-	288
Y	-	49	83	-	35
Zr	-	196	300	-	145
Ba	-	666	615	-	555
Ce	-	74	78	-	66

Sample Number	36b	36c	36d	36e	36f
Analyst	TJH	TJH	TJH	A.P.	S.M.
Technique	XRF	XRF	Wet	XRF	Wet
Laboratory	Nottingham	Nottingham	Leicester	Reading	Reading
SiO_2	44.98	45.06	44.01	43.42	44.70
TiO_2	1.98	1.92	2.06	1.93	2.15
Al_2O_3	15.35	15.62	15.69	15.05	15.10
Fe_2O_3	7.14	7.42	7.27	14.80	7.32
FeO	6.96	6.96	7.36	-	7.29
MnO	0.19	0.20	0.24	0.24	0.24
MgO	5.66	5.74	5.70	6.41	5.77
CaO	9.18	8.86	9.50	9.65	9.09
Na_2O	2.13	2.03	2.44	2.29	2.73
K_2O	0.39	0.39	0.23	0.39	0.39
P_2O_5	0.37	0.39	0.40	0.41	0.41
CO_2			N.D.		0.39
H_2O+	4.41	4.40	4.00	4.17	2.05
H_2O-			1.92		2.16
Total	98.74	98.99	100.82	98.76	99.79
Fe_2O_3 Total	14.87	15.15	15.45	14.80	15.42
Sc	55	55	-	36	-
V	214	217	-	< 10	-
Cr	90	76	-	208	-
Co	72	85	-	20	-
Ni	99	99	-	87	-
Cu	93	94	-	79	-
Zn	89	90	-	116	-
Rb	7	7	-	< 10	-
Sr	286	288	-	275	-
Y	34	35	-	49	-
Zr	138	147	-	124	-
Ba	543	559	-	365	-
Ce	62	69	-	35	-

Sample Number	38a	38b	38c	53a	53b
Analyst	TJH	A.P.	S.M.	TJH	TJH
Technique	XRF	XRF	Wet	XRF	XRF
Laboratory	Nottingham	Reading	Reading	Nottingham	Nottingham
SiO_2	49.33	50.08	49.70	47.54	48.64
TiO_2	1.32	1.21	1.37	1.12	1.14
Al_2O_3	14.37	14.81	14.39	14.98	15.17
Fe_2O_3	2.72	12.14	2.51	3.59	3.96
FeO	9.24	-	9.24	7.38	7.38
MnO	0.21	0.21	0.22	0.14	0.18
MgO	6.06	6.58	6.15	7.24	7.24
CaO	10.54	11.11	10.57	11.25	11.29
Na_2O	2.17	1.95	2.45	2.16	2.11
K_2O	0.74	0.76	0.72	0.24	0.24
P_2O_5	0.16	0.19	0.18	0.14	0.14
CO_2	)		0.65	)	
H_2O+	) 1.59	1.59	1.47	) 3.55	3.55
H_2O-	)		0.22	)	
Total	98.45	100.63	99.84	99.33	101.04
Fe_2O_3	12.99	12.14	12.78	11.80	12.16
Sc	73	51	-	76	76
V	138	<10	-	154	155
Cr	64	206	-	218	226
Co	57	20	-	76	77
Ni	60	73	-	175	186
Cu	127	128	-	177	180
Zn	72	91	-	60	61
Rb	21	25	-	10	10
Sr	168	161	-	330	336
Y	31	42	-	22	23
Zr	128	102	-	78	81
Ba	563	320	-	478	443
Ce	47	39	-	33	55

Sample Number	53c	53d	54a	54b	54c
Analyst	A.P.	S.M.	TJH	TJH	A.P.
Technique	XRF	Wet	XRF	XRF	XRF
Laboratory	Reading	Reading	Nottingham	Nottingham	Reading
SiO_2	46.31	47.80	46.71	46.57	43.65
TiO_2	1.03	1.17	1.20	1.25	1.11
Al_2O_3	14.82	15.41	14.57	14.61	14.25
Fe_2O_3	2.53	3.45	2.29	3.38	10.63
FeO	7.83	7.53	7.35	7.17	-
MnO	0.19	0.19	0.17	0.17	0.17
MgO	8.23	7.56	10.58	10.58	12.16
CaO	12.06	11.33	10.54	10.79	11.01
Na_2O	1.92	2.35	1.28	1.32	1.29
K_2O	0.26	0.25	0.18	0.19	0.20
P_2O_5	0.16	0.17	0.11	0.11	0.13
CO_2		0.45			
H_2O+	3.55	1.58	3.30	3.30	3.30
H_2O-		0.38			
Total	98.89	99.62	98.28	99.44	97.90
Fe_2O_3Total	11.23	11.82	10.46	11.34	10.63
Sc	48	-	78	79	41
V	108	-	180	180	114
Cr	451	-	696	671	985
Co	25	-	92	87	34
Ni	161	-	535	560	435
Cu	189	-	205	212	164
Zn	98	-	64	66	84
Rb	14	-	9	9	<10
Sr	398	-	189	196	205
Y	30	-	20	21	30
Zr	50	-	87	82	67
Ba	231	-	311	326	95
Ce	40	-	50	42	23

Sample Number	54d	72a	72b	72c	72d
Analyst	S.M.	TJH	TJH	A.P.	S.M.
Technique	Wet	XRF	Wet	XRF	Wet
Laboratory	Reading	Nottingham	Leicester	Reading	Reading
SiO_2	45.90	50.73	51.30	49.84	50.30
TiO_2	1.22	1.13	1.10	1.10	1.15
Al_2O_3	14.97	14.54	15.10	14.39	14.75
Fe_2O_3	2.51	1.44	2.68	10.21	1.50
FeO	7.54	8.77	7.76	-	8.42
MnO	0.17	0.19	0.15	0.19	0.19
MgO	10.75	6.27	6.48	7.52	6.36
CaO	10.39	10.21	10.34	11.52	10.16
Na_2O	1.69	2.15	2.66	1.95	2.47
K_2O	0.19	0.83	0.83	0.84	0.79
P_2O_5	0.13	0.17	0.19	0.19	0.18
CO_2	0.38	)	N.D.	)	1.22
H_2O+	3.12	) 2.09	1.67	) 2.09	1.62
H_2O-	0.47	)	0.18	)	0.32
Total	99.43	98.52	100.44	99.84	99.43
Fe_2O_3	10.89	11.19	11.30	10.21	10.89
Sc	-	88	-	41	-
V	-	262	-	108	-
Cr	-	261	-	388	-
Co	-	91	-	23	-
Ni	-	93	-	165	-
Cu	-	174	-	140	-
Zn	-	88	-	71	-
Rb	-	36	-	33	-
Sr	-	464	-	412	-
Y	-	29	-	34	-
Zr	-	167	-	118	-
Ba	-	687	-	314	-
Ce	-	55	-	40	-

Sample Number	93a	93b	93c	93d	111a
Analyst	TJH	TJH	A.P.	S.M.	TJH
Technique	XRF	XRF	XRF	Wet	XRF
Laboratory	Nottingham	Nottingham	Reading	Reading	Nottingham
SiO_2	61.14	62.31	60.64	60.20	48.59
TiO_2	0.87	0.80	0.85	0.84	1.29
Al_2O_3	13.85	13.67	13.63	13.93	14.05
Fe_2O_3	1.78	1.02	6.11	1.13	4.10
FeO	4.50	4.50	-	4.92	8.64
MnO	0.10	0.10	0.15	0.12	0.20
MgO	2.37	2.33	2.61	2.62	6.40
CaO	4.64	4.39	4.83	4.47	11.90
Na_2O	3.14	3.14	2.94	3.16	2.32
K_2O	3.22	3.30	3.30	3.10	0.39
P_2O_5	0.14	0.13	0.18	0.15	0.16
CO_2	3.97	3.97	3.97	2.60	0.95
H_2O+				2.62	
H_2O-				0.29	
Total	99.72	99.66	99.21	100.15	98.99
Fe_2O_3 Total	6.78	6.02	6.11	6.60	13.70
Sc	37	-	17	-	76
V	100	-	74	-	223
Cr	86	-	228	-	134
Co	31	-	24	-	69
Ni	22	-	58	-	81
Cu	109	-	63	-	180
Zn	60	-	94	-	73
Rb	80	-	63	-	17
Sr	252	-	211	-	138
Y	28	-	54	-	29
Zr	324	-	323	-	133
Ba	911	-	640	-	456
Ce	77	-	74	-	49

Sample Number	111b	111c	127a	127b	127c
Analyst	A.P.	S.M.	TJH	TJH	A.P.
Technique	XRF	Wet	XRF	XRF	XRF
Laboratory	Reading	Reading	Nottingham	Nottingham	Reading
SiO_2	49.61	48.40	53.13	52.55	52.29
TiO_2	1.26	1.42	1.75	1.70	1.68
Al_2O_3	14.51	14.05	13.62	13.53	13.86
Fe_2O_3	12.73	3.99	2.50	2.55	12.46
FeO	-	8.75	10.14	9.81	-
MnO	0.21	0.22	0.21	0.22	0.22
MgO	7.14	6.75	3.65	3.59	4.21
CaO	12.53	11.62	8.04	7.91	8.83
Na_2O	1.95	2.38	2.61	2.62	2.24
K_2O	0.39	0.36	1.63	1.63	1.71
P_2O_5	0.18	0.17	0.31	0.30	0.33
CO_2		0.82			
H_2O+	0.95	1.14	1.45	1.45	1.45
H_2O-		0.27			
Total	101.46	100.34	99.04	97.86	99.28
Fe_2O_3 Total	12.73	13.71	13.77	13.45	12.46
Sc	52	-	55	53	36
V	136	-	205	204	164
Cr	193	-	49	46	183
Co	20	-	49	52	15
Ni	68	-	12	16	165
Cu	174	-	77	77	51
Zn	94	-	109	109	102
Rb	24	-	57	57	55
Sr	140	-	354	354	357
Y	40	-	42	42	57
Zr	83	-	254	245	204
Ba	243	-	829	820	609
Ce	25	-	96	93	78

Sample Number	127d	135a	135b	135c	172a
Analyst	S.M.	TJH	A.P.	S.M.	A.P.
Technique	Wet	XRF	XRF	Wet	XRF
Laboratory	Reading	Nottingham	Reading	Reading	Reading
SiO_2	52.40	46.82	44.73	45.70	47.96
TiO_2	1.73	1.84	1.76	1.82	0.76
Al_2O_3	14.17	16.55	16.51	16.67	20.70
Fe_2O_3	2.70	1.96	13.45	3.35	8.35
FeO	9.53	10.92	-	9.27	-
MnO	0.32	0.24	0.21	0.19	0.15
MgO	3.55	7.67	8.48	7.62	5.06
CaO	7.97	9.79	10.47	9.53	12.63
Na_2O	2.87	1.89	1.62	2.18	1.88
K_2O	1.65	0.31	0.31	0.28	0.83
P_2O_5	0.34	0.21	0.23	0.22	0.12
CO_2	0.29	}		0.22	}
H_2O+	1.82	} 0.97	0.97	2.33	} 1.90
H_2O-	0.28	}		0.43	}
Total	99.62	99.17	98.74	99.81	100.34
Fe_2O_3	13.29	14.09	13.45	13.65	8.35
Sc	-	57	41	-	36
V	-	243	183	-	79
Cr	-	36	86	-	132
Co	-	69	24	-	22
Ni	-	11	200	-	30
Cu	-	79	32	-	79
Zn	-	117	96	-	81
Rb	-	50	<10	-	34
Sr	-	312	352	-	228
Y	-	44	42	-	27
Zr	-	231	113	-	63
Ba	-	734	239	-	227
Ce	-	86	47	-	33

Sample Number	172b	191a	191b	191c	437a
Analyst	S.M.	TJH	A.P.	S.M.	TJH
Technique	Wet	XRF	XRF	Wet	XRF
Laboratory	Reading	Nottingham	Reading	Reading	Nottingham
SiO_2	48.30	50.34	51.89	50.50	46.90
TiO_2	0.86	1.86	1.83	1.89	0.70
Al_2O_3	19.85	15.37	15.90	15.56	21.66
Fe_2O_3	2.32	4.60	11.89	5.33	0.76
FeO	5.98	6.42	-	5.69	6.07
MnO	0.17	0.19	0.21	0.20	0.11
MgO	4.54	3.73	4.17	3.85	4.49
CaO	11.90	7.03	7.05	7.01	13.78
Na_2O	2.46	2.62	3.10	3.35	1.91
K_2O	0.84	2.28	2.35	2.26	0.18
P_2O_5	0.12	0.69	0.79	0.71	0.09
CO_2	0.73	2.99	2.99	0.22	1.42
H_2O+	1.29			1.65	
H_2O-	0.29			1.75	
Total	99.65	98.12	102.17	99.97	98.07
Fe_2O_3 Total	8.96	11.73	11.89	11.65	7.50
Sc	-	40	28	-	72
V	-	204	191	-	115
Cr	-	22	25	-	115
Co	-	49	17	-	51
Ni	-	45	33	-	79
Cu	-	93	56	-	131
Zn	-	96	118	-	46
Rb	-	44	44	-	6
Sr	-	425	433	-	191
Y	-	36	55	-	13
Zr	-	322	276	-	55
Ba	-	1419	1132	-	593
Ce	-	147	111	-	67

Sample Number	437b	437c	748a	748a†	748b
Analyst	A.P.	S.M.	TJH	TJH	A.P.
Technique	XRF	Wet	XRF	XRF	XRF
Laboratory	Reading	Reading	Nottingham	Nottingham	Reading
SiO_2	46.47	47.60	44.41	49.24	44.90
TiO_2	0.60	0.72	1.74	1.93	1.80
Al_2O_3	22.77	22.72	14.19	15.73	13.80
Fe_2O_3	6.66	1.64	3.60	14.74	12.34
FeO	-	5.18	8.73	-	-
MnO	0.11	0.12	0.37	0.41	0.32
MgO	5.02	4.48	1.98	2.20	2.25
CaO	14.99	13.99	7.75	8.59	8.49
Na_2O	2.02	2.16	5.74	6.36	5.16
K_2O	0.16	0.20	0.68	0.75	0.70
P_2O_5	0.08	0.10	0.82	0.91	0.97
CO_2		0.04			
H_2O+	1.41	1.47	10.26	-	10.26
H_2O-		0.21			
Total	100.29	100.63	100.27	100.86	100.99
Fe_2O_3	6.66	7.39	13.30	14.74	12.34
Sc	30	-	38	-	15
V	65	-	119	-	181
Cr	171	-	7	-	< 5
Co	26	-	14	-	<10
Ni	58	-	10	-	<10
Cu	112	-	60	-	19
Zn	47	-	64	-	64
Rb	<10	-	27	-	27
Sr	196	-	229	-	236
Y	21	-	66	-	92
Zr	24	-	294	-	272
Ba	107	-	461	-	313
Ce	29	-	108	-	74

Sample Number	748b†	748e	748f	859a	859b
Analyst	A.P.	S.M.	-	TJH	A.P.
Technique	XRF	Wet	XRF	XRF	XRF
Laboratory	Reading	Reading	Durham	Nottingham	Reading
SiO_2	49.98	43.80	48.56	76.52	77.08
TiO_2	2.00	1.72	1.93	0.15	0.15
Al_2O_3	15.36	14.31	13.86	11.11	11.58
Fe_2O_3	13.74	1.82	14.62	1.37	1.99
FeO	-	8.77	-	0.09	-
MnO	0.36	0.28	0.36	0.00	0.01
MgO	2.50	2.12	2.49	0.20	0.15
CaO	9.45	7.48	9.76	0.16	0.31
Na_2O	5.74	6.21	6.63	3.23	3.03
K_2O	0.78	0.63	0.72	4.53	4.40
P_2O_5	1.08	0.85	0.79	0.01	0.02
CO_2		9.69	-		
H_2O+	-	1.48	-	1.30	1.30
H_2O-		0.25	-		
Total	100.99	99.41	99.72	98.67	100.02
Fe_2O_3 Total	13.74	11.56	14.62	1.47	1.99
Sc	-	-	-	2	< 10
V	-	-	-	24	11
Cr	-	-	-	3	133
Co	-	-	-	1	30
Ni	-	-	4	10	42
Cu	-	-	16	55	30
Zn	-	-	64	93	95
Rb	-	-	37	182	169
Sr	-	-	274	25	29
Y	-	-	80	73	119
Zr	-	-	287	-	394
Ba	-	-	240	489	60
Ce	-	-	-	229	193

Sample Number	859c	1162a	1162b	1162c
Analyst	S.M.	TJH	A.P.	S.M.
Technique	Wet	XRF	XRF	Wet
Laboratory	Reading	Nottingham	Reading	Reading
SiO_2	77.60	48.99	49.06	48.50
TiO_2	0.14	0.82	0.73	0.83
Al_2O_3	11.32	18.74	18.69	19.33
Fe_2O_3	1.55	2.32	9.52	2.49
FeO	0.22	7.07	-	6.85
MnO	0.01	0.18	0.17	0.18
MgO	0.14	4.52	5.21	4.60
CaO	0.12	11.97	12.53	11.65
Na_2O	3.16	2.03	2.04	2.30
K_2O	4.52	0.55	0.57	0.59
P_2O_5	0.01	0.09	0.10	0.11
CO_2	0.05	)		0.70
H_2O+	0.64	) 1.45	2.15	1.68
H_2O-	0.34	)		0.26
Total	99.82	98.73	100.77	100.07
Fe_2O_3 Total	1.79	10.18	9.52	10.10
Sc	-	69	41	-
V	-	106	76	-
Cr	-	40	65	-
Co	-	49	21	-
Ni	-	37	25	-
Cu	-	121	97	-
Zn	-	94	78	-
Rb	-	23	24	-
Sr	-	167	169	-
Y	-	19	29	-
Zr	-	63	53	-
Ba	-	566	192	-
Ce	-	39	35	-

APPENDIX XV

Analyses of Carlingford rocks prepared at Reading by X.R.F.

$FeO + Fe_2O_3$ determined as Fe_2O_3

N.D. Not Determined

Sample Number	5	22	23	24	25	36	37
SiO_2	66.45	57.09	66.59	51.99	68.64	43.42	50.98
TiO_2	0.74	1.19	0.72	2.62	0.60	1.93	2.40
Al_2O_3	13.36	13.87	13.93	12.30	13.64	15.05	11.83
Fe_2O_3	6.47	9.65	6.28	15.25	5.60	14.80	13.59
MnO	0.17	0.18	0.07	0.26	0.12	0.24	0.25
MgO	0.80	2.42	0.83	3.16	0.57	6.41	2.77
CaO	2.55	4.64	1.87	6.91	1.79	9.65	6.41
Na_2O	3.23	3.41	3.29	2.13	3.78	2.29	2.73
K_2O	4.49	3.91	5.33	2.64	5.12	0.39	2.83
P_2O_5	0.19	0.33	0.18	0.34	0.14	0.41	0.38
Loss on Ignition	1.90	2.03	0.91	1.40	0.69	4.17	0.38
Total	100.35	98.72	100.00	99.00	100.69	98.76	94.55
Sc	11i	21	<40	54	<10	36	46
V	233	104	62	257	51	<10	235
Cr	287	140	138	124	121	208	126
Co	15	14	15	10	16	20	12
Ni	307	47	44	41	40	87	41
Cu	19	64	61	83	46	79	65
Zn	79	110	100	137	105	116	115
Rb	149	133	176	95	193	<10	79
Sr	204	118	72	112	65	275	156
Y	94	83	98	80	97	49	76
Zr	466	300	446	226	472	124	249
Nb	43	39	44	37	44	18	27
Ba	805	615	755	727	806	365	694
La	78	50	66	148	69	<10	51
Ce	95	78	106	90	116	35	93

Sample Number	38	53	54	72	73	89	93
SiO_2	50.08	46.31	43.65	49.84	51.42	46.45	60.64
TiO_2	1.21	1.03	1.11	1.10	2.21	2.08	0.85
Al_2O_3	14.81	14.82	14.25	14.39	12.50	15.16	13.63
Fe_2O_3	12.14	11.23	10.63	10.21	14.25	12.23	6.11
MnO	0.21	0.19	0.17	0.19	0.23	0.16	0.15
MgO	6.58	8.23	12.16	7.52	3.91	6.09	2.61
CaO	11.11	12.06	11.01	11.52	8.04	9.66	4.83
Na_2O	1.95	1.92	1.29	1.95	1.99	2.39	2.94
K_2O	0.76	0.26	0.20	0.84	1.70	1.39	3.30
P_2O_5	0.19	0.16	0.13	0.19	0.46	0.66	0.18
Loss on Ignition	1.59	3.55	3.30	2.09	2.19	3.31	3.97
Total	100.63	99.76	97.90	99.84	98.90	99.58	99.21
Sc	51	48	41	41	35	38	17
V	<10	108	114	108	216	N.D.	74
Cr	206	451	985	388	153	131	228
Co	20	25	34	23	12	30	24
Ni	73	161	435	165	48	60	58
Cu	128	189	164	140	71	50	63
Zn	91	98	84	71	115	79	94
Rb	25	14	<10	33	N.D.	32	63
Sr	161	398	205	412	N.D.	549	211
Y	42	30	30	34	N.D.	46	54
Zr	102	50	67	118	N.D.	161	323
Nb	<10	<10	<10	15	N.D.	31	30
Ba	320	231	95	314	438	584	640
La	<10	<10	<10	<10	21	N.D.	31
Ce	39	40	23	40	53	55	74

Sample Number	111	127	134	135	138	172	177
SiO_2	49.61	52.29	48.73	44.73	53.13	47.96	48.11
TiO_2	1.26	1.68	1.05	1.76	1.67	0.76	0.66
Al_2O_3	14.51	13.86	17.30	16.51	13.18	20.70	22.15
Fe_2O_3	12.73	12.46	9.45	13.45	10.75	8.35	7.69
MnO	0.21	0.22	0.18	0.21	0.28	0.15	0.14
MgO	7.14	4.21	7.42	8.48	3.90	5.06	4.84
CaO	12.53	8.83	10.82	10.47	8.71	12.63	13.70
Na_2O	1.95	2.24	1.62	1.62	2.82	1.88	2.19
K_2O	0.39	1.71	0.42	0.31	1.71	0.83	0.43
P_2O_5	0.18	0.33	0.35	0.23	0.34	0.12	0.10
Loss on Ignition	0.95	1.45	2.78	0.97	2.40	1.90	0.50
Total	101.46	99.28	100.12	98.74	98.89	100.34	100.51
Sc	52	36	40	41	41	36	32
V	136	164	N.D.	183	N.D.	79	69
Cr	193	183	352	86	123	132	242
Co	20	15	34	24	20	22	24
Ni	68	165	146	200	29	30	67
Cu	174	51	57	32	40	79	77
Zn	94	102	60	96	103	81	67
Rb	24	55	15	$\lhd$ 10	31	34	18
Sr	140	357	320	352	460	228	225
Y	40	57	35	42	61	27	22
Zr	83	204	73	113	192	63	51
Nb	$\lhd$ 10	22	$\lhd$ 10	$\lhd$ 10	12	$\lhd$ 10	$\lhd$ 10
Ba	243	609	320	239	632	227	165
La	$\lhd$ 10	27	N.D.	$\lhd$ 10	N.D.	$\lhd$ 10	$\lhd$ 10
Ce	25	78	33	47	58	33	34

Sample Number	191	276	330	332	378	434	437
SiO_2	51.89	54.06	47.56	50.09	46.61	44.09	46.47
TiO_2	1.83	0.79	1.16	1.34	1.86	1.51	0.60
Al_2O_3	15.90	17.60	14.89	12.88	14.71	15.61	22.77
Fe_2O_3	11.89	7.77	11.85	12.40	13.05	13.33	6.66
MnO	0.21	0.17	0.20	0.25	0.23	0.24	0.11
MgO	4.17	3.48	8.08	5.39	7.05	8.27	5.02
CaO	7.05	9.64	12.37	11.06	10.62	9.63	14.99
Na_2O	3.10	2.87	2.00	2.92	2.01	1.73	2.02
K_2O	2.35	1.47	0.33	0.57	0.69	0.76	0.16
P_2O_5	0.79	0.11	0.20	0.19	0.44	0.27	0.08
Loss on Ignition	2.99	1.29	2.91	1.38	2.76	3.84	1.41
Total	102.17	99.25	101.55	98.47	100.03	99.28	100.29
Sc	28	32	48	51	40	41	30
V	191	N.D.	124	N.D.	N.D.	N.D.	65
Cr	25	206	280	N.D.	308	322	171
Co	17	21	23	24	29	31	26
Ni	33	59	105	79	155	168	58
Cu	56	80	150	86	76	78	112
Zn	118	75	95	100	94	93	47
Rb	44	42	13	23	32	36	$\lhd$ 10
Sr	433	174	152	164	268	231	196
Y	55	55	36	43	40	36	21
Zr	276	187	77	145	131	91	24
Nb	21	$\lhd$ 10	12	$\lhd$ 10	11	$\lhd$ 10	$\lhd$ 10
Ba	1132	358	170	323	448	394	107
La	53	N.D.	$\lhd$ 10	N.D.	N.D.	N.D.	$\lhd$ 10
Ce	111	43	38	35	35	35	29

Sample Number	446	447	530	550	575	582	685
SiO_2	58.47	60.03	53.02	60.87	53.85	51.77	60.60
TiO_2	0.55	0.53	1.63	0.92	2.12	1.70	0.74
Al_2O_3	18.48	17.08	13.66	13.73	12.62	13.17	14.39
Fe_2O_3	5.44	5.67	12.44	7.16	13.95	12.80	6.79
MnO	0.96	0.12	0.20	0.13	0.23	0.20	0.13
MgO	1.92	1.98	4.64	3.62	2.54	4.27	3.28
CaO	6.29	5.58	8.54	5.86	6.46	8.18	5.90
Na_2O	2.74	2.77	3.47	2.74	3.29	3.15	2.76
K_2O	3.18	3.28	1.89	3.21	2.47	2.00	2.50
P_2O_5	0.91	0.88	0.33	0.16	0.61	0.34	0.11
Loss on Ignition	1.48	2.64	0.30	0.54	2.12	2.43	3.02
Total	100.42	100.56	100.12	98.94	100.26	100.01	100.22
Sc	18	16	37	27	30	36	26
V	N.D.	N.D.	N.D.	N.D.	N.D.	N.D.	N.D.
Cr	148	142	148	252	107	144	224
Co	15	15	23	22	17	22	22
Ni	45	45	63	83	37	59	63
Cu	71	30	64	105	48	77	52
Zn	53	52	88	63	116	93	66
Rb	103	103	89	99	73	55	64
Sr	172	147	164	126	151	214	160
Y	63	60	60	53	69	48	41
Zr	280	309	192	274	241	172	235
Nb	15	18	10	11	<10	13	12
Ba	710	707	422	572	473	436	580
La	N.D.	N.D.	N.D.	N.D.	N.D.	N.D.	N.D.
Ce	64	70	50	63	67	51	56

Sample Number	748	809	813	825	830	838	856
SiO_2	44.90	47.27	42.51	59.41	53.66	55.68	48.89
TiO_2	1.80	0.95	1.06	1.31	1.96	1.81	1.30
Al_2O_3	13.80	13.82	13.27	13.71	13.11	12.81	13.85
Fe_2O_3	12.34	9.78	10.74	7.73	13.45	13.26	12.47
MnO	0.32	0.17	0.19	0.22	0.21	0.23	0.22
MgO	2.25	7.96	11.25	1.26	2.77	2.25	6.79
CaO	8.49	11.11	12.17	3.48	6.57	6.23	10.88
Na_2O	5.16	1.59	1.66	3.91	2.95	2.36	2.02
K_2O	0.70	0.68	0.11	3.52	2.44	2.75	0.86
P_2O_5	0.97	0.21	0.12	0.57	0.41	0.49	0.19
Loss on Ignition	10.26	6.16	5.41	5.72	2.72	2.66	1.97
Total	100.99	99.70	98.49	100.84	100.25	100.53	99.44
Sc	5	41	44	17	32	30	52
V	181	N.D.	N.D.	N.D.	N.D.	N.D.	135
Cr	<5	785	742	107	107	99	89
Co	<10	33	41	11	19	15	20
Ni	<10	204	338	34	39	33	40
Cu	19	97	101	41	57	50	120
Zn	64	62	54	103	102	112	97
Rb	27	21	<10	84	78	88	27
Sr	236	216	198	279	248	181	161
Y	92	34	30	65	63	71	46
Zr	272	88	57	349	231	276	100
Nb	98	<10	<10	22	14	20	10
Ba	313	302	126	552	481	428	326
La	31	N.D.	N.D.		N.D.	N.D.	<10
Ce	74	29	14	91	65	73	42

Sample Number	859	915	1162	1172	1190	1203	1236
SiO_2	77.08	46.36	49.06	50.53	49.69	70.82	58.04
TiO_2	0.15	1.51	0.73	2.04	1.17	0.30	1.27
Al_2O_3	11.58	15.56	18.69	12.45	14.09	14.76	15.87
Fe_2O_3	1.99	12.89	9.52	16.79	11.41	2.17	7.08
MnO	0.01	0.24	0.17	0.25	0.20	0.43	0.14
MgO	0.15	7.66	5.21	3.60	5.93	1.05	5.92
CaO	0.31	10.60	12.53	6.79	10.72	1.48	4.72
Na_2O	3.03	1.96	2.04	3.32	2.78	2.68	3.64
K_2O	4.40	0.62	0.57	1.79	0.95	4.61	2.21
P_2O_5	0.02	0.31	0.10	0.30	0.19	0.11	0.33
Loss on Ignition	1.30	1.58	2.15	1.77	2.75	1.82	1.97
Total	100.02	99.29	100.77	99.63	99.88	100.23	101.19
Sc	$<$ 10	16	41	35	42	$<$ 10	17
V	11	N.D.	76	N.D.	N.D.	23	123
Cr	133	304	65	112	161	158	192
Co	30	33	21	23	26	35	28
Ni	42	151	25	47	76	50	70
Cu	30	82	97	106	95	62	$<$ 15
Zn	95	92	78	154	84	52	73
Rb	169	21	24	71	30	135	58
Sr	29	246	169	173	201	225	572
Y	119	35	29	62	41	16	19
Zr	394	101	53	170	116	137	203
Nb	52	$<$ 10	$<$10	13	$<$10	15	16
Ba	60	327	192	460	252	713	698
La	119	N.D.	$<$10	N.D.	N.D.	13	23
Ce	193	25	35	45	31	54	65

Sample Number	1289	1292	1318	1324	1336	1381	1383
SiO_2	52.06	51.80	66.81	54.63	54.14	45.87	51.52
TiO_2	1.64	1.94	0.65	1.78	1.67	0.83	1.66
Al_2O_3	13.11	12.52	12.15	12.47	13.67	14.26	13.48
Fe_2O_3	12.67	15.68	7.63	12.58	12.01	9.47	12.93
MnO	0.22	0.30	0.68	0.22	0.26	0.12	0.20
MgO	3.21	3.68	0.45	3.38	2.77	8.44	4.21
CaO	8.06	7.84	0.52	8.48	6.32	13.15	8.58
Na_2O	2.20	3.39	3.14	2.84	2.59	1.89	2.52
K_2O	1.80	1.70	4.64	1.82	2.65	0.44	1.79
P_2O_5	0.44	0.25	0.92	0.35	0.64	0.14	0.27
Loss on Ignition	3.27	0.72	2.02	0.40	1.90	3.81	2.78
Total	98.68	99.82	99.61	98.95	98.62	98.42	99.94
Sc	31	52	11	44	29	45	37
V	64	N.D.	60	N.D.	151	N.D.	N.D.
Cr	139	114	127	126	131	525	129
Co	13	21	11	23	10	37	24
Ni	53	41	40	53	42	208	52
Cu	93	168	40	74	76	143	96
Zn	154	182	94	95	128	58	101
Rb	69	57	177	35	82	13	49
Sr	155	156	81	159	130	159	185
Y	73	62	89	57	111	26	42
Zr	202	196	436	189	237	54	167
Nb	23	$\lhd$ 10	45	$\lhd$ 10	34	$\lhd$ 10	$\lhd$ 10
Ba	476	574	887	N.D.	525	211	555
La	25	N.D.	27	N.D.	28	N.D.	N.D.
Ce	72	48	80	60	79	20	44

Sample Number	1385	1399
SiO_2	53.33	46.92
TiO_2	1.83	1.21
Al_2O_3	12.63	17.54
Fe_2O_3	14.72	9.79
MnO	0.23	0.19
MgO	3.03	4.13
CaO	6.99	12.15
Na_2O	2.90	2.78
K_2O	2.15	0.86
P_2O_5	0.36	0.22
Loss on Ignition	1.98	1.14
Total	100.15	96.93
Sc	39	36
V	N.D.	122
Cr	114	161
Co	23	19
Ni	39	52
Cu	65	89
Zn	104	82
Rb	49	33
Sr	276	281
Y	54	37
Zr	191	96
Nb	12	< 10
Ba	588	390
La	N.D.	< 10
Ce	52	31

APPENDIX XVI

Identity, Age and Locality of Analysed Carlingford Rocks and Structure of Source Bodies.

Rock Type:	As defined in Chapters 1 and 3
Structure	
Type:	As defined in Chapters 1 and 2
Thickness:	Measured in metres
Trend:	Azimuth in dregrees from True North
Attitude:	Inclination of minor intrusions measured from horizontal i.e. horizontal = 0^{o}, vertical = 90^{o}. Note - dykes are assumed vertical unless otherwise stated.
Age:	Defined in relation to episodes in cyclic sequence (Chapter 1).

Sample Number	Rock Type	Structure Type	Thickness	Trend	Attitude	Age	Locality
1	Gabbro	Lopolith	-	-	-	-	Quarry, Barnavave
2	Granophyre	Diapir	-	-	-	-	Quarry, Barnavave
3	High iron transition dolerite	Cone sheet	?	-	53°	11c	Rosemount
5	Craignuritic felsite	Cone sheet	?	-	?	11c	Rosemount
6	Basaltic craignurite	E.W. dyke	1.25M	089°	-	111b	Rosemount
9	Tachylitic transition dolerite	Cone sheet?	?	-	?	11d?	Quarry, Grange Irish
11	Variolitic quartz dolerite	Cone sheet	0.2M	-	?	11d?	Quarry, Grange Irish
12	Gabbro	Xenolith	-	-	-	-	Quarry, Grange Irish
13	Acidified gabbro	Lopolith?	-	-	-	-	Quarry, Cooley
15	Granophyre	Vein	-	-	-	-	Quarry, Cooley
18	Variolitic quartz dolerite	Cone sheet	1.25M	-	29°	11c	Rockmarshal
19	High alumina basalt	Lava	-	-	-	1	Rockmarshal
21	Transition basalt	Lava	-	-	-	1	Donalds Rock
22	Craignurite	N.S. dyke	1M	196°	-	111b	Quarry, Drumenagh Hill
23	Craignuritic felsite	N.E. dyke	1M	?	-	111b	Quarry, Drumenagh Hill

Sample Number	Rock Type	Type	Structure Thickness	Structure Trend	Structure Attitude	Age	Locality
24	Tachylitic basic craignurite	Cone sheet	0.6M	-	?	111b	Quarry, Drumenagh Hill
25	Craignuritic felsite	Cone sheet	1.5M	-	47°	111b	Quarry, Drumenagh Hill
27	Quartz dolerite	Cone sheet	1.1M	-	23°	111b	Quarry, Drumenagh Hill
28	Transition dolerite	N.W. dyke	2M	?	-	111c	Quarry, Drumenagh Hill
29	Granophyre with gabbro xenoliths	Diapir	-	-	-	-	Quarry, Drumenagh Hill
30	Quartz dolerite	Cone sheet	?	-	?	111b?	Quarry, Drumenagh Hill
31	Silurian sediment	-	-	-	-	-	Railway cutting, Sportsmans Hall
32	Minette	Dyke	1.5M	256°	67°S	-	Railway cutting, Sportsmans Hall
33	Quartz dolerite	Cone sheet	1.25M	-	36°	11c?	Railway cutting Carlingford Castle
34	Gabbro	Xenolith	-	-	-	-	Railway cutting Carlingford Castle
35	Craignurite	Cone sheet	3M	-	25°	11c	Railway cutting Carlingford Castle
36	Alkali basalt	N.E. dyke	1.5M	043°	-	111d	Railway cutting Carlingford Castle
37	Basaltic Craignurite	N.E. dyke	2M	065°	-	111b	Railway cutting Carlingford Castle

Sample Number	Rock Type	Type	Thickness	Structure Trend	Attitude	Age	Locality
38	Tholeiitic dolerite	Cone sheet	1.25M	-	?	11d	Railway cutting Carlingford Castle
40	Feldsparphyric dolerite	Cone sheet	0.5M	-	27°	11e-111a	Railway cutting Carlingford Castle
45	Feldsparphyric dolerite	Cone sheet?	?	-	-	11e-111a	Railway cutting Carlingford Castle
46	Craignuritic felsite	Cone sheet	1.5M	-	53°	11c	Railway cutting Carlingford Castle
53	Transition dolerite	Cone sheet	2M	-	24°	111c	Quarry, Carlingford
54	Transition dolerite	N.W. dyke	1.1M	133°	-	111c	Quarry, Carlingford
58	Craignuritic felsite	Dyke?	?	?	?	11c?	Quarry, Proleek
59	Basaltic craignurite	N.E. dyke	?	217°	?	11c?	Quarry, Proleek
61	Alkali basalt	N.E. dyke	1.25M	052°	-	111d	Quarry, Proleek Acres
63	Altered quartz dolerite	E.W. dyke	?	092°	59°S	111d	Quarry, Mountpleasant
64	Alkali basalt	N.E. dyke	1.5M	?	?	111d	Quarry, Mountpleasant
66	Trachy basalt	N.E. dyke	0.6M	034°	-	111d	Quarry, Mountpleasant
67	Tachylitic transition dolerite	Cone sheet?	0.25M	-	?	11d	Quarry, Mountpleasant
68	Tholeiitic dolerite	Cone sheet	3M	-	10°	11d	Quarry, Mountpleasant
71	Quartz dolerite	Cone sheet	?	-	7°	11d	Mullatee

Sample Number	Rock Type	Type	Thickness	Structure Trend	Attitude	Age	Locality
72	Quartz dolerite	Cone sheet	1M	-	0°	11d	Quarry, Carlingford
73	Tholeiitic dolerite	N.W. dyke	0.6M	333°	60°S	111c	Quarry, Carlingford
74	Feldsparphyric dolerite	N.W. dyke	0.6M	333°	60°S	11e-111a	Quarry, Carlingford
75	Tachylitic tholeiitic dolerite	N.W. dyke	2.8M	304°	83°	111c	Quarry, Carlingford
76	Transition dolerite	N.W. dyke	8M	304°	-	1b?	Quarry, Carlingford
78	Tholeiitic dolerite	N.W. dyke	0.3M	304°	-	11d	Quarry, Carlingford
80	Quartz dolerite	N.W. dyke	1M	304°	-	111c	Quarry, Carlingford
84	Transition dolerite	N.W. dyke	2M	317°	-	111c	Quarry, Carlingford
89	Trachy basalt	N.W. dyke	1.25M	148°	-	11b	Quarry, Carlingford
93	Craignuritic felsite	E.W. dyke	1.5M	269°	-	11c	Quarry, Carlingford
96	Alkali basalt	N.E. dyke	0.5M	219°	61°W	111d	Quarry, Carlingford
97	High iron transition dolerite	N.W. dyke	0.5M	097°	-	11d	Quarry, Carlingford
99	Tholeiitic dolerite	Cone sheet	2M	-	0°	111c	Quarry, Carlingford
102	Alkali basalt	N.E. dyke	0.5M	232°	57°N	111d	Quarry, Carlingford
107	Alkali basalt	N.W. dyke?	?	?	?	11b	Quarry, Carlingford
111	Transition dolerite	Cone sheet	1.25M	-	0°	111c	Quarry, Carlingford

Sample Number	Rock Type	Type	Thickness	Structure Trend	Attitude	Age	Locality
113	Transition dolerite	N.W. dyke	2M	123°	61°W	111c	Quarry, Carlingford
114	High alumina basalt (Porphyritic transition dolerite)	N.W. dyke	2M	144°	61°W	111c	Quarry, Carlingford
115	Alkali basalt	N.E. dyke	0.5M	235°	59°W	111d	Quarry, Carlingford
119	Alkali basalt	N.E. dyke	0.5M	221°	64°W	111d	Quarry, Carlingford
122	Quartz dolerite	Cone sheet	1M	-	0°	11d	Quarry, Carlingford
123	Quartz dolerite	Cone sheet	?	-	0°	11d	Quarry, Carlingford
124	Feldsparphyric dolerite	Cone sheet	3M	-	45°	11e-111a	Rosemount
125	Transition dolerite	Complementary Cone sheet	1.25M	-	20°	11d	Rosemount
127	Basaltic craignurite	Cone sheet	1M	-	42°	11c	Rosemount
130	Transition dolerite	E.W. dyke	1M	275°	70°S	111b	Rosemount
131	High iron transition dolerite	Complementary Cone sheet	0.3M	-	15°	11c	Rosemount
133	Quartz dolerite	Cone sheet	?	-	55°	11c	Rosemount
134	Tholeiitic dolerite	N.W. dyke	1.25M	307°	62°S	11d	Rosemount
135	Alkali basalt	N.W. dyke	1.25M	-	297°	11b	Rosemount
137	Feldsparphyric dolerite	Cone sheet	1M	-	50°	11e-111a	Rosemount

Sample Number	Rock Type	Type	Thickness	Structure Trend	Attitude	Age	Locality
138	Basaltic Craignurite	N.W. dyke	1.25M	347°	75°E	1a?	Rosemount
140	Alkali basalt	N.W. dyke	1.25M	284°	60°S	11b	Rosemount
141	High alumina basalt (Porphyritic tholeiitic dolerite)	N.W. dyke	2M	134°	78°S	11d	Rosemount
142	Tholeiitic dolerite	N.W. dyke	2M	300°	61°S	11d	Rosemount
143	Alkali basalt	N.W. dyke	?	287°	-	11b	Rosemount
145	Tholeiitic dolerite	N.W. dyke	0.3M	307°	79°S	11d	Rosemount
147	Tholeiitic dolerite	N.W. dyke	0.6M	142°	-	111c	North-east flank Barnavave
151	Craignuritic felsite	Cone sheet?	?	-	?	1a	East flank, Barnavave
155	Basaltic craignurite	N.W. dyke	1.25M	300°	-	1a	East flank, Barnavave
156	High iron transition dolerite	Complementary cone sheet	1M	-	20°	1b	Quarry, Grange Irish
158	Craignurite	N.W. dyke	1.25M	-	305°	1a	Quarry, Grange Irish
160	Tholeiitic dolerite	N.W. dyke?	?	?	?	?	Quarry, Grange Irish
162	Transition dolerite	N.W. dyke	1.5M	312°	-	1b	Quarry, Grange Irish
166	Craignurite	N.W. dyke	1M	?	-	11c	East flank, Slieve Foye
172	Feldsparphyric dolerite	Cone sheet	3M	-	25°	11e	East flank, Slieve Foye
173	Tholeiitic dolerite	Cone sheet	0.6M	-	?	111c	East flank, Slieve Foye

Sample Number	Rock Type	Structure Type	Thickness	Trend	Attitude	Age	Locality
174	Quartz dolerite	Cone sheet	0.6M	-	?	111b	East flank, Slieve Foye
175	Quartz dolerite	N.W. dyke	2M	130°	-	111b	East flank, Slieve Foye
176	Quartz dolerite	Cone sheet	0.6M	-	?	111b	East flank, Slieve Foye
177	High alumina gabbro	Cone sheet	15M	-	?	11e	East flank, Slieve Foye
181	Quartz dolerite	Cone sheet	1.25M	-	?	?	East flank, Slieve Foye
190	Feldsparphyric dolerite	Cone sheet	2.5M	-	?	11e-111a	East flank, Slieve Foye
191	Trachybasalt	N.E. dyke	4M	237°	-	111d	East flank, Slieve Foye
192	Transition dolerite	Cone sheet	1.25M	-	?	11d	East flank, Slieve Foye
235	Transition dolerite	Cone sheet	6M	-	20°	11d	Golden River, Slieve Foye
236	Craignurite	Cone sheet	4M	-	20°	11c	Golden River, Slieve Foye
253	Transition dolerite	Cone sheet	?	-	?	?	Golden River, Slieve Foye
269	Feldsparphyric dolerite	Cone sheet	1.5M	-	?	11e	East flank, Slieve Foye
273	Feldsparphyric dolerite	Cone sheet	1M	-	?	11e	East flank, Slieve Foye
276	Quartz dolerite	Cone sheet	1.25M	-	?	11c	East flank, Slieve Foye
292	Transition dolerite	Cone sheet	1.25M	-	?	1b	East flank, Slieve Foye
297	Transition dolerite	Cone sheet	1M	-	45°	1b	East flank, Slieve Foye
298	Transition dolerite	N.E. dyke	1M	257°	-	11d	East flank, Slieve Foye

Sample Number	Rock Type	Type	Thickness	Structure Trend	Attitude	Age	Locality
300	Tholeiitic dolerite	N.E. dyke	1.25M	233°	60°N	111c	East flank, Slieve Foye
305	Transition dolerite	Cone sheet	0.4M	-	40°	?	East flank, Slieve Foye
314	Tholeiitic dolerite	Cone sheet	1.25M	-	-	11d	East flank, Slieve Foye
330	Tholeiitic dolerite	N.E. dyke	2M	255°	-	11d	East flank, Slieve Foye
332	Tholeiitic dolerite	Cone sheet	?	-	?	11d	East flank, Slieve Foye
369	Tholeiitic dolerite	N.W. dyke	1.50M	287°	-	1b	East flank, Slieve Foye
371	Variolitic tholeiitic dolerite	Cone sheet	0.5M	-	?	11c	East flank, Slieve Foye
373	Gabbro	Xenolith	-	-	-	-	East flank, Slieve Foye
378	Altered alkali basalt	E.W. dyke	2M	265°	-	1	East flank, Slieve Foye
379	Alkali basalt	N.W. dyke	1.25M	297°	-	?	East flank, Slieve Foye
396	Gabbro	Lopolith	-	-	-	-	North-east flank, Slieve Foye
399	Feldsparphyric dolerite	Cone sheet	3M	-	?	11e	North flank, Slieve Foye
400	Transition dolerite	Cone sheet	?	-	?	11d	North flank, Slieve Foye
421	Transition dolerite	Complementary Cone sheet	1.1M	-	10°	?	St. Patricks River, Slieve Foye
424	Tholeiitic dolerite	N.E. dyke	1.25M	204°	-	11d	St. Patricks River, Slieve Foye
425	Transition dolerite	N.E. dyke	1.3M	239°	-	11d	St. Patricks River, Slieve Foye

Sample Number	Rock Type	Type	Thickness	Structure Trend	Attitude	Age	Locality
426	Feldsparphyric dolerite	Cone sheet	2.5M	-	35°	11e	St. Patricks River Slieve Foye
429	Tholeiitic dolerite	Cone sheet	1M	-	-	?	St. Patricks River Slieve Foye
434	Alkali basalt	N.W. dyke	2M	117°	-	1	St. Patricks River Slieve Foye
435	Alkali basalt	N.E. dyke	1M	237°	-	1	St. Patricks River Slieve Foye
437	High alumina gabbro	N.S. dyke	4M	187°	60°W	11e	St. Patricks River Slieve Foye
438	Tholeiitic dolerite	Cone sheet	0.6M	-	?	11d	St. Patricks River. Slieve Foye
439 *	Tholeiitic dolerite	N.W. dyke	?	-	112°	11d	St. Patricks River Slieve Foye
442	High alumina basalt (Porphyritic tholeiitic dolerite)	Cone sheet	0.5M	-	?	11d	St. Patricks River. Slieve Foye
443	High alumina basalt (Porphyritic tholeiitic dolerite)	Cone sheet	0.3M	-	?	11d	St. Patricks River Slieve Foye
444 *	High alumina basalt (Porphyritic tholeiitic dolerite)	N.S. dyke	3M	187°	-	?	St. Patricks River Slieve Foye

* NOTE: FOR 441 AND 445 SEE P.438.

Sample Number	Rock Type	Type	Thickness	Structure Trend	Attitude	Age	Locality
446	High alumina craignurite	Cone sheet	1.5M	-	?	11e	St. Patricks River Slieve Foye
447	High alumina craignurite felsite	Cone sheet	1.5M	-	?	11e	St. Patricks River Slieve Foye
450	High alumina gabbro	Cone sheet	3M	-	?	11e	St. Patricks River Slieve Foye
451	Tholeiitic dolerite	Cone sheet	1.5M	-	?	11d	St. Patricks River Slieve Foye
452	Feldsparphyric dolerite	Cone sheet	2M	-	?	11e	St. Patricks River Slieve Foye
457	Tholeiitic dolerite	N.W. dyke	2M	137°	-	11d	St. Patricks River Slieve Foye
458	Feldsparphyric dolerite	N.W. dyke	0.4M	137°	-	11e	St. Patricks River Slieve Foye
461	Tholeiitic dolerite	Dyke	?	?	-	11d	North-east flank, Slieve Foye
499	Transition dolerite	Cone sheet	2M	-	?	1b	North-east flank, Slieve Foye
500	Transition dolerite	N.E. dyke	0.5M	230°	-	1b	North-east flank, Slieve Foye
530	Basaltic craignurite	Cone sheet	1.1M	-	?	1a	North-east flank, Slieve Foye
536	Tholeiitic dolerite	Cone sheet	1M	-	?	?	North-east flank, Slieve Foye
550	Craignuritic felsite	Cone sheet	0.6M	-	?	1a	North-east flank, Slieve Foye
557	Tholeiitic dolerite	Cone sheet	?	-	?	11d	North-east flank, Slieve Foye

Sample Number	Rock Type	Type	Thickness	Structure Trend	Attitude	Age	Locality
559	Tholeiitic dolerite	Cone sheet	1.25M	-	?	11d	North-east flank, Slieve Foye
562	Tholeiitic dolerite	Cone sheet	1.25M	-	?	11d	North flank, Slieve Foye
563	Feldsparphyric dolerite	Cone sheet	1.25M	-	?	111e	North flank, Slieve Foye
565	Quartz dolerite	Cone sheet	0.3M	-	?	11c	North flank, Slieve Foye
568	Tholeiitic dolerite	Cone sheet	0.1M	-	40°	11d?	North-east flank, Slieve Foye
575	Basaltic craignurite	Cone sheet	1.5M	-	?	11c?	Two Mile River
582	Tholeiitic dolerite	Cone sheet	1.25M	-	?	11d	Two Mile River
589	Tholeiitic dolerite	Cone sheet	1.5M	-	?	?	Two Mile River
593	Biotite felsite	Complementary Cone sheet	?	-	20°	11a	Two Mile River
603	Tholeiitic dolerite	Cone sheet	1.25M	-	?	11d?	Two Mile River
605	Tholeiitic dolerite	Cone sheet	1.25M	-	?	11d	Two Mile River
619	Craignuritic felsite	Complementary Cone sheet	?	-	30°	?	Two Mile River
625	Tholeiitic dolerite	N.E. dyke	1M	212°	-	11d	Two Mile River
629	Altered quartz dolerite	N.W. Dyke	1.25M	129°	-	11c	Two Mile River
630	Tholeiitic dolerite	Cone sheet?	6M	-	?	11d	Two Mile Rive
636	Gabbro	Lopolith	-	-	-	-	Two Mile River

Sample Number	Rock Type	Structure Type	Thickness	Trend	Attitude	Age	Locality
658	High alumina basalt (Porphyritic tholeiitic dolerite)	Cone sheet	1.25M	-	?	11d	North flank, Slieve Foye
659	Tholeiitic dolerite	Cone sheet	1.25M	-	?	?	North flank, Slieve Foye
663	Tholeiitic dolerite	Cone sheet	1.5M	-	?	11d?	North flank, Slieve Foye
664	Transition dolerite	N.E. dyke	0.5M	242°	40°S	11d?	North flank, Slieve Foye
665	High alumina gabbro	Cone sheet	1.25M	-	?	11e	North flank, Slieve Foye
682	Transition dolerite	N.E. dyke	2M	253°	-	?	North flank, Slieve Foye
684	Tholeiitic dolerite	Cone sheet	1M	-	?	?	North flank, Slieve Foye
685	Craignuritic felsite	Cone sheet	1.25M	-	?	?	North flank, Slieve Foye
718	High alumina basalt (Porphyritic transition dolerite)	Cone sheet	3M	-	?	11d	North flank, Slieve Foye
719	Tholeiitic dolerite	Cone sheet	2M	-	?	11d	North flank, Slieve Foye
744	Basaltic craignurite	Cone sheet	0.75M	-	30°	11c	Upper Bridge, Castletown River
745	Benmorite	N.W. dyke	1M	142°	-	111d	Upper Bridge, Castletown River
746	Carboniferous Limestone	-	-	-	-	-	Upper Bridge, Castletown River
747	High iron trnsition dolerite	Dyke?	-	-	-	?	Upper Bridge, Castletown River

Sample Number	Rock Type	Type	Thickness	Structure Trend	Attitude	Age	Locality
748	Mugearite	N.W. dyke?	?	?	-	111d	Upper Bridge, Castletown River
759	Tholeiitic dolerite	Cone sheet	0.6M	-	32°	111c	Quarry, Castle Hill, Slieve Foye
762	Tholeiitic dolerite	Cone sheet	1.5M	-	33°	111c	Quarry, Castle Hill, Slieve Foye
765	Tholeiitic dolerite	Cone sheet	1.25M	-	35°	11d	Quarry, Castle Hill, Slieve Foye
766	Basaltic craignurite	Cone sheet	2.5M	-	?	11c	Quarry, Castle Hill, Slieve Foye
767	Quartz dolerite	Cone sheet	2M	-	?	?	Quarry, Castle Hill, Slieve Foye
768	Transition dolerite	Cone sheet	0.3M	-	30°	11d	Quarry, Castle Hill, Slieve Foye
769	Transition dolerite	Cone sheet	0.4M	-	?	11d?	Quarry, Castle Hill, Slieve Foye
770	Transition dolerite	N.W. dyke	1M	283°	-	11d	Quarry, Castle Hill, Slieve Foye
771	Tholeiitic dolerite	N.W. dyke	1M	?	-	11d	Quarry, Castle Hill, Slieve Foye
772	Tachylitic transition dolerite	Cone sheet	0.2M	-	?	?	Quarry, Castle Hill, Slieve Foye

Sample Number	Rock Type	Type	Thickness	Structure Trend	Attitude	Age	Locality
775	Quartz dolerite	Cone sheet	1.5M	-	40°	11c	Quarry, Castle Hill, Slieve Foye
780	Tholeiitic dolerite	Cone sheet	1.5M	-	10°	11c	Quarry, Mullatee
783	Alkali basalt	N.W. dyke	1.25M	305°	-	11b	Quarry, Mullatee
799	Alkali basalt	N.W. dyke	1.25M	312°	-	11b	Shore, Whitestown
802	Hawaiite	N.W. dyke	0.6M	?	-	11b	Shore, Whitestown
807	Alkali picrite	N.W. dyke	0.1M	312°	-	11b	Shore, Whitestown
809	Transition dolerite	Cone sheet	1.5M	-	20°	?	Shore, Whitestown
813	Alkali basalt	N.W. dyke	2M	317°	-	11b	Shore, Whitestown
825	Craignurite	N.E. Dyke	1M	217°	-	?	Quarry, Mullatee
827	Tholeiitic dolerite	Cone sheet	1.25M	-	0°	11d	Quarry, Mullatee
830	Tholeiitic dolerite	Cone sheet	1.5M	-	0°	11c	Railway Cutting, Mullatee
831	Alkali basalt	N.W. dyke	?	132°	-	11b	Railway Cutting, Mullatee
838	Craignurite	Cone sheet	?	-	?	11c	Mullatee
839	Felsite	Cone sheet	?	-	0°	?	Mullatee
840	Alkali gabbro	Cone sheet?	?	-	?	?	Mullatee
841	High iron transition dolerite	Cone sheet	0.6M	-	?	11d	Mullatee

Sample Number	Rock Type	Type	Thickness	Structure Trend	Attitude	Age	Locality
842	Tholeiitic dolerite	E.W. dyke	1M	284°	-	11d?	Mullatee
850	Craignuritic felsite	Cone sheet	1.5M	-	40°	11c	Railway Cutting north west of Carlingford
851	Quartz dolerite	Cone sheet	0.25M	-	40°	11c	Railway Cutting north west of Carlingford
852	Quartz dolerite	Cone sheet	0.3M	-	40°	11c	Railway Cutting north west of Carlingford
856	Tholeiitic dolerite	Cone sheet	3M	-	?	?	Railway Cutting north west of Carlingford
859	Rhyolite	Cone sheet	2.5M	-	?	11c?	Railway Cutting north west of Carlingford
864	Quartz dolerite	Cone sheet	0.3M	-	?	11c	Railway Cutting north west of Carlingford
876	Tholeiitic dolerite	N.E. dyke	0.6M	032°	-	11d?	Shore near Two Mile River
877	Tholeiitic dolerite	N.W. dyke	0.6M	127°	-	11d?	Shore near Two Mile River
878	Craignurite	N.W. dyke	0.1M	127°	-	11c?	Shore near Two Mile River
879	Craignurite	N.S. dyke	1.5M	179°	-	11c?	Shore near Two Mile River
884	Quartz dolerite	Cone sheet	1M	-	?	11c	Shore near Two Mile River
885	Biotite felsite	Cone sheet?	?	-	?	11a	Shore near Two Mile River
889	Tholeiitic dolerite	N.E. dyke	3M	247°	-	11d	Shore near Two Mile River

Sample Number	Rock Type	Structure Type	Thickness	Trend	Attitude	Age	Locality
891	Craignurite	Cone sheet?	?	-	?	11c?	Shore near Two Mile River
897	Biotite felsite	Cone sheet	2M	-	?	11a	Shore near St Patricks River
911	Craignuritic felsite with basic craignurite xenoliths	Cone sheet	1.5M	-	40°	11c	Shore, north west of Carlingford
912	Craignuritic felsite	Cone sheet	1.5M	-	40°	11c	Shore north west of Carlingford
915	Alkali basalt	Cone sheet	1M	-	?	1	St Patricks, Slieve Foye
916	Tholeiitic dolerite	Cone sheet	0.3M	-	?	1b	St Patricks, Slieve Foye
944	Transition dolerite	Cone sheet	1M	-	?	1b	North flank, Slieve Foye
945	Hornfelsed Silurian sediment	Cone sheet	-	-	-	-	North flank, Slieve Foye
948	Quartz dolerite	Cone sheet	?	-	?	11c	North flank, Slieve Foye
976	Quartz dolerite	Cone sheet	1M	-	?	11c	North flank, Slieve Foye
980	Basaltic craignurite	Cone sheet	0.3M	-	?	11c	North flank, Slieve Foye
991	Tholeiitic dolerite	Cone sheet	1.25M	-	?	?	North flank, Slieve Foye
1001	Feldsparphyric dolerite	Cone sheet	2.2M	-	?	11e	Ballyonan
1002	Transition dolerite	Dyke	0.3M	?	-	111c?	Ballyonan
1066	Tholeiitic dolerite	Cone sheet	1.25M	-	65°	111c	Round Mountain

Sample Number	Rock Type	Structure Type	Thickness	Trend	Attitude	Age	Locality
1067	Basaltic Craignurite	N.E. dyke	0.6M	019°	-	111b	Round Mountain
1082	Gabbro	Lopolith	-	-	-	-	Round Mountain
1095	Tholeiitic dolerite	Cone sheet	?	-	?	111c	Round Mountain
1118	Variolitic tholeiitic dolerite	Cone sheet	0.2M	-	?	11d?	Ballyonan
1119	High alumina basalt (Porphyritic transition dolerite)	Cone sheet	0.2M	-	?	11d?	Ballyonan
1162	Feldsparphyric dolerite	Cone sheet	?	-	?	111a	Doolargy
1166	Feldsparphyric dolerite	Cone sheet	?	-	?	111a	Doolargy
1168	Quartz dolerite	Cone sheet	?	-	?	111b	Doolargy
1171	Quartz dolerite	Cone sheet?	3M	-	?	111b	Doolargy
1172	Quartz dolerite	Cone sheet	?	-	?	111b	Doolargy
1175	Alkali picrite	N.W. dyke	1M	?	-	11b	Shore, Whitestown
1180	Biotite felsite	Cone sheet	2M	-	?	11a	Ballyonan
1190	Tholeiitic dolerite	Cone sheet	2M	-	?	11d	Ballyonan
1192	Variolitic tholeiitic dolerite	N.E. dyke	1.5M	275°	-	11d	Ballyonan
1193	Tholeiitic dolerite	N.E. dyke	2.5M	073°	-	11d	Ballyonan

Sample Number	Rock Type	Structure Type	Thickness	Trend	Attitude	Age	Locality
1197	Tholeiitic dolerite	Cone sheet	3M	-	?	?	Ballyonan
1203	Quartz feldspar porphyry	N.E. dyke	?	067°	-	11a	Ballyonan
1212	Quartz feldspar porphyry	Cone sheet	2.5M	-	?	11a	Ballyonan
1234	Tholeiitic dolerite	Complementary Cone sheet?	?	-	?	11d	Ballyonan
1235	Lamprophyre	Complementary Cone sheet?	?	-	?	11a??	Ballyonan
1236	Lamprophyre	Complementary Cone sheet?	10M?	-	?	11a??	Ballyonan
1250	Biotite felsite	Cone sheet	?	-	?	11a	Ballyonan
1255	Tholeiitic dolerite	Cone sheet	2.5M	-	?	?	Ballyonan
1289	Quartz dolerite	Cone sheet	1M	-	35°	11c	Cloughmore
1292	Acidified dolerite	N.W. dyke	1.2M	125°	-	111?	Cloughmore
1293	High iron transition dolerite	N.W. dyke	0.25M	?	-	111c	Windy Gap
1303	High iron transition dolerite	N.W. dyke	2.5M	327°	-	111c	Windy Gap
1317	Variolitic quartz dolerite	N.W. dyke	4M	297°	-	111c	Carnawaddy
1318	Craignuritic felsite	E.W. dyke	2M	286°	-	111b	Carnawaddy

Sample Number	Rock Type	Type	Thickness	Structure Trend	Attitude	Age	Locality
1319	Alkali basalt	N.W. dyke	2.5M	152°	-	111d	Carnawaddy
1320	Trachybasalt	N.W. dyke	1.25M	133°	-	111d	Carnawaddy
1324	Basaltic craignurite	Cone sheet	1.25M	-	?	11?	Carnawaddy
1336	Basaltic craignurite	Cone sheet	1M	-	?	111b	Doolargy
1341	High iron transition dolerite	Cone sheet	0.5M	-	?	11d	Shore near Two Mile River
1350	Lamprophyre	N.E. dyke	?	354°	-	11a??	Greer's Quay
1351	Alkali basalt	N.E. dyke	3M	072°	-	11b	Ryland River
1352	High alumina basalt (Porphyritic tholeiitic dolerite)	Cone sheet	1.25M	-	45°	?	Omeath
1366	Lamprophyre	E.W. dyke	2M	097°	-	11a??	Ryland River
1381	Transition dolerite	E.W. dyke	2M	277°	-	?	Shore east of Carlingford
1382	Tristanite	N.W. dyke	0.6M	324°	-	111d	Shore east of Carlingford
1383	Quartz dolerite	N.W. dyke	1M	107°	-	?	Shore east of Carlingford
1385	Basaltic craignurite	N.W. dyke	1.25M	326°	-	?	Shore east of Carlingford
1387	High alumina basalt (Porphyritic tholeiitic dolerite)	Cone sheet	1.5M	320°	30°	?	Shore east of Carlingford
1390	Tholeiitic dolerite	Cone sheet	2M	-	20°	?	Carlingford Castle

Sample Number	Rock Type	Type	Thickness	Structure Trend	Attitude	Age	Locality
1392	Quartz dolerite	Cone sheet	2.5M	-	0°	11c?	Roadside section Mullatee
1393	Quartz dolerite	Cone sheet	1.25M	-	0°	11c	Roadside section Mullatee
1397	Variolitic high iron transition dolerite	Cone sheet	2.2M	-	10°	11d	Roadside section Mullatee
1398	High iron transition dolerite	Cone sheet	0.6M	-	10°	11d?	Roadside section Mullatee
1399	High alumina basalt (Porphyritic tholeiitic dolerite)	Cone sheet	1M	-	10°	11d?	Roadside section Mullatee
1401	Basaltic craignurite	Cone sheet	1.25M	-	10°	11c	Roadside section Mullatee
1407	Quartz dolerite	Cone sheet	1.25M	-	10°	?	Mullatee
9554*	Tholeiitic dolerite	Cone sheet	1.5M	-	15°	11d	Quarry Mullatee
9556*	Alkali basalt	N.W. dyke	1.25M	?	75°S	11b	Quarry, Mullatee
441	Tholeiitic dolerite	Cone sheet	1.25M	-	?	1b	St. Patricks River Slieve Foye
445	Tholeiitic dolerite	Cone sheet	0.3M	-	?	11d	St. Patricks River Slieve Foye

* Collected by M.J. Le Bas sample numbers 554 and 556 respectively

BIBLIOGRAPHY

Akiman, O., 1973. Genesis of the composite intrusions in N.E. Ireland. Bull. Geol. Soc. Turk., Vol. 16, P.1-21.

Allen, J. C., Modreski, P. J., Haygood, C. and Boettcher, A. L., 1972. The role of water in the mantle of the Earth: The stability of amphiboles and mica. Proc 24th Int. Geol. Cong., Montreal, Sec. 2, P. 231-240.

Anderson, E. M., 1936. The dynamics of the formation of cone sheets, ring dykes and cauldron subsidences. Proc. Roy. Soc., Edinburgh, Vol. 56, P.128-157.

Anderson, E. M. and Radley, E. G., 1917. The pitchstones of Mull and their genesis; with notes on the rock-species leidleite and inninmorite, by H. H. Thomas and E. B. Bailey. Quart. Jour. Geol. Soc., London, Vol. 71, P.205-217.

Anderson, J. G. C. and Owen, T. R., 1968. The structure of the British Isles. Pergamon.

Badgley, P. C., 1959. Structural methods for the exploration geologist. Harper Bros.

Badham, J. P. N., 1973. Calc-alkaline volcanism and plutonism from the Great Bear Batholith, N. W. T. Can. Jour. Earth Sci., Vol. 10, P.1319-1328.

Bailey, E. B., 1926. Domes in Scotland and South Africa: Arran and Vredefort. Geol. Mag., Vol. 63, P.481-495.

Bailey, E. B., Clough, C. T., Wright, W. B., Richey, J. E., Wilson, G. V., and others, 1924. The Tertiary and post Tertiary geology of Mull, Loch Aline and Oban. Mem. Geol. Surv. Scotland.

Bailey, E. B. and McCallien, W. J., 1956. Composite minor intrusions and the Slieve Gullion complex, Ireland. Liverpool and Manchester Geol. Jour., Vol. 1, P.466-501.

Baker, P. E., Gass, I. G., Harris, P. G. and Lemaitre, R. W., 1964. The volcanological report of the Royal Society expedition to Tristan da Cunha, 1962. Phil. Trans. Roy. Soc., Ser A, Vol. 256, P.439-578.

Billings, M. P., 1945. Mechanics of igneous intrusion in New Hampshire. Am. Jour. Sci., Vol. 243A, P.40-68.

Bowen, N. L., 1928. The evolution of the igneous rocks. Princeton Univ. Press, (new ed. Dover Publications, 1956).

Bowen, N. L., 1937. Recent high temperature research on silicates and its significance in igneous geology. Am. Jour. Sci., Ser. 5, Vol. 33, P.1-21.

Brown, G. M., 1956. The layered ultrabasic rocks of Rhum, Inner Hebrides. Phil. Trans. Roy. Soc. London, Ser. B, Vol. 240, P.1-53.

Brown, G. M., 1957. Pyroxenes from the early and middle stages of fractionation of the Skaergaard intrusion, East Greenland. Min. Mag., Vol. 31, P.511-543.

Brown, G. M., 1963. Melting relations of Tertiary granitic rocks in Skye and Rhum. Min. Mag., Vol. 33, P.533-562.

Brown, G. M., 1968. Mineralogy of basaltic rocks. In: Basalts, The Poldervaart treatise on rocks of basaltic composition. Edit. Hess, H. H. and Poldervaart, A., Pub. Wiley (Interscience), Vol. 1, P.103-162.

Buddington, A. F., Fahey, J. and Vlisidis, A., 1955. Thermometric and and petrogenetic significance of titaniferous magnetite. Am. Jour. Sci., Vol. 253, P.497-532.

Buddington, A. F. and Lindsley, D. H., 1964. Iron titanium oxide minerals and synthetic equivalents. Jour. Petrol., Vol. 54, P.310-357.

Buist, D. S., 1952. A contribution to the petrochemistry and petrogenesis of the composite sill, South Bute. Trans. Edinburgh. Geol. Soc., Vol. 15, P.52-68.

Buist, D. S., 1959. The composite sill of Rudh' an Eireannaich, Skye. Geol. Mag., Vol. 96,.P.247-252.

Buist, D. S., 1961. The composite sill of Rudh' a' Chromain, Carsaig, Mull. Geol. Mag., Vol. 98, P.67-76.

Bullerwell, W., 1964. Aeromagnetic map of part of Great Britain and Northern Ireland, Sheet 7. Geol. Surv. Great Britain.

Cann, J. R., 1970. Upward movement of granitic magma. Geol. Mag., Vol. 107, P.335-340.

Carmichael, I. S. E., 1963. The cyrstallization of feldspar in volcanic acid liquids. Quart. Jour. Geol. Soc. London, Vol. 119, P.95-131.

Carmichael, I. S. E., 1964. The petrology of Thingmuli, a Tertiary volcano in eastern Iceland. Jour. Petrol., Vol. 5, P.435-460.

Carmichael, I. S. E., 1967. The iron-titanium oxides of salic volcanic rocks and their associated ferromagnesian silicates. Contr. Min. and Petrol., Vol. 14, P.36-64.

Carmichael, I. S. E. and Nicholls, J., 1967. Iron-titanium oxides and oxygen fugacities in volcanic rocks. Jour. Geophys. Res., Vol. 72, P.4665-4687.

Charlesworth, J. K. and eight others, 1960. The geology of North East Ireland. Proc. Geol. Ass., Vol. 71, P.429-459.

Chayes, F., 1966. Alkaline and subalkaline basalts. Am. Jour. Sci., Vol. 264, P.128-145.

Chayes, F., 1972. Silica saturation in Cenozoic basalts. Phil. Trans. Roy. Soc. London, Ser. A, Vol. 271, P.285-296.

Cloos, E., 1932. Feather joints as indicators of direction of movement on faults, thrusts, joints and magmatic contacts. Proc. Nat. Acad. Sci. Am., Vol. 18, P.387-395.

Coats, R. R., 1968. Basaltic andesites. In: Basalts, the Poldervaart treatise on rocks of basaltic composition. Edit. Hess, H. H. and Poldervaart, A., Pub. Wiley (Interscience), Vol. 2, P.689-736.

Cohen, L. H., Ito, K. and Kennedy, G. C., 1967. Melting and phase relations in an anhydrous basalt to 40 kilobars. Am. Jour. Sci., Vol. 265, P.475-518.

Cole, G. A. J., 1894. On derived crystals in the basaltic andesite of Glasdrumman Port, County Down. Sci. Trans. Roy. Soc. Dublin, Ser. 2, Vol. 5, P.239-248.

Cook, A. H. and Murphy, T., 1952. Gravity survey of Ireland, north of the line Sligo-Dundalk. Inst. Advanced Studies, School of Cosmic Physics, Dublin, Geophys. Mem. No. 2, P.1-36.

Coombs, D. S., 1963. Trends and affinites of basaltic magmas and pyroxenes as illustrated on the diopside-olivine-silica diagram. Min. Soc. Am. Spec. Paper 1, P.227-250.

Cooper, D. C., 1971. The geology of the area around Eydehaven, South Norway Unpublished PhD. thesis, University of Nottingham.

Cornwall, H. R. and Rose, H. J., 1957. Minor elements in Keweenawan lavas, Michigan. Geochim. et Cosmochim. Acta, Vol. 12, P.209-224.

Cox, K. G., 1972. Tholeiites and alkali basalts: unimodal or bimodal population? Earth and Planet. Sci. Lett., Vol. 16, P.185-188.

Daly, R. A., 1903a. The mechanics of igneous intrusion. Am. Jour. Sci., Ser. 4, Vol. 15, P.269-298.

Daly, R. A., 1903b. The mechanics of igneous intrusion. Am. Jour. Sci., Ser. 4, Vol. 16, P.107-126.

Daly, R. A., 1908. The mechanics of igneous intrusion. Am. Jour. Sci., Ser. 4, Vol. 26, P.17-50.

Daly, R. A., 1933a. Igneous rocks and the depths of the Earth. Mcgraw-Hill.

Daly, R. A., 1933b. The depths of the Earth. Presidential address (1932), Bull. Geol. Soc. Am., Vol. 44, P.243-264.

Deer, W. A., 1969. Field excursion guide to the Tertiary volcanic rocks of Ardnamurchan. Int. Ass. Volc. and Chem. of the Earths Interior, Symp. Volcanoes and their roots, Oxford.

Deer, W. A., Howie, R. A. and Zussman, J., 1966. An introduction to the rock forming minerals. Longmans, Green and Co.

de Sitter, L. U., 1964. Structural geology. McGraw Hill.

Drever, H. I. and Johnston, R., 1958. The petrology of picritic rocks in minor intrusions - a Hebridean group. Trans. Roy. Soc. Edinburgh, Vol. 63, P.459-499.

Durrance, E. M., 1967. Photoelastic stress studies and their application to a mechanical analysis of the Tertiary ring complex of Ardnamurchan, Argyllshire. Proc. Geol. Ass., Vol. 78, P.289-318.

Du Toit, A. L., 1920. The Karoo dolerites of S. Africa: a study in hypabyssal injection. Trans. Geol. Soc. S. Africa, Vol. 23, P.1-42.

Emeleus, C. H., 1955. The granites of the Western Mourne Mountains, County Down. Scient. Proc. Roy. Soc. Dub., Vol. 27, P.35-50.

Emeleus, C. H. and Preston, J., 1969. Field excursion guide to the Tertiary volcanic rocks of Ireland. Int. Ass. Volc. and Chem. of the Earths Interior, Symp. Volcanoes and their roots, Oxford.

Elder, J. W., 1966. Penetrative convection: its role in volcanism. Bull. Volcan., Vol. 29, P.327-343.

Engel, A. E. J. and Engel, C. G., 1964. Composition of basalts from the Mid Atlantic ridge. Science, Vol. 144, P.1330-1333.

Engel, A. E. J., Engel, C. G. and Havens, R. G., 1965. Chemical characteristics of oceanic basalts and the upper mantle. Bull. Geol. Soc. Am. Vol. 76, P.719-734.

Engel, C. G., Fisher, R. L. and Engel, A. E. J., 1965. Igneous rocks of the Indian Ocean floor. Science, Vol. 150, P.605-610.

Evans, A. L., Fitch, F. J. and Miller, J. A., 1973. Potassium-argon age determinations on some British Tertiary igneous rocks. Jour. Geol. Soc. London, Vol. 129, P.419-443.

Eyles, V. A. and Simpson, J. B., 1921. Silica percentages of igneous rocks. Geol. Mag., Vol. 58, P.436-440.

Flanagan, F. J., 1973. 1972 values for international geochemical reference samples. Geochim. et cosmochim. Acta, Vol. 37, P.1189-1200.

Flett, J. S., 1930. The teschenite of Easter Dalmeny. Sum. Progr. Geol. Surv. Great Britain, 1929, Pt. 3, P.59-74.

Flower, M. F. J., 1971. Evidence for the role of phlogopite in the genesis of alkali basalts. Contr. Min. and Petrol., Vol. 32, P.126-137.

Frankel, J. J., 1968. Forms and structures of intrusive basaltic rocks. In: Basalts, the Poldervaart treatise on rocks of basaltic composition. Edit. Hess, H. H. and Poldervaart, A., Pub. Wiley (Interscience), Vol. 1, P.63-102.

Fryklund, V. C. and Fleischer, M., 1963. The abundance of scandium in volcanic rocks a preliminary estimate. Geochim. et cosmochim. Acta, Vol. 27, P.643-664.

Garson, M. S., 1959. Stress pattern of carbonatitic and alkaline dykes at Tundulu ring structure, Southern Nyasaland. Proc. 20th. Int. Geol. Congr., Mexico. Ass. Serv. Geol. Africanos Actas, P.309-323.

Garson, M. S. and Smith, W. C., 1958. The geology of Chilwa Island. Mem. Geol. Surv. Nyasaland No. 1.

Gass, I. G., 1972. Proposals concerning the variations of volcanic products and processes within the oceanic environment. Phil. Trans. Roy. Soc., Ser. A, Vol. 271, P.131-140.

Gast, P. W. 1968. Trace element fractionation and the origin of tholeiitic and alkaline magma types. Geochim. et Cosmochim. Acta, Vol. 32, P.1057-1086.

Goles, G. G., 1967. Trace elements in ultramafic rocks. In: Ultramafic and related rocks, Edit. Wyllie, P. J., Pub. Wiley, P.352-362.

Green, D. H., 1968a. Effects of high pressure on basaltic rock. In: Basalts, the Poldervaart treatise on rocks of basaltic composition Edit. Hess, H. H. and Poldervaart, A., Pub. Wiley (interscience), Vol. 1, P.401-443.

Green, D. H., 1968b. Origin of basaltic magmas. In: Basalts, the Poldervaart treatise on rocks of basaltic composition. Edit. Hess, H. H. and Poldervaart, A, Pub. Wiley (interscience), Vol. 2, P.835-862.

Green, D. H., 1969a. The origin of basaltic and nephelinitic magmas in the Earths' mantle. Tectonophysics, Vol. 7, P.409-422.

Green, D. H., 1969b. A review of experimental evidence on the origin of basaltic and nephelinitic magmas. Phys. Earth. Planetary Interiors, Vol. 3, P.221-235.

Green, D. H., 1970. The origin of basaltic and nephelinitic magmas. Trans. Leicester Lit. and Phil. Soc., Vol. 64, P.28-54.

Green, D. H. and Ringwood, A. E., 1964. Fractionation of basalt magmas at high pressure. Nature, Vol. 201, P.1276-1279.

Green, D. H. and Ringwood, A. E., 1967. The genesis of basaltic magmas. Contr. Min. and Petrol., Vol. 15, P.103-190.

Green, T. H., Green, D. H. and Ringwood, A. E., 1967. The origin of high alumina basalts and their relationships to quartz tholeiites and alkali basalts. Earth and Planet. Sci. Lett., Vol. 2, P.41-51.

Griffith, R., 1840. Presidential Address. Jour. Geol. Soc. Dublin, 1843, P.95-130.

Griffin, W. L. and Murthy, V. R., 1968. Abundances of K, Rb, Sr, and Ba in some ultramafic rocks and minerals. Earth and Planet. Sci. Lett., Vol. 4, P.497-501.

Grout, F. F., 1918. The lopolith an igneous form exemplified by the Duluth gabbro. Am. Jour. Sci., Vol. 46, P.516-522.

Groves, A. W., 1951. Silicate analysis. 2nd Ed., Allen and Unwin.

Gussow, W. C., 1968. Salt diapirism: importance of temperature and energy source of emplacement. Am. Ass. Petrol. Gelogists, Symp. Diapirism and Diapirs, Edit. Braunstein, J. and O'Brien, G. D., P.16-52.

Hafner, S., 1960. Metalloxyde mit spinellstruktur. Swhweiz miner. Petrogr. Mitt., Vol. 40, P.207-242.

Halsall, T. J. and Le Bas, M. J., 1971. The Tertiary Dykes of Kildonan, South Arran. Proc. Geol. Soc. London, in Jour. Geol. Soc. 1971, Vol. 127, P.292-293.

Hamilton, C. W., 1839. Observations and sections made in the district lying between the Mourne and Dublin Mountains. Jour. Geol. Soc. Dublin, 1843, P.51-69.

Hamilton, D. L. amd Anderson, G. M., 1968. The effects of water and oxygen pressures on the crystallization of basaltic magmas. In: Basalts, the Poldervaart treatise on rocks of basaltic composition. Edit. Hess, H. H. and Poldervaart, A., Pub. Wiley (Interscience), Vol. 1, P.445-482.

Harker, A., 1904. The Tertiary igneous rocks of Skye. Mem. Geol. Surv. United Kingdom.

Harker, A., 1908. The geology of the Small Isles of Inverness-shire. Mem. Geol. Surv. United Kingdom.

Harris, P. G., 1957. Zone refining and the origin of potassic basalts. Geochim. et Cosmochim. Acta, Vol. 12, P.195-208.

Harris, P. G., 1972. Geothermal environment and basaltic magma type. Jour. Earth Sci., Vol. 8, P.275-284.

Harris, P. G., Hutchinson, R. and Paul, D. K., 1972. Plutonic xenoliths and their relation to the upper mantle. Phil. Trans. Roy. Soc. London, Ser. A, Vol. 271, P.313-323.

Harris, P. G., Ray, A. and White, I. G., 1967. Chemical composition of the upper mantle. Jour. Geophys. Res., Vol. 72, P.6359-6369.

Harris, P. G. and Rowell, J. A., 1960. Some geochemical aspects of the Mohorovicic discontinuity. Jour. Geophys. Res., Vol. 65, P.2443-2459.

Harry, W. T., 1952. Basic hornfels at a gabbro contact near Carlingford, Eire. Geol. Mag., Vol. 89, P.411-416.

Harry, W. T., 1954. The clinopyroxene - hornblende equilibrium in thermal metamorphism: some data from Carlingford, Eire. Geol. Mag., Vol. 91, P.79-85.

Harvey, P. K., Taylor, D. M., Hendry, R. D. and Bancroft, F., 1972. An accurate fusion method for the analysis of rocks and chemically related materials by Xray fluorescence spectrometry. Xray spectrometry, Vol. 2, P.33-44.

Hatch, F. H., Wells, A. K. and Wells, M. K., 1961. Petrology of the igneous rocks. 12th Edit. Murby and Co.

Haughton, S., 1856. Experimental researches on the granites of Ireland. Quart. Jour. Geol. Soc. London, Vol. 12, P.171-202.

Haughton, S., 1858. Experimental researches on the granites of Ireland. Quart. Jour. Geol. Soc. London, Vol. 14, P.300-305.

Haughton, S., 1876. On the trap dykes that penetrate the granites, metamorphic slates and Carboniferous Limestones of the district of Mourne in the north east of Ireland. Jour. Roy. Geol. Soc. Ire., Vol. 4, P.91-104.

Hill, U. T., 1959. Photometric determination of aluminium in steel. Anal. Chem., Vol. 31, P.429-431.

Hill, E. S., 1963. Elements of structural geology. Methuen.

Holland, J. G. amd Brown, G. M., 1972. Hebridean tholeiitic magmas: a geological study of the Ardnamurchan cone sheets. Contr. Min. and Petrol., Vol. 37, P.139-160.

Holmes, A. and Harwood, H. S., 1929. The tholeiitic dikes of the north of England. Min. Mag., Vol. 22, P.1-52.

Hough, F. E., 1972. In discussion of O'Hara, 1972. Jour. Earth. Sci., Vol. 8, P.221.

Hull, E., 1875. On the microscopic structure of a fragment of 'baked' or indurated slate, from the Lower Silurian rocks, Claremont Hill, near Dundalk. Jour. Roy. Geol. Soc. Ireland, Vol. 4, P.85-88.

Hurley, P. M., 1968a. Absolute abundance and distribution of Rb, K, and Sr in the Earth. Geochim. et Cosmochim. Acta, Vol. 32, P.273-283.

Hurley, P. M., 1968b. Correction to: Absolute abundance and distribution of Rb, K and Sr in the Earth. Geochim. et Cosmochim. Acta, Vol. 32, P.1025-1030.

Iida, C., 1961. Trace elements in minerals and rocks of the Izu-Hakone region, Japan, Part II, Plagioclase. Jour. Earth. Sci., Nagoya Univ., Vol. 9, P.14-28.

Irvine, T. N. and Baragar, W. R. A., 1971. A guide to the chemical classification of the common volcanic rocks. Can. Jour. Earth Sci., Vol. 8, P.523-548.

Ito, K. and Kennedy, G. C., 1967. Melting and phase relations in a natural periodotite to 40 kilobars. Am. Jour. Sci., Vol. 265, P.519-539.

Jaeger, J. C., 1964. Thermal effects of intrusions. Geophys. Rev., Vol. 2, P.443-466.

Jakobsson, S. P., Pederson, A. K., Rönsbo, J. G. and Larsen, M. L., 1973. Petrology of mugearite-hawaiite: early extrusives in the 1973 Heimaey eruption, Iceland. Lithos, Vol. 6, P.203-214.

Jamieson, B. G., 1966. Evidence on the evolution of basaltic magma at elevated pressure. Nature, Vol. 212, P.243-246.

Jamieson, B. G. and Clarke, D. B., 1970. Potassium and associated elements in tholeiitic basalts. Jour. Petrol., Vol. 11, P.183-204.

Jeffery, P. G., 1970. Chemical methods of rock analysis. Pergamon.

Judd, J. W., 1893. On composite dykes in Arran. Quart. Jour. Geol. Soc. London, Vol. 49, P.536-564.

Kennedy, W. Q., 1933. Trends of differentiation in basaltic magmas. Am. Jour. Sci., Ser. 5, Vol. 25, P. 239-256.

King, B. C., 1954. The Ard Bheinn area of the central igneous complex of Arran. Quart. Jour. Geol. Soc. London, Vol. 110, P.323-355.

King, B. C., 1962. The nature of basic igneous rocks and their relations with associated acid rocks: Part I. Sci. Prog., Vol. 50, P.616-629.

King, B. C., 1963a. The nature of basic igneous rocks and their relations with associated acid rocks: Part II. Sci. Prog., Vol. 51, P.259-275.

King, B. C., 1963b. The nature of basic igneous rocks and their relations with associated acid rocks: Part III. Sci. Prog., Vol. 51, P.610-628.

King, B. C., 1964. The nature of basic igneous rocks and their relations with associated acid rocks: Part IV. Sci. Prog., Vol. 52, P.282-292.

King, B. C., 1965a. The nature of basic igneous rocks and their relations with associated acid rocks: Part V. Sci. Prog., Vol. 53, P.117-125.

King, B. C., 1965b. The nature of basic igneous rocks and their relations with associated acid rocks: Part VI. Sci. Prog., Vol. 53, P.437-446.

Kuno, H., 1950. Petrology of Hakone volcano and the adjacent areas, Japan. Bull. Geol. Soc. Am., Vol. 61, P.957-1020.

Kuno, H., 1959. Petrology of Cenozoic petrographic provinces of Japan and surrounding areas. Bull. Volcan., Vol. 20, P.37-76.

Kuno, H., 1960. High alumina basalt. Jour. Petrol., Vol. 1, P.121-145.

Kuno, H., 1968. Differentiation of basalt magmas. In: Basalts, the Poldervaart treatise on rocks of basaltic composition. Edit. Hess, H. H. and Poldervaart, A., Pub. Wiley (Interscience), Vol. 2, P.623-688.

Kuno, H., Yamasaki, K., Iida, C., and Nagashima, K., 1957. Differentiation of Hawaiian magmas. Japan. Jour. Geol. and Geog., Vol. 28, P.179-218.

Kushiro, I., 1960. Si - Al relations in clinopyroxenes from igneous rocks. Am. Jour. Sci., Vol. 258, P.548-554.

Kushiro, I., 1961. A possible origin of tholeiitic magma. Japan. Jour. Geol. and Geog., Vol. 32, P.31-37.

Kushiro, I., 1968. Compositions of magmas formed by partial zone melting of the Earths' upper mantle. Jour. Geophys. Res., Vol. 73, P.619-634.

Kushiro, I. and Kuno, H., 1963. Origin of primary basalt magmas and classification of basaltic rocks. Jour. Petrol., Vol. 4, P.75-89.

Leake, B. E., Hendry, G. L., Kemp, A., Plant, A. G., Harvey, P. K., Wilson, J. R., Coats, J. S., Aucott, J. W., Lünel, T.and Howarth, R. J., 1968. The chemical analysis of rock powders by auotmatic Xray fluorescence. Chem. Geol., Vol. 5, P.7-86.

Le Bas, M. J., 1955. Structure and petrology of the Carlingford complex, Co. Louth. Unpublished Ph.D. thesis, University of Cambridge.

Le Bas, M. J., 1960. The petrology of the layered basic rocks of the Carlingford complex, Co. Louth. Trans. Roy. Soc. Edinburgh, Vol. 64, P.169-200.

Le Bas, M. J., 1962. The role of aluminium in igneous clinopyroxenes with relation to their parentage. Am. Jour. Sci., Vol. 260, P.267-288.

Le Bas, M. J. 1965a. On the occurrence in Ireland of a lava related to hawaiite. Proc. Geol. Ass., Vol. 76, P.91-94.

Le Bas, M. J., 1965b. The contamination of a gabbro by Carboniferous Limestone at Carlingford, Co. Louth. Min. Mag., Vol. 34, P.292-302.

Le Bas, M. J., 1967. On the origin of the Tertiary granophyres of the Carlingford complex, Ireland. Proc. Roy. Irish Acad., Sec. B, Vol. 65, P.325-340.

Le Bas, M. J., 1970a. The geochemistry of plagioclases from the gabbroic rocks of the Carlingford complex, Ireland. West Commemoration Volume, Edit. Murty, T. V. V. G. R. K. University of Saugor. P.64-78.

Le Bas, M. J., 1970b. Trace elements in the gabbros, olivines, augites and magnetites of the Carlingford complex, Ireland. Proc. Roy. Irish Acad., Sec. B, Vol. 69, P.217-243.

Le Bas, M. J., 1971. Cone sheets as a mechanism of uplift. Geol. Mag., Vol. 108, P. 313-376.

Liebenberg, C. J., 1960. Trace elements of the rocks of the Bushveld igneous complex. Publikasies vandie Universiteit van Pretoria, Nuwe Reeks, Nr. 12, P.1-69.

Luth, W. C., Jahns, R. H. and Tuttle, O. F., 1964. The granite system at pressures of 4 to 10 kilobars. Jour. Geophys. Res., Vol. 69, P.759-773.

Macdonald, G. A., 1949. Hawaiian petrographic province. Bull. Geol. Soc. Am., Vol. 60, P.1541-1596.

Macdonald, G. A., 1957. Dissimilarity of continental and oceanic rock suites (abstract). Bull. Geol. Soc. Am., Vol. 68, P.1761-1762.

Macdonald, G. A., 1960. Dissimilarity of continental and oceanic rock types Jour. Petrol., Vol. 1, P.172-177.

Macdonald, G. A., 1968. Composition and origin of Hawaiian lavas. In: Studies in volcanology, Geol. Soc. Am. Mem. 116, P.477-522.

Macdonald, G. A. and Katsura, T., 1964. Chemical composition of Hawaiian lavas. Jour. Petrol., Vol. 5, P.82-133.

Manson, V., 1968. Geochemistry of basaltic rocks: Major elements. In: Basalts, the Poldervaart treatise on rocks of basaltic composition. Edit., Hess, H. H. and Poldervaart, A., Pub. Wiley (Interscience), Vol. 1, P.215-219.

McDougall, I. and Lovering, J. P., 1963. Fractionation of chromium, nickel, cobalt and copper in a differentiated dolerite - granophyre sequence at Red Hill, Tasmania. Jour. Geol. Soc. Australia, Vol. 10, P.325-338.

Meighan, I. C. amd Gamble, J. A., 1973. The geochemistry and origin of Tertiary acid rocks in N. E. Ireland. Proc. Geol. Soc. London, in Jour. Geol. Soc. 1974, Vol. 130, P.181.

Melson, W. G., Thompson, G. and Van Andel, T. H., 1968. Volcanism and metamorphism in the mid-Atlantic ridge, 22° N latitude. Jour. Geophys. Res., Vol. 73, P.5925-5941.

Middlemost, E. A. K., 1972. A simple classification of volcanic rocks. Bull. Volcan., Vol. 36, P.382-397.

Middlemost, E. A. K., 1973. Evolution of volcanic islands. Lithos, Vol. 6, P.123-132.

Miller, J. A. and Brown, P. E., 1965. K - Ar age studies in Scotland. Geol. Mag., Vol. 102, P.108-134.

Morgan, W. J., 1971. Convection plumes in the lower mantle. Nature (Phys. Sci.), Vol. 230, P.42-43.

Muan, A. and Osborn, E. F., 1956. Phase equilibria a liquidus temperatures in the system Mgo - FeO - Fe_2O_3 - SiO_2. Jour. Am. Ceram. Soc., Vol. 39, P.121-140.

Muir, I. D. and Tilley, C. E., 1957. Contributions to the petrology of Hawaiian basalts, 1. The picrite-basalts of Kilauea. Am. Jour. Sci., Vol. 255, P.241-253.

Nockolds, S. R., 1935. Contribution to the petrology of Barnavave, Carlingford, I. F. S., 1. The junction hybrids. Geol. Mag., Vol. 72, P.289-315.

Nockolds, S. R., 1937. Contributions to the petrology of Barnavave, Carlingford, I. F. S., 2. An occurrence of quartz-bearing syenite and its xenoliths. Geol. Mag., Vol. 74, P.125-132.

Nockolds, S. R., 1938. Contributions to the petrology of Barnavave, Carlingford, I. F. S., 3. On some hybrids from the E. and S. E. slopes of Barnavave Mountain. Geol. Mag., Vol. 75, P.469-479.

Nockolds, S. R. and Allen, R., 1953. The geochemistry of some igneous rock series. Geochim. et Cosmochim. Acta, Vol. 4, P.105-142.

Norman, J. C. and Haskin, L. A., 1968. The geochemistry of Sc: a comparison to the rare earths and Fe. Geochim. et Cosmochim. Acta, Vol. 32, P.93-108.

Norrish, K. and Hutton, J. T., 1969. An accurate Xray spectrographic method for the analysis of a wide range of geological samples. Geochim. et Cosmochim. Acta, Vol. 33, P.431-453.

Odé, H., 1957. Mechanical analysis of the dike pattern of the Spanish Peaks area, Colorado. Bull. Geol. Soc. Am., Vol. 68, P.567-575.

O'Hara, M. J. 1965. Primary magmas and the origin of basalts. Scot. Jour. Geol., Vol. 1, P.19-40.

O'Hara, M. J., 1968a. The bearing of phase equilibria studies in synthetic and natural systems on the origin and evolution of basic and ultrabasic rocks. Earth Sci. Rev., Vol. 4, P.69-133.

O'Hara, M. J., 1968b. Are ocean-floor basalts primary magma? Nature, Vol. 220, P.683-686.

O'Hara, M. J., 1972. Upper mantle melting from the bottom the source of magmatism and the driving force of global tectonics, (abstract). Jour. Earth Sci., Vol. 8, P.219-224.

O'Hara, M. J. and Yoder, H. S. Jr., 1963. Partial melting of the mantle. Carnegie Inst. Washington Yearbook, Vol. 62, P.67-71.

O'Hara, M. J. and Yoder, H. S. Jr., 1967. Formation and fractionation of basic magmas at high pressures. Scot. Jour. Geol., Vol. 3, P.67-117.

Osborn, E. F., 1959. Role of oxygen pressure in the crystallization and differentiation of basaltic magma. Am. Jour. Sci., Vol. 257, P.607-647.

Osborn, E. F., 1962. Reaction series for subalkaline igneous rocks based on different oxygen pressure conditions. Am. Mineral., Vol. 47, P.211-226.

Osborn, E. F. and Roeder, P. L., 1960. Effect of oxygen pressure on crystallization in simplified basalt systems. Proc. 21st Int. Geol. Congr., Copenhagen, No. 13, P.147-155.

Parker, A., 1973. Manual of Xray fluorescence techniques. On file Departmental Library, Dept. Geology, University of Reading.

Patterson, E. M., 1950. Evidence of fissure eruption in the Tertiary lava plateau of north eastern Ireland. Geol. Mag., Vol. 87, P.45-52.

Patterson, E. M. and Swaine, D. J., 1957. The Tertiary dolerite plugs of north east Ireland. Trans. Roy. Soc. Edinburgh, Vol. 63, P.317-331.

Poldervaart, A., 1964. Chemical definition of alkali basalts and tholeiites. Bull. Geol. Soc. Am., Vol. 75, P.229-232.

Poldervaart, A. and Hess, H. H., 1951. Pyroxenes in the crystallization of basaltic magma. Jour. Geol., Vol. 59, P.472-489.

Powers, H. A., 1935. Differentiation of Hawaiian lavas. Am. Jour. Sci., Ser. 5, Vol. 30, P.57-71.

Presnall, D. C., 1963. The join $Mg_2 SiO_2$ - Ca Mg Si_2O_6 - iron oxide at oxygen pressures from 0.21 to 10^{-8} atmospheres. Unpublished Ph.D. thesis, Pa. State University.

Presnall, D. C., 1966. The join forserite-diopside-iron oxide and its bearing on the crystallization of basaltic and ultramafic magmas. Am. Jour. Sci., Vol. 264, P.753-809.

Preston, J., 1963. The dolerite plug at Slemish, County Antrim, Ireland. Liverpool and Manchester Geol. Jour., Vol. 3, P.301-314.

Preston, J., 1965. Tertiary feeder dykes in the west of Ireland. Proc. Geol. Soc. London, No.1626, P.149-150.

Preston, J., 1967a. A Tertiary feeder dyke in County Fermanagh, Northern Ireland. Sci. Proc. Roy. Soc. Dublin, Ser. A, Vol. 3, P.1-16.

Preston, J., 1967b. The Blind Rock dyke, Co. Donegal. Irish Nat. Jour., Vol. 15, P.286-293.

Preston, J., 1971. The Maddygalla dyke, Rathlin Island. Irish. Nat. Jour., Vol. 17, P.88-92.

Prinz, M., 1968. Geochemistry of basaltic rocks: Trace element. In: Basalts, the Poldervaart treatise on rocks of basaltic composition. Edit. Hess, H. H. and Poldervaart, A., Pub. Wiley (Interscience), Vol. 1, P.271-323.

Rao, M. S., 1959. Minor acid intrusions and dykes of Lamlash - Whiting Bay Region, Arran. Geol. Mag., Vol. 96, P.237-246.

Rast, N., Diggens, J. N. and Rast, D. E., 1968. Triassic rocks of the Isle of Mull; their sedimentation, facies, structure and relationship to the Great Glen Fault and the Mull Caldera. Proc. Geol. Soc. London, No. 1645, P.299-304.

Ray, P. S., 1960. Ignimbrite in the Kilchrist Vent, Isle of Skye. Geol. Mag., Vol. 97, P.229-238.

Reidel, W., 1929. Zur mechanik geologischer brucherscheinungen. Centralbl. f. Min. etc., Abt. B, P.354-368.

Reynolds, D. L., 1931. Dykes of the Ards Peninsula, Co. Down. Geol. Mag., Vol. 68, P.97-111 and 145-165.

Reynolds, D. L., 1951. The geology of Slieve Gullion, Foughill and Carrickarnon; an actualistic interpretation of a Tertiary gabbro-granophyre complex. Trans. Roy. Soc. Edinburgh, Vol. 62, P.85-142.

Richey, J. E., 1928. The structural relations of the Mourne granites (Northern Ireland). Quart. Jour. Geol. Soc. London, Vol. 83, P.653-688.

Richey, J. E., 1932. Tertiary ring structures in Britain. Trans. Geol. Soc. Glasgow, Vol. 19, P.42-140.

Richey, J. E., 1939. The dykes of Scotland. Trans. Geol. Soc. Edinburgh, Vol. 13, P.393-435.

Richey, J. E., 1958. Feldspathic types of basaltic rocks. In: Dolerite. University of Tasmania Symp., P.63-69.

Richey, J. E., 1961. Scotland: the Tertiary volcanic districts (3rd Edit.). British Regional Geology, Revised by Macgregor, A. G. and Anderson, F. W., H.M.S.O.

Richey, J. E. and Thomas, H. H., 1930. The geology of Ardnamurchan, North West Mull and Coll. Mem. Geol. Surv. Scotland.

Richey, J. E. and Thomas, H. H., 1932. The Tertiary ring complex of Slieve Gullion (Ireland). Quart. Jour. Geol. Soc. London, Vol. 88, P.776-849.

Ridley, W. I., 1971a. The petrology of some volcanic rocks from the British Tertiary Province: The islands of Rhum, Eigg, Canna and Muck. Contr. Min. and Petrol., Vol. 32, P.251-266.

Ridley, W. I., 1971b. Some chemical features of basalts from the British Tertiary Province. Earth and Planet. Sci. Lett., Vol. 11, P.435-439.

Rigg, T. and Wagenbauer, H. A., 1961. Spectrophotmetric determinations of titanium in silicate rocks. Anal. Chem., Vol. 33, P.1347-1349.

Riley, J. P., 1958. The rapid analysis of silicate rocks and minerals. Anal. Chim. Acta, Vol. 19, P.413-428.

Ringwood, A. E., 1955. The principles governing trace element distribution during magmatic crystallization - 1; the influence of electro-negativity. Geochim. et Cosmochim. Acta, Vol. 7, P.189-202.

Ringwood, A. E., 1966a. The chemical composition and origin of the Earth. In: Advances in Earth Science. Edit. Hurley, P. M., Pub. M.I.T. Press, P.287-356.

Ringwood, A. E., 1966b. The mineralogy of the mantle. In: Advances in Earth Science. Edit. Hurley, P. M., Pub. M.I.T. Press, P.357-417.

Ringwood, A. E., 1969. Composition of the crust and upper mantle. In: The Earth's crust and upper mantle. Monogr. Am. Geophys. Un., No. 13, P.1-17.

Roberts, J. L., 1970. The intrusion of magma into brittle rocks. In: Mechanics of igneous intrusion. Edit. Newall, G. and Rast, N., Geol. Jour. Spec. Issue No. 2, P.287-338.

Robson, G. R. and Barr, K. G., 1964. The effect of stress on faulting and minor intrusions in the vicinity of a magma body. Bull. Volcan., Vol. 27, P.315-330.

Roeder, P. L. and Osoborn, E. F., 1966. Experimental data for the system $MgO - FeO - Fe_2O_3 - CaAl_2Si_2O_8 - SiO_2$ and their petrologic implications. Am. Jour. Sci., Vol. 264, P.428-480.

Rose, G., 1863. Beschribung und eintheilung der meteorites. Abh. Preuss. Akad. Wiss., P.26-161.

Schairer, J. F., 1957. Melting relations of the common rock forming oxides. Jour. Am. Ceram. Soc., Vol. 40, P.215-235.

Schilling, J. G., 1973a. Afar mantle plume: rare Earth evidence. Nature (Physical Sci.), Vol. 242, P.2-5.

Schilling, J. G., 1973b. Iceland mantle plume: geochemical study of Reykjanes Ridge. Nature, Vol. 242, P.565-571.

Scrutton, R. A., Stacey, A. P. and Gray, F., 1971. Evidence for the mode of formation of Porcupine Sea bight. Earthand Planet. Sci. Lett., Vol. 11, P.140-146.

Sen, S. K., 1960. Some aspects of the distribution of barium, strontium, iron and titanium in plagioclase feldspars. Jour. Geol., Vol. 68, P.638-665.

Shapiro, L. and Brannock, W. W., 1952. Rapid analysis of silicate rocks. U. S. Geol. Surv. Circ. , No.165.

Shapiro, L. and Brannock, W. W., 1956. Rapid analysis of silicate rocks. Bull. U. S. Geol. Surv., No.1036C.

Shapiro, L. and Brannock, W. W., 1962. Rapid analysis of silicate, carbonate and phosphate rocks. Bull. U. S. Geol. Surv., No.1144A.

Skelhorn, R. R., 1959. A study of some composite sills in Skye and Mull. Unpublished Ph.D. thesis, University of London.

Skelhorn, R. R., Speight, J. M., Sloan, T. and Knaap, R. J., 1971. The structural significance of the Tertiary Hebridean dyke swarms of Britain. Proc. Geol. Soc. London, in Jour. Geol. Soc. 1971, Vol. 127, P.98.

Smellie, W. R., 1913. Tertiary composite sill of south Bute. Trans. Geol. Soc. Glasgow, Vol. 15, P.121-139.

Sollas, W. J., 1894. On the volcanic district of Carlingford and Slieve Gullion. Part 1. - on the relation of the granite to the gabbro of Barnavave, Carlingford. Trans. Roy. Irish Acad., Vol. 30, P.477-512.

Spencer, E. W., 1959. Geologic evolution of the Beartooth Mountains, Montana and Wyoming. Bull. Geol. Soc. Am., Vol. 70, P.467-508.

Streckeissen, A. L., 1965. Die klassifikation der eruptiugesteine. Geol. Rdsch., Vol. 55, P.478-491.

Streckeissen, A. L., 1967. Classification and nomenclature of igneous rocks. N. Jb. Min. Abh., Vol. 107, P.144-240.

Taylor, D. M., 1972. The geochemistry and petrology of the andesites and associated igneous rocks of an area of the Ochil Hills, near Dunning, Perthshire. Unpublished Ph.D. thesis, University of Nottingham.

Thompson, R. N., 1972. Evidence for a chemical discontinuity near the basalt andesite transition in many anorogenic volcanic suites. Nature, Vol. 236, P.106-110.

Thornton, C. P. and Tuttle, O. F., 1960. Chemistry of igneous rocks. 1. Differentiation index. Am. Jour. Sci., Vol. 258, P.664-684.

Tilley, C. E., 1950. Some aspects of magmatic evolution. Quart. Jour. Geol. Soc. London, Vol. 106, P.37-61.

Tilley, C. E. and Muir, I. D., 1962. The Hebridean plateau magma type. Trans. Geol. Soc. Edinburgh, Vol. 19, P.208-215.

Tilley, C. E. and Yoder, H. S. Jr., 1964. Pyroxene fractionation in mafic magma at high pressures and its bearings on basalt genesis. Carnegie Inst. Washington Yearbook, Vol. 63, P.114-121.

Tomkeieff, S. I., 1940. The dolerite plugs of Tieveragh and Tievebulliagh near Cushendall, Co. Antrim, with a note on Buchite. Geol. Mag., Vol. 77, P.54-64.

Tomkeieff, S. I. and Marshall, C. E., 1935. The Mourne dyke swarm. Quart. Jour. Geol. Soc. London, Vol. 91, P.251-292.

Tomkeieff, S. I. and Marshall, C. E., 1940. The Killough - Ardglass dyke swarm. Quart. Jour. Geol. Soc. London, Vol. 96, P.321-338.

Traill, W. A., 1878. Explanatory memoir to accompany part of sheets 60 and 71. Mem. Geol. Surv. Ireland.

Turekian, K. K., 1963. The chromium and nickel distribution in basaltic rocks and ecologite. Geochim. et Cosmochim. Acta, Vol. 27, P.835-846.

Turekian, K. K. and Kulp, J. L., 1956. The geochemistry of strontium. Geochim. et Cosmochim. Acta, Vol. 10, P.245-296.

Turner, F. J. and Veerhoogen, J. 1960. Igneous and metamorphic petrology, (2nd Edit). Mcgraw-Hill.

Tuttle, O. F. and Bowen, N. L., 1958. Origin of granite in the light experimental studies in the system $NaAlSi_3O_8$ - $KAlSi_3O_8$ - SiO_2 - H_2O. Mem. Geol. Soc. Am., No. 74.

Tyrrell, G. W., 1928. The geology of Arran. Mem. Geol. Surv. Scotland.

Varne, R., 1970. Hornblende lherzolite and the upper mantle. Contr. Min. and Petrol., Vol. 27, P.45-51.

Veerhoogen, J. 1962. Distribution of titanium between silicates and oxides in igneous rocks. Am. Jour. Sci., Vol. 260, P.211-220.

von Lasaulx, A., 1878. Petrographische skizzen aus Irland. III. Olivin gabbro von den Carlingford Mts., nördlich von Dundalk. Min. Petrog. Mitt., Vol. 1, P.426-433.

Wager, L. R. and Brown, G. M., 1968. Layered igneous rocks. Oliver and Boyd.

Wager, L. R. and Deer, W. A., 1939. Geological investigations in East Greenland, Part III. The petrology of the Skaergaard intrusion, Kangerdlugssuaq, East Greenland. Medd. Om. Grønland, Vol. 105, P.1-352.

Wager, L. R. and Mitchell, R. L., 1951. The distribution of trace elements during strong fractionation of basic magma - a further study of the Skaergaard intrusion, East Greenland. Geochim. et Cosmochim. Acta, Vol. 1, P.129-208.

Wager, L. R., Vincent, E. A. and Smales, A. A., 1957. Sulphides in the Skaergaard intrusion, East Greenland. Econ. Geol., Vol. 52, P.855-903.

Wager, L. R., Weedon, D. S. and Vincent, E. A., 1953. A granophyre from Coire Uagneich, Isle of Skye, containing quartz paramorphs after tridymite. Min. Mag., Vol. 30, P.263-276.

Walker, F., 1953. The pegmatitic differentiates of basic sheets. Am. Jour. Sci., Vol. 251, P.41-60.

Walker, G. P. L., 1959. Some observations on the Antrim basalts and associated dolerite intrusions. Proc. Geol. Assoc., Vol. 70, P.179-205.

Walton, E. K., 1963. Sedimentation and structure in the Southern Uplands. In: The British Caledonides, Edit. Johnson, M. R. W. and Stewart, F. H., Pub. Oliver and Boyd, P.71-97.

Wedepohl, K. H., 1959. Untersuchungen zur geochemie des bleis. Geochim. et Cosmochim. Acta, Vol. 10, P.69-148.

Wells, M. K., Smith, A. C. S. and Bowles, J. F. W., 1973. Carbonate enrichment at the margins of a basic dyke, Ardnamurchan, (abstract Bull. Min. Soc., No. 20, P.2.

Wells, M. K., Smith, A. C. S. and Bowles, J. F. W., 1974. Carbonate enrichment at the margins of a basic dyke, Ardnamurchan. Min. Mag., Vol. 39, P.514-524.

White, I. G., 1967. Ultrabasic rocks and the composition of the upper mantle. Earth and Planet. Sci. Lett., Vol. 3, P.11-18.

Wilkinson, J. F. G., 1956. Clinopyroxenes of alkali olivine - basalt magma. Am. Min., Vol. 41, P.724-743.

Wilkinson, J. F. G., 1959. The geochemistry of a differentiated teschenite sill near Gunnedah, New South Wales. Geochim. et Cosmochim. acta, Vol. 16, P.123-150.

Wilkinson, J. F. G., 1968. The petrography of basaltic rocks. In: Basalts, the Poldervaart treatise on rocks of basaltic composition. Edit. Hess, H. H. and Poldervaart, A., Pub. Wiley (Interscience), Vol. 1, P.163-214.

Williams, H., 1936. Pliocene volcanoes of the Navajo-Hopi country. Bull. Geol. Soc. Am., Vol. 47, P.111-172.

Williams, H., Turner, F. J. and Gilbert, C. M., 1954. Petrography: an introduction to the study of rocks in thin section. Freeman.

Wilson, A. D., 1955. A new method for the determination of ferrous iron in rocks and minerals. Bull. Geol. Surv. Great Britain, No. 9, P.56-58.

Wilson, A. D., 1960. The micro-determination of ferrous iron in silicate minerals by volumetric and colorimetric method. Analyst, Vol. 85, P.823-827.

Woode, R. D. A., 1961. The determination of traces of zinc in igneous rocks and minerals. Unpublished B.sc. thesis, University of Oxford.

Wyllie, P. J. and Tuttle, O. F., 1961. Hydrothermal melting of shales. Geol. Mag., Vol. 98, P.56-66.

Yoder, H. S. Jr. and Tilley, C. E., 1957. Basalt magmas. Carnegie Inst. Washington Yearbook, Vol. 56, P.156-161.

Yoder, H. S. Jr. and Tilley, C. E., 1952. Origin of basalt magmas: an experimental study of natural and synthetic rock systems. Jour. Petrol., Vol. 3, P.342-532.

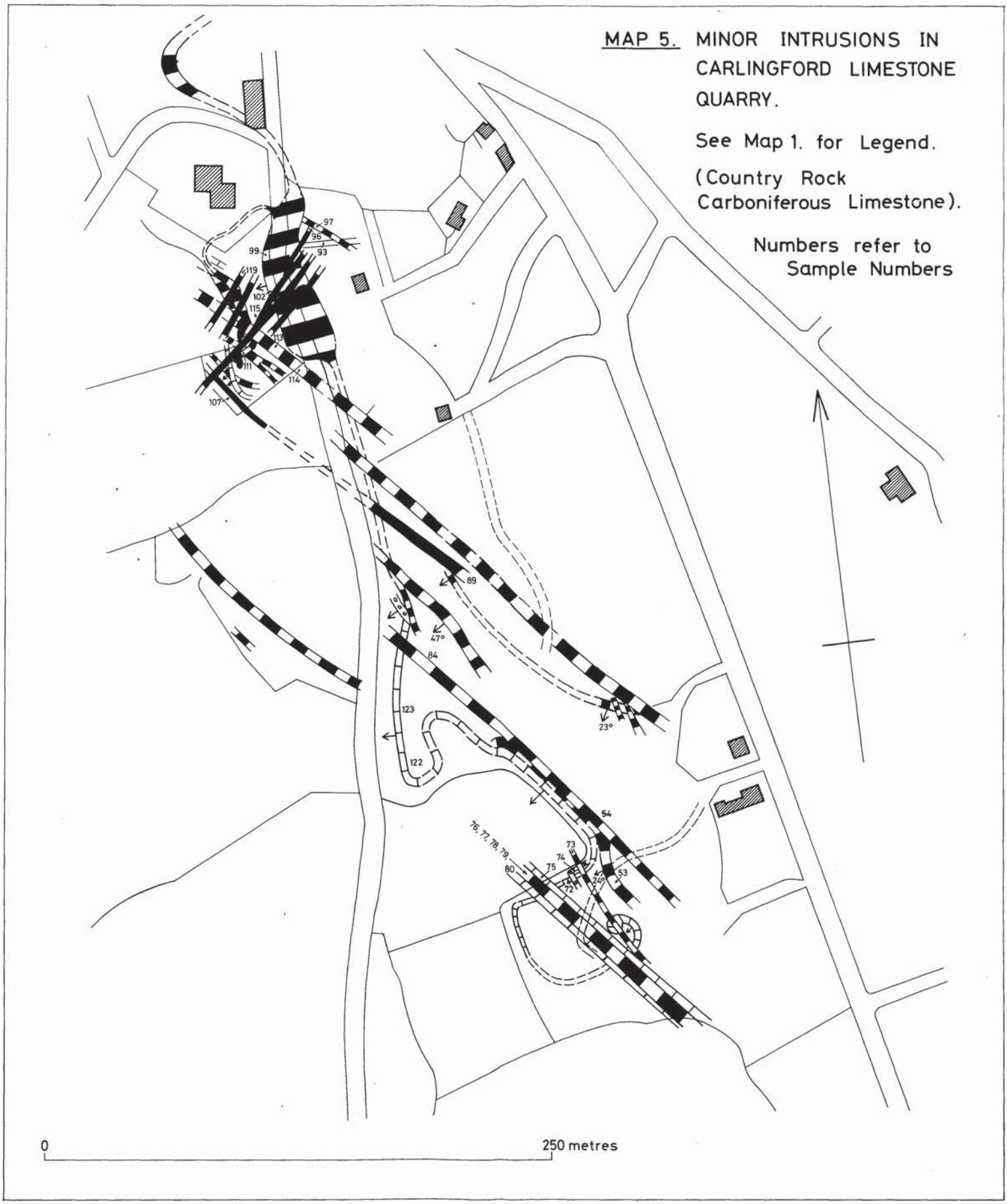
MAP 5. MINOR INTRUSIONS IN CARLINGFORD LIMESTONE QUARRY.
See Map 1. for Legend.
(Country Rock Carboniferous Limestone).
Numbers refer to Sample Numbers
97
96
93
99
119
102
115
113
111
114
107
89
47°
84
123
122
23°
54
76, 77, 78, 79,
80
75
74
73
72
71
24°
53
0
250 metres

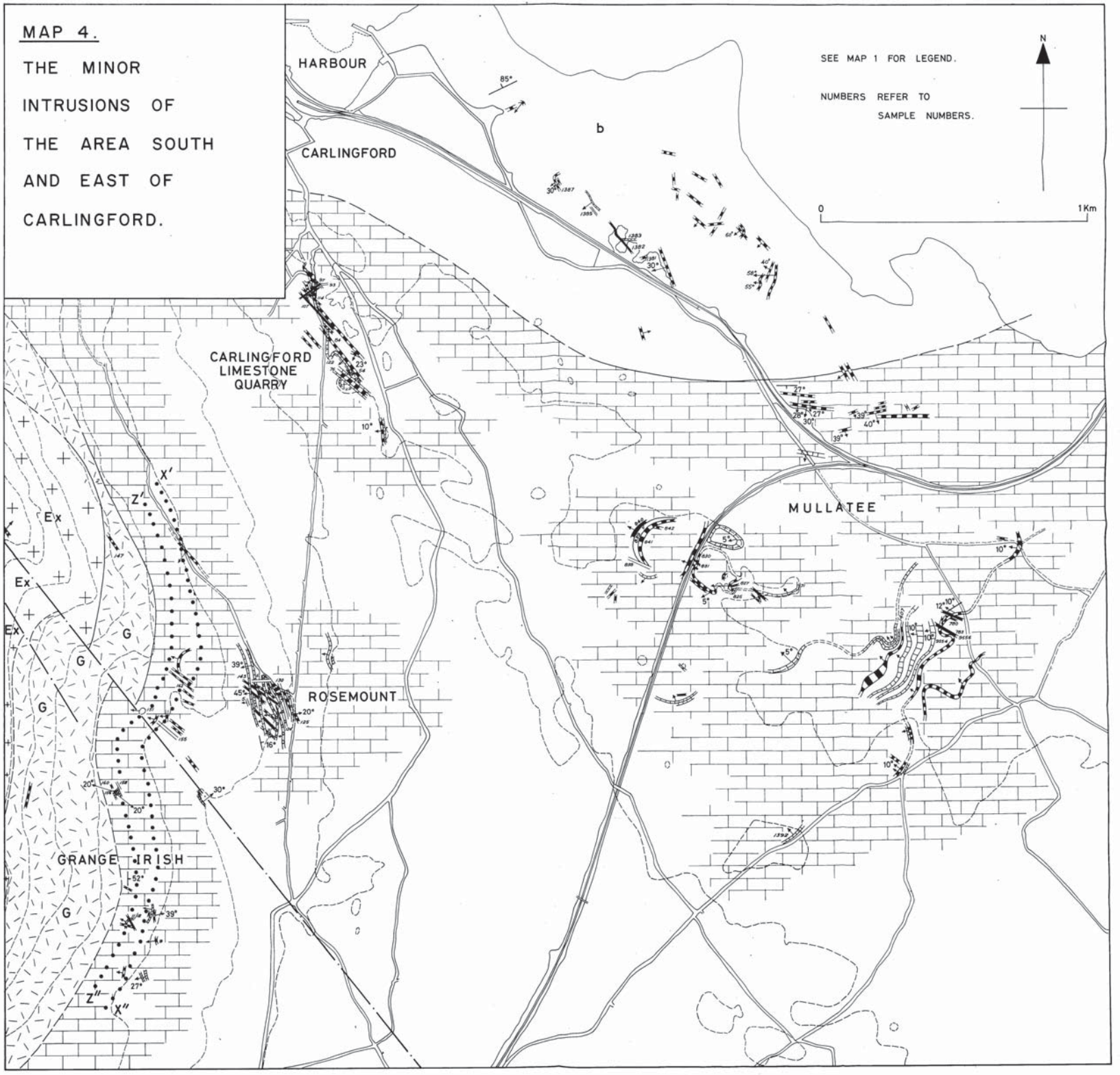
MAP 4.
THE MINOR INTRUSIONS OF THE AREA SOUTH AND EAST OF CARLINGFORD.
HARBOUR
CARLINGFORD
CARLINGFORD LIMESTONE QUARRY
ROSEMOUNT
MULLATEE
GRANGE IRISH
SEE MAP 1 FOR LEGEND.
NUMBERS REFER TO SAMPLE NUMBERS.
N
0
1 Km
X'
Z'
X''
Z''
Ex
G
b

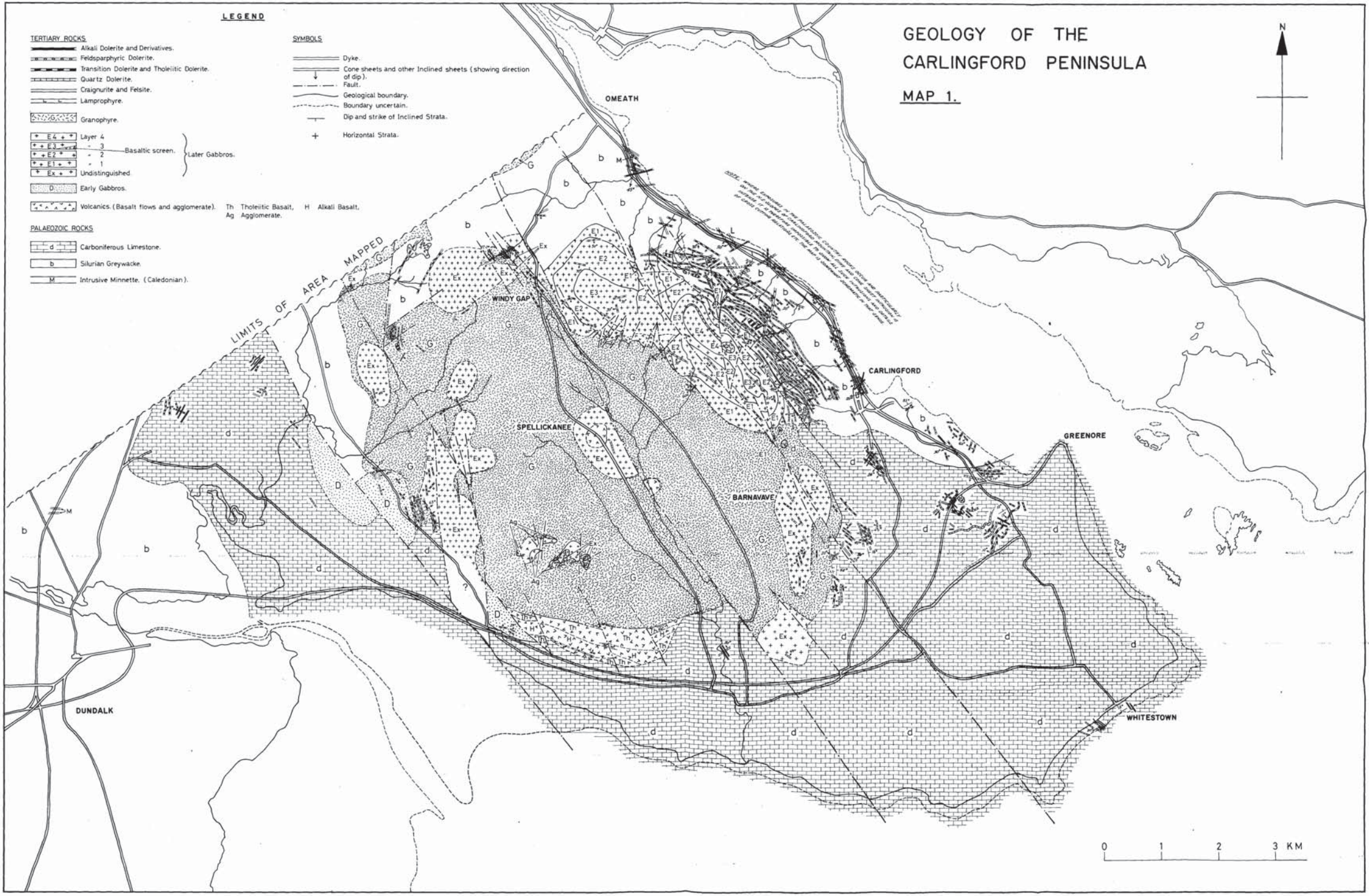
LEGEND
TERTIARY ROCKS
Alkali Dolerite and Derivatives.
Feldsparphyric Dolerite.
Transition Dolerite and Tholeiitic Dolerite.
Quartz Dolerite.
Craignurite and Felsite.
Lamprophyre.
Granophyre.
Layer 4
" 3
" 2
" 1
Undistinguished.
Basaltic screen.
Later Gabbros.
Early Gabbros.
Volcanics. (Basalt flows and agglomerate).
Th Tholeiitic Basalt, H Alkali Basalt, Ag Agglomerate.
PALAEOZOIC ROCKS
Carboniferous Limestone.
Silurian Greywacke.
Intrusive Minnette. (Caledonian).
SYMBOLS
Dyke.
Cone sheets and other Inclined sheets (showing direction of dip).
Fault.
Geological boundary.
Boundary uncertain.
Dip and strike of Inclined Strata.
Horizontal Strata.
GEOLOGY OF THE CARLINGFORD PENINSULA
MAP 1.
N
LIMITS OF AREA MAPPED
OMEATH
WINDY GAP
SPELLICKANEE
BARNAVAVE
CARLINGFORD
GREENORE
WHITESTOWN
DUNDALK
0 1 2 3 KM

MAP 3 THE MINOR INTRUSIONS OF CARLINGFORD AND CASTLE HILL

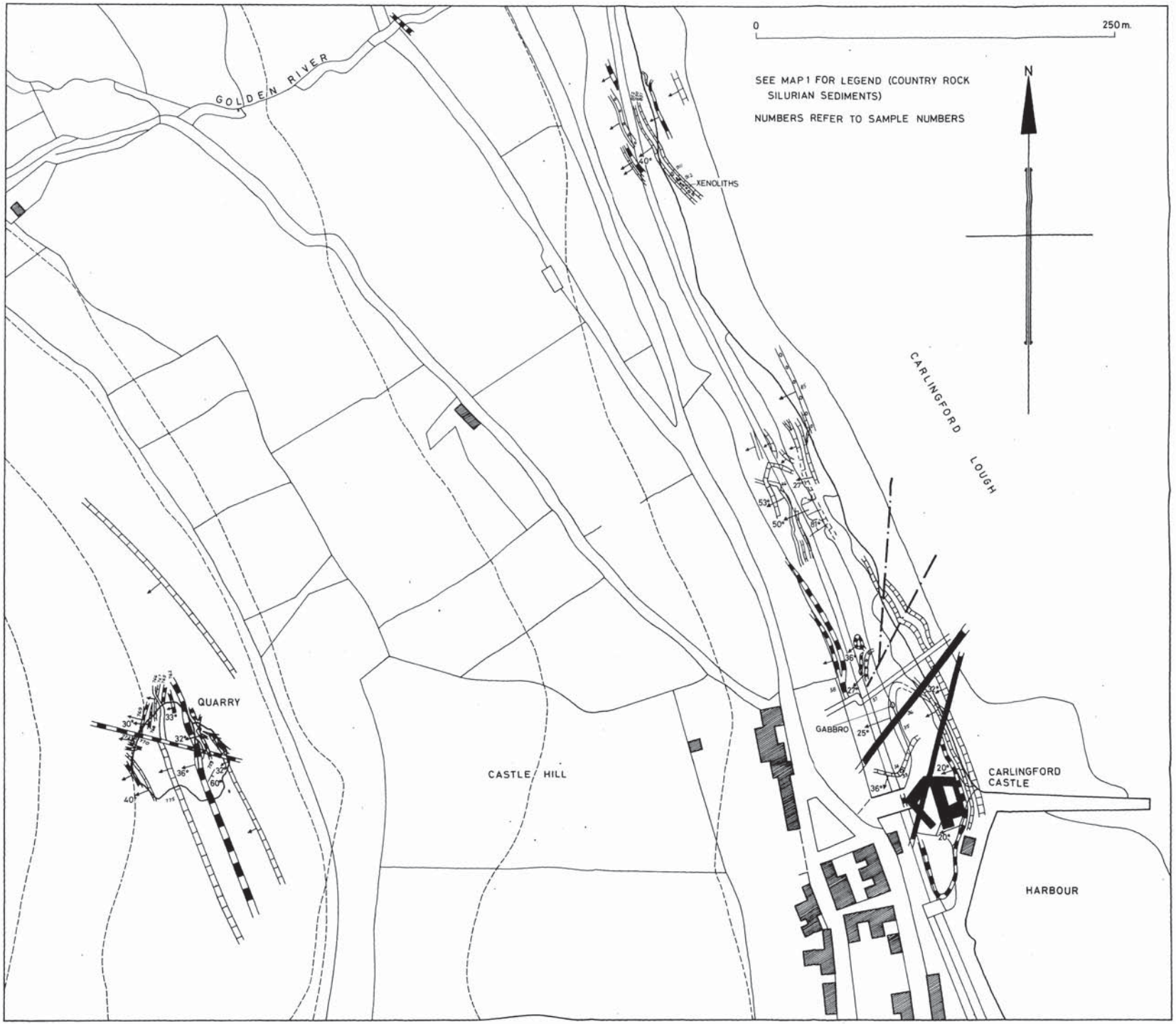

MAP 6. MINOR INTRUSIONS IN ROSEMOUNT QUARRY.

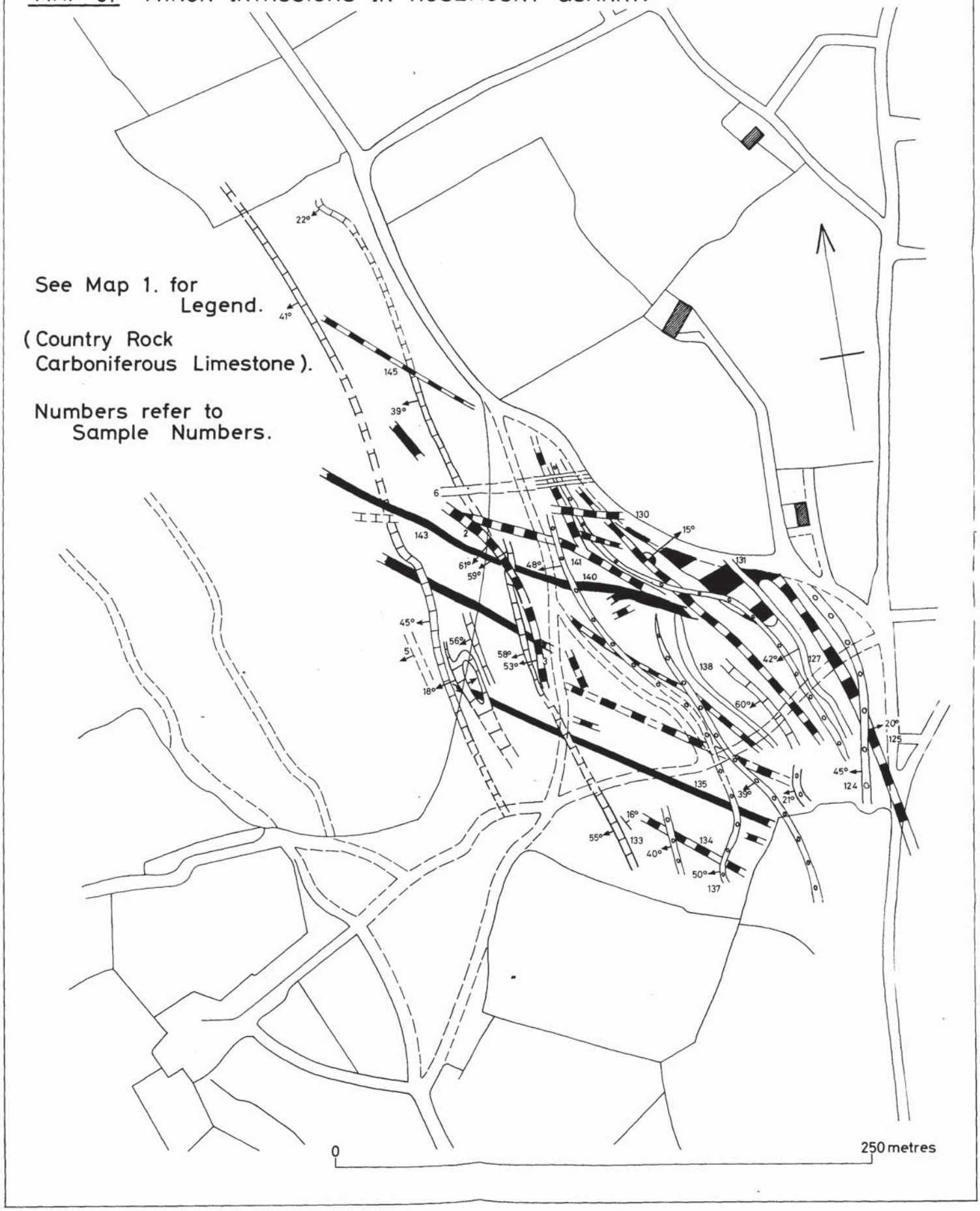

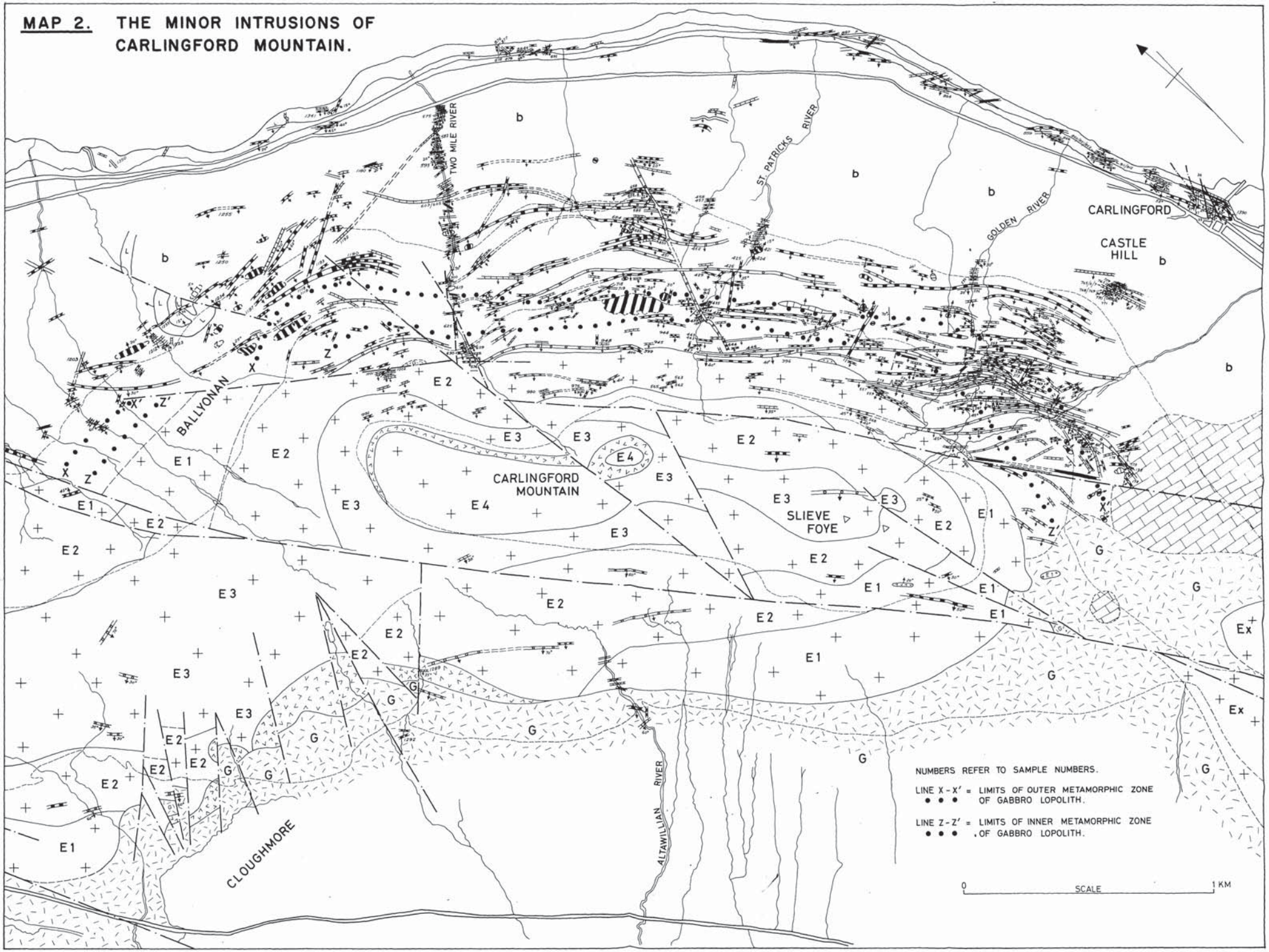
MAP 2. THE MINOR INTRUSIONS OF CARLINGFORD MOUNTAIN.
TWO MILE RIVER
ST. PATRICKS RIVER
GOLDEN RIVER
CARLINGFORD
CASTLE HILL
BALLYONAN
CARLINGFORD MOUNTAIN
SLIEVE FOYE
CLOUGHMORE
ALTAWILLIAN RIVER
b
E1
E2
E3
E4
G
Ex
X
X'
Z
Z'
NUMBERS REFER TO SAMPLE NUMBERS.
LINE X - X' = LIMITS OF OUTER METAMORPHIC ZONE OF GABBRO LOPOLITH.
LINE Z - Z' = LIMITS OF INNER METAMORPHIC ZONE OF GABBRO LOPOLITH.
0
SCALE
1 KM